Zekâi Şen

# Flood Modeling, Prediction, and Mitigation

# Flood Modeling, Prediction, and Mitigation

Zekâi Şen

# Flood Modeling, Prediction, and Mitigation

Springer

Zekâi Şen
Faculty of Engineering and Natural
    Sciences, Department of Civil
    Engineering
Istanbul Medipol University
Beykoz, Istanbul
Turkey

NOAH PHENOMENON — (GREAT FLOOD, WET SPELL)
JOSEPH PHENOMENON — (DROUGHT, DRY SPELL)

*There is sensitive balance in nature as a sequence of dry and wet periods, which needs care for their preservations without destroying the balance in the environment. This book is dedicated to those who care for such a balance by logical, rational, scientific and ethical applications for the sake of other living creatures' rights.*

# Preface

Floods are among the natural extreme events that occur after intensive storm rainfall events as excessive water volumes over the earth surface more than the capacity of surface natural or artificial conveyance systems (stream and river basins, creeks, estuaries, wadis, valleys, canals, channels, culverts, dams, cities). Apart from the rainfall causative floods, there are others as consequences of snowmelt, sea surge and tides, tsunamis, ground water level rise, urban sewer capacity overflow, dam breaks in addition to confined aquifer overflows.

Since the start of human history, societies have been exposed to the danger of natural events such as earthquakes, droughts, and floods that could not be avoided completely even with the modern-day scientific and technological facilities, pre-paredness, mitigation, and early warning systems. The most hazardous extreme natural event is the flood occurrence not only due to the intensive rainfall effects, but more significantly due to human settlement along flood dangerous areas such as floodplains, adjacent to riverbanks, and valleys. The floods are extremely beneficial events in arid regions, because they are the main source of groundwater recharge along drainage basins (wadis), where there are no human settlements or urban area exposed to flood danger. For this purpose, there are even runoff harvesting works in many arid regions of the world. However, flood beneficial aspects are outside the scope of this book, which is concentrated on floods and flash floods.

In order to achieve successful works to reduce flood danger and hazard, it is necessary to know scientific fundamental aspects of flood definition and generation processes, which pave way for methodological procedures to predict their future behaviors and to take precautions by means of hardware through the engineering water structures and software by means of early warning systems and also public awareness through educative training.

The main purpose of this book is to bring together all the layman, technicians', engineers', and scientists' methodological procedures that have been developed for flood peak discharge prediction during the last 150 years. Early approaches are rather logical and empirical, but later on, more systematic and analytical approaches are developed on the basis of rational, probabilistic, statistical, and stochastic

uncertain methodologies in a better objective manner. Empirical formulations are location dependent and cannot be applied to other parts of the world with satisfaction. Their old versions, prior to the rainfall recording, are dependent on the drainage basin area, but later versions include the rainfall amount or intensity. Today, the evolution of the flood peak discharge calculation methodology has reached to the employment of remote sensing and satellite image procedures coupled with digital elevation model (DEM) in the electronic media as for the surface morphological feature description, which is an essential ingredient in flood discharge prediction.

This book after the introductory chapter explaining the flood definition, types, physical causes, relationship to the overall hydrological cycle, and hazard types enters the domain of methodological procedures starting with the precipitation characteristics that take role in flood occurrence in addition to the surface features of drainage basin in terms of geomorphological variables. In two of the chapters, the hydrographs and flood discharge estimation empirical methodologies are presented with basic and fundamental explanations. The uncertainty aspects are presented through the probabilistic and statistical procedures including risk concept and return periods, which correspond to life of an engineering water structure. In the mean time, the sedimentation and debris expositions of various engineering structures are presented with some innovative recommendations for the first time in this book. In the last two chapters, climate change impact relationship to floods and also the flood hazard and mitigation procedures and approaches are exposed with the latest developments. In each chapter, some criticism and new suggestions are proposed for future better methodological advancements.

The content of this book is based on the vast experience of the author especially in arid region of the Arabian Peninsula through his academic work at the King Abdulaziz University, Faculty of Earth Sciences, Kingdom of Saudi Arabia; at the application establishment of the Saudi Geological Survey, Jeddah; and also at the Meteorology and Civil Engineering Faculties at the Istanbul Technical University, Istanbul, Turkey.

I hope that this book will support to those interested in flood discharge estimation with risk attachments, climate change relationships, hazard and mitigation aspects, and their applications in flood prevention works. I thank my colleagues who have encouraged me to write a book on floods and especially my wife Mr. Fatma Şen, who had kept silence, endurance, and patience during my extensive hourly, daily, monthly, and yearly works for the preparation of this book.

Çubuklu, Istanbul, Turkey                                                                    Zekâi Şen
2016

# Contents

# Chapter 1
# Introduction

**Abstract** Floods are among the major natural extreme and dangerous events that cause loss of life and property, and they are the most frequent extreme occurrences in different parts of the world. A broad definition of floods and their types are explained with meteorological and hydrological causative triggers and the consequences. Ordinary and flash flood features are presented in a comparative manner so that the reader can appreciate the difference between them. Flood hazards are exposed with recommendations and human pre-flood preparation procedures. It is emphasized that the floods are although natural phenomenon, but skewed settlements especially along the main watercourse such as the flood plain are also effective in the flood losses.

**Keywords** Definition · Flash · Flood · Hydrology · Hazard · Meteorology
Ordinary · Plain

## 1.1 General

In many places, excess water may become a disaster rather than a temporary inconvenience, especially if there are not early warning flood plans and the basic flood inundation maps, which are very essential for flood-prone region short-term and long-term protections. If there are limited communication facilities in a society, then any prolonged and widespread flooding may become a disaster more than ordinary event. On the other hand, it must be kept in mind that if there are no flood dangers in drainage basins, then floods provide rich groundwater recharge possibilities, especially in arid and semiarid regions, which should be considered as benefit. Any society must be prepared for flood awareness and at least for the preparation of flood inundation maps based on the fundamental flood estimation methodologies, which are the topics of this book.

Abundance of water is referred to as floods after intensive storm rainfall events (frontal or convective types) over the earth surface more than the capacity of surface natural or artificial conveyance systems (stream and river basins, creeks, estuaries,

wadis, valleys, canals, channels, culverts, dams, cities). Apart from the rainfall causative floods, they can be triggered also as a result of snowmelt, sea surge and tides, tsunamis, ground water level rise, urban sewer capacity overflow, dam breaks, and confined aquifer overflows. Floods have depth, areal extent, speed, and debris leading to unwanted sedimentation problems (Chap. 7). They may have threats in cases of intensively developed settlement or human activity concentrated catchments as a result of land use otherwise they do not cause any risk and danger in natural flood plains.

Impact of water-related phenomenon can be categorized into three groups according to their end consequences. In general terms, these groups are water scarcity, water availability, and excessive water occurrences (Şen 2005). Water availability is the most demanding aspect of water activities, and therefore, other two extreme cases must be rendered to support this domain through the application of scientific and technological facilities at large. Although, water is the most fundamental material for life sustenance on the earth, its occurrence and distribution are rather haphazard with temporal and spatial irregularities. For the maximum benefit from such irregularly variable water amounts, it is of prime importance to control and manage water according to certain basic scientific and technological developments. Water resources development scale is an indicator of prosperity for any country. Under the light of above classification, the management and control practices and approaches vary, and their applications in the field are the end products that help to sustainable development for the society.

The main causes of flood are the total amount and distribution of precipitation in the drainage area. Three natural factors that give rise to flood occurrence are the rainfall type and intensity (Chap. 2), drainage basin surficial features (Chap. 3), and subsurface soil and geological composition. Hence, assessment of a flood requires knowledge from meteorology, surface water hydrology, and hydrogeology disciplines.

Floods are initially more conspicuous, because they can occur over days or weeks instead of months or years. Floods arise from conditions that are somehow different than the established norms. Climate may not turn out to be a smooth continuum of meteorological possibilities after all, but rather the summation of multiple processes operations have additional significance both regionally and globally on differing time scales. Floods occur within local and global context of climate. It is necessary to understand the geography and meteorological response of a given watershed. One should also look beyond basin boundaries to appreciate the coherent patterns that influence weather regionally.

A flood is an overflowing of water from rivers onto adjacent land leading to inundations. Flash floods can explode suddenly out of a single summer thunderstorm. Flooding, however, can also be caused by a month-long buildup of moisture, such as the fast melting of a heavy winter's accumulation of mountain snow or soil saturated by high seasonal rainfall. All floods are shaped by the basin through which they flow. Spatial and temporal scales of floods are generally linked to the corresponding time and space scales of the flood -generating rainfall combined with weather and climate change conditions (Chap. 8).

Natural flood disasters related to the atmospheric origin are costly and their cost increases steadily due to social activities, industrial developments, and to a certain extent climate change. In many countries, most of the population lives in major cities, which are highly populated urban areas without sufficient infrastructure and also along the coastal areas. As a result, most of the commercial, trade, and industrial activities are prone to water disasters. On the contrary, human activities also affect the natural events as a result of not only climate change and global warning, but also local increase of impervious surfaces due to construction and asphalt roads and squares as well as the heat islands. Storm and flood losses have increased steadily in the last 30 years all over the world. Historical and conventional studies concerning the climate and floods do not provide reliable prediction for future behaviors of these events. Consequently, there may appear estimation errors in large percentage limits. The reduction of the estimation error will require not only the refinement of the basic knowledge and methodologies but also network design and monitoring system development. Any model has many restrictions, assumptions, local requirements, and time specifications. Therefore, a model that is developed for a specific country or region cannot be useful directly with the quantitative data for some other region. For the success of such a model, the necessary initial and boundary conditions must be identified for the area concerned. For instance, the risk levels of flood plains and inundation risks of coastal areas must be prepared at least approximately on a qualitative basis. However, there are objective quantitative techniques for proper digital description of the risks level (Chaps. 6 and 9). It is necessary to prepare risk maps for any natural disaster including flood risks also. Depths of floods in risky cross sections should also be identified for the establishment of assessment problems (Chap. 4).

The model for flood predication and assessment should require the flood discharges and their occurrence dates for proper investigation. In this book, especially, the statistical properties of each site flood records are conventionally desired as model inputs, but another necessity is their regionalization for proper spatial and regional interpretations. On the other hand, there might not be available data for the area of interest, and therefore, possible flood consequences could be carried from the record-known sites to the area of interest. Even the models that are used in practice cannot be capable of producing the resolutions that are needed by the planners, and therefore, downscaling procedures should be applied for attaining desired information. Model results may not be reliable especially for the tropical and mid-latitude regions. Besides, the models are average parameter producers, and therefore, possible deviations from these averages must also be accounted for. Even though the standard deviation around the mean does not change, this does not mean that the changes will be in a linear fashion, but unfortunately, the extreme events such as floods appear in a nonlinear manner. This point should be taken into consideration in future predictions.

When rainfall covers any area, the water evaporates and infiltrates, and runoff may occur on the surface as flood. The process of generating floods depends on

many factors; the most important one is the character of rainfall including intensity, time, and depth intensity–duration–frequency (IDF) curves, (see Chap. 2), the climatic conditions of the area, and the soil characters of the stream. The flood water moves in different directions according to the topography and the slope of the ground toward the mainstream. Flood usually starts with/after rainfall and continues to a time interval after falling (Viessman et al. 1989).

Runoff assessment requires sufficient data about climate conditions such as rainfall, infiltration, and evaporation. In addition, geomorphological and geological settings are needed as well as data with regard to surface water stage heights, if available, and water quantity and velocity.

In any flood study, satellite images, digital elevation model (DEM) data and aerial photographs are utilized to delineate drainage boundaries, while control sections of wadi channels are measureable in the field by leveling instruments (Chap. 3). Also observations of the highest flood level marks in the field are gathered and other relevant information is obtained from local inhabitants (Chap. 8). This preliminary information is used to construct rating curves in the control sections by using empirical formula (Chap. 3). The infiltration rates through the alluvium surface can be determined by the use of double ring infiltrometers in the drainage basins, which are referred to as wadis in arid and semiarid regions (Şen 2008a). There are a set of empirical and rational flood peak calculation methodologies among which the most suitable one can be selected for a preliminary assessment (Chap. 5). Hydrological parameters for the rational methods are presented in detail by Maidment (1993).

Only engineering structural protections cannot serve the community, but more significantly the pre-flood warning through the flood inundation maps are very helpful for future planning by local and central authorities. Furthermore, past experience has shown that the engineering structures fail in many cases due to either insufficient calculation or construction or the record breaking behavior of natural events. The main rule considered in this book is that rather than the trust to an engineering structure and expansion of the activity within the flood plain, it is wiser to depend on the flood inundation maps and especially on the risk calculations in planning for future developments in a potential flood-prone area (Chaps. 6 and 9).

According to a report by the U.S. Congress's Office of Technology Assessment, "despite recent efforts, vulnerability to flood damages is likely to continue to grow." The factors cited include the following points.

(1) Growing populations in and near flood-prone regions,
(2) The loss of flood-moderating wetlands,
(3) Increased runoff from paving over soil,
(4) New development in areas insufficiently mapped for flood risk,
(5) The deterioration of decades-old dams and levees,
(6) Policies such as subsidies that encourage development in flood plains.

A very significant factor that should be added to this list is the anthropogenic climate change impacts (Chap. 8). Although a number of water balance studies have

been conducted for a variety of watersheds throughout the world, the rainfall–runoff studies in addition to the water balance of the arid and semiarid lands present some interesting challenges (Flerchinger and Cooley 2000; Scanlin 1994; Kattelmann and Elder 1997; Mather 1979). These watersheds, which are dominated by precipitation and evaporation, exhibit a high degree of variability in vegetation communities on scales much smaller than addressed by most hydrological modeling. Thus, arid region wadis (catchments) pose a unique set of problems for hydrological modeling.

Extreme situations are rather uncontrollable due to hazard potentiality, but their impacts can be reduced significantly provided that a certain risk level is accepted in water structure designs such as dams, culverts, land use, industrial area development, agricultural land allocation, and similar activities, last but not the least, also the impact of present climate change should be taken into consideration in all future projects (Chaps. 8 and 9). The risks are more serious in arid and semiarid regions, because of the potential flash flood occurrences, which cannot be pre-warned easily (Chap. 5). It is, therefore, preferable to prepare flood hazard maps that guide any development level and areas in a flood-prone drainage basin. This book also provides effective field and office works in addition to reliable models for flood hazard map preparation (Chap. 6).

## 1.2 Flood and Hazard Definition

Floods are the common name for extreme runoff volumes after an intensive storm rainfall event over a drainage basin. This definition indicates two components for flood occurrences, which are the rainfall intensity and the drainage area features. It does not imply that intensive rainfall events will lead to floods. For flood occurrence, certain features of the drainage basin are important and without them even though the rainfall might be very intensive, but there might not be any flood event. Among the most significant drainage basin features are drainage basin areal extend, slope and especially cross-sectional area variations along the main channel course.

A flood is an overflowing of water from rivers, streams, main channels, wadis onto land that do not experience usually inundations. Floods also occur when water levels of lakes, ponds, reservoirs, aquifers, and estuaries exceed some critical value and inundate the adjacent land, or when the sea surges on coastal lands are much above the mean sea level. Nevertheless, floods are natural phenomena important to the life cycle of many biotas, not the least of which is mankind. Floods are the most destructive of natural disasters and cause the greatest number of deaths. Spatial and temporal flood scales are generally linked with the corresponding scales of the flood-generating thunder storm events.

A flood is defined also as any relatively high flow that overtops the natural or artificial banks in any reach of a stream. When banks are overtopped, water spreads

over the floodplain and generally comes into conflict with man. It is important that floods should be controlled so that the damage caused by them does not exceed an acceptable amount. Man must acquaint himself/herself with the characteristics of floods if he/she is to control them. Although floods vary from year to year, their measurements should be carried out regularly. Analysis of flood records provides a better understanding of the phenomenon (Linsley et al. 1982).
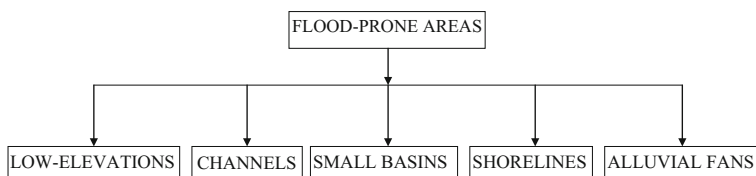
The most flood-prone environments are presented in Fig. 1.1 including five areas in general irrespective of hydrological regime.

Low-lying areas suffer the most from the flooding and inundation hazards. Many thousands of populations live in these areas due to the groundwater availability and transportation facilities. In small basins, flash floods occur more frequently, because during an intensive storm rainfall the basin receives more than it could transfer as surface water in a short time of period.
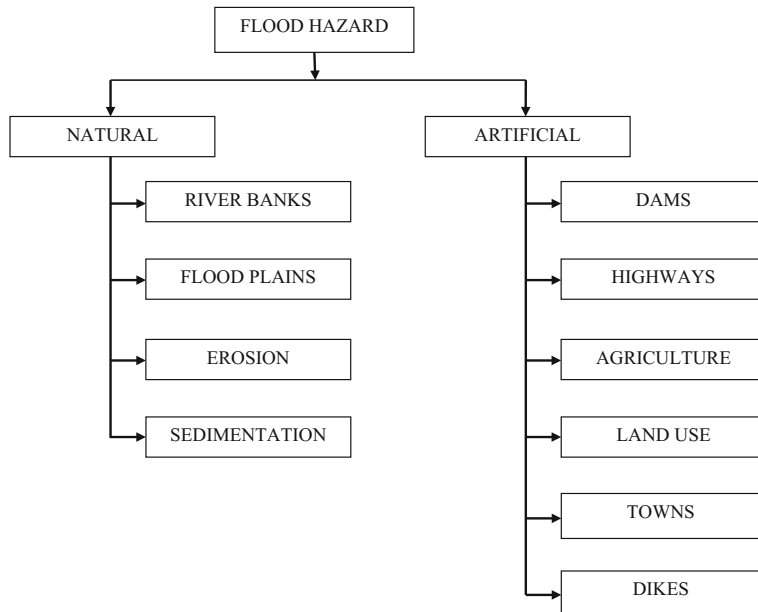
Floods may also result from dam failures, which give destruction and damage to downstream-located activity centers such as urban areas, industrial plants, agricultural lands. Shoreline flooding due to sea level rise is also possible in some countries. Alluvium fans are attractive for urban development with their groundwater potentiality, but in the same time especially in arid regions, they create special type of flash flood treats. Alluvial fans are risk-prone environments, because the drainage channels can meander unpredictably across the relatively steep slopes, bringing high velocity flows (5–10 m/s), which are highly loaded with sediment.

On the contrary to the natural cases, there are also artificial flood occurrences due to human activities. The closer the urban land use to the main channel stream, the more prone is to inundation, and consequently, drainage cross sections that have not been prone to flood hazard before, may become under the threat of flood danger. Hence, it is possible to divide the flood hazards into two complementary sections as natural and artificial flood hazards as shown in Fig. 1.2.

There are not enough floods studies in arid regions. In these water stricken regions, flood waters can be stored in the form of surface or subsurface reservoirs. In addition, most of the engineering structures across watercourses are under designed and in small intensity floods they may be subjected to damage or even complete washout. This damage might extend to agricultural lands and to other human properties. Furthermore, the sediments transported during floods may result in the filling of hand-dug wells and ditches. Most of the alluvium aquifers in arid



**Fig. 1.1** Flood environments

**Fig. 1.2** Flood hazards

regions occur in the wadis (dry valleys), which provide depressions for deposition and occasional surface runoff occurrences. The groundwater reservoirs in these wadis are directly related to flash floods. Groundwater resources in arid region aquifers are depleted through pumping or by natural subsurface flow into the sea. However, it is replenished during floods following adequate rainfalls. These replenishments of groundwater depend on the local climatological and geomorphological conditions, in addition to the geological composition of the area (Şen 2008a).

The absence of detailed records on major floods is noticeable in most basins. In general, comparatively more recorded data exist on normal rainfall. The set of available rainfall data together with the drainage basin characteristics facilitate the use of empirical equations to estimate relevant flood discharges. As explained by Parks and Sultcliffe (1987), the problem of flood measurement is more acute in arid areas than elsewhere.

Apart from the flood hazards there are also a variety of benefits provided that the flood management planning is based on local experience, expertise, scientific methodologies, and technologies. For instance, flood plain inundation provides groundwater recharge possibilities, which may support round-the-year water supply through surface and subsurface water structures. Floods also carry nutrients in addition to sediments, which help to enrich soil.
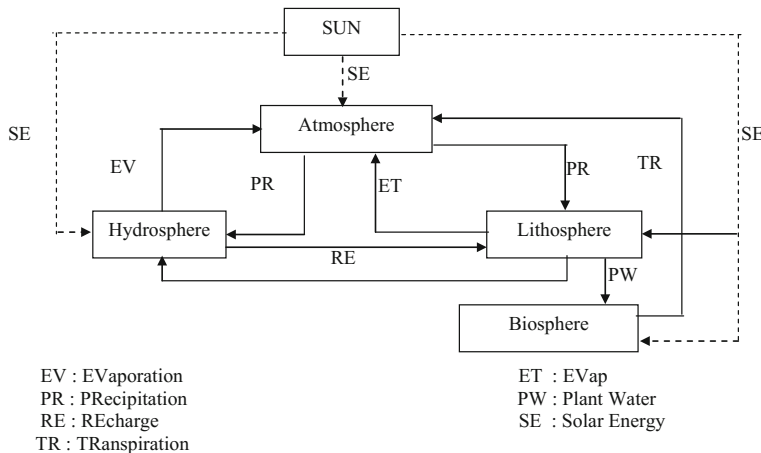
## 1.3  Hydro-meteorological Events

Water-related problems cannot be solved only by consideration of the measurements, but the physical mechanisms should be also thought for the integrated flood estimation methodologies. The trend for integrated water resources management (IWRM) also includes integration of flood management for sustainable development and human security. Any successful IWRM should be based on the flood hazards vulnerability and society that are under the effects of flood risks. Although the rainfall is the triggering event for surface flow and its extreme values as floods, its quantitative and qualitative features must be identified in a combined manner. Toward the best solution meteorology, climatology, surface hydrology, and finally, hydraulics principles inter-effectively play common role for flood problem solutions.

   The main causes of flood are the amount and distribution of precipitation in the drainage area. Three natural factors that give rise to flood occurrence are the rainfall type and intensity, drainage basin surficial features, and subsurface soil and geological compositions. Assessment of a flood requires knowledge from meteorology, geomorphology, geology, and surface water hydrology and hydraulics principles.

### 1.3.1  Global Environment and Cycle

Hydrological cycle is the combination of all possible waterways among the atmosphere, lithosphere, biosphere, hydrosphere, and cryosphere in addition to specific ways within each one of these spheres. Human beings, animals, and plants are dependent on some gases, water, nutrients, and solids that are available in nature quite abundantly in sensitive balances and almost freely for their survival. The most precious ones are the air in the atmosphere that is essential for living organisms to breathe and the water that is available in the hydrosphere. The atmosphere has evolved over geological time history, and the development of life on earth has been closely related to the composition of the atmosphere, hydrosphere, and lithosphere. From the geological records, it seems that about 1.5 billion years ago free oxygen first appeared in the atmosphere in appreciable quantities, (Harvey 1982). The appearance of life was very dependent on the availability of oxygen, but once sufficient amount was accumulated for green plants to develop, then photosynthesis was able to liberate more into the atmosphere. The various spheres and their interactions for human survival on the earth are shown in Fig. 1.3 (Şen 1995). Hydrosphere consists of oceans, lakes, and rivers, whereas lithosphere forms the continental crust, and biosphere includes the living kingdom of continents and oceans. Although these natural systems are very different in their composition, physical properties, structure, and behavior, they are interlinked to each other by exchanging fluxes of mass, energy, momentum, and hydrological cycle (Şen 2008b).

**Fig. 1.3** Spheres and their environments

In any part of the world, the hydrological cycle functions fully or partially, and especially in arid and semiarid regions functioning is not continuous, but depends on the season of the year. Rainfall phenomena are the major hydrological events, which subsequently cause other hydrological events such as the depression, interception, evaporation, infiltration, runoff, and flood. These are the vital hydrological elements for the existence of life in a region.

## 1.4 Hydrological Cycle

Hydrology is the science of water occurrence, movement, and transport. Furthermore, it is concerned with local circulations through the atmosphere, lithosphere, biosphere, and hydrosphere dealing with water movement, distribution, quality and environmental aspects. In general, it deals with natural events such as rainfall, runoff, drought, flood, and groundwater occurrences.

The hydrological cycle of rainfall, runoff, and evaporation does not exist in isolation. The interaction at various time scales between the hydrological cycle and the cycle of erosion and sedimentation has long been recognized. More recently, the study of the earth–chemical cycles of carbon, nitrogen, and sulfur has revealed the importance of their linkage to the hydrological cycle. These three cycles (hydrological, erosion, geochemical) can be considered as part of a general earth system, which interacts in turn with the regional socioeconomic system. Population growth and economic development combine to increase the demand for good quality water. At the same time, these two factors also combine to impact the geo-system in such a way so as to reduce the supply of clean water. The continuation of these two tendencies in the future is expected to produce water crises of unprecedented magnitude.
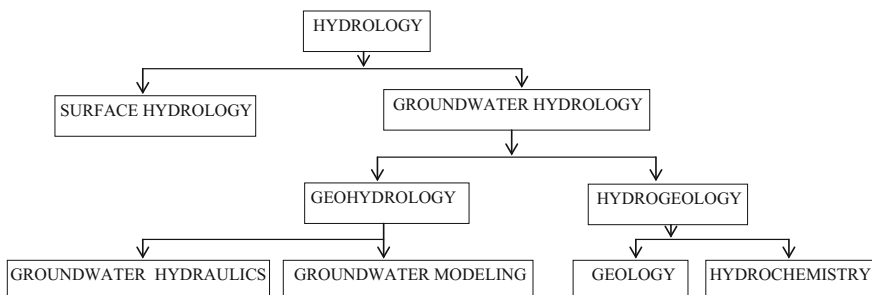
Human beings try to benefit from different ways of water movements to their advantage for the prosperity of society. It is, therefore, necessary to develop different and convenient techniques for the assessment of these movements, and if possible to delay or speed up their sequences such that right water demands are met at right times and places. Hence, temporal and spatial variations of hydrological components play a definite role in human activities so as to control and use the potentials provided by the hydrological cycle.

On the application side, hydrology provides basic laws, equations, algorithms, procedures, and modeling of earth-system events for the practical use of the humanity. It is most concerned with the practical and field applications for water resources identification, simple rational calculations leading toward the proper management (Fig. 1.4).
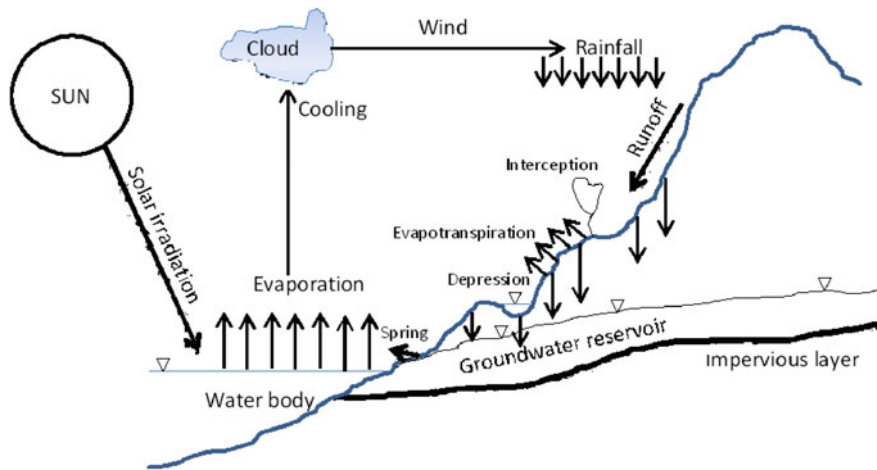
Hydrological cycle is the sole vital indicator of water existence with its distribution, movement, physical properties, and quality related to atmosphere, lithosphere, biosphere, and hydrosphere environments. Each environment includes water in different phases (gas, liquid, or solid) and these are related both temporally and spatially to each other by the hydrological cycle. The classical form of hydrological cycle is presented in many textbooks with its full components.

This general cycle works completely or partially depending on the geographical location. For instance, in arid regions, the component of infiltration or deep percolation may not function properly, and consequently, groundwater resources cannot be replenished sufficiently. Hydrological cycle works since millions of years, but even during such time span, it has worked in some parts completely in the past, but today it functions partially at the same locations. At great depths of sedimentary geological successions are the groundwater reservoirs as fossil water that cannot be replenished with the present day hydrological cycle. The effective domain of hydrological cycle does not change with geographical location only, but also temporally and leaves trace in different forms.

In arid regions, the hydrological cycle behavior becomes independent from the general atmospheric circulations, which are significant for humid regions. However, the hydrological cycle is more dependent on local conditions and distance from the



**Fig. 1.4** Hydrology-related topics

**Fig. 1.5** Hydrological cycle components (Şen 2015)

coastal areas. It is possible to say that the arid region hydrological cycle works rather in small scales at the sea coastal regions and nearby inland areas, but with the penetration of moist air to far inland areas, hydrological cycle components either become very weak or nonexistent for some reasons.

In nature the hydrological cycle starts from the evaporation and ends after stages of cloud formation, rainfall, runoff and groundwater recharge. Along this path, there are the oceanic, atmospheric, hydrospheric, and lithologic domains, each of which impacts on the occurrence, movement, and distribution of the natural water phase (gas, fluid, and solid) and water resources occurrences. Hydrosphere includes environments of sole water such as lakes, rivers, and oceans. The water of the earth circulates among these environments from the hydrosphere (oceans) to atmosphere then to the lithosphere. The circulation including complex and dependent processes such as evaporation, precipitation, runoff, infiltration, groundwater flow is called "the hydrological cycle" (see Fig. 1.5).

## 1.5   Flood Definition
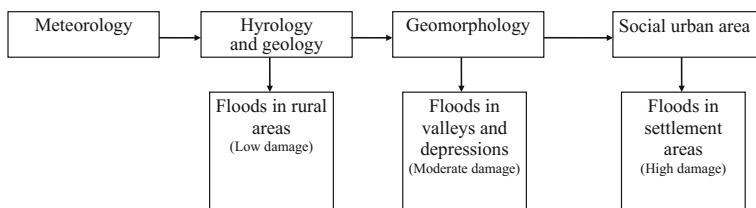
Naturally, there are two flood types as ordinary floods, which are common in many parts of the world and flash floods that are sudden and in huge quantities that are coupled with recent climate change impact, especially in arid and semiarid regions of the world. However, as for the triggering mechanism of floods there are also many different types.

## *1.5.1  Ordinary Floods*

Coupled with the meteorological conditions hydrological circumstances might not be sufficient for the flood occurrence. Still further the surface features (geomorphology) of the area play a significant role in the generation of the harmful floods. Geomorphological characteristics are the guide features of the precipitation water that reaches the earth surface. According to the water divide and collection (streams and rivers), this water is distributed and divided into various shares within each catchment and in its sub-catchments. Geomorphological features provide basis for the flood velocity, and subsequently, the damage increases. Due to high velocity in areas where there are not sufficient vegetation covers, flash floods endanger further the human life and property (Chap. 3).

In addition to the above causes, there are social factors, which bring at times, unconsciously, some human settlement areas under the threat of future floods. This might be due to misplanning and mismanagement. For instance, if urban areas are selected right in the upstream areas, where there are not flood risks, then they will not be exposed to flood danger. For such a task, necessary meteorological, hydrological, and social planning projects, constructions, and administration works must be studied carefully with the aim to reduce the flood damage. Most often, these studies do not care flood exposed sites such as industrial and settlement locations, where all of sudden floods may appear with their destructive property and life claiming consequences. Especially, river flooding is caused in a flash manner mainly by sudden precipitation increase, which leads to intensive rainfalls within short time durations. Long duration precipitations, say for few weeks, replenish the soil moisture and after the saturation, the surface flow starts to appear in an increasing rate and velocity leading steadily to floods. These might not be as harmful as the flash floods, which might appear even in desert areas, because due to the high rainfall intensity there is not enough time for the seepage, and therefore, suddenly all the water contributes to the surface flow and consequently to the floods. The sequential flood blocks are presented in Fig. 1.6 which should be considered in any flood assessment study.

Meteorological data do not provide reliable regional study possibilities, and therefore, insufficient studies must be supplemented by the expert views and additional local information and experience from the society and administrations.



**Fig. 1.6**  Flood causes

For instance, the insurance companies would like to know the risk levels during different return periods so as to guide and properly design their insurance policies (Chap. 9). Especially, in flood studies, real-time predictions are not necessary but interval estimates, i.e., return period-based estimates are the basic knowledge that is required by the planners and administrators in addition to the private companies such as the insurance units. On the other hand, not only quantitative digital data, but additionally verbal expert views are most important in taking final decisions. Any model has many restrictions, assumptions, local requirements in addition to time specifications. Point risk levels on the site basis are useful (Chap. 6) but more effectively, it is desirable to have regional risk level maps, which may be in the form of equal risk level lines for different return periods such as 5-year, 10-year, 20-year, 25-year, 50-year, and 100-year. Unfortunately, these have not been prepared for many parts of the world.

Flooding can occur quickly in the mountain head-water areas in large river basins as well as in the rivers draining to the coast. The rivers are steeper and flow quickly with flooding sometimes lasting only for one or two days. These floods can be potentially much damaging and pose a greater risk to loss of life and property. This is because there is generally much less time to take preventative actions against dangerous water flows. This type of flooding can affect major towns and cities.

Flooding studies concerned with life protection depend on estimating the maximum rate of flooding in the area (Chaps. 5, 6, 7, and 9). The processes of developing and distribution of flooding movement are affected by many climatic and topographic factors. Accordingly, the estimation of flooding hazards needs detailed examination of climatic studies (including rainfall data and evaporation process), geological, topographic and morphologic studies (including basin area and their drainage system patterns), engineering geologic studies (including the characteristics and behavior of wadi soils), and hydrological studies.

The absence of detailed records on major floods is noticeable in most drainage basins. In general, comparatively sufficiently recorded data exist on normal rainfall. The set of available rainfall data together with the drainage basin characteristics facilitate the use of empirical equations to estimate relevant flood discharges (Chap. 5). As explained by Parks and Sultcliffe (1987), the problem of flood measurement is more acute in arid areas than elsewhere. In general, floods are flashy, and hence, the problem of the peak discharge level determination by the maximum water level record is aggravated by siltation of inlet pipes (Farquhason et al. 1992).

## 1.5.2   Flash Floods

A flash flood is a specific type of flood that appears and moves quickly across the land with little warning. Many parameters can cause a flash flood including heavy rainfall concentrated over an area, thunderstorms, hurricanes, and/or tropical storms. Dam failures can also cause flash flood events. When a dam or levee

breaks, a gigantic quantity of water is suddenly discharged downstream destroying anything in its path.

These are events that occur in many parts of the world including arid regions, and they may cause sudden potential hazards to human life and property. Especially, in arid and semiarid regions, these floods may rise rapidly due to impervious hard rock catchments and move along the sand and gravel filed wadis, which are normally very dry. The flood speeds are usually faster than a person can escape from the rough channels. Flash floods normally reach the sea or are lost in the inland deserts. However, they also help to fill the wadi alluviums that later provide groundwater recharge for local agricultural lands or partially for the nearby city water supply.

Flash floods are short-term inundations of small areas such as a town or parts of a city, usually by tributaries and creeks. Heavy rain in a few hours can produce flash flooding even in places, where little rain has fallen for weeks, months, and years. If heavy rainfall occurs repeatedly over a wide area, then river or mainstream flooding becomes more likely, in which the main rivers of a region swell and inundate large areas, sometimes well after rainfall end. If the intense convectional cells coincide with small drainage basins, then catastrophic flash floods can result and they occur mainly in the summer season, especially in the inlands. They produce large volumes of flood water with rapid concentrations in time and space leading to great damage potentials.

Although flash floods are among the most catastrophic phenomena, the volume of the infiltration from floods is a major source of groundwater replenishment to aquifers that are hydraulically connected with watercourses on the surface. Moreover, this volume of water could be increased significantly by impounding the floods with surface dams or successive dykes (Şen 2014). Importance of flood studies, other than dealing with surface and subsurface water interactions includes flood influences on engineering structures, such as dams, bridges, culverts, and spillways.

From the hydrological point of view, the following variables are important in any flash flood calculation (Chaps. 3 and 4).

(1) Rainfall intensity,
(2) Rainfall duration,
(3) Topography,
(4) Soil conditions,
(5) Coverage of the terrain.

Topographic conditions such as high-exposure (steeply sloping) high land terrains, narrow valleys, or ravines hasten the runoff and increase the likelihood of flash flood occurrence. Saturated soil or shallow watertight geological layers increase surface runoff. Urbanization processes and affiliated construction with watertight materials are thought to make runoff 2–6 times greater in comparison to terrains with natural coverage (fields, meadows, forests).

Flash floods are not uncommon in arid regions and present a potential hazard to life, personal property, and structures such as small dams, bridges, culverts, wells, and dykes along the wadi courses. After a short period of intensive rainfall, flash floods are formed rapidly and they flow down over extremely dry or nearly dry watercourses at speeds more than 1. 5 m/s faster than a person can escape from the rough and sandy wadi channels (Dein 1985).

In arid/semiarid regions, flash floods constitute the majority of casualties of all natural hazards, and these areas occasionally confront a higher risk of damage by flooding than their counterparts in more humid environments. This is usually because of the longer return periods or rarity of extreme rainfall, in addition, prediction of flash floods is extremely difficult due to their short duration and the small geographical region over which they occur. However, in a warmer world, the frequency of these intense storms in semiarid and arid regions may increase (Smith 1996; Smith and Handmer 1996; Smith and Ward 1998).

Flash floods normally strike the urban areas and roads at the downstream part of any drainage basin, because they are uncontrollable and difficult to predict. Therefore, the subject requires special attention by researchers especially in arid climates to estimate the magnitude, volume, time to peak flood discharge and areas, which are prone to flood hazards. The most frequent areas that are affected by flash floods are those in low-lying areas surrounded by high mountains in and around the mainstreams of wadis and in adjacent flood plains. The risks are more serious in these regions, due to the potential flash flood occurrences, which cannot be warned earlier. It is, therefore, required to prepare flood hazard maps that may help to indicate safe and unsafe areas along the basin.

During the last few decades, flash floods have developed as one of the most dangerous natural disasters, which may occur almost everywhere in the world. In recent times, great attention is given to flash floods due to several catastrophic events in different countries. Flash floods are one of the most impressive hazardous manifestations of the environment, which directly affect human activities and security. Their origin and development are not yet well enough understood. There are many ways to prevent flash floods, but no matter how well any one method works, its effect is always limited.

### 1.5.3   Triggering Mechanism Types

As mentioned earlier, flood occurrences take place in different location depending on their triggering mechanisms. These are summarized in the following items.

(1) Winter rainfall floods: Westerly depressions with well-developed warm fronts bring winter precipitation, mainly in Central and Northern Europe. When these precipitations are heavy, continuous, and prolonged, they can lead to soil saturation and consequent high volumes of runoff. As a result, rivers may flow out of banks, causing flooding,

(2) Summer convectional storm-induced floods: Heavy convectional thunderstorms can sometime generate intensive storms and floods. Especially, in Southern European regions, prolonged summer months hot periods can end with sudden storms. If the storm event can be localized they can lead to severe flash floods affecting highly developed sub-areas,

(3) Convective frontal storm-induced floods: Frequent meteorological conditions over Western and Southern Europe are characterized by extended low pressure, associated to cold fronts, which travel from the west Mediterranean Sea toward the continent. In these situations, mesoscale convective systems may develop, resulting in extreme rainfall, lasting more than 24 h. The air mass can be subjected to orographic enhancement upon reaching over the slopes of the mountain chains,

(4) Snowmelt floods: Rapid snowmelt can sometimes cause flooding, especially in the spring when warm southern air streams become influential Alpine or upland areas may generate sudden snowmelt accompanied frequently by heavy rainfall. This phenomenon is usually much localized and in very steep watersheds can produce flash floods, since flood water velocity can be high. The problem affects urban areas at the valley bottoms,

(5) Urban sewage flooding: Inadequate sewage system can lead to serious flooding problems in urban areas, since even normal intensive rainfall events can create abnormal flooding,

(6) Sea surge and tidal flood threat: One of the major problems of flooding that may affect many European coastal areas is related to the sea surge and tidal effects. Moreover, associated with this problem is the phenomenon of coastal erosion, which may consequently lead to flooding,

(7) Dam-break flood risk: Flood problems can also arise from the breaking of dams and dikes.

In many regions, there are various causes of flooding, the most important ones are related to the geological and topographic conditions and the climate features. In addition, the social and economic situation of the population makes them more closely attached to the sources of the hazards. It is possible to classify the floods according to their durations and appearances as follows.

(1) Long-term floods: One week or longer duration,
(2) Short-duration floods (flash floods): About 6 h or less duration.

On the other hand, floods can be classified also according to their appearances into four categories as follows.

(1) Active water collector floods—Streams and rivers,
(2) Dry water collector floods—Mountain sides and slopes,
(3) City floods—Creeks in the urban areas,
(4) Coastal floods—Open pressure effect on the sea surface.

## 1.6  Physical Causes of Flood

Floods are among the natural disasters that cause property and life losses occasionally with great financial, environmental, and social consequences. The main trigger mechanism of these natural hazardous events is the atmospheric conditions that end up with the convenient meteorological setup for the generation of precipitation. Especially, extreme cases of precipitation give rise to intensive rainfall, which might be calculated from the water expert's point of view, by the concept of "probably maximum precipitation" (see Chap. 2). Meteorological conditions are necessary, but not sufficient for the floods in an area. In the hazardous flood occurrences not only rainfall event the but also hydrological, geomorphological and the geological sub-surface features play significant role to a certain extent. From the hydrological standpoint, floods appear when the soil saturation is complete and, therefore, almost all the precipitation without evapotranspiration and seepage turns to the surface flow. In plane areas, hydrological floods become harmful for the agricultural lands mostly due to water accumulation.

Floods are extreme surface water occurrences corresponding to a high flow of water, which overtops either the natural or the artificial banks of a river. For a hydrologist, the flood is expressed best with its maximum flood discharge, which does not indicate the flood inundation effects. However, for someone working in flood hazard potential, rather than the discharge, its maximum height (stage) is more significant. The stage is the maximum level that surface water reaches. Floods are generated as a combined result of two distinctive physical causes.

(1) Primary Causes: These are due to meteorological and atmospheric conditions related to the climatologic features of the region. The rainfall occurrences, types, intensities, directions, excessive rainfall, etc., are the necessary ingredients among these causes,

(2) Secondary Causes: These are related to the surface features of the drainage basin in terms of geomorphology, geology, vegetation, etc. The necessary ingredients are the catchment area, slope, drainage density, main channel length, time of concentration, etc.

The primary causes are time variables that cannot be predicted reasonably. These can vary from the semi-predictable seasonal rainfalls over wide geographical areas, which give rise to the annual monsoonal floods in tropical areas, to almost random convectional storms giving flash floods over small basins, (Ward 1978).

Climate change is among the physical trigger agents of unusual floods. It causes changes in timing, regional patterns, and intensity of precipitation events, and in particular in the number of days with heavy and intense precipitation occurrences. Floods are now being experienced in areas, where there were no floods in the past. This is mainly due to the global climate change. The recent floods seem to have some effects of global climate change, although they cannot be taken as proof that it

is already taking place in other parts also. The potential for increased flooding due to climate change would be exacerbated by erosion associated with deforestation and overgrazing. Such environmental degradations also increase surface runoff and the severity of flooding and contribute to landslides. Hence, in order to effectively assess the future flood occurrence possibilities and loss consequences, especially erosion and deforestation areas and rates should also be taken into consideration in any part of the world.

Floods might cause many deaths and injuries and the public health impact of floods also includes damage or destruction of homes and displacement of their occupants. Although much of the flood literature and current studies focus on catastrophic flood events, it is most likely that more frequent, but less severe flooding also has significant impacts on human security. Most of the death and injuries are caused by major natural disaster of sudden impact, such as a flood or storm that occurs within a few hours after the precipitation start. The major deaths during the flooding are due to drowning, but later deaths are as a result of various injuries during the floods.

About two-thirds of the world population lives within the 60-km coastal line, which are also expensive settlement areas. As a result, most of the commercial, trade, and industrial activities are prone to the water disasters. Insurance companies become more involved all over the world with the consequences of water-related catastrophic events and they started to consider flood risks for proper insurance systems and future planning. One may classify the floods according to their place of occurrence as follows.

(1) Tropical and mid-latitude frontal storms: General circulation models provide rather sophisticated information about the frequency and trends in the occurrence of cyclones. There is not even a general impression about the mid-latitude storm trends,

(2) Convective events and extreme convective precipitation: According to the general circulation model, increase in the $CO_2$ amounts means increase in the convective activities. As a result, the frequency of severe precipitation increases leading to more frequent surface runoff and floods. As the frequency increases, landslide occurrences also increases,

(3) Coastal Floods: There is an increasing possibility in the frequency increase of coastal flooding and the sea level rise with consequent subsidence.

Smith and Ward (1998) distinguished between the primary causes of floods, mainly resulting from widespread climatological forces, and secondary flood-intensifying conditions that are more drainage basin feature dependent. It is also possible to relate the physical causes of floods to other environmental hazards. Among such effects are river floods that arise from atmospheric (rainfall, snowmelt, ice jam), tectonic (landslides, subsidence), and technological (water structure failure) effects, and coastal floods are due to either storm surges or tsunamis.

## 1.7  Flood Plains

Flood plains are land areas adjacent to rivers and streams that are subjected to recurring inundation. Owing to their continually changing nature, floodplains and other flood-prone areas need to be examined in the light of how they might affect or be affected by development. This section presents an overview of the important concepts related to flood hazard assessments and explores the use of remote sensing data from satellites to supplement traditional assessment techniques.

Floods raise many concerns for communities living along main channels in any drainage area. These natural waterways are important for the formation of flood-plain lands, deposition of rich flood plain soils, and creation of river habitats. Development of urban and agricultural areas along the channels has placed many homes, buildings, and other structures within the floodplain. Communities and land owners often protect these investments by hardening the banks and minimizing channel change, which lead to reduced channel dynamics and impaired ecological conditions.

The major rule, which is considered in this book, is that no intensive land use should ever occur on flood plains for flood hazard intact human activity sustainability. Unfortunately, this ideal rule is corrupted as a result of pressures of population and the growing shortage of land for development. The development of flood plain land can produce a net economic benefit if the additional benefits derived from locating on the flood plain (i.e., benefits over and above those available at the next best alternative flood-free site) outweigh the average annual flood losses. Throughout the history, although the human beings were aware of flood danger, flood plains have always been attraction centers for human activities with the least investment cost. Economic growth and population redistribution have always tempted greater degree of flood plain encroachment, which is also taking place today within the major drainage basins. It is not unnoticeable that the urban areas are expanding year by year toward the flood plains with no early flood warning. By looking at the flood inundation maps at different risk levels, one can decide the location of its property with a certain risk acceptance.

Early water resources developments in many regions started to develop within the rich wadi alluviums, where the surface and ground water are available, at traces soil is suitable for agriculture, water disposal is easy, and especially, proximity to commercial centers led to settlement developments along the wadi reaches. Expansion of settlement centers within the alluvium areas with houses, industry, public buildings, and farms on the flood plains invites disaster. Unfortunately, settlers in such flood-prone areas seem not to recognize the natural flood way of the drainage basin main channel, which conveys occasional floods after intensive rainfalls. The flood plain is the flat surface adjacent to the mainstream channel, which is periodically inundated by flood water. Therefore, the flood plains must be recognized as its relation to occasional surface water might be dangerous to human life and property. Although the early settlers were not aware of such potential flood threats to the society, but they learned with pains taking experiences to identify such areas and
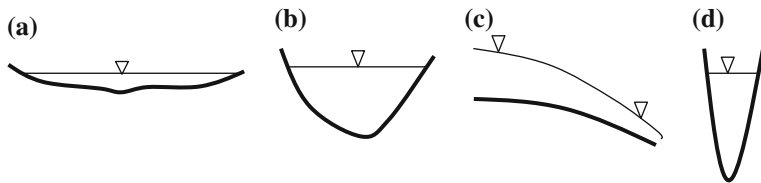
started to avoid any human activity. In future developments as guidance for land allocation and use studies, it is necessary to deal with procedures that help to identify flood-prone and potential disaster areas with inundation areas. For this purpose, flood hazard maps should be prepared with certain risk factor so as to warn central and local administrators and more significantly for convincing the local settlers, (the society). Flooding is a natural phenomenon that is related to the hydrological cycle within the catchment area with emphasis on the mainstream channel.

If any flood plain is already urbanized even at small scales, then there is an inevitable demand from the local community for flood protection. Despite the fact that a progressive shift in recent years toward more regulatory controls on flood plain development, it has been difficult to shake off the massive structural legacy even in modern societies. It is sad to state that especially big cities undergoing economic recession are also prone to increased hazard, since the local authorities are so desperate for investment that they are willing to attract floodplain development rather than no development at all.

Natural stream channels are part of hydrological cycle, which transport surface water from the upstream to downstream parts. Confluence of different main channel branches toward the downstream, with their accumulative surface water amounts increase the surface water volume toward downstream, which may consequently lead to flood inundation of lower areas. The surface area of the drainage basin collects the meteorological inborn rainfall water and leads it to the low-lying points within the drainage basin, which is referred to as the stream or river in humid regions but as wadi in arid regions (Şen 2008a).

The slope of drainage basin is its vertical drop per unit of horizontal distance and it plays a key dominance in runoff and flood velocity calculations. In general, slope is steepest at upstream parts and is much reduced as the basin approaches to its downstream level. It is possible to appreciate the slope along the drainage basin from upstream toward downstream along the main channel longitudinal profile, which has generally a concave shape (Chap. 3). In high elevations, the surface water erodes a deeper drainage basin in the hilly and mountainous terrain due to the high runoff velocity. Even though the discharge might be constant along the channel, according to the following changes there will be differences in water level from cross section to another.

(1) If there is a widening in the cross-sectional area, then the depth of water is expected to decrease comparatively (see Fig. 1.7a),
(2) If there is a deepening in the cross-sectional area, then the cross section is subjected to be covered by more extensive inundation area, (see Fig. 1.7b),
(3) If there is an increase in the slope within the vicinity of the cross-sectional area, then the flow velocity will also increase leading to reduction in the flow depth, (see Fig. 1.7c),
(4) If there is any contraction (expansion) in the cross-sectional area then accordingly the flow depth and inundation will also change according to the circumstances (see Fig. 1.7d).

**Fig. 1.7** Flow cross-sectional area changes, **a** widening, **b** deepening, **c** slope variation, **d** contractions

It is possible to conclude that any change in the geometrical shape of cross-sectional area will cause different flood inundation area widths. Since, in natural channels there are always changes from cross section to other, the flood inundation area boundaries will change both temporally and spatially. In flood inundation map preparations, provided that the discharge is determined, the remaining work is just to route this amount of water according to the cross-sectional geometric shape variations along the drainage basin main channel. The wadi tends to have a slope and cross-sectional areal shapes provide just the velocity of flow necessary to do the work of flooding. In the cases of an increase or decrease in the amount of water that the wadi main channel receives, there are usually changes in the channel's slope or cross-sectional shape depending on the flow velocity. The change of velocity may, in turn, increase or decrease the water depth and width.

Secondary flood intensifying causes cover a range of factors, which increase the drainage basin response to a given rainfall event. Most of these factors, such as those relating to the topography and hydraulic geometry of the basin are entirely natural. The effects of these factors have both and time and spatial variabilities. Together with the primary causes, these factors determine the key features of flood event such as the magnitude of the flood discharge, the surface water speed, the sediment load, and the duration, which is referred to as the time of concentration in flood calculations (Chap. 3). Past experience indicates that the greater all these features are, the greater the damage potential is in any area.

## 1.8  Flood Hazards

Among all environmental hazards, flooding is the most common in societies all over the world. The main reasons for this are the widespread geographical distribution of river valleys in humid regions or wadi courses in arid and semiarid regions, and low-lying coasts, together with their longstanding attractions for human settlement, and the availability of surface and groundwater resources. Although in many cases, the threat is limited to comparatively well-defined flood plains and low-lying areas such as estuaries, no country is immune from flood hazards (Smith 1992).

Although floods vary from year to year, there are considerable concerns that the number and the magnitude of floods have been on the increase over the past few years. This is particularly true in arid and semiarid regions, because the effects of recent climate change give rise to extensive rainfall in some parts of the world leading to unprecedented flooding events. Despite growing investment in schemes to mitigate flood risks, losses continue to increase, which could be attributed to a variety of factors that may be combined in two broad categories.

(1) Physical causes, related mostly to atmospheric events as the increase in the frequency and magnitude of rainfall and consequent flood events,
(2) Human causes, due to an increase in the vulnerability of flood plains as a result of intensive habitation and development. In spite of the fact that flood plains are one of the most topographically obvious regions of all hazard-prone environments, widespread invasion has occurred as a result of countless individual decisions rooted in the belief that local benefits outweigh risks (Smith 1992).

Appreciation of these two factors is as important as flood hydrology in understanding flood hazards. Most floods occur as a result of human causes. This is the primary factor that must be considered when attempting to prepare flood inundation maps. The flood inundation map of this book helps to identify dangerous flood plain regions depending on different risk levels.

Flood protection studies and mitigations have started in the beginning of the twentieth century with four distinctive evolution stages as,

(1) Hydraulic structural stage (1930–1960s): Engineering structures such as flood protection dams, levees, successive dikes, diversion canals, etc. During these studies, the basic flood generation reasons are identified and the peak flood discharge calculation procedures, algorithms, and formulations are established,
(2) Floodplain management stage (1960–1980s): During these two decades most emphasis is given to the combination of mitigation measures such as early flood warning, land use planning, etc., and currently,
(3) Flood mitigation stage (1980–2000s): Especially land-use control by considering different flood scenarios,
(4) Flood modeling stage (2000–): With the dissemination flood information through the world, various software is developed by taking into account remote sensing and satellite image facilities for better flood modeling possibilities including also the climate change impacts.

Not all the flood phenomena have destructive effects, and therefore, they are not dangerous. By definition as in Sect. 1.5.1, an ordinary flood cannot be described as a hazard unless it threatens human life and property. The damage potential of flood waters can increase exponentially with velocity, and speeds above 3 m/s can undermine the foundations of buildings (Smith 1992). The physical stresses on structures are raised further, probably by hundreds of times, when rapidly flowing water contains debris such as rock and sediment. Rapid inundation by floods greatly increases the risk of life as well as property. This is because forecasting and

warning systems can provide less time for evacuation or for emergency flood proofing measures.

Other flood-intensifying conditions arise from human actions such as land-use change, which may be semi-deliberate, including the increase in agricultural land drainage designed to speed the runoff from productive fields.

There are benefits in non-flood-prone areas, whereby flooding is a necessary part of the environmental and wadi catchment ecosystem and helps to maintain a wide range of wetland habitats, soil fertility by silt deposition, the flushing of salts from the surface layers, and water provision for natural irrigation and for fisheries as a protein source. In normal years, in places with balanced hydrological conditions, floods can bring benefits to a society rather than destruction. This is completely true if the necessary precautions, in the form of risk-attached flood inundation maps are planned and their future predictions are completed. Even in developed countries, the nature and scale of flood risks vary greatly. In most of these countries, flooding is dominant. However, in arid region countries, sudden floods in the form of flash occurrences are the most dangerous hazards in the middle stream portion of a wadi system, whereas inundation risks predominate in the downstream sections.

Low-lying areas suffer most from flood and inundation hazards. For instance in the western parts of the Kingdom of Saudi Arabia, thousands of people live in such low-lying areas because of the availability of groundwater and transportation facilities (Şen 2008a). The significance of small basins is due to the occurrence of flash floods, because during an intensive period of rainfall, the basin receives more than it can transfer as surface water in a short time of period. Flash floods occur more in those arid and semiarid regions, where there are favorable conditions of steep topography, weak vegetation, and high-intensity rainfall, coupled with short durations. In particular, narrow wadis and settlement centers generate rapid runoff due to an increase in surface water speed and a reduction in surface-layer permeability as a result of urbanization.

Floods may also result from dam failures that damage or destroy developed areas downstream, as urban areas, industrial plants, agricultural lands, etc. Alluvial fans support urban development due to their groundwater potentiality, but in the same time, especially in arid regions, they generate a special type of flash flood threat.

The flood hazard potentiality may have adverse effects on urban, industrial, infrastructural, and agricultural areas. This view emerges from the past experiences, and therefore, urges preparation of flood risk inundation maps. Availability of such maps is the key requirement in any urban development including dams, tunnels, highways, and bridges for sustainable future (Chap. 7).

## *1.8.1   Human Causes*

The major rule, which is considered in this book, is that no intensive land use should ever occur on flood plains for flood hazard-free human activity sustainability. This ideal rule is corrupted as a result of population pressure and the
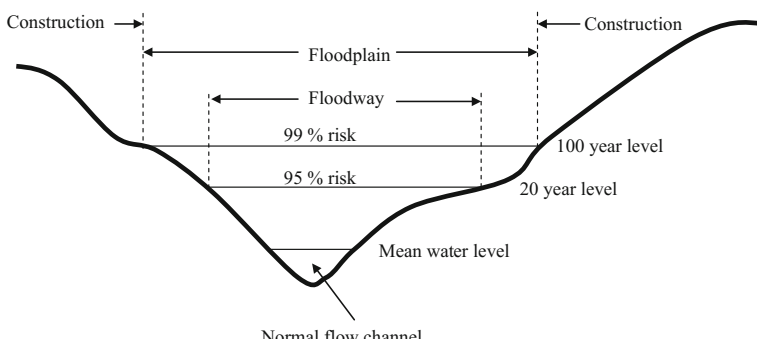
growing shortage of land for development. By looking at the flood inundation map
at different risk levels, one can decide the location of his property with a certain risk
acceptance Fig. 1.8 helps to visualize different flood risk levels.

In this book, the flood inundation levels corresponding to the following cate-
gories are classified as follows.

(1) Absolute protection zone (90% risks): This is the most dangerous zone, which
    might be definitely under flooding, whatever the flood intensity is. The local
    and central authorities must forbid the construction of any building or human
    activity within this zone,
(2) Significant protection zone (90–80% risks): This is the area, where some human
    activities can be allowable such as small story building constructions. A general
    rule might be accepted in this zone as the allowance of 10% of the areal
    property for light building constructions. However, these buildings should not
    include significant activities such as schools, hospitals, general public services,
(3) Moderate protection zone (80–70% risks): About 30% of the areal property
    should be opened for human activities such as agriculture, irrigation and storage
    buildings,
(4) Weak protection zone (70–50% risks): These areas can be opened for public
    use at 50% construction rate.

Even the flood inundation maps cannot be salvages, but at least they stand open
to each individual, local, and central administrator, and consequently, such unde-
sirable situations can be avoided to a great extent. Physiologically, existence of
such maps will hinder any individual administrator to dare for flood plain even at
his own risk. Smith (1992) gave the following three reasons for the circular link
between flood control works and flood plain investment and encroachment.

(1) The greater the amount of flood plain development, and the greater the existing
    investment, the greater are the economic benefits from flood control structures.
    Thus, flood protection schemes are more likely to be implemented on cost–
    benefit grounds,



**Fig. 1.8** Schematic delimitation of hazard planning zones on a cross section

(2) The cost–benefit ratio also weights in the favor of construction, when land can be protected from risk and freed for development. The higher the land values in the "protected" area the more likely is further flood plain invasion,

(3) Above all, the real cost of protection (and encroachment) typically has not been born by the most directly involved parties.

One can view any cross section in a flood-prone area as consisting of three major parts including the no-construction, only flood-proofed construction, and proper construction zones as in Fig. 1.8. In the same figure, "floodway" term is used for 5% annual probability, which corresponds to 20-year level of probable flood water. Likewise, "floodplain" is employed for 1% annual probability corresponding to 100-year flood water level.

In land-use practices against the floods, it is customary to divide the risk into two components, which are more or less independent from each other. These are the vulnerability (the sensitivity of the land use and of the population) and the natural hazard (Chap. 9). Such a division leads to a more adequate, flexible, and manageable definition of risk. If a place is not vulnerable, then the expected risk will be small. Vulnerability is related to the exposition of any human activity to flood danger. If in a drainage basin, there is no infrastructural elements, no settlement, no agricultural activity, in this case the vulnerability is almost zero.

## 1.9   Water Disasters

It is the main purpose of this book, to deal with extreme water availability, i.e., floods in a drainage area at certain finite time periods (return periods). Extreme situations are rather uncontrollable due to hazard potentiality, but their impacts can be reduced significantly provided that a certain risk level is accepted in water structure designs such as dams, culverts, bridges, land use, industrial area development, agricultural land allocation, and similar activities.

Sudden changes in the common behavior of hydrological events such as flooding or flash flooding with progressive and long lasting may be dangerous for many human activities. This affects both the way the disaster is identified and managed. In order to reduce such dangers, the following immediate or long-term solution points can be considered.

(1) Immediate, for example, drowning or injuries during flooding,

(2) Middle-range, such as progressive food shortage or epidemics following a flooding,

(3) Long-term, such as epidemics and severe lack of food and drinkable water.

If there are no external assistances or precaution then hydrological events may turn into an emergency case as a disaster. One working definition of a disaster is that it causes at least 10 deaths or results in an appeal for outside assistance. Whatever the definition, disasters involving water are increasing. In recent decades,

there has been an increase in the numbers of deaths and people affected by weather disasters such as droughts and floods. Climate change appears to be responsible for at least some of this increase and while global warming has been acknowledged, the term is misleading, because it leaves out the key element of water.

Drainage basin channels are parts of hydrological cycle, with surface water transportations after the evaporation and infiltration losses from the upstream to downstream parts. Connection of different wadi branches toward the downstream with their surface water amounts cumulatively causes surface water volume increase, which may consequently lead to flood inundation of lower areas. If the region is drained by a single wadi or wadi system, it is called as a drainage basin or watershed. The surface area of the drainage basin collects meteorologically inborn rainfall water and leads it to the low-lying points within the drainage basin, which is referred to as the stream or river in humid regions, but as wadi in arid regions.

In addition to natural factors, human activities may also contribute to the occurrence of floods and to flood hazards. The closer the active land use to the main channel stream, the more prone is the land to inundation, and consequently, drainage cross section that have not been prone to flood hazard, become under the threat of flood hazard. In water stricken regions, flood waters can be stored in the form of surface or subsurface reservoirs.

## 1.10   Various Definitions

In the following is a set of definitions that should be taken into consideration in any hazard and safety study.

**Acceptable risk**—The level of risk (the combination of the probability and the consequence of a specified hazardous event), for which the public is prepared to accept without further management. Acceptability of risk may be reflected in government regulations.

**Adverse effect**—It is a change to the ecosystem or a component of the ecosystem that is judged to be detrimental.

**Cumulative risk**—It is the combined risks from aggregate exposures to multiple hazards or stressors.

**Emergency**—In terms of water resources operation, any condition which develops naturally or unexpectedly endangers the integrity of the water structures such as dam, upstream or downstream property or life, and requires immediate action.

**Emergency plan**—Document(s) that contain procedures for preparing and responding to emergencies at the water structure or at its appurtenances including communication directories and inundation maps.

**Extreme event**—It is an event with a very low annual exceedance probability.

**Extreme loads**—The rare loadings imposed by extreme events such as large earthquakes, floods and landslides.

**Failure (of dam)**—This means that in terms of structural integrity the uncontrolled release of a reservoir contents through collapse of the dam or some part of it. In terms of geochemical integrity, the uncontrolled release of contaminants from the reservoir/tailings impoundment.

**Failure mode**—Mode in which element or component failures must occur to cause loss of the system function. For instance, at a general level there are three dam failure modes: dam overtopping (flooding), dam collapse, and contaminated seepage. At a lower level, failure effects become the failure modes at the next higher level in the system.

**Hazard**—A system state or set of conditions that together with other conditions in the system environment could lead to a partial or complete failure of the system. Hazards may be external (originating outside the system) or internal (errors and omissions or deterioration within the system). On the other hand, it is also a source of potential harm, or a situation with a potential to cause loss or an adverse effect.

**Hazard identification**—It is the process of analysing hazards and the events that give rise to harm.

**Inflow Design Flood (IDF)**—Most severe inflow flood (volume, peak, shape, duration, and timing) for which water resources facilities are designed.

**Management**—Originally it is from business economics and all activities, which control the decisions and actions of a decision maker under a set of rules and regulations effectively and efficiently. Among these activities are planning as data gathering, analysing, goal setting, evaluation of options, and so forth in addition to organization and direction. In this sense "management" is also used in water resources systems.

**Probability**—It is the likelihood of a specific outcome. Probability is expressed as a number between 0 and 1, with 0 indicating an impossible outcome and 1 indicating that an event or outcome is certain.

**Probable Maximum Flood (PMF)**—Estimate of hypothetical flood (peak flow, volume, and hydrograph shape) that is considered to be the most severe "reasonably possible" at a particular location and time of year, based on relatively comprehensive hydrometeorological analysis of critical runoff-producing precipitation (snowmelt if pertinent) and hydrological factors favorable for maximum flood runoff.

**Restoration**—It is the improvement or enhancement of the environmental condition of the drainage basin in the direction of "ecologically healthy."

**Return period**—Reciprocal of the annual exceedance probability (Chap. 6).

**Risk**—Measure of the probability and severity of an adverse effect to property such as water resources engineering structures. It is estimated by the mathematical expectation (arithmetic average) of the consequences of an adverse event occurrence (i.e., the product of the probability of occurrence and the consequence). It is also defined as the chance (probability) of something happening that will have an undesirable impact on the objectives. Risk is measured in terms of a combination of the likelihood that a hazard gives rise to an undesirable outcome and the seriousness (consequences) of that undesirable outcome.

**Risk acceptability**—It is the acceptability of the risk by the stakeholders, water system designers and those who will bear the consequences.

**Risk analysis**—In its context are the actual determination of the likelihood and consequences of undesirable effects on the water resources system.

**Risk assessment**—This is defined as the overall process of hazard identification, risk estimation, and risk evaluation (may be qualitative, semiquantitative, or quantitative).

**Risk management**—It is the processes and structures to manage potential adverse impacts.

**Safe water structure**—Any water structure does not impose an unacceptable risk to people or property and meets safety criteria that are acceptable to the government, the engineering profession and the public.

**Spillway**—Weir, channel, conduit, tunnel, chute, gate, or other structure designed to permit discharges from the reservoir.

**Threat**—An action or activity that has the capacity to adversely affect an ecological value or asset.

# References

Dein, M.A. (1985). Estimation of floods and recharge volumes in wadis Fatimah, Na'man and Turabah. Unpublished M.Sc. thesis, Faculty of Earth Sciences, King Abdulaziz University, Saudi Arabia, p. 127.

Farquharsen, F. A. K., Meigh, J. R., & Sutcliffe, J. V. (1992). Regional flood frequency analysis in arid and semi-arid areas. *Journal Hydrological, 138,* 487–501.

Flerchinger, G. N., & Cooley, K. R. (2000). A ten-year water balance of a mountainous semi-arid watershed. *Journal Hydrological, 237*(1–2), 86–99.

Harvey, J. G. (1982). *Atmosphere and ocean. Our fluid environment* (p. 143). London: The Vision Press.

Kattelmann, R., & Elder, K. (1997). Hydrological characteristics and water balance of an alpine basin in the Sierra Nevada. *Water Resources Research, 27,* 1553–1562.

Linsley, R. K., Kohler, M. A., & Paulhus, J. L. H. (1982). *Hydrology for engineers*. Third edn. (p. 508). New York: McGraw-Hill.

Maidment, D. R. (1993). *Handbook of hydrology*. New York: McGraw-Hill.

Mather, J.R. (1979, July). *Use of the climatic water budget to estimate streamflow* (p. 528). Technical Research Report, Newark DE: Dept. Geography, Water Resources Center, University of Delaware.

Parks, Y.P., & Sutcliffe, J.V. (1987). The development of hydrological yield assessment in NE Botswana. In: *British Hydrological Symposium* (pp. 12.1–12.11), 14–16 September, London: Hull, British Hydrological Society I.C.E.

Scanlin, B. R. (1994). Water and heat flux in desert soils: 1, field studies. *Water Resources Research, 30,* 709–719.

Şen, Z. (1995). *Applied hydrogeology for scientists and engineers* (p. 495). New York: Taylor and Francis Group, CRC Publishers.

Şen, Z. (2005). *The Saudi geological survey (SGS) hydrograph method for use in arid regions* (p. 20). Technical report, Saudi Geological Survey, SGS-TR-2004-5.

Şen, Z. (2008a). *Wadi hydrology* (p. 347). New York: Taylor and Francis Group, CRC Press.

Şen, Z. (2008b). *Solar energy fundamentals and modeling techniques: atmosphere, environment, climate change and renewable energy* (p. 276). Berlin: Springer.

Şen, Z. (2015). *Practical and applied hydrogeology* (p. 406). Elsevier

Smith, K. (1992). *Environmental hazards assessing risk and reducing disaster* (p. 324). London: Routledge.

Smith, K. (1996). *Environmental hazards*. London: Routledge.

Smith, D. I., & Handmer, J. W. (1996). Urban flooding in Australia: policy development and implementation. *Disasters, 8*(2), 105–117.

Smith, K., & Ward, R. (1998). *Floods*: *physical processes and human impacts* (p. 382). Chichester: John Wiley and Sons.

Viessman,W., Knapp, J. W., & Lewis, G. L. (1989). *Introduction to hydrology*. New York: Harper and Row Publishers.

Ward, R. (1978). *Floods: A geophysical perspective*. London: MacMillan Press.

# Chapter 2
# Rainfall and Floods

**Abstract** There are different types of rainfall depending on elevation, temperature, or pressure differences that generated by composition of various meteorological factors such as light, moderate, or extreme rainfall occurrences with or without flood consequences. In arid regions, elevation (orographic) and temperature (convective) differences may cause to floods, but in humid regions, pressure difference (frontal) rainfalls are the major factors. In order to calculate various rainfall characteristics such as the intensity recording, raingauge records are necessary, but with accurate measurements. Different sources of measurement errors are explained in the text with their correctional actions in the field and office. Various areal average rainfall calculation methodologies, especially innovative percentage-weighted methodology, are presented in comparison with the classical and about 100-year-old Thiessen approach. New concepts such as the dimensionless intensity–duration curves are explained, and their application to annual maximum rainfall amounts is presented with actual data processing. The importance of the intensity–duration–frequency curves is explained with the concepts of different risk levels. The significance of probable maximum rainfall and its connection with probable maximum flood calculation is presented through the applications to a set of drainage basins from the western part of the Kingdom of Saudi Arabia. Efficiency factor is defined the first time in the text for distinction of the climate change impact on the rainfall occurrences in the region.

**Keywords** Areal average · Efficiency factor · Error · Hyetograph
Dimensionless intensity · Intensity–duration curve rainfall · Probable maximum
rainfall · Probable maximum flood

## 2.1 General

Floods are consequences of a set of rainfall premises among which are the rainfall type, regime, amount, duration, frequency, and intensity. Rainfall records are available at a set of meteorology stations, and measurements are recorded by the

meteorology service of each country. In general, there are two types of rainfall records; the first one is total rainfall measurements during the whole period of the storm rainfall event, which includes the duration and the total rainfall height. A sequential collection of total measurements includes more than one storm rainfall in the form of a time series, which is very important for description of wet and dry period features as well as extreme values that may cause floods or droughts. The next type is the record of rainfall amounts during each storm rainfall in a cumulative manner, which gives a basis for rainfall intensity, duration, and frequency (IDF) calculations. Such records are important for determining the rainfall intensity for the design of many engineering structures based on the return period and risk level (Chaps. 5 and 7).

The most important meteorological event in the lower atmosphere (troposphere) is the precipitation that is the source of all water resources in the world. It is the fall of any solid (snow, hail) and fluid (rain) drops from the cloud bottom to the earth surface. After the reach of precipitation on the earth surface, not the meteorological principles, but the hydrological laws govern the surface and subsurface flows. The very first task is to measure the temporal and spatial variations of the precipitation by a set of convenient measurement instruments, which are referred to as the raingauges. The measurements from a raingauge are the records that provide temporal behavior of the precipitation event at the meteorology station location and around its nearby surrounding. Preliminary assessments of the records provide the initial interpretation opportunities to reach at information about the rainfall height, time durations (hour, week, month, season, and year), and areal extent. Further, refined calculations provide severity, magnitude, duration, intensity, and frequency of dangerous events such as floods and droughts. As for the water resources, rainfall and the snowmelt are the two major contributions. In order to plan and manage the entire water resources, one should try and obtain basic information, interpretation, and conclusions about the areal and temporal characteristics of the rainfall. Such activities are significant in water resources planning, management, irrigation, and agricultural activities. The types, intensities, frequencies, areal coverages, and averages are very important statistical quantities for the design of flood magnitude, risk, and occurrences. In Chap. 6, the probabilistic and statistical evaluation of the rainfall and consequent flood evaluation are presented for future predictions.

The chief characteristic of a heavy rainfall event as flash flooding and such an event (in any region) can be described as a natural hazard that causes major floods and severe destruction, often resulting in loss of lives and damage to property. It is, therefore, necessary to understand and be able to follow the evolution of a heavy rainfall event at the event scale. Such an assessment provides considerably beneficial information to scientists, in general, and to the administrative authorities of a region, in particular. Sudden and rapid occurrences of flash floods in natural channels present technical challenge to scientific modelers and decision-making administrations. They are linked to intensive thunderstorms, and they are also highly localized. Trapp et al. (2007) mentioned that apart from producing dangerous lightning and torrential rainfall, such thunderstorms are responsible for

high-impact weather, including destructive surface wind, hail storms, and/or tornadoes.

In any water study, the rainfall is the basic variable and it is expressed as the amount of rainfall over unit area during unit time or snowmelt water depth equivalent per area. For instance, when monthly rainfall is said to be 35 mm, it means that over 1 m$^2$, the rainfall depth is 35 mm and the following points must be taken into consideration in the same context:

1. It is the amount of rainfall that falls onto the surface from the clouds prior to any loss of evaporation, depression, and infiltration; hence, it is also the amount of global rainfall on the ground surface.
2. The rainfall has three important units as area—m$^2$; depth—m; and time duration, which may be day, month, or year. It is not enough to say that the rainfall amount is 15 mm, because its duration as hour, day, etc., must be specified as total, average, low, extreme, or any other value.

Effective rainfall is obtained after the subtraction of evaporation and infiltration from the gross rainfall amount in this chapter. If rain falls on a frozen or completely impervious or saturated soil surfaces, then infiltration cannot take place, so that once the initial interception and depression storage are satisfied, the remaining rainfall contributes to runoff and to possible flood. The amount of the surface moisture in the soil influences the infiltration capacity.

Frequency of inundation depends on the climate, the material that makes up the banks of the stream, the channel slope, and drainage basin surface features (Chap. 3). Where substantial rainfall occurs in a particular season each year, or where the annual flood is derived principally from snowmelt, the flood plain may be inundated frequently every year, even along large streams with very small channel slopes. In regions without extended periods of below-freezing temperatures, floods usually occur in the highest precipitation season. The regions, where most floods are the result of snowmelt, are accompanied often by rainfall during spring or early summer seasons.

Rainfall is the main source of the world's freshwater supplies. Nature and characteristics of a storm rainfall help to predict its effect on runoff, infiltration, groundwater recharge, evapotranspiration, and water yield calculations. The volume of flow rate for storage or conveyance by the drainage system can be related mathematically to the rainfall storm features such as intensity, duration, and frequency. The main interest is to know the likelihood of occurrence (probability) of an event with a specified intensity and duration, which are inversely related.

This chapter is concerned with the description, definition, quantification, and estimation of different rainfall characteristic amounts and some applications, especially in arid lands.

## 2.2  Causative Reasons for Rainfall Occurrence

The travel of precipitation from the cloud base to the earth surface is of concern to meteorologists. They are concerned with the generation of clouds as a result of evaporation and transpiration, the rising moist air (water vapor), and their cooling and condensation to form the clouds. For precipitation, the presence of clouds is necessary, but not sufficient, because each cloud does not yield precipitation. The water particles and ice crystals, especially in the upper layer within the cloud, move randomly in various directions at small scales. Since they are very small, they can escape the gravitational effects. Even today, physical reasons for precipitation generation within the clouds are not understood completely and there is vague information about it. Microscale irregular movements do not provide a common base for the precipitation generation mechanism fully scientifically. For precipitation, the cooling, condensation, and drop growth stages must be completed successively. In general, for the precipitation generation there are four stages:

1. Existence of enough water vapor in the air as the source of clouds,
2. Drop in water vapor temperature below dew point for condensation,
3. Water drops' cooling leading to ice piece generation,
4. Growth of drops and pieces that reach to a scale that cannot escape the gravitation force, and hence, precipitation starts from the cloud base and reaches to the measurement instruments on the earth surface.

### 2.2.1  Water Vapor

Evaporation and transpiration release to the air invisible water vapor together with small water drops and microscopic solid pieces, which make up the humidity in the air. The humid air rises and originates the clouds, but at lower elevations, it appears as fog. Water phases appear in different diameters, and according to their scale, they can be grouped into different classes. Water vapors in the form of gases have diameters around $10^{-4}$ micron; cloud drops have 5–100 micron diameter; 100–500 micron diameters are for ice crystals; and precipitation drops have diameters in the range 500–5000 micron. Snow and hail pieces have bigger diameters. Inside the cloud, these various diameter pieces are in a mixture and they move randomly. In open and clear air (without cloud), the water vapor pressure is small, but in cloudy weather precipitable water vapor increases between the earth surface and the cloud base. Air saturation causes dew point to increase with increasing temperature. In fact, the content of precipitable water vapor is higher in summer seasons than winter periods. In general, the amount of precipitable water at a location is dependent on the air thickness, latitude, distance, and elevation from the sea level, general circulations in the atmosphere and on the specific meteorological features of the location.

## 2.2.2   *Cooling*

Initially, for precipitation occurrence in the troposphere, sufficient amount of water vapor must exist. Water vapor is necessary for precipitation, but it is not sufficient. For cooling, according to thermodynamic rules, the air must expand, which is the main reason why clouds come into existence at certain heights from the earth surface. In other words, if water vapor laden air rises due to any cause, then it expands and cools. For a given temperature, there is a certain amount of air content. The air temperature varies according to air saturation ratio. As the temperature increases, the water content of the air also increases. Reduction in the air temperature causes incapability of air to accept more water vapor. The air cools down to a certain temperature according to the water vapor amount in the air and then onward cannot accept additional water vapor; i.e., the air is in the form of saturation. After this stage, further reduction in the temperature causes water vapor condensation. During the contact of saturated air with cold air, respectively, dew, ice, and fog start to appear.
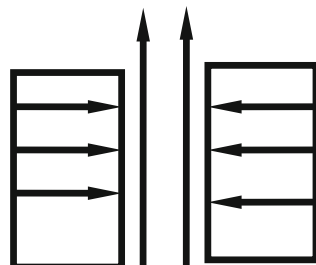
During condensation moist air releases, heat, and hence, becomes cooler. The major factor that causes air to cool down is due to heat exchange, i.e., adiabatic state and the pressure fall. The rising and cooling effects of the air cause troposphere to be in a dynamic state continuously. The following factors individually and collectively cause to dynamism in the troposphere.

(a) Convergence lifts: The air movement from different directions toward a point is referred to as the convergence (Fig. 2.1). In this manner, at low elevations, the air converges and forcefully rises and such a vertical movements cause air to cool down.

Among the events that cause to convergence are the momentum difference between longitude and latitude, air movement to low-pressure centers from high-pressure centers, topographic hindrances, and divergence event at high elevations.

Air convergence events occur especially at tropical zone frontal areas, at low-pressure valleys, convergence of different valleys to direct the wind movement to a certain location, and tropical cyclones.

**Fig. 2.1** Convergence event

(b) Frontal lifts: Confrontation of cold and warm air masses generates slopes
     similar to topographic features (Fig. 2.2).
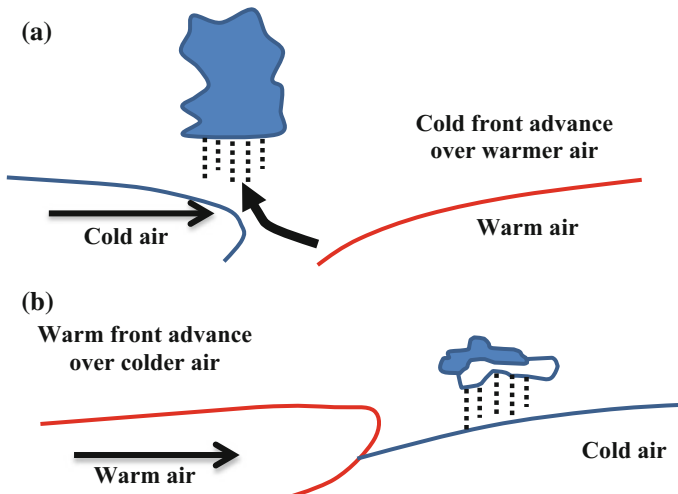
In case of warm air over the cold one, frontal surfaces are generated from 1/100
to 1/300 slopes. On the contrary, in cold fronts, the cold air has steeper slopes (1/25
to 1/300). Over the sloppy plane, the air is forced to rise. In case of cold fronts, the
slope is higher, and consequently, the warm air rises to higher elevations, and
hence, short duration, but intensive rainfalls occur.

(c) Orographic lifts: As in Fig. 2.3, the air that is loaded with water vapor force-
     fully raises over the hill slope surfaces with wind effect. Ascending air starts to
     cool down, and logically, the speed of ascend is dependent on the hill slope and
     the speed of the wind.
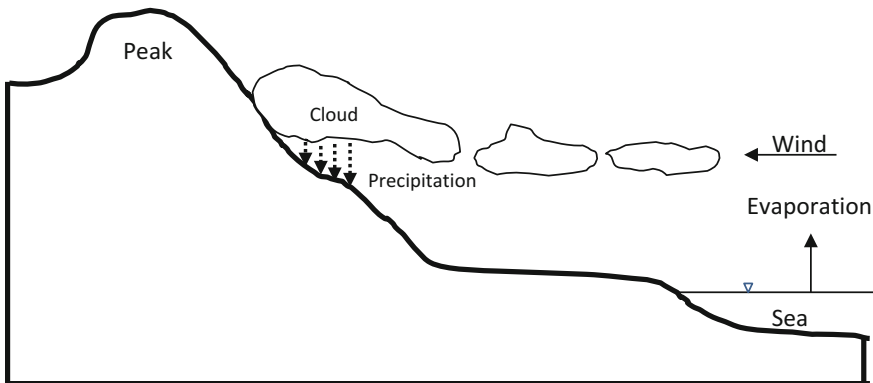
The vertical speed reduces with the elevation and as has been documented by
various researchers that even 50% reduction appears at 1000 m. Mountain hill
slopes are continuous and steeper than the frontal slopes. In these regions, the air
raises speedily and, therefore, results in longer duration rainfalls. This is the main
reason why mountainous regions receive abundant and long duration rainfalls.

(d) Turbulence lifts: This lifting operation occurs in small and large scales con-
     tinuously in a sophisticated manner (Fig. 2.4).

The small-scale turbulences happen at the boundary layers as a result of physical
topographic hindrances. This causes water vapor to rise forcefully and generates thin
layers of clouds at low elevations. Bigger scale turbulences are due to air dynamics at
higher elevations along with the conventional movements. This mechanism may
even cause water vapor to cross over the troposphere.
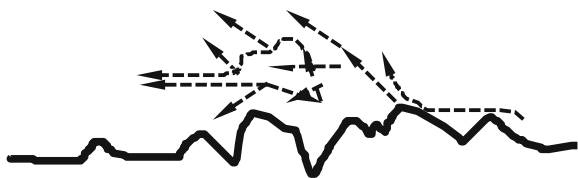


**Fig. 2.2**  Fronts–(**a**) cold, (**b**) hot

**Fig. 2.3**  Orographic lift

**Fig. 2.4**  Turbulence lifting



All the aforementioned lifting mechanisms come into existence after the instability of stable air due to various effects. In the imbalance of air, the following factors play a significant role:

(a) Cooling from bottom: In summer seasons, frequently observed phenomenon is the air cooling from below. As a result of this vertical cumulus, cumulonimbus clouds are formed (Fig. 2.5). Cumulus clouds are rather puffy and look like cotton heaps. Its base is almost flat and at about 1000 m above the earth surface. Its top is like a round tower, and it grows upwardly.

Similarly, as a result of upper latitude air mass movements toward the lower latitudes, the air becomes into contact with relatively warmer surface temperatures, the cooling is from the bottom, and hence, the air balance is disturbed.

(b) Upper cooling: If the water vapor in the atmosphere, especially in the upper troposphere, is dry and little, but the lower air layer is relatively moister, then the solar radiation can penetrate dry air easily, and hence, the lower moist air layer is heated from above. As a result, there are variations in the vertical temperature profile and the stability of air is disturbed, which causes thunderstorm and lightning prior to rainfall occurrences.

**(a)**



**(b)**
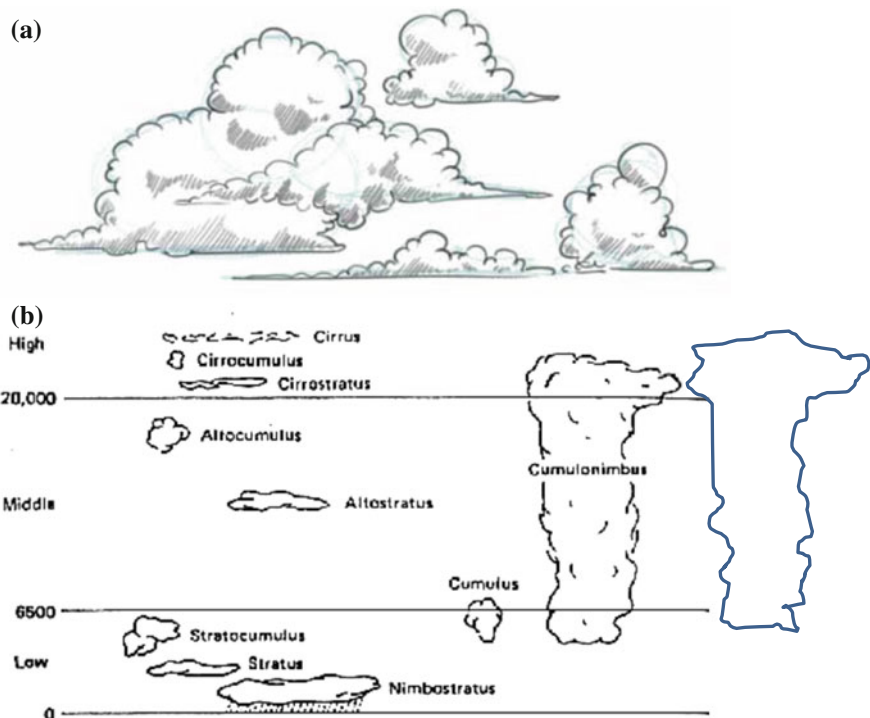


**Fig. 2.5** Clouds, (**a**) cumulus, (**b**) cumulonimbus

(c) Conditional instability: If an air layer is between the dry and saturated vertical temperature differences, instability occurs as a result of lifting. If there are topographic and frontal effective risings, the air cools down to condensation-level dry vertical temperature difference, but after that, the cooling is due to saturation of vertical temperature difference. As a result, movement starts freely, because of the vertical temperature difference convectionally.

(d) Air layer lift: Below the air layer very moist and above it dry and relatively less moist air existence cause to air instability.

## 2.2.3   Condensation

With the cooling of air, the internal water vapor condenses and forms very small water drops. For this process, condensation kernels are necessary. These kernels can be dust and pollution particles that have risen from the earth's surface due to various reasons, and also, they can be salt pieces from the seas and oceans as well

as the pieces that are born from the meteors outside the troposphere. The cooling is possible with temperature decrease, but it is not sufficient for condensation, if the kernel particles are not available. It is for this reason that those who search for the artificial rainfall generation (cloud seeding) throw dust and very small pieces of sand into the clouds. In the absence of such particles, even if the air is 100% saturated, the condensation process does not take place. In the atmosphere, frequently there are chlorides and sulfur oxides for condensation and their diameters are smaller than 10 micron.

After the above-mentioned processes, prior to the precipitation generation, various water particles move randomly inside the cloud toward the upper layer. Under general synoptically valid conditions, the speed of this movement is very small (35 m/hour), but in the cumulus type of clouds, it is very high (70 km/hour). It is not possible that each saturated air always condenses. The air with its movement toward the ceiling of the cloud may be overcooled, and therefore, oversaturation takes place. Entrance of condensation kernels into such air causes precipitation.

## 2.3 Precipitation Types
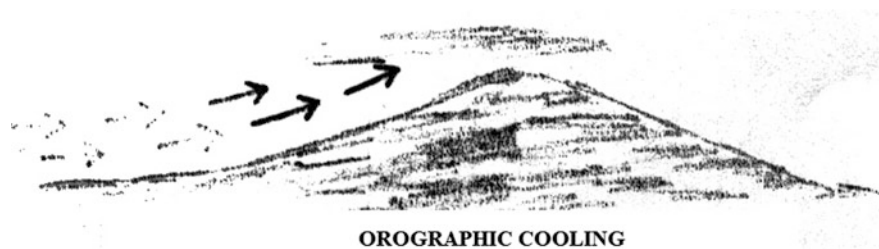
It is already understood that for precipitation fall from the bottom of the clouds, three components should coexist. These are water vapor, solid condensation kernels, and a dynamic cooling mechanism. Depending on the type of the dynamic mechanism, three precipitation types occur. Each mechanism is dependent on some physical precipitation causative factors.

### 2.3.1 Elevation Difference (Orographic)

As already explained in Sect. 2.2.2, the clouds that are loaded with moist air and solid condensation kernels are carried horizontally due to the winds. When these clouds hit high mountains, they rise forcefully and become cooler leading to heavy drops as a result of further cooling and the gravitational force causes water drops to leave the clouds (Fig. 2.6). This is the type of orographic precipitation. The areal extent of such precipitation events is rather small.

### 2.3.2 Temperature Difference (Convective)

The meaning of the word "convective" is vertical movement in the troposphere, and they occur as a result of temperature difference, because hot air rises. Especially at flat surfaces of the earth, heating of low albedo parts gives rise to moisture and the

 **OROGRAPHIC COOLING**
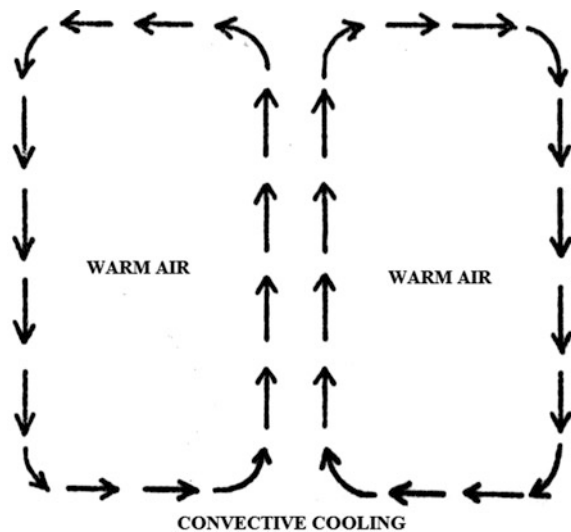
**Fig. 2.6** Orographic precipitation

solid particle movements toward higher elevations, and hence, cooling process takes place (Fig. 2.7). By time the water drops grow further and again, the gravitational force causes precipitation. Such precipitation types are rather local and cover small areas. For instance, occurrence of rainfall in some part of the cities, but no precipitation in the adjacent quarters, is due to this type of cooling mechanism.

This rainfall type occurs most often in the tropical belt of the world, and the Hadley general circulation starts from the equator due to extra heating, because of the perpendicular solar radiation fall on the earth's surface. Most of the rainfall occurrences in desert areas are of this type. They are very common, especially in summer seasons, and occur frequently over areas that are surrounded by mountains. In summer, the air becomes moister due to evaporation, transpiration, and evapo-transpiration from the soil. This causes hot air rises over the earth's surface, rising air expands and cools down, and finally, at a certain elevation, precipitation occurs

**Fig. 2.7** Convective precipitation



WARM AIR                    WARM AIR

**CONVECTIVE COOLING**

following the condensation. The soil includes moisture in the autumn and summer seasons, and these also trigger convective rainfall occurrences. In particular, after abundant rainfalls during winter season, the soil ends up with saturation, which is the major factor of convective rainfall occurrences in summer seasons. These rainfall types are coupled with thunder, lighting, and even with occasional hail incidences.

### 2.3.3 Pressure Difference (Frontal)

Establishment of low- and high-pressure centers at various locations over the earth generates pressure differences, which move hot and cold air masses toward each other, and their hit gives rise to frontal precipitation. The moist air condenses due to the cold air effect, and hence, rainfall takes place. Compared with the two other types, the frontal rainfalls cover long distances and extensive areal coverages. They take place along the hot and cold frontals as in Fig. 2.8. In this manner, air masses laden with moist air in some country may end up with frontal rainfalls in some other country. The duration of these rainfalls is very long compared with the two other types and may continue for days and even for months. The rainfall amount has no comparison with other types, and it is very big.

## 2.4 Rainfall Measurement

Rainfall-related events such as floods and droughts can be evaluated provided that an effective monitoring system is available at different locations. Accurate and reliable observations and measurements are fundamental factors that provide sound bases for various engineering calculations in order to make dependable predictions. The raingauges must be located conveniently at local climate representative locations in a region. In general, the selection of convenient measurement locations should take into consideration the following points.



Fig. 2.8 Frontal precipitation

1. Easy transportation, flat or slightly sloppy areas are preferable.
2. The raingauge location must be extensive without ditches and hills.
3. The nearest hindrance to the gauge location should be at least three times the height of the object.
4. The gauge locations must be away from materials such as dust and chemical pollution sources and sinks, highways, railways, construction areas.
5. The peripheral boundary of the gauge must be such that neither animal nor human can get near to the gauge itself.

Information about the rainfall regime of any region can be obtained through the past records numerically and from local people linguistically. For this purpose, the rainfall records must be kept at regular time intervals and also at a set of locations for future prediction and planning activities. The amount of rainfall at any location is dependent on the surface features (geomorphology), persistent wind direction, and other meteorological factors including temperature, solar irradiation, humidity. Possible errors that may appear in raingauges are as follows:
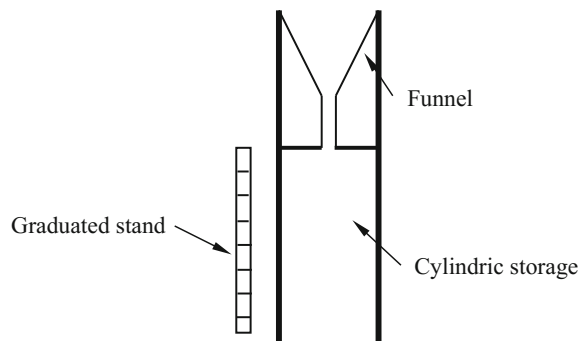
(a) Defects from the gauge itself,
(b) The gauge locations might not be determined properly, and the instrument rim should be at about 30 cm above the ground,
(c) In case of insufficient raingauges or nonexistence of monitoring network.

## 2.4.1   Non-recording Raingauges

Instruments that record rainfall amounts at regular time instances or in a continuous manner are raingauges. In general, they have three major parts: cylindrical rainwater collection storage tank; funnel that gives way for rainwater to enter the storage smoothly and more specifically that hinders evaporation losses during non-rainy periods, and a graduated staff for rainfall amount measurement (Fig. 2.9).

These instruments provide rainfall heights at the gauge location. The more uniform is the rainfall distribution over a region, the less is the number of needed

**Fig. 2.9**  Non-recording raingauge parts

Funnel

Graduated stand

Cylindric storage

**Table 2.1** Minimum density of raingauge network

| Region property | Minimum | Tolerable |
|---|---|---|
| Flat regions of temperate, Mediterranean, and tropical zones | 600–900 km$^2$ | 900–3000 km$^2$ |
| Mountainous areas of temperate, Mediterranean, and tropical zones | 100–250 km$^2$ | 250–1000 km$^2$ |
| Arid zones | 1500–10,000 km$^2$ | |
| For small islands | 25 km$^2$ | |

10% of these gauges should be of recording type to enable the determination of rainfall intensity

gauges. This means that in rough terrain and mountainous areas, comparatively more dense raingauges must be located. In general, one raingauge is enough per 800–1000 km$^2$. The World Meteorological Organization (WMO) has given certain norms for the minimum network density as in Table 2.1.

## 2.4.2 Recording Raingauges
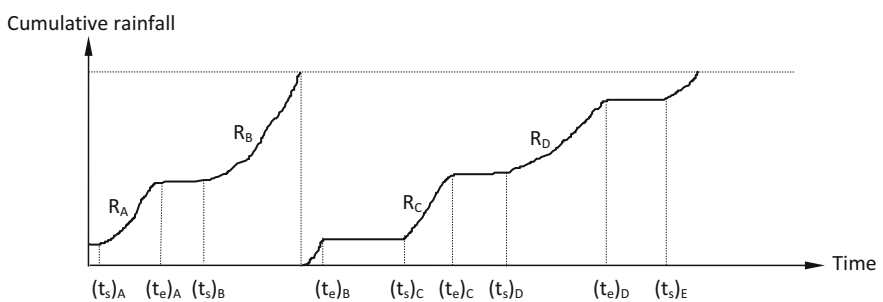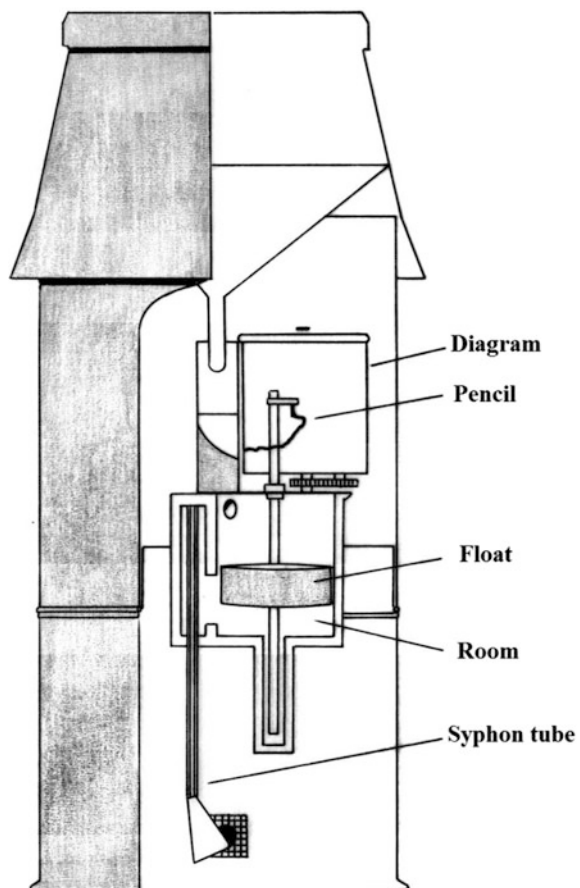
These are three types depending on mechanical, hydraulic, and electronic functions. In the mechanical type, a standard tank that stores rainwater is located on a balance, and as the water accumulates, the balance reflects the records on a chart located on the surface of a continuously and timely rotating cylinder. According to the revolution speed of the cylinder, daily or weekly accumulative rainfall records can be traced. In Fig. 2.10, hydraulically working recording raingauge is given.

The recording raingauges provide continuous records over long-time durations, and in a single chart, there may be more than one rainfall event. The chart records rainfall amounts continuously without any gap during the rainfall event. The records are in the form of continuously increasing curve forms as shown in Fig. 2.11.

This chart provides much information about an individual rainfall event at different time instances during the rainfall duration. The following points are some of the useful information deductions from such charts:

(a) The number of rainfall events at the station location can be counted easily from the chart. For instance, in Fig. 2.11 there are four complete rainfall events as $R_A$, $R_B$, $R_C$, and $R_D$.
(b) One can know the beginning, $t_b$, and ending, $t_e$, time instances for each rainfall event.
(c) The rainfall duration, $d$, can be obtained as the difference between the ending and beginning time instances as, $d = t_e - t_b$.
(d) The difference between rainfall amounts at the beginning and ending instances yields the total rainfall amount during the rainfall event, $(R_b - R_e)$.

**Fig. 2.10** Recording
raingauge



**Fig. 2.11** Recording raingauge chart

(e) At each point on the rainfall chart trace, the slope of the tangent is equal to the rainfall intensity. It is possible to depict a certain time interval, $\Delta d$, much smaller than the rainfall duration, $d$, and starting from the rainfall occurrence during the whole rainfall duration, non-overlapping but adjacent $\Delta d$ intervals will have corresponding rainfall increments, $\Delta R$, and hence, the rainfall intensity can be calculated simply as $\Delta R/\Delta d$, which yields a set of intensities and the maximum value is adapted for design purposed in future activities. This point will be explained in detail in Sect. 2.12.
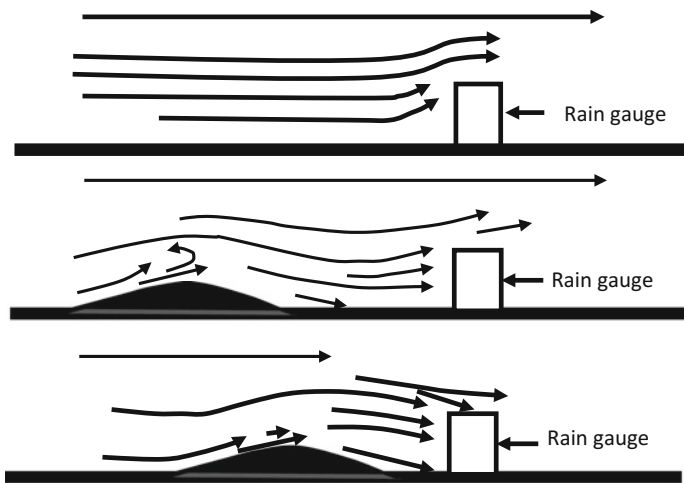
## 2.5   Rainfall Measurement Errors

In practice, it is not possible to measure rainfall amount without error. The best is to care with extra effort and record the measurement as errorless. However, the same care must be kept for each measurement, which is not possible in practice. Temporal or spatial arithmetic average rainfall amounts may have relatively less error than individual records. In practice, the location of the instruments must be selected in such a way that the overall recording errors are minimized as much as possible. There are three most significant error sources from the instruments.

(a) Errors from long-duration (daily or more) rainfall records: Possible evaporation from the raingauge is one of the major errors, which can be minimized by extra precautions to reduce its rate. For instance, addition of very fine layer of oil in the rainwater storage tank is one of the simple solutions.
(b) Errors from delay in transportation of rainfall water entrance: The rainfall water that falls on the funnel area may accumulate and cause entrance delay into the main water storage tank.
(c) Errors from icing: In cold weathers, water vapor in the air may freeze on the surface of the funnel and its hindrance of water entrance into the main water storage may cause errors.
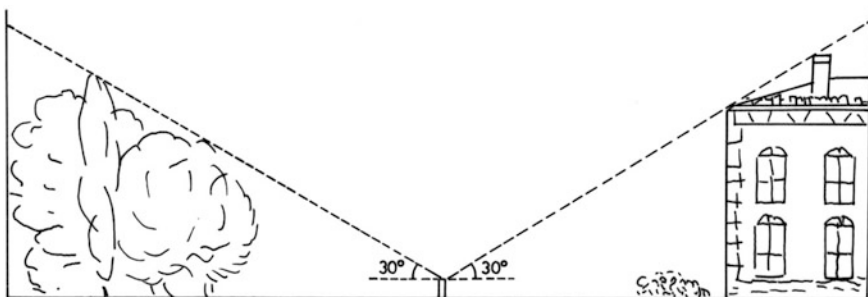
Apart from these errors, there may be additional ones, because of the location change of the raingauge. In the establishment of the raingauge at a location, one must consider uniform rainfall around the instrument over 100 m or preferably 1000 m radius area without any hindrance to disturb such a uniform areal distribution (Fig. 2.12). A raingauge is rather a big body; therefore, it must be located in such a way that there must not be any increase or decrease error effect within the boundary layer.

Air masses may cause turbulence effects around the raingauge and, hence, may hinder vertical entrance of rainfall into the funnel part. Other hindrance structures such as buildings, walls, and trees do not allow rainfall to fall vertically into the funnel, and hence, reliable measurements cannot be recorded. In the fixation operations of raingauge location, these points must be taken into consideration.

**Fig. 2.12** Air flow around raingauges

In order to reduce the effect of the turbulence, the upper rim of the raingauge must be almost conveniently at the same level with the ground surface, but this may cause to other two error sources. The first one is that the splash of rain drops from the soil may enter the gauge, because of the indetermination of the convenient rim height from the earth surface. As stated earlier, high structures around the gauge may give rise to air movement disturbances and reliable measurements cannot be recorded. Such errors may be reduced if the rim of the raingauge is such that within the 30° space from the gauge, there are not structures as shown in Fig. 2.13.



**Fig. 2.13** Distance to adjacent hindrances

## 2.6   Arid Region Rainfall

Rainfall consists of the water drops that reach the Earth surface from clouds after cooling and condensation of atmospheric vapor. It is the sole source of surface and groundwater resources, and in particular, groundwater reservoirs are replenished after each shower of rainfall. For practical applications, the quantity of water that reaches the Earth surface from the clouds is important and it is expressed in height, depth, or weight as records of specified duration. In general, it is expressed, say, as length/time or weight/time, which is the rainfall intensity. The change of intensity during the rainfall occurrence provides significant information in many applications such as engineering water structure constructions and groundwater recharge. The major agent of the hydrology in any region is the rainfall, and in particular, in the arid and semiarid regions, its lack over extensive periods gives rise to aridity and water stress (Şen 2008). In particular, in the arid and semiarid regions, the most important rainfall features can be summarized as follows:

1. Rainfall can be very varied and erratic spatially and temporally.
2. Individual storm rainfall total can be very high, and in many cases, the single storm rainfall may exceed the mean annual rainfall leading to floods.
3. Rainfall intensities can be very high, and consequently, floods occur and groundwater recharge can be augmented significantly (Şen 2014).
4. The amount of runoff is increased by the scaling effects of rainfall impact, which increases runoff transport capacity and may lead to flood events.
5. Due to the seasonal pattern of the rainfall, erosion, sediment, and groundwater recharge yield follow similar pattern, where the most suitable period for these activities is the early part of the wet season, when the rainfall is high, but the vegetation has not grown sufficiently to protect the surface.
6. Weather patterns in arid regions are most often under the effect of small-scale orographic and convective rainfall occurrences rather than occasional large-scale frontal rainfalls.

Spatial rainfall variability is directly related to the local and regional topography. At high elevations, orographic rainfall occurs and this happens, especially, if surface water and nearby high hills exist within short distances from the sea coastal lines.

There are many days in arid zones without rainfall (zero rainfall) and groundwater recharge. The rainfall in arid zones usually pours down, and consequently, flash floods may pose risks even in the most desiccated desert regions. There are very scant flood records, and people in arid zones are aware of how to deal with these dangerous natural water hazards. Catastrophe may occur when a flash flood is unusually large, or when nothing has happened for such a long time that the settlers have been lulled into a false sense of security.

Surface runoff can be considered as one of the major problems in many regions. Surface flow-prone regions have many development projects, such as reclamation, agriculture, industry, tourism, settlements, and others. Runoff, especially in the

form of flash flood, is a real danger for the urban and social developments in these areas, and it is the main reason to lose big quantities of freshwater, besides the destruction of life stocks and water-related infrastructure.

The desert is characterized by rare rainfall occurrences, which normally do not increase more than 25 mm, annually. Rainfall in arid and semiarid zones results largely from convective cloud mechanisms producing storms typically of short duration, relatively high intensity, and limited areal extent (Cooke and Warran 1973). However, low-intensity frontal-type rains are also experienced, usually in the winter season. For instance, in the Red Sea area, relatively low-intensity rainfall may represent the greater part of annual rainfall during this period.

## 2.7   Rainfall Duration
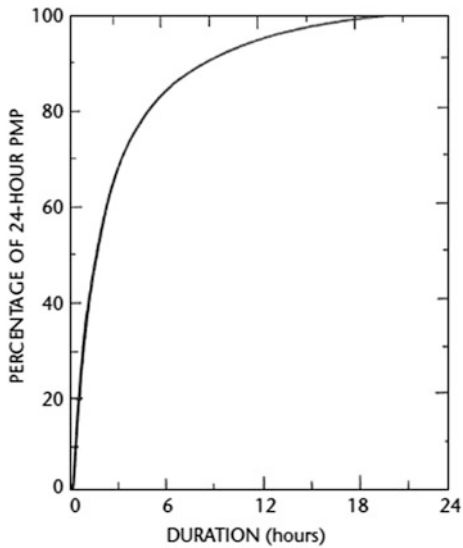
Individual storm rainfall durations vary from climate belt to another, and for instance, the closer is the location to the equator, the longer is the rainfall event duration. In desert areas, it may vary between 1 hour and 6 hour, but in humid regions, the single rainfall event may continue even for many days.

In many regions of the world, especially in arid and semiarid regions, only daily precipitation measurements are available. Various types of depth–duration relationships have been developed to show rainfall distribution within storms. Such relationships vary a great deal depending on storm type. For example, orographic rainfalls will show a much more gradual accumulation of rainfall with time than will thunderstorm rainfalls. The maximum depth–duration relation of Fig. 2.14 is based on rainfall amounts in heavy storms averaged over areas ranging up to 1000 km$^2$ in Illinois, USA (Huff 1967). This relation arranges the rainfall increments for various time intervals in decreasing order of magnitude and not in chronological order. In other words, the curve, a depth–duration curve (24-hour probable maximum precipitation percentage relation to duration) shows the greatest 3-hour amount in the first 3 h, the second greatest 3-hour amount in the second 3-hour period, and so forth. This arrangement is not intended to represent the order in which the rainfall increments accidentally for an occasional storm. Studies of chronological distribution of rainfall within storms (the mass curve of rainfall) indicate no consistent pattern, with maximum intensities likely to occur during any period of the storm. The depth–duration curve in Fig. 2.14 is representative of convective storms in the central USA.

## 2.8   Missing Data Filling

In some of the meteorology stations, due to various reasons, sometimes the records cannot be kept properly and, therefore, cause to missing records. Among the main causes are the broken instruments, unreachable locations due to heavy meteorology

**Fig. 2.14** Maximum depth-duration curve (Huff 1967)



conditions such as floods, intensive snow fall, terrorist activities, and alike. There are different methods for filling the missing records either within the record itself or among records at different locations. In the following sequel, missing record filling procedures are presented based on a set of stations.

## 2.8.1   Arithmetic Average

If the maximum relative error, $\alpha$, among a set of adjacent stations is less than 10%, then areal arithmetic average can be thought as the representative missing rainfall filling procedure uniformly all over the study area. If the rainfall amounts at two stations are $R_1$ and $R_2$, then the relative error percentage is calculated by the following expression:

$$\alpha = 100 \frac{|R_1 - R_2|}{\max(R_1, R_2)} \tag{2.1}$$

For the filling of missing station record, at least three adjacent station records must be taken into consideration. In the arithmetic average method, each station has the same weight, which is 1/n, where n is the number of stations in the arithmetic average calculation.

## *2.8.2  Ratio Method*

If the relative errors among the stations are more than 10%, then arithmetic average method is not valid. One can select the way of weighting the rainfall amounts at adjacent stations. The missing record value is a function of the same time records at other stations with weighting factors that are the ratio of the missing station arithmetic average to the arithmetic averages of other stations. The missing station arithmetic average is $\overline{R}_X$, and other stations' arithmetic averages are $\overline{R}_A, \overline{R}_B$ and $\overline{R}_C$; additionally, if the rainfall amounts at adjacent stations are $R_A$, $R_B$, and $R_c$, the station weights are $\frac{\overline{R}_X}{\overline{R}_A}, \frac{\overline{R}_X}{\overline{R}_B}$ and $\frac{\overline{R}_X}{\overline{R}_C}$. Hence, the missing rainfall amount can be calculated as follows:

$$R_X = \frac{1}{3}\left(\frac{\overline{R}_X}{\overline{R}_A}R_A + \frac{\overline{R}_X}{\overline{R}_B}R_B + \frac{\overline{R}_X}{\overline{R}_C}R_C\right) \tag{2.2}$$
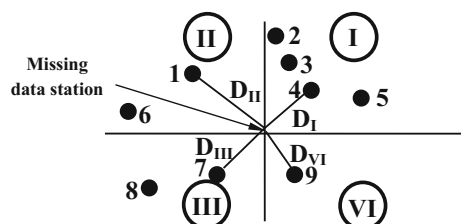
In case of more than three stations, this expression can be expanded similarly with the addition of new stations. In practical applications, calculations based on three stations are considered as sufficient for the application of the ratio method. In case of three stations, with almost equal arithmetic averages that are not different from each other more than 10% Eq. (2.2) reduces to the following arithmetic average expression with equal weights, 1/3:

$$R_X = \frac{1}{3}(R_A + R_B + R_C) \tag{2.3}$$

## *2.8.3  Inverse Distance Square Method*

In the previous missing data filling procedures, the distances are not taken into account between the missing data station and the adjacent ones. In general, the closer the stations, the higher are their effects on each other. The missing data station location is taken as the origin point of a Cartesian coordinate system, and then, the closest station within each quadrant (I, II, III or IV) is considered for data filling procedure (Fig. 2.15).

**Fig. 2.15**  Closest four stations

The closest four station distances to the origin point are $D_I$, $D_{II}$, $D_{III}$, and $D_{VI}$ with the corresponding rainfall amounts $R_I$, $R_{II}$, $R_{III}$, and $R_{IV}$, and hence, the inverse distance square method missing data procedure equation is:

$$R_X = \frac{\frac{1}{D_I^2}R_1 + \frac{1}{D_{II}^2}R_2 + \frac{1}{D_{III}^2}Y_3 + \frac{1}{D_{IV}^2}Y_4}{\frac{1}{D_I^2} + \frac{1}{D_{II}^2} + \frac{1}{D_{III}^2} + \frac{1}{D_{IV}^2}} \tag{2.4}$$

### 2.8.4   Correlation Method

A scatter diagram is obtained by plotting the two rainfall time series against each other with corresponding records. The most suitable straight line, if possible, is fitted to this scatter diagram. Such a straight-line indicates the correlation coefficient as the slope of the trend line. The fitting of the straight-line is achieved by least squares procedure. After the straight-line equation, one can obtain the missing rainfall value corresponding to available rainfall record at the same time in the next time series. In some cases, instead of a straight line, a nonlinear equation can be valid. If the records at two different locations are $X_1$, $X_2$, $X_3$, …, $X_n$ and $Y_1$, $Y_2$, $Y_3$, …, $Y_n$, their scatter may take the form as in Fig. 2.16.

In the case of a straight line, one can obtain a and b parameters of the following mathematical function by statistical least squares technique (Benjamin and Cornell 1970):
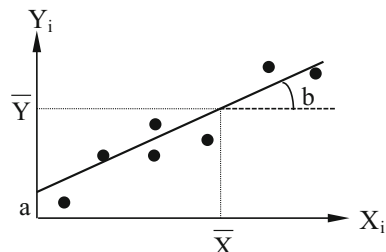
$$Y = a + bX \tag{2.5}$$

According to the least squares technique, the straight line crosses through the arithmetic averages ($\overline{X}$ and $\overline{Y}$) of the two time series. This provides opportunity to take the arithmetic averages of the two sides in Eq. (2.5):

$$\overline{Y} = a + b\overline{X} \tag{2.6}$$

For determination of the two unknowns, it is necessary to have another equation The second expression can be obtained again under the light of the least squares

Fig. 2.16   Scatter diagram

method, after multiplying two sides of Eq. (2.5) by the independent variable, $X$, and then taking the arithmetic average of both sides leading to the following expression:

$$\overline{XY} = a\overline{X} + b\overline{X^2} \tag{2.7}$$

The cross multiplication of X and Y and its average, $\overline{XY}$, is the representative of the correlation coefficient that is also related to the regression coefficient. Furthermore, this correlation value is equivalent to the straight-line slope.

The coefficients a and b are calculated from the simultaneous solution of Eqs. (2.6) and (2.7) on the basis of two time series $X_i$ and $Y_i$ ($i$ = 1, 2, 3, …, $n$). Equation (2.5) helps to fill the missing data in one of the time series, $Y$, from the other time series, $X$.

## 2.9  Double Mass Curve Method

In the rainfall records, there are two types of errors, namely systematic and random. The random errors are assumed to be embedded into the records with plus and minus signs. However, the random errors may not be very active in long-time series records. The major random errors are also referred to as the statistical sampling errors. Their sources can be explained along the following lines:

(a) Measurement errors from the instrument,
(b) Errors that originate from the writing and rounding,
(c) Printing errors, because rainfall records are distributed through the computer files or bulletins.

The systematic errors remain even on the long run, and therefore, they must be eliminated prior to any engineering calculations. The main systematic error sources are as follows:

(a) Station location shift: If the station location falls within the urban areal growth, dam reservoir coverage area, along the highway construction, then the station location must be shifted to another suitable location.
(b) Vegetation growth around the station and hindrance of wind: In such situations, the raingauge starts to measure more or less than the usual cases. The raingauge can be damaged due to animal hit and, hence, loses its sensitivity and starts to record systematic errors. Also, appearance of very small holes in the storage tank leads to systematic error records.
(c) Some pieces of the raingauge can be replaced by new ones, and hence, the new measurements may have slightly systematic error records.
(d) Various changes around the location of the raingauge may also lead to systematic errors.

In order to eliminate the systematic errors from the records, it is necessary to depend on the convenience tests. The most effective method for this purpose is the double mass curve graph analysis. The suspicious station values are shown on the vertical axis.
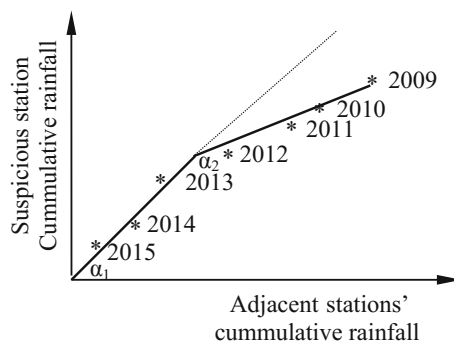
The application of the double mass curve method requires a set of adjacent station daily, monthly, or yearly record arithmetic averages together with the arithmetic averages of the suspicious station on the same durations. Generally, it is preferable to consider the station locations that fall within the same drainage basin or under the similar climatological region around the suspicious station. After the identification of the suspicious station, historically the last record average is considered as the first value in the sequence of averages with others following backward in a sequence. This implies that the last record comes at the end of the sequence. The averages of the suspicious station and the regional averages of the adjacent stations are plotted against each other on a Cartesian coordinate system as in Fig. 2.17.

If a single straight line is fitted to the scatter of points, then there is no systematic error in the suspicious meteorology station records. This implies that all the stations abide with homogeneity in the region. Otherwise, there appear broken straight lines, which is the indicator of systematic error in the suspicious station records. In this case, the slopes, $\alpha_1$ and $\alpha_2$, of the two straight lines are determined and the correction factor, f, for the records in the suspicious station can be calculated as,

$$f = \frac{\tan \alpha_1}{\tan \alpha_2} \tag{2.8}$$

Finally, all the records before the break point are corrected by multiplying each record by f. This leads to a single straight line on the scatter diagram with the corrected records.
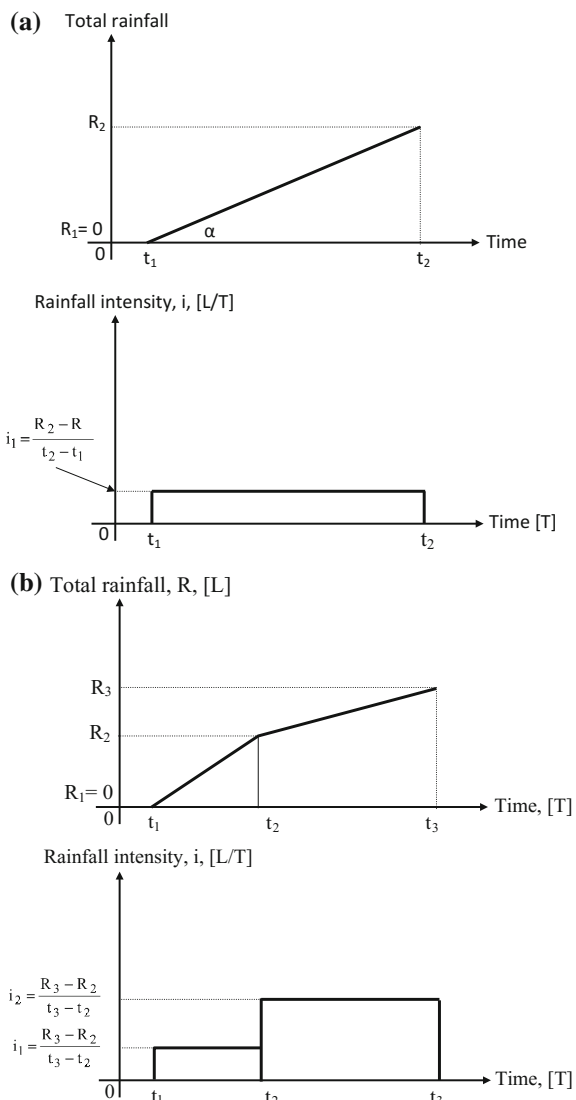
**Fig. 2.17** Double mass curves

## 2.10   Rainfall Intensity

It is known from any textbook on principles of hydrology (Chow et al. 1988; Linsley 1986; Şen 2008) that a recording raingauge output graph gives the cumulative rainfall change during a storm by time (Fig. 2.12). For the sake of argument, the cumulative rainfall curve (CRC) is assumed in its simplest linear form with its slope, $\alpha$, as in Fig. 2.18. At the storm beginning, it has the minimum

**Fig. 2.18** Single storm rainfall record



**(a)**   Total rainfall

$R_2$

$R_1 = 0$                                                          Time
      0   $t_1$              $\alpha$                        $t_2$

Rainfall intensity, i, [L/T]

$i_1 = \dfrac{R_2 - R}{t_2 - t_1}$                                    Time [T]
      0   $t_1$                                        $t_2$

**(b)** Total rainfall, R, [L]

$R_3$

$R_2$

$R_1 = 0$                                                          Time, [T]
      0   $t_1$              $t_2$              $t_3$

Rainfall intensity, i, [L/T]

$i_2 = \dfrac{R_3 - R_2}{t_3 - t_2}$

$i_1 = \dfrac{R_3 - R_2}{t_3 - t_2}$                                    Time, [T]
      0   $t_1$              $t_2$              $t_3$

**(c)**
Total rainfall, R, [L]



Rainfall intensity, i, [L/T]



**(d)**
Total rainfall, R, [L/T]



Rainfall intensity, i, [L/T]
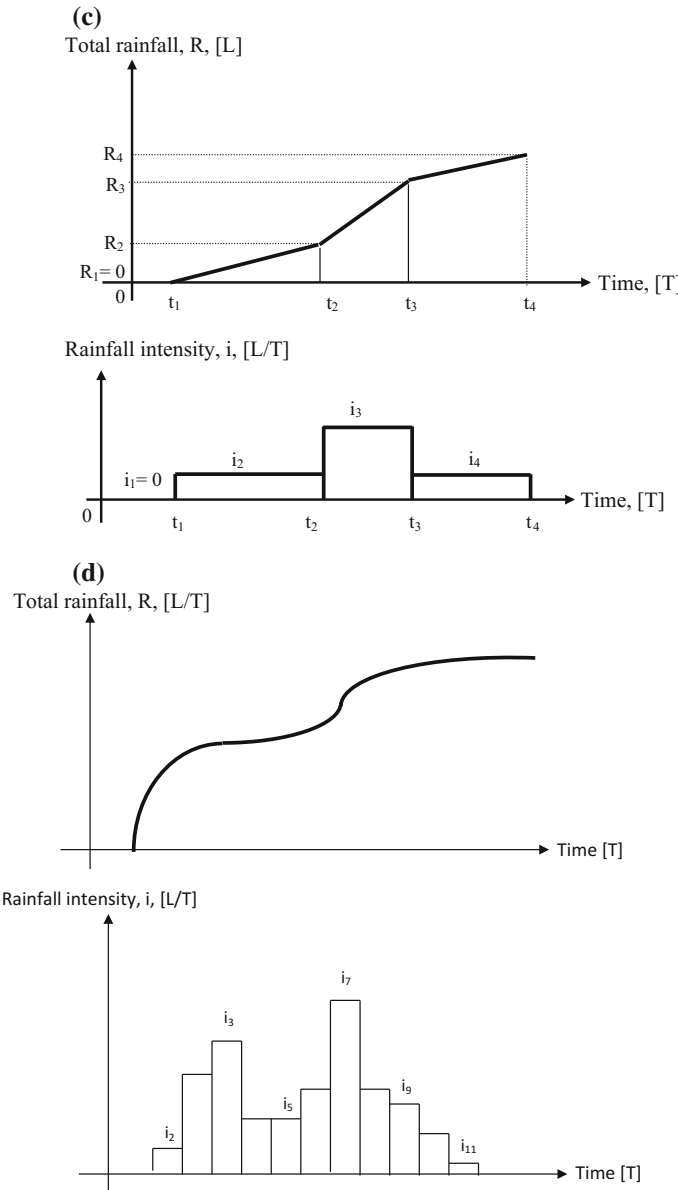


**Fig. 2.18**  (continued)

value ($R_1 = 0$), which reaches to its maximum at the end of the storm, $R_2$. If the storm rainfall has a uniform rate right from the beginning, $t_1$, until the end, $t_2$, of the storm, then it will appear as a straight line (see Fig. 2.18a).

The rainfall intensity, $i$, is equal to the slope of the total rainfall line, which is expressed geometrically as,

$$i = \tan \alpha \tag{2.9}$$

where $\alpha$ is the slope of CRC. It is also possible to express the rainfall intensity mathematically as the derivative of total rainfall amount, $R$, with respect to time, $t$, as,

$$i = \frac{dR}{dt} \tag{2.10}$$

which implies that the rainfall intensity is constant during dt duration. It is also possible to write the rainfall intensity in terms of a finite difference as,

$$i = \frac{R_2 - R_1}{t_2 - t_1} \tag{2.11}$$

In order to express simple change in the rainfall intensity, let us consider two straight lines that represent the CRC (see Fig. 2.18b). Accordingly, there are two rainfall intensities as, $i_1 = \cot \alpha_1$ and $i_2 = \cot \alpha_1$ or mathematically $i_1 = dR_1/dt$ and $i_2 = dR_2/dt$.

In general, there will be n small straight lines that can represent closely the CRC (see Fig. 2.18c), and hence, the corresponding rainfall intensities for each line are

$$i_1 = \cot \alpha_1, i_2 = \cot \alpha_1, i_3 = \cot \alpha_1, \ldots, \text{ and } i_n = \cot \alpha_1 \tag{2.12}$$

or

$$i_1 = dR_1/dt, i_2 = dR_3/dt, i_3 = dR_3/dt, \ldots, \text{ and } i_n = dR_n/dt \tag{2.13}$$

Similarly, a natural CRC will look like a non-decreasing curve, which will have relatively small slopes at the beginning and ending portions with comparatively bigger slopes in-between as in Fig. 2.18d. In order to convert the CRC into its hyetograph, it is necessary to divide the time axis into equal intervals, $\Delta t$, and then to find the corresponding rainfall increments from the vertical axis as $\Delta R_1, \Delta R_2, \ldots, \Delta R_n$. Accordingly, the rainfall intensities will be,

$$i_1 = \frac{dR_1}{\Delta t}, i_2 = \frac{dR_2}{\Delta t}, i_3 = \frac{dR_3}{\Delta t}, \ldots, \text{ and } i_n = \frac{dR_n}{\Delta t} \tag{2.14}$$

If the rainfall intensity is plotted against the time increments, the resulting curve is the hyetograph, which shows the change of rainfall intensity by time (see Fig. 2.18d).

*Example 2.1* The storm rainfall recording raingauge records on January 26, 2011, are given in Table 2.2. Since the length of minute-wise record is very long, the first two-hour records are presented in the table, but the whole record graph is shown in Fig. 2.19.

**Table 2.2** Jeddah storm rainfall record

| Date | mm | Time (min) | Cumulative rainfall (mm) | 5-min | 10-min | 15-min | 30-min | 60-min | 120-min |
|---|---|---|---|---|---|---|---|---|---|
| 26/01/2011 10:57 | 0.1 | 1 | 0.1 | | | | | | |
| 26/01/2011 10:58 | 0 | 2 | 0.1 | | | | | | |
| 26/01/2011 10:59 | 0 | 3 | 0.1 | | | | | | |
| 26/01/2011 11:00 | 0 | 4 | 0.1 | | | | | | |
| 26/01/2011 11:01 | 0.1 | 5 | 0.2 | 1.2 | | | | | |
| 26/01/2011 11:02 | 0 | 6 | 0.2 | 1.2 | | | | | |
| 26/01/2011 11:03 | 0 | 7 | 0.2 | 1.2 | | | | | |
| 26/01/2011 11:04 | 0 | 8 | 0.2 | 1.2 | | | | | |
| 26/01/2011 11:05 | 0 | 9 | 0.2 | 0 | | | | | |
| 26/01/2011 11:06 | 0.1 | 10 | 0.3 | 1.2 | 1.2 | | | | |
| 26/01/2011 11:07 | 0 | 11 | 0.3 | 1.2 | 1.2 | | | | |
| 26/01/2011 11:08 | 0 | 12 | 0.3 | 1.2 | 1.2 | | | | |
| 26/01/2011 11:09 | 0 | 13 | 0.3 | 1.2 | 1.2 | | | | |
| 26/01/2011 11:10 | 0.1 | 14 | 0.4 | 1.2 | 1.2 | | | | |
| 26/01/2011 11:11 | 0 | 15 | 0.4 | 1.2 | 1.2 | 1.2 | | | |
| 26/01/2011 11:12 | 0.1 | 16 | 0.5 | 2.4 | 1.8 | 1.6 | | | |
| 26/01/2011 11:13 | 0.1 | 17 | 0.6 | 3.6 | 2.4 | 2 | | | |
| 26/01/2011 11:14 | 0 | 18 | 0.6 | 2.4 | 2.4 | 2 | | | |
| 26/01/2011 11:15 | 0 | 19 | 0.6 | 2.4 | 1.8 | 1.6 | | | |
| 26/01/2011 11:16 | 0 | 20 | 0.6 | 1.2 | 1.8 | 1.6 | | | |
| 26/01/2011 11:17 | 0.1 | 21 | 0.7 | 1.2 | 2.4 | 2 | | | |

**Table 2.2** (continued)

| Date | mm | Time (min) | Cumulative rainfall (mm) | 5-min | 10-min | 15-min | 30-min | 60-min | 120-min |
|---|---|---|---|---|---|---|---|---|---|
| 26/01/2011 11:18 | 0 | 22 | 0.7 | 1.2 | 2.4 | 2 | | | |
| 26/01/2011 11:19 | 0.1 | 23 | 0.8 | 2.4 | 2.4 | 2.4 | | | |
| 26/01/2011 11:20 | 0 | 24 | 0.8 | 2.4 | 2.4 | 2 | | | |
| 26/01/2011 11:21 | 0 | 25 | 0.8 | 1.2 | 1.8 | 2 | | | |
| 26/01/2011 11:22 | 0.1 | 26 | 0.9 | 2.4 | 1.8 | 2.4 | | | |
| 26/01/2011 11:23 | 0 | 27 | 0.9 | 1.2 | 1.8 | 2.4 | | | |
| 26/01/2011 11:24 | 0 | 28 | 0.9 | 1.2 | 1.8 | 2 | | | |
| 26/01/2011 11:25 | 0.1 | 29 | 1 | 2.4 | 2.4 | 2.4 | | | |
| 26/01/2011 11:26 | 0 | 30 | 1 | 1.2 | 1.8 | 2 | 1.8 | | |
| 26/01/2011 11:27 | 0.1 | 31 | 1.1 | 2.4 | 2.4 | 2 | 2 | | |
| 26/01/2011 11:28 | 0.1 | 32 | 1.2 | 3.6 | 2.4 | 2.4 | 2.2 | | |
| 26/01/2011 11:29 | 0.1 | 33 | 1.3 | 3.6 | 3 | 2.8 | 2.4 | | |
| 26/01/2011 11:30 | 0 | 34 | 1.3 | 3.6 | 3 | 2.8 | 2.2 | | |
| 26/01/2011 11:31 | 0 | 35 | 1.3 | 2.4 | 2.4 | 2.4 | 2.2 | | |
| 26/01/2011 11:32 | 0.2 | 36 | 1.5 | 3.6 | 3.6 | 3.2 | 2.6 | | |
| 26/01/2011 11:33 | 0.3 | 37 | 1.8 | 6 | 5.4 | 4 | 3.2 | | |
| 26/01/2011 11:34 | 0.3 | 38 | 2.1 | 9.6 | 6.6 | 5.2 | 3.8 | | |
| 26/01/2011 11:35 | 0.2 | 39 | 2.3 | 12 | 7.8 | 6 | 4 | | |
| 26/01/2011 11:36 | 0.3 | 40 | 2.6 | 13.2 | 9 | 6.8 | 4.6 | | |
| 26/01/2011 11:37 | 0.6 | 41 | 3.2 | 16.8 | 12 | 9.2 | 5.8 | | |
| 26/01/2011 11:38 | 0.7 | 42 | 3.9 | 21.6 | 15.6 | 12 | 7.2 | | |

**Table 2.2**  (continued)

| Date | mm | Time (min) | Cumulative rainfall (mm) | 5-min | 10-min | 15-min | 30-min | 60-min | 120-min |
|------|-----|------|------|------|------|------|------|------|------|
| 26/01/2011 11:39 | 0.8 | 43 | 4.7 | 28.8 | 20.4 | 14.8 | 8.6 | | |
| 26/01/2011 11:40 | 0.6 | 44 | 5.3 | 32.4 | 24 | 17.2 | 9.8 | | |
| 26/01/2011 11:41 | 0.7 | 45 | 6 | 33.6 | 27 | 19.6 | 11 | | |
| 26/01/2011 11:42 | 0.5 | 46 | 6.5 | 31.2 | 28.2 | 21.2 | 11.8 | | |
| 26/01/2011 11:43 | 1.1 | 47 | 7.6 | 34.8 | 33 | 25.2 | 14 | | |
| 26/01/2011 11:44 | 1.7 | 48 | 9.3 | 48 | 42 | 32 | 17.4 | | |
| 26/01/2011 11:45 | 1.5 | 49 | 10.8 | 57.6 | 49.2 | 38 | 20.4 | | |
| 26/01/2011 11:46 | 1.6 | 50 | 12.4 | 70.8 | 55.2 | 43.6 | 23.4 | | |
| 26/01/2011 11:47 | 1.3 | 51 | 13.7 | 73.2 | 58.8 | 47.6 | 26 | | |
| 26/01/2011 11:48 | 0.8 | 52 | 14.5 | 62.4 | 58.8 | 49.6 | 27.4 | | |
| 26/01/2011 11:49 | 0.5 | 53 | 15 | 50.4 | 58.2 | 50.8 | 28.4 | | |
| 26/01/2011 11:50 | 0.2 | 54 | 15.2 | 33.6 | 55.2 | 50.4 | 28.8 | | |
| 26/01/2011 11:51 | 0.3 | 55 | 15.5 | 21.6 | 54 | 49.2 | 29.2 | | |
| 26/01/2011 11:52 | 1.2 | 56 | 16.7 | 26.4 | 54.6 | 51.2 | 31.6 | | |
| 26/01/2011 11:53 | 1.9 | 57 | 18.6 | 43.2 | 55.8 | 55.6 | 35.4 | | |
| 26/01/2011 11:54 | 1.5 | 58 | 20.1 | 58.8 | 55.8 | 59.2 | 38.2 | | |
| 26/01/2011 11:55 | 1.2 | 59 | 21.3 | 69.6 | 53.4 | 61.2 | 40.6 | | |
| 26/01/2011 11:56 | 1.6 | 60 | 22.9 | 74.4 | 55.2 | 65.6 | 43.6 | 22.8 | |
| 26/01/2011 11:57 | 1.3 | 61 | 24.2 | 67.2 | 58.2 | 66.4 | 46 | 24.1 | |
| 26/01/2011 11:58 | 1.5 | 62 | 25.7 | 67.2 | 64.2 | 65.6 | 48.8 | 25.6 | |
| 26/01/2011 11:59 | 1.6 | 63 | 27.3 | 72 | 72.6 | 66 | 52 | 27.2 | |

(continued)

**Table 2.2**  (continued)

| Date | mm | Time (min) | Cumulative rainfall (mm) | 5-min | 10-min | 15-min | 30-min | 60-min | 120-min |
|---|---|---|---|---|---|---|---|---|---|
| 26/01/2011 12:00 | 1.4 | 64 | 28.7 | 69.6 | 79.2 | 65.2 | 54.8 | 28.5 | |
| 26/01/2011 12:01 | 1.3 | 65 | 30 | 69.6 | 79.8 | 65.2 | 57 | 29.8 | |
| 26/01/2011 12:02 | 1.5 | 66 | 31.5 | 69.6 | 77.4 | 68 | 59.4 | 31.3 | |
| 26/01/2011 12:03 | 1.1 | 67 | 32.6 | 63.6 | 75 | 70.4 | 61 | 32.4 | |
| 26/01/2011 12:04 | 1.4 | 68 | 34 | 63.6 | 76.2 | 75.2 | 63.4 | 33.8 | |
| 26/01/2011 12:05 | 1.4 | 69 | 35.4 | 64.8 | 75 | 79.6 | 65.6 | 35.1 | |
| 26/01/2011 12:06 | 1.4 | 70 | 36.8 | 63.6 | 75.6 | 80.4 | 67.2 | 36.5 | |
| 26/01/2011 12:07 | 1.5 | 71 | 38.3 | 68.4 | 75.6 | 78.8 | 68.8 | 38 | |
| 26/01/2011 12:08 | 1.6 | 72 | 39.9 | 70.8 | 75.6 | 79.2 | 70.4 | 39.6 | |
| 26/01/2011 12:09 | 1.5 | 73 | 41.4 | 72 | 76.2 | 80.4 | 72.2 | 41 | |
| 26/01/2011 12:10 | 1.3 | 74 | 42.7 | 70.8 | 76.2 | 79.2 | 73.4 | 42.3 | |
| 26/01/2011 12:11 | 0.8 | 75 | 43.5 | 62.4 | 72 | 77.2 | 74 | 43 | |
| 26/01/2011 12:12 | 1.1 | 76 | 44.6 | 56.4 | 72 | 75.6 | 74 | 44 | |
| 26/01/2011 12:13 | 1 | 77 | 45.6 | 50.4 | 69.6 | 73.2 | 72.6 | 45 | |
| 26/01/2011 12:14 | 1.1 | 78 | 46.7 | 48 | 67.8 | 72 | 71.8 | 46.1 | |
| 26/01/2011 12:15 | 1.5 | 79 | 48.2 | 56.4 | 68.4 | 72.8 | 71.6 | 47.6 | |
| 26/01/2011 12:16 | 1 | 80 | 49.2 | 55.2 | 65.4 | 70.8 | 71 | 48.5 | |
| 26/01/2011 12:17 | 0.9 | 81 | 50.1 | 54 | 61.2 | 70 | 71.2 | 49.4 | |
| 26/01/2011 12:18 | 1.1 | 82 | 51.2 | 54 | 58.8 | 68.8 | 72.4 | 50.4 | |
| 26/01/2011 12:19 | 0.5 | 83 | 51.7 | 42 | 54 | 65.2 | 73 | 50.9 | |
| 26/01/2011 12:20 | 0.5 | 84 | 52.2 | 36 | 52.2 | 61.6 | 73.4 | 51.4 | |

**Table 2.2** (continued)

| Date | mm | Time (min) | Cumulative rainfall (mm) | 5-min | 10-min | 15-min | 30-min | 60-min | 120-min |
|---|---|---|---|---|---|---|---|---|---|
| 26/01/2011 12:21 | 0.9 | 85 | 53.1 | 36 | 51 | 59.2 | 72.8 | 52.2 | |
| 26/01/2011 12:22 | 0.6 | 86 | 53.7 | 30 | 48.6 | 55.2 | 70.2 | 52.8 | |
| 26/01/2011 12:23 | 0.2 | 87 | 53.9 | 26.4 | 43.2 | 50 | 67.6 | 53 | |
| 26/01/2011 12:24 | 0 | 88 | 53.9 | 20.4 | 34.2 | 44.8 | 65.2 | 52.9 | |
| 26/01/2011 12:25 | 0.1 | 89 | 54 | 10.8 | 28.8 | 42 | 62.2 | 53 | |
| 26/01/2011 12:26 | 0.2 | 90 | 54.2 | 6 | 24.6 | 38.4 | 60 | 53.1 | |
| 26/01/2011 12:27 | 0.2 | 91 | 54.4 | 6 | 19.2 | 35.2 | 57.4 | 53.2 | |
| 26/01/2011 12:28 | 0 | 92 | 54.4 | 6 | 16.2 | 30.8 | 54.2 | 53.1 | |
| 26/01/2011 12:29 | 0 | 93 | 54.4 | 4.8 | 13.2 | 24.8 | 51.4 | 53.1 | |
| 26/01/2011 12:30 | 0.1 | 94 | 54.5 | 3.6 | 8.4 | 21.2 | 49 | 53.2 | |
| 26/01/2011 12:31 | 0.1 | 95 | 54.6 | 2.4 | 5.4 | 18 | 46.2 | 53.1 | |
| 26/01/2011 12:32 | 0.3 | 96 | 54.9 | 6 | 6 | 14.8 | 44.6 | 53.1 | |
| 26/01/2011 12:33 | 0.4 | 97 | 55.3 | 10.8 | 8.4 | 14.4 | 42.6 | 53.2 | |
| 26/01/2011 12:34 | 0.2 | 98 | 55.5 | 12 | 9 | 13.2 | 40.2 | 53.2 | |
| 26/01/2011 12:35 | 0.4 | 99 | 55.9 | 15.6 | 10.2 | 11.2 | 38.2 | 53.3 | |
| 26/01/2011 12:36 | 0.7 | 100 | 56.6 | 20.4 | 13.2 | 11.6 | 36.6 | 53.4 | |
| 26/01/2011 12:37 | 0.8 | 101 | 57.4 | 25.2 | 18 | 14 | 35 | 53.5 | |
| 26/01/2011 12:38 | 0.7 | 102 | 58.1 | 31.2 | 22.2 | 16.8 | 33.4 | 53.4 | |
| 26/01/2011 12:39 | 1.3 | 103 | 59.4 | 42 | 29.4 | 21.6 | 33.4 | 54.1 | |
| 26/01/2011 12:40 | 1.4 | 104 | 60.8 | 50.4 | 37.2 | 26.4 | 34.6 | 54.8 | |
| 26/01/2011 12:41 | 1.5 | 105 | 62.3 | 58.8 | 44.4 | 31.6 | 35.4 | 55.8 | |
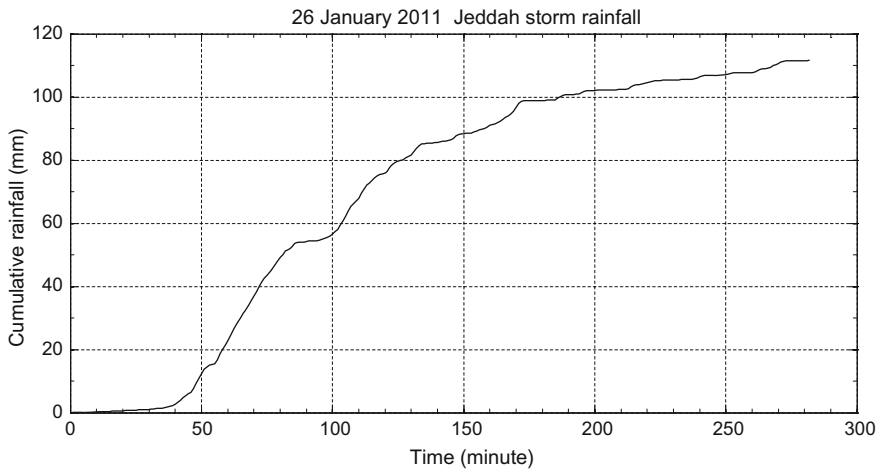
**Table 2.2** (continued)

| Date | mm | Time (min) | Cumulative rainfall (mm) | 5-min | 10-min | 15-min | 30-min | 60-min | 120-min |
|---|---|---|---|---|---|---|---|---|---|
| 26/01/2011 12:42 | 1.6 | 106 | 63.9 | 69.6 | 51.6 | 38 | 36.6 | 56.3 | |
| 26/01/2011 12:43 | 1.5 | 107 | 65.4 | 72 | 59.4 | 44 | 37.4 | 56.1 | |
| 26/01/2011 12:44 | 0.8 | 108 | 66.2 | 64.8 | 61.8 | 46.8 | 36 | 55.4 | |
| 26/01/2011 12:45 | 0.8 | 109 | 67 | 56.4 | 62.4 | 49.6 | 35.6 | 54.6 | |
| 26/01/2011 12:46 | 1 | 110 | 68 | 49.2 | 63.6 | 52.4 | 35.8 | 54.3 | |
| 26/01/2011 12:47 | 1.6 | 111 | 69.6 | 50.4 | 69 | 57.2 | 36.8 | 55.1 | |
| 26/01/2011 12:48 | 1.3 | 112 | 70.9 | 56.4 | 69 | 61.6 | 38.4 | 55.9 | |
| 26/01/2011 12:49 | 1.3 | 113 | 72.2 | 62.4 | 68.4 | 65.2 | 40 | 57 | |
| 26/01/2011 12:50 | 0.5 | 114 | 72.7 | 56.4 | 62.4 | 64.4 | 39.2 | 57.2 | |
| 26/01/2011 12:51 | 0.9 | 115 | 73.6 | 48 | 58.2 | 64.8 | 39.8 | 56.9 | |
| 26/01/2011 12:52 | 0.8 | 116 | 74.4 | 42 | 54 | 65.2 | 41 | 55.8 | |
| 26/01/2011 12:53 | 0.6 | 117 | 75 | 33.6 | 52.8 | 62.4 | 42.2 | 54.9 | |
| 26/01/2011 12:54 | 0.4 | 118 | 75.4 | 32.4 | 50.4 | 58.4 | 42.8 | 54.1 | |
| 26/01/2011 12:55 | 0.3 | 119 | 75.7 | 25.2 | 46.2 | 53.6 | 43 | 52.8 | |
| 26/01/2011 12:56 | 0.2 | 120 | 75.9 | 18 | 37.8 | 48 | 43 | 51.7 | 37.9 |
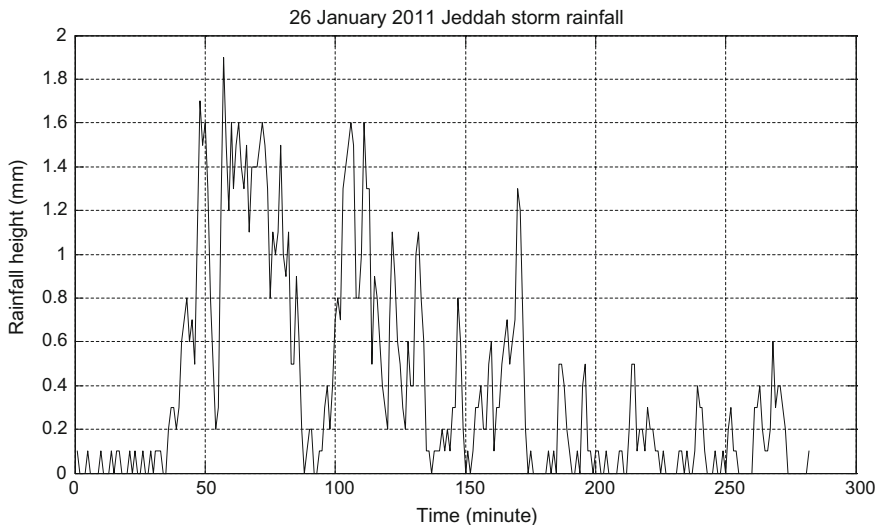
The relationship between the rainfall intensity and the duration is given in Fig. 2.19, where the rainfall intensity (the slope of the tangent at any point) starts as high values and by the time decreases.

The variation of rainfall amount during the storm rainfall is shown in Fig. 2.20. It is obvious that especially between the first 50–70 min, the rainfall height is the maximum.

The rainfall intensity calculations are presented in Table 2.2 for 5-, 10-, 20-, 30-, 60-, and 120-min durations; the maximum rainfall intensity during each one of these durations is plotted against the selected durations; and the result is given in Fig. 2.21, where a straight line is matched through the scatter points on the double logarithmic paper.
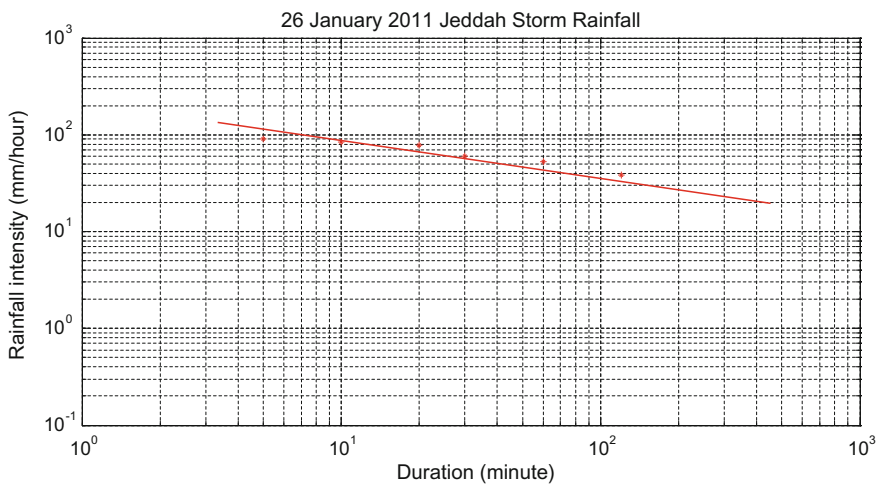
**Fig. 2.19**  Cumulative rainfall amounts during 26 January 2011 Jeddah storm rainfall
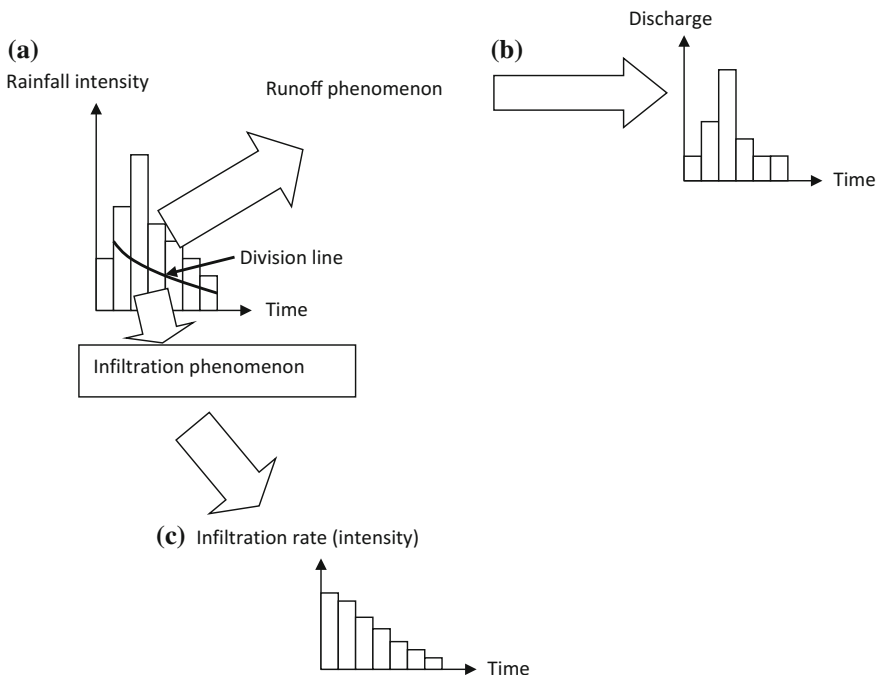


**Fig. 2.20**  Jeddah storm rainfall time series

## 2.11   Hyetograph–Hydrograph Relationship

The rainfall intensity at the earth's surface splits into two parts, namely losses of infiltration, evaporation, depletion, and runoff. They are referred to as non-effective (losses) rainfalls and effective (runoff). As shown in Fig. 2.22a, the upper (effective) part corresponds to direct runoff and the lower (non-effective) part leads to infiltration and later to the consequent groundwater recharge. In Fig. 2.22a, the division

**Fig. 2.21** Rainfall intensity–duration curve



**Fig. 2.22** (**a**) Hyetograph, (**b**) hydrograph, and (**c**) infiltration curve
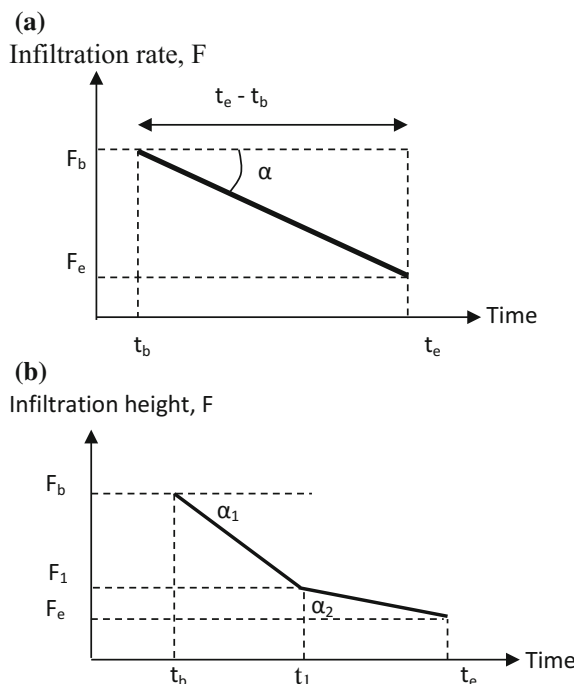
line is located rather arbitrarily, but in actual studies, it corresponds to the infiltration curve (Şen 2008). Hydrograph is the graphical form of effective rainfall change on the earth's surface, whereas infiltration curve is the graphical appearance of non-effective rainfall time variation in the subsurface.

In hyetograph and infiltration curves, the vertical axis is shown as the rainfall intensity, whereas the hydrograph has the vertical axis allocated for discharge dimension. The drainage area, A, plays the main role as the conversion factor between the discharge and the rainfall intensity or infiltration rate. The hyetograph is the summation of hydrograph and infiltration curve.

Similar to rainfall event, infiltration also changes with time and infiltrometers are used to record the cumulative water that enters the earth surface by time. The reader is referred to any basic textbook on the hydrology principles for detailed information on infiltrometers (Chow et al. 1988; Şen 2008). Herein, the procedure of calculations and the derivation of the infiltration graph are explained explicitly. Similar to CRC, total infiltration curve is obtained in the field by infiltration test measurements. In the case of assumed uniform infiltration rate from the beginning ($t_b$) of the test until the soil is saturated, i.e., ending time ($t_e$) of infiltration, a similar straight line appears as in Fig. 2.18a (see Fig. 2.23a).

By definition, the infiltration rate, $f$, is the slope of this straight line and trigonometrically it is possible to write,



**Fig. 2.23** Uniform infiltration rate

$$f = \tan \alpha \qquad\qquad (2.15)$$

or

$$f = \frac{F_e - F_b}{t_e - t_b} = \frac{\mathrm{d}f}{\mathrm{d}t} \qquad\qquad (2.16)$$

In the case of heterogeneous infiltration rate, there are at least two straight lines that represent the infiltration rate curve as shown in Fig. 2.23b, but the second straight line is expected physically to have smaller slope than the first one. This is due to the fact that as the time passes the soil becomes more saturated and accommodates less water by time. Any infiltration curve starts with a big slope, which becomes smaller by time, and finally, it remains the same indicating that the soil cannot accommodate additional water, since it is completely saturated. The infiltration rates can be calculated as $f_1 = \tan \alpha_1$ and $f_2 = \tan \alpha_2$ or $f_1 = \mathrm{d}F_1/\mathrm{d}t$ and $f_2 = \mathrm{d}F_2/\mathrm{d}t$. However, if there are n different straight lines, the infiltration rates can be calculated as $f_1 = \tan \alpha_1$, $f_2 = \tan \alpha_2$, $f_3 = \tan \alpha_3$, ..., and $f_n = \tan \alpha_n$ or according to Eq. (2.16) $f_1 = \mathrm{d}F_1/\mathrm{d}t$, $f_2 = \mathrm{d}F_2/\mathrm{d}t$, $f_3 = \mathrm{d}F_3/\mathrm{d}t$, ..., $f_n = \mathrm{d}F_n/\mathrm{d}t$. After the infiltration test in the field and the completion of necessary calculations, it is possible to obtain an exponential curve according to Horton (1933) as in Fig. 2.24.
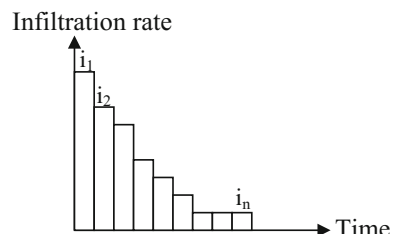
By considering the same time intervals, one can calculate the rainfall intensity values that cause to direct runoff, by the subtraction of the infiltration from the same time interval rainfall intensity, r, which leads to,
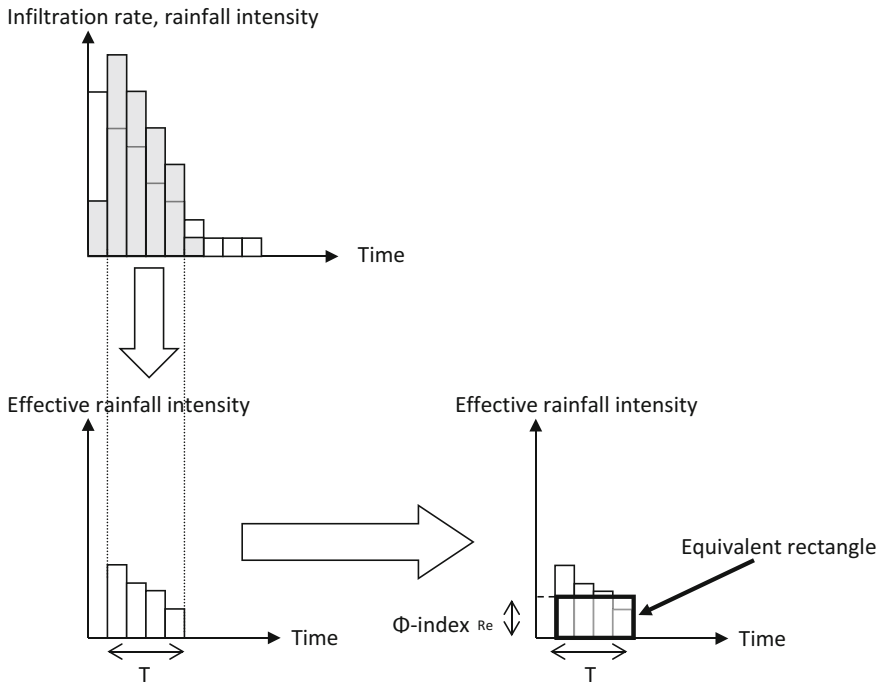
$$i_1' = i_1 - f_1, i_2' = i_2 - f_2, i_3' = i_3 - f_3, \ldots, i_n' = i_n - f_n \qquad\qquad (2.17)$$

Finally, the residual hyetograph that leads to direct surface runoff becomes as in Fig. 2.25.

In practical works, the histogram is divided into two parts by a horizontal line such that the overlying hyetograph area is equal to direct runoff height. This is referred to as the Φ-index method (Chow et al. 1988; Linsley et al. 1988). In the last graph of Fig. 2.25, the remaining effective rainfall, which is the cause of direct runoff, is converted into a rectangle with the same area of the hyetograph by leaving the base time the same. This yields the height of the equivalent rectangle with an

**Fig. 2.24**  Infiltration rate curve

**Fig. 2.25** Direct hyetograph

effective rainfall height, $R_e$ or Φ-index, that should be considered in any hydrograph analysis.

It is now time to consider the transformation mechanics of the direct hyetograph into its direct hydrograph through the watershed properties. This information will be used in Chap. 4 following sections for arriving at a proper hydrograph according to some assumptions or empirical relationships. The transformation has two phases: The first one is concerned with time translation, because in nature, the hydrograph peak discharge always appears after the end of effective rainfall (shifting principle in Chap. 4). The second phase is due to the storage effect of the watershed area, which gives different shapes to the hydrograph at different sections, and hence, the peak of the hydrograph also changes In general, the highest effective rainfall in the hyetograph is higher than the depth of the peak direct hydrograph discharge.

By definition in any direct hydrograph, the area under the curve, which corresponds to direct rainfall volume, is equal to the multiplication of the watershed area, A, by idealized average effective rainfall height, $R_e$. Depending on what have been explained above, one can deduce the following significant quantities for further hydrograph analysis:

1. Effective rainfall amount, $R_e$,
2. Effective rainfall duration, $t_e$,
3. Hydrograph peak discharge, $Q_p$,
4. Time to peak discharge, $t_p$,
5. Hydrograph base time duration, $t_b$,
6. The time lag, $t_L$, in the sense of distance between the effective rainfall centroid and the hydrograph peak.

First two quantities are completely related to rainfall and infiltration properties. Infiltration is dependent on the type of soil, vegetation, land use, and geology. The third, fourth, and fifth quantities are functions of rainfall and watershed characteristics. The last point is related to the response of watershed to rainfall as input. The time lag can be expressed by different conceptions. For instance, it may be taken as the time difference between the centroids of hyetograph and hydrograph. However, commonly it is taken as the time difference between the centroid of hyetograph and peak hydrograph discharge. These are the key information in any hydrograph calculation. In theoretical or synthetic hydrograph analysis, each one of these factors is simplified or expressed in terms of measurable watershed characteristics.

## 2.12   Intensity–Duration–Frequency (IDF) Curves

In the planning and assessment of any water resources, IDF curves have fundamental importance. In the literature, there are numerous theoretical and empirical approaches for their constructions (Chow et al. 1988; Bell 1969; Aron et al. 1987; Burlando and Rosso 1996; Koutsoyiannis et al. 1998). The regional studies of IDF curves are given for some countries (Froehlich 1995a, b, c; Garcia-Bartual and Schneider 2001).

In many humid areas of the world, IDF curves are constructed on the basis of Gumbel theoretical PDF (Gumbel 1958; Chap. 6). However, in arid and semiarid lands, Gamma PDF is more convenient. In the construction of IDF curves, the following meaningful knowledge, information, and interpretation are important:

1. Any PDF indicates the symmetric or skew distribution features of the rainfall records. For instance, in dry regions as climate knowledge, low (high) rainfall occurrences appear at high (low) frequency. Such situations are representative by the Gamma PDF or its version as exponential PDF (Chap. 6).
2. In water engineering, IDF curves are calculated frequently for 2-, 5-, 10-, 25-, 50-, and 500-year design durations in risk assessments.

If the rainfall intensity is denoted by $i$ and the IDF curve function is denoted by $f(i)$, then it is shown in an integral form, the risk, $r$, is defined as,

$$r = \int\limits_{i}^{+\infty} f(i)\mathrm{d}i \tag{2.18}$$

In the derivation of IDF curves, another point is the relationship between storm rainfall duration, $T$, and the maximum rainfall intensity, $i$.

Many procedures and formula, mainly empirical, are proposed in the literature for IDF curve identification (Yarnell 1935; Chow et al. 1988; Gumbel 1958; Bell 1969; Chen 1983; Aron et al. 1987). A mathematical approach is proposed by Burlando and Rosso (1996) and Koutsoyiannis et al. (1998). In practice, division of the rainfall duration into three groups, namely durations from 1 min to 1 h as "short," from 1 to 24 h as "intermediate," and more than 24 h as "long," has led to meaningful interpretations and works on the regionalization of IDF relationships in different geographical areas (Froehlich 1995a, b, c; Hanson 1995; Garcia-Bartual and Schneider 2001). In many parts of the world, the recording raingauge instruments are either rarely available or not at all. For these regions, the IDF curves can be obtained through empirical approaches (Chow et al. 1988). Proper and accurate determination of IDF curves is possible if the storm rainfall accumulation records are available.

In the literature, the most used three formulations with two-parameter mathematical functions are summarized as follows:

1. The most widely used expression with R and C (two-parameter) is due to Sherman (1931) as,

$$i = \frac{R}{T + C} \tag{2.19}$$

2. Bernard (1932) provided a hyperbolic expression again with two parameters as,

$$i = \frac{R}{T^C} \tag{2.20}$$

3. The relationship between the intensity and duration on a semilogarithmic paper appears as a straight line.

$$i = R - CLnT \tag{2.21}$$

On the other hand, there are also three-parameter functions. Similar to Eqs. (2.20) and (2.25) with a third parameter, B,

$$i = \frac{R}{(T+C)^{\text{B}}} \tag{2.22}$$

and

$$i = \frac{R}{T^{\text{B}} + C} \tag{2.23}$$

Other three-parameter equations are given by Garcia-Bartual and Schneider (2001) as,

$$i = R + \frac{B}{T+C} \tag{2.24}$$

and

$$i = \frac{R}{B + CT} \tag{2.25}$$

Keers and Wescott (1977) suggested the following formulation:

$$i = \frac{R}{(1+BT)^{\text{C}}} \tag{2.26}$$

The IDF relationships are of fundamental importance in hydrology for flood assessments, especially in engineering water structure designs. These curves are necessary for design storm determination and also as prerequisites in many hydrological models and procedures for design discharge computation. Flood risk evaluation and mitigation works also necessitate IDF information in order to plan appropriate infrastructures including rainfall drainage systems, dam spillways, culverts, bridges, levees, dikes for protecting local settlers and their properties against flood danger with efficiency.

In this section, determination of convenient IDF curves is presented based on the annual daily maximum rainfall (DMR) records. For this purpose, a dimensionless intensity–duration (DID) curve is derived from the available recording raingauge and then the theoretical probability distribution function (PDF) is fitted to DMR data. The PDF provides opportunity to determine the DMR amounts corresponding to a set of return periods (2, 5, 10, 25, 50 and 100 year). The DID curve helps to disaggregate the DMR amounts to a set of shorter rainfall duration (10, 20, 30, 60, 120, 360, 720 and 1440 min).

In many parts of the world, past and current IDF statistics are computed by considering the Gamma, log-normal, extreme value (Gumbel), generalized extreme value (Pearson), and Weibull PDF to describe the frequency of extreme rains. These theoretical PDFs are also used by most of the official meteorological services in different countries. The Gumbel and Pearson PDFs have the advantage to be well

known by the engineering communities for the works on the reliability of hydraulic infrastructures.

The rainfall regime in arid and semiarid regions does not abide by the Gumbel cumulative distribution function CDF. In almost all applications, Gumbel CDF is employed theoretically due to either nonexistence of basic data or convenience of use or both. This is the main reason why after flood events there are damages to hydraulic structures such as bridges, culvers, and levees, especially in arid lands. It is, therefore, necessary to assess the IDF properties of storm events leading to convenient curves even though the basic data may not be very sufficient.

In this section, the determination of convenient IDF curves is presented for the Kingdom of Saudi Arabia (KSA) as a representative of arid regions. Various CDFs have been used on the basis of factual data for a set of time durations such as 5, 10, 15, 20, 30, and 60 min. On the basis of these CDFs, the possible rainfall intensities for a set of design periods (return periods or risk levels) are presented by considering 2-year, 5-year 10-year, and 25-year, 50-year, 100-year, and 500-year durations (SGS, 1015).

## 2.12.1 Dimensionless Intensity–Duration (DID) Curve

In the previous section, most frequently used theoretical intensity duration (ID) formulations are presented, and depending on the parameter values, each one yields a single curve. If the parameters are determined in some way, then this single curve can be converted into a DID curve after dividing the duration (intensity) values by the maximum duration (intensity) value. With hypothetical values of $A = 200$, $B = 0.8$, and $C = 4$ the resulting DID curves appear for different formulations as in Fig. 2.26.
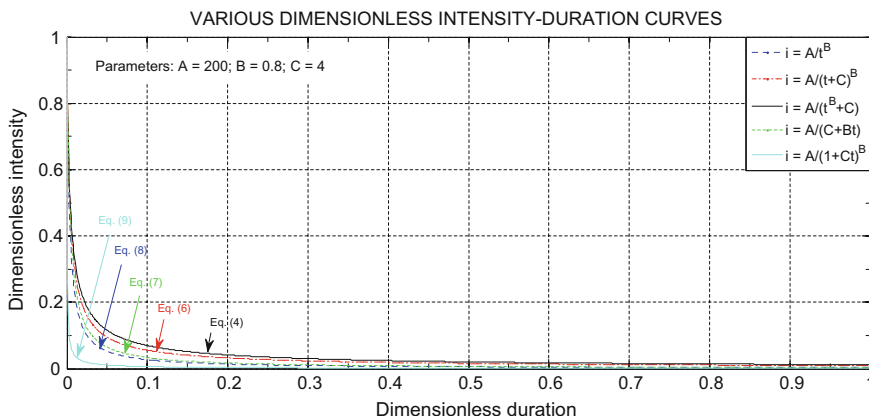


Fig. 2.26 Dimensionless intensity–duration curves

Different sets of parameter values yield slight shifts in these curves, but their general shape remains the same.

The view adopted in this section is that all ID curves for different return periods fall on the same DID curve. Hence, once DID curve is obtained, then it is possible to obtain all of the actual intensity–duration curves for any given return period or exceedence probability (frequency) provided that the DMR data are available.
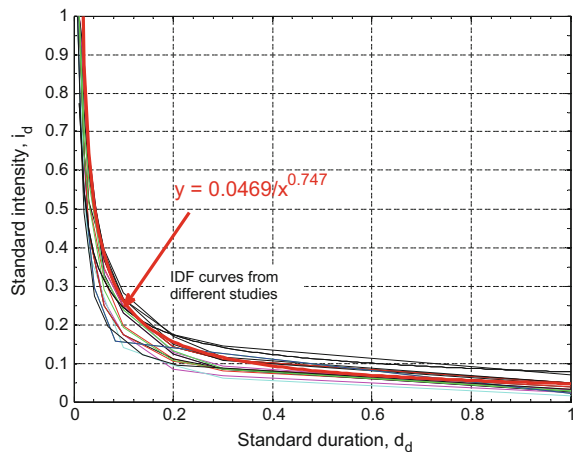
### 2.12.2  Intensity–Duration–Frequency (IDF) Curve Generation

It is necessary to consider that an IDF curve provides numerical information about the intensity and the return period (inverse of exceedence probability) (Chap. 6). On the basis of this sentence, the questions are "how can one obtain a set of intensities for a given set of return periods at certain duration?" and "what might be this duration?" In practice, most often the total daily rainfall amounts are available and they can be converted to DMR records, which imply rainfall duration as one day, i.e., 1440 min. In arid and semiarid regions, one cannot observe day-long rainfall events, because they have shorter duration. In such regions, depending on the location, one can take the DMR durations as 3 or 6 hours. Whatever the duration, one can obtain the theoretical PDF of the DMR data and then a set of exceedence probability rainfall amounts can be calculated each attached with the return periods. After the calculation of these rainfall amounts for a given duration, the remaining is to disaggregate them into shorter time durations by means of DID curve.

For IDF curves, generation from the DMR amounts and their combination with the DID curve can be achieved through the execution of the following steps:

1. Since DMR amounts for 6 hours = 360 min are available, first the most suitable PDF is determined for each station,
2. The theoretical PDFs help to calculate rainfall amounts that correspond to a set of desired probabilities of exceedence, p, according to the inverse relationship between the return period, T, and the probability of exceedence, $p$, as $p = 1/T$. The return period (exceedence probability) set is adapted as $T = 2$-year ($p = 0.50$), $T = 5$-year ($p = 0.20$), $T = 10$-year ($p = 0.10$), $T = 25$-year ($p = 0.04$), $T = 50$-year ($p = 0.02$), and $T = 100$-year ($p = 0.01$),
3. The IDF curves can be generated on the basis of the available information from the previous steps concerning DMR data and DID curve. Additionally, one should also know rainfall amount corresponding to the exceedence probability for each return period from the suitable PDF for each station,
4. Available natural IDF curves from different parts of the KSA are converted to DID curves as in Fig. 2.27 with the best average DID curve expression as,

**Fig. 2.27** Dimensionless intensity–duration curves



$$i_\mathrm{d} = \frac{0.0469}{d_\mathrm{d}^{0.747}} \tag{2.27}$$

where $i_\mathrm{d}$ and $d_\mathrm{d}$ are dimensionless intensity and duration, respectively.

5. Since definition of DID curve is the change of dimensionless intensity variable by dimensionless time, it is possible to calculate rainfall duration, $t_\mathrm{r}$, for the IDF graph through the following expressions:

$$t = t_\mathrm{r} t_\mathrm{d} \tag{2.28}$$

On the other hand, consideration of DID curve expression from Eq. (2.27) with the rainfall amounts, $r_\mathrm{e}$, the intensity, $i$, is calculated as,

$$i = i_\mathrm{i} r_\mathrm{e} \tag{2.29}$$

6. The application of the previous steps to each one of the stations leads to IDF curves for each one of them.

## 2.13 Probably Maximum Precipitation (PMP)

The probable maximum precipitation (PMP) is necessary for calculating the probable maximum flood (PMF), which is necessary in many design water-related projects at a particular geographical location in a given drainage basin. It also provides information for designing the size (dam height and reservoir storage

capacity) of the given project. Furthermore, dimension of the flood-carrying structures (spillway and flood-carrying tunnel) is also dependent on the PMP and subsequent PMF. Storm rainfall events and their subsequent floods have physical upper limits, and they are referred to as PMP and PMF.

Among the water resource management features, the most significant satisfactions are for the needs of society and the economy in addition to the protection of water and the natural environments. In any drainage basin where the probable maximum flood (PMF) occurrences are important, the preliminary step is to calculate point-wise and regional PMP amounts. The PMF quantities are important, especially for dam planning, design, and operation works at a particular section of drainage basin mainstream line. In particular, in arid regions, the construction of surface dams for flood protection and groundwater recharge is bound to increase due to climate change impact, which indicates that in the future there will appear rainfall increments especially over the Arabian Peninsula. World Meteorological Organization, WMO (2009, 2011), defined the PMP as the theoretically greatest depth of rainfall that is physically possible in a given time interval (minute, hour, day, etc.) over a particular area and geographical location at a given time of the year.

Numerical determination of the PMP can be achieved by different methodologies depending on the availability of data. Among these scientific works are the ones due to Hansen et al. (1982), Foufoula-Georgiou (1989), BOM (1994), Collier and Hardaker (1996), Svensson and Rakhecha (1998), Corrigan et al. (1999), Desa et al. (2001), Rakhecha and Clark (2002), Rezacova et al. (2005), Papalexiou and Koutsoyiannis (2006), Desa and Rakhecha (2007), and Şen (2008). It is possible to consider the collection of these approaches into two categories, namely statistical analysis of rainfall frequency and genetic analysis based on synoptic situations, where vertical radio-zoning measurements are important for precipitable precipitation calculations (Sect. 2.16).

### 2.13.1   Definitions of PMP and PMF

Theoretically, PMP is the maximum precipitation for a given duration during which there are proper rainfall records that is assumed to be distributed over the whole drainage basin rather uniformly, or a storm area of a given size, at a certain time of year. Under a set of conditions and assumptions, PMP can be converted theoretically into PMF and it poses extremely serious threats to the flood control of a given project design. Such a flood could plausibly occur in a locality at a particular time of year under current meteorological conditions.
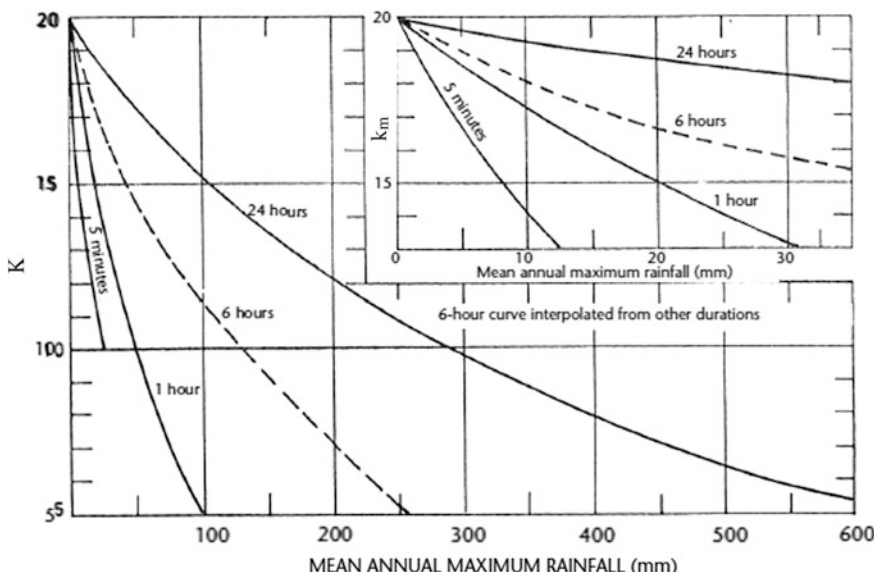
### 2.13.2   Statistical Estimates

The PMP amounts can be estimated approximately by the statistical approaches. The basis of such approaches is a frequency analysis with its two specific

properties, namely the arithmetic average and the standard deviation. The PMP statistical method concentrates on a wide region or a drainage basin by taking into account the individual station records available in the region. It helps to appreciate the upper physical limit of a storm. On the other hand, the statistical maxima are calculated according to the frequency analysis that corresponds to a certain risk level. The essence of the method is storm transposition, but instead of transposing the specific rainfall amount of one storm, the frequency factor, K, concept is adapted in almost all the water-related projects.

For the use of the PMP calculation, sufficient amount of data must be available, for instance, records of at least 30 years and also several stations scattered over the study area. In such an approach, the only meteorology data are precipitation records without any other meteorology variables. Figure 2.32 shows the change of K with the amount of mean annual maximum rainfall. These charts are useful for making quick decisions for drainage areas of less than 1000 km$^2$. One of the shortcoming of the procedure is that it yields point PMP, and therefore, it is necessary to apply area reduction calculation through convenient curves for adjusting the point values different size areas (see Fig. 2.28).

In the selection of appropriate frequency factor value, extreme value statistical PDF is necessary that is representative of the extreme values. A second problem is determining the appropriate value to use for $K$, which is a statistical variable that depends on the frequency distribution of extreme value hydrological data. According to the data at hand, different $K$ values have been used by various investigators (Dhar and Damte 1969).



**Fig. 2.28**  K as a function of rainfall duration and mean of annual series (Hershfield 1965)

The procedure is suggested first by Hershfield ([1961], [1965]), and later, Hershfield ([1965]) modified it leading to a general frequency equation (Chow [1964]).
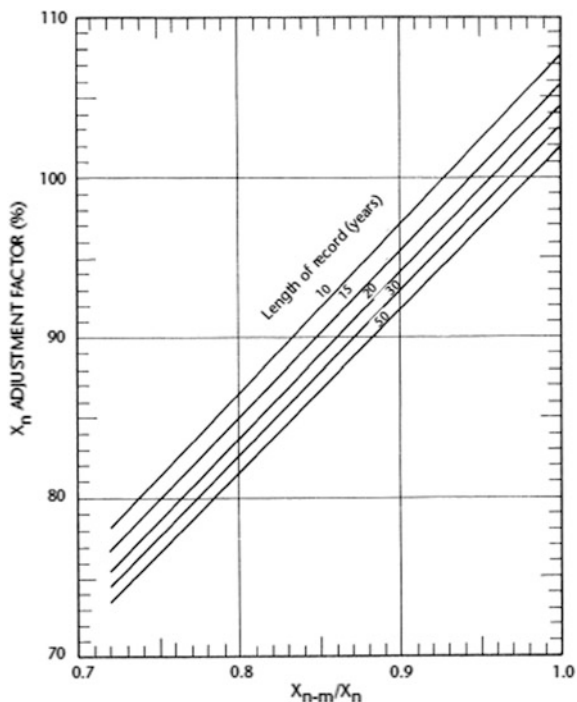
$$X_T = \overline{X}_n + K\,S_n \tag{3.30}$$

where $X_t$ is the rainfall for return period $T$, $\overline{X}_n$ and $S_n$, are, respectively, the mean and standard deviation of annual maximum precipitation records of length, $n$, and $K$ is the frequency factor.
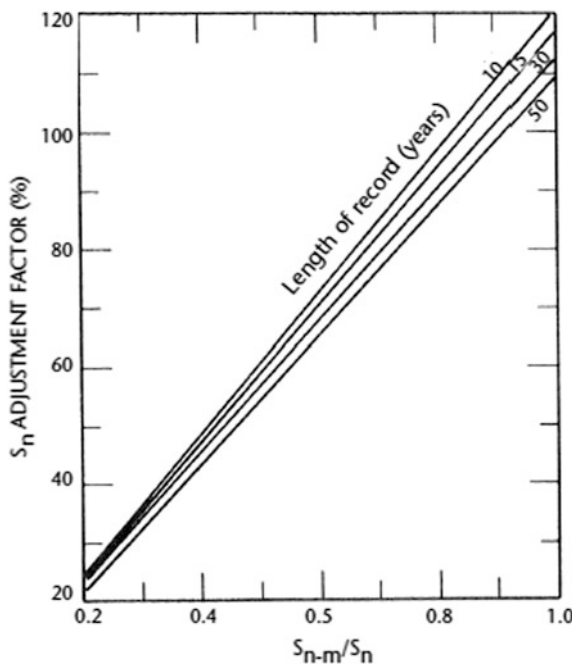
Extreme rainfall amounts of rare magnitude or occurrence are often found to have occurred at some time during a much shorter period of record, such as 30 years. Such a rare event is regarded as an outlier with an appreciable effect on the mean $\overline{X}_n$ and standard deviation $S_n$ of the annual series. The effect is smaller (bigger) for long (short) records. Hershfield ([1965]) has studied this effect by using hypothetical series of varying lengths. Figures [2.29] and [2.30] indicate the necessary adjustments to be made on $X_n$ and $S_n$ in order to compensate for any outlier. In these figures, $X_{n-m}$ and $S_{n-m}$ refer to the mean and standard deviation of the annual maximum series after excluding the maximum item in the series. It should be noted that these relationships consider only the effect of the maximum observed event, but no consideration is given to other anomalous observations.

Increase in the record length may cause increase in the arithmetic average and the standard deviation of the annual maximum rainfall series. In general, the PDF of



Fig. 2.29 Adjustment of mean of annual series for maximum observed rainfall (Hershfield [1965])

**Fig. 2.30** Adjustment of standard deviation of annual series for maximum observed rainfall
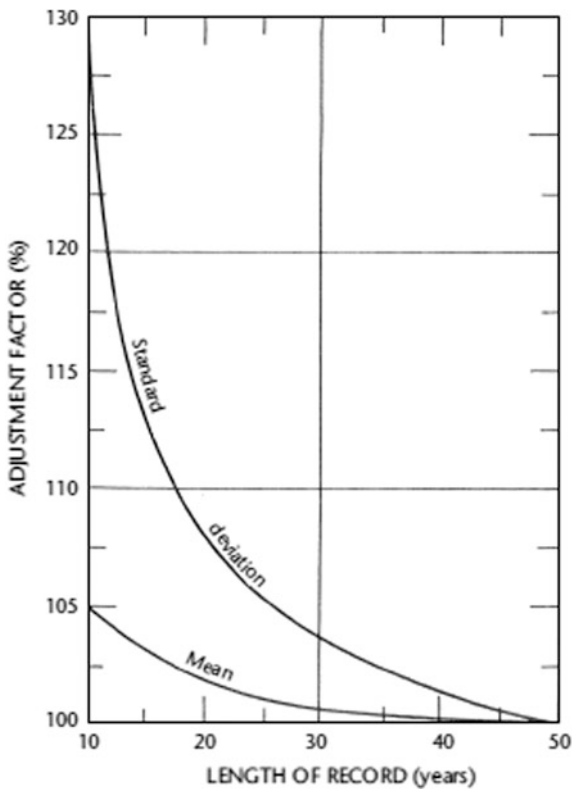


rainfall extremes is skewed to the right and this provides greater opportunity for largeness than a small extreme as the length of record increases. Figure 2.31 provides a basis for adjustments in the mean and standard deviation according to the record length.
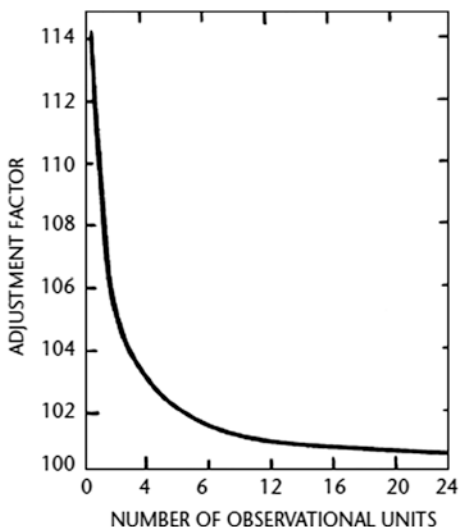
In general, the precipitation data are not recorded instantaneously, but over a certain time interval such as 6 hours, daily, weekly, monthly, or annually. Such data recording system hides actual maximum rainfall records. Maxima for longer duration are different to a certain extend than the maxima in a shorter duration record.

Studies of thousands of station-years of rainfall data indicate that multiplying the results of a frequency analysis of annual maximum rainfall amounts for a single fixed time interval of any duration from 1 to 24 h by 1.13 will yield values closely approximating those to be obtained from an analysis based on true maxima (Hershfield 1961). Hence, the PMP values yielded by the statistical procedure should be multiplied by 1.13, if data for single fixed time intervals are used in compiling the annual series. Lesser adjustments (Weiss 1964) are required when maximum observed amounts for various durations are determined from two or more fixed time intervals (Fig. 2.32). Thus, for example, maximum amounts for 6-hour and 24-hour periods determined from 6 and 24 consecutive 1-hour rainfall increments require adjustment by factors of only 1.02 and 1.01, respectively.

**Fig. 2.31** Adjustment of
mean and standard deviation
of annual series for the length
of record
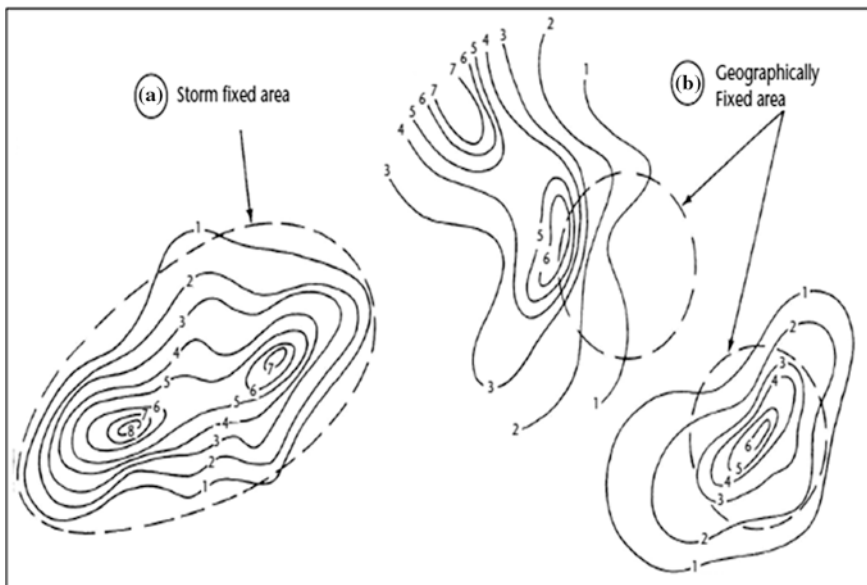


**Fig. 2.32** Adjustment of
fixed-interval precipitation
amounts for number of
observation units

### 2.13.3   Area Reduction Curves
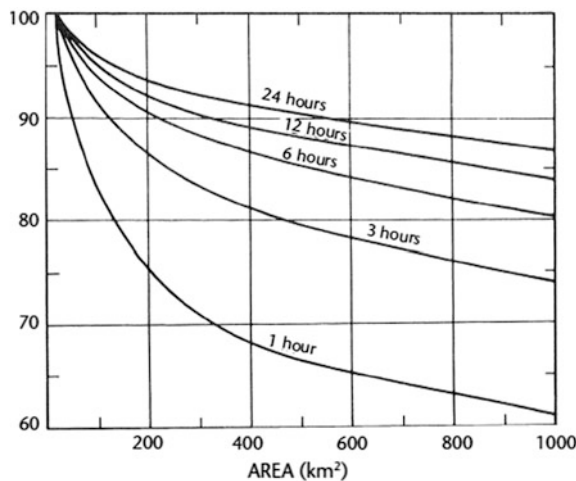
The procedure that is valid for point rainfall data requires some other procedures for reduction of the point values to some required distances or areal rainfall averages. As mentioned by Miller et al. (1973), there are two types of depth–area relations. The first is the storm-centered relation, that is, the maximum precipitation occurring when the storm is centered on the area affected (Fig. 2.33a). The second type is the geographically fixed area relation, where the area is fixed and the storm is either centered on it or displaced so that only a portion of the storm affects the area (Fig. 2.33b). Storm-centered depth–area curves represent profiles of discrete storms, whereas the fixed area data are statistical averages in which the maximum point values frequently come from different storms.

The most convenient curves are the storm centers and surrounding ones for PMP studies. Court (1961) mentioned that there are different variations of depth–area relation curves (DAD). The relation in Fig. 2.34 is an idealized example, but similar curves must be developed for the study area. They will look alike to these curves as the study area enlarges the curves will decrease and curves should be developed for the specific location of the project.



**Fig. 2.33** Example of (**a**) isohyetal pattern centered over basin as would be the case for storm-centered depth-area curves and (**b**) two possible occurrences of isohyetal patterns over a geographically fixed area as would be the case in development of curves for a geographically fixed area (Miller et al. 1973)

**Fig. 2.34** Depth-area or area reduction curves for western USA (United States Weather Bureau 1960)



### 2.13.4   PMP and PMF Estimations

Thunderstorm rainfall events and consequent floods have upper physical level that cannot be transgressed theoretically. These limits are referred to as the PMP and PMF, respectively. Only their approximate estimations are possible in practical applications, because of the lack in hydrometeorological data sources, because of physical, meteorological, and hydrological complexities.

In the estimation the major factors are the precipitation intensity and efficiency as well as maximum moisture content between the surface and the cloud bases. The PMP estimation can be achieved through one of the two approaches. The first one is based on the PMPs estimations with different durations and areas. It provides a set of methods to convert them into the PMP in the design drainage basin for the purpose of PMF estimation for high-risk cases.

The other method based on drainage basin area is a direct approach, which focuses on the PMP estimation based on a given duration that is determined according to a specific project in the study area with comparatively lesser risk level. For instance, construction of a reservoir in the study area requires such an approach. The duration of the design flood is taken relatively long; the final design storm may be generated through the superposition, and it is the main controlling factor for the project regarding flood control. The required design flood duration may hence be shorter, and a storm may be generated by a single storm weather system or by local violent convection.

On the other hand, as for the PMF estimation, there are six different approaches that are currently used. These are as follows:

(a) The local storm maximization with an effective local model: In this approach, PMP is estimated on the basis of the maximum storm past observation in the study area. The application requires several years of meteorology data.

(b) The storm transposition model: Extraordinarily large storm is transported from the adjacent area to the study region. For this purpose, the probability of storm transposition is necessary, which can be obtained either by determination of meteorologically homogeneous zones over the study area or by a sequence of operations and modifications on the transposition storm so as to suit the local characteristics. It is widely used for design areas, where high-efficiency storms are rare.

(c) The temporal and spatial maximization of storm through a combination model: This model combines two or more storms that occurred over the study area on the basis of synoptic features of the region so as to obtain an artificial, but representative storm with a long duration. It is applicable for PMP and PMF estimations in large drainage basins with long durations, but requires strong meteorological knowledge.

(d) The theoretical inferential model: The basis is a three-dimensional storm structure that takes place over the study area and its conversion to a simple physical storm equation with the main physical factors effective in the study area. In the approach, either a laminar or a convergence model is used. The following points are significant in the convergence model.

(e) The generalized estimation model.

(f) The statistical estimation model.

These methodologies are usable mostly in medium-latitude or low-latitude areas. Their use in tropical low-latitude areas requires some parameters. Furthermore, additionally, the following two methods can also be used for deriving PMP and PMF estimations in extremely large drainage basins. It is assumed that the inflow of storm moisture converges to the center from all sides and rises to generate a storm event. However, in the case of laminar flow, it is assumed that the inflow of storm moisture crawls along an inclining surface in a laminar fashion and rises to generate an event. For the success of this method, upper layer meteorology data are necessary and it can be applied to very large areas.

(a) The major temporal and spatial combination and generalization method: It helps to estimate PMP over large and meteorologically homogeneous areas. The rainfalls are of orographic (elevation difference) type, and their convergence is toward an observed rainfall storm. This method has the results of PMP depth that show a generalized depth–area–duration (DAD) curve, spatial and temporal distribution of PMP.

(b) The storm simulation method based on the statistics historical floods: The PMP estimation is obtained by taking into account a set of numerous rainfall stations in a meteorologically homogeneous region, and the use of hydrological frequency analysis leads to generalized method. As explained by Wang (1984), the procedure is different from the traditional frequency analysis method.

## 2.13.5   Application of Procedure

The PMP calculation procedure can be found in the manual for estimation of probable maximum precipitation (WMO 2009) provided that long data series (more than 15 years) are available. The basis of the statistical PMP calculation methodology has been presented by considerations from the frequency equation by Hershfield (1965), which can be summarized as follows. In general, the PMP is a function of the arithmetic average of the daily maximum precipitation, $\overline{X}$, and the standard deviation, $S_X$, of the whole maximum daily rainfall time series through the factor, $k_m$, of the standard deviation as,

$$\text{PMP} = \overline{X} + k_m S_X \tag{2.31}$$

Herein, $k_m$ is referred to as the frequency factor, which is a very important part of Eq. (2.31) as it constitutes the number of standard deviations added to the mean distribution value in order to attain the largest possible precipitation value within a series. If the annual number of maximum daily rainfall is n, then the exclusion of the maximum among the maxima daily rainfalls leads to another maximum daily rainfall series of length $n - 1$. For such a situation, the maximum daily rainfall amount can be related to the arithmetic average and the standard deviation of this new series similar to Eq. (2.31) as follows:

$$R_{\max} = \overline{X}_{n-1} + k_m S_{X(n-1)} \tag{2.32}$$

Hence,

$$k_m = \frac{R_{\max} - \overline{X}_{n-1}}{S_{X(n-1)}} \tag{2.33}$$

The internal structure of maximum daily rainfall amounts at each station is identified by the Gamma probability distribution function (PDF). Table 2.3 includes the statistical parameters and the PDF parameters.

The recorded data as well as the theoretical PDF are shown for each meteorology station. It is possible to calculate the maximum daily rainfall amount corresponding to a set of return periods as in Table 2.4, but none of these values are indication of the PMP. In this table, 2-, 5-, 10-, 25-, 50-, 100-, 250-, and 500-year return periods are given.

The PDF graphs provide a basis for the analysis of the frequency distribution of maximum daily rainfall mounts as well as their visual variability, and hence, numerical values include the median, the lower and upper quartiles (25 and 75%), the interquartile range, and extremes.

The basic values for the PMP numerical value calculations are given in the 3rd, 4th, 5th, and 6th columns in Table 2.5 according to Eqs. (2.31)–(2.33).

**Table 2.3**  Statistical parameters

| Station number | Statistical parameter | | Gamma PDF parameters | |
|---|---|---|---|---|
| | Mean (mm) | St. dev. (mm) | Alpha | Beta |
| J102 | 28.40 | 20.70 | 0.88 | 33.10 |
| J113 | 46.66 | 35.51 | 2.23 | 21.00 |
| J114 | 36.96 | 27.44 | 1.53 | 24.20 |
| J134 | 28.81 | 25.40 | 1.27 | 22.70 |
| J204 | 36.50 | 20.60 | 2.82 | 13.10 |
| J205 | 36.50 | 20.59 | 1.90 | 23.10 |
| J214 | 32.20 | 25.11 | 1.61 | 20.00 |
| J219 | 23.75 | 20.83 | 1.29 | 18.50 |
| J220 | 21.67 | 16.55 | 1.11 | 19.50 |
| J221 | 27.51 | 27.62 | 1.31 | 21.00 |
| J139 | 24.38 | 16.37 | 1.58 | 15.40 |
| 41024 | 28.94 | 22.74 | 1.26 | 23.00 |
| **Minimum** | **7.10** | **5.34** | **0.53** | **4.96** |
| **Average** | **31.02** | **23.29** | **1.57** | **21.22** |
| **Maximum** | **46.66** | **35.51** | **2.82** | **33.10** |
| **St. Dev.** | **21.67** | **16.37** | **0.88** | **13.10** |
| *Regional* | *28.93* | *22.74* | *3.57* | *19.4* |

**Table 2.4**  Maximum daily rainfall amounts

| J102 | 22.68 | 43.69 | 58.45 | 77.26 | 91.16 | 104.88 | 122.78 | 136.21 |
|---|---|---|---|---|---|---|---|---|
| J113 | 39.89 | 68.97 | 88.50 | 112.83 | 130.53 | 147.83 | 170.22 | 186.89 |
| J114 | 29.27 | 57.07 | 76.69 | 101.33 | 120.33 | 138.66 | 162.62 | 180.59 |
| J134 | 21.71 | 45.37 | 62.54 | 84.79 | 101.41 | 117.91 | 139.58 | 155.89 |
| J204 | 32.28 | 52.45 | 65.65 | 81.85 | 93.52 | 104.86 | 119.46 | 130.27 |
| J205 | 36.35 | 65.93 | 86.19 | 111.70 | 130.39 | 148.74 | 172.58 | 190.39 |
| J214 | 25.84 | 49.43 | 65.95 | 86.97 | 102.49 | 117.79 | 137.77 | 152.74 |
| J219 | 17.95 | 37.34 | 51.39 | 69.57 | 83.15 | 96.62 | 114.30 | 127.62 |
| J220 | 15.63 | 34.56 | 48.61 | 67.01 | 80.86 | 94.65 | 112.84 | 126.56 |
| J221 | 20.92 | 34.17 | 59.24 | 80.00 | 95.46 | 110.86 | 131.01 | 146.18 |
| J239 | 19.48 | 37.50 | 50.15 | 66.27 | 78.19 | 89.95 | 105.31 | 116.81 |
| 41024 | 21.72 | 45.62 | 63.00 | 85.53 | 102.38 | 119.11 | 141.08 | 157.63 |
| **Minimum** | **15.63** | **34.17** | **48.61** | **66.27** | **78.19** | **89.95** | **104.31** | **116.81** |
| **Average** | **25.31** | **47.68** | **65.00** | **85.43** | **100.82** | **115.99** | **135.80** | **150.64** |
| **Maximum** | **39.89** | **68.97** | **88.50** | **112.83** | **130.53** | **148.74** | **172.58** | **190.39** |
| **St. Dev.** | **7.59** | **11.64** | **13.14** | **15.85** | **17.94** | **20.00** | **22.73** | **24.81** |
| *Regional* | *62.84* | *96.63* | *118.22* | *144.39* | *163.08* | *181.11* | *204.20* | *221.23* |

**Table 2.5** PMP numerical values

| Meteorology station | Record duration | Global parameters | | Maximum exclusion parameters | | Frequency factor | PMP (mm) | |
|---|---|---|---|---|---|---|---|---|
| | | Mean (mm) | Standard deviation (mm) | Mean (mm) | Standard deviation (mm) | | Past | Climate change |
| J102 | 1966–2011 | 28.40 | 20.70 | 26.30 | 16.06 | 4.22 | 151.00 | 173.65 |
| J113 | 1966–2005 | 46.66 | 35.51 | 42.77 | 26.55 | 5.57 | 244.00 | 280.60 |
| J114 | 1967–2013 | 36.96 | 27.44 | 33.69 | 23.86 | 2.73 | 112.06 | 128.87 |
| J134 | 1970–2012 | 29.39 | 25.49 | 26.83 | 20.30 | 4.79 | 151.35 | 174.05 |
| J204 | 1966–2005 | 36.50 | 20.60 | 35.10 | 18.91 | 2.88 | 95.87 | 110.25 |
| J205 | 1966–2005 | 43.76 | 26.77 | 41.87 | 24.27 | 3.11 | 127.06 | 146.19 |
| J214 | 1966–2006 | 32.20 | 25.10 | 30.02 | 20.99 | 4.37 | 141.99 | 163.29 |
| J219 | 1970–2006 | 23.75 | 20.83 | 22.14 | 18.97 | 2.80 | 82.01 | 94.31 |
| J220 | 1966–2011 | 21.67 | 16.55 | 20.57 | 15.08 | 3.13 | 73.50 | 84.53 |
| J221 | 1971–2006 | 27.51 | 27.62 | 23.62 | 17.91 | 6.51 | 207.25 | 238.34 |
| J239 | 1976–2011 | 24.38 | 16.37 | 23.24 | 15.34 | 2.30 | 62.10 | 71.41 |
| 41024 | 1970–2009 | 28.94 | 22.74 | 27.25 | 20.89 | 2.67 | 89.61 | 103.05 |

The application of Eq. (2.33) with the arithmetic mean and standard deviation values in columns 5 and 6 yields the frequency factor values in column 7. Table 2.5 indicates that the frequency factor values vary between 2.30 and 6.51. The same table indicates that one-day past PMP is the biggest (244 mm) at station J113 among other stations. Accordingly, the same is valid for the climate change effective calculations. There is a logarithmic relationship between the PMP and its corresponding frequency factor as in Fig. 2.35.

The logarithmic relationship between the PMP and the frequency factor is given as follows:

$$PMP = 70k^{0.757} \tag{2.34}$$

Although this expression represents past and climate change PMP values, one can construct another straight line on this graph just for the climate change effects and it will be shifted upward slightly. This task is left outside the work in this book, because it is not necessary for the completion of the study.

Figure 2.36 shows the frequency factor distribution with the meteorological station. The arithmetic mean and the standard deviation of the frequency factor are 3.76 and 1.33, respectively.

The maximum and minimum frequency factors are at the J221 and J239 meteorology stations, respectively. For a regional assessment, one can use the arithmetic average of the frequency factor, which is equal to 3.76; however, such a work is not necessary for this section, because the regionalism is worked with the maximum daily rainfall amounts irrespective of the meteorology stations as shown in the last row in Table 2.4. Figure 2.37 indicates the change of annual maximum daily rainfall pattern in the study area.

The correspondence to the annual maximum rainfall time series is the PDF according to the Gamma function with the relevant parameters as in Fig. 2.38. Although the PMP ($\sim 145$ mm) is the greatest than any other station (point-wise)-based amounts, in this section it will not be used, because the climate change PMP
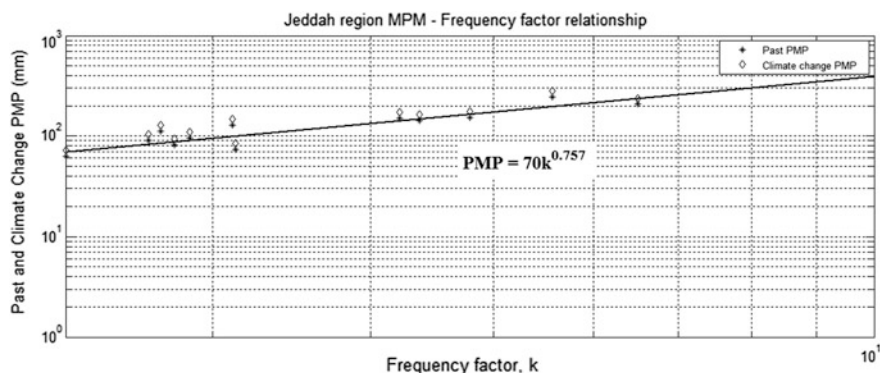


**Fig. 2.35** PMP–frequency factor relationship
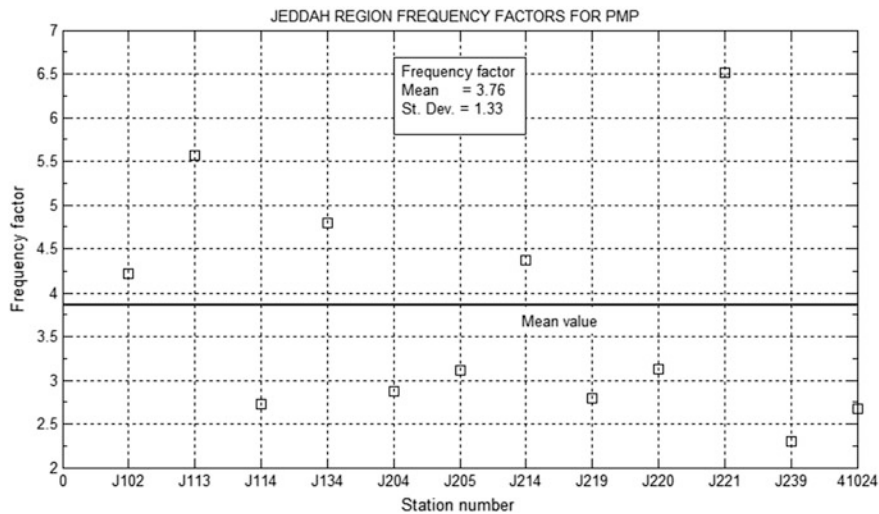
**Fig. 2.36** Frequency factor distributions with meteorology stations
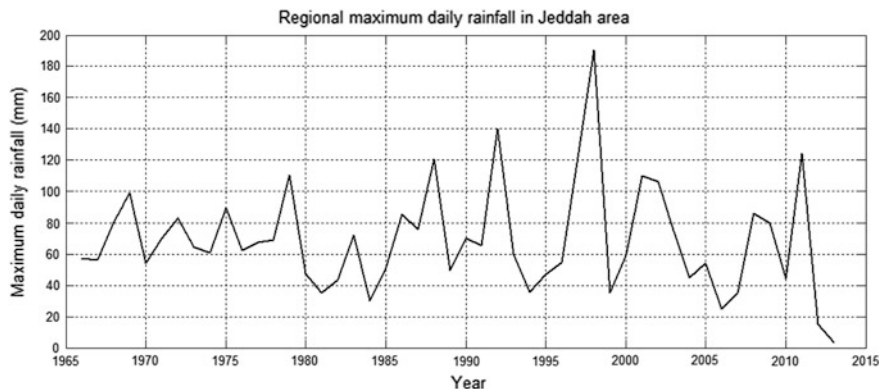


**Fig. 2.37** Annual maximum daily rainfall time series

map indicates that the dam locations are close to the coastal area, where the spatial variations are rather smaller.

Figure 2.39 shows the change of PMP along the meteorology stations both for past records and for climate change projections.

This relationship can be regarded as the regional expression for the PMP calculation in the Jeddah area. Out of 12 stations, seven (J102, J113, J114, J134, J205, J214, and J221) have PMP values more than 100 mm on the basis of past record bases. Climate change effect increases this number to nine stations including J204 and 41024. Relatively low maximum daily rainfall amounts, especially those smaller than 100 mm, are observed at meteorology stations J219, J220, and J239.
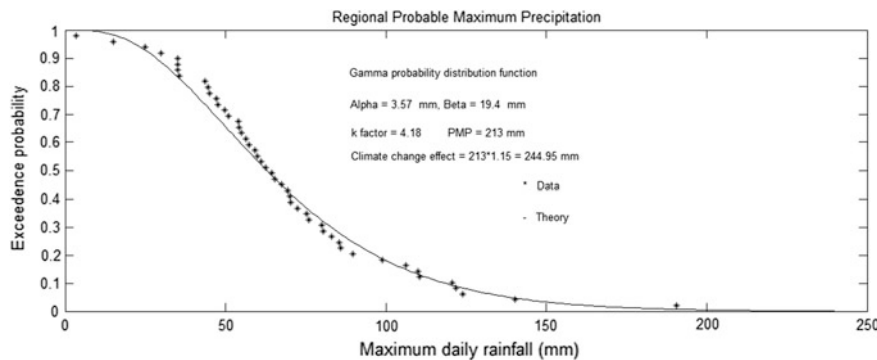
**Fig. 2.38** Annual maximum daily rainfall characteristics
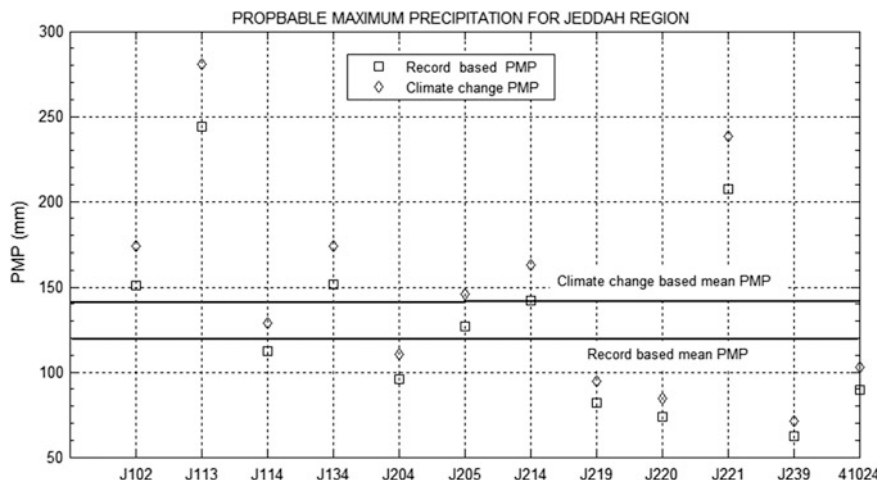


**Fig. 2.39** PMP change along stations

On the other hand, storm cells are observed at the time, which resulted in extremely high rainfall levels at stations other than those included in the analysis. While the long-term annual average rainfall for Jeddah City is approximately 55 mm, the Saudi Geological Survey (SGS) has estimated that some 160 mm of rainfall fell on November 25, 2009, for the duration of about 3 h, leading to the disastrous consequences. It is obvious from Table 6.7 that the first three maximum daily rainfall records have been observed at J113 (190.6 mm), J221 (140.2 mm), and J205 (117.4 mm) stations. The maximum rainfall amounts are related to the movement of moist westerly or northwesterly fronts or large areas of low pressures. Additionally, another potential reason is due to the fact of the hot flow and humid tropical air from the Red Sea region and its convergence with polar marine air over the study area.

**Table 2.6** Rainfall efficiency

| Years | Stations | | | | | | | | | | | |
|---|---|---|---|---|---|---|---|---|---|---|---|---|
|  | J102 | J113 | J114 | J134 | J204 | J205 | J214 | J219 | J220 | J221 | J239 | 41024 |
| $R_{max}$ | 110.5 | 190.6 | 99 | 124 | 89.6 | 117.4 | 121.8 | 75.2 | 67.8 | 140.2 | 58.6 | 83 |
| PMP (past) | 151 | 224 | 112.1 | 151.4 | 95.9 | 127.1 | 142 | 82.01 | 73.5 | 207.3 | 62.1 | 89.6 |
| PMP (climate) | 173.7 | 280.6 | 128.9 | 174.1 | 110.3 | 146.2 | 163.3 | 94.3 | 84.6 | 238.3 | 71.4 | 103.1 |
| Efficiency (past) | 1.37 | 1.18 | 1.13 | 1.22 | 1.07 | 1.08 | 1.17 | 1.09 | 1.08 | 1.48 | 1.06 | 1.08 |
| Efficiency (climate) | 1.57 | 1.47 | 1.30 | 1.40 | 1.23 | 1.25 | 1.34 | 1.25 | 1.24 | 1.70 | 1.22 | 1.24 |

### 2.13.5.1   Efficiency Factor

In order to see how close are the actually recorded maximum daily rainfall amounts to the calculated PMP values, the efficiency factor, E, can be defined as the ratio of the calculated past and climate effective PMPs to the maximum daily rainfall, $R_{max}$.

$$E = \frac{PMP}{R_{max}} \tag{2.35}$$

The sixth and seventh rows in Table 2.6 are the efficiency values, which are always more than one. It implies that in the study region yet the PMP values are not reached by the recorded rainfall occurrences, and hence, there is still room for more dangerous rainfall occurrences. At places, the difference is more than 70%. This point implies that for future designs concerning any engineering structure (dams, diversion canals, roads, etc.) need more care and to be on safe side, these structures must be constructed based on the PMP values.

### 2.13.5.2   Regional Variations

In order to appreciate the regional variation of the frequency factor and the PMP amounts for past and climate change contribution cases maps are prepared and shown in Figs. 2.40, 2.41, and 2.42. Each one provides visual inspection of regional variations around the Jeddah area, and one can then decide which PMP values to adopt for the PMF calculations for this region as explained in the next section.
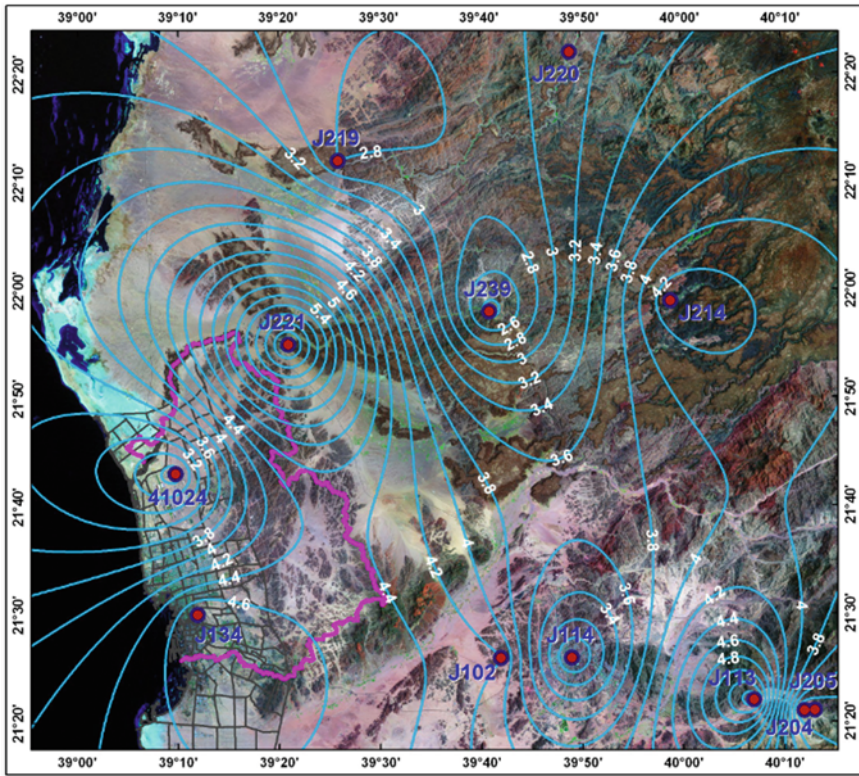
This figure shows that close to the area of dams (within the study area), the PMP frequency factors vary from 3.2 to 4.6 in the north–south direction. In the PMF calculations, it is recommended that the contours within the study area encircled by the pink line should be taken into consideration in any further calculations.

Within the study area, the past PMP contours have values between 110 mm and 170 mm with the lowest one around the Jeddah Airport meteorology station number with 41024.

This figure has almost the same pattern as the past PMP pattern in Fig. 2.41, but comparatively with bigger values. In the future calculations, these contour values must be considered, because it has the effects of the past records and the climate change impact.

## 2.14   Probable Maximum Flood (PMF)
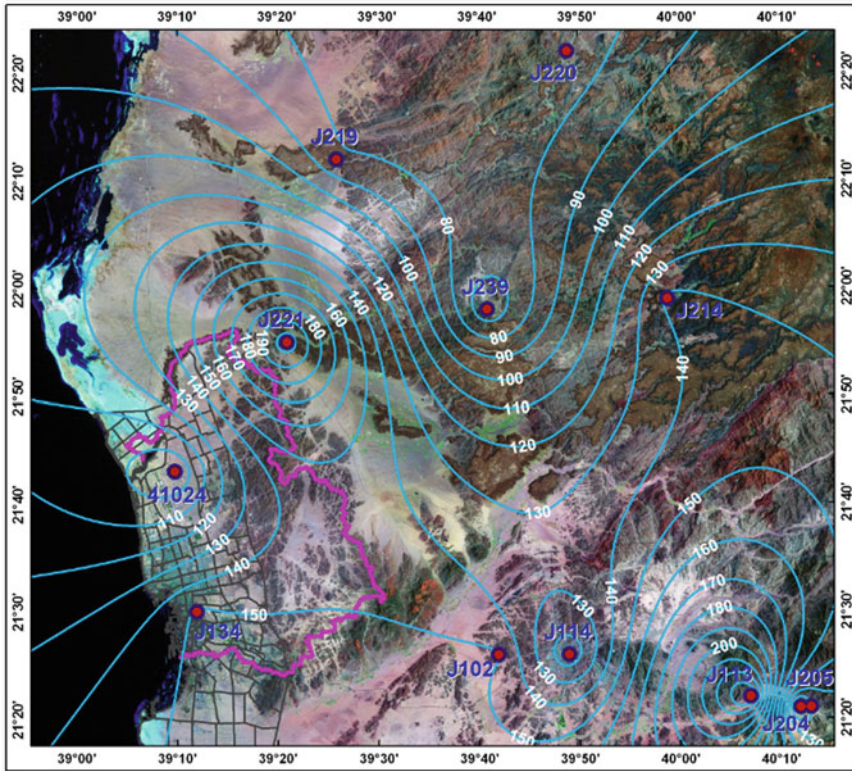
The estimation accuracy of PMP/PMF is dependent on the quantity and quality of data, especially on the extraordinary storms and floods. Even then it is not possible to say that their estimations are precise, because there is no a complete methodology

**Fig. 2.40** Frequency factor regional distributions

for this purpose. It is necessary to analyze, compare, and harmonize estimation results from a set of different methods. For the quality control, various methodological results can be compared and, if necessary, their ensemble averages can be taken in some manner. In the comparison studies, it is necessary to care for the amount by which the PMP estimation exceeds the maximum rainfall record values for the adjacent meteorologically homogeneous region. Additionally, the frequency and severity of storms records should be taken into consideration. There may be limitations in the storm transposition in the region. Furthermore, the reliability of relations between rainfalls and other meteorological variables is also important for the comparison purposes.

After the completion of the PMP calculations, it is now time to convert the values through a convenient rainfall–runoff relationship so as to calculate the peak discharges and the resulting hydrographs. It is, therefore, necessary to calculate the duration of the rainfall within a day. This can be achieved empirically according to the Snyder method (Chap. 5), which gives the time to peak discharge by taking into consideration the longest channel length, $L$, and the length of this channel from the projection of the centroid point on the channel and the outlet, $L_c$, in addition to the slope value.

**Fig. 2.41**  Past PMP regional distributions
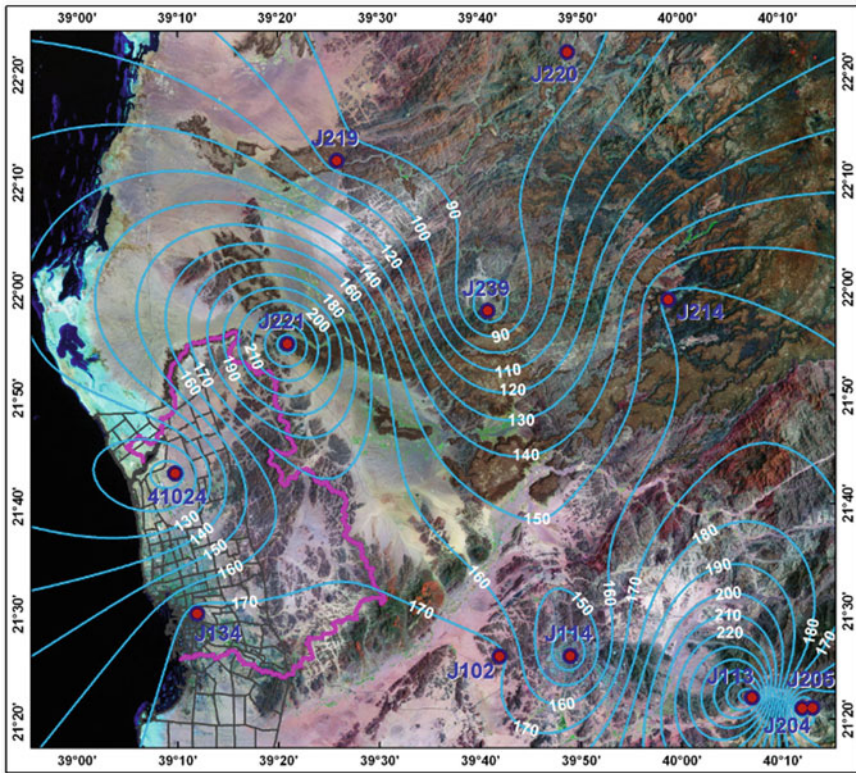
The peak discharge values can be calculated according to various methodologies such as the Snyder, SCS, kinematic wave, and other methodologies (Şen 2008). However, in this section, the simplest one is considered according to the rational approach, which can be used with confidence especially in small drainage areas (Chap. 5).

For the PMF calculations, the catchments in the area are identified with their geomorphological features including the drainage area, main channel length, centroid length, and if necessary also the slope. The locations of 15 drainage basins that are the subject of this report are given in Fig. 2.43.

Table 2.7 includes the names and codes of the dams and also the names of wadis (drainage area) and sub-basins.

Table 2.8 includes all the necessary geomorphological features that will enter into the PMF calculations.

The execution of the three steps mentioned at the beginning of this section leads to the numerical results as shown in Table 2.9 (Figs. 2.44 and 2.45).
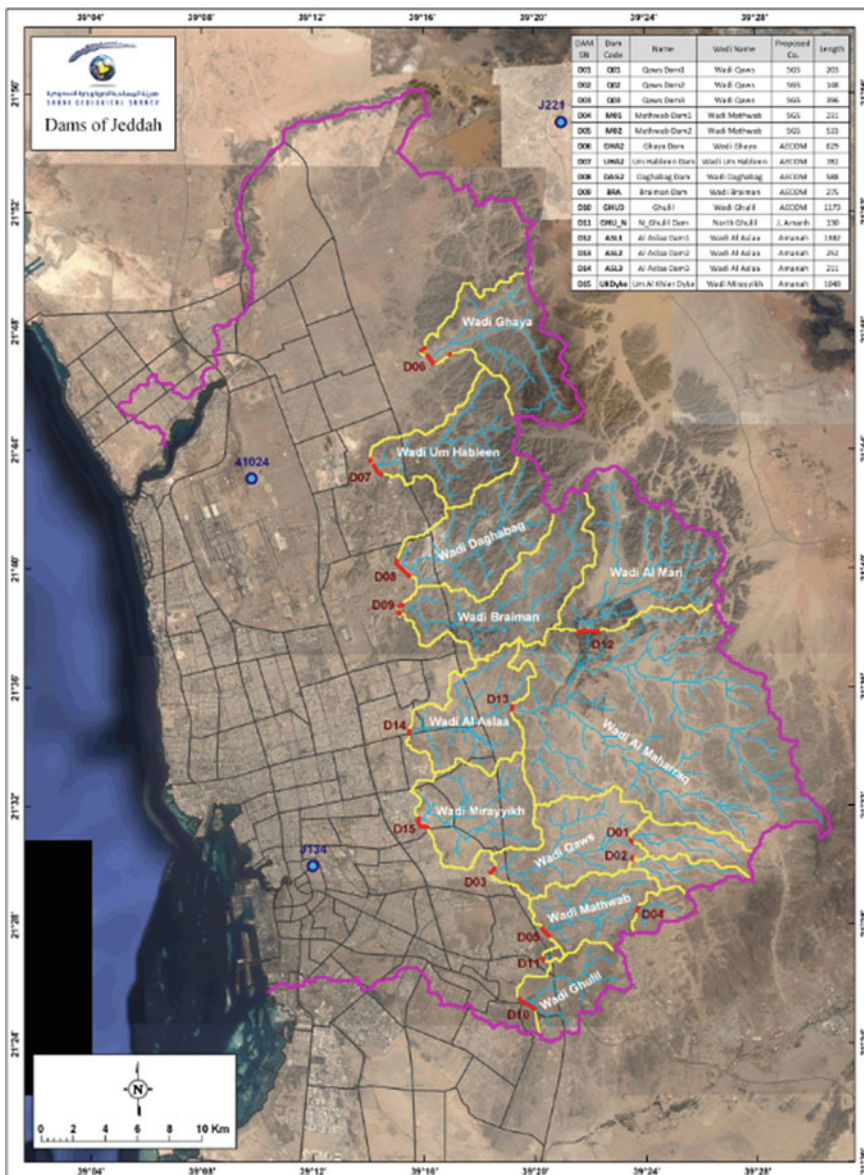
**Fig. 2.42** Climate change PMP regional distributions

## 2.15  Precipitable Water Calculation

In this section, useful knowledge and information are presented by making use of the moisture content of the lower atmosphere between the Earth surface and the cloud bases. This type of calculation leads to another version of the PMP calculation and a set of verbal information deductions, especially those that are useful for analytical methodological developments.

The moisture content in the air can be converted to precipitable water amount by simple engineering approaches. The first modeling design is given in Fig. 2.46 in the form of a prism, where the horizontal base area is equal to 1 and the height as small as possible, d$z$.

In this air column, the conversion of the humidity into rainfall is referred to as the PMP. For PMP calculation, it is necessary to know the vertical variations of meteorological factors that cause to rainfall as temperature, $T$, pressure, $p$, and humidity, $q$. These factors vary temporarily and spatially. The vertical variations can be obtained from the radiosonde measurements. This leads to the vertical variation of humidity and pressure as in Fig. 2.47.

**Dams of Jeddah**

| DAM SN | Dam Code | Name | Wadi Name | Proposed Co. | Length |
|---|---|---|---|---|---|
| 001 | 003 | Qaws Dam1 | Wadi Qaws | 565 | 205 |
| 002 | 002 | Qaws Dam2 | Wadi Qaws | 565 | 148 |
| 003 | 003 | Qaws Dam3 | Wadi Qaws | 565 | 266 |
| 004 | M01 | Mathwab Dam1 | Wadi Mathwab | 565 | 231 |
| 005 | M02 | Mathwab Dam2 | Wadi Mathwab | 565 | 530 |
| 006 | GHA2 | Ghaya Dam | Wadi Ghaya | ARCOM | 629 |
| 007 | UH02 | Um Hableen Dam | Wadi Um Hableen | ARCOM | 382 |
| 008 | DAG2 | Daghabag Dam | Wadi Daghabag | ARCOM | 548 |
| 009 | BRA | Braiman Dam | Wadi Braiman | ARCOM | 275 |
| 010 | GHU3 | Ghulil | Wadi Ghulil | ARCOM | 1173 |
| 011 | GHU_N | N_Ghulil Dam | North Ghulil | L.Amanh | 190 |
| 012 | ASL1 | Al Aslaa Dam1 | Wadi Al Aslaa | Amanah | 1982 |
| 013 | ASL2 | Al Aslaa Dam2 | Wadi Al Aslaa | Amanah | 242 |
| 014 | ASL3 | Al Aslaa Dam3 | Wadi Al Aslaa | Amanah | 211 |
| 015 | UKDyke | Um Al Khier Dyke | Wadi Mirayykh | Amanah | 1040 |

**Fig. 2.43**  Drainage area and dam locations

The specific humidity is defined as the ratio of water vapor density to air density, and it is a dimensionless quantity, but in practical applications, it is expressed as gr/kg. Based on the prism as in Fig. 2.46, if the water amount in d$z$ height is d$s$, from the base to a height, $h$, the water amount variation is $s(h)$; provided that the water vapor density is $\rho_s$, then one can write that,

**Table 2.7** Wadi names and dam codes

| Dam SN | Dam Code | Name | Wadi Name |
|--------|----------|------|-----------|
| D01 | Q01 | Qaws Dam1 | Wadi Qaws |
| D02 | Q02 | Qaws Dam2 | Wadi Qaws |
| D03 | Q03 | Qaws Dam3 | Wadi Qaws |
| D04 | M01 | Mathwab Dam1 | Wadi Mathwab |
| D05 | M02 | Mathwab Dam2 | Wadi Mathwab |
| D06 | GHA2 | Ghaya Dam | Wadi Ghaya |
| D07 | UHA2 | Um Hableen Dam | Wadi Um Hableen |
| D08 | DAG2 | Daghabag Dam | Wadi Daghabag |
| D09 | BRA | Braiman Dam | Wadi Braiman |
| D10 | GHU3 | Ghulil | Wadi Ghulil |
| D11 | GHU_N | N_Ghulil Dam | North Ghulil |
| D12 | ASL1 | Al Aslaa Dam1 | Wadi Al Aslaa |
| D13 | ASL2 | Al Aslaa Dam2 | Wadi Al Aslaa |
| D14 | ASL3 | Al Aslaa Dam3 | Wadi Al Aslaa |
| D15 | UKDyke | Um Al Khier Dyke | Wadi Mirayyikh |

**Table 2.8** Jeddah region drainage basins characteristics

| Basin SN | Basin name | Wadi name | Area $(km^2)$ | Basin slope $(m/m)$ | MFDIST $(m)$ | MFDSLOPE $(m/m)$ | Centroid $(m)$ |
|----------|-----------|-----------|---------------|---------------------|--------------|------------------|----------------|
| 1 | Qaws01 | Wadi Qaws | 14.247 | 0.02215 | 9519.2 | 0.0117 | 4424.5 |
| 2 | Qaws02 | Wadi Qaws | 9.408 | 0.02277 | 8855.9 | 0.01244 | 3941.8 |
| 3 | Qaws03 | Wadi Qaws | 38.291 | 0.03341 | 12098.6 | 0.00933 | 6092.7 |
| 4 | Mathwab01 | Wadi Mathwab | 7.062 | 0.04009 | 4427.5 | 0.01097 | 1896.4 |
| 5 | Mathwab02 | Wadi Mathwab | 26.492 | 0.03599 | 9087.2 | 0.00913 | 3802.9 |
| 6 | Ghaya | Wadi Ghaya | 46.087 | 0.10729 | 15239.6 | 0.0246 | 6449.8 |
| 7 | Um Hableen | Wadi Um Hableen | 39.672 | 0.11069 | 11419.7 | 0.03552 | 5780.4 |
| 8 | Daghabag | Wadi Daghabag | 46.269 | 0.10712 | 13892.3 | 0.02622 | 6844.4 |
| 9 | Braiman | Wadi Braiman | 51.269 | 0.056 | 20495.2 | 0.00932 | 9874.1 |
| 10 | Ghulil | Wadi Ghulil | 23.828 | 0.04337 | 8951 | 0.01139 | 4218.3 |
| 11 | N_Ghulil | | 0.856 | 0.09268 | 1682.5 | 0.0436 | 477 |

**Table 2.8**   (continued)

| Basin SN | Basin name | Wadi name | Area (km²) | Basin slope (m/m) | MFDIST (m) | MFDSLOPE (m/m) | Centroid (m) |
|---|---|---|---|---|---|---|---|
| | | Wadi N_Ghulil | | | | | |
| 12 | Al Mari | Wadi Al Mari | 62.601 | 0.05348 | 13022.6 | 0.00657 | 6998.8 |
| 13 | Al Maharraq | Wadi Al Maharraq | 188.261 | 0.03544 | 30974.4 | 0.01805 | 13099.6 |
| 14 | Al Aslaa | Wadi Al Aslaa | 37.54 | 0.06054 | 12596.7 | 0.0077 | 4611.4 |
| 15 | Mirayyikh | Wadi Mirayyikh | 38.373 | 0.04406 | 10313.2 | 0.01105 | 4723.6 |
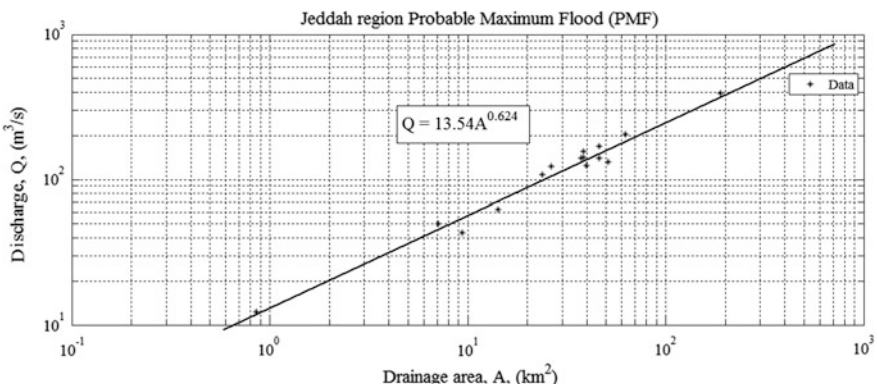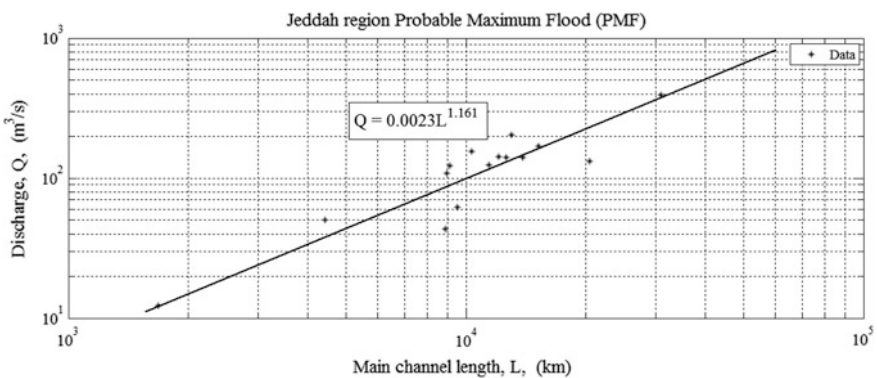
**Table 2.9**   Jeddah region drainage basin parameters

| Basin name | Wadi name | Area (km²) | MFDIST (m) | CENTOUT (m) | Snyder tp (h) | Rational discharge (m³/day) | PMF discharge (m³/s) |
|---|---|---|---|---|---|---|---|
| Qaws01 | Wadi Qaws | 14.247 | 9519.2 | 4424.5 | 3.77 | 18837.98 | 62.33 |
| Qaws02 | Wadi Qaws | 9.408 | 8855.9 | 3941.8 | 3.57 | 11758.44 | 43.54 |
| Qaws03 | Wadi Qaws | 38.291 | 12098.6 | 6092.7 | 4.47 | 59886.95 | 141.63 |
| Mathwab01 | Wadi Mathwab | 7.062 | 4427.5 | 1896.4 | 2.33 | 5756.03 | 50.12 |
| Mathwab02 | Wadi Mathwab | 26.492 | 9087.2 | 3802.9 | 3.56 | 33010.41 | 122.99 |
| Ghaya | Wadi Ghaya | 46.087 | 15239.6 | 6449.8 | 4.87 | 78579.23 | 170.16 |
| Um Hableen | Wadi Um Hableen | 39.672 | 11419.7 | 5780.4 | 4.32 | 60026.18 | 124.91 |
| Daghabag | Wadi Daghabag | 46.269 | 13892.3 | 6844.4 | 4.82 | 78108.16 | 139.90 |
| Braiman | Wadi Braiman | 51.269 | 20495.2 | 9874.1 | 6.05 | 108560.73 | 131.82 |
| Ghulil | Wadi Ghulil | 23.828 | 8951.0 | 4218.3 | 3.66 | 30490.44 | 107.72 |
| N_Ghulil | Wadi N_Ghulil | 0.856 | 1682.5 | 477.0 | 1.15 | 344.96 | 12.29 |
| Al Mari | Wadi Al Mari | 62.601 | 13022.6 | 6998.8 | 4.76 | 104344.85 | 204.48 |
| Al Maharraq | Wadi Al Maharraq | 188.261 | 30974.4 | 13099.6 | 7.45 | 491147.66 | 392.88 |
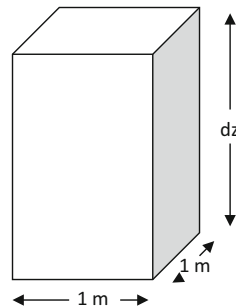
**Table 2.9** (continued)

| Basin name | Wadi name | Area (km²) | MFDIST (m) | CENTOUT (m) | Snyder tp (h) | Rational discharge (m³/day) | PMF discharge (m³/s) |
|---|---|---|---|---|---|---|---|
| Al Aslaa | Wadi Al Aslaa | 37.54 | 12596.7 | 4611.4 | 4.16 | 54663.26 | 140.36 |
| Mirayyikh | Wadi Mirayyikh | 38.373 | 10313.2 | 4723.6 | 3.94 | 53002.70 | 155.98 |



**Fig. 2.44** Discharge–drainage area relationships



**Fig. 2.45** Discharge–main channel length relationships

**Fig. 2.46** Unit base area
prisms



$$s(h) = \int_0^h \mathrm{d}s = \int_0^h \rho_s \mathrm{d}z \qquad (2.36)$$

Instead of height, if pressure is considered then the hydrostatic equilibrium
equation says that $\mathrm{d}p = -\rho_H g \mathrm{d}z$. The subject of dz from this expression can be
substituted into previous equation after the necessary arrangements leading to,
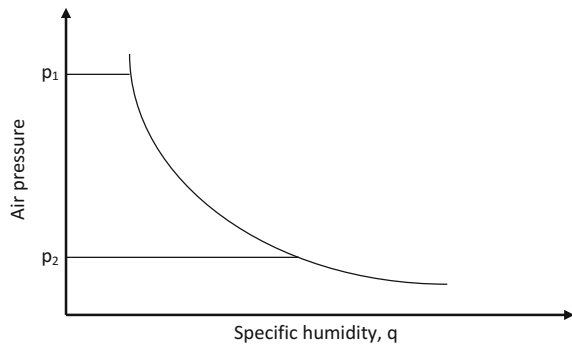
$$s(p) = -\frac{1}{\rho g} \int_{p_1}^{p_2} q \mathrm{d}p \qquad (2.37)$$

where $q = \rho_w/\rho_H$ is the specific humidity; $p_1$ and $p_2$ are low and high-pressure
levels, respectively. It is possible to render this expression into a more practical
form by taking into account the g value approximately as,

$$s(p, q) = 0.0001 \int_{p_1}^{p_2} q \mathrm{d}p \qquad (2.38)$$

This expression is useful to calculate the PMP precipitable water amount of the
unit area base prism provided that the pressure variations between two levels ($p_1$
and $p_2$) are known. As shown in Fig. 2.47 from the radiosonde data, the determi-
nation of the specific humidity by pressure, the integration in Eq. (2.38) can be
achieved and it shows the area of pressure change between two pressure levels. The
multiplication of this area by 0.0001 leads to PMP amount. In order to obtain the
rainfall height in cm, the specific humidity must be in gr/kg and the pressure in
minibar.

Fig. 2.47 Vertical humidity
variations



## 2.15.1   Application Principles

In practical applications, in order to depend on easily applicable procedure instead
of pressure consideration, water vapor density, $\rho_{wv}$, one can obtain the precipitable
water volume, $dV$, within the unit area and $dz$ height volume as,

$$dV = \rho_{wv}dz$$

Its integration from the earth surface to height h yields,

$$P(h) = \int_0^h \rho_{sp}dz \qquad (2.39)$$

In these calculations, the humidity distribution, m, around the radiosonde trace is
assumed to be constant. Precipitation in gram can be calculated by taking into
consideration the absolute humidity measurement in gr/cm$^3$ as,

$$V(h) = \int_0^h mdz \qquad (2.40)$$

In radiosonde measurements, the relative humidity, $m_r$, records are obtained in
percentage. For this reason, the relationships between the absolute and relative
humidity are necessary in the applications. In this relationship, saturated water
vapor,$\rho_{swv}$, is considered, and hence,

$$m_r = 100\frac{\rho_{wv}}{\rho_{swv}} \qquad (2.41)$$

**Table 2.10** Dew point
temperature and saturation
water vapor density

| $T_d$ | $\rho_{swv}$ |
|-------|--------------|
| 0     | 4.86         |
| 5     | 6.81         |
| 10    | 9.41         |
| 15    | 12.83        |

and

$$\rho_{swv} = \frac{m_r \rho_{swv}}{100} \tag{2.42}$$

The substitution of this expression into Eq. (2.39) yields,

$$V(h) = \int_0^h \frac{m_r \rho_{swv}}{100} \, dz \tag{2.43}$$

Herein, $\rho_{swv}$ is a function of the saturation point temperature, $T_s$. The relationship between the two variables is given in Table 2.10.

The fit curve to these data gives the following expression:

$$\rho_{swv} = 5.0 \, e^{0.0614 \, T_s} \tag{2.44}$$

The integration Eq. (2.43) can be taken practically by finite difference approach as,

$$V(h) \cong \frac{\rho_{swv}}{100} \sum_{i=1}^n (m_r \Delta z)_i \tag{2.45}$$

## 2.16   Areal Average Rainfall Calculation

Rainfall records at individual meteorology stations represent the station vicinity rainfall amounts. However, in case of several meteorology station existence in an area, it is necessary to find the areal average rainfall (AAR) amount to know the rainfall amounts at any point within the study area. For the AAR calculations, there are various practical methods and in practical applications it is necessary to decide which one to use. In the following subsections, four of these methodologies are explained briefly, because they are available in any textbook on the hydrometeorology.

### 2.16.1 Arithmetic Average

This method yields plausible AAR values provided that the rainfall amounts at each station are not different more than 10% relative error percentage (Sect. 2.8.1). This means that there is more or less uniformly distributed areal rainfall prevalence over the study area. In order to check the 10% error percentage, e, it is necessary to pinpoint the maximum, $R_{max}$, and minimum, $R_{min}$, rainfall records among n number of stations by taking into consideration Eq. (2.2). Provided that $\alpha < 10\%$, then the AAR, $\overline{R}_A$, can be calculated according to the arithmetic average formula as,

$$\overline{R}_A = \frac{1}{n}\sum_{i=1}^{n} R_i \qquad (2.46)$$

where $R_i$ is the amount of rainfall at station $i$. It is important to notice that this expression is a special case of the following section rainfall calculation with equal weightings.

### 2.16.2 Weighted Average
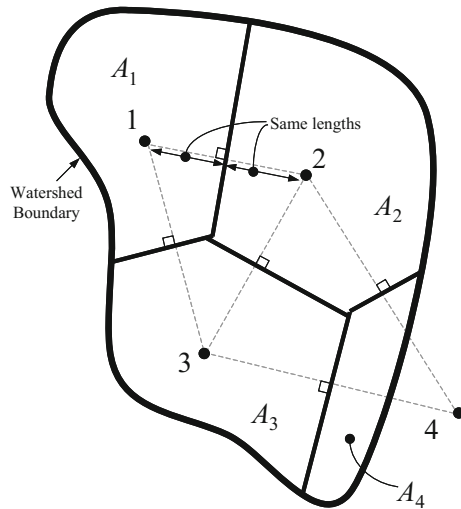
This method considers for each station a certain portion of the drainage basin area, and accordingly, each rainfall station record is considered as effective over such sub-areas. In practical applications, these sub-areas are determined as polygons or percentage polygons.

#### 2.16.2.1 Thiessen Polygon

Logically, each rainfall recorded at a raingauge should have its areal domain of influence, i.e., a representative sub-area. If the relative differences between the stations are more than 10%, then in the calculation of AAR, the role of representative sub-areas must be taken into consideration. It is not always clear how to get the most representative sub-area value. Although the advent of Geographic Information Systems (GIS) has greatly streamlined the problem of determining spatial statistics, sometimes it is not practical to use GIS; instead, Theissen (1912) polygon approach is probably the most common method used in hydrometeorology for determining AAR when there are several raingauge records. The basic concept is to divide the drainage basin into several polygons, each one around a measurement point, and then take the weighted average of the measurements based on the size of each polygon area.

The construction of sub-area polygons can be achieved as follows. Consider the drainage basin boundary as in Fig. 2.48 There is three raingauges inside the drainage basin, and the fourth is outside.

**Fig. 2.48** Theissen
polygonal divisions



The application of the Theissen areal weighting method first consists of constructing a series of triangles by joining pairs of adjacent rainfall stations. The nearest stations should always be jointed, and each triangle is kept near the equiangular shape when possible.

1. First connect all of the measurement points, the dots in the figure are measurement points, and they have been connected with dashed lines.
2. Draw perpendicularly bisect each of the "connecting" lines and extend the bisecting lines until either intersect the watershed boundary or another bisecting line.
3. Hence, four polygons are generated and note that measurements made at point 4 will contribute less to the final average than, say, the measurements at point 2.

If there are $n$ stations, then there are n polygons and $n$ representative sub-areas, $A_i$, for each station with the rainfall record, $R_i$. Provided that the representative polygons are decided, then the AAR can be calculated according to the following weighted average:

$$\overline{R}_A = \frac{\sum_{i=1}^{n} R_i A_i}{\sum_{i=1}^{n} A_i} = \frac{1}{A} \sum_{i=1}^{n} R_i A_i = \sum_{i=1}^{n} R_i \frac{A_i}{A} = \sum_{i=1}^{n} R_i a_i \qquad (2.47)$$

where $a_i$'s are the percentage representative areas, and therefore, $0 < a_i < 1$ and $a_1 + a_2 + \dots a_n = 1$. If the representative polygon sub-areas are all equal and amount to $A_s$, then $A_i/A = A_s/nA_s = 1/n$, and hence, Eq. (2.47) becomes equivalent to Eq. (2.46), which is the arithmetic average AAR calculation.

### 2.16.2.2  Şen Polygon

The major drawback in the Theissen polygon approach is that whatever the rainfall amounts, the sub-area polygons remain the same. These polygons are dependent entirely on the raingauge location configuration. Sometimes, it is possible that a very small rainfall at one of the stations may have a very big sub-area, and hence, the contribution may be more than another station, where the rainfall is much higher. In order to alleviate this drawback, Şen (1998) suggested that the representative sub-area polygons should not be dependent on the station configuration only, but in the meantime on the amount of the rainfall recorded at each station. This is the percentage-weighted polygon (PWP) method, which has the same basic triangularization procedure as in the Theissen polygon method.

After deciding on the triangles, the following procedure is necessary for dividing the study area into polygons leading to the PWP. If the rainfall values at three apices of a triangle are $A$, $B$, and $C$, then their respective percentages are calculated simply as,

$$pA = 100A/(A + B + C) \qquad (2.48)$$

$$pB = 100B/(A + B + C) \qquad (2.49)$$

and
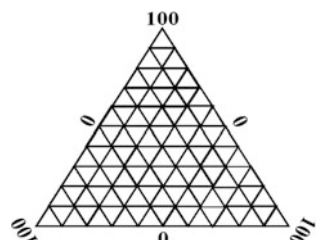
$$pC = 100C/(A + B + C) \qquad (2.50)$$

respectively. Hence, it is possible to find the three-variable percentage data of constant sums for each triangle. A two-dimensional plot of three variables can be shown on a triangular graph paper as one point (see Fig. 2.49). Such papers are very common tools in earth sciences (Koch and Link 1971).

In order to demonstrate the method more explicitly, the following step-by-step algorithm is provided:

1. Draw lines between each adjacent pair of rainfall stations. Hence, a set of triangles is obtained that cover the study area.
2. For each triangle, calculate the rainfall percentage at its apices according to Eqs. (2.48)–(2.50). Consider in each station that each apex has the value of 100 percentages with zero percentage on the opposite side.

**Fig. 2.49**  Triangular coordinate paper

3. Consider bisector, which connects an apex to the midpoint of the opposite side and graduate it into 100 equal pieces.

4. By making use of one rainfall percentage calculation in step 2, mark it along the convenient bisector starting from the opposite side toward the apex.

5. Draw a parallel line from this marked point in step 4 to the opposite side of the apex considered with its rainfall percentage.

6. Repeat steps 4 and 5 for the next rainfall percentage and find similar parallel line this time to another opposite side.

7. The intersection of these two lines defines the key point for the triangle considered.

8. In order to check the correctness of this key point, repeat steps 4 and 5 for the remaining third rainfall percentage value. If the parallel line to the side crosses through the aforementioned key point, then the procedure of finding the key point for the triangle is complete. Otherwise, there is a mistake either in rainfall percentage calculations or in the location of marked points along the bisectors in steps 3 through 6 inclusive.

9. Return to step 2 and repeat the process for other triangles constructed in step 1. In this manner, each triangle will have its key point. The location of this point within the triangle depends on the percentages of recorded rainfall amounts at the three adjacent apices. The greater the rainfall percentage for an apex, the closer the point will lie to this apex. It is not necessary that the triangles resulting from a given set of stations in a network should be exactly equilateral. However, in the Theissen method for an obtuse-angle triangle, the intersection of the three perpendicular bisectors occurs outside the triangular area.

10. Key points at adjacent triangles are connected with each other to form polygons each including a single rainfall station.

11. Finally, the boundaries of polygons around the basin perimeter are defined by drawing a perpendicular to the sides of triangles from the key points.

The AAP calculation is achieved by the application of Eq. (2.47) as already explained in detail by Şen (2008).

### 2.16.2.3   Isohyet Map

The word isohyet is a compound Greek word consisting of "iso" and "hyet" meaning "equal" and "rain." Hence, collectively it implies equal rainfall lines (contour lines) similar to the equal elevation lines in a topographic map. The construction of the isohyet map is exactly the same as drawing any topographic map. The only difference is that instead of triangularization points for the topographic map, there are raingauge locations and the elevations at each of these locations are the amount of rainfall for a specific duration of time. In order to calculate the AAR from this map, the following steps are necessary:

1. Find average rainfall, $R_1$, between successive isohyets and this is representative of the arithmetic average for the area that is encircled by the two isohyets and the drainage boundary.
2. Find the area, $A_i$, on the map between the two successive isohyets.

With these two quantities ($R_i$ and $A_i$), the AAR can be calculated from Eq. (2.47) similar to the previous polygon approaches.

This is the most accurate among all the previous methods, and it depends heavily on the skill of the person in drawing the isohyets. It is preferable because the map marker may know the terrain within the drainage basin and be able to adjust the isohyets to reflect natural conditions in the field. In mountainous countries, the isohyets would approximate topographic contours, since orographic rainfall usually increases by going upslope toward the mountainous areas (Sect. 2.3.1). If some measuring points show unusually heavy rainfall, then the isohyets can be clustered around such points. The advantages of the isohyet maps can be stated as follows:

1. It permits the analyst to exercise his/her own judgment and knowledge of average and specific rainfall distribution within the area.
2. It helps to fill the missing data and also adjusts suspected rainfall records.
3. There is no artificial weighting as in the polygon methods.
4. It provides opportunity to adjust the contours according to topographic features.

However, there are also disadvantages, as it is more time-consuming than most of the other methods; and it is more subjective in that the accuracy depends upon the skill of the analyst.

# References

Aron, G., Wall, D. J., White, E. L., & Dunn, C. N. (1987). Regional rainfall intensity-duration-frequency curves for Pennsylvania. *Water Resources Bulletin, 23*(3), 479–485.

Bell, F.C. (1969). Generalized rainfall-duration-frequency relationships. *Journal of the Hydraulics Division, ASCE, 95*(1), 311–327.

Benjamin, J. R., & Cornell, C. A. (1970). *Probability, statistics, and decision for civil engineers*, Dover Books on Engineering.

Bernard, M. M. (1932). Formulas for rainfall intensities of long durations. *Transactions of the ASCE, 96,* 592–624.

BOM. (1994). *Rainfall intensity Bureau of Meteorology* (2015), Accessed June 9, 2015, http://www.bom.gov.au/water/designRainfalls/ifd/index.shtml.

Burlando, P., & Rosso, R. (1996). Scaling and multiscaling models of depth-duration-frequency curves for storm precipitation. *Journal of Hydrology, 187*(1–2), 45–64.

Chen, C. I. (1983). Rainfall intensity-duration-frequency formulas. *Journal of Hydraulic Engineering, 109*(12), 1603–1621.

Chow, V. T. (1964). *Handbook of applied hydrology* (Vol. 9–49, pp. 9–62). New York: McGraw-Hill.

Chow, V. T., Maidment, D. R., & Mays, L. W. (1988). *Applied hydrology*. St. Louis, MO: McGraw-Hill Publishing Company.

Collier, C. G., & Hardaker, P. J. (1996). Estimating probable maximum precipitation using a storm model approach. *Journal of Hydrology, 183,* 277–306.

Cooke, G., & Warran, A. (1973). *Geomorphology in deserts*. London: Batsford, 394 pp.

Corrigan, P., Fenn, D. D., Kluck, D. R., & Vogel, J. L. (1999). *Probable Maximum Precipitation for California: Hydrometeorological Report No. 59*, Hydrometeorological Design Study Center, National Weather Service, National Oceanic and Atmospheric Administration, U.S. Department of Commerce, Silver Spring, MD 392 p. SGS.

Court, A. (1961). Area depth rainfall formulas. *Journal Geophysical Research, 66*(6), 1823–1831.

Desa, M. M. N., Noriah, A. B., & Rakhecha, P. R. (2001). Probable maximum precipitation for 24hr duration over Southwest Asian monsoon region—Selangor, Malaysia. *Atmospheric Research, 58,* 41–54.

Desa, M. M. N., & Rakhecha, P. R. (2007). Probable maximum precipitation for 24-h duration over an equatorial region: Part 2-Johor, Malaysia. *Atmospheric Research, 84*(1), 84–90.

Dhar, O. N., & Damte, P. P. (1969). A pilot study for estimation of probable maximum precipitation using Hershfield technique. *Indian Journal of Meteorology and Geophysics, 20* (1), 31–34.

Foufoula-Georgiou, E. (1989). A probabilistic storm transposition approach for estimating exceedance probabilities of extreme precipitation depths. *Water Resources Research, 25*(5), 799–815.

Froehlich, D. C. (1995a). Intermediate-duration-rainfall equations. *Journal of Hydrologic Engineering ASCE, 121*(10), 751–756.

Froehlich, D. C. (1995b). Long-duration-rainfall intensity equations. *Journal of Irrigation and Drainage Engineering, 121*(3), 248–252.

Froehlich, D. C. (1995c). Short-duration-rainfall intensity equations for drainage design. *Journal of Irrigation and Drainage Engineering, 121*(4), 310–311.

Garcia-Bartual, R., & Schneider, M. (2001). Estimating maximum expected short-duration rainfall intensities from extreme convective storms. *Physics and Chemistry of the Earth, Part B: Hydrology, Oceans and Atmosphere, 26*(9), 675–681.

Gumbel, E. J. (1958). *Statistics of extremes*. New York: Columbia University Press.

Hansen, E. M., Schreiner, L. C., & Miller, J. F. (1982). *Application of probable maximum precipitation estimates*. United States East of 16th meridian. Hydro-meteorological report, No. 52, 228 pp.

Hanson, C. L. (1995). Short-duration-rainfall intensity equations for drainage design. *Journal of Irrigation and Drainage Engineering, 121*(2), 219–221.

Hershfield, D. M. (1961). Estimating the probable maximum precipitation. *Journal Hydraulics Division, ASCE*, *87*(5), part 1, 99–116.

Hershfield, D. M. (1965). Method for estimating probable maximum precipitation. *Journal American Water Works Association, 57,* 965–972.

Horton, R. E. (1933). The role of infiltration in the hydrologic cycle. In *Transactions, American Geophysical Union, 14th Annual Meeting* (pp. 446–460).

Huff, F. A. (1967). Time distribution of rainfall in heavy storms. *Water Resources Research, 3,* 1007–1019.

Keers, J. F., & Wescott, P. (1977). *A computer-based model for design rainfall in the United Kingdom*. Meteorol Office Science Paper 36, London.

Koch, G. S., & Link, R. E. (1971). *Statistical analysis of geological data*, Vols I and II. New York: Dower Publications, Inc.

Koutsoyiannis, D., Kozonis, D., & Manetas, A. (1998). A mathematical framework for studying rainfall intensity-duration-frequency relationships. *Journal of Hydrology, 206,* 118–135.

Linsley, R. K. (1986). Flood estimates: How good are they? *Water Resources Research, 22*(9), 159S–164S.

Linsley, R. K., Kohler, M. A., & Paulhus, J. L. (1988). *Hydrology for Engineers* (p. 492). London: Mc-Graw-Hill Book Co.

Miller, J. F., Frederic, R. H., & Tracey, R. J. (1973). *Precipitation frequency atlas of the conterminous western United States*. NOAA Atlas 2, U.S. Department of Commerce, National

Oceanic and Atmospheric Administration, National Weather Service, Silver Springs, Maryland (Vol. 11).

Papalexiou, S. M., & Koutsoyiannis, D. (2006). A probabilistic approach to the concept of Probable Maximum Precipitation. *Advances in Geosciences, 7*(51–54), 1680–7359.

Rakhecha, P. R., & Clark, C. (2002). Areal PMP distribution for one-day to three-day duration over India. *Applied Meteorology, 9,* 399–406.

Rezacova, D., Sokol, Z., & Pesice, P. (2005). A radar-based verification of precipitation forecast for local convective storms. *Atmospheric Environment*.

Şen, Z. (1998). Average areal precipitation by percentage weighted polygon method. *Journal of Hydrologic Engineering, 3*:1(69): 69–72.

Şen, Z. (2008). *Wadi hydrology* (346 pp). New York: Taylor and Francis Group, CRC Press.

Şen, Z. (2014) *Philosophical, logical and scientific perspectives in engineering*. Berlin: Springer-Nature, 260 p.

Sherman, C. W. (1931). Frequency and intensity of excessive rainfall at Boston. *Transactions of the ASCE, 95,* 951–960.

Svensson, C., & Rakhecha, P. R. (1998). Estimation of probable maximum precipitation for dams in the Hongru River catchment, China. *Theoretical and Applied Climatology, 59,* 79–91.

Trapp, R. J., Halvorson, B. A., & Diffenbaugh, N. S. (2007). *Journal of Geophysical Research Atmosphere, 112,* D20109. doi:10.1029/2006JD008345.

U.S. Weather Bureau. (1960). *Rainfall intensity-frequency regime—Part 5: The Great Lakes Region*, Technical Paper No. 29 (TP-29), Washington, D.C. Viessman, W., Jr., Lewis, G. L., & Knapp, J. W. (1996). *Introduction to hydrology* (4th ed., p. 760). New York: Harper Collins College Publishers.

WMO. (2009). *Guidelines on analysis of extremes in a changing climate in support of informed decisions for adaptation*. By Klein Tank AMG, Zwiers FW, Zhang X. (WCDMP-72, WMO-TD/No. 1500), 56.

WMO. (2011). WMO statement on the status of the global climate in 2011 WMO-No. 1085 © World Meteorological Organization, ISBN 978-92-63-11085-5.

Yarnell, D. L. (1935). *Rainfall intensity-frequency data*. U.S. Department of Agriculture, Miscellaneous Publication No. 204, 35 pp.

Wang, B. -H. M. (1984). Estimation of probable maximum precipitation: Case studies. *Journal of Hydraulic Engineering*, *110*, 1457–1472.

# Chapter 3
# Floods and Drainage Basin Features

**Abstract** Floods occur not only because of the rainfall but also the surface features, which collects, converges, and diverges of the after rain runoff flows through natural or artificial channels. The significance of topographic maps, satellite images, and digital elevation model (DEM) data, if available. The treatment of these data sources for the purpose of flood evaluation and prediction of various softwares are used, which take into consideration a set of morphological (physiographic) features. The basic definitions of various surface features are presented in a conceptual and rational manner so that the reader can appreciate the significance and the partial effect of each feature to overall flood discharge. The significance of cross sections with their hydraulic properties so as to calculate the surface water flow speed is described in detail with the cooperation of the rating curve concepts and their practical importance in any flood and early flood system setups. The most important part of the flood modeling is to reach flood maps in terms of inundation maps, which are missing in many parts of the world. Standard hypsographic curves and their relationship to the flood discharge calculation and classification are explained. Finally, early flood discharge formulations that are related simply to the drainage area are presented in the forms of equations and graphical representations with comparisons and restrictive limitations.

**Keywords** Channel slope · Cross section · Drainage area discharge relationship · Digital elevation model (DEM) · Drainage area · Drainage basin · Flash flood · Flood · Hypsographic curve · Inundation · Rating curve

## 3.1 General

Apart from the rainfall factors as effective agents on flood calculations, the next significant set of factors is concerned with the earth surface shapes in the form of drainage basins and their internal structures such as the area, main channel length, slope, drainage density, cross sections. These geomorphological features transform the rainfall amounts into surface runoff. The geomorphological elements provide

surface flow from high elevation points within the drainage basin to lower parts ending up in the main and lateral channels, which direct the surface flow (runoff) along the drainage basin, and finally, to its lowest point, which may confluence with the sea, lake, or lost in the desert areas.

It is well appreciated that whatever is the amount and the intensity of rainfall, floods do not happen without the effect of the surface features. They give convenient traces for flow and at places inundation extensions may take place according to the topography. This is the main reason why people try to augment artificial surface water structures such as conveyance canals, bridges, culverts, artificial depressions, and flood water leading ditches to convenient depressions for groundwater recharge.

Flood inundation maps are dependent on the topographic and geomorphologic features of a drainage basin, which are most susceptible for potential flash flood occurrences. It is not possible to control the potential flood hazards by using technological instruments that forewarn the occurrences or imminences. Additionally, it is better to prepare flood risk maps so as to delineate the risky areas to educate the administrators, decision makers, and local society. The availability of these maps is the key requirement for any urban development that entails land use allocation, identification of dam, tunnel, highway, culvert, bridge sites, and infrastructure locations for sustainable future.

Flooding can occur more quickly in the mountain head-water areas of large rivers as well as in the rivers draining to the coast, where they have steeper flanks causing to quicker flow than any other part of the drainage basin. These floods are potentially much more damage full and pose a greater risk to loss of life and property because there is generally much less time to take preventative actions. This type of flooding can affect most of the major towns and cities.

Flood plains can be looked at from several different perspectives (Chap. 1). As a topographic category, they are quite flat and lie adjacent to a stream; geomorphologically, they are landforms composed primarily of unconsolidated depositional material derived from sediments being transported by the related stream; hydrologically, they are defined best as a land form subject to periodic flooding by a parent stream. A combination of these features comprises the essential criteria for the floodplain definition (Schmudde 1968). Most simply, a flood plain is defined as "a strip of relatively smooth land bordering a stream and overflowed at a time of high water" (Leopold et al. 1964).

This chapter is confined to the definitions of each significant geomorphological element that can be employed in the derivation or explanation of flood discharge estimation, mitigation, and inundation hindrance tasks in future works. Additionally, basic information is presented for rational and logical bases of relationships between the surface water (runoff) and some of the morphological elements.

## 3.2  Topographic Map Presence
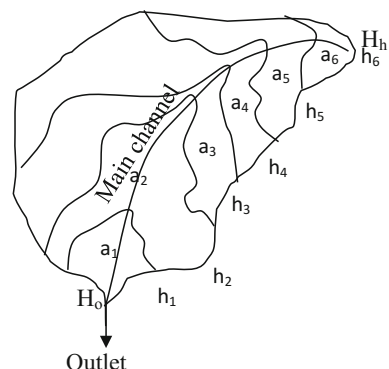
In the past, topographic maps and aerial photographs were utilized to delineate drainage basin boundaries, while control sections of wadi channels were measured in the field by leveling instruments. Also, observations of the highest flood level marks in the field were gathered and other relevant information was obtained from local inhabitants. The flood stages in a control cross section are used to construct rating curves by using empirical formulations (Sect. 3.9). The main objective is to show the inundation boundaries on digital elevation map (DEM), but if DEMs are not available, then classical topographic map contours around some representative cross sections are presented as inundation boundaries.

Topographic maps are equal elevation lines (contours) that provide the surface roughnesses and smoothness's collectively as in Fig. 3.1, and they provide objective bases for identification of many essential geomorphological features that are necessary for the flood peak discharge calculation (Chap. 5).

The most important flood evaluation quantities that can be derived from a given topographic map are the following.

(1) Drainage area, $A$, collects and leads the surface flow (runoff) to the outlet point,
(2) Elevation difference, $\Delta H$, between the lowest (outlet), $H_o$ and the highest, $H_h$, point of the drainage basin,
(3) Main channel length, $L$, carries water collection in the drainage network toward the outlet point,
(4) The main channel slope, $S = (H_{h-o})/L$, is helpful to calculate average water velocity, and also, time of concentration that is the time duration of rainfall drop on the highest point and its arrival at the outlet point (see Sects. 3.7.4 and 3.13),
(5) Total drainage length, $\sum L_i$, of the natural channels that convey surface water to the outlet point,
(6) Drainage density, $D_d = \sum L_i / A$, which indicates drainage amount per area. The higher is the drainage density, the speedier is the surface water conveyance toward the outlet point,

**Fig. 3.1**  Topographic map
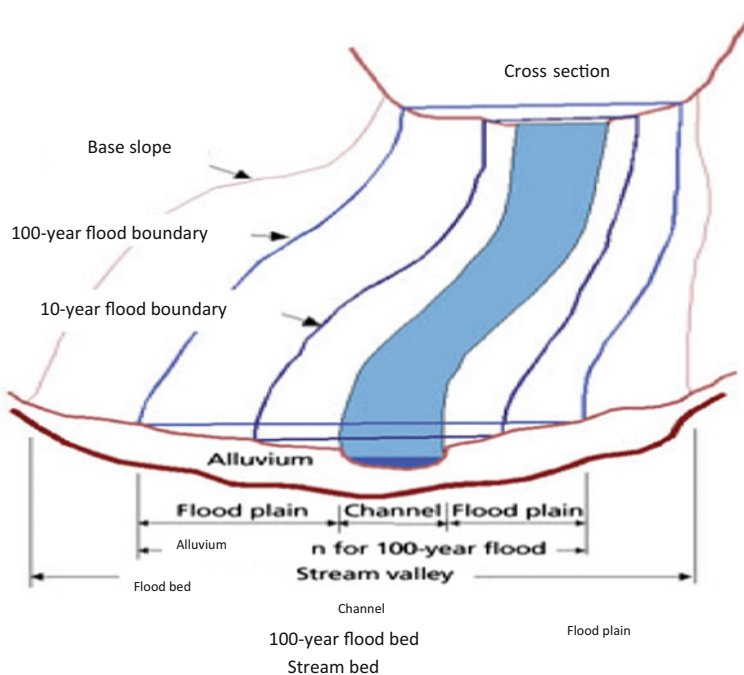
(7) Cross sections at a set of points along the main channel or on any branch as in
    Fig. 3.2, where there may be the possibility of some flood or inundation
    activity.

   These are the major quantities that are important in any surface flow and flood
discharge calculations. However, there are other geomorphological quantities that
can be obtained also from a given topographic map among which are the elongation
ratio, circularity, bifurcation ratio, etc.

## 3.2.1  Elevation Features

In order to describe the elevation features of a drainage basin in a refined manner,
the sub-areas are calculated between successive equal height lines (contour), (see
Fig. 3.1). The percentages of each sub-area are calculated out of the total watershed
area. This helps to know the total percentage of sub-areas below any given contour
line. If the area between two successive contours is shown by $a_i$ and the average



**Fig. 3.2** Flood boundaries

elevation of this sub-area by $e_i$, then the average elevation $\overline{E}$ of the watershed can be calculated as follows:

$$\overline{E} = \left(\frac{a_1}{A}\right)e_i + \left(\frac{a_2}{A}\right)e_2 + \cdots \left(\frac{a_n}{A}\right)e_n \qquad (3.1)$$

and succinctly, by definition of each areal ratio by percentage, $p_i$,

$$\overline{E} = p_1 e_1 + p_2 e_2 + \cdots p_n e_n \qquad (3.2)$$

It is possible to obtain elevation-area relationship from Fig. 3.1, which is given representatively in Fig. 3.3.

As the elevation increases, the areal coverage below this level also increases. Such a graph is useful to identify rainfall variation with elevation, show coverage, temperature change with height, and vegetation types.
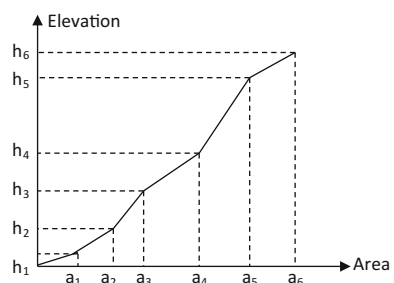
## 3.2.2   Field Survey
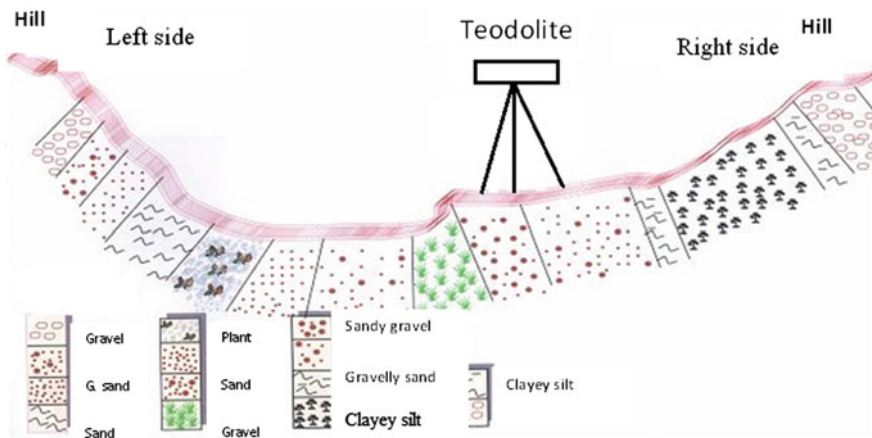
In this case, it is not possible to determine flood inundation boundaries exactly. The practical and applicable way is to make field survey in the field with theodolite instruments at a set of cross sections (see Fig. 3.4).

The cross section locations may be selected at the branch entrances to the main channel at possible sediment settlement locations or urban areas, industrial regions, militarily important sites, agricultural lands, and alike. These cross sections are referred to as the control cross section (Chaps. 4 and 5).

The best way to obtain the profile of a cross section is from the field measurements rather than readily available digital elevation model (DEM) data, and the use of theodolite instrument is the best at dry cross sections. The DEM cross sections should be controlled by field measurements as much as possible, if necessary, corrections must be done. The measurements are plotted on a plain paper and then the geometrical shape of the cross section appears as in Fig. 3.4 with descriptions of peripheral features.



Fig. 3.3  Elevation-area graphs

**Fig. 3.4** Representative cross section (Saudi Geological Survey, SGS 2007)

## 3.3  Digital Elevation Model (DEM)

These are prepared commonly in raster data structures in compatibility with remotely sensed data. They are represented in an array of equally spaced pixels with topographic elevation values of the earth's surface. The basic geometric properties that characterize the terrain surface at a pixel are as follows:

(1) Elevation,
(2) Properties of the gradient vector; the magnitude defines slope, and the direction angle represents terrain aspect,
(3) Surface curvature,
(4) Convexity,
(5) Surface-specific points and lines, i.e., local maxima (peaks), minima (pits), saddle points (passes), inflection points, break-lines, ridge and valley lines (Jordan 2003).

DEMs offer the most common methods for extraction of vital elevation and topographic information. They are increasingly used for visual analysis of topography, landscapes, and landforms, in addition to the modeling of surface processes (Welch 1990; Hirano et al. 2003; Kamp et al. 2003). Currently, DEMs are the main source for the extraction of different geomorphological and topographic features depending on altitude and its spatial distribution as well as a variation (Felicisimo 1994, 1995). Digital elevation data (DED), digital terrain data (DTD) (Campbell 2002), or digital terrain model (DTM) all include various arrangements of individual points of east–west and north–south directions coordinates of geographical elevation values $Z$, relative to a given datum for a set of $X$ and $Y$ points (Welch 1990; Bolstad and Stowe 1994; Bernhardsen 1999).

It is similar to any remote sensing data except that each pixel shows an elevation measurement in the center of the pixel instead of brightness values. Using this format makes the process of manipulations, classification, analysis, and display of DEMs similar to that of remote sensing imagery (Campbell 2002). Although the term is used inconsistently in the literature (Burrough 1986; Weibel and Heller 1991), it is defined here consistently with the terms of Burrough (1986), as a regular gridded matrix representation of the continuous variation of relief over space (Wood and Fisher 1993).

In the last decades, several developments are introduced to satellite sensors to produce data for DEM generation. Nowadays, many satellites provide stereo images with high potential of producing DEMs that can be integrated into the visualization of software or GIS environments with available geo-data and carto-graphic information (i.e., existing vector data) for landscape and geomorphic analysis (Polis et al. 2004). However, DEMs of usable details are still not available for much of the earth, high accuracy determination and visualization of the topography of the earth surface is still very essential for local and national level environmental applications (Chrysoulakis et al. 2003).

DEM provides a digital representation in three-dimensions of any portion of earth terrain. The resolution of DEMs depends on scale and resolution of the data source (digital satellite images, aerial photographs) and the spatial resolution (i.e., grid spacing) of the data samples, as well as other variables like data structure and algorithms that are used during the extraction process (Campbell 2002; Sabins 1997).

The use of three-dimensional terrain modeling in GIS applications was made possible after the advancements in computer software and database technology improvements. When combined with satellite images and GIS coverage's, a DEM becomes more useful in terrain visualization and geomorphic terrain analyses (Welch 1990).

## 3.4   Flood Map Derivation Ingredients

Especially, in urban and suburban areas, flood maps are necessary to allocate locations with the minimum risk, and hence, contribute to the local and regular planning by shareholders. The majority of flood hazards in urban areas are not due to the flood risks only but more importantly because of the missing of flood inundation maps. Unfortunately, development of urban area takes place toward potentially risky locations. Similar to the topographic, geographical, geological, and other relevant maps, flood risk maps coupled with inundation maps must be pre-pared for significant areas (urban centers, suburban areas, military bases, and agricultural fields). In the preparation of such maps, the following points are important:

1. Digital elevation model (DEM) data or topographic maps,
2. The following features must be ready for each drainage basin,

   2.1. Drainage basin area,
   2.2. Natural main channel trace,
   2.3. Main channel length,
   2.4. Main channel slope,
   2.5. If necessary, also the slopes and lengths of the branches.

3. Critical stream cross section geometrical descriptions,

   3.1. At different levels (at least 5 stages) for rating curves determination,
   3.2. Wet perimeter calculation for each cross section,
   3.3. Hydraulic radius calculations,
   3.4. Cross section slopes.

4. Cross section features

   4.1. Determination of friction factors for each cross section (Manning coefficients),
   4.2. Average velocity calculations at a set of water levels,
   4.3. If possible, natural or artificial rating curve generation for each cross section.

5. Hydrometeorological quantities

   5.1. Decision on rainfall intensity,
   5.2. Rainfall intensity determinations for hydraulic structure designs and planning at 2-, 5-, 10-, 25-, 50-, and 100-year return periods,
   5.3. Similarly, a set of risk calculations in harmony with the return periods,
   5.4. Calculation of convenient flow hydrograph peak discharge for 2-, 5-, 10-, 25-, 50-, and 100-year return periods,
   5.5. Determination of water levels in each cross section based on the peak discharge calculation.

6. Plotting on the topographic map the levels for the same risk levels and their connections give the inundation boundaries.
7. Some flood estimation methods are based on theoretical considerations, whereas others are purely empirical. In general, flood discharge is a function of climatic and watershed characteristics.

The main climatic variable is defined by the rainfall amount, its intensity, distribution, and duration, while the watershed features include the drainage area, density, shape, slope, and main channel length, etc. The latter factors act as an operator to convert a time sequence of naturally occurring precipitation into a time sequence of runoff (Seyhan 1977). The rainfall-runoff relationship becomes even more complicated with the consideration of the distribution of the vegetation, geological formations, soil condition, and spatial and temporal variation of climatic factors.

## 3.5 Drainage Basin (Catchment) Features
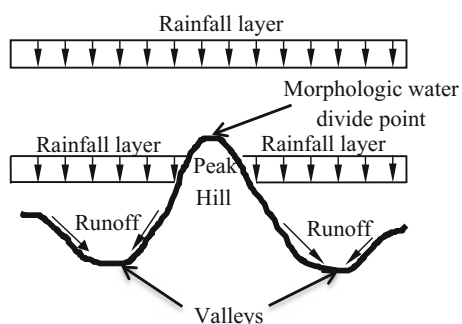
Drainage basin is interchangeably used as catchments in humid regions, and its counterpart in arid and semiarid regions is the wadi concept (Şen 2008).

### 3.5.1 Water Divide Point
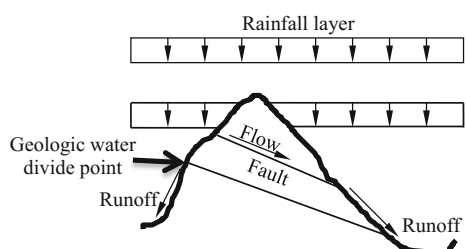
In Fig. 3.5, the hill point of a cross section is shown with an uniformly distributed ideal rainfall layer, which before reaching the morphological peak point remains without disturbance. After the touch of this layer onto the hill peak, it is separated into two parts on the right- and left-side valleys. The point that divides the rainfall is referred to as the geomorphological water divide point.

The water divide point may not correspond with the geomorphological peaks always. For instance, if a faulty geological structure exists, then the water divide point may shift to a lower elevation as in Fig. 3.6. Although the rainfall layer is divided again into two parts, the one on the higher faulty side, surface water does not reach the valley on the same side, but instead transportation takes place along the subsurface geological structure to the other side.



Fig. 3.5 Geomorphologic water divide points



Fig. 3.6 Geological water divide points
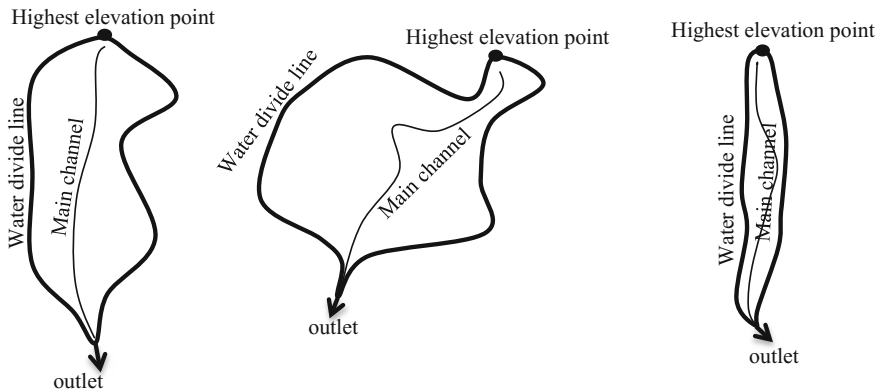
This information indicates that not only topographic maps but also subsurface geological maps are important for refined water divide point identification. Geological water divide point determination is important in some critical projects, but in almost all applications, water divide points are depicted only from the topographic maps or DEM data without any geological consideration.

### 3.5.2   Water Divide Line

In any topographic map, there are hill ridges especially at the upper stream part of a drainage area that are composed of water divide points. It is possible to appreciate such points during a field trip and from the point that one stands, by looking around the highest points on the silhouette one may have a good experience of the water divide points and water divide line locations.

The collection of all the water divide points appears in the form of a curvature line that closes onto itself at the outlet (lowest elevation) point, which collects all the surface waters. In Fig. 3.7, various forms of the water divide lines are given.

In flood calculations, along the water divide line two specific points have importance. The first one is the outlet cross section through which each rainfall drop of runoff passes into the sea or into adjacent basin or lost in the desert. The second important point is the highest elevation at a location just opposite to the outlet point.
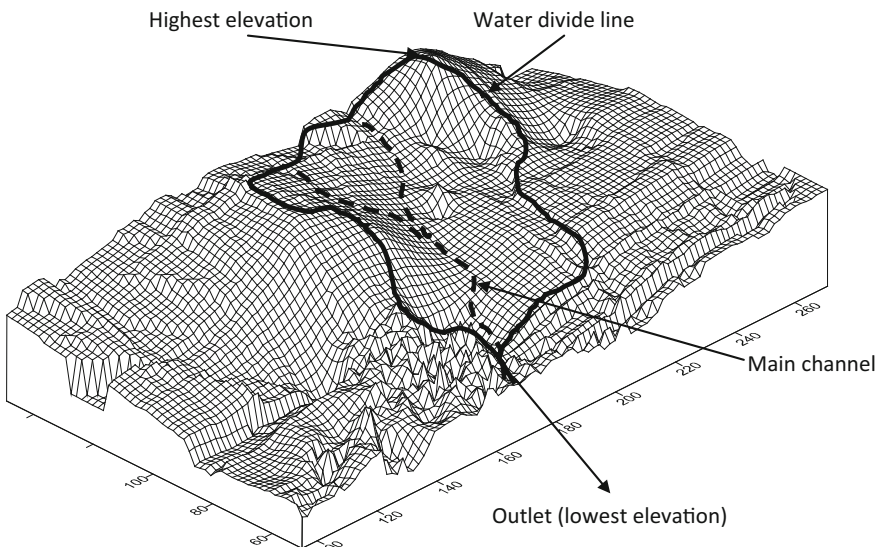


**Fig. 3.7**   Water divide lines

### 3.5.3  Drainage Basin (Catchment)
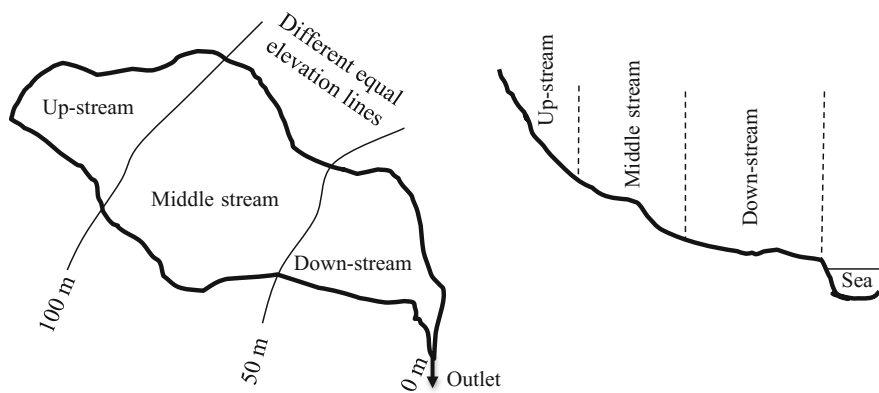
The surface features of a drainage basin have direct effect on the runoff, flood, groundwater recharge, and orographic rainfall occurrences (Chap. 2). The runoff calculations require the relationship between the water volume per time (discharge) and different geomorphologic factors such as the drainage area, $A$, main channel length, $L$, and slope, $S$, drainage density, $D_d$. These quantities can be calculated in the office provided that a detailed topographic map is available or better from the DEM values by means of suitable software. Drainage basins are identified by the water divide line preferably on a topographic map of scale 1/50,000. A hypothetical part of such a map is presented in three-dimensions in Fig. 3.8.

In general, the drainage basin areas are very irregular in shape and they have the following characteristics:

(1) Water divide lines are irregular in shape, but they have a regular property that any point along this line has a decline (or incline in the opposite) direction but decline on both sides on the perpendicular direction (Fig. 3.5),
(2) The whole drainage basin might be thought of at least in three major parts, namely, upstream, middle stream, and downstream depending on distinctive meteorological, hydrological, topographic, and geological features (Fig. 3.9),
(3) On the water divide line, there is one point with the highest elevation, which is around the most distant point from the lowest elevation (outlet) point. The lowest point is referred to as the outlet of the catchment through which all the surface waters flow toward downstream confluence (Fig. 3.7),
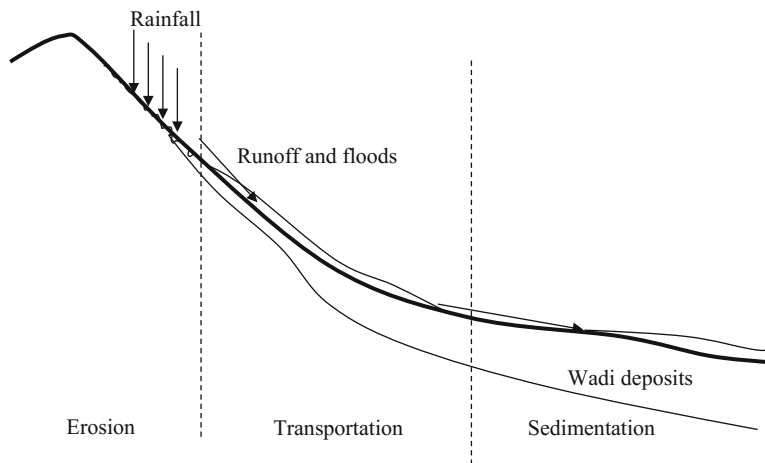


**Fig. 3.8**  Geomorphology of a wadi

**Fig. 3.9** Longitudinal wadi cross section portions

(4) Within each drainage basin from upstream to downstream, there is a sequence of lowest points that constitute the main channel ending at the outlet,

(5) The upper reach of a basin has steeper slopes with higher surface water (runoff) velocity, bigger erosion rates, better groundwater quality, weak groundwater recharge possibility and more rainfall intensities than other parts,

(6) In arid and semiarid regions, drainage channels and depressions are filled with Quaternary deposits and other parts are rock surfaces without vegetation, but in humid regions, vegetation and forestry are major surface covers,

(7) The depth of the wadi deposits increases toward the downstream. However, the groundwater quality deteriorates at the downstream, where the groundwater reservoir has relatively thicker alluvial deposits (Fig. 3.10).



**Fig. 3.10** Longitudinal wadi cross sections

(8) Erosion has the maximum rate at high elevations and sedimentation, and deposition rates are more at the lower elevations around the main channel,

(9) Upstream has higher elevations, and in general, in arid regions, the storm rainfalls occur over these areas, but due to high slopes, the surface water has not enough time or space for groundwater recharge.
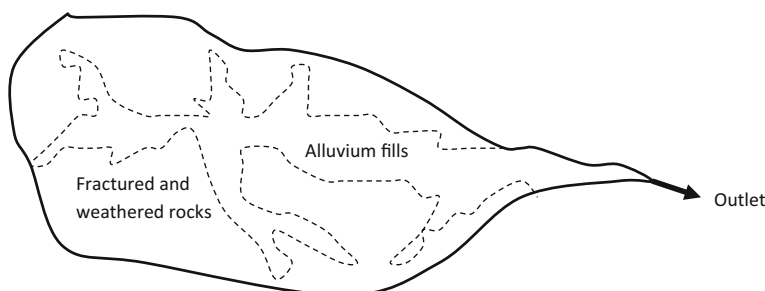
For arid and especially semiarid regions, the very word "wadi" is the part of the basin, which is covered by Quaternary deposits along the channels. The wadi (drainage basin) collects the surface water from different points and directs them to the outlet. During such a transitional direction, surface water runs over the alluvial fills, which are referred to as wadi channels (courses) among the local people.

In arid regions, wadis (catchments) have two different geological surface areas as alluvium fills or fractured and weathered rocks, which are schematically shown in Fig. 3.11.
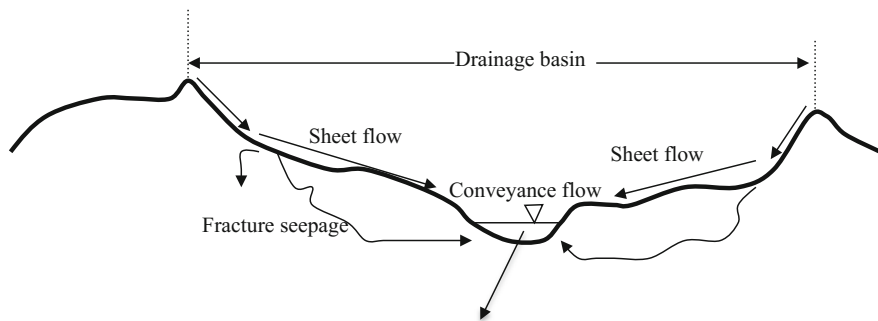
There are perennial rivers in humid region drainage basins, but in arid and semiarid regions ephemeral streams exist after each rainfall event and depending on the rainfall intensity, there are occasionally intermitted surface flows and floods at the downstream parts.

After each rainfall event that covers whole the drainage basin, the surface water may be viewed in two parts as "sheet flow" over the surface and "conveyance" within the channels (Fig. 3.12). The former includes higher points than the plain areas, whereas the latter is the most concentrated surface flow in visible water channels. In the sheet flow area, the rainfall cannot infiltrate directly in significant amounts but there are flash surface flows leading toward the confluence area from each convenient direction depending on the morphological features of the sheet flow area. From the surface and subsurface feature points of view, the conveyance area is the most important region for the strategic groundwater resources.

In this area, surface features are important for infiltration rate calculations, and the subsurface is for the groundwater storage volume. In humid regions, the sheet flow is very important for the conveyance flow calculations, but in arid regions, the concentration of extensive study must be on the conveyance type. The wider and deeper the conveyance area, the more the groundwater storage, and hence, there are plenty of domain for strategic groundwater planning. Unfortunately, in any classical



**Fig. 3.11** wadi surface areas

**Fig. 3.12** Sheet flow and channel flow

groundwater storage calculations, the sheet flow area and underlying fractured, weathered, and structural geological features are not considered. In any strategic groundwater storage calculation, the contribution through the fractured area and subsurface geology must be considered even by simplified methodologies.

## 3.6 Drainage Basin Quantities

The drainage basin characteristics can be measured and analyzed quantitatively through a process called drainage basin morphometry (geomorphology, surface characteristics, or features). It attempts to relate basin and stream network geometries to water quantity (discharge) and occasionally to sediment transportation (Chap. 7). The size of a drainage basin influences the amount of water yield; the length, shape, and relief factor affect the rate at which water is discharged from the basin and the total yield of sediment; the length and character of the stream channels affect the availability of sediment for stream transport and the rate at which water and sediment are discharged. The stream pattern and properties draining the basin depend not only on the geological structure but also on land surface relief, climate, soil types, vegetation, and increasingly human impacts on the basin environment.

### 3.6.1 Drainage Area

It is the projected horizontal surface area, which lies in the upstream of outlet. The area can be calculated from a topographic map after delimitation of water divide line as explained in Sect. 3.5.1. Simple logic states that increase in the area results in increase in the rainfall share and likewise in the surface and groundwater shares.

**Table 3.1**  Drainage basin classifications

| Area (km²)        | Classification |
|-------------------|----------------|
| A > 1000          | Very big       |
| 1000 < A < 100    | Big            |
| 100 < A < 5       | Middle         |
| A < 5             | Small          |

According to the areal size, $A$, the drainage basins can be classified into four categories as in Table 3.1.

There are many empirical formulations, which relate the drainage basin area, $A$, to peak discharge, $Q_P$, and the most widely used empirical formulation reads as follows:

$$Q_P = c A^n \tag{3.3}$$

where $c$ and $n$ are the parameters that can be obtained empirically (Chap. 5).
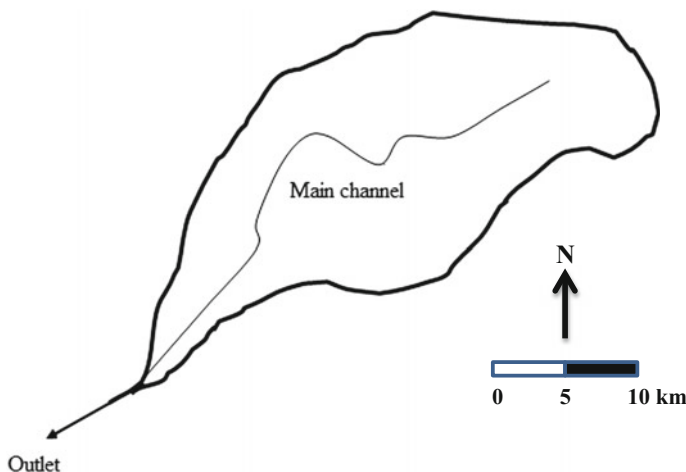
Each drainage basin is topographically separate from adjacent basins by a ridge, hill, or mountain, which is known as the water divide line (Al-Abed and Al-Sharif 2008). The morphometric analysis of the main basins in any drainage area depends mostly on measurements of some parameters from topographic maps (scale 1:50,000), satellite images (ETM$^+$, SPOT and SRTM), and field measurements to prepare a database, which can then be analyzed mathematically, probabilistically, and statistically by means of convenient formulations and models.

Basin area is hydrologically important because it directly affects the size of the storm hydrograph and the magnitudes of the mean runoff and peak discharge. It is interesting that the maximum flood discharge per unit area is inversely related to size (Chorley et al. 1957). Strahler (1950) stated that basins with similar areal features and forms are also similar in their geomorphological characteristics.

## 3.6.2   Main Channel Length

The natural channel extends from the upper part of a drainage basin down to the outlet point and constitutes the main drainage line. Its length plays significant role in the surface flow and flood calculations. Figure 3.13 indicates the main channel enclosed by the water divide line.

There are many ways to measure the basin length. The first is the length in a straight line from the mouth of a stream (outlet point) to the farthest and highest point on the water divide (Schumm 1959). One can determine the basin length automatically from DEM by GIS software.

**Fig. 3.13**  Main channel length

## 3.6.3  Main Channel Slope

The slope of the drainage basin is its vertical drop per unit of horizontal distance, and it plays as a dominant factor in runoff and flood velocity as well as discharge calculations. In general, the slope is steepest at higher elevations in the upstream areas and much reduced as the wadi approaches its base level at the downstream portions. It is possible to appreciate the slope along the wadi from upstream toward the downstream along the longitudinal profile of the main channel, which has generally a concave shape. In high elevations, the surface water erodes a deep valley in the hilly and mountainous terrain due to the high runoff velocity. The steeper the slope, the more rapidly flows the runoff. Therefore, the time to peak is shorter and the peak discharge is higher than downstream. On the other hand, infiltration capacity is lower as slope gets steeper.

There are different slope measures, but the main channel slope, $S$, is used frequently in practical works. It is defined simply as the ratio of difference between the outlet, $H_o$, and the highest, $H_h$, point elevations to the main stream length, $L$, as,

$$S = \frac{H_h - H_o}{L} \qquad (3.4)$$

The more the slope, the faster is the surface flow arrival to the outlet. Apart from the main channel, there are slopes of other branches within the drainage basin and they play a significant role in the distribution and movement of surface flow, streamflow, infiltration, vegetation cover, and sedimentation and flood inundation. The overall average slope, $S_a$, can be calculated from,

$$S_a = \frac{\Delta H}{A} W_T \qquad (3.5)$$

where $\Delta H$ is the elevation difference between two consecutive contour lines on a topographic map, $W_T = (W_1 + W_1 \ldots W_n)$ is the total length of contour lines within the drainage area, and $A$ is the catchment area. Arid region, natural watercourses may be divided roughly into three major groups as follows (FAO 1981):

(1) Stable, rocky, steep, deeply incised, irregular channels, which almost wholly control the flow characteristics of the water/sediment mixture,
(2) Unstable, disorganized, braided alluvial channels, whose slope, depth, shape, sinuosity, and bed-form are controlled by the water–sediment flow characteristics and in a state of dynamic equilibrium with them,
(3) Minor watercourses in flat alluvial plains or approaching the terminal reaches of major basins. In these watercourses, vegetal growth dominates the water depth-discharge relationships. There may be no obvious single preferred channel, but water finds its way among the large hummocks.

The first alternative degrades and the discharge measurements in the channels are subject to large errors due to high velocity, turbulence, and debris load. The last two are of an aggrading type and subject to large errors due to the configuration of the watercourse. In any flood discharge calculations, these uncertainties must be taken into consideration and also in the flood risk assessment (Chap. 6).
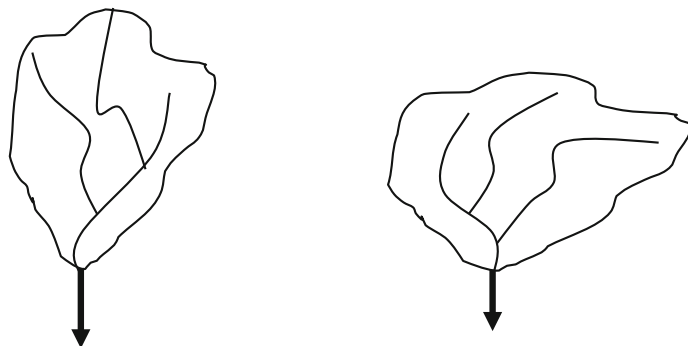
### 3.6.4  Drainage Density

Drainage density, $D_d$, as defined by Horton (1945) as the ratio of the total stream length, $\sum L_i$, within a basin to basin area, $A$, which is expressed in terms of km/km$^2$. It is a measure of the total stream channel length per unit area, which can be expressed as,

$$D_d = \frac{\sum L_i}{A} \qquad (3.6)$$

The smaller the drainage density, the surface flow, and runoff move slowly, but in the meantime, infiltration increases and leads to the time delay in discharge with small peak discharge amounts. Drainage density alone cannot explain the drainage behavior of the catchment area. Two drainage basins with the same area and drainage density are not distinguishable even though one of them may be drainage wise better than other (Fig. 3.14).

The drainage density indicates the closeness of streams spacing, thus providing a quantitative measure of the average stream channel length for the whole basin. Drainage density measurements over a wide range of geologic and climatic types

**Fig. 3.14** Two watersheds with the same area and drainage density

indicate that a low drainage density is more likely to occur in regions of highly resistant and permeable subsoil material under dense vegetative cover, where relief is also low. High drainage density is the resultant of weak or impermeable sub-surface material, sparse vegetation, and mountainous relief. Low drainage density leads to coarse drainage texture, while high drainage density implies fine drainage texture (Strahler 1964).

## 3.6.5   Shape Factor

The shape of a drainage basin affects especially runoff, flood events, and their temporal and spatial distributions. Different researchers suggest different shape factors. By definition each one is simple and comparable with a specific ideal regular shape without dimension. The drainage basin shape effect on discharge is different for drainage basins with the same surface area and rainfall intensity. In particular, the elongated watersheds have less peak discharges than equivalent round/circular watersheds. One of the shape factors, $S_1$, is defined as the ratio of the squared main stream channel length to catchment area as,

$$S_1 = \frac{L^2}{A} \tag{3.7}$$

The bigger is this shape factor, the more elongated and narrow is the watershed area. In general, as the drainage area increases, the shape factor also increases.

Another shape factor, depending on the area and the length of the main channel, is defined as the ratio of equivalent circle area diameter, $D$, with the drainage area to the main stream length as,

$$S_2 = \frac{D}{L} \tag{3.8}$$
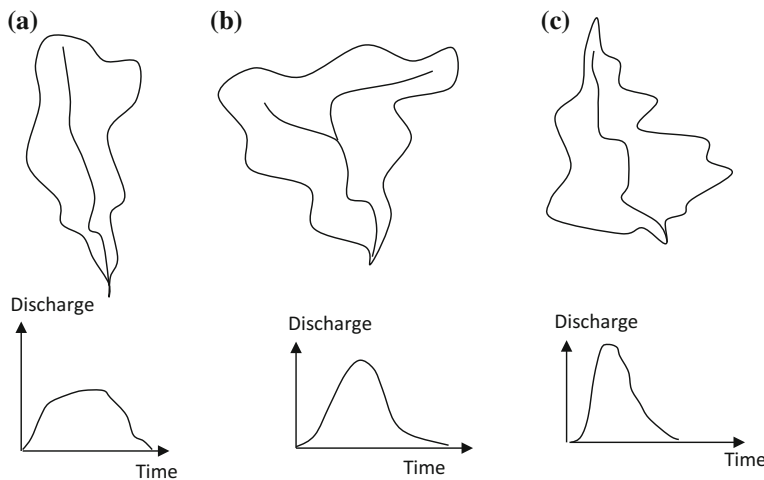
There is another shape factor, which takes into consideration the perimeter length, $P_w$, of the watershed and the perimeter, $P_c$, of the equivalent areal circle, which is defined as follows:

$$S_3 = \frac{P_w}{P_c} \tag{3.9}$$

This means that when the same rain falls on different watersheds, their hydrographs are expected to have different shapes. In Fig. 3.15, such different hydrographs are shown from the same hyetograph on different watersheds.

Rainfall over long and narrow watersheds has long duration hydrographs, which are rather flat (see Fig. 3.15c). In the case of extensive watersheds, hydrograph duration is shorter and peak discharge is bigger (Fig. 3.15b).

The steeper the basin, the narrower it is. Basin width is an important element to study the shape of basins and the ratio of $L/W$ to determine the final shape of these basins (Muller 1974). At least, there are three possibilities to measure the width of a basin as the average of basin width; division of the basin area by basin length $A/L$; comparison of the maximum width, $W_{max}$, of the basin with the maximum length, $L_{max}$, in the basin.



**Fig. 3.15** Effect of watershed shape on hydrographs

### 3.6.6   Stream Order

Drainage order and frequency in a watershed has a main channel from which there are tributaries and tributaries of tributaries as in Fig. 3.16. The quantitative study of stream network has been considered by Horton (1945), who developed a system for ordering stream networks and derived laws relating the number and length of streams of different orders.

In this ordering system, the smallest recognizable channels are designated by order 1. These terminal channels have flows normally during wet weather conditions only. Two channels of the same order combined together lead to the next order. For instance, after the confluence point of two first-order streams, second-order stream comes into view. If a lower order channel joints a higher order channel, the channel downstream retains the higher order of the two previous orders. The order of a watershed is equivalent to the highest order available within the same watershed. For instance, in Fig. 3.15, the watershed order is 3.

### 3.6.7   Bifurcation Ratio
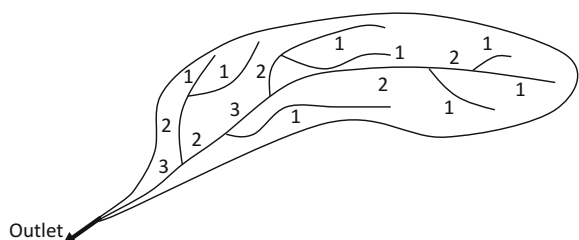
Consideration of the subsequent stream order numbers leads to the concept of the bifurcation ratio. Horton (1945) has found empirically that the bifurcation ratio, $R_N$, or a ratio of the number $N_i$, of channels of order $i$ to the number $N_{i+1}$ is relatively constant between two successive orders. This is the Horton's law of steam number, and it is expressed as,

$$R_N = \frac{N_i}{N_{i+1}} \tag{3.10}$$

Similar definitions can be made for the lengths, $L_i$, and areas, $A_i$, of the orders, $i$, and $(i+1)$ as follows:

$$R_L = \frac{L_{i+1}}{L_i} \tag{3.11}$$



**Fig. 3.16** Drainage ordering and frequency in a watershed

as

$$R_A = \frac{A_{i+1}}{A_i} \qquad (3.12)$$

All these ratios can be obtained from a topographic map with a scale. If these ratios are close to each other for a set of watersheds, then they are considered as similar to each other.

### 3.6.8 Elongation Ratio

It is the ratio between the diameter, $D$, of an equivalent circle with some area to the basin and the maximum channel length, $L$, of the basin. Elongation ratio, $E_r$, values vary from 0.25 to 1.00 and defined as (see Fig. 3.17),
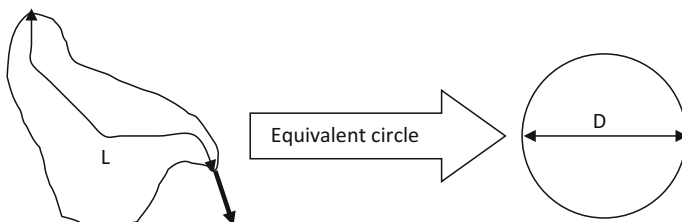
$$E_r = \frac{D}{L} \qquad (3.13)$$

### 3.6.9 Drainage Frequency

This factor is important from infiltration process of view. It indicates the frequency of the stream and sub-stream channels within the drainage basin. The drainage frequency, $D_f$, is dependent on the number, $N_s$, of all streams within a drainage area, $A$ as,

$$D_f = \frac{N_s}{A} \qquad (3.14)$$

It is possible to count the number of streams from the catchment area features as in Fig. 3.15. This simply implies the number of streams per unit area, and hence, it is possible to compare two or more drainage basins on the basis of this factor.



**Fig. 3.17** Different elongation ratios

Increase in the drainage frequency leads to increase in infiltration capacity. Surface runoff channel branches are also considered in the calculation of drainage frequency. Increase in the drainage frequency also causes a quick response of the drainage basin to storm rainfall with early hydrograph peak arrival and big peak discharge.
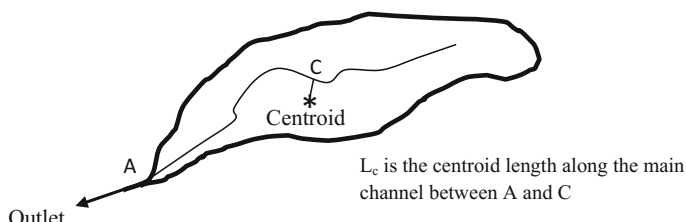
### 3.6.10   Centroid Length

As will be explained in Chap. 5, in synthetic hydrograph analysis, one of the significant watershed parameters is the distance, $L_c$, between the nearest point to the drainage basin centroid on the main channel and the outlet. The centroid point can be determined by hanging the template of watershed made of cardboard from two different points. Vertical straight lines are drawn from each hanging point, and the intersection between these two straight lines is the location of the watershed centroid. Its projection on the main channel gives the nearest point of the channel to the centroid. As in Fig. 3.18, the length, $L_c$, is defined as the distance between centroid point, $C$, and the outlet.

## 3.7   Cross Sections

In order to prepare flood inundation map, it is necessary to know the corresponding possible discharge depths at a set of cross sectional areas along the main channel. Since the flood hazard potential is more common in the downstream part of a catchment, more frequent cross sections should be taken at downstream locations. In the selection of cross sections, the following guidelines are helpful:

(1) It is preferable to select three best representative cross sections along each channel branch. This may not be possible due to time and budget restrictions, and therefore, most often two cross sections are selected one in the upstream and the other in the downstream portions of each reach,
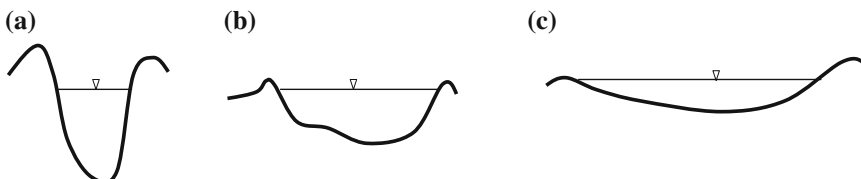


Fig. 3.18   Centroid length

(2) The selection of cross sections should be more intensified at the downstream branches of a drainage basin. Another useful guidance is a preliminary reconnaissance inspection through quick field trips, if possible. This will help to identify the most potential inundation subjected areas by expert views and with information support from the local settlers,

(3) The cross sections must be selected on rather stable portions of the main channel course and if possible at more or less straight line reaches. This is a requirement for the simplicity of calculations. Stable portions are covered with solid rocks that do not allow cross section shape changes for many years or if such cross sections are not available, it is possible to construct ones by rein-forced concrete in regular shapes and especially with trapezium cross sections.

In order to determine the cross section geometry, field surveying applications are carried out across each section perpendicular to the drainage basin longitudinal extension. For this purpose, the surveying instrument is located over a point almost in the middle of the section and a sequence of right and then left height readings is taken at a set of appropriate points with the record distances from the instrument location (Sect. 3.2.2, Fig. 3.4). The appropriateness of the points is dependent on the surface features and texture changes along the cross section. For instance, if there is a change from fine sand to gravel or from naked part to vegetation or to rock, than a measuring point is adopted. In this manner, the depth of each point from the common horizon of the instrument is recorded with distance. Finally, the plot of distances against the depths results in the profile of the cross section as, representatively, shown in Fig. 3.19.

Young cross sections have rather steep banks on two sides, and they are not eroded sufficiently enough and intensive rainfall resultant floods erode their beds and the cross section gets larger in the width and shallower in the depth. This indicates that by time, the same volume of water crosses from the same cross section with rather a small velocity (Fig. 3.19a). This type of cross sections is mainly on the upstream parts of the drainage basing. Figure 3.19b is either medium age or middle stream cross section type, where the flow velocities are comparatively smaller than the upstream case not because of the cross section property only but also due to the slope. The third cross section type has a wider width and shallower depth, which can be observed at old, and especially, at the downstream parts of drainage basins, where the surface flow speeds are the smallest compared to upper and middle stream cross sections (Fig. 3.19c). As for the flood and inundation



**Fig. 3.19** Representative cross section profiles

occurrences causing to hazards, the most subjective cross section is in Fig. 3.19c, which frequently exists at the downstream portion of the drainage basin. Apart from the geomorphological and rainfall intensity effects for flood hazards, also careless human settlement locations provide additional opportunity for flood risk and consequent hazard (Chaps. 6 and 9).
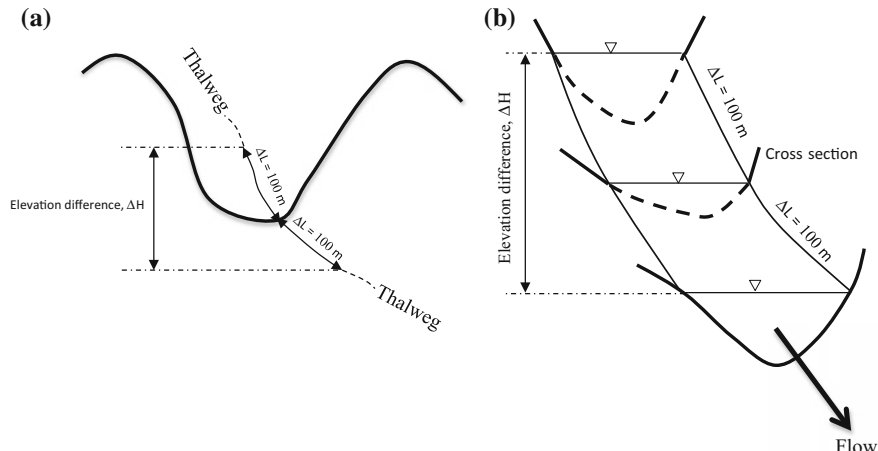
## 3.7.1  Cross Section Slope

In Sect. 3.6.3, main channel slope properties and the way of calculations are explained. The cross section slope is a part of the main channel slope at the cross section location. In practical applications, the cross section slope is calculated by taking into account a certain distance toward upstream and downstream directions, say about 100 m along the main channel thalweg as shown in Fig. 3.20a.

In humid regions, the slope of the cross section, $S_{cs}$, is calculated by the slope of surface water profile as shown in Fig. 3.20b. Consideration of the notations in Fig. 3.20 yields simply to the formulation of the cross section slope as follows:

$$S_{cs} = \frac{2\,\Delta L}{\Delta H} \tag{3.15}$$

Although the distance between the upstream and downstream measurement points is suggested as $2 \times 100 = 200\,\text{m}$, depending on the situation in the field work, one can take any convenient value instead of 100 m.
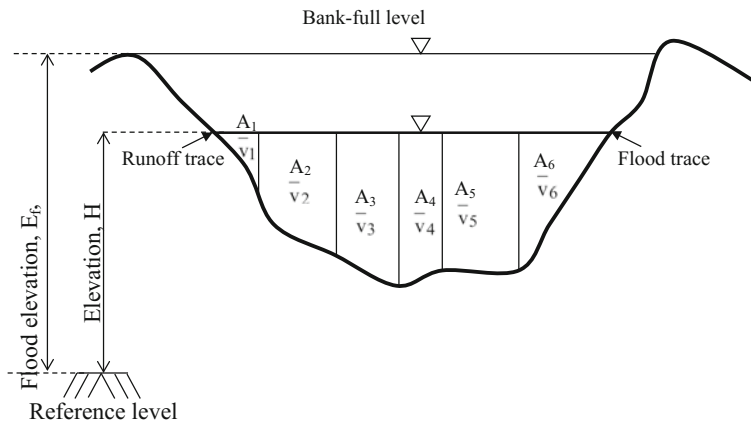


Fig. 3.20  Cross section slope, **a** arid region, **b** humid region

## 3.7.2 Cross Sections Area and Rating Curve

In humid regions, water cross section area is divided into a set of sub-areas (trapezium and triangular) as in Fig. 3.21. The summation of these sub-areas yields the total area of flow cross section. The calculations are repeated for each depth variation (water level fluctuations). In order to calculate the i-th cross section average velocity, $\bar{v}_i$ is measured through a current meters in each sub-area, and hence, the average discharge is as $Q_i = A_i \bar{v}_i$ (i = 1, 2, ..., 6). The summation of these discharges gives the global discharge through the cross section.
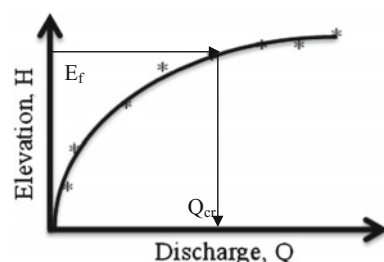
Repetition of the same discharge calculations in the same cross section at a set of different flood water levels provides information between the cross section discharge and the flood water elevation (stage) or water depth. The rating curve is the relationship between the discharge and the elevation or water depth, which has the shape similar to Fig. 3.22.

In general, within the same drainage basin, each cross section has a special rating curve. The rating curves are also useful to estimate the discharge value corresponding to the trace of the flood on both sides of the cross section. It is also useful



**Fig. 3.21** Representative cross section and sub-sections

**Fig. 3.22** Representative rating curve

to determine the critical discharge, $Q_{cr}$, (Fig. 3.21) that corresponds to bank-full level as in Fig. 3.20.

In arid and semiarid regions, there is not surface water, and hence, it is not possible to generate the rating curve according to the rules in humid regions.

Figure 3.23 shows the hydrograph with water depth increase as the rising limb and then water level decrease as recession limb.

### 3.7.3   Cross Section Wetted Perimeter and Hydraulic Radius

Wetted perimeter, $P_w$, can be written in terms of width, $W$, and depth, $D$, in case of shallow waters as,
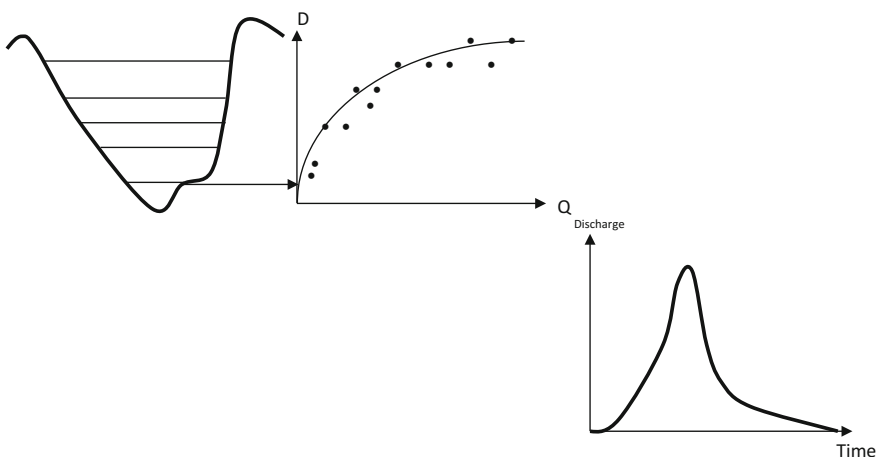
$$P_w = W + 2D \qquad (3.16)$$

The spread of surface water over very wide widths may render this relationship into a simpler form as,

$$P_w = W\left(1 + \frac{2D}{W}\right) \qquad (3.17)$$

Since $W \gg > D$ then $P_w \approx W$. The hydraulic radius, R, is calculated as the ratio of flow cross section area to the wetted perimeter as,

$$R = \frac{A}{W} \qquad (3.18)$$



**Fig. 3.23**  Unique hydrograph

Since by definition A = WD, and therefore, the hydraulic radius takes its simplest form as,

$$R = D \tag{3.19}$$

### 3.7.4 Cross Section Discharge

In general, the definition of discharge, $Q$, for water flow through a cross section is volume, $V$, of water per time interval, $\Delta t$.

$$Q = \frac{V}{\Delta t} \tag{3.20}$$

It is possible to express the volume as the water flow cross section area, $A$, and the length, $L$, of water movement distance, $\Delta L$, during the same time interval. Hence,

$$Q = \frac{AL}{\Delta t} \tag{3.21}$$

Since physically $L/\Delta t$ is the definition of average velocity, $\bar{v}$, (cross section average velocity) one can then write,

$$Q = A\bar{v} \tag{3.22}$$

Furthermore, the cross section area can be expressed as the water depth, $D$, multiplied by cross section width, $W$, and therefore, it is possible to rewrite,
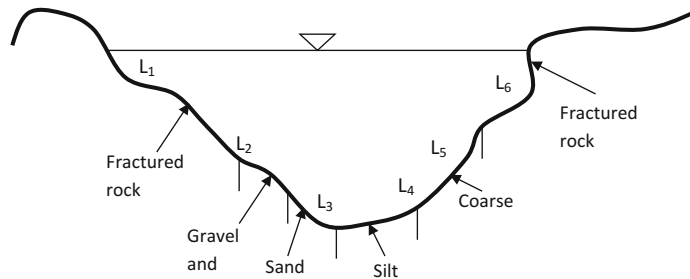
$$Q = WD\bar{v} \tag{3.23}$$

If necessary, one can express the width as,

$$W = \frac{Q}{D\bar{v}} \tag{3.24}$$

In general, prior to the hydrometric calculations, the field velocity measurements are necessary. For this purpose, in any cross section with water depth, $D$, the wet cross section area, $A$, and the mean velocity, $\bar{v}$, must be measured for discharge, $Q$, calculation as in Eq. (3.22).

After drawing of the cross section geometry along the perimeter, different soil types (rock, gravel, sand, silt, clay, vegetation, tree, etc.) can be indicated for later calculation of the Manning's coefficient as already shown in Fig. 3.4. The soil types are important for the friction coefficient determination between the water and the wetted perimeter of the cross section. The coarser the material of the cross section,

**Fig. 3.24** Cross section wet perimeter, material and positions

the more is the friction losses. In Fig. 3.24, different materials and their lengths along the perimeter are shown with different notations such as $L_1, L_2, \ldots, L_6$.

For each soil type, the Manning's coefficient can be taken from tables provided by various researchers (Şen 2008). The global Manning's coefficient can be calculated either as the arithmetic average or as the weighted average with wet perimeter material lengths. For discharge calculation, first of all, a series of hypothetical water depths, $D$, is adapted from the bottom (thalweg) of the cross section and then the wet area (flow area) and the wetted perimeter length are found for each level. Not only the wetted perimeter different material lengths but also their soil types are determined for Manning's coefficient selection from the available tables.

Manning's formulation helps to calculate average velocity, $\bar{v}$, in a cross section after the substitution of the aforementioned quantities into the following formulation.

$$\bar{v} = \frac{1}{n} R^{2/3} S^{1/2} \tag{3.25}$$

The Manning roughness coefficient, $n$, is dependent on the cross section material (geology in arid regions). One can get $n$ values from the Internet as in Table 3.2.

At cross sections, where the width is comparatively very big than the depth, the use of Eq. (3.19) gives rise to the simplest form as,

$$\bar{v} = \frac{1}{n} D^{2/3} S^{1/2} \tag{3.26}$$

Substitution of the relevant quantities into Eq. (3.22) yields the cross section discharge, $Q$, as,

$$Q = A \frac{1}{n} R^{2/3} S^{1/2} \tag{3.27}$$

**Table 3.2**  Manning coefficients

| Surface material | Manning's roughness Coefficient - n - | Surface material | Manning's roughness Coefficient - n - |
|---|---|---|---|
| Asbestos cement | 0.011 | Galvanized iron | 0.016 |
| Asphalt | 0.016 | Glass | 0.01 |
| Brass | 0.011 | Gravel | 0.029 |
| Brickwork | 0.015 | Lead | 0.011 |
| Cast-iron, new | 0.012 | Masonry | 0.025 |
| Clay tile | 0.014 | Metal—corrugated | 0.022 |
| Concrete—steel forms | 0.011 | Natural streams—clean and straight | 0.03 |
| Concrete—finished | 0.012 | Natural streams—major rivers | 0.035 |
| Concrete—wooden forms | 0.015 | Natural streams—sluggish with deep pools | 0.04 |
| Concrete—centrifugally spun | 0.013 | Plastic | 0.009 |
| Copper | 0.011 | Polyethylene PE—Corrugated with smooth inner walls | 0.009–0.015 |
| Corrugated metal | 0.022 | Polyethylene PE—Corrugated with corrugated inner walls | 0.018 –0.025 |
| Earth | 0.025 | Polyvinyl Chloride PVC—with smooth inner walls | 0.009–0.011 |
| Earth channel—clean | 0.022 | Steel—Coal-tar enamel | 0.01 |
| Earth channel—gravelly | 0.025 | Steel—smooth | 0.012 |
| Earth channel—weedy | 0.03 | Steel—New unlined | 0.011 |
| Earth channel—stony, cobbles | 0.035 | Steel—Riveted | 0.019 |
| Floodplains—pasture, farmland | 0.035 | Wood—planed | 0.012 |
| Floodplains—light brush | 0.05 | Wood—unplaned | 0.013 |
| Floodplains—heavy brush | 0.075 | Wood stave | 0.012 |
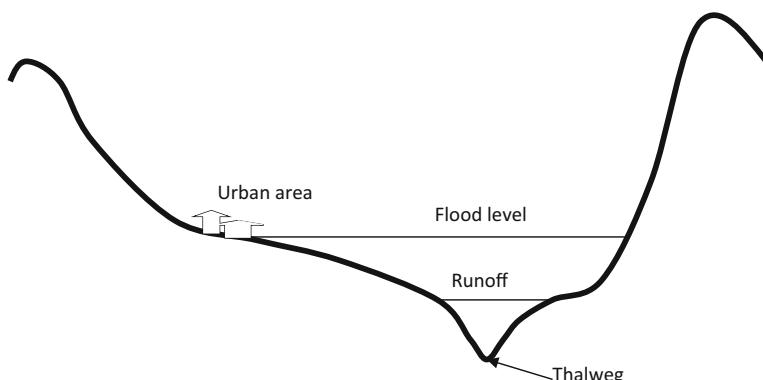
In order to generate the inundation map in an area, one cross section rating curve is not enough, but better to have several cross sections scattered at convenient locations.

## 3.8  Floods and Basic Concepts

Every surface water runoff does not appear in the form a flood, and hence, does not cause inundation and destruction. Light and even moderate rainfall events do not give rise to significant surface water depths. They flow starting from the thalweg point in any cross section and by time the flow depth increases. The thalweg is the lowest points along the length of a riverbed or main channel in the drainage basin. Hence, the level of water in inundation areas becomes rather significant in the critical definition of flood hazards.

It is possible that some intensive rainfalls do not cause flood in an area, and the same storm rainfall may give rise to flood event in some other area. This indicates that floods are dependent on the geomorphology. It does not imply that intensive rainfall events will lead to floods. For floods, certain features of the drainage basin are important and without them, even though the rainfall might be very extensive, there may not be any flood event. Hence, the rainfall intensity and drainage basin characteristics are the two major factors in flood evolution. Among the most significant drainage basin features are the areal extend, slope and cross sectional area variations along the main channel course. The cross sectional areal variation is shown in Fig. 3.25 for various water levels as floods and non-floods. From the hydraulic calculations point of view, cross sectional area and wetted perimeter play the most significant role in cross section flood discharge. If the perimeter coarseness, and hence, the friction coefficient is high, then there is a better chance for water elevation and overtoppling of bank level leading to flood hazards.

Another definitional concept of the floods is whether the cross sectional area allows the surface flow from its upstream area to pass through or not? This is a very significant consideration and question for the calculation of flood level in a cross section. In the case of floods, the conventional or naturally existing cross section area may not allow the passage of upstream surface flow easily, which is the instance of flood occurrence. If the cross sectional area allows the surface water pass
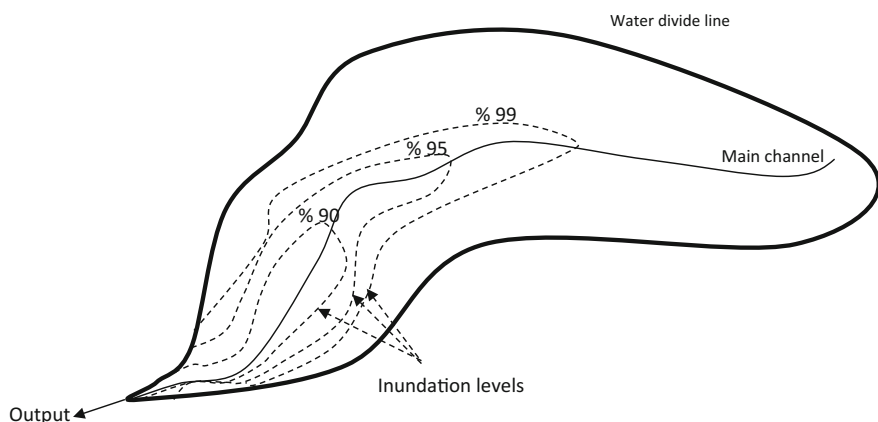


**Fig. 3.25**  Thalweg and flood levels

easily through its area, then whatever the rainfall intensity, flood does not occur in the cross section. If a region includes this property in all its cross sections, then there is neither flood danger nor any need for inundation map in the region. If some of the cross sections do not allow the passage of water, then the area may be under the flood effect partially. However, in some instances, a complete flood inundation may take place depending on rainfall intensity and drainage basin geomorphologic features. The most hazardous parts of any channel are the banks near the main channel where there are always runoff occurrence possibilities (Figs. 3.21 and 3.25).

In the aforementioned passages, only the natural flood causes are explained, but there may be floods due to anthropogenic (human) activities. The best-known example is that with or without information about the flood danger, in many parts of the world urban areas, villages, or local settlement locations are established right inside the dangerous potential flood plains. In this case, the floods hit the human life and property more than any other occasion. The closer the active land use to the main channel stream, the more prone is the land to inundation, and consequently, drainage cross section that has not been prone to flood hazard become under the tread of flood hazard. It is possible to delimit the flood inundation lines in the study areas (see Fig. 3.26).

It is also possible to consider the flood hazards and effected areas under natural and artificial categories. Natural floods occur at river banks and flood plains together with erosion and sedimentation processes. It is necessary to assess the vulnerability of an area to floods and the extent of natural hazard. Such a division leads to more adequate, flexible, and manageable definition of risk. If a place is not vulnerable, then the risk will be small. Vulnerability is related to the exposition of any human activity to flood danger.



**Fig. 3.26** Inundation regions (overview)

### 3.8.1   Flash Floods

Flash floods, which are short-lived extreme events, prove the exception. They usually occur under slowly moving or stationary thunderstorms and they last for less than 24 h. The resulting rainfall intensity exceeds infiltration capacity, so runoff takes place very rapidly. Flash floods are frequently very destructive as the energy flow can carry much sedimentary materials.

Flash floods are short-term inundations of small areas such as a town or parts of a city, usually by tributaries and creeks. Heavy rainfall in a few hours can produce flash flooding even in places where little rain falls for weeks or months. If heavy rainfall occurs repeatedly over a wide area, then river or main stream flooding becomes more likely, in which the main rivers of a region swell and inundate large areas, sometimes well after rainfall ends.

Flash floods are not uncommon in arid regions and present a potential hazard to life, personal property, and structures such as small dams, bridges, culverts, wells, and dykes along the wadi courses. After a short period of intensive rainfall, flash floods are formed rapidly and they flow down over extremely dry or nearly dry watercourses at speeds more than 1.5 m/s faster than a person can escape from the rough and sandy wadi channels (Dein 1985).

Although flash floods are among the most catastrophic phenomena, the volume of the infiltration from floods is a major source of groundwater replenishment to aquifers that are hydraulically connected with watercourses on the surface. Moreover, this volume of water could be increased significantly by impounding the floods with surface dams or successive dykes. Importance of flood studies, other than dealing with surface and subsurface water interactions, includes flood influences on engineering structures, such as dams, bridges, culverts, and spillways (Chap. 7).

Flash floods usually occur with little or no warning after heavy rain and can reach peak level in a short time. A number of reasons cause flash floods including increased impermeability due to an increase in the built component of the urban ecosystem; increased accelerated erosion from exposed surfaces resulting in sedimentation of streams, which subsequently cause flash flood along flat low-lying channels; and poor maintenance of drainage facilities in built-up areas. There is a relationship between urbanization and informal settlement growth in flood-prone areas in many cities of the world, and especially cities topographically surrounded by gentle hills and mountains.

In recent years, Europe has been witnessing a large number of severe and catastrophic flood events, both localized flash floods and basin-wide flooding in large river systems. Exceptional heavy rains have led to extensive flooding of major rivers and lakes. The floods caused a toll of several hundred fatalities; nearly, one million people were evacuated. These events have demonstrated the need for continuing development of improved flood forecasting and warning systems.

Flash floods are events that occur in many parts of the world including arid regions, and they may cause potential hazards to human life and property. These

floods may rise rapidly due to hard rock cover catchments and move along the sand and gravel filed channels. The flood speeds are usually faster than a person can escape from the rough channels. Flash floods normally reach the sea or are lost in the inland deserts. However, they also help to fill the wadi alluviums that later provide groundwater recharge for local agricultural activities or partially for the nearby cities.

Flash floods occur more in arid and semiarid regions, where there are favorable conditions of steep topography, weak vegetation, and high intensity rainfall coupled with short durations. Especially, narrow wadis and settlement centers generate rapid runoff due to surface water speed increase and reduction in surface-layer permeability due to urbanization.
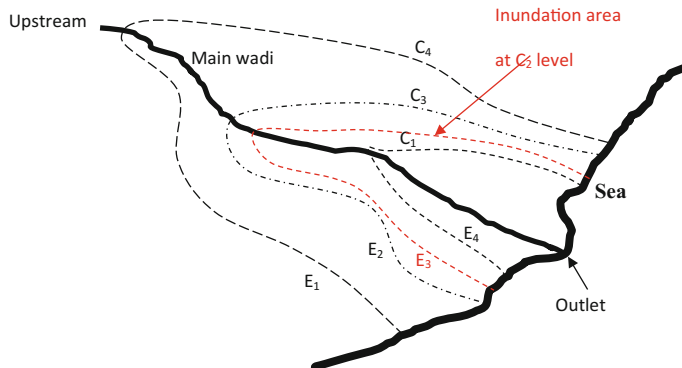
## 3.9 Flood Hazard Map Preparation

The main definition and measure of flood hazard potential damage are the flood probability (relative frequency) occurrences, which provide a basis for flood hazard map preparation in a region. The flood hazard is related especially to the flood risk, source area, rainfall intensity, and main drainage channels as pathways. The overall risk is a complicated function of individual risks.

The most important part of flood risk identification and management is the flood-prone area (extent) delineation. They areas are subject to inundation as a result of flooding with certain frequency. The flood-prone area determination requires considerable collection of historical data, accurate digital elevation and, discharge data, number of cross sections located throughout the watershed and morphometric analysis of basins.

Inundation map preparation necessitates the availability of drainage surface description means such as topographic maps, DEM data, or actual field surveying's. In order to construct the flood inundation map for a given drainage basin, first of all detailed and intensive elevation contour lines must be available at least along the major channels. It is preferable to have contour lines, if possible at every 0.5 m or 1 m intervals. In the preparation of flood inundation maps for coastal drainage basins and similarly the inland basins following steps are necessary.

(1) Identify the contour lines $(C_1, C_2, C_3, \ldots)$ at the flood inundation prone areas within the drainage basin, and its branches as shown in Fig. 3.27. Let the elevation of each contour line be denoted by $E_1, E_2, E_3, \ldots$, where $E_1 > E_2 > E_3 > . > . > .$,

(2) Measure the area enclosed by each contour and the coastal line, which includes the major channel with its apex on the main channel in the upstream or it extends on both sides of the channel. Hence, a sequence of areas is calculated as $A_1, A_2, A_3, \ldots$ It is obvious that $A_1 > A_2 > A_3 > . >$,

(3) Calculate the volume between successive areas by considering that subsequent pair of areas $(A_i$ and $A_{i+1})$ constitute the upper and lower bases of a trapezoidal

**Fig. 3.27** Contour areal extend

volume, as in Fig. 3.28. Here, $\Delta E_i$ is the elevation difference between two successive elevations, i.e., $\Delta E_i = E_{i+1} - E_i$.
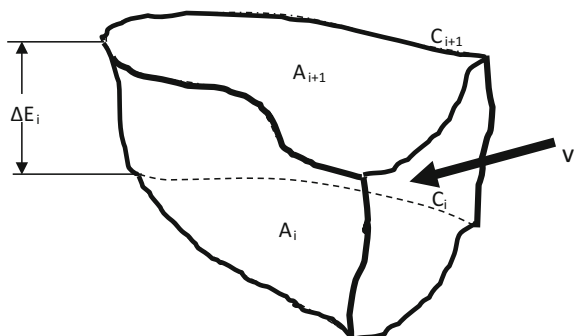
(4) The volume calculation can be achieved by the following trapezoidal space calculation,

$$v_i = \frac{A_i + A_{i+1}}{2} \Delta E_i \tag{3.28}$$

Hence, a sequence of volumes emerges, and let the notation of these volumes as $v_1 > v_2 > v_3 > \ldots$.

(5) In flood inundation calculations, each one of these volume is accumulated starting from the lowest contour elevation as,

**Fig. 3.28** Volume between contour lines
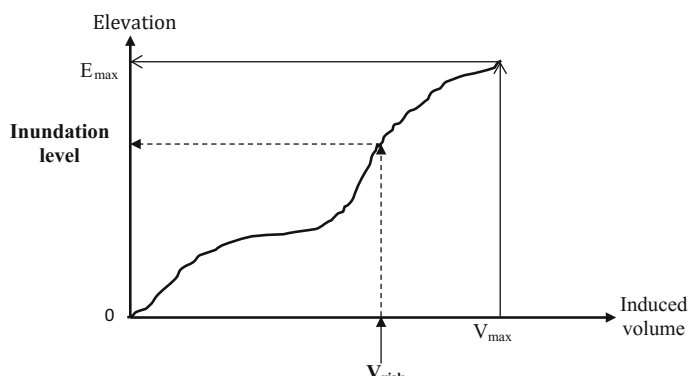
$$
\begin{aligned}
V_1 &= v_1, \\
V_2 &= V_1 + v_2 = v_1 + v_2, \\
V_3 &= V_2 + v_3 = v_1 + v_2 + v_3, \\
V_4 &= V_3 + v_4 = v_1 + v_2 + v_3 + v_4, \\
&\ldots\ldots\ldots \\
&\ldots\ldots\ldots\ldots \\
V_n &= V_{n-1} + \sum_{i=1}^{n} v_i
\end{aligned}
\tag{3.29}
$$

(6) Calculated the induced volumes, $V_{i1}, V_{i2}, V_{i3}, \ldots V_{in}$, which corresponds to the infiltration subtractions leading to,

$$
\begin{aligned}
V_{i1} &= V_1 - I_1, \\
V_{i2} &= V_2 - I_2, \\
V_{i3} &= V_3 - I_3, \\
V_{i4} &= V_4 - I_4, \\
&\ldots\ldots\ldots\ldots \\
&\ldots\ldots\ldots\ldots \\
V_{in} &= V_n - I_n
\end{aligned}
\tag{3.30}
$$

where $I_1, I_2, \ldots, I_n$ imply the infiltration volumes (Şen 2008)

(7) Plot on a Cartesian coordinate system cumulative volumes versus elevation on the vertical axis as in Fig. 3.29. This graph is referred as the flood inundation rating curve,



Fig. 3.29 Inundation rating curve
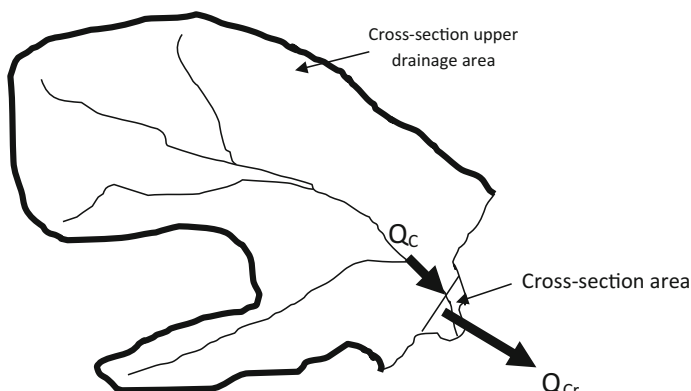
(8) Any hazard discharge prediction with a risk level is converted into volume, $V_{risk}$, and its entrance onto the horizontal axis (see Fig. 3.29) leads to corre-sponding inundation level reading on the vertical axis,

(9) Detection of the inundation level on the topographic map gives the inundation area corresponding to risk level. Implementation of the level on the topographic map as in Fig. 3.26 shows the boundaries of the inundation area.

## 3.10   Drainage Basin Flood System

In humid regions, it is possible to make predictions to a certain extent provided that the elements of the hydrological cycle are recorded. However, in dry regions, records are not available, and therefore, empirical and indirect ways are employed for the same purpose. The peak discharge over a drainage basin can be visualized by considering a cross section and its upstream drainage basin area features as in Fig. 3.30. In this figure, there are two quantities as the areas of the cross section and the upstream drainage basin.

For flood peak discharge and aftermath inundation areal extend inundation boundaries can be obtained through the execution of the following steps:

(1) The peak discharge, $Q_P$, must be calculated (Chaps. 2 and 5),

(2) The critical discharge, $Q_{Cr}$, that the cross section can allow to pass runoff water without any flood danger can be obtained from the rating curve by taking into consideration the bank-full level according to the guidance given in Sect. 3.7.2 Figs. 3.21 and 3.22,

(3) Comparison of these two discharge values helps to decide on flood, if $Q_T > Q_{Cr}$, otherwise there is no flood danger,



**Fig. 3.30**  Watershed flood elements

Cross section discharge concept model serves different purposes depending on the local situation. As in Fig. 3.31a, global flood hazard and the other one is given in Fig. 3.31b depending on a given risk level gradually. In practical applications, the global flood discharge is obtained after successive calculations for each risk level and corresponding peak discharge. In these calculations, the geometry of the flood discharge passage cross section plays the major role.
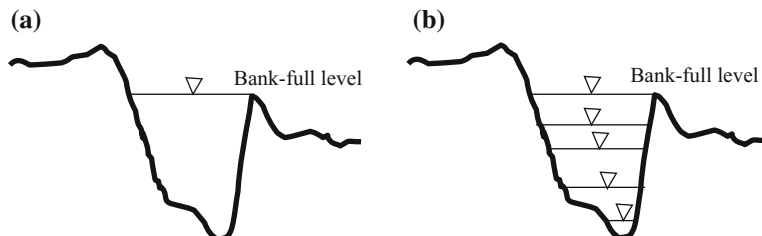
To check, whether $Q_P > Q_{Cr}$ is referred as the conventional flood calculation methodology (Kohler et al. 1948; Maidment 1983). This approach takes into account a theoretical pdf (Gumbel, Pearson and Log-Pearson II, etc.) for streamflow records (Chap. 6). However, it is not useful in arid and semiarid regions, where runoff records are not available.

Gradual flood inundation map calculation methodologies are very important especially for early flood warning systems. Inundation maps provide a common basis for local settlers, administrations, and shareholders for planning and managing land use share in a manner that the flood hazard will be the minimum.

## 3.11  Standard Hypsographic Curves (HC)
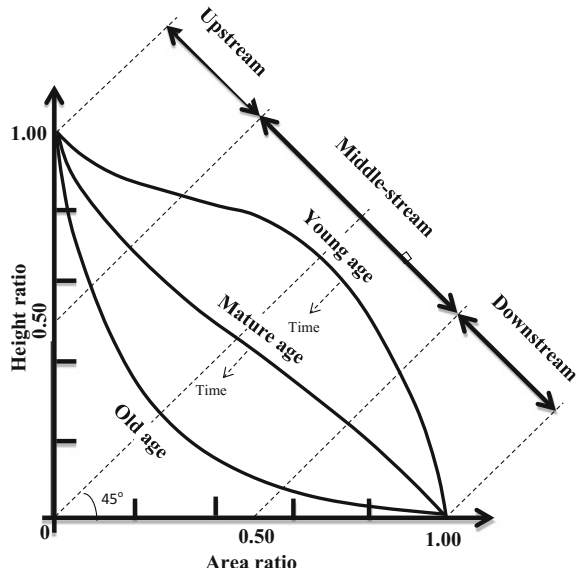
These curves represent the scaled down sub-area ratios of any drainage basin versus corresponding height ratios (Sect. 3.2.1). For this purpose, the sub-areas, $A_1, A_2, \ldots, A_n$ (heights $h_1, h_2, \ldots, h_n$) are divided by the total area, $A_T$, (the biggest height, $H_h$). This is referred as the standard HC as in Fig. 3.32. In a drainage basin, the HC construction starts from the highest elevation point, $H_h$, where the discharge value is equal to zero and descending toward the downstream lowest height, $H_o$, outlet point, where the discharge has the maximum value. In general, any drainage area reflects one of the three standard HC shapes in Fig. 3.32; either as "young," "mature," or "old" depending on the geological process throughout past million years. The evolution of any drainage basin is from the "young" to the "old" class by time.

Each HC can be classified also according to the upstream, middle stream, and downstream portions depending on the height classification. The shape of each standard HC helps to classify the geomorphological surface features and the



**Fig. 3.31** Flood discharge, **a** gross flood, **b** graduated flood

**Fig. 3.32** Different standard
HCs



possibility of hydroelectric power generation qualitatively. This classification pro-
vides preliminary general information about the hydropower potential at different
portions of a drainage basin as follows (Alahsan et al. 2016):

(1) Upstream: The height differences are comparatively lower in "young" (recent
    geological times) age HC than the other two and the biggest is in the "old" case.
    It is further possible to classify the upstream parts as "low," "medium," and
    "high" hydropower potentials at "young," "mature," and "old" HCs,
    respectively,

(2) Middle stream: The "young" age has more potential than its upstream portion;
    "mature" age remains almost the same, whereas the "old" HC has lower
    hydropower potential than its upstream portion. Although hydropower potential
    in case of "mature" HC remains the same, as the height decreases the "young"
    ("old") HC experiences hydropower potential increase,

(3) Downstream: The "young" age drainage basins have the highest hydropower
    potential; the "old" HC has the lowest potential, but the "mature" HC behaves
    as it was in the middle and upstream cases.

For example, the HC of the Euphrates and the Tigris rivers are in the "old"
category, compared to others within Turkish river basins (Şen 1999). Especially,
from agricultural point of view, the best locations are along the middle stream and
to a lesser extend at the downstream portions. The hydroelectric energy generation
plants are among the largest projects in the world.

## 3.12 Direct Hydrograph Catchment Feature Relationships

In case of simultaneous rainfall and runoff records absence, it is possible to derive empirical formulations on the rational and logical bases by consideration of various factors that affect the flood discharge. In general, the peak discharge, $Q_P$, is a function mainly of different factors including drainage area, $A$, main channel length, $L$, slope, $S$, centroid length, $L_c$, drainage density, $D_d$, and time of concentration, $t_c$, i.e., implicitly as a function, $Q_P = f(A, L, S, L_c, D_d, t_c)$.

In order to derive a general expression, the reader should be able to decide directly or inversely proportionality relationships between $Q_P$ each one of the factors. Table 3.3 indicates the pairs of relationships as increasing (decreasing) arrow for direct (inverse) proportionalities.

Each arrow indicates linear ($\nearrow$ is for directly and $\searrow$ is indirectly proportional) relationship, which is possible to arrive at logically, but rational and logical thinking cannot tell easily about the nonlinearity of these relationships. It is possible to combine collectively these effective variables on the peak discharge through suitable arithmetic operations, which leads generally to,

$$Q_p = \frac{\alpha A^\beta L^\gamma L_c^\delta}{S^\eta D^\lambda t_c^\nu} \tag{3.31}$$

where $\alpha, \beta, \gamma, \delta, \eta, \lambda$ and $\nu$ are the coefficients for taking into consideration the most general formulation, and each one of them represent nonlinearity possibility of the pairwise relationships. By taking into consideration, the unit of discharge as $[L^3/T]$ Eq. (3.31) reduces to its simplest form as,

$$Q_p = \alpha \frac{AL}{t_c} \tag{3.32}$$

This logical equation is used in the definition of the innovative methodology in Chaps. 4 and 5.

## 3.13 Drainage Area Discharge Approaches

Flood discharge measurement difficulties led the early researchers to seek for simply measurable quantities and relate them to flood peak discharge empirically. The earliest examples relate the flood peak discharge, $Q_P$, to the drainage area, $A$, in a directly proportional equation form. Different alternatives of such a formulation

**Table 3.3** Pairwise relationship

|        | A | L | $L_c$ | S | $D_d$ | $t_c$ |
|--------|---|---|-------|---|-------|-------|
| $Q_p$  | $\nearrow$ | $\nearrow$ | $\nearrow$ | $\searrow$ | $\searrow$ | $\searrow$ |

are suggested by various researchers. They yield flood peak discharge value without detailed information. Since they provide the same flood discharge value at different climate zones, they are not reliable. It is neither possible to calculate the return period nor the risk attachment to the discharge value.

Prior to the rainfall measurement instruments, the first examples of such formulations appeared in the Indian sub-continent and the flood peak discharge is related to the drainage area, $A$, in a nonlinear form as,

$$Q_P = C_1 A^{3/4} \tag{3.33}$$

If the unit of drainage area is in $km^2$, then the discharge is $m^3$/sec unit and the constant variation is suggested as, $10 < C_1 < 25$, which is dependent on the drainage area features on the one hand, and on the other, on the rainfall characteristics. On the average, one can adapt $C_1 = 15$, but as the slope of the drainage basin increases the peak discharge should also increase.

Similarly, some other formulations are also suggested by taking into consideration the distance of the drainage basin location to the sea coast and elevation.

$$Q_P = C_2 A^{2/3} \tag{3.34}$$

The average constant value is around 6.8. Table 3.4 includes detailed information.

In Fig. 3.33, the results from Eqs. (3.33) and (3.34) are presented for a set of parameter values. The results of Eq. (3.34) are rather close to each other, and for any given drainage area, its value is smaller than the previous formulation.

These graphs take the straight line form on a double logarithmic paper as shown in Fig. 3.34.
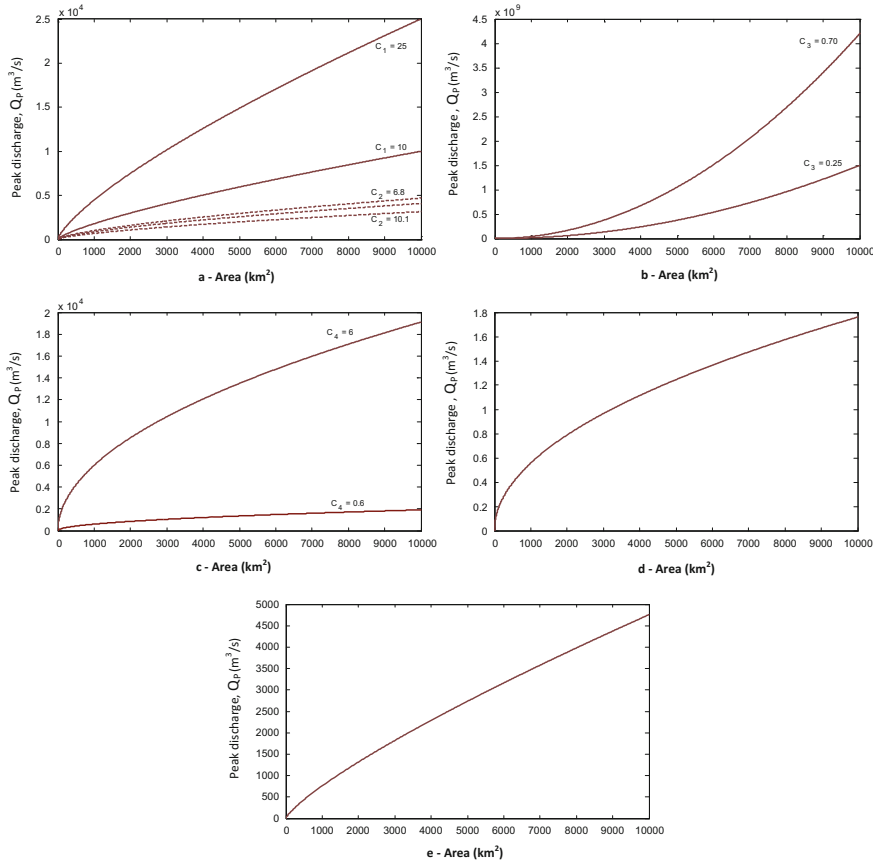
Similar to the above formulations, there are other approaches suggested by different researchers (Özer 1986).

$$Q_P = 60 C_3 \sqrt{A} \tag{3.35}$$

Herein, $C_3$ is a parameter that varies between 0 and 1. More specifically, it varies between 0.25 and 0.35 for plain areas; 0.35–0.50 for hilly areas; and 0.50–0.70 for mountainous areas. One can see that the relationship between the peak discharge and drainage area has a convex form opposite to the previous simple formulations (see Fig. 3.34b). Its means that as the drainage basin area increases, the increase in the flood discharge is bigger. Another formulation that takes into account the drainage area is given as follows:

**Table 3.4** Empirical constants

| Drainage area distance from the sea coast | $C_2$ |
|---|---|
| About 80 km | 6.8 |
| Between 800 and 2400 km | 8.8 |
| Limited areas under the effect of hills | 10.1 |
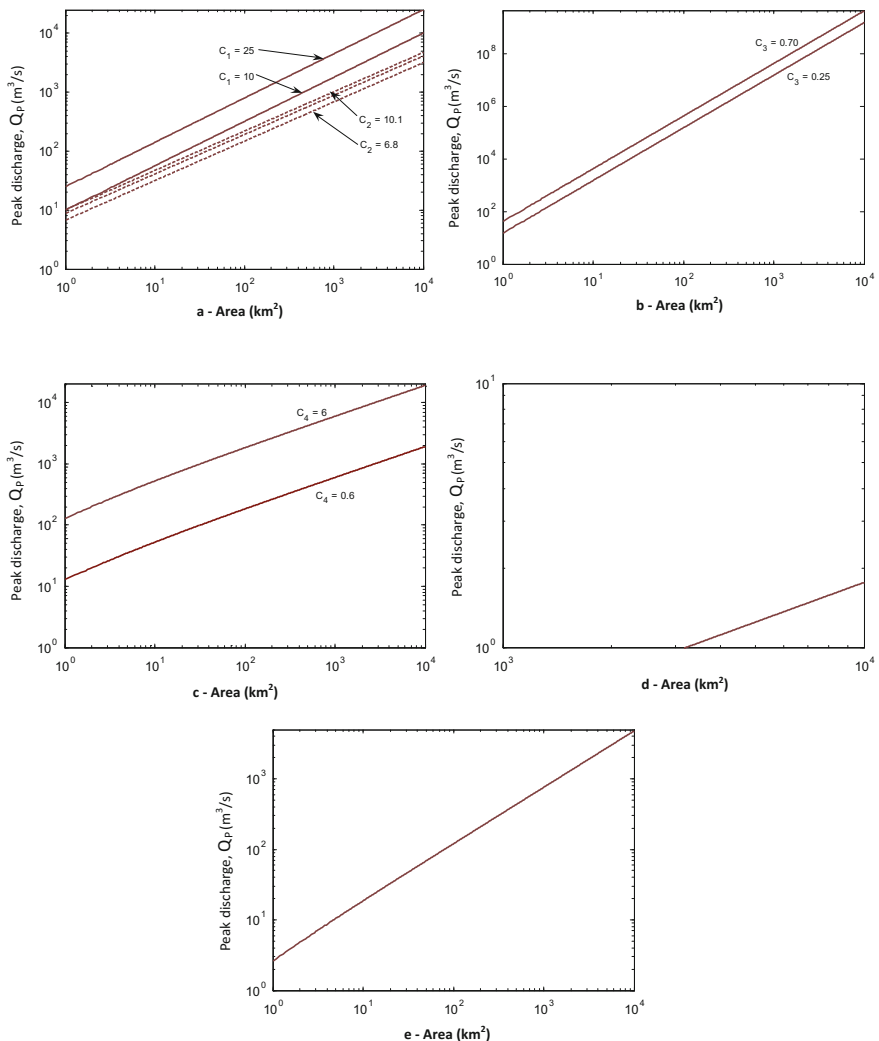
**Fig. 3.33** Flood peak discharge drainage area relationships

$$Q_P = \frac{32C_4A}{0.5 + \sqrt{A}} \tag{3.36}$$

where $C_4$ is a parameter that assumes values in the range, 0.6–6, and its graphical form is presented in Fig. 3.34c. It has concave curve similar to the first two formulations. Some other similar formulations are given as,

$$Q_P = 0.0176\sqrt{A} \tag{3.37}$$

**Fig. 3.34** Double logarithmic paper flood peak discharge drainage area relationships

or

$$Q_P = 3A/(1+A)^{0.29} \tag{3.38}$$

Their respective graphical forms are given in Fig. 3.34d and e.

Depending on the parameter values, some of the formulations have upper and lower boundaries as straight lines and others appear as a single straight line. It is

possible to express all the straight lines on a double logarithmic paper as a power function as,

$$Q_P = aA^b \tag{3.39}$$

This expression is used widely today in the world (see Chaps. 4 and 5). Determination of parameters $a$ and $b$ requires measurements. This last equation is the basic expression for fractal geometry (Mandelbrot 1992), and it represents all the drainage areas in the world. Fractal characteristic indicates that all the drainage basins show self-similarity to each other. In this expression, $b$ represents the slope of the straight line on double logarithmic paper and corresponds to the flood peak discharge value at $A = 1$ km$^2$ drainage area, i.e., the flood peak discharge for unit drainage area.

# References

Al-Abed, N., Al-Sharif, M. (2008). Hydrological modeling of Zarqa river basin –Jordan using the hydrologicalsimulation program –FORTRAN (HSPF) Model. *Water Resoures Management*, *22*:1203–1220.

Alashan, S., Şen, Z., & Toprak, Z. F. (2016). Hydroelectric energy potential of Turkey: a refined calculation method. *Arabian Journal for Science and Engineering*, Vol. *41*(4), 1511–1520.

Bernhardsen, T. (1999). *Geographic information systems: An introduction* (2nd ed.). New York: Wiley.

Bolstad, P. V., & Stowe, A. (1994). An evaluation of DEM accuracy: Elevation, slope, and aspects. *Photogrammetric Engineering and Remote Sensing, 60*(11), 1327–1332.

Burrough, P. A. (1986). *Principles of geographical information systems for land resources assessment*. Oxford: Clarendon Press.

Campbell, L. B. (2002). *Introduction to remote sensing* (3rd ed.). New York: The Guilford Press.

Chrysoulakis, N., Spiliotopoulos, M., Domenikiotis, C., & Dalezios, N. (2003). Towards monitoring of regional atmospheric instability through MODIS/Aqua images. In: *Proceedings of the International Symposium held at Volos*, (pp. 7–9). Greece.

Chorley, R. J., Malm, D. E., & Pogorzelski, H. A. (1957). A new standard for estimating drainage basin shape. American Journal of Science, Vol. *255*, 138–141.

Dein, M. A. (1985). *Estimation of floods and recharge volumes in wadis Fatimah, Na'man and Turabah. Unpublished M.Sc*. thesis, Faculty of Earth Sciences, King Abdulaziz University, Saudi Arabia, 127 pp.

Felicisimo, A. M. (1994). Parametric statistical method for error detection in digital elevation models. *ISPRS Journal of Photogrammetry and Remote Sensing, 49*, 29–33.

Felicisimo, A. M. (1995). Error propagation analysis in slope estimation by means of digital elevation models. In *Cartography Crossing Borders: Proceedings of the 17th International Cartographic Conference and 10th General Assembly of International Cartographic Association*, (pp. 9–94). InstitutCartogra®cdeCatalunya: Barcelona.

Hirano, A., Welch, R., & Lang, H. (2003). Mapping from ASTER stereo image data: DEM validation and accuracy assessment. *ISPRS Journal of Photogrammetry and Remote Sensing, 57*, 356–370.

Horton, R. E. (1945). Erosional development of stream & their drainage basin; Hydrogeological approach to quantitative morphology. Geological Society of America Bulletin, Vol. *56*: 75–370.

Jordan, G. (2003). Morphometric analysis and tectonic interpretation of digital terrain data: A case study. *Earth Surface Processes and Landforms, 28,* 807–822.

Kamp, U., Bolch, T., & Olsenholler, J. (2003). DEM generation from ASTER satellite data for geomorphic analysis of Cerro Sillajhuay Chile/Bolivia. In *Proceedings of ASPRS Annual Conference*, Anchorage, Alaska.

Leopold, L. B., et al., 1964). "Fluvial Processes in Geomorphology". W.H. Freeman and Company San Francisco and London.

Maidment, D. R. (1983). Handbook of hydrology. McGraw-Hill, New York.

Muller, A. B. (1974). Desalination by salt replacement and ultrafiltration. Desalination Research Report No. 1, Department of Hydrology and Water Resources, University of Arizona, Tucson.

Polis, G. A., Power, M. E., & Huxel, G. R. (Eds.). (2004). *Food webs at the landscape level*. Chicago: University of Chicago Press.

Sabins, F. F. (1997). Remote Sensing Principles and interpretation. (3rd ed., p. 448). W.H. Freeman and Company: New York.

Schmudde, T. H. (1968). "Floodplain". In R.W. Fairbridge (Ed.), "The Encyclopedia of Geomorphology". New York: Reinhold: 359–362.

Schumm, S. A. (1959). The relation of drainage basin relief to sediment loss. *International Association of Scientific Hydrology*, Vol. *36*, 216–219.

Şen, Z. (1999). Terrain topography classification for wind energy generation. *Renewable Energy, 16*(1–4), 904–907.

Şen, Z. (2008). *Wadi Hydrology* (p. 346). New York: Taylor and Francis Group, CRC Press.

Seyhan, E. (1977). *The Watershed as an Hydrology Unit*. Geografisch Instituut Transitorium II Heidelberglaan 2, Utrecht, Netherland.

Strahler, A. N. (1950). Equilibrium theory of erosional slopes approached by frequency distribution analyses, *American Journal of Science*, *248*, 673–696.

Strahler, A. N. (1964). Quantitative geomorphology of drainage basin and channel network. In VT Chow (Ed.), *Handbook of Applied Hydrology*, sec-4-II, McGraw Hill, New York.

Weibel, R, & Heller, M. (1991). Digital terrain modelling. In Goodchild M F, Maguire D J, Rhind D W (Eds.), G*eographical information systems:* p*rinciples and applications,*(Vol. 2, pp. 269–297). John Wiley & Sons Inc.: Harlow, Longman/New York.

Wood, J. D., & Fisher, P. J. (1993). Assessing interpolation accuracy in elevation models. *IEEE Computer Graphics and Applications, 13,* 48–56.

Welch, R. (1990). 3-D terrain modeling for GIS applications. *GIS World, 3*(5), 26–30.

# Chapter 4
# Hydrograph and Unit Hydrograph Analysis

**Abstract** In any flood prediction study, the most important tools are hydrographs that reflect the change of surface water flow discharge by time after each rainfall occurrence. These hydrographs are in the form of single peak curves, where the peak discharge value is one representation of the historical flood occurrences. In flood calculations, hydrograph concept and its various properties and features are important for successful applications. Various basic hydrograph concepts such as natural, unit, dimensionless, instantaneous, and synthetic are presented with relationships among them and the significance of each one for peak flood discharge calculations. Furthermore, starting from the simplest rational method for flood peak discharge calculation, various comparatively more sophisticated alternatives are also explained in detail among which are Snyder, the Soil Conservation Service (SCS), and geomorphological approaches. Finally, the most commonly used rational method irrationality is explained leading to innovative rational methodology for the first time in this book.

**Keywords** Instantaneous · Irrationality · Hydrograph · Geomorphologic Rational · Unit · Synthetic · Natural · Soil conservation service · Snyder

## 4.1 General

Hydrograph is a graph that shows the change of discharge by time at any cross section of a stream. Although discharge and time are the basic variables in hydrograph definition, the shape of the relationship between the two is dependent on geomorphologic features of the catchment (Chap. 3) as well as the shape of the hyetograph, which includes the change of rainfall intensity by time (Chap. 2). There are also spatial variations, but in hydrological studies, consideration of a cross section provides the temporal variations. In this chapter, the temporal discharge change by time is considered only. In general, a hydrograph has different portions, and the main purpose of this chapter is to indicate the elements of a hydrograph and their physical relationship to different hydrological variables.

Even though hydrograph can be obtained from measurements in a drainage basin, one may consider it as a natural response of the catchment, but still there are practical difficulties in its use such as the following. Any observed hydrograph is the result of a given specific rainfall hyetograph (Chap. 2, Sect. 2.6). In applications, most often the design engineer or hydrologist needs hydrographs for different water resource activities. Hence, the question is how to obtain hydrograph of desired rainfall intensity or preferably at a given risk level. Each hydrograph has specific natural rainfall duration, and if the hydrologists would like to know hydrographs with different durations, then a single observed hydrograph is not of any direct use. It is necessary to develop a procedure so that one can convert the observed hydrograph into another hydrograph with desired duration and rainfall intensity. For the same drainage basin, even if the rainfall duration, intensity, and areal coverage are the same, the resulting hydrographs are expected to be slightly different from each other due to the antecedent conditions in the drainage basin. Hence, the question is which one to choose or how to combine all the observed hydrographs so as to obtain a standard one for the applications. Each hydrograph at different cross section even along the same drainage basin channel is different from others due to topographical and geological conditions. Here, the question is how the successive hydrographs are related to each other in different cross sections along a channel.

All of these and similar questions can be answered if there is a unique and standard hydrograph for the drainage basin. This brings one to the idea of unit hydrograph (UH) concept where the derivation of which is either based on the observed hydrographs or in cases of unmeasured drainages, and empirical approaches are used through the relationships between the hydrograph features and the drainage basin geomorphologic characteristics (Chap. 3).

The main purpose of this chapter is to explain fundamentals of hydrograph and its various versions such as the unit, synthetic, dimensionless, and *S*-hydrographs.

## 4.2  Hydrograph
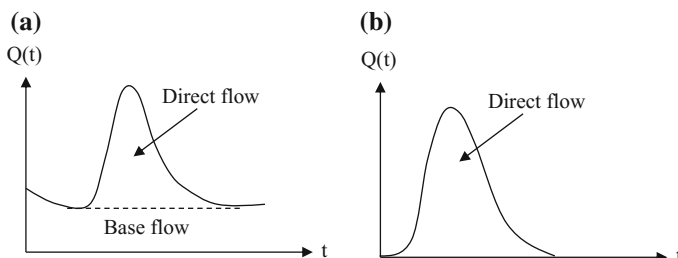
The general definition of cross section discharge has already been given in Chap. 3, Sect. 3.7.4. In the same chapter, the discharge is shown to be in directly proportional relationship with the cross sectional area and the average flow velocity as in Eq. (3.22). This indicates that for discharge calculation, the cross sectional area and the velocity of water are sufficient. Water velocity is different at different points on the cross section, and therefore, in the calculations, practically average velocity, $\bar{v}$, is taken into consideration.

In any hydrological study, the single most significant variable is the discharge at any cross section of a catchment. For humid regions, there are different analytical, empirical, field, and hybrid techniques for hydrograph identification, which should concentrate on the following natural and rational features.

(1) As long as there is surface water in any natural channel, there are temporal discharge variations depending on meteorological and geomorphological conditions,

(2) During non-rainy periods in humid regions, there is a base flow in the channel due to groundwater recharge. Most often such a base flow is missing in arid and semiarid regions,

(3) With the start of the storm rainfall after some time, the discharge in the channel starts to increase by time,

(4) After the stop of the storm rainfall, the discharge continues to increase for some time, but since there is no supporting rainfall for the surface water, it starts to decrease. Hence, after some time from the rainfall stop, there is a peak discharge value,

(5) After the peak discharge, the recession part of the hydrograph continues for some time and then returns to its natural base flow level depending on the groundwater recharge from the upstream parts of the cross section, if there is any contribution from the groundwater through springs,

(6) If successive peaks appear rather individually on a non-intermittent hydrograph, this is tantamount to saying that individual storms also appear in time succession.

In humid regions, hydrograph is always present (in rainy or non-rainy periods), but in arid and semiarid regions, it is rather simultaneous with the rainy periods and thereafter effects only. In humid regions, one can separate the hydrograph into two parts, namely non-rainy (base flow) and rainy (direct runoff) periods (Fig. 4.1a). Direct runoff is related to individual rainfall occurrences and it is an additional portion to the base flow. In general, in arid and semiarid regions, the base flow does not exist, and hence, the hydrograph reflects the direct flow discharge variation only (Fig. 4.1b).

In arid and semiarid regions, commonly, floods move down the channel network as flood wave over a bed that is either dry initially or has a small base flow. Hydrographs are typically characterized by extremely rapid rise over as little as 15–30 min. However, losses from the flood hydrograph through bed infiltration are important factors in reducing the flood volume as the flood wave moves
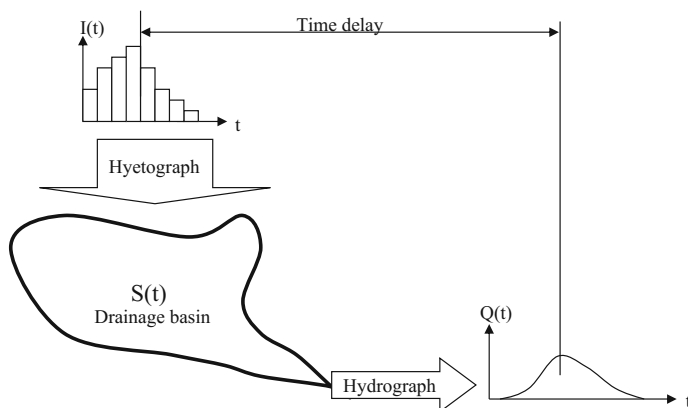


**Fig. 4.1** Hydrograph **a** humid region, **b** arid region

downstream. These transmission losses dissipate the flood and obscure the inter-
pretation of observed hydrographs. It is not uncommon that no flood is observed at
a gauging station when the upstream flood has been generated and lost to bed
infiltration.

In general, the hydrograph is an end result of hyetograph as the transformation of
rainfall into runoff according to watershed features (Fig. 4.2). Whatever the
regional descriptions are, as humid or arid, hyetograph exists for the rainy periods
only.
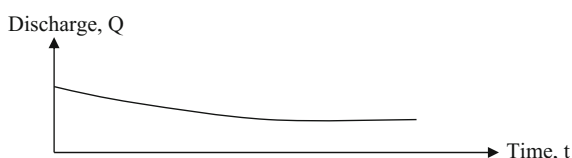
Rainy and non-rainy periods correspond to rising and recession limbs of a
hydrograph, respectively. There is a set of useful information for many water
resources planning and design that can be derived from a given hydrograph. These
are,

(a) In humid regions, the base flow reflects the contribution of springs (ground-
    water) during non-rainy periods. In general, base flow shows slight decrease
    with time in the form of a decreasing trend (see Fig. 4.3). The area of base flow
    indicates the total water volume that originates from springs,
(b) The area underneath the hydrograph apart from the base flow gives the total
    volume of surface flow generation from a single thunderstorm rainfall. This
    volume corresponds to excess rainfall amount, which is the remaining rainfall
    after subtraction of losses such as evaporation, infiltration, depression, and
    interception storages,



**Fig. 4.2** Catchment responses to precipitation
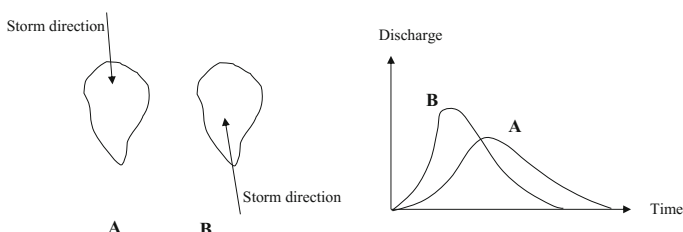
**Fig. 4.3** Hydrograph without
storm rainfall
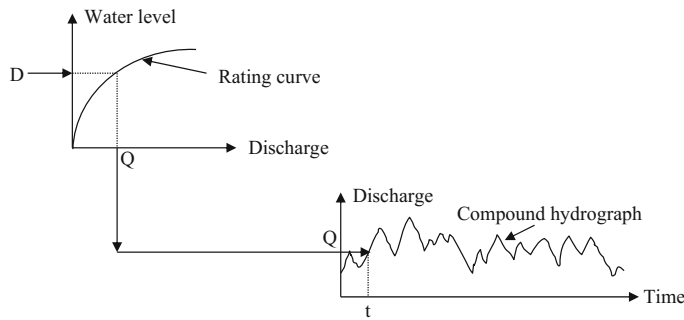
(c) If rainfall continues for long durations, the rising limb of the hydrograph reflects more rainfall volume directly. After the rainfall cessation, this limb continues to rise up to a peak discharge. The peaks of hyetograph and hydrograph are not simultaneous, but there is a time delay (lag) in the hydrograph peak with respect to hyetograph peak or centroid (see Fig. 4.2),

(d) The recession limb reflects the surface sheet flow (Chap. 2) into the channel after the rainfall cessation,

(e) The peak represents the maximum runoff discharge due to rainfall hyetograph, and it reflects the time needed for a raindrop to take from its fall onto the farthest point in the upstream to the outlet, which is the time of concentration (Şen 2010).

The shape of hydrograph is also related to direction of rainfall advancement. From the outlet point toward the middle stream and upstream, the recession limb starts earlier and peak discharge has greater value than stagnant rainfall event (see Fig. 4.4).

Although the spatial distribution of rainfall causes variations in hydrograph shape, in practice, the rainfall is considered as uniformly distributed as shown in Figs. 3.5 and 3.6. If the center of the storm is close to the basin outlet, a rapid rise, sharp peak, and rapid recession of the hydrograph are observable. If a larger amount of rainfall occurs in the upper reaches of a basin, the hydrograph exhibits a lower and delayed peak. The direction of storm movement with respect to orientation of the basin can also affect both the peak flow magnitude and the surface runoff duration. Storm direction has the greatest effect on elongated basins, whereas upstream moving storms tend to produce lower peaks of longer duration than storms moving toward downstream. Thunderstorms produce peak flows on small basins, whereas large cyclonic or frontal-type storms are generally dominant in producing major floods in larger basins. If spatial variability is small, the variation in the storm intensity over its duration is best presented by a rainfall hyetograph, as commonly applied in design practice. However, the assumption of spatially uniform rainfall is likely to be highly questionable, whereas localized thunderstorm rainfall predominates.



**Fig. 4.4** Rainfall direction effect on hydrograph

**Fig. 4.5** Hydrograph obtained from rating curve

In humid regions, rating curves (Chap. 3) can be obtained by field measurements and subsequent office calculations, whereas in arid regions, synthetic and empirical approaches become effective.
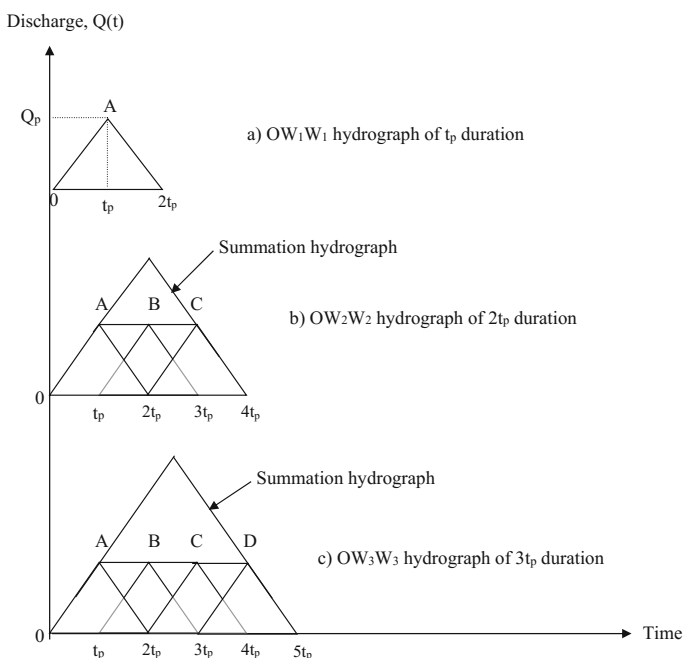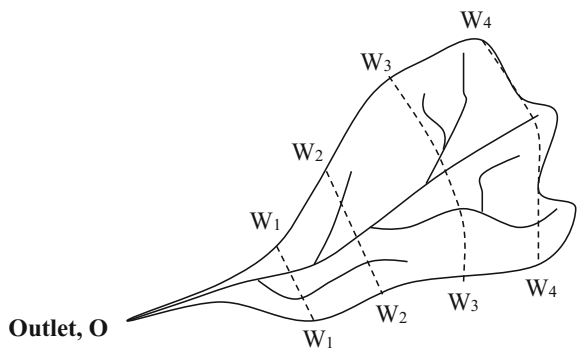
In arid regions, rating curves help to find discharge sequence corresponding to a set of runoff or flood depth measurements at different times in the cross section. Hence, the plot of the discharges versus time yields to a compound hydrograph as in Fig. 4.5.

## 4.3  Theoretical Storm Hydrographs

These are the productions of rational hydrograph derivations based on a set of mathematical and physical simplifications coupled with assumptions. In order to simplify the underlying physical basis of a hydrograph, it is convenient to idealize the natural phenomenon by rational thinking based on a scientific philosophy (Şen 2014). For this reason, let us assume that the entire watershed characteristics and the rainfall intensity are temporally and spatially uniform. The watershed area is also impervious with no losses, and the entire area is subjected to uniform excessive rainfall rate, $R_e$, of duration, $t_{re}$. Let us consider that the entire area is divided into 4 sub-areas by equal time of travel, $t_t$ contours ($W_1$, $W_2$, $W_3$, and $W_4$), which are also called as isochrones (Fig. 4.6).

The areas between the outlet and each isochrones within the water divide line have the upper boundaries as $W_1$-$W_1$, $W_2$-$W_2$, $W_3$-$W_3$, and $W_4$-$W_4$. With the rainfall, the first area, $OW_1W_1$, contributes to the outlet. Let us logically consider that this is the only area contributing to the outlet. The temporal rise in discharge, $Q(t)$, is from zero to its peak, $Q_P$, at time, $t_p$, and the following recession portion ends at zero discharge at time, $2t_p$, as shown at the top of Fig. 4.7. This is called herein as partial hydrograph because it is as a result of rainfall–runoff phenomena from the $OW_1W_1$ area only (see Fig. 4.7a). The runoff from $W_1W_1$ takes $t_p$ duration to reach the outlet.

**Fig. 4.6** Basic hydrograph concepts



**Fig. 4.7** Area partial hydrographs

The hydrograph from area $OW_1W_1$ results in the shape of a triangle. The peak discharge can be calculated simply from the principle that the area under the hydrograph is equal to sub-area, $A_1$, of $OW_1W_1$ multiplied by $R_e$, which leads to

$$Q_{P1} = \frac{A_1 R_e}{t_p} \tag{4.1}$$

The whole area contributes for $t_e = 2t_p$ duration at the outlet due to $t_p$ duration rainfall. Runoff from the $W_1W_1$ isochrones contributes at the outlet point from the end of the rainfall duration. The last drop of rain at the end of $t_p$ duration storm from the line $W_1W_1$ takes $t_p$ duration to reach the outlet. After this duration, the last drop of water from the isochrones $W_1W_1$ reaches outlet with zero runoff discharge. It must be noticed that the whole area contributes after $2t_p$ duration due to $t_p$ duration rainfall.

Now let us consider that $t_p$ duration rainfall covers the area between isochrones $W_1W_1$ and $W_2W_2$, which will contribute at the outlet until $4t_p$. The peak of this contribution will appear after $2t_p$ duration with the amount

$$Q_{P2} = \frac{A_2 R_e}{2t_p} \qquad (4.2)$$

If $2t_p$ duration rainfall is assumed over the whole $OW_2W_2$ sub-area, $A_2$, then the resulting outlet hydrograph is the large triangle in Fig. 4.7b.

Similar procedure indicates that $3t_p$ duration rainfall leads to hydrograph in the shape of triangle that is greater than the previous triangle (Fig. 4.7c). The peak discharge for this case can be given as,

$$Q_{P3} = \frac{A_3 R_e}{3t_p} \qquad (4.3)$$

All the catchment features are assumed to have the same effect at any point in time and space on the outlet hydrograph. The reader must visualize that in a natural situation, the triangles will appear as single-peaked curves.

## 4.4 Hydrograph Properties

In addition to what has been explained about the hydrographs, there is also relationship between hyetograph, hydrograph, and the watershed properties in the form of triple variables. In order to explain this situation, the following conceptual assumptions are helpful.

(1) The rainfall hyetograph belongs to a single storm that covers the whole watershed area, $A$,
(2) Rainfall height, $R_e$, is uniformly distributed over the whole watershed area during the rainfall duration, $t_{re} = t_b$,
(3) Rainfall and the runoff durations are the same, and hence, hydrograph has a single peak discharge, $Q_P$,
(4) There are no hydrological, morphological, topographic, and geologic variations in the drainage basin during very long time durations.

Under these assumptions, the rainfall hyetograph appears in the form of a rectangle and the consequent hydrograph is free of base flow as in Fig. 4.8.

The hydrograph has two parts with respect to peak discharge point. To the left is the rising limb and to the right is the recession limb. This direct runoff hydrograph has the following properties depending on rainfall intensity and watershed characteristics.

(1) Basin lag time ($t_L$): This is the time duration between the centroid of excess rainfall hyetograph and the peak discharge in the hydrograph,
(2) Peak time ($t_p$): This is the time duration from the beginning of excess rainfall to peak discharge,
(3) Time of concentration ($t_c$): This is the time duration between the end time of excess rainfall and the inflection point on the recession limb of the hydrograph. It is equivalent to time required for the raindrop that falls at the furthest upstream point of the watershed to reach the outlet point after the rainfall stops.

Under the light of the aforementioned assumptions, the subsequent total runoff volume, $V_R$, from a storm rainfall at the outlet point of a catchment is equal to the multiplication of the watershed area, $A$, by effective rainfall height, $R_e$ as,

$$V_R = AR_e \tag{4.4}$$
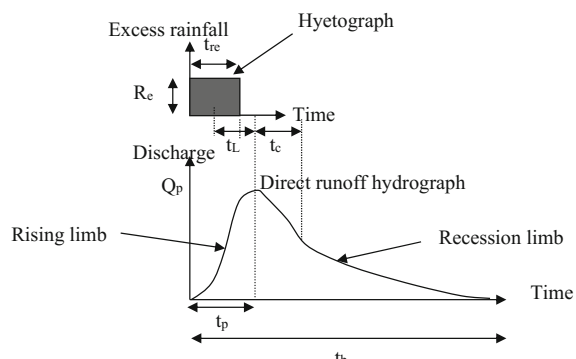
By considering the rainfall duration, $t_{re}$, the discharge at the outlet point can be obtained as,

$$Q = \frac{V_R}{t_{re}} = \frac{AR_e}{t_{re}}$$

As already mentioned in Chap. 2, the ratio of rainfall height to its duration is defined as the rainfall intensity, $I = R/t_{re}$, and hence, the last discharge expression can be written as,

$$Q = AI \tag{4.5}$$

**Fig. 4.8** Uniform rainfall hyetograph and hydrograph
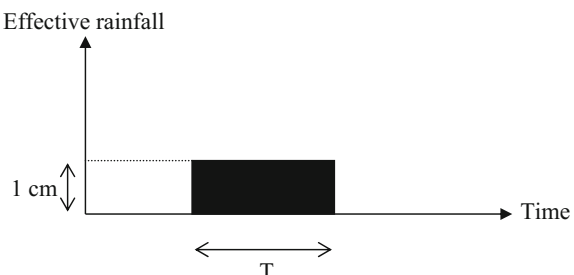
## 4.5   Unit Hydrograph Definition (UH)

This hydrograph is defined by Sherman (1931) as the unit pulse response function of a linear hydrological system, which results from unit height (1 cm) excess rainfall scatter uniformly all over the catchment area at a constant rate over effective rainfall duration, $T$. The word "unit" implies that the excess rainfall height is equal to 1 cm, however, it is sometimes mistakenly understood by beginners that it is unit time duration. Once the unit hydrograph duration is known, then it is possible to find any non-unit excess rainfall pulse response by principles of proportionality for the same duration and superposition property for digital folds of the basic excess rainfall duration. Under the light of these information, following hidden assumptions are within the concept of UH as,

(1) The excess rainfall is uniformly distributed over the whole drainage area during the effective rainfall duration. It is preferable to select short duration storm rainfalls because they are the most likely to produce an intense and nearly constant excess rainfall rate with well-defined single-peaked hydrograph of short time base (Chow et al. 1988),

(2) If the catchment area is not covered by more or less spatially uniform rainfall amounts, then the resulting hydrograph will not be representative. It might, therefore, be necessary to subdivide the area according to rainfall spatial uniformity into adjacent sub-areas,

(3) The base time of direct runoff hydrograph (response function) is greater than the effective rainfall duration $t_b > t_{re}$ and it is constant. The base time duration depends very much on the base flow separation procedure and therefore includes some uncertainty,

(4) The direct runoff hydrograph shape depends solely on the catchment morphological features. This corresponds to time invariance of the hydrological system, and therefore, the system parameters remain constant. These features also guarantee the proportionality and superposition principles.

If the effective rainfall height is equal to $R_e = 1$ cm over time duration, $T$, then the resulting hydrograph is referred to as $T$ duration UH. This indicates that there are different UHs for different durations. In other words, the hyetograph of a unit hydrograph appears as a rectangle shown in Fig. 4.9.



**Fig. 4.9** Effective hyetograph of unit hydrograph
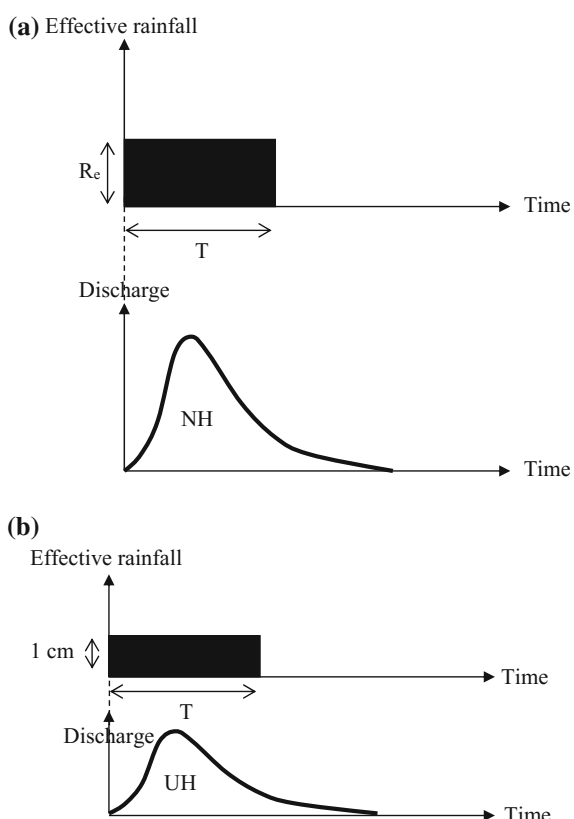
Description in this figure indicates the constant rainfall intensity as equal to 1/ $T$ (Chap. 2, Sect. 2.5). It also explains that the time distribution of effective rainfall is homogeneous and the corresponding hyetograph is in the form of a single rectangular block. On the other hand, the spatial distribution of the effective rainfall over the whole drainage basin is also assumed as homogeneous with uniform depth of 1 cm. It means that prior to the runoff the whole catchment area is covered with water layer of 1 cm thickness. This implies that the total UH volume, $V_{UH}$, is equal to the multiplication of the watershed area, $A$, by effective rainfall height which is 1 cm,

$$V_{UH} = 1 \times A = A \tag{4.6}$$

In practical use of this equation, the units of variables must be considered with care. Equation (4.6) indicates that the area under the UH is equivalent to the volume of effective rainfall over the whole area. As mentioned before, the area under the natural hydrograph is equal to the multiplication of the watershed area by effective rainfall height. These last two statements logically lead to the conclusion that in order to obtain from a given natural hydrograph its corresponding UH, it is sufficient to divide all the ordinates by the effective rainfall height, $R_e$. Figure 4.10 presents a natural hydrograph (NH) with its corresponding UH.



Fig. 4.10 a NH and b UH

In the mathematical sense, the division of NH coordinates by effective rainfall height, $R_e$, is called as the "proportionality" property. Hence, the UH of a given NH is similar in shape with the only difference in the vertical scale without any change in the horizontal axis time values. All the vertical quantities of NH and its corresponding hyetograph are divided by $R_e$ so as to obtain the UH and its corresponding hyetograph as shown in Fig. 4.10b. Accordingly, the vertical scale of the effective rainfall also changes and becomes equal to 1 cm.
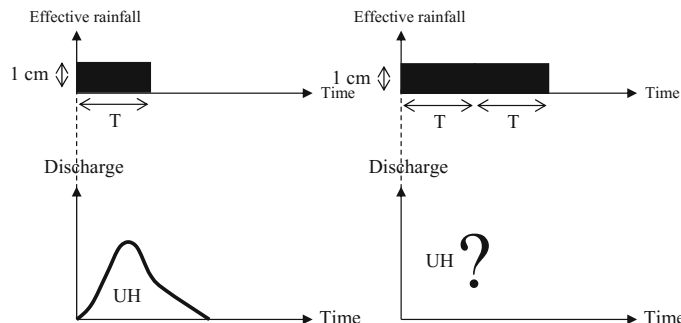
The reverse transformation is also applicable, in that given a UH, it is possible to obtain the corresponding NH of any effective rainfall height, $R_e$. In this case, all the UH vertical ordinates (discharges) are multiplied by effective rainfall height.

In practice, it is not possible to find NH and UH with the same duration, and therefore, it is necessary to find a way to change the time axis values also. Hence, the question is how to obtain NH of any effective rainfall duration if the UH with different effective rainfall duration is available or vice versa. It is necessary to find some other principle than proportionality for the answer. The question can be viewed in two parts as whether the desired duration is a digital fold of the basic UH duration (as $2T$, $5T$, etc.) or it is a decimal fold (as $1.5T$, $0.6T$, etc.). The answer is easy if the desired duration is a digital fold of $T$. Let us look at Fig. 4.11, where on the left-hand side is the UH and on the right-hand side although the effective rainfall duration is given as twofold of the basic UH duration, the UH for this double duration, $2T$, is not known? How to find the double duration UH from the given information?

Although $2T$ duration effective rainfall UH is not known, the UHs are known separately for each basic time duration, $T$, as in the first four graphs in Fig. 4.12.
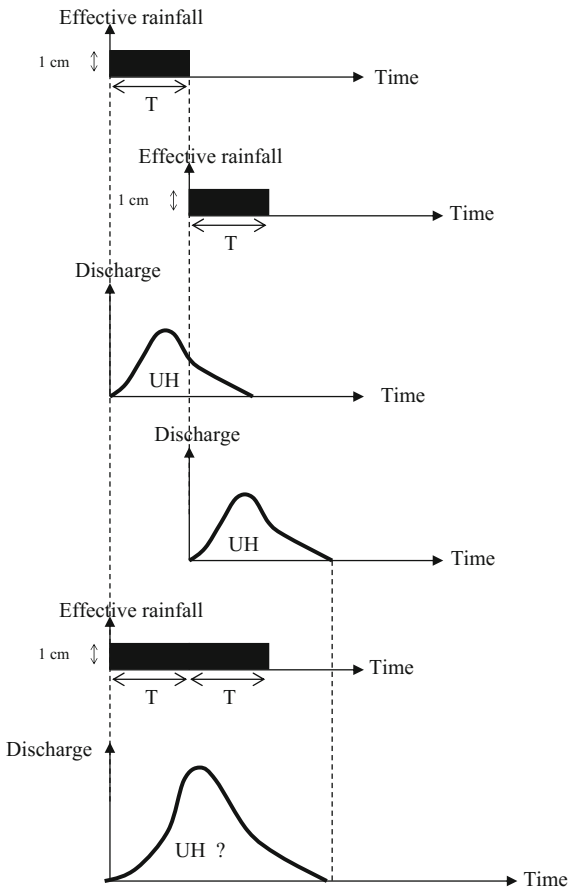
Let us now ask the question, whether the final hydrograph is indeed UH? In order to answer this question, the golden rule of "the volume," $V_{UH}$, (the area under the UH) must be equal to the catchment area (see Eq. 4.6). If $V_{UHT} \neq A$, then the ordinates of hydrograph are multiplied by the ratio, $V_{UH}/A$.

Logically, the resulting hydrograph from double duration effective rainfall is the summation of two ordinates of the same time duration UHs, but by one time, $T$,



**Fig. 4.11**  Unit hydrograph and double duration unit hydrograph

**Fig. 4.12** Double duration
UH from single duration UH



shift as in the first two graphs in Fig. 4.12. It is now possible to generalize the procedure for *n*-fold duration (*nT*) effective unit rainfall as follows.

(1) Draw the basic UH,
(2) Shift the same UH *n* times below the similar graph to the graph in Fig. 4.12,
(3) Sum the ordinates of these shifted UHs,
(4) Check whether the area under the summed hydrograph is equal to the watershed area,
(5) If the area under the hydrograph is not equal to the watershed area, use the proportionality principle as mentioned above, and hence, obtain the UH of *n*-fold duration effective rainfall.

### 4.5.1  UH Limitations
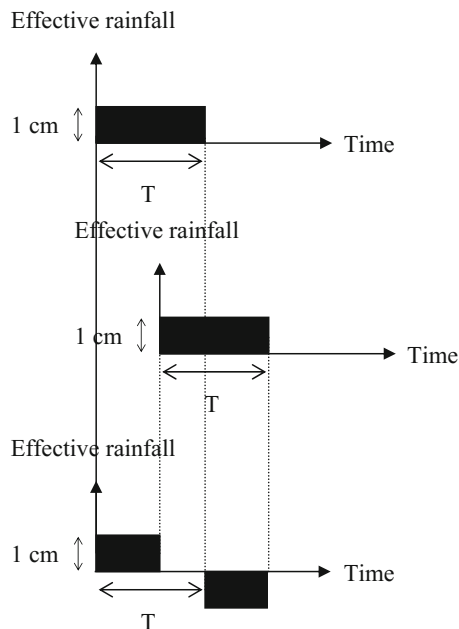
In practice, there are some restrictive assumptions that limit the application of UH in hydrological design and flood assessments.

(1) Due to the uniform spatial rainfall distribution over the whole watershed area, the UH derivations are not reliably valid for areas more than 5000 km$^2$. For such regions, suitable sub-areas must be selected for UH application. Also, the lower limit for the application of UH is 2 km$^2$,

(2) The shape of the catchment area is also important, and the UH approach is not valid for very long watersheds,

(3) The UH method is valid for rainfall occurrences, but other types of precipitation such as snow cover is not considered at all in the UH derivation,

(4) The duration of excessive rainfall must be about 20–30% of the basin lag (concentration) time for reliable results,

(5) In cases of big storages such as dams, especially surface storage, the UH must not be derived for applications,

(6) The spatial distribution of the rainfall must not be very different from location to others over the catchment area,

(7) Total effect of rainfall intensity variation cannot be accounted by the use of UH.

## 4.6  S-Hydrograph and Decimal-Fold Duration UH

As explained in the previous sections, the shifting, proportionality, and the summing (superposition) rules produce different scale direct runoff hydrographs and UHs, but the question still remains for decimal-fold effective rainfall durations. At this junction, it is logical to ponder that if infinitesimally small time UH is known, then by the previous procedural approach, one could obtain any desired duration UH with desired duration by shifting and superposition (summation, integration). Such a hydrograph is referred to as the instantaneous UH (IUH). It is, therefore, necessary to obtain IUH for general use. The shape of IUH will appear similar to Fig. 4.10b with infinitesimal duration, $\Delta T$, and effective rainfall height equal to 1. Let us try to obtain decimal duration, $T_D$, UH from a UH of duration, $T$. Consideration of what have been said above leads to such a UH according to the following steps.

(1) Draw the UH,

(2) Draw the same UH after the time shift of $T_D$ as in Fig. 4.13,

(3) Subtraction of the shifted UH from the first one will lead to implausible conclusion such that the effective rainfall will have two parts at $T_U - t_u$ apart with negative values.
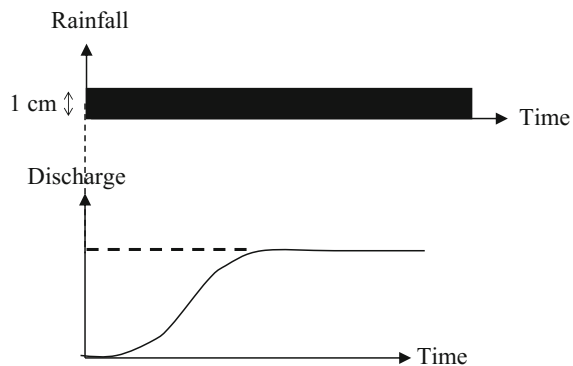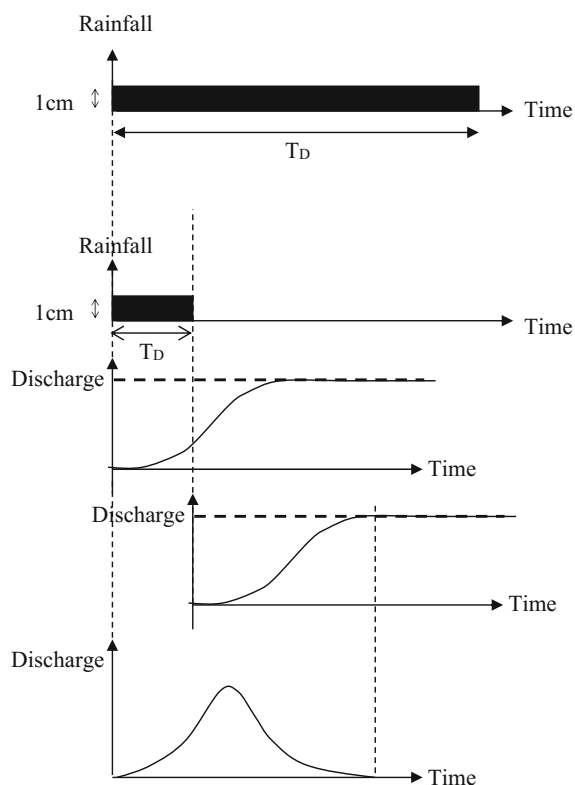
**Fig. 4.13** UH subtraction



Effective rainfall

As a conclusion, this procedure cannot yield IUH. Hence, the aforementioned hydrograph principles do not function. In order to get rid of such implausible results, let us first obtain infinite duration UH. For this purpose, one can shift the given UH as many times as possible. There is a practical upper limit for the number of shifts, because after a certain number, the summation of the shifted UHs peak discharge of the resulting hydrograph will reach to a constant value, and any further shifting operation does not bring additional increment. Hence, one should continue shifting until the constant hydrograph peak value attained as in Fig. 4.14. The reader is asked to ponder about the final result of the hydrograph, which appears in the form of an *S*-curve, and therefore, this is called an *S*-hydrograph in the hydrology literature.

If the shifting operation is applied to the *S*-curve, it is possible to obtain decimal duration, $T_D$, effective rainfall UH as in Fig. 4.15.

After the shifting operation, if both effective rainfall blocks and corresponding *S*-hydrograph are subtracted from each other, the result will be a unit effective rainfall height over $T_D$ duration. The question is whether this hydrograph is a UH. It must be checked from two points of view.

(1) Effective rainfall check: The *S*-hydrograph is obtained from *T* duration UH, and therefore, the rainfall intensity is $1/T$, but the effective rainfall height of the subtracted hydrograph is $T_D/T$, which is not equal to unit height. This indicates that the final hydrograph is not yet a UH. However, it can be converted into a UH after dividing the ordinates by $T_D/T$. This is to say that *T* duration UH ordinate, $Q(T, t)$, at any time instant, *t*, is calculated as,

**Fig. 4.14** *S*-hydrograph



**Fig. 4.15** Any desired duration $T_D$ hydrograph



$$Q(T,t) = \frac{\Delta S}{T_D/T} \qquad (4.7)$$

(2) Watershed area check: The area under the UH should equal the area of the watershed. If it is not, the hydrograph must be adjusted to this level. For this

purpose, the area under the hydrograph is calculated, $A_U$, and if it is not equal to the watershed area $A$, then all the coordinates must be multiplied by $A/A_U$.

## 4.7   Instantaneous Unit Hydrograph (IUH)

This concept is already explained in the first paragraphs of the previous section. It is understood that UHs are named according to their excess rainfall duration. The smaller the duration, the more close the UH peak to the vertical axis; hence there is a shift toward the left. In the limiting case, for infinitesimally small duration, rainfall event with 1 cm of excess rainfall is spread over the catchment uniformly and instantaneously, and hence, the resulting direct runoff hydrograph is referred to as IUH. This concept is used to investigate rainfall–runoff process of a basin theoretically because it is not possible for a basin to get rainfall excess of 1 cm in zero time duration. The advantage of IUH is the elimination of effective rainfall duration. Any hydrograph is always attached with its productive effective rainfall duration. However, as explained in the previous section, *S*-hydrograph may give effective rainfall hydrograph with any desired duration. In Eq. (4.7), $1/T$ indicates the rainfall intensity, $i$, and hence, it can be rewritten as,

$$Q(T,t) = \frac{\Delta S}{iT_D} \qquad (4.8)$$

If the time duration is also taken as an infinitesimal, $\Delta t$, then one can write

$$Q(T,t) = \frac{\Delta S}{i\Delta t} \qquad (4.9)$$

By considering that for $T \to 0$, $i = 1$, this expression takes the following form
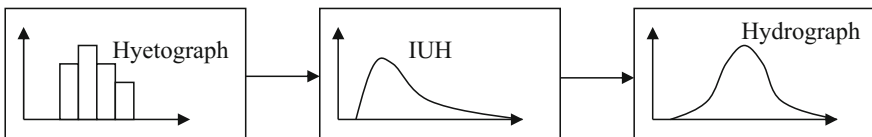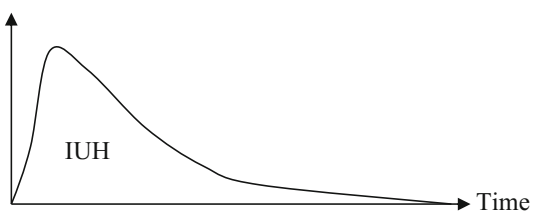
$$Q(0,t) = \frac{dS}{dt} \qquad (4.10)$$

this indicates that the IUH can be obtained by the derivative of *S*-hydrograph. Such a hydrograph is shown in Fig. 4.16 where the peak discharge is very close to the vertical axis and there is no effective rainfall duration for the hydrograph. This is the only hydrograph type which does not have any time duration attachment.

It is the hydrograph of unit effective rainfall intensity that is supposed to fall over the whole watershed area instantaneously. In the triple relationship of black box system similar to Fig. 4.17, the UH plays the role of identification, and hence, transformation of the input effective rainfall hyetograph $I(t)$ into output as a hydrograph.

**Fig. 4.16** Instantaneous UH



**Fig. 4.17** Black box model

The properties of IUH are,

(1) The ordinates are always positive for any time, $t$,
(2) For negative time instances, the ordinates are equal to zero,
(3) For large time instances, the ordinates approach zero,
(4) The area under IUH is equal to the unit rainfall excess depth over the catchment,
(5) The integration of IUH, $U(t)t\mathrm{d}t$, is the time lag, which is the time interval between centroids of effective rainfall hyetograph and direct runoff hydrograph,
(6) Time to peak in the IUH is always less than the time to centroid of the IUH.

## 4.7.1  IUH Derivation

It is possible to obtain a hydrograph by subtraction of two $S$-hydrographs separated $\mathrm{d}t$ duration apart. The ordinates of this hydrograph are divided by $\mathrm{d}t/T$, where $T$ is the basic time duration of UH. The result is $\mathrm{d}t$ hour duration UH for the watershed. If two $S$-hydrograph ordinates are $S_1$ and $S_2$, then $\mathrm{d}t$ hour UH ordinates are given as,

$$\frac{S_1 - S_2}{\mathrm{d}t/T} = \frac{S_1 - S_2}{i\mathrm{d}t} \tag{4.11}$$

where $i = 1/T$ (cm/hr) rainfall intensity for the UH. As d$t$ goes to infinitesimally small value, this ratio approaches to
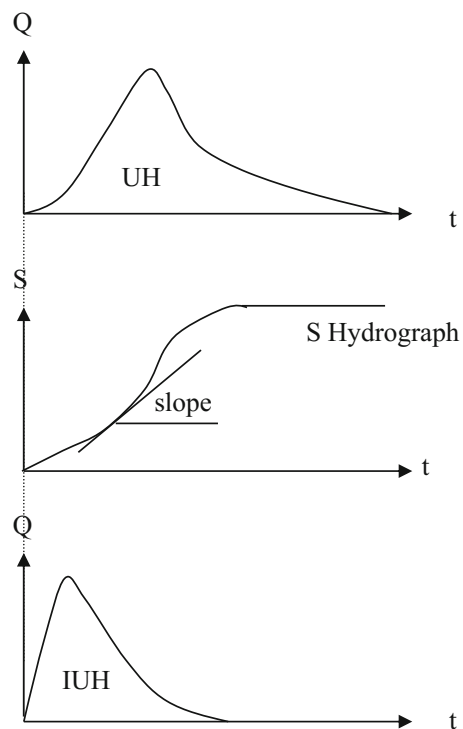
$$\frac{dS}{i dt} \tag{4.12}$$

Additionally, if $i = 1$ cm/h, then the IUH ordinate becomes

$$U(t) = \frac{dS}{dt} \tag{4.13}$$

It means that the ordinates of IUH at any time, $t$, is the derivative of UH at this time instant as shown in Fig. 4.18.

**Fig. 4.18** Hydrograph, UH, and IUH relationship

## 4.8    Dimensionless Unit Hydrograph (DUH)

As mentioned in the section on the natural hydrographs, among the significant hydrograph quantities are the peak discharge, $Q_P$, and time to peak, $t_p$. It is possible to convert the basic UH into a dimensionless form after dividing its ordinates by $Q_P$ and abscissa by $t_p$. In this manner, DUH form is obtained as shown in Fig. 4.19.
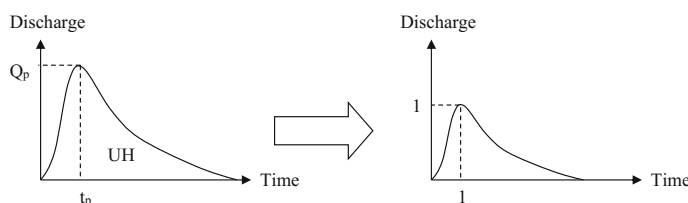
This shape is similar to the basic UH. Dimensionless UH can be used for obtaining first the UH provided that for a watershed area, the peak discharge, $Q_P$, and time to peak, $t_p$, are calculated in some manner as explained in the following section. Their empirical calculations are sufficient for obtaining the UH and onwards the design storm hydrograph. The DUH will be elaborated more in Chap. 5.

DUHs are derived from watershed characteristics rather than measured rainfall and runoff data, which are not frequently available especially in arid and semiarid zones. The two-parameter Gamma PDF is most commonly used in various forms depending on the smooth and single peak valued shape of hydrographs. For instance, using the concept of IUH, Nash (1958, 1959a, b) and Doodge (1959) derived the Gamma distribution-like hydrographs from the cascade of linear reservoirs. Depending on the data availability Croley (1980) and Aron and White (1982) derived the two parameters of the Gamma PDF, which are useful in deriving a DUH. For ungauged catchments such as the wadis in the arid regions, the two-parameter Gamma PDF provides the complete shape of the UH. Singh (1988) and Bhunya et al. (2003) stated that it is possible to obtain the parameter estimations from geomorphological characteristics of the catchment (Chap. 5).
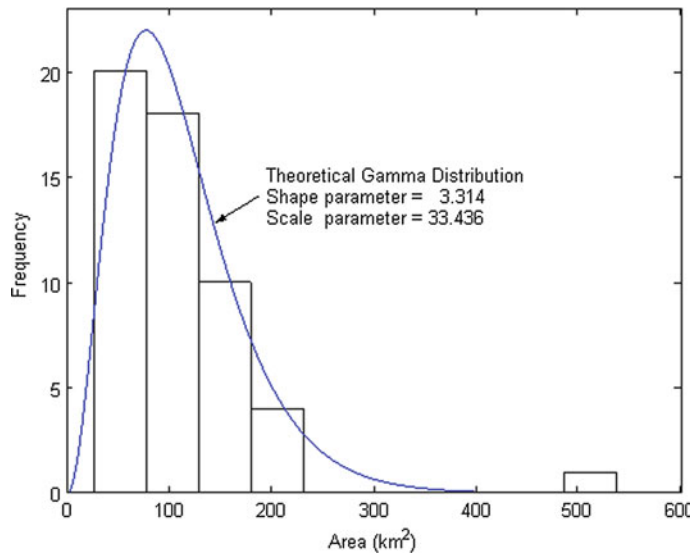
The basic assumption is that the whole hydrograph ordinates are dependent on the sub-basin area. Therefore, the shape of the hydrograph is expected to be similar to the relative frequency distribution of the catchment areas. Figure 4.20 shows the relative frequency distribution of wadi sub-catchments.

After the Gamma PDF assumption, the dimensionless UH coordinates are presented in Table 4.1. In order to find the dimensionless UH, the discharges and times are divided by the peak discharge and time to peak, respectively.

The most widely used one is due to SCS and the necessary values of SCS DUH are presented in Table 4.2.



**Fig. 4.19**  Dimensionless unit hydrograph

**Fig. 4.20** The two-parameter Gamma distribution function

**Table 4.1** Dimensionless SGS UH coordinates
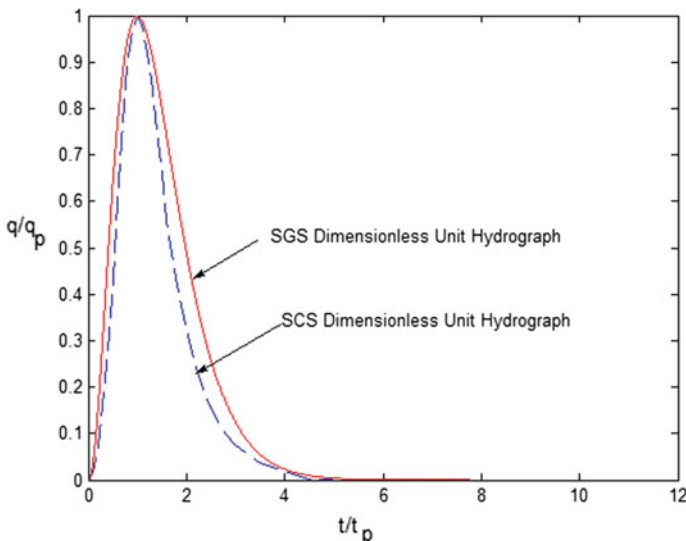
| $t/t_b$ | $q/q_b$ | $t/t_b$ | $q/q_b$ | $t/t_b$ | $q/q_b$ | $t/t_b$ | $q/q_b$ |
|---|---|---|---|---|---|---|---|
| 0 | 0 | 3.4974 | 0.0558 | 1.8135 | 0.6019 | 5.3109 | 0.0022 |
| 0.1295 | 0.0662 | 3.6269 | 0.0449 | 1.9430 | 0.5232 | 5.4404 | 0.0017 |
| 0.2591 | 0.2439 | 3.7565 | 0.0361 | 2.0725 | 0.4500 | 5.5699 | 0.0013 |
| 0.3886 | 0.4617 | 3.8860 | 0.0289 | 2.2021 | 0.3836 | 5.6995 | 0.0011 |
| 0.5181 | 0.6655 | 4.0155 | 0.0231 | 2.3316 | 0.3244 | 5.8290 | 0.0008 |
| 0.6477 | 0.8263 | 4.1451 | 0.0184 | 2.4611 | 0.2724 | 5.9585 | 0.0006 |
| 0.7772 | 0.9335 | 4.2746 | 0.0147 | 2.5907 | 0.2272 | 6.0881 | 0.0005 |
| 0.9067 | 0.9880 | 4.4041 | 0.0117 | 2.7202 | 0.1885 | 6.2176 | 0.0004 |
| 1.0000 | 1.0000 | 4.5337 | 0.0092 | 2.8497 | 0.1555 | 6.3472 | 0.0003 |
| 1.1658 | 0.9701 | 4.6632 | 0.0073 | 2.9793 | 0.1277 | 6.4767 | 0.0002 |
| 1.2953 | 0.9171 | 4.7927 | 0.0058 | 3.1088 | 0.1044 | 6.6062 | 0.0002 |
| 1.4249 | 0.8471 | 4.9223 | 0.0045 | 3.2383 | 0.0850 | 6.7358 | 0.0001 |
| 1.5544 | 0.7676 | 5.0518 | 0.0036 | 3.3679 | 0.0690 | | |
| 1.6839 | 0.6844 | 5.1813 | 0.0028 | | | | |

The graphical representations of the Saudi Geological Survey (SGS) (As-Sefry et al. 2004) and American Soil Conservation Service (SCS 1971, 1986) UHs are given in Fig. 4.21.

It is obvious that the SGS dimensionless UH follows closely the SCS dimensionless UH, but SGS has longer high discharge flow tail than SCS. Conversely,

**Table 4.2** SCS DUH values

| $t/t_p$ | $Q/Q_p$ | $t/t_p$ | $Q/Q_p$ |
|---------|---------|---------|---------|
| 0.00 | 0.000 | 1.80 | 0.420 |
| 0.20 | 0.075 | 2.00 | 0.320 |
| 0.40 | 0.280 | 2.50 | 0.220 |
| 0.60 | 0.600 | 2.75 | 0.155 |
| 0.80 | 0.900 | 3.00 | 0.075 |
| 1.00 | 1.000 | 3.50 | 0.036 |
| 1.20 | 0.920 | 4.00 | 0.018 |
| 1.40 | 0.750 | 4.50 | 0.009 |
| 1.60 | 0.560 | 5.00 | 0.004 |



**Fig. 4.21** SCS and SGS dimensionless UHs

SGS graph has more discharge values along the recession limb. These are the features, which make the use of SCS approach rather inconvenient for arid regions such as the Kingdom of Saudi Arabia. It is not necessary that the area under the dimensionless UH is equal to one, which is the property of a UH only.

The of DUH expresses the UH discharge, $Q_t$, as a ratio to the UH peak discharge, $Q_p$, for any time $t$, a fraction of $t_p$, the time to UH peak. Different DUHs are available in the literature.

Research by the SCS suggests that the UH peak and time of UH peak are related as

$$Q_\mathrm{p} = C\frac{A}{T_\mathrm{p}} \tag{4.14}$$

where $A$ is the watershed area, and $C$ is the conversion constant equal to 2.08 in metric system. The time of peak is related to the unit excess precipitation duration as,

$$t_\mathrm{p} = \frac{\Delta t}{2} + t_\mathrm{lag} \tag{4.15}$$

where $\Delta t$ is the excess precipitation duration, and $t_\mathrm{lag}$ is the basin lag, defined as the time difference between the center of rainfall excess mass and the peak of the UH (see Fig. 4.8).

DUH lag can be estimated via calibration for gauged headwater sub-watersheds. For ungauged watersheds, the SCS suggests that the UH lag time may be related to time of concentration, $t_\mathrm{c}$, as,

$$t_\mathrm{lag} = 0.6t_\mathrm{c} \tag{4.16}$$

## 4.9  Synthetic Hydrographs (SH)

These are mostly empirical and obtained for specific regions with the consideration of many natural hydrographs. Although the SH can be used for the region they are derived first, due to similarities in climate and hydrological features, they are also used in many parts of the world. Unfortunately, their blind uses lead to invalid conclusions, but these inconsistencies are not noticed by practicing engineers and hydrologists alike and even in the academic circles. It is, therefore, advised in this book that prior to the use of any synthetic or empirical approach, the underlying assumptions and conditions must be noticed for a successful application.

In many watersheds of the world, direct measurement of surface flow is not possible due to various reasons. The most important reason is that the watershed area might be considered for development in the past, but currently, it might become important for some other activities. In the case of such unmonitored watersheds, it is necessary to relate some significant properties of the hydrograph to a set of measurable watershed geomorphologic features such as the area, main channel slope and length, etc. (Chap. 3). Any hydrograph that is obtained with such empirical relationships is referred to as the SH. In the following, SHs are explained as suggested by different authors with basic reasons and fundamentals. Two innovative SH derivation methodologies are developed in this book and presented in Chaps. 7 and 8.

### 4.9.1  Snyder Method

This is an empirical approach that has been developed for USA in the region of Appalachian mountainous drainage basins. The method relates time to peak and the peak discharge quantities to the geomorphologic features of the drainage area. Once these two quantities are obtained by some means, then the SH is constructed by either from DUH concept or by some simple procedures such as triangular UHs. Snyder (1938) expressed time to peak, $t_p$, as a function of the main channel length, $L$, the distance between the projection of the watershed area centroid on the main channel and the outlet point, $L_c$ as,

$$t_p = C_t (LL_c)^{0.3} \tag{4.17}$$

where $C_t$ is an empirical basin coefficient which varies between 1.35 and 1.60. The duration of effective rainfall, $t_r$, is also given as an empirical relationship simply as,

$$t_e = \frac{t_p}{5.5} \tag{4.18}$$

Similarly, the peak discharge is in direct proportional relationship with the watershed area, $A$, but in an inverse proportionality with time to peak,

$$Q_p = \frac{2.78 C_p A}{t_p} \tag{4.19}$$

in which $C_p$ is a coefficient with values between 0.23 and 0.67. In Snyder's method, the channel slope, $S$, as one of the significant watershed features is influential on the time to peak. Linsley et al. (1958) gave similar empirical formulation as,

$$t_p = C \left( \frac{LL_C}{\sqrt{S}} \right)^{0.38} \tag{4.20}$$

where $C$ assumes 1.72 for mountainous zones, 1.0 for foothills, and 0.5 for valleys. On the other hand, the lag time is expressed as,

$$t_l = t_p \, 0.25(t_r - t_e) \tag{4.21}$$

In this expression, $t_r$ should be assumed according to past experience. The peak discharge expression is also given similar to Eq. (4.19) as,

$$Q_p = \frac{2.78 C_p A}{t_l} \tag{4.22}$$

On the other hand, the time base of the SH is suggested by Taylor and Schwartz (1952) as,

$$t_b = 5(t_l + 0.5t_r) \tag{4.23}$$

It is also advised that $t_t$ should be taken as four- and fivefolds of the time to peak. Empirical equations of Snyder's method lead to UH after the completion of the following steps.

(1) It is preferable to consider natural UH with the closest and similar hydrological as well as climatologic features. The values of $t_p$, $t_e$, and $Q_p$ are calculated from Eqs. (4.17), (4.18), and (4.19), respectively, by considering cross-checks from the nearest drainage basins. First, a tentative SH is sketched by taking into consideration the widths $W_{50}$ and $W_{75}$ of the unit hydrographs at 50 and 75% of the peak discharge levels, respectively, according to the following equations,

$$W_{50} = \frac{5.87}{q_{pu}^{1.08}} \tag{4.24}$$

and

$$W_{75} = \frac{3.35}{q_{pu}^{1.08}} \tag{4.25}$$

These widths are in time units.

(2) In the plotting of $W_{50}$ and $W_{75}$, they should first be divided into three equal parts and one part is taken to the left of peak discharge and two parts on the right-hand side. However, some authors have suggested that 40% is laid down to the left and remaining percent to the right,

(3) If the SH area is not equal to the watershed area, then it should be adjusted accordingly.

Furthermore, a standard SH is defined as one whose rainfall duration, $t_e$, is related to the basin lag, $t_p$, as,
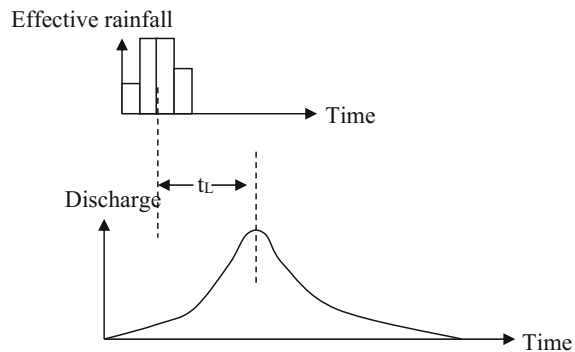
$$t_L = 5.5t_e \tag{4.26}$$

Herein, the time lag is the difference in the time of the SH peak and the time associated with the centroid of the excess rainfall hyetograph (see Fig. 4.22).

If the duration of the desired SH for the watershed of interest is significantly different from that specified by Eq. (4.26), then the following relationship can be used to define the relationship between SH peak time and its duration

$$t_p = t_p - \frac{t_r - t_u}{4} \tag{4.27}$$

**Fig. 4.22** Snyder's unit
hydrograph



where $t_r$ and $t_u$ are the durations of effective rainfall and desired SH, and $t_p$ is the
time lag of desired UH. Snyder (1938) discovered that SH lag time and peak per
unit of excess precipitation per unit area of the watershed are related by

$$\frac{Q_p}{A} = C\frac{C_p}{t_p} \tag{4.28}$$
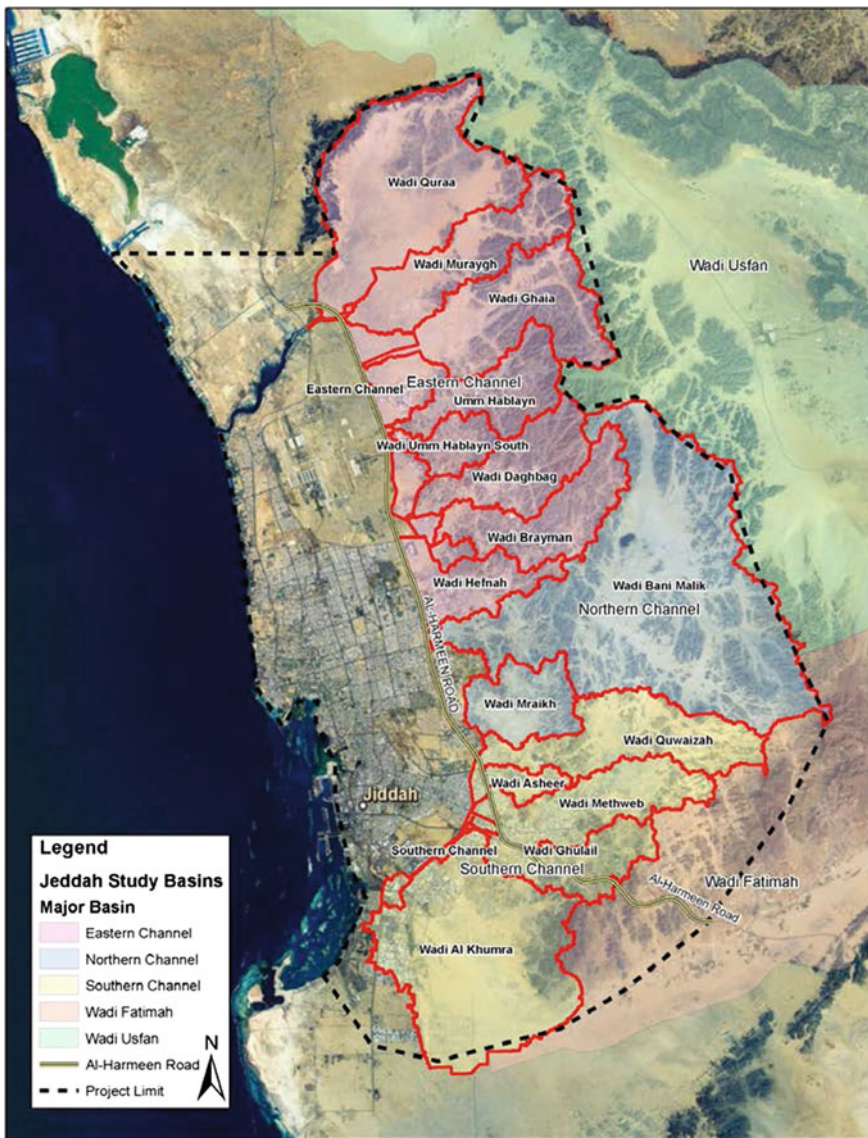
where Up is the peak of standard SH, $A$ is the catchment area, $C_p$ is a coefficient
related to the SH peak, and $C$ is the conversion constant which assumes 2.75 for SI.

For the flood analysis in the Arabian Peninsula, a set of wadis that confluence to
the Red Sea and their locations are given in Fig. 4.23. These locations are between
latitudes 18 and 19°N and longitudes 40°30′E and 42°E. The highest elevation at
the upper stream parts of these wadis is about 2000 m above mean sea level.

This region is subject to air masses during winter seasons from northwest
coming from the Mediterranean Sea, and the valley effect of the Red Sea allows
their penetration down to the study area (see Fig. 4.23). In spring periods, the same
region is under the influence of monsoon air masses from southeast. In other
seasons, due to extreme temperatures, orographic type of local rainfalls takes place.

The flood prediction methodologies are based on theoretical principles, but they
are also adjusted with empirical and experimental principles. In general, flood
discharge is a complex function of climate conditions and geomorphologic features.
Among the most important climate variables are rainfall intensity, areal distribution,
duration, frequency, drainage basin features such as drainage area, drainage density,
main channel slope and length. Drainage features play the role of rainfall trans-
formation to runoff. Rainfall–runoff relationships are also complicated function of
the vegetation, geology, and land use, and soil types.

The geomorphological features of all the wadis mentioned in the previous sec-
tion are obtained from the digital elevation model (DEM) data and they are exposed
in Table 4.3, where $A$ is the drainage area, $L$ is the main channel length, $L_c$ is the
distance between the projection point of the centroid on the main channel and the
outlet point, $\Delta h$ is the elevation difference, and $S_o$ is the main channel slope.

**Fig. 4.23**  Red Sea coastal watersheds

From the $L$ and $L_c$ data from this table, one can obtain the relationship between them on a double logarithmic paper for Wadi Baish as in Fig. 4.24.

In practical applications, $L_c$ calculation is rather tedious, but the following expression deduced from Fig. 5.16 makes its calculation easy.

**Table 4.3**  Geomorphological quantities

| Sub-basin name | Sub-basin number | A ($km^2$) | $L_c$ (km) | $L$ (km) | $\Delta H$ (km) | $S_o$ |
|---|---|---|---|---|---|---|
| *Wadi Hali* | | | | | | |
| Mamdah | 1 | 99.41 | 9.5 | 19.13 | 0.386 | 0.02 |
| Qada | 3 | 346.04 | 17.75 | 32.44 | 1.126 | 0.035 |
| Ralah | 4 | 376.15 | 15.25 | 35.24 | 0.863 | 0.024 |
| Uraun | 5 | 442.87 | 23 | 47.59 | 0.998 | 0.021 |
| Al-Hamd | 6 | 450.11 | 23.75 | 39.37 | 0.738 | 0.019 |
| Ar-Raysh | 7 | 507.9 | 21.25 | 37.18 | 0.802 | 0.022 |
| Tayyah | 8 | 628.57 | 30.05 | 50.9 | 1.685 | 0.033 |
| Hali | 9 | 672.98 | 27 | 39.7 | 2.557 | 0.064 |
| Baqarah | 10 | 725.14 | 33 | 49.54 | 1.117 | 0.023 |
| Qana | 11 | 810.05 | 34.5 | 67 | 0.835 | 0.012 |
| Ghargharah | 12 | 160.64 | 8.25 | 20.86 | 0.287 | 0.014 |
| *Wadi Yibah* | | | | | | |
| Al-Qawz | 1 | 752.99 | 19.25 | 43.93 | 0.41 | 0.01 |
| Sayfir | 2 | 231.26 | 13.25 | 22.4 | 0.34 | 0.02 |
| Urf | 3 | 181.36 | 14 | 28.77 | 0.58 | 0.02 |
| Mafal | 4 | 291.86 | 10 | 24.73 | 1.45 | 0.06 |
| Khat | 5 | 578.78 | 20.75 | 40.79 | 1.69 | 0.04 |
| Biyan | 6 | 527.59 | 19.75 | 28.19 | 0.9 | 0.03 |
| Al-Jawf | 7 | 284.75 | 15.25 | 22.93 | 1.63 | 0.07 |
| Jafn | 8 | 334.99 | 16.5 | 29.84 | 1.34 | 0.05 |

$$L_c = 0.2682L^{1.198} \tag{4.29}$$
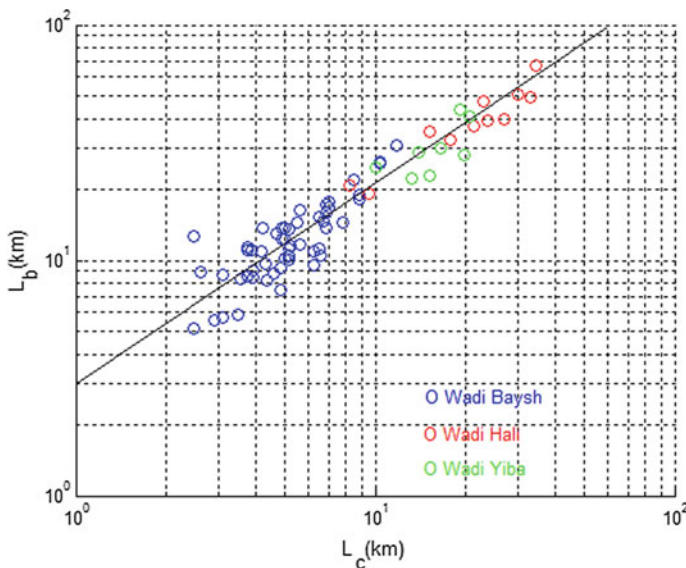
In this equation, all the quantities must be expressed in km unit. The substitution of this expression modifies the Snyder SH time to peak discharge given in Eq. (4.20) as follows.

$$t_p = C\left(\frac{0.2682\,L^{2.198}}{\sqrt{S}}\right)^{0.38} \tag{4.30}$$

Linsley et al. (1982) have provided $C_p$ and $C_t$ values according to the soil type in Table 4.4.

After substitution of Eqs. (4.18) into (4.19) and consideration of $C_p = 1$ and $S = 1$, one can obtain the parallel lines on the double logarithmic paper the relationship between the peak discharge and drainage basin area as in Fig. 4.25.

*Example 4.1* Among the wadis in Table 4.3 for Wad Hali sub-basin Mamdah, the soil is medium sandy and clay, and hence, calculates the flood peak discharge.

**Fig. 4.24** $L_c$ and $L$ relationship
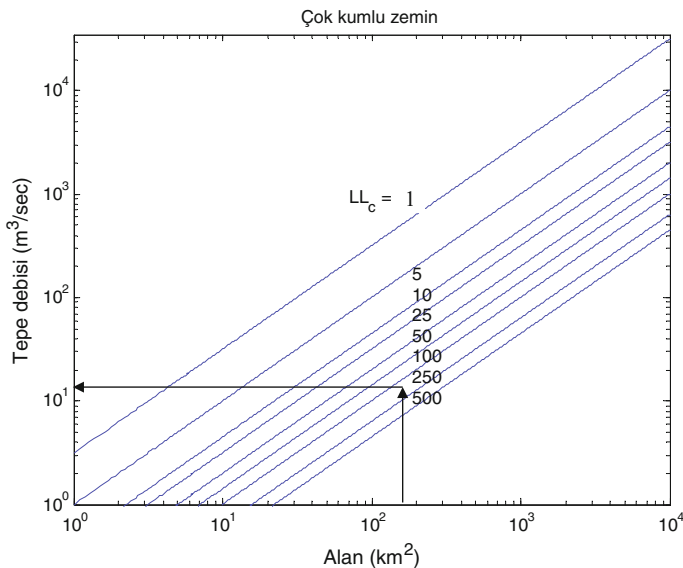
**Table 4.4** Snyder method constants

| Soil type | $C_t$ | $C_p$ |
|---|---|---|
| Sandy | 1.65 | 0.56 |
| Medium sand and clay | 1.50 | 0.63 |
| Highly clay and rock | 1.35 | 0.69 |
| Average | 1.5 | 0.63 |

**Answer 4.1** From Table 4.3, $A$ = 99.1 km$^2$, $L_c$ = 9.5 km, and $L$ = 19.13 km, and hence, one can calculate that $LL_c$ = 181.73 km$^2$. By means of the drainage area and these values, one can deduct from Fig. 4.25 that 15 m$^3$/s, which is valid in case of $C_p$ = 1 and $S$ = 1. Table 4.4 for $C_p$ = 0.63, the peak discharge value can be found as $Q_P$ = 15 × 0.63 = 9.45 m$^3$/s.

## 4.9.2   Soil Conservation Service (SCS) Method

The basis of this approach is rather simple and includes basic principles of hydrology. The logical basis is that during a single storm, rainfall will accumulate with time and depending on the soil properties the surface runoff will take place. It is logical that always the amount of runoff at any time will be less than the rainfall. Hence, the ratio of total runoff, $r$, to total precipitation, $P$, will always be less than

**Fig. 4.25** Snyder area-flood discharge relationships

one. In the Soil Conservation Service (SCS 1971, 1986) method, this ratio is thought as equal to the ratio of water storage accumulation on the surface, $F$, to maximum surface storage, $S$. These two last sentences imply that

$$\frac{r}{P} = \frac{F}{S} \tag{4.31}$$

This is a very simple and logically based expression and its consideration with the simple water budget (continuity) equation based on three components, namely precipitation, runoff, and surface storage, one can write that

$$P = r + F \tag{4.32}$$

Substitution of F from this expression into Eq. (4.31) leads after simple algebraic operation to

$$r = \frac{P^2}{P + S} \tag{4.33}$$

If the precipitation is considered with the infiltration loss, $I_a$, then it should be subtracted from the overall precipitation, and hence, Eq. (4.33) takes the following form.

$$r_{\text{e}} = \frac{(P - I_{\text{a}})^2}{P - I_{\text{a}} + S} \tag{4.34}$$

where $r$ and $P$ are the runoff and accumulated precipitation excess depth at time $t$, respectively. $S$ is the potential maximum retention which is a measure of the catchment ability to abstract and retain storm precipitation.

From the analysis of results in many small experimental watersheds, the SCS developed an empirical relationship between $I_{\text{a}}$ and $S$ as,

$$I_{\text{a}} = 0.2S \tag{4.35}$$

Hence, the cumulative excess at time $t$ is

$$r_{\text{e}} = \frac{(P - 0.2S)^2}{P + 0.8S} \tag{4.36}$$

Incremental excess for a time interval is computed as the difference between the accumulated excess at the end and beginning of the period. The maximum retention, $S$, and catchment characteristics are related through an intermediate parameter, which is referred to as the curve number (commonly abbreviated CN).

$$S = \frac{25400 - 254\,\text{CN}}{\text{CN}} \quad (\text{SI}) \tag{4.37}$$

CN values range from 100 (for water bodies) to approximately 30 for permeable soils with high infiltration rates.

It is possible to estimate the CN for a catchment as a function of land use, soil type, and antecedent watershed moisture, using tables published by the SCS in Technical Report 55 (commonly called TR-55). For the use the tables, it is necessary to identify the soil type and land use and refer to the appropriate portion to identify the single-valued CN. For a catchment consisting of several soil types and land uses, a composite CN is calculated as,

$$\text{CN}_{\text{composite}} = \frac{\sum A_{\text{i}}\text{CN}_{\text{i}}}{\sum A_{\text{i}}} \tag{4.38}$$

where $i$ is an index of catchment subdivisions of uniform land use and soil type, $\text{CN}_{\text{i}}$ is the CN for subdivision $i$, and $A_{\text{i}}$ is the drainage area of subdivision $i$.

### 4.9.3   The Geomorphologic Instantaneous Unit Hydrograph

Rodriguez-Iturbe and Valdes (1979) have suggested the basis of geomorphologic instantaneous unit hydrograph (GIUH) for determination of UH in drainage basins,

where there is no runoff measurements. The basis of the method is probabilistic and stochastic modeling of rainfall on the drainage basin and its movement toward proper outlets according to time of travel distributions.

In the geomorphologic approach, the IUH is assumed as the PDF of travel times. In general, the travel time is defined as the time required for any drop of rainfall that falls onto the watershed surface to reach the proper outlet. The PDF of the travel time is adopted theoretically as an exponential PDF. Since the passages of surface water are the stream channels that constitute different orders of a drainage basin configuration (Chap. 3, Sect. 3.6.7), this method is referred to as the exponentially distributed geomorphologic IUH (ED-GIUH). On the other hand, Kirshen and Bras (1983) sought the validity of exponential PDF of the travel time, and they employed the linearized equation of motion and arrived at conclusion that the travel time distribution is not exactly exponentially distributed. It will be referred to this type hydrograph linear routing geomorphologic instantaneous unit hydrograph (LR-GIUH).

The main drawback of these two approaches is that they do not take into account the infiltration phenomenon. In order to alleviate this restriction, Diaz-Granados, Bras (1989) have included infiltration component, which is assumed to be a linear function of the runoff. Finally, they have applied this technique with the exponential distribution GIUH (ED-GIUH) approach for different watersheds in Egypt and Porto Rico and ended up with that they do not differ significantly in the peak discharge, time to peak, and the shape of hydrograph. Hence, since ED-GIUH has simpler mathematical derivation, it is preferred practically over the others. However, there are practical difficulties in the estimation of model parameters from field data. On the other hand, ED-GIUH does not take into consideration the following physical points.

(1) Infiltration losses have not been incorporated in the model properly,
(2) Possibility of physically based incorporation of infiltration losses has not been credited in the developments.

In the ED-GIUH method, the travel time is assumed as the division of stream length by the stream velocity, similar to Eq. (3.34) in Chap. 3.34. It is to be noticed that the velocity of each stream varies from one storm to other. Rodriguez-Iturbe and Valdes (1979) stated that varying velocity incorporation in the ED-GIUH calculations will make the mathematical manipulations complex and rather impossible analytically. In order to alleviate this situation, the velocity calculation is suggested at the time of peak discharge by different researchers (Rodriguez-Iturbe and Valdes 1979; Kirshen and Bras 1983; Troutman and Karlinger 1985). Even if agreed on this velocity, the problem is then how to estimate it, and this is another criticism against the GIUH approach.

This methodology uses network topology and probability concepts. Three different laws concerning the stream number, stream length, and the stream area are

already presented in Chap. 3 concerning the bifurcation ratios by Eqs. (3.10), (3.11), and (3.12), respectively. These ratios vary between 3–5, 1.5–3.5, and 3–6, respectively. In the calculations, Strahler (1950, 1952) stream ordering is used (see Fig. 4.26).

Furthermore, it is assumed that water travels through basin, making transitions from lower to higher order streams. On the other hand, travel times and transition probabilities can be approximated using Strahler stream ordering scheme. The PDF is obtained analogous to an IUH, where the surface/subsurface travel times are ignored in order to get a channel-based GIUH. The channel-based GIUH has the peak discharge and time values as,

$$q_{\mathrm{p}} = \frac{1.31}{L_\Omega} R_{\mathrm{L}}^{0.43} V \tag{4.39}$$

and
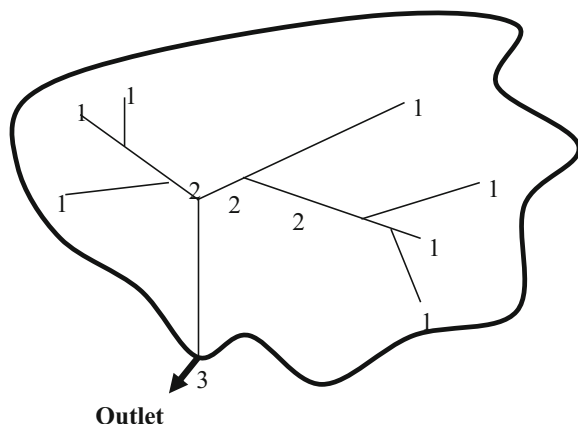
$$t_{\mathrm{p}} = \frac{0.44 L_\Omega}{V} \left( \frac{R_{\mathrm{B}}}{R_{\mathrm{A}}} \right)^{0.55} R_{\mathrm{L}}^{-0.38} \tag{4.40}$$

where $L_\Omega$ should be in km, $V$ in m/s and the results are $q_{\mathrm{p}}$ in $\mathrm{hr}^{-1}$ and $t_{\mathrm{p}}$ in hrs.

### 4.9.3.1 Time of Travel

After the falling of a single drop on any point on the watershed, it will lead toward a destination through a definite number of stream branches. In the GIUH approach, water enters from lower stream order to the next order in sequence, until it reaches the point of outlet (see Fig. 3.35). This statement makes it clear that there are two



Fig. 4.26 Strahler stream ordering

probabilities that should be considered for the water drop. First, the probability of the drop falling on a certain stream order, say $i$, and hence, the probability of its state can be shown notationally as $P_i$. The second probability is the time of travel probability, $P_{ti}$, within this stream order. Hence, falling probability states the entrance of water drop into the order system, and traveling probability represents the movement possibility of the same drop within the same stream order until it reaches the upstream point of the next stream order. Hence, the combined probability of a single drop to fall and then travel completely within a stream order, $i$, can be expressed assuming that the falling and traveling phenomena are independent of each other which allows to the multiplication of probabilities as $P_i P_{ti}$. Since physically such probabilities are mutually exclusive, it is possible to write for the time of travel of many particles through a finite number of stream order, say $S$, as the summation of mutually exclusive events,

$$P_t = \sum_{j=i}^{S} P_j P_{tj} \qquad (4.41)$$

For practical derivations, time spent by any drop of water on overland flow is considered as negligible, and hence, the travel time in a particular stream is the sum of the travel times in the streams that lead to this particular stream. The probability of a single drop of water to be in stream order $i$ at time $t$ can be expressed through the following transitional probabilities as,

$$P_{ti} = P_{Ai} P_{ij} P_{jk} \ldots P_{mS} \qquad (4.42)$$

where $P_{Ai}$ is the probability that a water drop falls over the drainage area of stream order $i$. This can be regarded as the initial probability. All other terms on the right-hand side of Eq. (4.43) indicate the transition probabilities from one stream order to the next one. By definition, the initial and transitional probabilities can be expressed explicitly as,

$$P_{Ai} = (\text{Total area draining directly into stream order } i)/(\text{Total basin area}) \quad (4.43)$$

and

$$\begin{aligned} P_{ij} = &\ (\text{Number of } i\text{-th order streams draining to the next order}) \\ &/(\text{Total number of } i\text{-th order streams}) \end{aligned} \qquad (4.44)$$

One can obtain the estimations of these probabilities by considering the stream ordering and the sub-area of the catchment attached to each stream as follows.

$$P_{Ai} = \frac{N_i \overline{A}_i}{AS} \qquad (4.45)$$

this can also be written more explicitly as,

$$P_{\mathrm{A}i} = \frac{N_i}{AS}\left(\overline{A}_i - \sum_{k=1}^{i-1}\frac{\overline{A}_k N_k P_{ki}}{N_i}\right) \quad (i = 2, 3, \ldots, S) \tag{4.46}$$

and

$$P_{ij} = \frac{(N_i - 2N_{i+1})E(j, S)}{\sum\limits_{k=j}^{S} E(k, S)N_i} + \frac{2N_{i+1}}{N_i}\delta_{i+1,j} \quad (1 < i < j < S) \tag{4.47}$$

where $\overline{A}_i$ is the average runoff area contributing to a stream of order $i$ and its tributaries of lower order, $\delta_{i+1,j} = 1$ if $j = i+1$, and 0 otherwise. $E(j, S)$ denotes the mean number of interior links of order i in a watershed of order $S$. This can be written explicitly as,

$$E(j, S) = N_i \prod_{k=2}^{j}\frac{(N_{k-1} - 1)}{2N_k - 1} \quad (i = 2, \ldots, S) \tag{4.48}$$

The last three expressions are approximations only and therefore may represent a major source of error in the GIUH calculations. It is also assumed that the averaged drainage area of the streams of all groups is the same which implies that

$$\frac{A_{i,j}^T}{N_{i,j}} = \frac{A_{i,l}^T}{N_{i,l}} = \frac{A_{i,S}^T}{N_{i,S}} = \overline{A}_i \tag{4.49}$$

where $A_{i,j}^T$ means total drainage area of the $i$-th order streams which drain into stream order $j$.

On the other hand, Rodriguez-Iturbe and Valdes (1979) suggested that the travel time in any stream is exponentially distributed as,

$$P(T_i) = \lambda_i \mathrm{e}^{-\lambda_i t} \tag{4.50}$$

where $\lambda_i = V/\overline{L}_i$, $V$ is the streamflow velocity and $\overline{L}_i$ is the average length of $i$-th order stream. This last expression gives a graph that does not start from zero, and therefore, the same authors presented the following expression for the travel time distribution by considering that $\lambda_S^* = 2\lambda_S$.

$$P(T_i) = \lambda_S^{*2} t\mathrm{e}^{-\lambda_S^* t} \tag{4.51}$$

### 4.9.3.2 Infiltration Loss

The spatio-temporal channel infiltration losses, $i(x, t)$, are considered as a linear expression according to the following expression (Diaz-Granados et al. 1983),

$$i(x,t) = kq(x,t) \tag{4.52}$$

where $k$ is a proportionality constant and $q(x, t)$ is the discharge per unit width of the channel. The use of this expression led to infiltration expression portion ($I_i$) in a stream order of $i$ as,

$$I_i = 1 - \frac{\left(1 - e^{-k\overline{L}_i}\right)}{k\overline{L}_i} \tag{4.53}$$

The exponential PDF of travel time is modified for accounting the infiltration process as,

$$P(T_i) = \lambda_i e^{-\mu_i t} \quad i < S \tag{4.54}$$

and

$$P(T_S) = \mu_S^* \lambda_S^* t e^{-\mu_S^* t} \tag{4.55}$$

where $\mu_i = V_i / \overline{L}_i (1 - I_i)$ and $\mu_S^* = 2\mu_S$ which make the area under $P(T_i)$ equal to $(1 - I_i)$.

Infiltration Coefficient Estimation

If a stream of order $i$ has a unit input and uniform infiltration loss along its length, then the outflow will be $(1 - I_i)$. The infiltration within the next stream order will be $(1 - I_i)I_j$ and the net outflow from the $j$-th order stream will be $(1 - I_i)(1 - I_j)$. The same logical sequence for the whole stream orders within the watershed area leads to $(1 - I_i)(1 - I_j) \ldots (1 - I_S)$. Hence, the surface runoff yields, $r$, of a watershed area $A_S$ from a rainfall depth, $h$, landing anywhere in the watershed can be expressed as,

$$r = A_S h \sum_{s \varepsilon S} P(s)(1 - I_s) \tag{4.56}$$

For a catchment of known area and drainage pattern, the only unknowns in Eq. (4.57) are $I_i$'s which can be obtained from Eq. (4.53).

### 4.9.3.3   Mean Holding Time

The time lag (mean holding time) of a drainage basin can be expressed as follows (Gupta et al. 1980),

$$\overline{T} = \sum_{s \varepsilon S} P(s)\overline{T}_s \tag{4.57}$$

where $\overline{T}_s$ is the meantime of travel in path $s$ which is equal to the sum of the mean times of travel in the streams of this path as,

$$\overline{T} = \overline{T}_i + \overline{T}_j + \cdots \overline{T}_S \tag{4.58}$$

It can be noticed from Eq. (4.50) that $\overline{T}_i$ is equal to $1/\lambda_i$. However, in the modified ED-GIUH as presented in Eq. (4.54), $\overline{T}_i = (1 - I_i)^2 \big/ \lambda_i$. Since the area under $P(T_i)$ equals $(1 - I_i)$, the normalization is necessary through dividing by $(1 - I_i)$. Finally, $\overline{T}$ can be calculated as,

$$\overline{T} = \frac{1}{V} \sum_{s \varepsilon S} P(T_S)(\overline{L}_i + \overline{L}_j + \cdots + \overline{L}_S) \tag{4.59}$$

On the other hand, according to Diaz-Granados et al. (1983), this can be rewritten as,

$$\overline{T} = \frac{1}{W} \sum_{s \varepsilon S} P(T_S)[\overline{L}_i(1 - I_i) + \overline{L}_j(1 - I_j) + \cdots + \overline{L}_S(1 - I_S)]$$

Comparison of these two last expressions shows that

$$W = \beta V \tag{4.60}$$

where

$$\beta = \frac{\sum\limits_{s \varepsilon S} P(T_S)\big[\overline{L}_i(1 - I_i) + \overline{L}_j(1 - I_j) + \cdots + \overline{L}_S(1 - I_S)\big]}{\sum\limits_{s \varepsilon S} P(T_S)(\overline{L}_i + \overline{L}_j + \cdots \overline{L}_S)} \tag{4.61}$$

## 4.10   Santa Barbara Hydrograph

This hydrograph is developed for California, Santa Barbara County Flood Control and Water Conservation District. It is a direct way of hydrograph computation without an intermediate process as the UH method requires. The computations can

be done manually with ease. This method is similar to the contributing area procedure for hydrograph computation where sub-watershed area hydrographs are developed and then routed to determine the outflow hydrograph for the whole watershed (Sect. 4.3). The following steps are necessary for the application of Santa Barbara hydrograph procedure.

(1) The runoff depths are calculated by considering impervious and pervious surface area percentages of the watershed area. If the impervious area percent is denoted by $\alpha$ then the pervious area percentage is $(1 - \alpha)$. Consideration of rainfall and infiltration increments during $\Delta t$ time interval as $P_{\Delta t}$ and $I_{\Delta t}$, the impervious, pervious, and total runoff depths can be calculated as,

$$
\begin{aligned}
R_I &= \alpha P_{\Delta t} \\
R_P &= (1 - \alpha)(P_{\Delta t} - I_{\Delta t})
\end{aligned}
\tag{4.62}
$$

and

$$
R_T = R_I + R_P = P_{\Delta t} + (1 - \alpha)I_{\Delta t} \tag{4.63}
$$

respectively. In practices, $\Delta t$ can be taken as ¼, ½, etc. hours.

(2) The instantaneous hydrograph is calculated first by multiplying the total runoff depth, $R_T$ for each time period over the watershed area, $A$, hence the runoff volume is obtained for this time interval as,

$$
V_{\Delta t} = A R_T \tag{4.64}
$$

On the other hand, the instantaneous hydrograph has its discharge, $Q'_{\Delta t}$, value during this time increments as,

$$
Q'_{\Delta t} = \frac{V_{\Delta t}}{\Delta t} \tag{4.65}
$$

Substitution of Eq. (4.64) by considering also Eq. (4.63) into this last expression leads to,

$$
Q'_{\Delta t} = A \frac{R_T}{\Delta t} = A \frac{P_{\Delta t} + (1 - \alpha) I_{\Delta t}}{\Delta t} \tag{4.66}
$$

Since by definition, $i_{\Delta t} = P_{\Delta t}/\Delta t$ and $f_{\Delta t} = I_{\Delta t}/\Delta t$ are the rainfall intensity and the infiltration rate during the considered time interval $\Delta t$, respectively, this last expression can be rewritten as

$$Q'_{\Delta t} = A[i_{\Delta t} + (1 - \alpha)f_{\Delta t}] \tag{4.67}$$

Furthermore, the discharge, $q_{\Delta t}$ per unit area becomes,

$$q_{\Delta t} = i_{\Delta t} + (1 - \alpha)f_{\Delta t} \tag{4.68}$$

(3) The final design hydrograph discharge $Q_{\Delta t}$ can be obtained by routing the instantaneous hydrograph discharge $Q'_{\Delta t}$ through an imaginary reservoir with a time delay calculated using the time of concentration, $t_c$, of the watershed. This can be achieved according to the following routing expression,

$$Q_{\Delta t}(j) = Q_{\Delta t}(j-1) + K_r\left[Q'_{\Delta t}(j-1) + Q'_{\Delta t}(j) - 2Q_{\Delta t}(j)\right] \tag{4.69}$$

where

$$K_r = \frac{\Delta t}{(2t_c + \Delta t)} \tag{4.70}$$

The shape of the resulting hydrograph is controlled by the routing constant, $K_r$. It is also possible to modify the Santa Barbara Hydrograph equation by accounting for the depression storage or evaporation according to the following expression.
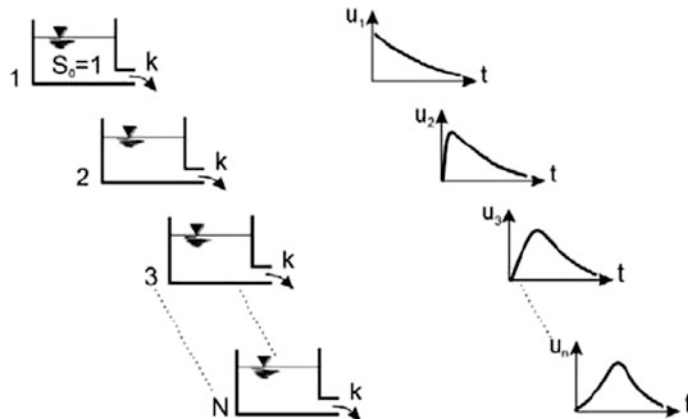
$$R_I = \alpha(P_{\Delta t} - D_{\Delta t})e_{\Delta t} \tag{4.71}$$

where $D_{\Delta t}$ is the depression storage during $\Delta t$ time increment and $e_{\Delta t}$ is the portion of rainfall excess which evaporates before the runoff.

## 4.11  Conceptual UH Models

These are input—output-storage change models that are represented by a series of reservoirs as shown in Fig. 4.27. Each reservoir attenuates the input, and hence, a series of reservoirs expands the effective base time of the output hydrograph. There are several conceptual models that are used in the practical applications.

These have theoretical and conceptual basis with mathematical requirement in a successive manner. Most of the models are cited by their first innovator's name. The purpose is to derive IUH and then to convert it into UH as explained in Sect. 4.7.

**Fig. 4.27** Series of reservoirs

## 4.11.1 Nash Conceptual Model

Nash (1957a, b) suggested that the cascade of reservoirs as shown in Fig. 4.27 has the same dimensions and hydraulic parameters. The most important parameter in each reservoir is the storage coefficient, $K$, which shows the amount of storage within the reservoir. The bigger is the storage coefficient, the larger is the reservoir volume for water impoundment. The model is lumped, time invariant and the number of reservoirs in the cascade depends on the effective rainfall hyetograph and the direct runoff hydrograph.

The mechanism of this model is such that an input of 1 cm of excess rainfall is applied over the whole catchment for the first reservoir instantaneously. This reservoir is assumed not to have an input. This implies that the rainfall is routed through the first reservoir so as to find the output, which is the input into the next reservoir and the same procedure is repeated for a certain number of the reservoirs. Finally, the output from the last reservoir is regarded as the IUH from the drainage area. The basic equation in any routing problem is the fundamental water budget expression in the science of hydrology, which is expressed in plain terms as "input minus output equals to the change of storage." Mathematically this can be written as,

$$I - O = \frac{dS}{dt} \tag{4.72}$$

where $I$, $O$, and $S$ are the input, output, and storage amounts. For the first reservoir, the storage, $S$, is assumed to be a linear function of the output as,

$$S = KO \tag{4.73}$$

The substitution of Eq. (4.73) into Eq. (4.72) with the initial condition that $I = 0$ leads to,

$$-O = \frac{dS}{dt} = \frac{d(KO)}{dt} = K\frac{dO}{dt}$$

this can be arranged as

$$\frac{dt}{K} = -\frac{dO}{O}$$

its integration gives

$$-\frac{t}{K} = \ln O + C$$

where $C$ is an integration constant. Using the initial condition for $t \to 0$, and $O \to O_0$ gives that $C = -\ln O_0$, and therefore, after the necessary algebraic manipulations one can obtain,

$$O = O_0 e^{-t/K} \tag{4.74}$$

On the other hand, due to linearity property $S_0 = KO_0$, and since, the input is unit, i.e., $S_0 = 1$, Eq. (4.73) becomes,

$$O = \frac{1}{K} e^{-t/K} \tag{4.75}$$

This is the output from the first reservoir. In the subsequent reservoirs numerical subscripts will be used in order to show the reservoir number, hence for the next reservoir the continuity equation can be written as,

$$I_2 - O_2 = \frac{dS_2}{dt}$$

where

$$I_2 = O_1 = \frac{1}{K} e^{-t/K}$$

On the other hand, linear reservoir property states that $S_2 = KO_2$ and the substitution of these two expressions into the continuity equation of the second reservoir after the necessary algebra leads to,

$$O_2 = \frac{t}{K^2} e^{-t/K} \tag{4.76}$$

Likewise, the third and the fourth reservoirs yield the output hydrographs as,

$$O_3 = \frac{1}{2.1} \frac{1}{K} \left(\frac{t}{K}\right)^2 e^{-t/K}$$

and

$$O_4 = \frac{1}{3.2.1} \frac{1}{K} \left(\frac{t}{K}\right)^3 e^{-t/K}$$

respectively. It is possible to deduce the final, i.e., $n$-th reservoir output hydrograph as,

$$O_3 = \frac{1}{(n-1)} \frac{1}{K} \left(\frac{t}{K}\right)^{n-1} e^{-t/K}$$

This is the IUH expression which can be written in a more illuminating manner as follows,

$$O(t) = \frac{1}{(n-1)} \frac{1}{K} \left(\frac{t}{K}\right)^{n-1} e^{-t/K} \tag{4.77}$$

It is obvious from this expression that two parameters are necessary for the IUH ordinate calculation. These parameters are the storage coefficient, $K$, and the number, $n$, of the reservoir. They can be obtained by considering the basic hydrograph definition. The centroid of IUH can be evaluated as the first moment, $M_1$, about the ordinate axis, which is equal to $nK$ where $K$ is the lag time of each reservoir. Hence,

$$M_1 = nK \tag{4.78}$$

This is also equal to the difference between the excess rainfall hyetograph and direct runoff hydrograph first moments as

$$M_{1-\text{Direct runoff hydrograph}} - M_{1-\text{Rainfall excess hyetograph}} = nK \tag{4.79}$$

# References

Aron, G., & White, E. L. (1982). Fitting a gamma distribution over a synthetic unit hydrograph. *Water Resources Bulletin, 18*(1), 95–98.

As-Sefry, S., Şen, Z., Al-Ghamdi, S. A., Al-Ashi, W., & Al-Baradi, W. (2004). *Strategic groundwater storage of Wadi Fatimah- Makkah region Saudi Arabia*. Saudi Geological Survey, Hydrogeology Project Team, Final.

Bhunya, P. K., Mishra, S. K., & Berndtsson, R., (2003). Simplified two parameter gamma distributions for derivation of synthetic unit hydrograph. *Journal of Hydrologic Engineering, ASCE, 8*(4), 226–230.

Bras, R. L. (1989). *Hydrology: An Introduction to Hydrological Sciences*. Reading, M.A: Addison-Wasley.

Chow, V. T., Maidment, D. R., & Mays, L. W. (1988). *Applied hydrology*. St. Louis, MO: McGraw-Hill Publishing Company.

Croley, T. E. (1980). Gamma synthetic hydrographs. *Journal of Amsterdam Hydrology, 47,* 41–52.

Diaz-Granados, M. A., Valdes, J. B., & Bras, R. L. (1983). *A derived flood frequency distribution based on the geomorphologic-climatic IUH and density function of rainfall excess*. Report No. 292, Massachusetts Institute of Technology, Cambridge, MA.

Doodge, J. C. I. (1959). A general theory of the unit hydrograph. *Journal Geophysical Research, 64,* 241–256.

Gupta, V. K., Waymire, E., & Wang, C. T. (1980). A representative of an instantaneous unit hydrograph from geomorphology. *Water Resources Research, 16*(5), 855–862.

Kirshen, D. M., & Bras, R. L. (1983). The linear channel and its effect on the geomorphologic IUH. *Journal of Hydrology, 65,* 175–208.

Linsley, R. K., Kohler, M. A., & Paulhus, J. L. H. (1958). *Hydrology for engineers* (pp. 150–160). New York: McGraw-Hill.

Linsley, R. K., Kohler, M. A., & Paulhus, J. L. H. (1982). *Hydrology for engineers* (3rd ed., p. 508). New York: McGraw-Hill.

Nash, J. E. (1957a). Discussion of "Frequency of discharges from ungaged catchments". *Eos (Transactions, American Geophysical Union), 38*(6), 963–969.

Nash, J. E. (1957b). The form of the instantaneous unit hydrograph. *International Association of Science Hydrology 45*.

Nash, J. E. (1958). Determining run-off from rainfall. *P. I. Civil Engineering, 10,* 163–184.

Nash, J. E. (1959a). The effect of flood-elimination works on the flood frequency of the river Wandle. *Proceedings of the Institution of Civil Engineers, 13,* 317–338.

Nash, J. E. (1959b). Systematic determination of unit hydrograph parameters. *Journal of Geophysical Research, 64*(1), 111–115.

Rodriguez-Iturbe, I., & Valdes, J. B. (1979). The geomorphic structure of hydrologic response. *Water Resources Research, 18*(4), 877–886.

Şen, Z. (2010). *Fuzzy logic and hydrological modeling* (pp. 340). Taylor and Francis Group, CRC Press Publishers.

Şen, Z. (2014) *Philosophical, logical and scientific perspectives in engineering* (p. 260). Berlin: Springer-Nature.

Sherman, C. W. (1931). Frequency and Intensity of Excessive Rainfall at Boston. *Transactions ASCE, 95,* 951–960.

Singh, V. P. (1988). *Hydrologic systems: Rainfall-runoff modeling*, vol. 1. Englewood: NJ Prentice Hall.

Snyder, F. F. (1938). Synthetic unit hydrographs. *Transactions American Geophysics Union, 19,* 447–454.

Soil Conservation Service (SCS). (1971). *National engineering handbook*, *section 4: Hydrology.* Springfield, VA: USDA.

Soil Conservation Service (SCS). (1986). *Urban hydrology for small watersheds* (Technical Report 55). Springfield, VA.

Strahler, A. N. (1950). Equilibrium theory of slopes approached by frequency distribution analysis. *American Journal of Science, 248*(673–696), 800–814.

Strahler, A. N. (1952). Hypsometric (area-altitude) analysis of erosional topography. *Geological Society of America Bulletin, 63,* 1117–1142.

Taylor, A. B., & Schwartz, H. E. (1952). Unit-hydrograph lag and peak flow related to basin characteristics. *Transactions American Geophysical Union*, *33*, 235–246.

Troutman, B. M., & Karlinger, M. R. (1985). Unit hydrograph approximations assuming linear flow through topologically random channel networks. *Water Resources Research, 21,* 743–754.

# Chapter 5
# Rational Flood Methodologies

**Abstract** There are different flood discharge calculation methodologies that have started more than 100 years ago, and most of the first ones are based on logical and rational thinking. The very early ones do not include any information because there were no rain gauges established at that time. As already mentioned in the previous section, they were all related to drainage area nonlinearly without any further consideration of the surface features as soil type, land use, etc., or rainfall characteristics. Reliability of these early methodologies is discussed with comparison to the present most advanced techniques. For flood discharge estimations and preliminary appreciation of the magnitude, flood envelop curves are presented, and their usage procedures are given for different parts of the world again in comparative manner. For the application of rational methods (RMs) in arid regions, empirical runoff coefficient formulation is presented with applications to some of the drainage basins in the southwestern corner of the Arabian Peninsula. Irrationality of the RM is explained, and instead, a new and innovative modification of it is presented with application example. Practical surface water discharge calculation methods are presented on the basis of different ration based on the drainage area, mean flow, and standard deviation of the flow records.

**Keywords** Arid region · Flash flood · Flood envelope · Irrationality Modification · Rational · Discharge · Ungauged watersheds

## 5.1 General

In this chapter, flood evaluation is explained on rational, logical, and simple formulation bases. Most of the early flood discharge formulations are empirical and time independent, because rainfall and runoff measurements are not available. The flood discharge is related to drainage area by taking into consideration the direct and linear relationships between these two variables (Chap. 3). Later on, with the beginning of rainfall measurements, the flood discharge is expressed as a function of the drainage area and the rainfall intensity (Chap. 4). These formulations had a

balancing constant for equality, and therefore, the numerical determination of the constants (runoff coefficients) led to different approaches. Generally, the flood discharge is under the influence of numerous meteorological, hydrological, geologic, land use, soil type, vegetation, etc., effects, but in practical applications, only few of these factors are considered. Drainage parameters include uncertainties, because they cannot be sampled and measured with the required spatial accuracy. However, basic hydrometeorological variable measurements rainfall, evaporation, infiltration, and runoff are regarded as accurate and reliable.

There are various methods by which the estimate of flood peak discharge can be made. Some of these methods incorporate a rational analysis of the rainfall–runoff process, whereas others are completely based on empirical formulae or correlative techniques. These methods can predict the peak flood with drainage basin characteristics such as drainage basin area, main channel slope, and length of the main channels.

One definition of hydrological forecasting is that branch of science and engineering, which deals with the assimilation and analysis of hydrometeorological data and information, and the input of such information into hydrological modeling and prediction procedures to arrive at forecast for the present and future states of the various hydrological cycle components, especially the streamflow conditions in streams and rivers. Thus, hydrological forecasting involves application of hydrological and meteorological principles in engineering systems framework. An interesting meteorological–hydrological system for real-time use is characterized by its capacity to incorporate the precipitation forecast into the hydrological modeling. The likelihood of flooding is more predictable than some other types of hazards such as earthquakes, landslides, and volcanic eruptions. Identical flood-generating mechanism, especially those associated with climate, can generate different floods within different catchments, or within the same catchment at different times.

## 5.2  Early Methodologies

Excessive rainfall and consequent floods have caused human life and property loss since time immemorial. Availability of surface and groundwater resources at lower elevations attracts humans to select their settlements along valley floodplains, and therefore, they subject themselves to flood hazards. Later, they become aware of such flood dangers and tried to take precautions by water diversion though channels and canals or surface water impoundment behind small bents, dams, levees, etc., without scientific calculation. Toward the end of the eighteenth century, professionals developed various formulations for calculations. Over time, engineers developed design aids based on the performance observations of existing structures by taking into consideration the causative factors. Initially, they did not possess any hydrological data, but relied on logical inferences with few simple measures.

The first conscious list of the methods for design discharge is prepared by Chow (1962), who listed 12 formulas for waterway area and 62 formulas for design

discharge. Only a few of these formulas have been ever widely employed by engineers in practical applications. Among the most frequently used method is the Talbot (1887–1888) formulation for discharge (Quraishi and Al-Hasoun 1996). Even though recorded data were not available, early researchers identified logically and rationally the most important factors that may affect the flood design discharge. The first considerations were not concerned with discharge but the area of the waterway (Byrne 1902). It has long been noted that the following points are significant in any flood study.

(1) The rate of rainfall,
(2) The soil condition,
(3) The character and inclination of the surface,
(4) The condition and inclination of stream bed,
(5) The shape of the drainage area and the position of stream branches,
(6) The form of the mouth and the bed slope,
(7) Whether it is permissible to back water up above the water structure (culvert), thereby
(8) Causing additional pressure on the structure.

The appreciation of such factors could not be imported into a proper design decision treatment without knowing their significance and intuitive feeling about each factor's contribution to design discharge. The following recommendations are given for successful and plausible sizing of water structures, especially, for culverts and bridges.

(1) Observations of the existing openings on the same stream,
(2) Measurements at time of high water, a cross section of the stream at some narrow locations, if possible,
(3) Determination of high-water level as indicated by drift and the evidence of settlements in the neighborhood.

With this basic information and careful consideration, it is possible to determine the proper area of the waterway with a reasonable degree of accuracy (Byrne 1902).

Even today, a tradeoff is taken into consideration between the worst case and economics. In the past, the worst case was assessed according to observations and expert views; however, in modern times, the worst cases are expressed in terms of percentage risks (0.02, 0.04, 0.01, 0.05, 0.04, and 0.1%) corresponding to return periods (500-year, 200-year, 100-year, 50-year, 25-year, and 10-year). In cases of under-design water structure (culverts, bridges, etc.), the liability of a washout is most possible, and such situations may cause to traffic interruptions, highway expensive repairs, and also accidents with large sums for damages (Chap. 7). On the other hand, in cases of overdesign economic losses occur.

However, suitable design from engineering and economic planning points of view can be achieved only after a convenient maximum (peak) discharge subject of the water structures. In cases of human life loss culverts, bridges and similar water structures must be designed with highest safety, even without economic considerations, if necessary.

## 5.2.1  Talbot Method

Talbot (1887–1889), at the University of Illinois, proposed an effective discharge formulation without the availability of meteorological measurements, where the peak discharge, $Q_P$, is expressed as a power function of the drainage area with exponent ¾ similar to general expression in Chap. 2.

$$Q_p = CA^{3/4} \tag{5.1}$$

where $A$ is the drainage area in acres, and $C$ is a coefficient between 0.3 and 1. He then suggested the following guides for the adaptation of the coefficient.

(a) For rolling agricultural country, subject to floods at the time of melting snow, and with the length of valley three or four times the width, $C = 1/3$,
(b) In districts not affected by snow and where the length of the valley is several times the width, $C = 1/5$ or $1/6$ or even less,
(c) $C$ should be increased for steep side slopes, especially at the upstream of the drainage basin, where there is much greater fall than the channel at the culvert site.

Knowledge of the action of streams of similar situations in floods and of the effects of peculiar formations is of far more value than any extended formula (Talbot 1887–1888). In a subsequent discussion, Talbot added, "For steep and rocky ground $C$ varies from two-thirds to unity."

The Talbot formula gained widespread popularity among railroad and highway engineers. Since then the same formula is adopted by highway engineers for culvert and bridge design. In the USA, the highway departments of 25 states listed the Talbot formula as an acceptable design method in the University of Illinois's 1953 survey of design practices (Chow 1962).

In Saudi Arabia, Ministry of Transportation (MOT) has developed a modified form of Talbot formula. The original version in USA is as follows,

$$Q_5 = 0.6Q_{25} \tag{5.2}$$

$$Q_{10} = 0.8Q_{25} \tag{5.3}$$

$$Q_{25} = 1.0Q_{25} \tag{5.4}$$

$$Q_{50} = 1.2Q_{25} \tag{5.5}$$

$$Q_{100} = 1.4Q_{25} \tag{5.6}$$

$Q_{25}$ is the 25-year as the basis of all the discharge formulations, and its properties are given in Table 5.1, where $A$ is the drainage area in hectares, SF is the slope factor for drainage area.

**Table 5.1** Talbot equations

| Drainage area (hectares) | 25-year frequency rainstorm |
|---|---|
| $0 < A < 400$ (small catchment area) | $Q = A.SF$ |
| $400 < A < 1258$ | $Q = 0.837CA^{3/4}$ |
| $1258 < A < 35{,}944$ | $Q = 4.985CA^{1/2}$ |
| $A > 35{,}944$ | $Q = 14.232CA^{2/5}$ |

Finally, $C$ is the coefficient of runoff as the summation of three parts,

$$C = C_1 + C_2 + C_3 \qquad (5.7)$$

each coefficient on the right-hand side has the following numerical values depending on the verbal descriptions (Wilson Murrow Consultant 1971). They are given collectively in Table 5.2.

The modified Talbot formula has the preferential advantage of determining the value of $C$ for different drainage basins with great ease and is fairly reliable for areas where the rainfall intensity varies approximately from 20 to 70 mm/h. It has been tested for several years for practicality over the whole Kingdom of Saudi Arabia (KSA). The design flood discharges for a large number of drainage basins are checked, and it is observed that this formula gives satisfactory results and can be used reliably provided that the users have experience for selecting the correct $C$ value for the given drainage basin.

However, the formula suffers from the shortcoming of not being truly representative of basins/regions of great rainfall amounts, scanty rainfall like semi-desert areas and also not for conditions, where a drainage basin contains big storage or

**Table 5.2** C components

| $C_1$, for terrain conditions | |
|---|---|
| Mountains | 0.30 |
| Semi-mountains | 0.20 |
| Low lands | 0.10 |
| $C_2$, for slope, S, conditions | |
| $S > 0.15$ | 0.50 |
| $0.10 < S\ 0.15$ | 0.40 |
| $0.05 < S\ 0.10$ | 0.30 |
| $0.02 < S\ 0.05$ | 0.25 |
| $0.01 < S\ 0.02$ | 0.20 |
| $0.005 < S\ 0.01$ | 0.15 |
| $C_3$, for width, W, conditions | |
| $W = L$ | 0.30 |
| $W = 0.40L$ | 0.20 |
| $W = 0.20L$ | 0.10 |
| Where $L$ is the length of the channel | |

other artificial obstacles like high agricultural dikes, which either detain a big quantity of runoff or retard considerably the flow rate of the runoff.

According to the flood studies carried out by Al-Suba'i (1992) and the Saudi Geologic Survey (2007), the relationship between the drainage basin area, $A$, and the flood peak discharge, $Q_P$, for the KSA can be expressed as,

$$Q_P = 43A^{0.522} \tag{5.8}$$

Comparison of Talbot formulation in Eq. (5.1) with this expression indicates that the former yields gross underestimation of discharge values. This is the key expression that relates the cross sectional peak discharge at the outlet point to the upstream water flow. If two areas within the same drainage basin (gully) are considered as the whole area, A, and portion of this area, a, and the peak discharge, $Q_P$ for the whole area and the corresponding peak discharge, $Q_{Pi}$, to the $i$-th sub-area can be calculated from the ratio of the two discharges by considering the following expression.

$$Q_{ai} = Q_P \left(\frac{a_i}{A}\right)^{0.522} \tag{5.9}$$

### 5.2.1.1  Talbot Method Criticism

This more than 100-year-old method is not very well known in the hydrology and flood discharge calculation literature. In the past, there were no rainfall records, and hence, many researchers have sought simple empirical formulas, but nowadays with meteorology instrumentations, the rainfall records are frequently available in many areas of the world. In any flood discharge calculation, there are always subjectivities. The Talbot method seems straightforward in application, but without physical justifications by engineers. It is advised that the results of this method must be cross-checked by some recent methodology before its use in practical applications. This will also give chance to improve the Talbot methodology under the light of up-to-date hydrological information. The following points can be raised against Talbot methodology.

(1) This method takes into consideration only the area of drainage basin, and then according to its size, slope, and shape, empirical formulations are given with subjective specification. It is based on 25-year return period discharge and then onwards proposed factors are used for increments to other return periods as 50-year, 100-year, etc.,

(2) Shape factor is another basic variable, but it is dependent on the areal width and area of the basin, hence it does not take into consideration the length of the major stream, which contributes to flood discharge more than any other drainage parameter,

(3) It does not take into consideration the rainfall intensity. However, there are other methodologies that do not take into account the rainfall intensity but they are more recent such as the Snyder method (Chap. 4), which has logical foundations. However, it is recommended in modern times to take into consideration the rainfall intensity as the major factor in flood calculations,

(4) $C$ as the runoff coefficient has been considered compositely as a maximum value equal to 0.9. It is decided in a subjective manner by not taking into consideration bedrock nature, channel slope, and some topographic factors. In fact, nowadays, there are detailed tables for determination of $C$ depending on surface soil types, hydrological soil classification considering vegetation cover, land use, geology, topography, etc., which are not considered in the Talbot approach,

(5) It is not clear how discharge ($Q$)-area ($A$) straight line on double logarithmic paper is obtained. Accordingly, the basic equation as $Q_{25} = Q_{basic}$ SF takes into consideration only the area but inclusion of SF is not very clear, although it is mentioned that it is dependent on the slope factor for drainage area,

(6) W is a factor that reflects the elongation ratio of the catchment, but not the drainage density and main channel slope, which are important in discharge calculations,

(7) There is no reason why the exponent is taken as $\frac{3}{4} = 0.75$; there should be some empirical basis,

(8) $C_1$, $C_2$, and $C_3$ are expressed depending on expert view empirically. They cannot be taken as constants for the whole catchment, because in any catchment, there may be mountainous areas, vegetation cover, and low lands together. It is not clear which one to choose. Perhaps, the best that can be done is the weighted average, but such an approach is not available in the Talbot method,

(9) The factors for $Q_{50} = 1.2Q_{25}$ and $Q_{100} = 1.4Q_{25}$ can be considered as frequency factors, but they should be based on a certain probability distribution function (PDF) such as Gumbel, Pearson Type-II, log-Pearson are extreme value with validation. These factors cannot be adopted as constant in different drainage basins. Besides, they should also be dependent on the rainfall PDFs.

On the other hand, the same method has the following drawbacks that should be taken into consideration in the applications.

(1) Basic discharge calculation graph on double logarithmic paper has a minor error on the vertical ($Q$m$^3$/s, herein $Q = Q_{basic}$) axis, because logarithmic axis cannot assume zero value. On the other hand, the straight line on this graph has not been confirmed empirically,

(2) The same straight line is used to derive 25-year return period discharge as $Q_{25} = Q_{basic}S$, where $S$ is the slope of wadi. This implies that as long as the slopes and the wadi drainage areas are the same, then calculated discharge value remains the same all over the world. However, arid region calculations should have difference than humid regions (Şen 2008),

The modified Talbot empirical formulae, after Quraisi and Al-Hasoun (1996), give the peak discharge for different sizes of large watershed as follows.

$$Q_{25} = 4.985C(A)^{0.5} \qquad (5.10)$$

$$Q_{50} = 1.2Q_{25} \qquad (5.11)$$

$$Q_{100} = 1.17Q_{50} \qquad (5.12)$$

Herein, $Q_{25}$, $Q_{50,}$ and $Q100$ are discharges in m$^3$/s corresponding to return periods of 25-year, 50-year, and 100-year, respectively.

### 5.2.2  Lacey Formulation

For large cross sections, W is equal to the wetted perimeter, $P_w$ (Chap. 3), and Lacey's equation states that $P_w$ is proportional to the square root of the bank-full discharge $Q$ (Lacey 1930).

$$P_w = 4.84\sqrt{Q} \qquad (5.13)$$

Although its applicability still stands unchallenged, it lacks physical explanation. For stream width formula, Lacey made use of the wetted perimeter $P_w$ instead of the width $W$. The wetted perimeter is somewhat larger than the width: in a rectangular profile, it is equal to the summation of base width, $W$, and twice of the water depth, $d$, as $P_w = W + 2D$; and in alluvial streams, where the width is generally much larger than the depth ($W \gg D$), the wetted perimeter is approximately equal to the stream width $P_w \approx W$ (see Sect. 3.7.3). Hence, Eq. (5.13) can be rewritten as

$$P \approx W = 4.84\sqrt{Q} \qquad (5.14)$$

The bank-full discharge is the discharge at which the river starts spilling over the natural levees (see Fig. 3.20, Sect. 3.7.1). It is the discharge above which the river can deposit sediments on its banks. Regular overtopping is necessary for the river to maintain its bed. The following principles are significant in Lacey's formulation application.

(1) If the waterway under bridge is less than Lacey's regime waterway, then it will be called as "restricted waterway",
(2) The unrestricted waterway will be that which is equal or greater than Lacey's regime waterway.

Numerous empirical formulas have been proposed for this and similar problems; but at best, they are all approximate, since no formula can give accurate results with inaccurate data Byrne (1902).

### 5.2.3   Reliability of Early Methods

Early engineers were well aware of the shortcomings and uncertainties of their hydrological design methods. Many of these methods have only a rule of thumb. The responsibility of the individual is much diminished if he has something of that kind to lean on, and in so doubtful a matter as the proper size of culverts, this is especially natural. In making a simple rule, one must confess doubts as to whether this is not the case with the various formulas for proportioning waterways, and in addition to the probable variations in maximum rainfall and possible future changes in the surface conditions must be considered.

The determination of the values of different factors entering into the problem is almost wholly a matter of judgment. An estimate for any one of the above factors is liable to be in error from 100 to 200%, or even more, and of course any result deduced from such data must be very uncertain. Fortunately, mathematical exactness is not required by the problem nor warranted by the data. The question is not one of 10 or 20% of increase; for if a 2-foot pipe is insufficient, a 3-foot pipe will probably be the next size, an increase of 225%; and if a 6-foot arch culvert is too small, an 8-foot will be used, an increase of 180%. The real question is whether a 2-foot pipe or an 8-foot arch culvert is needed.

Blanchard and Drowne (1913) advocated the use of empirical methods or formulas developed over time from local observations. They correctly observed that methods that consider drainage area alone cannot provide universally satisfactory results.

In any event, the use of such results is better than a mere guess, and if some method or formula can be applied to conditions in any one locality for a sufficient length of time, and proper study be given to the factors, which tend to make the results approximate, in time the method or formula can be depended upon to give results which, for that particular locality at least are reasonably accurate.

Empirical formulas are many in number and give results, which are extremely variable. This may be accounted for in some instances by the fact that the formulas are calculated for conditions in one locality may not agree with those in another. Again, some of these formulas have only one variable in them, namely the drainage area, and it cannot be expected that the results by such formulas will agree with those obtained by formulas which have coefficients that are to be applied for different soil conditions, steepness of slope, etc. (Blanchard and Drowne 1913).

Unfortunately, many of the formulations are widely divergent, mainly because of variations in the governing conditions, such as the area of drainage basin, amount of annual rainfall, intensity, extent, and duration of rainstorms, slope of stream and its tributaries, character of soil and quality, and extent of vegetation. These factors certainly constitute a valid excuse for considerable divergence in the resulting values of stream areas and discharges as calculated by the various formulae that have received more or less endorsement by the engineering profession; but they are by no means a legitimate reason for the ridiculously large variations that one notes when applying such formulae for some particular case.

## 5.3   Flood Discharge Envelope Curves

Similar expressions to Eq. (5.8) play very significant role in practical applications provided that there are at the outlet points. It is simply possible to plot the drainage area, $A$, versus flood peak discharge, $Q_P$, and arrive at straight lines on the double logarithmic paper. Such data are given in Table 5.3.

The values in this table are combined with others and shown in Fig. 5.1 on double logarithmic paper as relationship between the drainage area and the flood peak discharge.

In this figure, the straight line on double logarithmic paper yields to a mathematical function as,

$$Q_P = 500A^{0.4} \tag{5.15}$$

This shows a power function relationship, which implies that on the general all the drainage basins considered in Table 5.3 have more hill effective roughness than depression dominance. On the other hand, such a relationship implies rather prompt response of the drainage basin to rainfall intensity to occur in the form of surface runoff.

For instance, Bayazıt and Önöz (2008) in their work to find a relationship between Turkish drainage areas and the peak discharge proposed the following conditional expressions.
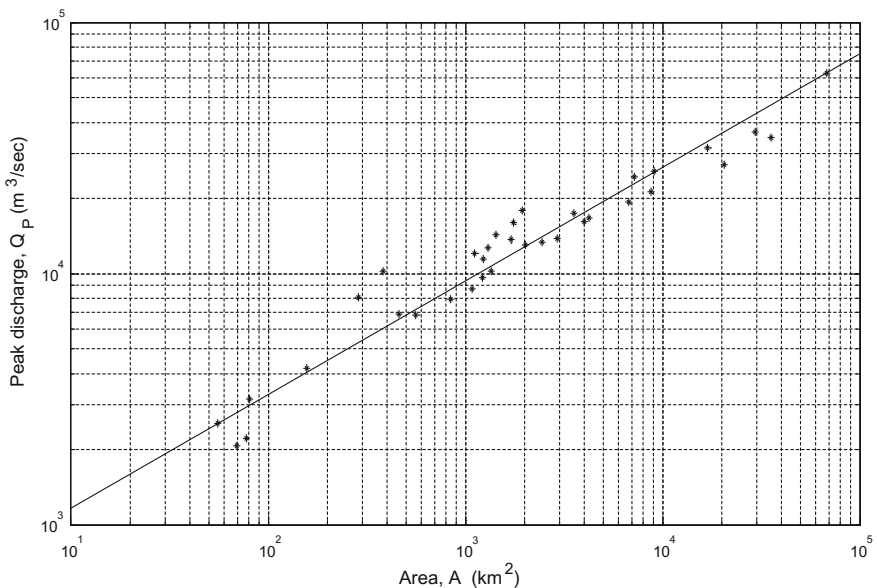
$$Q_P = 1.81A^{1.22} \quad A \leq 300 \tag{5.16}$$

$$Q_P = 79A^{0.5} \quad 300 \leq A \leq 10,000 \tag{5.17}$$

The first studies about the envelope curves concerning flood peak discharges are carried out in the USA (Costa 1987a, b, c, and detailed explanations are presented by Bayazıt and Önöz (2007). It is expected that by time, record-breaking flood discharges may occur in the same drainage basin. For instance, in the USA, the maximum flood discharges were for 10 km$^2$ in 1850, 55 m$^3$/s, in 1939, 397 m$^3$/s, and in 1986, 740 m$^3$/s. The corresponding flood discharges for 100 km$^2$ were 304, 2430, and 3250 m$^3$/s in respective years. It is observed that the floods may transgress the envelope curve at the USA in drainage basins that have more than 100 km$^2$ drainage area. As the drainage area increases, this becomes more pronounced. In small drainage basins, the flood peak discharge is related to the local morphology and climatology. It is possible to observe bigger flood peak discharges in arid and semiarid regions. In cases of drainage basins more than 1000 km$^2$, the flood discharge comes from different sub-catchments, and therefore, it is related to various drainage basin morphological and climatological effects.

**Table 5.3** Drainage area flood peak discharge records (Costa 1987a, b)

| Location | Area, A, (km$^2$) | Peak discharge, $Q_P$, (m$^3$/s) |
|---|---|---|
| USA | 55.34 | 2523.48 |
| Cuba | 69.34 | 2055.89 |
| Tahiti | 77.45 | 2208.00 |
| Mexico | 80.17 | 3162.28 |
| K. Caledonia | 156.68 | 4178.30 |
| Taiwan | 287.08 | 8053.78 |
| K. Caledonia | 459.20 | 6902.40 |
| K. Caledonia | 383.71 | 10,209.39 |
| USA | 561.05 | 6839.12 |
| New Zealand | 839.46 | 7888.60 |
| USA | 1086.43 | 8669.62 |
| Australia | 1216.19 | 9594.01 |
| Japan | 1358.31 | 10,209.39 |
| Taiwan | 1227.44 | 11,428.78 |
| Mexico | 1111.73 | 12,022.64 |
| Japan | 1300.17 | 12,676.52 |
| USA | 1435.49 | 14,321.88 |
| India | 1698.24 | 13,614.45 |
| USA | 2009.09 | 12,941.96 |
| Taiwan | 1757.92 | 15,885.47 |
| Japan | 1945.36 | 17,782.79 |
| North Korea | 2460.37 | 13,335.21 |
| Japan | 2910.72 | 13,740.42 |
| Philippines | 3556.31 | 17,418.07 |
| Japan | 4017.91 | 16,032.45 |
| USA | 4255.98 | 16,710.91 |
| USA | 6729.77 | 19,319.68 |
| USA | 7194.49 | 24,210.29 |
| Madagascar | 8709.64 | 21,183.61 |
| North Korea | 9099.13 | 25,468.30 |
| South Korea | 16,826.74 | 31,622.78 |
| Pakistan | 20,606.30 | 27,101.92 |
| China | 29,444.22 | 36,559.48 |
| Madagascar | 35,645.11 | 34,673.69 |
| China | 68,233.87 | 62,950.62 |

**Fig. 5.1** Worldwide drainage area flood peak discharge relationships

The best curve fit to the scatter of points on the double logarithmic paper is similar to Eq. (5.8), and it has the following mathematical form.
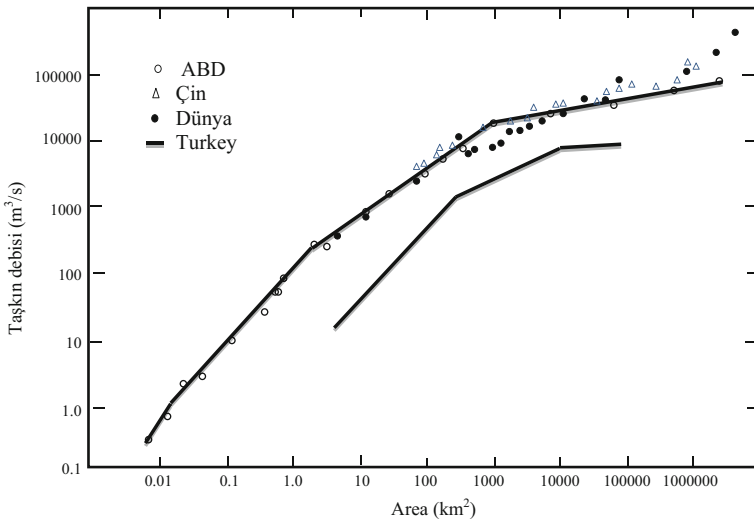
$$Q_P = 500A^{0.40} \tag{5.18}$$

This expression is useful to calculate the flood peak discharge at any point in the world, but especially in the countries mentioned in Table 5.3. However, at different locations similar to the general trend, Figs. 5.1 and 5.2 present more detailed information.
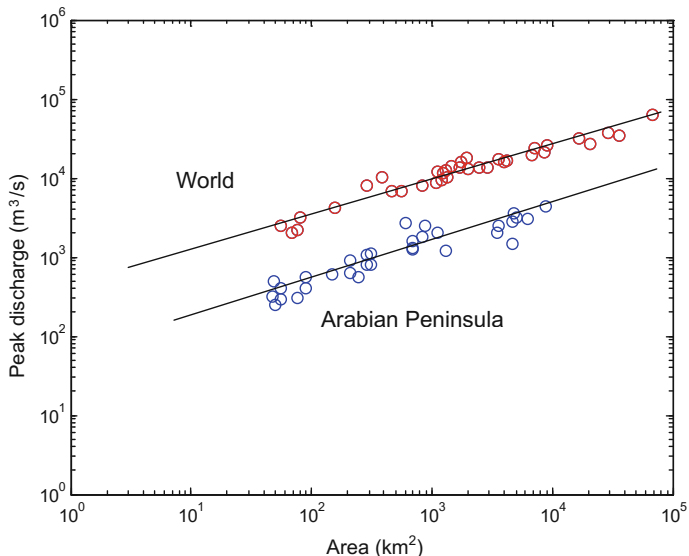
The comparison of the two last figures leads to the following important points concerning the flood peak discharge expectations in the world.

(a) In the countries mentioned in Table 5.1 and Fig. 5.2 (more tropical climate countries), intensive flood occurrences take place, and their average predictions can be achieved from Eq. (5.15),

(b) In cases of more than 10 km$^2$ drainage basin areas, the rate of increase in the flood peak discharge is less than small drainage areas,

(c) Especially at drainage basins with areas smaller than 100 km$^{2,}$ flood peak discharge changes more with the drainage area, because in Fig. 5.2 the slope of this part is more than larger area parts.

On the other hand, in the Arabian Peninsula as a representative of arid regions, the average flood peak discharges are comparatively smaller than the world case (see Fig. 5.3).

**Fig. 5.2** Detailed drainage area flood peak discharge relationships



**Fig. 5.3** Arabian Peninsula drainage area flood peak discharge relationships
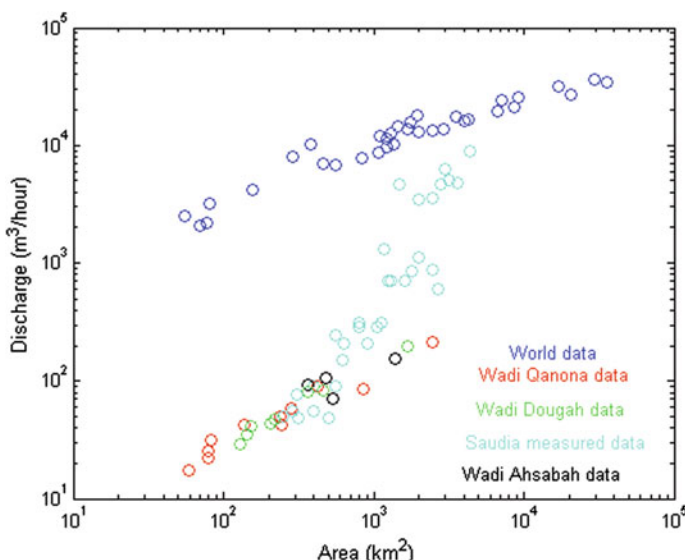
In this figure, the flood peak discharges are smaller than the world case, but still they appear along the parallel line to the world case on double logarithmic paper. This means that although the slope, b, is the same, the unit area ($A = 1$) peak

discharge values, a, are different. Finally, this explanation implies that the constant, 500, in Eq. (5.15) will be smaller in the Arabian Peninsula case around 70.

KSA is subject to occasional floods in different wadis, and especially, the ones along the Red Sea coastal area are more prone than other parts of the Kingdom (Şen 2008). It has tropical climatic features with lengthy dry seasons, which are intersected by sudden, unexpected flash floods. The comparison of floods peaks with reference to different catchment area as in Fig. 5.4 including world data indicates that the discharge-area relationship in the Kingdom has a steeper slope than the rest of the world at large areal extents.

This figure implies that within the same areal range, discharge increase with the drainage basin area is more responsive than other parts of the world. The reasons can be specified as follows.

(1) Sporadic and rare rainfall intensities in the Arabian Peninsula reach high values, which cause rapid response of the drainage basin to runoff,
(2) The vegetative cover is very rare in the Arabian Peninsula drainage basins, and hence, this leads to high surface water velocity,
(3) The geomorphology of the basins on the western Arabian Peninsula is very different between the upstream and the downstream parts along short distances, where upstream locations have elevations reaching to more than 2000 m above mean sea level, and therefore, the runoff velocities are high,
(4) In the upper parts of the catchments, there are hardly any soils to store water by moisturizing. In these areas, the slopes of the mountains are normally steep, and the rocks are impervious. Therefore, infiltration loss and retention by filling the depressions are minor, and consequent flood occurrences are rapid,



**Fig. 5.4** World discharge compared with the Saudi Arabian flood peaks

(5) In the foothill parts of the catchments, the high-intensity rain seals the surface of bare soil very quickly, and consequently, only a shallow depth of soil moisture may be achieved before ponding and surface runoff initiation, which enhance the flood occurrence,

(6) Peak discharges in the Arabian Peninsula are comparatively smaller than the world data, which is due to high evaporation rates.

## 5.4  Discharge-Area-Rainfall Intensity Rational Method

It is rational on logical bases with simplifying basic assumptions, but it does not seem physically plausible for actual flow cases, especially for large drainage basins. Among its assumptions, peak flow rate (discharge) is produced by a constant storm rainfall intensity, which is maintained for a time equal to the period of concentration over the whole drainage basin area. Additionally, there is a set of assumptions that should be taken into consideration for successful applications and interpretations of the results. Otherwise, the peak discharge estimation by the classical RM may lead to unreliable conclusions. Among such assumptions are the following points for close consideration.

(1) Average excess rainfall intensity has the same recurrence interval with the peak discharge,

(2) The excess rainfall is uniformly distributed over the drainage area,

(3) The excess rainfall intensity is constant during the time of concentration,

(4) Peak discharge volume is distributed uniformly over the drainage area, and it is directly and linearly dependent on the excess rainfall intensity over the same drainage area. The ratio between the two is referred to as the runoff coefficient,

(5) The excessive rainfall intensity time is identical to time required for the runoff to flow from the hydraulically most distant point in the contributing drainage area to the point of design,

(6) It is not possible to satisfy all the assumptions simultaneously in any work, and there is less chance that the rainfall rate used in the design might occur actually. Hence, the safety factor cannot be considered in the design,

(7) In general, a difference exists between intense point rainfall areal coverage over some portion and over the whole drainage area. In such cases, the classical RM (Sect. 5.8) yields excessive peak discharge values, and hence, it is necessary to have an area reduction factor (Omolayo 1993; Sirdaş and Şen 2007), which cannot be determined easily in the practical applications,

(8) In an irregularly shaped drainage basin, a part of the area with a short time of concentration may cause greater peak discharge at the outlet point than the runoff rate calculated for the entire drainage basin. This is because parts of the area with long concentration times are far less susceptible to high-intensity rainfall,

(9) A portion of a drainage area with small permeability produces greater amount of runoff than that calculated for the entire area. In order to reduce the effects of the last three points in the calculations, it is better to subdivide the whole drainage area into a set of convenient sub-areas.

Average knowledge is possible only when a phenomenon or process is isolated from surrounding effects through a set of restrictive assumptions that render the problem into the world of certainty by ignoring all uncertainty features. For instance, $C$ is a multiplier applied to deterministically (classical two-valued logic) calculated peak discharge according to rational formulation in hydrology. Thus, by effectively "overengineering" or "under-engineering" the design by strengthening components or including redundant systems, $C$ accounts for imperfections in hydrological calculations, flaws in assembly, geomorphological and geologic degradation, and uncertainty in discharge estimates. In fact, $C$ includes "ignorance component" due to the exclusion of all fuzzy logic information about the hydrological design. However, fuzzy logic rules and system help to solve the hydrological design problem without considering $C$ explicitly (Şen 2010).

(a) After a rainfall occurrence, the discharge value at the outlet point of any drainage basin can be calculated according to the following steps.
(b) A uniform rainfall depth is assumed at each point over the drainage area (Chap. 3). Along the rainfall duration, $T$, the average water volume, $V$, over the drainage area, $A$, with effective rainfall height, $P$, is given simply as,

$$V = AP$$

(c) After the division of both sides by the rainfall duration, the left-hand side becomes equivalent to peak discharge definition, $Q_P = V/T$, and the right-hand side to rainfall intensity, $I = P/T$, and finally,

$$Q_R = AI$$

Prior to the surface runoff, there will be various losses such as depression storage, evaporation, and infiltration, and hence, the rainfall discharge must be multiplied by a constant, $C$, less than 1. This is the runoff coefficient, which converts the rainfall to runoff. Finally, the surface runoff peak discharge is,

$$Q_P = CIA \tag{5.18}$$

One of the most important questions is about the calculation of the rainfall intensity for practical applications. In Chap. 2, rainfall intensities are provided for a set of times with intensity-duration-frequency curves. However, in the surface water (runoff, flood) calculations, the intensity should be adapted not on the basis of the rainfall duration, but on the time duration that is needed for the runoff drop on the

farthest upstream point to reach the drainage basin outlet, which is the time of concentration. Runoff coefficient is considered as constant during the storm rainfall; the morphology of the drainage basin remains the same during the storm rainfall.

The specifications concerning the hydrological soil groups are given according to Part 630 Hydrology National Engineering Handbook, United States Department of Agriculture Natural Resources Conservation Service and Hydrologic Soil Groups as follows.

**Group A**—Soils in this group have low runoff potential when thoroughly wet. Water is transmitted freely through the soil. Group A soils typically have less than 10% clay and more than 90% sand or gravel and have gravel or sand textures. Some soils having loamy sand, sandy loam, loam, or silt loam textures may be placed in this group if they are well aggregated, of low bulk density, or contain greater than 35% rock fragments.

**Group B**—Soils in this group have moderately low runoff potential when thoroughly wet. Water transmission through the soil is unimpeded. Group B soils typically have between 10 and 20% clay and 50–90% sand and have loamy sand or sandy loam textures. Some soils having loam, silt loam, silt, or sandy clay loam textures may be placed in this group if they are well aggregated, of low bulk density, or contain greater than 35% rock fragments.

**Group C**—Soils in this group have moderately high runoff potential when thoroughly wet. Water transmission through the soil is somewhat restricted. Group C soils typically have between 20 and 40% clay and less than 50% sand and have loam, silt loam, sandy clay loam, clay loam, and silty clay loam textures. Some soils having clay, silty clay, or sandy clay textures may be placed in this group if they are well aggregated, of low bulk density, or contain greater than 35% rock fragments.

**Group D**—Soils in this group have high runoff potential when thoroughly wet. Water movement through the soil is restricted or very restricted. Group D soils typically have greater than 40% clay, less than 50% sand, and have clayey textures. In some areas, they also have high shrink–swell potential. All soils with a depth to a water impermeable layer less than 50 cm (20 in.) and all soils with a water table within 60 cm (24 in.) of the surface are in this group, although some may have a dual classification, as described in the next section, if they can be adequately drained.
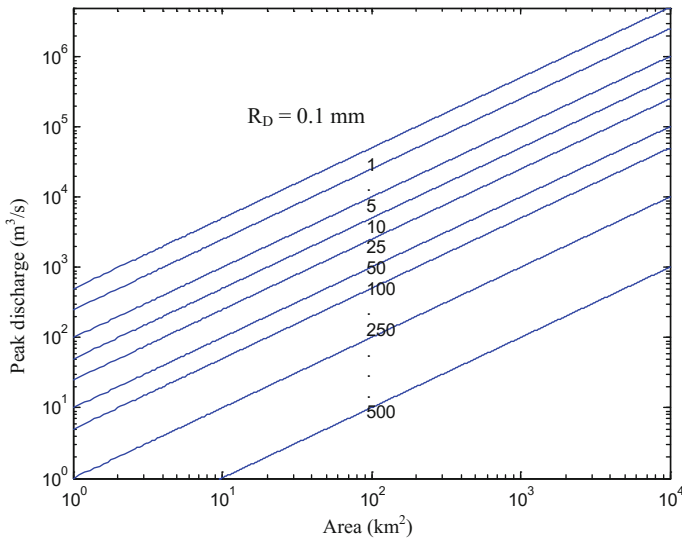
In general, the runoff coefficient can be taken from Table 5.4, and then from Eq. (5.18), the required peak discharge can be calculated.

The area in the RM in Eq. (5.18) and the flood peak discharge has a relationship depending on a set of rainfall intensity, which is shown on a double logarithmic paper in Fig. 5.5 as straight lines. Herein, $R_D = Ci$ shows effective rainfall height.

These straight lines are similar to the ones in Fig. 5.1. This point indicates how the initial formulations between the flood peak discharge and the drainage area are rationally reliable.

**Table 5.4** Runoff coefficients for different hydrological soil groups

| Hydrological Soil Group | A | | | B | | | B | | | D | | |
|---|---|---|---|---|---|---|---|---|---|---|---|---|
| Recurrence interval | 5 | 10 | 100 | 5 | 10 | 100 | 5 | 10 | 100 | 5 | 10 | 100 |
| Land use or surface characteristics | | | | | | | | | | | | |
| Business: | | | | | | | | | | | | |
| A—commercial area | 0.75 | 0.80 | 0.95 | 0.80 | 0.85 | 0.95 | 0.80 | 0.85 | 0.95 | 0.85 | 0.90 | 0.95 |
| B—neighborhood area | 0.50 | 0.55 | 0.65 | 0.55 | 0.60 | 0.70 | 0.60 | 0.65 | 0.75 | 0.65 | 0.70 | 0.80 |
| Residential: | | | | | | | | | | | | |
| A—single family | 0.25 | 0.25 | 0.30 | 0.30 | 0.35 | 0.40 | 0.40 | 0.45 | 0.50 | 0.45 | 0.50 | 0.55 |
| B—multi-unit (detached) | 0.35 | 0.40 | 0.45 | 0.40 | 0.45 | 0.50 | 0.45 | 0.50 | 0.55 | 0.50 | 0.55 | 0.65 |
| C—multi-unit (attached) | 0.45 | 0.50 | 0.55 | 0.50 | 0.55 | 0.65 | 0.55 | 0.60 | 0.70 | 0.60 | 0.65 | 0.75 |
| D—½ lot or larger | 0.20 | 0.20 | 0.25 | 0.25 | 0.25 | 0.30 | 0.35 | 0.40 | 0.45 | 0.40 | 0.45 | 0.50 |
| D—apartments | 0.50 | 0.55 | 0.60 | 0.60 | 0.60 | 0.70 | 0.60 | 0.65 | 0.75 | 0.65 | 0.70 | 0.80 |
| Industrial | | | | | | | | | | | | |
| A—light areas | 0.55 | 0.60 | 0.70 | 0.60 | 0.65 | 0.75 | 0.65 | 0.70 | 0.80 | 0.70 | 0.75 | 0.90 |
| B—heavy areas | 0.75 | 0.80 | 0.95 | 0.80 | 0.85 | 0.95 | 0.80 | 0.85 | 0.95 | 0.80 | 0.85 | 0.95 |
| Parks, cemeteries | | | | | | | | | | | | |
| Playgrounds | 0.10 | 0.10 | 0.15 | 0.20 | 0.20 | 0.25 | 0.30 | 0.35 | 0.40 | 0.35 | 0.40 | 0.45 |
| Schools | 0.30 | 0.35 | 0.40 | 0.40 | 0.45 | 0.50 | 0.45 | 0.50 | 0.55 | 0.50 | 0.55 | 0.65 |
| Railroad yard areas | 0.20 | 0.20 | 0.25 | 0.30 | 0.35 | 0.40 | 0.40 | 0.45 | 0.45 | 0.45 | 0.50 | 0.55 |
| Streets | | | | | | | | | | | | |
| A—paved | 0.85 | 0.90 | 0.95 | 0.85 | 0.90 | 0.95 | 0.85 | 0.90 | 0.95 | 0.85 | 0.90 | 0.95 |
| B—gravel | 0.25 | 0.25 | 0.30 | 0.35 | 0.40 | 0.45 | 0.40 | 0.45 | 0.50 | 0.40 | 0.45 | 0.50 |
| Drives, walks, and roofs | 0.85 | 0.90 | 0.95 | 0.85 | 0.90 | 0.95 | 0.85 | 0.90 | 0.95 | 0.85 | 0.90 | 0.95 |
| Lawns | | | | | | | | | | | | |
| A—50–75% grass (fair condition) | 0.10 | 0.109 | 0.15 | 0.20 | 0.20 | 0.25 | 0.30 | 0.35 | 0.40 | 0.30 | 0.35 | 0.40 |
| B—75% or more grass (good condition) | 0.05 | 0.05 | 0.10 | 0.15 | 0.15 | 0.20 | 0.25 | 0.25 | 0.30 | 0.30 | 0.35 | 0.40 |
| Underdeveloped surface | | | | | | | | | | | | |
| A—flat (0–1%) | 0.04–0.09 | | | 0.07–0.12 | | | 0.11–0.16 | | | 0.15–0.20 | | |
| B—average (2–6%) | 0.10–0.14 | | | 0.12–0.17 | | | 0.16–0.21 | | | 0.20–0.25 | | |
| C—steep | 0.13–0.18 | | | 0.18–0.24 | | | 0.23–0.31 | | | 0.28–0.38 | | |

**Fig. 5.5**   Rational method double logarithmic paper representations

## 5.5   Runoff Coefficient Seasonal Variation
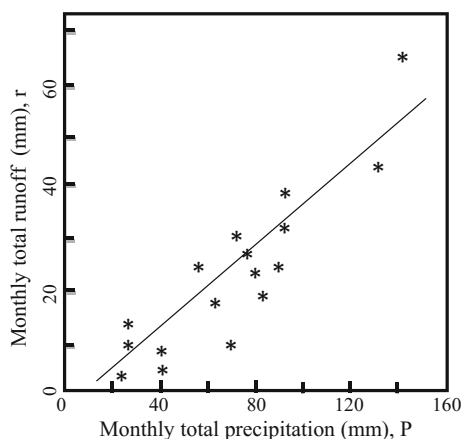
Runoff coefficient estimation presents one of the greatest difficulties, and it is a major source of uncertainty in many water resources projects. The coefficient must account for factors that affect peak flow relationship to average rainfall intensity other than drainage area and time of concentration. In any water resources design, the values of the runoff coefficient are taken from tables (Table 5.4) of possible values depending on the soil description of the area. The main concern in selecting these values is that they are chosen rather subjectively in a vague manner and largely reflect personal judgment rather than hard data. On the other hand, few studies show that adopted or derived runoff coefficient values on a drainage basin vary widely from storm to storm particularly depending on different antecedent wetness conditions. The value of the runoff coefficient increases as the average recurrence interval increases in a nonlinear form. Since considerable judgment and experience are required in selecting satisfactory runoff coefficient values for design, there is a need to check values against observed runoff data in a given catchment. In any water resources operation, runoff plays a significant role as an input variable in the design of engineering structures such as culverts, reservoirs, in groundwater recharge estimations, and in flood designs. Runoff is produced at the ground surface when the rainfall intensity exceeds the infiltration capacity, and water originally falling as rain or snow is converted into runoff. The runoff coefficient plays a central role in the calculations of the surface water yield of a catchment due to many forms

of precipitation (Chap. 2). It is quantitatively related to various interrelated factors such as precipitation intensity and its seasonal distribution, precipitation types (orographic, convective, cyclonic, or frontal), vegetation types and cover, transpiration rate, geological outcrops, infiltration rates, and the topography of a catchment area (Chap. 3). Additionally, in many catchments and especially those closer to city centers, runoff volumes are strongly modified by anthropogenic effects such as urbanization, irrigation, inter-basin water transfer, water impoundment reservoirs, and artificial groundwater recharges.

The runoff coefficient is dimensionless and defined as the ratio of runoff to precipitation amount. It can be evaluated statistically by plotting precipitation versus runoff, and the slope of the regression line is the runoff coefficient. A typical rainfall–runoff scatter diagram is shown in Fig. 5.6 for monthly data. This simple procedure has the following drawbacks.

(1) The straight-line slope provides a global estimate of the runoff coefficient, but does not provide interpretations or clues about other timescales such as seasons or years,

(2) In the regression line solution, the basic assumption is that the relationship between rainfall and runoff is linear. With linearity, an increase in the rainfall results in proportional increase in the runoff and runoffs from different inputs can be superimposed. The rainfall–runoff relationship in a catchment is nonlinear. Proportionality and superposition principles do not apply with nonlinear systems (Kundzewicz and Napiorkowski 1986),

(3) This straight-line fitting gives a simple and global value for the runoff coefficient for all time periods. More detailed information about the topic is presented by Maidment (1993).

**Fig. 5.6** Schematic precipitation-runoff scatter diagrams
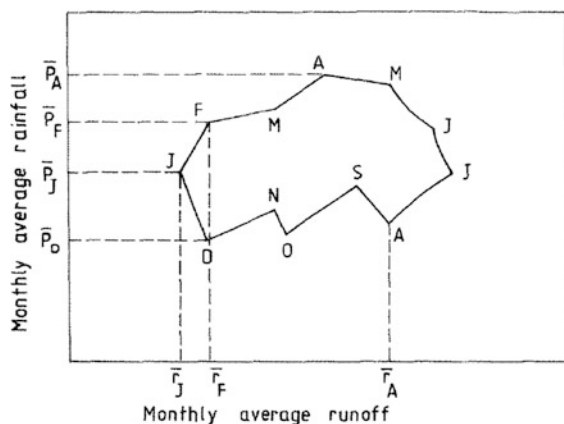
## 5.5.1  Runoff Coefficient Polygons

The main concern herein is not to calculate a single parameter for all the scattered points on the polygon diagram, but to make interpretations and quantifications as the system passes along the polygon sides from one month to the next. Kadioğlu and Şen (2001) have provided all the necessary steps and explanations about runoff coefficient polygons.

Based on the dynamics of monthly precipitation and runoff time series, one can construct the polygon diagram on a Cartesian coordinate system. For the runoff coefficient estimations, it is necessary that these two time series be simultaneously recorded in the same catchment. Their plots with the connection of successive months by straight lines lead to a scatter diagram with almost no definite pattern. This is an expected result because the precipitation and runoff phenomena depend on many external factors such as the types of storms, weather patterns, and geological composition of the catchment surface, human settlement, water resources, and agricultural developments in the catchment area and antecedent conditions, all of which introduce uncertainty into the system. In order to obtain a definitive pattern, monthly averages of the precipitation and runoff are calculated and then plotted leading to a set of 12 successive points. Figure 5.7 shows representative monthly averages of precipitation-runoff pairs. The connection of the successive monthly points by straight lines appears in the form of a closed polygon with different lengths and slopes of its sides.

(1) Generally, so far in the literature, a global regression line is fitted to the scatter diagrams as in Fig. 5.6, and its slope is considered as the annual runoff coefficient for the catchment. In effect, this is the linearization of the nonlinear behavior of the precipitation-runoff transformation system. Polygon diagrams similar to Fig. 5.7 provide a basis for qualitative and quantitative interpretations and calculations about the precipitation-runoff flow system and the runoff coefficient as follows.



**Fig. 5.7** A representative monthly precipitation-runoff polygon diagram

    i. The polygon sides indicate the change in average values of precipitation or runoff for consecutive months. All the sides considered together define a closed polygon implying the natural balance of the precipitation-runoff flow during one year,

   ii. The lengths of the polygon sides indicate the values of the changes in average values for consecutive months,

  iii. The closeness of the slope of each side to the vertical or horizontal indicates the relative proportions of the precipitation and runoff in making up the numerical value of the monthly runoff coefficient. It implies that the average precipitation contributes less significantly to the average runoff for each consecutive month. Similar interpretations for all months during one year provide a basis for qualitative interpretations about the precipitation-runoff occurrences in a catchment,

(2) Along each side, the runoff is assumed to change linearly with precipitation. The physical interpretation of the end point on a side is an average value of precipitation and runoff for a particular month. Such a linearity assumption during time intervals smaller than one year yields more reliable results in the runoff volume calculations. Division of the runoff coefficient into months during one year, as in the polygon diagram, furnishes a basis for the successive application of the RM similar to numerical procedures. The polygon constitutes finite straight-line portions for the validity of a linearity assumption on a monthly basis. Practically, if all of the sides fall along a single direction within ±5 or ±10% deviations, then the corners in the polygon diagram might be considered as scatters along a straight line, which represents the annual precipitation-runoff relationship. The narrower the polygon, the more uniform is the representative runoff coefficient for the catchment concerned. Wide polygons imply heterogeneous temporal runoff coefficients for the catchment area. It also means nonlinearity in precipitation-runoff relationships for the catchment area considered,

(3) In each polygon, there is always a rising sequence of sides followed by a falling sequence as shown in Fig. 5.7, where starting from A (August) through points S, O, N, D up to J (January), the average monthly runoff volumes rise. However, in contrast, starting from J (January) through F, M, A, M, J, J and ending in A (August), a falling sequence exists. In general, the runoff coefficients along a rising sequence are comparatively greater than those of a falling sequence. This is due to the fact that during the rising sequence, the catchment becomes wetter with time, whereas along the falling sequence, the same catchment becomes drier. A rising sequence corresponds to precipitation periods, but the falling sequence might even represent the contributions from groundwater to surface/water, hence causing the runoff coefficient to assume values greater than one,

(4) Any horizontal line intersection with the polygon provides lower and upper limits of expected runoff heights with corresponding runoff coefficients for a given precipitation depth. In contrast, any vertical line depicts the lower and
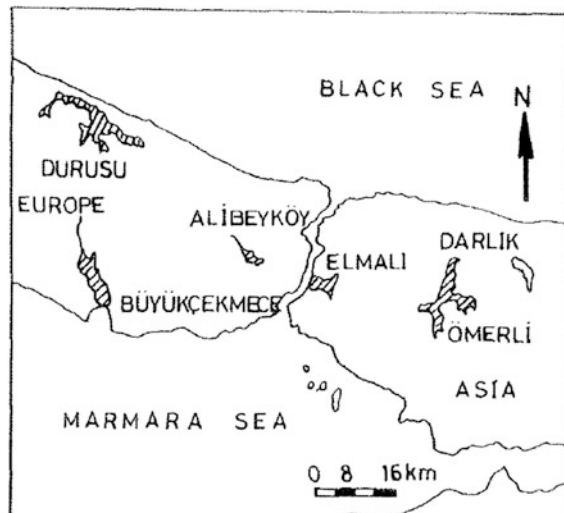
upper limits as well as the range of precipitation depth that might give rise to a certain amount of runoff,

(5) The smaller the area of the polygon, the more consistent is the monthly precipitation and the more constant is the runoff coefficient,

(6) The smaller the overall slope of the polygon from the horizontal axis, the more precipitation is converted to runoff by the catchment system,

(7) In any water resources development and operation activity that is planned within a catchment area, these polygons will provide runoff coefficient values for an effective operation rule.

(8) These general characteristics of the polygon diagrams reflect many qualitative properties of the precipitation-runoff phenomena that occur over the catchment area.

### 5.5.2   Application

Istanbul City water supply sources are dependent on six surface reservoirs located in different catchments in the European and Asian areas, three in each as shown in Fig. 5.8. According to their usable capacities in sequence, the three in the European area are the Durusu, Buyukçekmece, and Alibeykoy reservoirs, while those in the Asian area are the Ömerli, Darlik, and Elmali reservoirs. Some characteristics of the catchments and reservoirs are shown in Table 5.5. The runoff coefficients shown in this table are long annual averages, which are the overall regression line slopes. Depending on the urbanization extent in European catchment areas, the runoff coefficients for highly urbanized catchments assume high values.

**Fig. 5.8**  Reservoir locations near Istanbul City
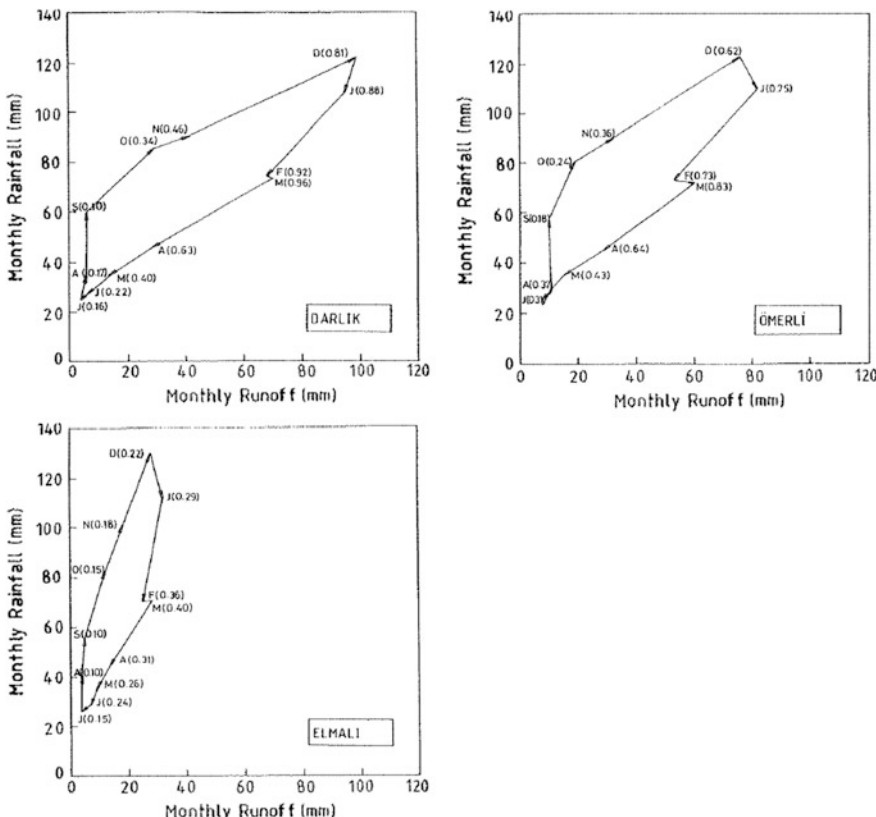
**Table 5.5**  Istanbul watershed and reservoir characteristics

| Drainage basin characteristics | Asia | | | Europe | | | Average |
|---|---|---|---|---|---|---|---|
| Area (km$^2$) | 600 | 207 | 76 | 619 | 621 | 160 | 380 |
| Rainfall (mm/year) | 850 | 850 | 820 | 750 | 700 | 830 | 800 |
| Runoff ($\times 10^3$ m$^3$/year) | 236 | 108 | 32 | 163 | 219 | 54 | 135 |
| Runoff coeff. (%) | 45 | 59 | 51 | 35 | 40 | 46 | |

The precipitation-runoff phase diagram polygons for each catchment are plotted using monthly average data under consideration of catchment characteristics given in Table 5.5.

The results are shown in Fig. 5.9 for the Asian and in Fig. 5.10 for the European catchments near Istanbul.

The following qualitative characteristic behaviors of the precipitation-streamflow phenomenon can be deduced from these polygons for the Istanbul catchments.



**Fig. 5.9**  Polygons for Asian drainage basins

(a) In all the polygons at the corner points, the streamflow coefficients calculated as the ratio of runoff to precipitation are given within the brackets. The average monthly runoff coefficients for one monthly period are calculated as the arithmetic average of the preceding and current months' runoff coefficients as they appear in Figs. 5.9 and 5.10. The average annual runoff coefficient is calculated as the arithmetic average of 12 months. These runoff coefficient values are presented in Table 5.6.

For instance, the runoff coefficient of 0.74 at the Omerli catchment in January is obtained as the arithmetic average of the January and February corner values in Fig. 5.10, i.e., (0.73 + 0.15)12 − 0.74. Comparison of these values among all the catchments indicates that for the Buyukçekmece catchment, there are runoff coefficients calculated in this way, which attain values greater than one. At first, such a value might appear as absurd, but it pinpoints a very important natural phenomenon that this reservoir is fed by groundwater and snowmelt in addition to precipitation. Notice that runoff coefficients greater than one is attached to the decreasing limb of
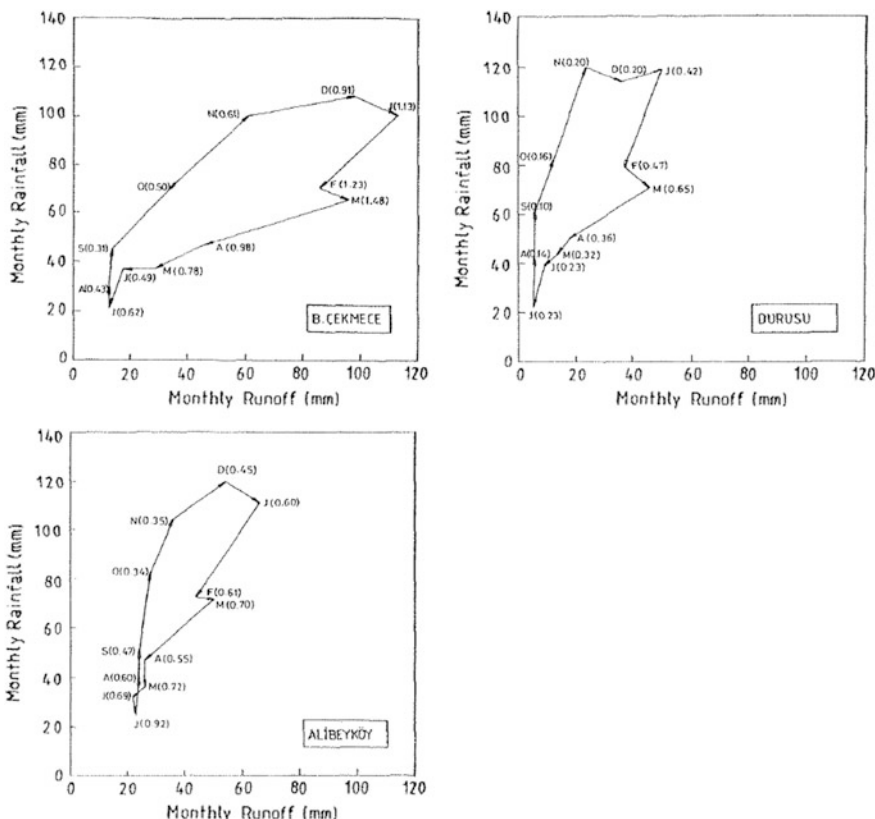


Fig. 5.10 Polygons for European drainage basins

**Table 5.6** Runoff coefficients (%)

| Reservoir | Monthly | | | | | | | | | | | | Annual |
|---|---|---|---|---|---|---|---|---|---|---|---|---|---|
| | J | F | M | A | M | J | J | A | S | O | N | D | |
| Omerli | 74 | 78 | 74 | 54 | 38 | 32 | 34 | 28 | 21 | 30 | 49 | 69 | 48 |
| Darlik | 90 | 94 | 80 | 52 | 31 | 19 | 17 | 14 | 22 | 40 | 64 | 85 | 51 |
| Elmali | 33 | 38 | 36 | 28 | 35 | 20 | 13 | 10 | 13 | 17 | 20 | 26 | 23 |
| Durusu | 45 | 56 | 51 | 34 | 28 | 23 | 19 | 12 | 13 | 18 | 20 | 31 | 29 |
| Buyukcekmece | 118 | 136 | 123 | 88 | 64 | 56 | 53 | 37 | 41 | 56 | 76 | 102 | 79 |
| Alibeykoy | 60 | 66 | 63 | 64 | 71 | 81 | 76 | 54 | 41 | 35 | 40 | 58 | 59 |

polygons during which the precipitation decreases steadily, but groundwater as a delayed recharge contributes to the streamflow. The geological formation of this catchment is a composition of limestones and dolomites, which easily store and transmit groundwater in large amounts. Another explanation of these runoff coefficients is that since the catchment area is very big, the precipitation that might occur at distant parts arrives at the streamflow measuring station, which is located near the reservoir, in a rather delayed manner. Last, but not least, the precipitation in the form of snow after melting contributes to runoff again with a delayed response.

(b) A first glance indicates that the steepest and narrowest polygon appears for the Elmali catchment in the Asian area (Fig. 5.9). The narrowness of the polygon implies that the catchment response to precipitation is almost the same in each month without significant variation. Two catchments that show a similar steep pattern of behavior are the Durusu and Alibeykoy catchments in the European area (Fig. 5.10). However, their polygons are comparatively wider; hence, catchment reaction to precipitation is different in different months,

(c) In all the polygons, irrespective of location the polygon sides for precipitation amounts in the months July, August, and September are almost vertical, which means that any precipitation occurrence in these months will result in negligible runoff, but significant groundwater recharge and, to a lesser extent, evaporation. After September, all the polygons show significant changes in the slopes and contribute to the runoff more and more. This situation continues steadily until the end of December, except in the Durusu catchment, where there is a decrease from November to December, and subsequently, a slight increase, which is followed by a continuous decrease again until July. In all the polygons except the one for Durusu, the end of December forms a turning point for precipitation increases and from then onward there are decreases in the precipitation amounts and, consequently, in the runoff amounts. In the Durusu catchment, there is a local decrease in the precipitation amount from November to December,

(d) The most instantaneous response to precipitation takes place at the Darlik and Buyukçekmece catchments, especially during the period from the end of September until December, since over this period the polygon sides have the smallest slopes.

(e) Invariably in each polygon for the six catchments near Istanbul City, there is a local increase in the runoff amount although the precipitation continues to decrease. This is attributable to frost events, which happen quite frequently in this period. Hence, the rainfall cannot find an opportunity to infiltrate easily and consequently is forced to appear in the form of runoff,

(f) Since the Elmali catchment is the smallest in area, the completion of its annual cycle of precipitation-runoff does not take a long time. This is evident from Fig. 5.9, in which the Elmali polygon comparatively has the least peripheral length. Accordingly, the gathering of water into the reservoir in this watershed is rather fast, and such a property must be taken into consideration in the reservoir operations.

## 5.6   Arid Zone Runoff Coefficient Area Relationship

Problems in the analysis of flood records from arid areas include those of gauging and measurements, low or zero annual maxima in a number of years, and the suitability or otherwise of the mean annual flood as the appropriate scaling factor for the dimensionless curves (Farquharson et al. 1992). Mean runoff values form the basis for any irrigation and flood protection measures. In addition, annual flood and frequency data are needed for dam siting as well as for dimensioning of the hydraulic structures for flood control and irrigation purposes (Sen and Al-Suba'I 2002). In the following, these quantities are evaluated for the drainage basin on which the dams are proposed.

It is economically costly and physically difficult to gauge all streams in a region. Consequently, some methods are used to estimate runoff coefficients and volume for the catchments of ungauged streams. The runoff coefficient, $C$, is defined as the ratio of the annual discharge volume of the stream to the annual volume of precipitation of its catchment.
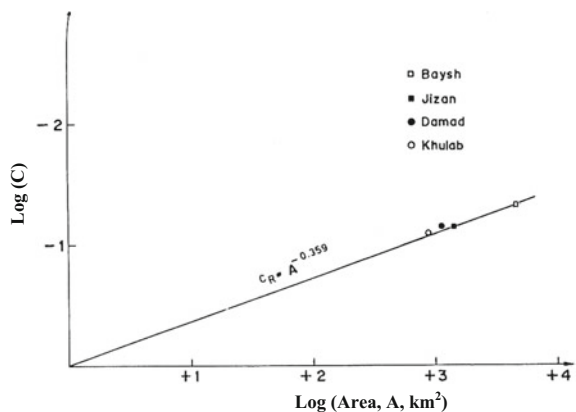
Calculation of the mean values of $C$ for the catchments of four gauged streams in and around the KSA is given in Table 5.7.

In practical applications, one seeks the ratio on the basis of one-year surface flow volume to rainfall volume. In arid regions, such as the southwestern corner of the Arabian Peninsula on the basis of some runoff measurements and their plots on a

**Table 5.7**  Runoff coefficients

| Drainage basin | wadis | | | |
|---|---|---|---|---|
| | Baysh | Damad | Jizan | Khulab |
| Area ($km^2$) | 4652 | 1108 | 1430 | 900 |
| Average annual runoff ($\times 10^6$ $m^3$) | 76 | 40 | 57 | 32 |
| Average annual rainfall ($\times 10^6$ $m^3$) | 1586 | 570 | 755 | 405 |
| Runoff coefficient | 0.048 | 0.071 | 0.076 | 0.078 |

**Fig. 5.11** Runoff coefficient
drainage area relationships



double logarithmic paper have led to the following expression, which relates the
runoff coefficient to the inverse of the drainage area as in Fig. 5.11.

$$C = \frac{1}{A^{0.359}}$$

(5.19)

For this region, the value of the runoff coefficient varies between 0.048 and
0.078.
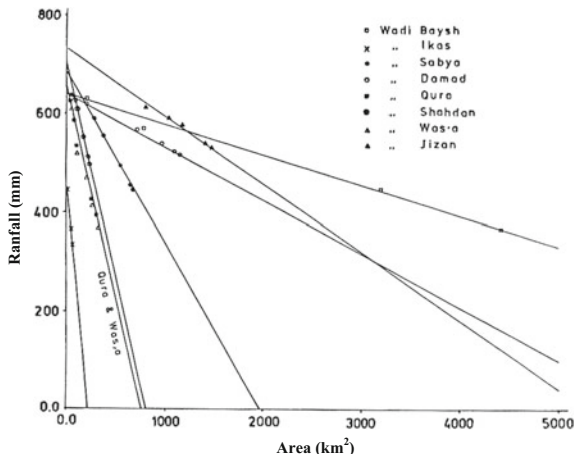
## 5.7  Arid Region Flood Calculations

For reservoir storage or flood design in arid regions, the records of rainfall, runoff,
and their maximum records are important. If there are no rainfall–runoff records, the
flood peak discharges are calculated according to locally derived empirical for-
mulations or formulations derived in similar regions and adapted after their simple
modification to suit the region of concern. It is possible that in a region, several
high-intensity rainfall occurrences take place, and consequently, floods appear. The
rainfall occurrences are rather sudden and may lead to flash floods, and therefore,
their calculations are complex and difficult. Whatever are the circumstances in the
design of reservoir storages, flood analysis principles must be used.

This last expression helps to calculate the runoff coefficient from the drainage
area value. Figure 5.12 shows the given water depth area curves, which provides
opportunity to calculate annual rainfall amount provided that the drainage area is
known.

The calculations are presented in Table 5.8 for a set of the Arabian Peninsula
southwestern part drainage basins as in column 3.

**Fig. 5.12** Arid region
rainfall height-area curves



Annual rainfall volumes, $V_A$, can be calculated by the multiplication of the values in the second and third columns, and the results are entered into column four. Annual runoff volumes are included in the last column.

In arid regions, wadi (drainage basin) annual runoff volumes have great variability. Figure 5.13 presents calculated and measured flood peak discharge values for the Arabian Peninsula (Sen and Al-Suba'I 2002).

In these areas, 50-year, 100-year, and 200-year return period calculations are important for erosion, sedimentation, reservoir volume design, and flood peak discharge calculations. In Fig. 5.14, 100-year return period discharges are presented.

## 5.8 Irrationality of Rational Method and Some Rectification

RM is the simplest approach for peak discharge calculation, but it has many simplifying and unrealistic assumptions, which cause biased results in many applications. Among the most important drawbacks are its applicability restriction to small areas, but it is also used without much care even for large, flat, and horizontal areas, but drainage basins have slopes and rough topography. In the RM, the rainfall intensity is taken as constant over the whole storm rainfall duration and coverage of the drainage area. In this paper, the RM irrationalities are explained, and then a modified formulation is proposed by reconsidering geomorphological and rainfall features. Nonlinear relationships of peak discharge with drainage area and slope are incorporated in the new formulation. Its application is achieved for a set of drainage sub-basins from the KSA.

**Table 5.8** Runoff coefficients and average annual runoff volumes

| Wadi name | Drainage area, A (km²) | Average annual rainfall, P (mm) | Rainfall volume, $V_A$ (10³ m³) | Average runoff coefficient, C | | Runoff volume, $V_R$ (10⁶ m³) | |
|---|---|---|---|---|---|---|---|
| | | | | Measurement | Calculation | Measurement | Calculation |
| Baysh | 4652 | 342 | 1591 | 0.05 | 0.05 | 76 | 76 |
| Ikas | 68 | 370 | 25 | – | 0.22 | – | 6 |
| Qura | 309 | 423 | 131 | – | 0.13 | – | 17 |
| Shahdan | 213 | 510 | 109 | – | 0.15 | – | 16 |
| Was'a | 324 | 446 | 145 | – | 0.13 | – | 18 |
| Sabya | 675 | 453 | 306 | – | 0.10 | – | 29 |
| Damad | 1108 | 515 | 571 | 0.07 | 0.08 | 40 | 46 |
| Jizan | 1430 | 528 | 755 | 0.07 | 0.07 | 57 | 58 |

*Note* The calculations are achieved according to equations $V_A = AP$ and $V_R = CV_A$
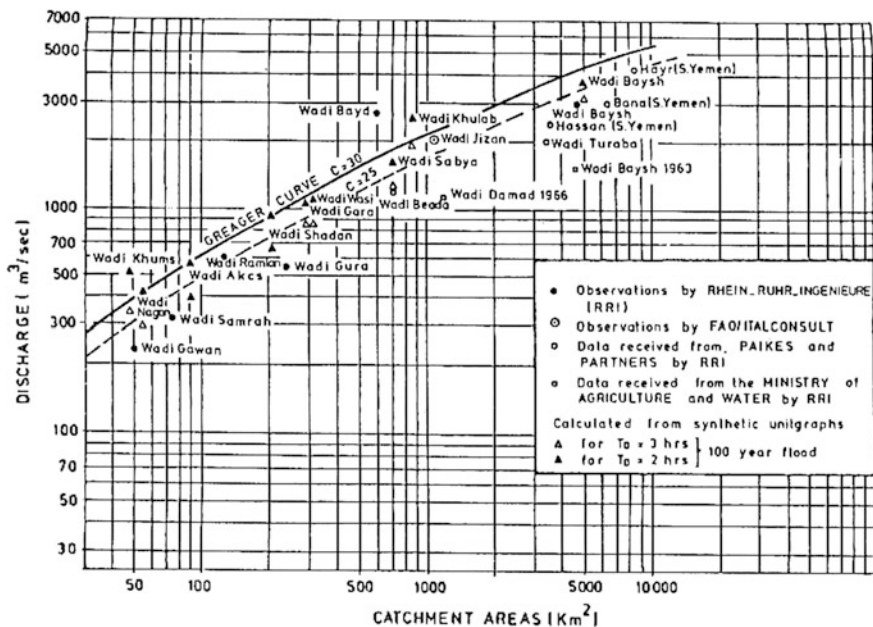
Fig. 5.13 Measured and calculated flood amounts
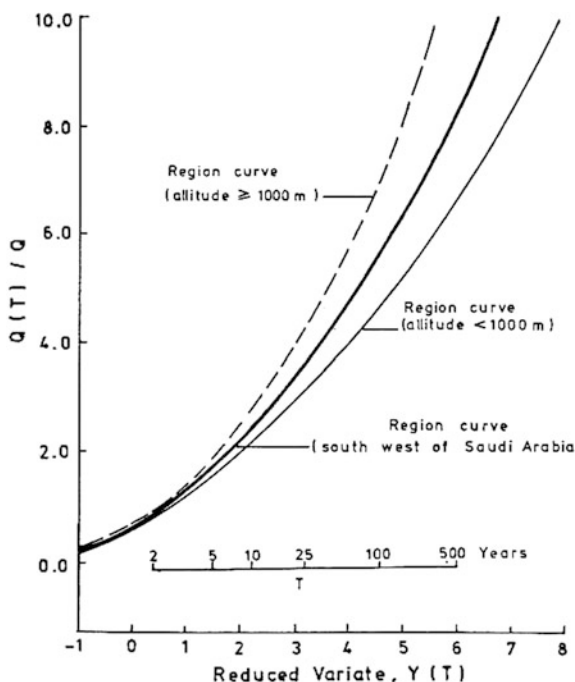


Fig. 5.14 100-year return period flood discharges

Rainfall–runoff relationship plays a key role in any water resources planning, design, operation, and maintenance study. Flood estimations on small drainage basins are required for a number of engineering structures such as dams, levees, culverts, and soil conservation purposes. If in a basin designs are of low-cost hydraulic structures, then the flood estimation models with large amounts of input data are not warranted. Preferably, parsimonious models are considered with simple basic principles for easy use (Linsley 1982).

Peak discharge calculations are necessary for flood control studies in water engineering domain. Especially, climate change effects trigger floods in different parts of the world in an unprecedented manner and hence more refined formulations are necessary for better estimations through simple models that can be used practically by engineers. The most frequently used methods in flood estimations on small catchments are the RM and the Soil Conservation Service (SCS) method (SCS 1971, 1986). Details of these methods can be obtained readily from the relevant literature (Chow et al. 1998; Linsley 1982). The main parameter for the RM is the runoff coefficient (C) and for the SCS method, the curve number (CN). These methods are used for design flood discharge estimation provided that the design rainfall information is given (Şen 2008).

Pilgrim and Cordery (1993) present the application of the RM as a design procedure. In many applications, $C$ value is considered as constant, but in nature, it changes with time, and especially in the calculation of design discharge average recurrence interval, it plays the single most roles. The variation of C with time must be considered in any formulation for finding refined rainfall–runoff conversion mechanism (Kadioglu and Sen 2001). Estimation of the $C$ value is difficult and is the major source of uncertainty in many water resources projects. The coefficient must account for all the significant factors affecting the peak flow response to average excessive rainfall intensity without area and response time restrictions. In any water resources design, the $C$'s are taken from tables based on a set of drainage features (Maidment 1993). They are chosen in a rather vague manner and largely include subjective judgments rather than actual field data. Additionally, various studies show that $C$'s vary widely from storm to storm particularly depending on different antecedent wetness and environmental conditions (Hjelmfelt 1991; Ponce and Hawkins 1996; Kadioglu and Şen 2001). Generally, the $C$ increases as the average recurrence interval of rainfall increases, thus allowing for nonlinearity in runoff response of the drainage basin. Since considerable judgment and experience are required in selecting satisfactory $C$'s for a design, there is a need to check values against observed runoff data.

It is the main purpose of this section to modify the RM assumptions so as to obtain a more flexible and useful methodology for peak discharge estimation. In the new method, drainage area is considered as nonlinearly effective on the peak discharge, and also the drainage basin slope is taken into consideration in addition to nonlinearity in the rainfall intensity. The application of the proposed methodology is given for Wadi Baish in the KSA with its 54 sub-basin considerations.

## *5.8.1   Criticisms*

RM is rational on logical bases with simplifying basic assumptions, but it does not seem physically plausible for actual flow cases. Among its assumptions, peak flow rate is produced by a constant storm rainfall intensity, which is maintained for a time equal to the period of concentration over the whole drainage basin area. This time is defined theoretically as the time required for the surface runoff from the most remote part of the drainage basin to reach the point of interest. Practically, one cannot measure it in the field, and therefore, it is calculated in an empirical manner (Kirpitch 1940; Şen 2010). Additionally, there is a set of assumptions that the engineer should be aware of for successful applications and interpretations of the results. Otherwise, the peak discharge estimation by the classical RM may lead to unreliable conclusions. Among such assumptions are the following points for close consideration.

(1) Average excess rainfall intensity has the same recurrence interval with the peak discharge,
(2) The excess rainfall is uniformly distributed over the drainage area,
(3) The excess rainfall intensity is constant during the time of concentration,
(4) Peak discharge volume uniformly distributed over the drainage area is directly and linearly dependent on the excess rainfall intensity over the same drainage area. The ratio between the two is referred to as the runoff coefficient,
(5) The excessive rainfall intensity time is identical to time required for the runoff to flow from the hydraulically most distant point in the contributing drainage area to the point of design,
(6) It is not possible to satisfy all the assumptions simultaneously in any study, and there is a less chance that the rainfall rate used in the design might occur actually. Hence, the safety factor cannot be considered in the design,
(7) In general, a difference exists between intense point rainfall areal coverage over some portion or the whole drainage area. In such cases, the classical RM yields excessive peak discharge values, and hence, it is necessary to have an area reduction factor (Omolayo 1993; Sirdaş and Şen 2007), which cannot be determined easily in the practical applications,
(8) In an irregularly shaped drainage basin, a part of the area that has a short time of concentration may cause greater peak discharge at the outlet point than the runoff rate calculated for the entire drainage basin. This is because parts of the area with long concentration times are far less susceptible to high-intensity rainfall,
(9) A portion of a drainage area with high permeability produces greater amount of runoff than that calculated for the entire area. In order to reduce the effects of the last three points in the calculations, it is better to subdivide the whole drainage area into a set of convenient sub-areas.

Average knowledge is possible only when a phenomenon or process is isolated from surrounding effects through a set of restrictive assumptions that render the

problem into the world of certainty by ignoring all fuzzy features. For instance, $C$ is a multiplier applied to deterministically (classical two-valued logic) calculated peak discharge according to rational formulation in hydrology. Thus, by effectively "overengineering" or "under-engineering" the design by strengthening components or including redundant systems, $C$ accounts for imperfections in hydrological calculations, flaws in assembly, geomorphological and geologic degradation, and uncertainty in discharge estimates. In fact, $C$ includes "ignorance component" due to the exclusion of all fuzzy information about the hydrological design. However, fuzzy logic and system help to solve the hydrological design problem without considering $C$ explicitly (Şen 2010).

## 5.8.2   Modified Rational Method (MRM)
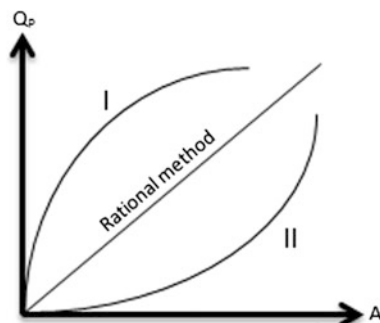
Rectification of RM formulation is possible by considering the following logical statements and relationships.

### 5.8.2.1   Peak Discharge-Drainage Area Relationship

Is it acceptable that peak discharge, $Q_p$, is directly and linearly proportional with the catchment area, $A$? If this statement is accepted without criticism, then the more the area, the more is the peak discharge without any limitation. The first part of this statement has logical validity, but the second part "linearity" is not valid in practical applications. This leads to the logical and rational conclusion that such a relation is nonlinear, which brings into mind two alternatives, I and II as in Fig. 5.15.

Rational thinking and many empirical studies indicate that as area increases, excess rainfall initially leads to discharge increment more that linear case (RM) and at large values the rate of increase starts to decrease. In other words, the slope of peak discharge with respect to area, $dQ_p/dA$, is not a constant value but initially more than this constant (linear RM line), and as the area increases the increment in

**Fig. 5.15** Peak discharge catchment area relationship

the discharge value decreases. Hence, type-II nonlinearity case is out of order, and type-I is plausible. As a result, it is possible to express such directly proportional expression mathematically as,

$$Q_{\mathrm{p}} \, \alpha_{\mathrm{A}} \, A^n \tag{5.20}$$

where $\alpha_{\mathrm{A}}$ is the proportionality sign and n is a power less than 1, which can be determined empirically from available data set including different catchment areas and their peak discharges.

The relationship between the catchment area and the peak discharge is related to the area directly as in the rational methodology, but the surface roughness (hills and depressions) gives rise to a nonlinear relationship between these two quantities. For instance, in Fig. 5.15, limb I corresponds to comparatively more hilly (depressive) surface features, where the exponent in Eq. (5.20) has a value smaller (bigger) than 1. In the meantime, $n = 1$ is the reflection of the rational formulation where hills and depressions are not taken into consideration at all.
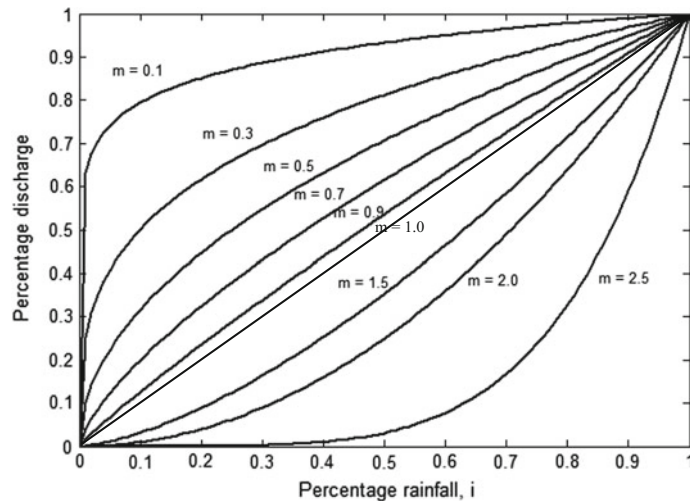
In Eq. (5.20), $n = 1$ corresponds to flat areas; $n \neq 1$ represents rough topography within the drainage basin. If $n > 1$, then in the drainage basin, hilly areas are more dominant over depressions otherwise when $n < 1$, the depression areas within the drainage basin are more dominant than the hilly areas. A question at this junction what is meant by hilly (depression) areas, do we need to consider the heights or the areal extensiveness of these areas. The more extensive the hilly (depression) area, the bigger (smaller) is the $n$ value than the flat area case of $n = 1$. Table 5.9 illustrates some numerical values that can be used in the practical applications.

### 5.8.2.2   Peak Discharge-Rainfall Intensity Relationship

Now, let us ask the same question as for the relationship between the rainfall intensity, $I$, and the peak discharge, $Q_{\mathrm{p}}$. Logically, the intensity is directly proportional to $Q_{\mathrm{p}}$, but what about its type as for the linearity? Furthermore, if antecedent conditions, such as soil moisture, surface cover features (man-made or

**Table 5.9** Roughness exponent value

| Roughness type | $n$ values |
|---|---|
| Very hilly | 2.00 |
| Hilly | 1.75 |
| Medium hilly | 1.50 |
| Slightly hilly | 1.25 |
| Flat | 1.0 |
| Slightly depressive | 0.90 |
| Medium depressive | 0.75 |
| Depressive | 0.50 |
| Very depressive | 0.25 |

**Fig. 5.16**  Peak discharge excess rainfall ratio relationship

natural, i.e., geological), and evapotranspiration are considered, then logical and rational thinking lead to the fact that as $Q_P - I$ relationship nonlinear as (see Fig. 5.16).

$$Q_P \; \alpha_i \; I^m \tag{5.21}$$

where $m$ indicates the nonlinearity power that depends on the mutual interaction between the rainfall and the drainage basin surface features. Logically, low m values correspond to business, residential and asphaltic areas where surface permeability is rather high. High m values imply delay in the surface flow occurrence at small rainfall intensities, and after the saturation is reached, the runoff takes place at high rates which correspond to curves below $m = 1.0$ line in Fig. 5.16. Further, interpretations from Fig. 5.16 lead to the following significant points as for the surface flow within a drainage basin.

(1) The more (less) permeable the drainage basin surface, the bigger (smaller) is the runoff exponent value than $m = 1$, which corresponds to completely impervious drainage area,

(2) For m values more (less) than 1 the surface peak discharge starts rather slowly (rapidly), and then the rate of discharge decreases (increase) with the rainfall intensity.

### 5.8.2.3  Peak Discharge-Drainage Slope Relationship

Another significance missing factor the classical RM is the catchment slope. In its present form, the RM provides the runoff over horizontal and flat surface areas but with considerations of actual flow. How could actual flow take place without slope? The question is then what about the relationship between the peak discharge and the catchment slope? The more the slope the less is the discharge, and therefore, inverse but a nonlinear relationship is expected as in Fig. 5.17.

This figure indicates that there is an exponential relationship between $Q_P$ and $S$, which appears in the mathematical form as,

$$Q_P \, \alpha_S \, e^{-kS} \qquad (5.22)$$

Here, $\alpha_S$ is another proportionality coefficient and $k > 0$. Equation (5.22) implies that zero slopes correspond to a constant discharge, which is in accordance with the classical RM. It is, therefore, necessary to write this expression in such a way that for zero slopes, the peak discharge has a definite value.

### 5.8.2.4  Compound Relationship
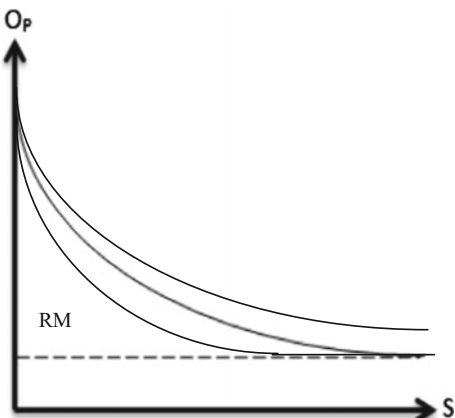
All of the above bivariate proportionalities can be combined together by multiplication operations, and the final formulation through a global proportionality coefficient, $\alpha_G$, can be written as,

$$Q_P \, \alpha_G \, A^n \, I^m \, e^{-kS}$$

One can write mathematical equation by introducing a proportionality parameter, $C_p$, leading to,

$$Q_P = C_p A^n \, I^m \, e^{-kS} \qquad (5.23)$$



**Fig. 5.17**  Peak discharge slope relationship
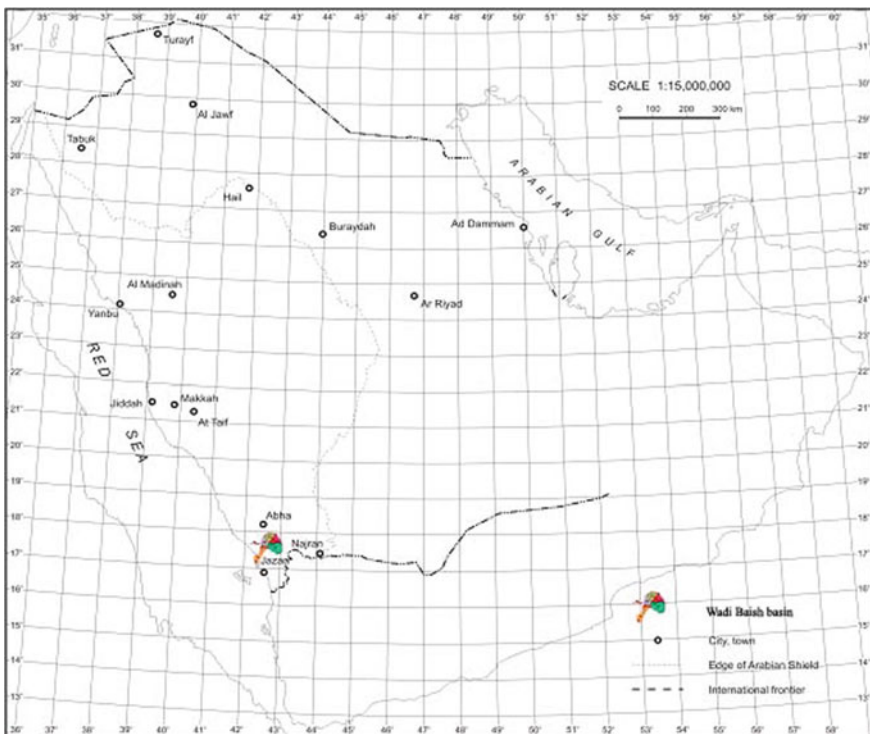
This expression leads to the physical definition of the proportionality parameter as the runoff discharge that corresponds to per drainage basin area (km$^2$), per rainfall intensity (mm) on a flat surface ($S = 1$).

On the other hand, the same expression can be reduced to the classical rational formula by considering that $n = m = 1$ and $S = 0$. In this special case, $C_p$ has then the equivalent value to the runoff coefficient. In the RM physically, $C$ is the ratio of runoff volume to excess rainfall volume over the drainage area, which is dependent on the permeability of the surface material, and accordingly, necessary tables help to identify its numerical value (Meidment 1993). However, in Eq. (5.23), $C_c$ has a different definition as reflecting not only the soil permeability but additionally the effects of the nonlinearities as explained above.

### 5.8.3  Application

The application of the methodology presented in this paper is applied to Wadi Baish in the KSA. It is one of the largest drainage basins in southwestern Saudi Arabia (Fig. 5.18) with approximately 5970 km$^2$ area. Different physiographic variables,



**Fig. 5.18**  Location map of the study area

in addition to rock, soil, and vegetation variables, are measured in Wadi Baish drainage area. Several physiographic parameters are measured, reviewed, and analyzed and used in appropriate equations to synthesize a unit hydrograph for the Wadi Baish catchment area. Full detail information is available in the report by the Saudi Geological Survey (Al-Zahrani et al. 2007).

The whole Baish catchment has 54 sub-basins as shown in Fig. 5.19, and detailed application of the Soil Conservation Service (SCS) methodology to each sub-basin has provided the basic data including area, slope, and discharge values (see Table 5.10).

The scatter of peak discharge versus area is presented in Fig. 5.20a for natural and double logarithmic scales (Fig. 5.20b). One can observe that on the double logarithmic plot, the scatter of points lies along a straight line with slope equal to $n = 0.55$.
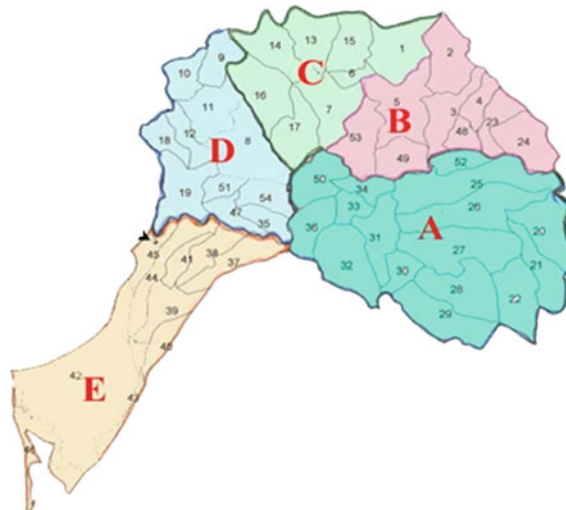
On the other hand, since the straight line passes through $Q_p = 500$ and $A = 100$ km$^2$ point, the equation form of Eq. (5.21) yields the constant as 40. Hence, the valid peak discharge-area relationship appears as,

$$Q_p = 40A^{0.55}$$

The slope relationship with the peak discharge is shown in Fig. 5.21, where on the double logarithmic paper, the relationship slope is equal to $k = 7.63$. Since the straight line goes through the points with coordinates ($Q_p = 700$ m$^3$/s, $S = 0.00$) and ($Q_P = 275$, $S = 0.12$), then the proportionality in Eq. (5.23) in the form of equation leads to a constant value approximately as 700. Hence, the final expression between the peak discharge and drainage slope becomes as,

$$Q_p = 700e^{-7.63S}$$

Fig. 5.19 Wadi Baish sub-basins
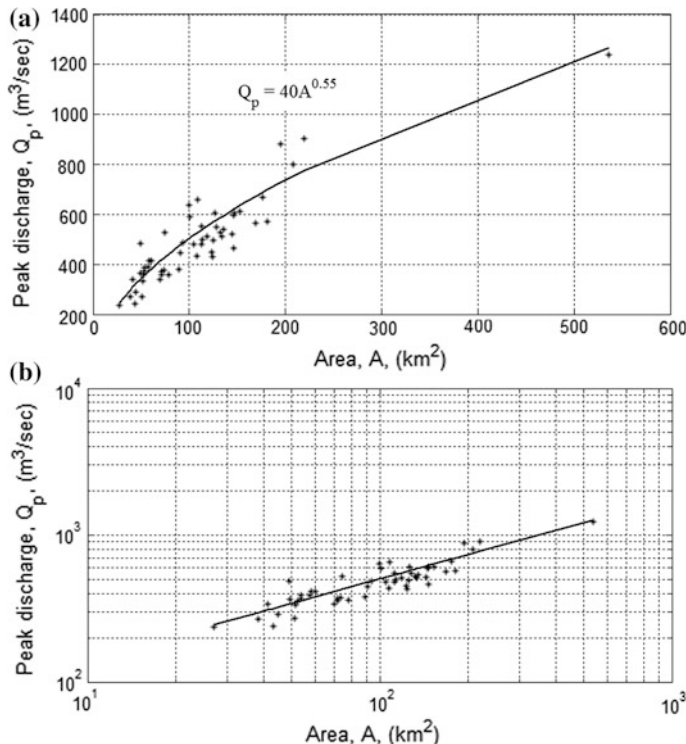
**Table 5.10** Geomorphological features of Wadi Baish sub-basins

| Sub-basin No. | Area (km²) | So | Discharge (m³/s) | Sub-basin No. | Area (km²) | So | Discharge (m³/s) |
|---|---|---|---|---|---|---|---|
| 1 | 146.5 | 0.048 | 466.066 | 28 | 153 | 0.058 | 610.9423 |
| 2 | 134 | 0.058 | 511.7341 | 29 | 146.8 | 0.045 | 605.7025 |
| 3 | 100.9 | 0.064 | 590.4745 | 30 | 51.21 | 0.068 | 270.3481 |
| 4 | 51.61 | 0.098 | 334.2873 | 31 | 112.5 | 0.051 | 481.911 |
| 5 | 176.3 | 0.052 | 668.0169 | 32 | 168.9 | 0.079 | 565.8286 |
| 6 | 27.06 | 0.079 | 236.0097 | 33 | 44.77 | 0.039 | 290.6617 |
| 7 | 135.3 | 0.059 | 540.8138 | 34 | 49.21 | 0.031 | 363.7294 |
| 8 | 181.4 | 0.067 | 570.6024 | 35 | 52.45 | 0.074 | 357.2733 |
| 9 | 78.22 | 0.115 | 359.756 | 36 | 90.7 | 0.085 | 447.4473 |
| 10 | 69.96 | 0.047 | 339.687 | 37 | 108.3 | 0.051 | 657.7244 |
| 11 | 118.7 | 0.041 | 512.5776 | 38 | 74.42 | 0.032 | 526.4656 |
| 12 | 58.15 | 0.044 | 414.2175 | 39 | 93.51 | 0.007 | 485.4893 |
| 13 | 113.8 | 0.079 | 500.6066 | 40 | 53.7 | 0.041 | 387.1429 |
| 14 | 126.3 | 0.071 | 606.3679 | 41 | 41.48 | 0.018 | 339.3307 |
| 15 | 104.9 | 0.074 | 479.2184 | 42 | 535.9 | 0.002 | 1239.822 |
| 16 | 146.1 | 0.065 | 595.2061 | 43 | 49.01 | 0.021 | 484.3066 |
| 17 | 123.2 | 0.046 | 449.2771 | 44 | 112.4 | 0.023 | 552.1155 |
| 18 | 57.41 | 0.039 | 390.3996 | 45 | 60.27 | 0.016 | 414.1791 |
| 19 | 144.5 | 0.033 | 520.5371 | 47 | 53.73 | 0.029 | 372.6239 |
| 20 | 128.2 | 0.042 | 548.0393 | 48 | 43.15 | 0.095 | 240.9954 |
| 21 | 99.57 | 0.026 | 637.634 | 49 | 89.15 | 0.076 | 380.698 |
| 22 | 132.1 | 0.044 | 526.0269 | 50 | 107.7 | 0.055 | 434.3845 |
| 23 | 71.45 | 0.04 | 358.0542 | 51 | 38.3 | 0.08 | 269.1822 |
| 24 | 125.3 | 0.055 | 495.3614 | 52 | 71.45 | 0.056 | 371.5351 |
| 25 | 219.6 | 0.037 | 903.6417 | 53 | 124 | 0.087 | 429.8804 |
| 26 | 194.7 | 0.026 | 880.6327 | 54 | 73.32 | 0.078 | 375.4878 |
| 27 | 207.6 | 0.025 | 799.1697 | | | | |

On the other hand, determination of the composite runoff coefficient, $C$, in Eq. (5.30) is possible by knowing the relationship for any region between the catchment area and the peak discharge, which is given for the study area by Sen and Al-Suba'I (2002) as in Sect. 5.11, Eq. (5.8). Its expression appears as a straight line on the double logarithmic paper and corresponds to the maximum excess rainfall event, which implies that $i = 1$ in Eq. (5.23).

After all the calculation and determination of the constants, the final formulation for Wadi Baish becomes as follows.

$$Q_P = 55A^{0.55}i^m e^{-7.63S} \tag{5.24}$$
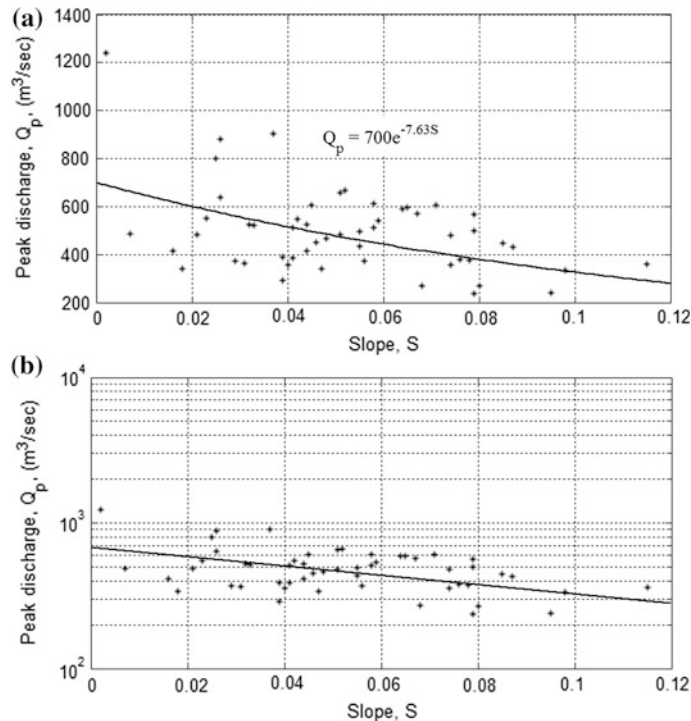
**Fig. 5.20** Peak discharge—area relationship

On the basis of maximum excess rainfall event, this expression can be thought of two complementary but separate product components. The first version is for zero slope that indicates the area effect only and the other is unit area case that shows the slope effect. Both of these effects are given separately in Fig. 5.22 with 45° straight line that shows the model validity. It is obvious that the area effect is more than the slope, but the areal effect by itself cannot make acceptable predictions because all the points (inverse triangles in the figure) lie over the straight line, which implies that such an approach causes overestimation of the observed discharges. The slope effect has comparatively very small effect.
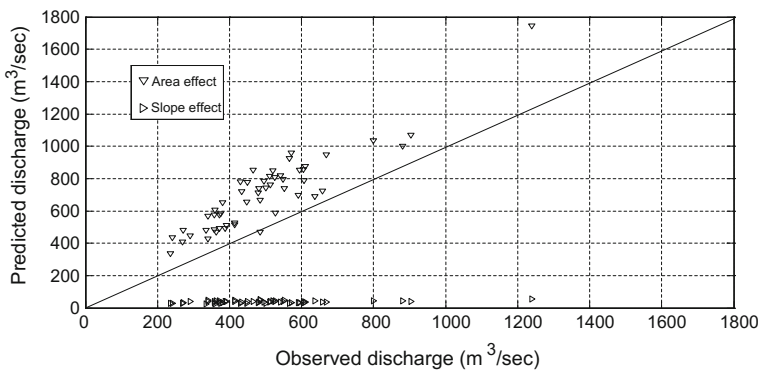
In Fig. 5.23, area and slope effects are considered together again for the case of maximum effective rainfall that covers uniformly the drainage basins, and the scatter of points are now around the 45° straight line. In the same figure, the RM result is shown for $C = 0.8$ and unit excessive rainfall amount. It is obvious that the RM is far away from the real data, and it needs some rectification an alternative of which is presented in this section.

The error distribution from the modified RM method is presented in Fig. 5.24.

Rational formulation is considered as panacea for many practical applications in engineering hydrology such that the very word "rational" in its title leads many
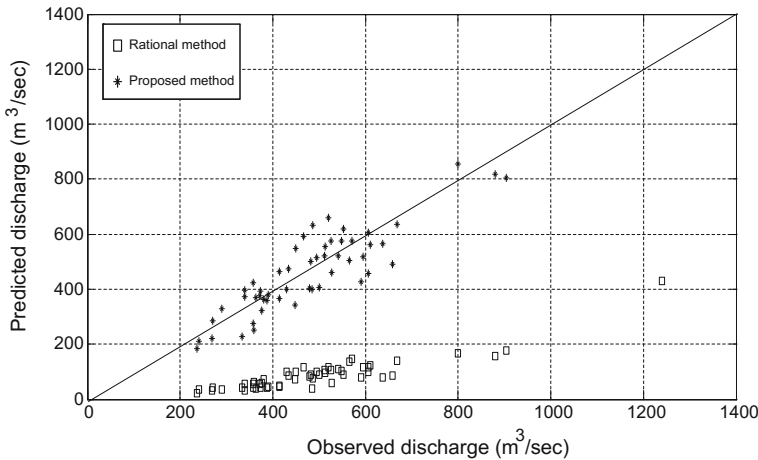
**Fig. 5.21** Peak discharge—slope relationship
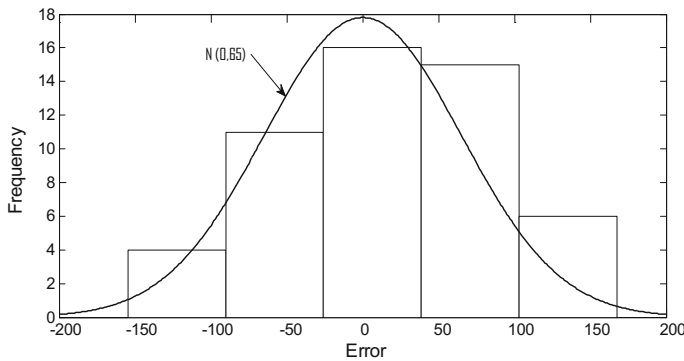


**Fig. 5.22** Area and slope effect on the discharge prediction

researchers not to criticize its structure except that it is restricted for use in small drainage basins. Logical reasoning on the input variables such as the drainage area and rainfall intensity to the discharge impels one to suspect from the directly linear

**Fig. 5.23**  Combined effect of area and slope



**Fig. 5.24**  Error frequency distribution

relationship between these parameters in addition to the missing drainage area slope in the formulation. It is well known from many synthetic and empirical studies that the peak discharge is linearly related neither to the drainage area not to the rainfall intensity nor to the slope. There is directly nonlinear relationship between the peak discharge and the drainage area, whereas the relationship between the slope and the peak discharge is inversely nonlinear. Additionally, the peak discharge is directly proportional and nonlinearly related to rainfall intensity. This paper presents all these logical nonlinear relationships for the rectification of the rational formulation, which leads to another and more general peak discharge formulation. The application of this new procedure is checked against the peak discharges from Wadi Baish that lies in the southwestern province of the KSA.

## 5.9  Ungauged Site Monthly Flow Estimation

Runoff prediction in ungauged basins of arid regions is among the most difficult problems in water resources assessments. There are varieties of methods for runoff estimation in ungauged catchments, but they are limited to rather small basins and under specific local weather as well as geomorphological conditions (Snyder 1938; Gray 1961; SCS 1986). On the other hand, almost all the methods are developed for humid or semi-humid regions of the world, and their applications to arid regions of ungauged catchments may pose practical difficulties. In the majority of cases, rainfall excess is assumed to follow different runoff paths to reach the catchment outlet according to drainage pattern (Beven and Kirby 1979; Takeuchi et al. 1999). Lee and Yen (1997) developed a kinematic-wave approach-based geomorphological instantaneous unit hydrograph to estimate the mean travel times on overland areas and in stream channels. In this model, the catchment rainfall–runoff relationship can be obtained using only the rainfall excess and the geomorphological information (Lee et al. 2001).

The authors, Farmer and Vogel (2013), touched on very practical aspects of engineering hydrology for streamflow estimation at ungauged sites provided that there are records in some similar regional watersheds. Water resources projects and hydrological investigations, such as the integrated water resources management in a drainage basin, cannot be achieved effectively without streamflow records, and in cases of missing data or ungauged sites, it is necessary to carry information from nearby gauged sites. In general, either deterministic or stochastic methodologies are used for practical solution in ungauged site streamflow estimations. However, their mixture may lead to better results in practical applications.

In hydrological studies, the fundamental logical basics of formulations must not be forgotten prior to their practical applications. After all, there are simple and illuminating logical and philosophical grounds behind each formulation (Şen 2013). The three approaches suggested by many researchers and particularly by Farmer and Vogel (2013) need such explanations prior to their use, so that they can be developed further to open new horizons for better improvements. The following three subsections explain the fundamentals of three methods suggested by the authors.

### 5.9.1  Standardizing Flows by Drainage Area

Although this has been defined as the drainage-area ratio (DAR) technique that assumes the equality of the flow per unit area, or unit discharge between hydrologically similar catchments, its physical reasoning can be derived from the RM discharge, $Q$, formulation in Eq. (5.18).

If the two similar basins are $X$ and $Y$, then by using these labels as subscripts, Eq. (5.18) can be rewritten for each basin as follows.

$$Q_X = C_X I_X A_X$$

and

$$Q_Y = C_Y I_Y A_Y$$

The ratio of these formulations yields to,

$$\frac{Q_X}{Q_Y} = \frac{C_X I_X A_X}{C_Y I_Y A_Y} \tag{5.25}$$

This expression can be applied directly provided that the rainfall intensities and the runoff coefficients of the gauged and ungauged sites are known. Hence, also the climatic factor plays role in the discharge estimation.

In Eq. (5.25), there are two important ratios, namely runoff coefficient ratio, $C_X/C_Y$, and rainfall intensity ratio, $I_X/I_Y$. It is possible to interpret Eq. (5.25) in three ways. First, the rainfall intensities may be the same, and hence, $I_X/I_Y = 1$, but the land use, morphology, vegetation cover, soil classification, and geology may be different from each other, which imply difference in the runoff coefficients. Hence, Eq. (5.25) takes the following form.

$$\frac{Q_X}{Q_Y} = \frac{C_X A_X}{C_Y A_Y} = \alpha \frac{A_X}{A_Y} \tag{5.26}$$

where $\alpha$ is the runoff coefficient ratio, which can be calculated easily from the available runoff coefficient tables as the one given for lawns by Wanielista et al. (1997) in Table 5.11.

More detailed tables are available depending on the land use such as business, residential, industrial, and agricultural land uses (Table 5.4). One can calculate the runoff coefficient ratio between two different types of land uses as for the gauged and ungauged drainage basin characteristics for lawns (see Table 5.12).

The values in the parenthesis are the averages of the runoff coefficient ratios, which may be used in practical applications. For example, if gauged, $Y$, and ungauged, $X$, sites have the same soil classification as sandy soil but different

**Table 5.11** Runoff coefficient for lawns

| Land use | $C$ |
|---|---|
| Sandy soil flat, (<2%) | 0.05–0.10 |
| Sandy soil avg., (2–7(%) | 0.10–0.15 |
| Sandy soil steep, (>7%) | 0.15–0.20 |
| Heavy soil flat, (<2%) | 0.13–0.17 |
| Heavy soil avg., (2–7%) | 0.18–0.22 |
| Heavy soil steep, (>7%) | 0.25–0.35 |

**Table 5.12** Runoff coefficient ratios, α

| | | Ungauged site, $X$ | | | | | |
| --- | --- | --- | --- | --- | --- | --- | --- |
| | | Sandy soil flat, (<2%) | Sandy soil avg. (2–7%) | Sandy soil steep, (>7%) | Heavy soil flat, (<2%) | Heavy soil avg., (2–7%) | Heavy soil steep, (>7%) |
| Gauged site $Y$ | Sandy soil flat, (<2%) | 1 | 0.5–0.67 (0.59) | 0.33–0.50 (0.43) | 0.77–0.59 (0.69) | 0.28–0.57 (0.43) | 0.20–0.29 (0.25) |
| | Sandy soil avg., (2–7%) | | 1 | 0.67–0.75 (0.71) | 0.77–0.88 (0.83) | 0.56–0.68 (0.62) | 0.40–0.43 (0.42) |
| | Sandy soil steep, (>7%) | | | 1 | 1.15–1.18 (1.17) | 083–0.91 (0.87) | 0.60–0.57 (0.59) |
| | Heavy soil flat, (<2%) | | | | 1 | 0.72–0.77 (0.75) | 0.53–0.49 (0.51) |
| | Heavy soil avg., (2–7%) | | | | | 1 | 0.72–0.63 (0.68) |
| | Heavy soil steep, (>7%) | | | | | | 1 |

slopes, 0.015 and 0.075, respectively, then the runoff coefficient ratio can be obtained from Table 5.12 as between 0.33 and 0.50 or as the average, $\alpha = 0.42$.

If in both basins the runoff coefficients and the rainfall intensities are equal to each other, then Eq. (5.25) becomes,

$$\frac{Q_X}{Q_Y} = \frac{A_X}{A_Y} \tag{5.27}$$

which is equivalent with the DAR suggestion by Farmer and Vogel (2013). For this case, the main diagonal elements (all equal to 1) are valid as the runoff coefficient ratio. After all, this equation has a set of assumptions as,

  (i) The runoff coefficients are equal, which is hardly the case in practical applications due to the differences in geomorphology, land use, geologic lithology, vegetation cover, etc.,
 (ii) Equal rainfall intensities generate equal discharges in both basins,
(iii) Since the RM is valid only for small drainage basins (Chow et al. 1998), the validity of Eq. (5.27) has areal limitation.

On the other hand, as the authors rightly state in some practical applications, a power constant, $n$, is considered and the same expression can be written as follows.

$$\frac{Q_X}{Q_Y} = \left(\frac{A_X}{A_Y}\right)^n \tag{5.28}$$

Logically, $0 < n < 1$ and as the similarity between the two basins increases, $n$ approaches to 1. If they are identically the same, then $n = 1$, and the DAR formulation becomes valid with the above restrictive assumptions.

Apart from all the aforementioned physical and logical explanations, the DAR equation can also be written by including an error term, $\varepsilon$, which also distinguishes the two basins to a certain extent.

$$\frac{Q_X}{Q_Y} = \frac{A_X}{A_Y} + \varepsilon \tag{5.29}$$

where $\varepsilon$, has zero mean, unit standard deviation and abides by the normal PDF.

## 5.9.2 Standardizing Flows by Mean Streamflow

This is referred to as the standardizing by mean flows (SM) technique by Farmer and Vogel (2013). If one considers the simplest form of stochastic process as the first-order Markov model for streamflow generation, then she/he can write discharge, $Q_{Xi}$, at a site, $i$, as,

$$Q_{X_i} = \mu_{Xi} + \rho_{Xi} Q_{X_{i-1}} + \sigma_{Xi}\sqrt{1 - \rho_{Xi}^2}\,\varepsilon_{Xi} \tag{5.30}$$

where $\mu_{Xi}$ is the arithmetic average, $\sigma_{Xi}$ is the standard deviation, $\rho_{Xi}$ is the first-order serial correlation coefficient, and finally, $\varepsilon_{Xi}$ is the standard normal PDF with zero mean and standard deviation. It is mentioned by Farmer and Vogel (2013) that such an approach is used in flood frequency analysis. This statement implies that the serial correlation coefficient is equal to zero, which reduces Eq. (5.30) into the following form.

$$Q_{Xi} = \mu_{Xi} + \sigma_{Xi}\varepsilon_{Xi} \tag{5.31}$$

If one assumes that there is only the effect of arithmetic mean and ignores the contribution by the standard deviation, then the last expression can be written as follows.

$$Q_{Xi} = \mu_{Xi}$$

One can also write similar expression for the ungauged site as,

$$Q_{Yi} = \mu_{Yi}$$

Finally, the ratio of these two last equations leads to the SM approach formulation as follows.

$$\frac{Q_X}{\mu_{Q_X}} = \frac{Q_Y}{\mu_{QY}} \tag{5.32}$$

Logically, compared with the DAR approach, SM has wider validity, because it does not have any restrictive areal extend.

### 5.9.3  Standardizing Flows by Mean and Standard Deviation

The standardization of flows by mean and standard deviation (SMS) works on dimensionless discharge variable for which the expectation value is zero and the variance is equal to unit. The basis of its derivation is again the first-order Markov model and the assumption of serial independence, which led to Eq. (5.31). Rearrangement of this expression leads to,

$$\frac{Q_i - \mu_i}{\sigma_i} = \varepsilon_i \tag{5.33}$$

which implies that at each time instant, the mean and standard deviation are taken into consideration, and hence, only residuals remain. This expression also confirms the statement by Farmer and Vogel (2013) that a new standardized variable is obtained with zero mean and unit variance, regardless of the PDF of the original flows. The ratio of the last equation between the gauged, $X$, and ungauged, $Y$, sites gives,

$$\frac{\frac{Q_X - \mu_X}{\sigma_X}}{\frac{Q_Y - \mu_Y}{\sigma_Y}} = \frac{\varepsilon_X}{\varepsilon_Y} \tag{5.34}$$

If one assumes that at the two sites the error terms are also the same, then this last expression reduces to,

$$\frac{Q_X - \mu_X}{\sigma_X} = \frac{Q_Y - \mu_Y}{\sigma_Y} \tag{5.35}$$

Since SMS approach takes into account standard deviation in addition to arithmetic average, as Farmer and Vogel (2013) states, it is always superior to the drainage area ratio method (DAR), because its information content is more than even the SM method. After all, as for the information content concerning

streamflow sequence, it is possible to rank these approaches into preference sequence as DAR < SM < SMS. Such a sequence has already been observed in the numerical calculations by Farmer and Vogel (2013).

# References

Al-Suba'i, K. (1992). Erosion-sedimentation and seismic considerations to dam sitting in the central Tihamat Asir region. Ph. D dissertation, Faculty of Earth Science, King Abdulaziz University, Saudi Arabia.

Al-Zahrani, M. K., Al-Harthi, S. G., Hawsawi, H. M., Al -Ammawi, F. A., Theban, M. S., Khiyami, H. A., & et al. (2007). Potential flood hazard in Wadi Baish Southwest, Saudi Arabia. Saudi Geological Survey Confidential Report, 216 pp.

Bayazit, M., & Önöz, B. (2007). To prewhiten or not to prewhiten in trend analysis? *Hydrological Sciences Journal, 52,* 611–624.

Bayazıt, M., & Önöz, B. (2008). *Taşkın ve Kuraklık Hidrolojisi*, Nobel Yayınevi,(in Turkish) (Flood and Drought Hydrology).

Beven, K. J., & Kirkby, M. J. (1979). A physically based variable contributing area model of basin hydrology. *Hydrological Sciences Bulletin, 24*(1), 43–69.

Blanchard, A. H., & Drowne, H. B. (1913). *Text-book on highway engineering*. New York: Wiley.

Byrne, A. (1902). *Treatise on highway construction*, 4th ed.

Chow, V. T. (1962). *Hydrologic determination of waterway areas for the design of drainage structures in small drainage basins, experimental station bull*. Illinois: University of Illinois, Engrg.

Chow, V., Maidment, D., & Mays, L. (1998). *Applied hydrology* (p. 572). New York: McGraw-Hill.

Costa, J. E. (1987a). Hydraulics and basin morphometry of the largest flash floods in the conterminous United States. *Journal of Hydrology, 93,* 313–318.

Costa, J. E. (1987b). A comparison of the largest rainfall-runoff floods in the United States with those of the People's Republic of China and the world. *Journal of Hydrology, 96,* 101–115.

Costa, J. E. (1987c). A comparison of the largest rainfall-runoff floods in the United States with those of the People's Republic of China and the world. *Journal of Hydrology, 96*(101), 115.

Farmer, W., & Vogel, R. M. (2013). Performance-weighted methods for estimating monthly streamflow at ungauged sites. *Journal of Hydrology, 477,* 240–250.

Farquharsen, F. A. K., Meigh, J. R., & Sutcliffe, J. V. (1992). Regional flood frequency analysis in arid and semi-arid areas. *Journal of Hydrology, 138,* 487–501.

Gray, D. M. (1961). Interrelationships of watershed characteristics. *Journal Geophysical Research, 66*(4), 1215–1223.

Hjelmfelt, A. T., Jr. (1991). Investigation of curve number procedure. *Journal of Hydrologic Engineering, ASCE, 117*(6), 725–737.

Kadioglu, M., & Şen, Z. (2001). Monthly precipitation–runoff polygons and mean runoff coefficients. *Hydrological Sciences Journal, 46*(1), 3–11.

Kirpich, Z. P. (1940). Time of concentration of small agricultural watersheds. *Civil Engineering*, *10*(6), 362.

Kundzewicz, Z. W., & Napiorkowski, J. J. (1986). Nonlinear models of dynamic hydrology. *Hydrological Soil Journal, 37,* 163–185.

Lacey, G. (1930). Stable channels in alluvium. *Proceedings of the Institution of Civil Engineers, 229,* 259–384.

Lee, K. T., Chang, G. H., Yang, M. S., & Yu, W. S. (2001). Reservoir attenuation of floods from ungauged basins. *Hydrological Sciences Journal, 46*(3), 349–362.

Lee, K. T., & Yen, B. C. (1997). Geomorphology and kinematic wave based hydrograph derivation. *Journal of Hydraulic Engineering, ASCE, 123*(1), 73–80.

Linsley R. K. (1982). Rainfall–runoff models—an overview. In Singh V. P. (Ed.), *Proceedings of the International Symposium on Rainfall–Runoff Relationship*. Water Resources Publications: Littleton, CO.

Maidment, D. R. (1993). *Handbook of hydrology*. New York: McGraw-Hill Inc.

Omolayo, A. S. (1993). On the transformation of areal reduction factors for rainfall frequency estimations. *Journal of Hydrology, 145,* 191–205.

Pilgrim, D. H., & Cordery, I. (1993). Flood runoff. In D. R. Maidment (Ed.), *Handbook of hydrology* (9.1–9.42). McGraw-Hill: New York.

Ponce, V. M., & Hawkins, R. H. (1996). Runoff curve number: Has it reached maturity? *Journal of Hydrologic Engineering, ASCE, 1*(1), 11–19.

Quraishi, A., & Al-Hasoun, S. (1996). Use of Talbot formula for estimating peak discharge in Saudi Arabia. *Journal of King Abdulaziz University: Engineering Science, 8,* 73–85.

Şen, Z. (2008). Wadi hydrology (346 pp). New York: Taylor and Francis Group, CRC Press.

Şen, Z. (2010). Fuzzy logic and hydrological modeling (340 pp). Taylor and Francis Group, CRC Press Publishers.

Şen, Z. (2013). *Philosophical, logical and scientific perspectives in engineering* (p. 260). New York: Springer.

Şen, Z., & Al-Suba'I, K. (2002). Hydrological considerations for dam siting in arid regions: Saudi Arabia study. *Hydrological Sciences Journal, 47*(2), 173–186.

Sirdaş, S., & Şen, Z. (2007). Determination of flash floods in Western Arabian Peninsula. *Journal of Hydrologic Engineering ASCE, 12*(6), 676–681.

Snyder, F. F. (1938). Synthetic unit hydrographs. *Transactions American Geophysics Union, 19,* 447–454.

Soil Conservation Service (SCS). (1971). *National engineering handbook, Section 4: hydrology*. USDA: Springfield, VA.

Soil Conservation Service (SCS). (1986). Urban hydrology for small watersheds. Technical Report 55. USDA: Springfield, VA.

Takeuchi, K., Ao, T., & Ishidaira, H. (1999). Interpretation of block-wise use of TOPMODEL and Muskingum-Cunge method for the hydro-environmental simulation of a large ungagged basin. *Hydrological Sciences, 44*(4), 636–656.

Talbot, A. N. (1887–88). The determination of water-way for bridges and culverts (pp. 14–22). Selected papers of the Engineers' Club, Technograph No. 2, University of Illinois.

Wanielista, M., Kersten, R., & Eaglin, R. (1997). *Hydrology: Water quantity and quality control* (2nd ed.). New York, NY: Wiley and Sons Inc.

Wilson Murrow Consultant, Drainage Report. (1971). A report submitted to the Ministry of Communications, Riyadh, Saudi Arabia: 217 pp.

# Chapter 6
# Probability and Statistical Methods

**Abstract** In flood frequency and discharge calculations, there are two different treatment procedures as either probabilistic or deterministic approaches. So far, the previous chapters are concerned with hydrological deterministic methods, but this chapter provides information about the probabilistic, statistical, and stochastic uncertain methods. The very bases of these approaches are the annual, partial, or hybrid selections from a given time series of extreme discharge magnitudes. The selected flood discharges are fitted to the most suitably representative probability distribution functions for risk-level calculations. Most often, the flood discharges for two-year, five-year, 10-year, 25-year, 50-year, 100-year, and 500-year return periods are sought which correspond to 0.50, 0.20, 0.10, 0.04, 0.01, and 0.002 probability exceedence (risk) levels. Explanation of various probability papers and their theoretical background information are exposed with some examples.

**Keywords** Annual · Frequency · Distribution function · Hybrid · Partial Probability · Probability paper · Risk · Safety

## 6.1 General

Mankind is very sensitive to natural extreme phenomena, and therefore, scientific knowledge prior to their occurrences is of prime importance. Extreme values of various hydrometeorological variables provide keys for significant decisions in planning, design, and operation of numerous hydrological, agricultural, and industrial activities. Their modeling and subsequent prediction with the minimum possible error is the main objective of existing extreme value statistics theory (Gumbel 1958; Fisher and Tippett 1928). Construction of a convenient model, which reflects the structural dependence and variation of observed phenomena, is a first step in any prediction scheme. It seems that climate change is associated not with higher intensity of extreme values, but rather with a higher frequency of the extreme value occurrences (Flohn 1989).

In flood calculations, the most important assumption is the independent occurrences of extreme events along the time axis. In general, this assumption is valid, because they have at least more than one-year occurrence duration between two successive events. Recently, such an assumption may not be valid anymore, because the climate change impact may give rise to more than one flood occurrence during one year. Frequent and intensive flood occurrences in recent years gear toward improvement of the independence assumption by considering dependence in the formulations or in their modified alternatives. Independence assumption provides opportunity to employ probability statements only in flood occurrence and magnitude calculations. However, consideration of the dependence directs to the use of stochastic methodologies in the flood assessments.

The modern era of flood frequency analysis began in the early 1940s with a series of papers by Gumbel (1958). Before, the flood data were analyzed by ad hoc graphical methods. He developed a theoretically sound method based on fitting an extreme value type I probability distribution function (PDF) to the record of annual peak flows.

In the 1970s, the U S Water Resources Council (USWRC) developed recommended procedures for flood frequency analysis applications by all federal agencies. These procedures were published initially in USWRC's Bulletin 17, "Guidelines for Determining Flood Flow Frequency" (1976). Revised guidelines were published as Bulletin 17A (Interagency Advisory Committee on Water Data, 1977) and Bulletin 17B (Interagency Advisory Committee on Water Data, 1981). The Bulletin 17B procedures have been applied by federal agencies since 1981. In the USWRC method of flood frequency analysis, the record of annual flood peaks is fitted with a Log-Pearson type III PDF rather than Gumbel's extreme value PDF.

For probabilistic and statistical method applications, it is necessary to have database through proper measurements and monitoring systems. The use of these measurements leads to PDF and to statistical parametrization, which help flood predictions on the basis of relative frequency (probability) with consideration of a certain return period (Chaps. 2 and 9). The statistical approach for design flood estimation treats the past annual flood peak discharge records, which are either observed directly at the site or estimated by a suitable method. In case of flood record absence, the frequency analysis may be carried out on the available annual rainfall record in the region (Chap. 2). The probability of occurrence, $P$, is defined as the maximum flood discharge record that is equal to or in excess of a specified magnitude $X_0$. The recurrence interval, $T$, is defined as the reverse of $P$. The main purpose of the flood frequency analysis is to treat and interpret past records according to an objective methodology leading to future flood discharge magnitude prediction corresponding to a specific return period.

Gathering hydrological data directly from rivers and streams is a valuable but time-consuming effort. If such dynamic data have been collected for many years through stream gauging, models can be used to determine the statistical frequency of given flood events, thus determining their probability. However, without a record of at least twenty or better for thirty years, such assessments are difficult.

In this chapter, based on the independence assumption, probabilistic risk and reliability relationships are presented in flood assessment studies, and finally, PDF and its cumulative version (cumulative PDF, CDF) curves are used for flood estimates at a set of risk levels. Additionally, the dependent cases are considered with convenient calculation methods.

## 6.2 Flood Frequency Calculations

The main purpose is to derive theoretically very long data group "population" characteristics of the flood occurrence from a given limited number of records. In flood frequency, the population is composed of the annual flood peak discharges (annual maximums) at a site. Flood peak corresponds to the maximum of the past discharge value records at any year. In order to reach to a reliable flood peak discharge estimation, the following assumptions are adapted in practical flood frequency applications.

(1) The recorded samples are representatives of the flood discharge population,
(2) Past is the reflection of future, and hence, future estimations are statistically indistinguishable replications of the past. However, this assumption is no more valid due to the climate change impact,
(3) The flood discharge data have an independent serial structure, which implies that flood discharge at any year is independent of any other year. This is tantamount to saying that the flood discharge samples are randomly distributed in nature.

Flooding is a natural and recurring event in a river or stream. Statistically, streams will equal or exceed the mean annual flood once every 2.33 years (Leopold et al. 1964). Flooding is a result of heavy or continuous rainfall exceeding the absorptive capacity of soil and the flow capacity of rivers, streams, and coastal areas. This causes a watercourse to overflow its banks onto adjacent lands.

In the flood frequency data treatment first of all after the reliability check of available data, it is necessary to identify trend, jump, or any systematic structure within the sequence. In this context, trend is the gradual increasing or decreasing change in the sample data. Trend may occur either by human interference to environment (afforestation or deforestation in the drainage basin area) or by the climate change impact. Jumps correspond to exceptionally sudden high or low values as a result of events such as forest fire, earthquake, landslide, and they change temporarily the flow characteristics in the drainage basin.

After the clarification of the records from the trend, jump, and any other systematic components such as the seasonality, the next step is the application of a convenient PDF fit to the available data set. Since the flood annual peak flow records are random numbers and they are also representative of the population,
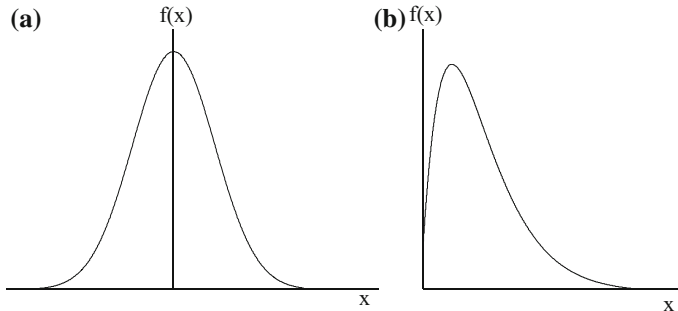
therefore, they are likely to happen in future. Each data value is referred to as a variate, $x$, from entire data range, $X$.

The PDF, $P$, of a variable is the occurrence number of a variate divided by the sample number, $n$, and the summation of all the probabilities is equal to 1, $\sum_{i=1}^{n} P_i = 1$, where $n$ is the sample length. In general, the PDF of all variates is denoted a $f(x)$ as shown in Fig. 6.1
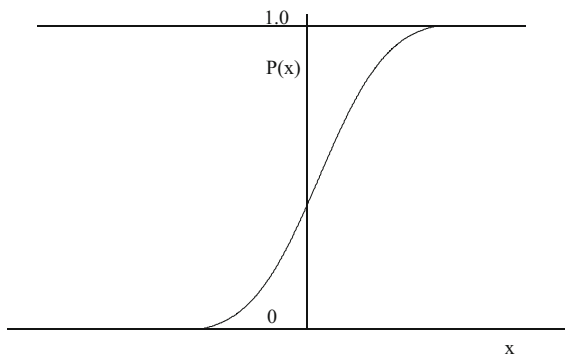
Furthermore, the cumulative probability distribution (CDF), $P(x)$, is of the type as shown in Fig. 6.2.

The CDF of a random variable has a value equal to or less than certain assigned value $x$ is equal to $P(x \leq x)$, or greater than the same value $P(x > x)$.

In the flood frequency analysis, the above concepts are useable provided that the functions $f(x)$ or $P(x)$ are known. It is then possible to find out the probability with which certain high flood peak is likely to occur. The same idea may be used to



Fig. 6.1  Typical PDFs, **a** symmetric, **b** skewed



Fig. 6.2  A typical CDF

recalculate the high flood peak that is likely to be equaled or exceeded corresponding to a given frequency (say, 1 in 100 years, i.e., 100-year return period).

There is a number of PDFs, $f(x)$, which are suggested by different researchers among which the most commonly used ones in practice are the log-normal, Pearson type III, and Gumbel PDF.

There are statistical tests that provide the conformity of one of these PDFs to fit the given flood peak discharge data. After the identification of the best-fit PDF to available data, it is adopted for likely flood occurrence calculation corresponding to specific return periods.

## 6.2.1  Plotting Positions

Even though the sample length may not include extreme values of future, the extension of the data yields such extreme flood discharge values. If a certain probability is attached to each one of the data, then data values versus the probabilities can be plotted, which appears in the form of scatter diagram. Prior to such a scatter diagram, the data are sorted in ascending or descending order that corresponds to non-exceedence or exceedence probabilities. Hence, the scatter diagram has gradually increasing or decreasing tendency. For this purpose, after the sorting of data sequence each value has a rank, $m$, from 1 to $n$. The calculation of the empirical probability is achieved through one of the methodologies shown in Table 6.1, where there are three methods as California, Hazen, and Weibull approaches.

Throughout the text of this book, the Weibull empirical probability attachment formulation is used.

## 6.2.2  Probability Distribution Functions (PDFs)

In developing intensity–duration-frequency (IDF) or probabilistic flood evaluation curves, statistical frequency analysis is employed, whereby an annual extreme rainfall series of given duration is described by an assumed PDF including extreme value (EV, Gumbel), generalized extreme value (GEV, Pearson), two-parameter log-normal, three-parameter log-normal, Gamma, Pearson type III, and

**Table 6.1** Empirical probability calculation methodologies

| The probability of exceedence of $X$ over a certain threshold value $P(X \geq X_o)$ is given by various researchers | Name of formula | $P(X \geq x)$ |
|---|---|---|
| 1 | California | $m/n$ |
| 2 | Hazen | $(m - 0.5)/n$ |
| 3 | Weibull | $m/(n + 1)$ |

Log-Pearson type III distributions. The use of any PDF depends on the storm rainfall intensity features in the form of relative frequency distributions or histograms as will be explained later in this section. The practicing hydrologist should know the general appearance of these theoretical PDFs so as to allocate the most suitable one to the data at hand first visually and then objectively by a statistical test such as the Chi-squared or Kolmogorov–Smirnov tests (Benjamin and Cornell 1970). The general mathematical expression of the GEV PDF, $f(x)$, for a hydrometeorological variable, $x$, is given by Jenkinson (1969). Each one of the aforementioned PDFs is explained with mathematical expressions in Chap. 2).

$$f(x) = \frac{1}{\alpha}\left[1 - k\left(\frac{x-u}{\alpha}\right)\right]^{1/k-1} \quad e^{-\left[1-k\left(\frac{x-u}{\alpha}\right)\right]_{1/k}} \tag{6.1}$$

where $\alpha$, $u$, and $k$ are the model parameters. The extreme value type I Gumbel PDF has the following form (Gumbel 1958; Yevjevich 1972; Chow 1964).

$$f(x) = \frac{1}{\alpha}\exp\left[\left(-\frac{x-u}{\alpha}\right) - \exp\left(-\frac{x-u}{\alpha}\right)\right] \tag{6.2}$$

On the other hand, the earliest application of the Gaussian (normal) PDF to hydrological variables has been presented by Hazen (1914) through the use of the Gaussian (normal) probability paper for analysis of the hydrological data. This PDF has a bell shape, and its general expression can be found in standard textbook on statistics as,

$$f(x) = \frac{1}{\sigma\sqrt{2\pi}}e^{\frac{1}{2}\left(\frac{x-\mu}{\sigma^2}\right)^2} \tag{6.3}$$

where $\mu$ and $\sigma$ are the arithmetic mean and standard deviation values of the variable record, respectively.

In order to obtain a skewed PDF, two-parameter log-normal PDF is suggested with mathematical formulation as,

$$f(x) = \frac{1}{x\,\sigma_x\sqrt{2\pi}}\exp\left[-\frac{[\mathrm{Ln}(x) - \mu_x]^2}{2\sigma_x^2}\right] \tag{6.4}$$

The three-parameter log-normal PDF is similar to the two-parameter log-normal PDF except that $x$ is shifted by an amount, $m$, which represents a lower bound (Kite 1977).

$$f(x) = \frac{1}{(x-m)\sigma_x\sqrt{2\pi}}\exp\left[-\frac{[\mathrm{Ln}(x-m) - \mu_x]^2}{2\sigma_x^2}\right] \tag{6.5}$$

Herein, $\mu_x$ and $\sigma_x$ are the mean and standard deviations of the variable value logarithms.

A flexible PDF, which also includes the exponential PDF in case when $\beta = 1$, is the two-parameter Gamma PDF, which can be expressed mathematically as,

$$f(x) = \frac{1}{\alpha^\beta \Gamma(\beta)} x^{\beta-1} e^{-(x/\alpha)} \tag{6.6}$$

Pearson (1930) suggested the Pearson III PDF and then its logarithmic version (Log-Pearson III) PDFs as,

$$f(x) = \frac{1}{\alpha \Gamma(\beta)} \left(\frac{x-\gamma}{\alpha}\right)^{\beta-1} e^{-\left(\frac{x-\gamma}{\alpha}\right)} \tag{6.7}$$

and

$$f(x) = \frac{1}{\alpha x \Gamma(\beta)} \left[\frac{\mathrm{Ln}(x) - \gamma}{\alpha}\right]^{\beta-1} e^{-\left\{\frac{ln(x)-\gamma}{\alpha}\right\}} \tag{6.8}$$

respectively.

### 6.2.2.1 Return Period

Any flood is described usually in terms of its statistical frequency. A "100-year flood" or "100-year floodplain" describes an event or an area subject to a 1% (1/100 = 0.01) probability of a certain size flood occurrence in any future year. This concept does not mean that such a flood will occur only once at a certain time during the next hundred years. Whether or not it occurs in a given year has no bearing on the fact that there is still a 1% chance of a similar occurrence in any other year. Since floodplains can be mapped, the boundary of the 100-year flood is commonly used in floodplain mitigation programs to identify areas, where the risk of flooding is significant as a consequence of inundation. Any other statistical frequency of a flood event may be chosen depending on the degree of risk that is selected for evaluation, as five-year, 20-year, 50-year, 100-year floodplain.

Frequency of inundation depends on the climate, the material that makes up the banks of the stream, and the channel slope. Each year substantial rainfall occurs in a particular season, or the annual flood is principally from snowmelt; the floodplain may have inundation almost every year, even along large streams with very small channel slopes. In regions without extended periods of below-freezing temperatures, floods usually occur in the season of highest precipitation. In some places, most floods are the result of snowmelt often accompanied by rainfall, and the flood season is spring or early summer.

In order to estimate flood peak discharges, flood hydrographs are used for a variety of purposes, such as flood risk estimation and flood control structures' dimensioning and for the management and regulation of flood plains, design of bridges, and others purposes (Al-Zhrani 2007).

## 6.3   Flood Data Preparation
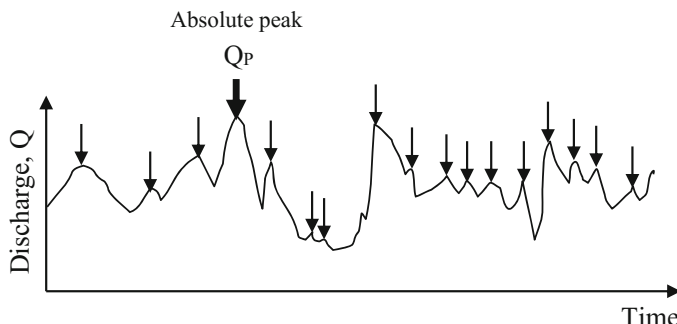
In a compound hydrograph, there are many peak discharges, $Q_i$ ($i = 1, 2, \ldots, n$), and magnitude considerations of three successive discharges as $Q_{i-1} < Q_i > Q_{i+1}$ identify all the peaks during the record period in the finest detail. According this definition, in Fig. 6.3 all peaks, minor or major, are indicated by arrows.

Among the local peak discharges, there is the maximum one, which is referred to as the absolute maximum (peak) discharge, $Q_P$, and it is shown by bold arrow in the figure. It is possible to adapt this maximum discharge as the expectation occurrence in future deterministically under a set of restrictive assumptions. This is not a preferable way, because it denies the uncertainty, probability, risk, and stochastic occurrence nature of flood events. On the other hand, it is necessary to consider each local discharge collectively as a set and base the flood prediction on such an approach, because each discharge may have occurred in different seasons. It is necessary to distinguish and select the suitable local flood discharges' set for flood prediction calculations. At locations with continuous runoff measurements, flood data must be extracted from records according to three methods, namely annual, partial, and hybrid flood discharges.
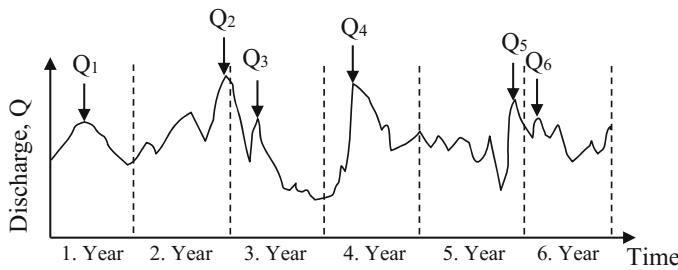
### 6.3.1   Annual Flood Discharge

The selection of representative maximum discharges for each year, irrespective of seasonality, constitutes annual flood discharge series. For this purpose, the time axis is partitioned into regular yearly intervals, and then, the maximum discharge is selected for each year as shown in Fig. 6.4.

Such annual series identification provides opportunity to consider one peak discharge in each year, and hence, floods and their triggering precipitation events can be considered practically independent from each other. For instance, in Fig. 6.4



**Fig. 6.3**  Compound hydrograph and local peak discharges
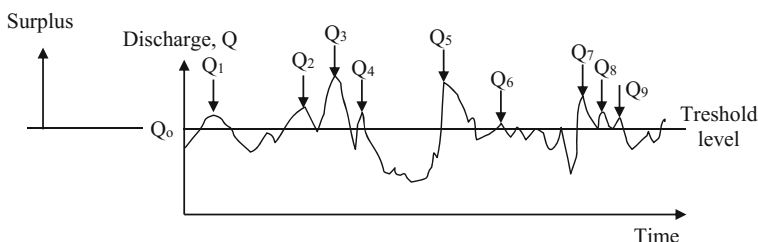
**Fig. 6.4**  Annual flood discharge series

the 2nd year and 3rd year and similarly 5th year and 6th year floods are very close to each other, and even though small, there is a possibility that they are dependent to a certain extent, but they are assumed as independent. In the annual flood records, the number of flood discharges is equal to the number of available record years.

### 6.3.2  Partial Flood Discharges

Instead of annual identification, it is possible to divide the whole record series into two parts with respect to a threshold, $Q_o$, level. The peaks above this level are referred to as surpluses. This truncation level must be determined before ahead according to some criteria. In Fig. 6.5, the peak discharges above the threshold level are considered collectively as partial flood discharges' set.

In this flood discharge identification approach, there may be partial dependences according to the temporal closeness of two successive flood discharges, but in practical flood prediction calculations, they are also considered as independent. Later in this chapter in Sect. 6.10, a new calculation methodology is presented, which takes into consideration partial dependence among the flood discharges. In the partial flood discharge selection procedure, there are more flood discharges than the number of record years. The truncation level selection can be achieved in several ways among which are the following alternatives.



**Fig. 6.5**  Partial flood discharge series

(1) The transportation capacity of a drainage basin without hazardous flood discharge,
(2) The volume of flood impoundment reservoir in a basin,
(3) At settlement areas, determination of the lowest level that will not give rise to a flood and consequent inundation.

In some years, there may not be flood discharges but in some others more than one instant.
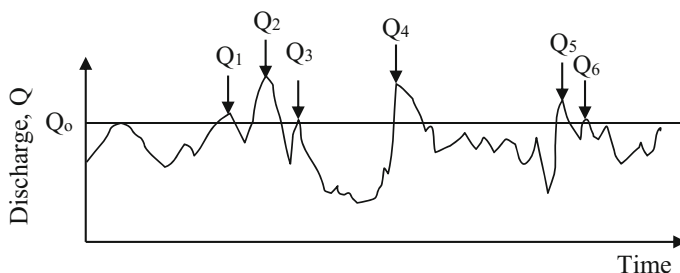
## 6.3.3  Hybrid Flood Discharges

After the consideration of the two previous methods, one can think about a third procedure by shifting a horizontal line from the highest peak value toward lower values and as new peaks fall above the shifting horizontal line, the number of peaks over the line is equal to the number of flood years (Fig. 6.6).

This method provides the truncation level mechanically without any engineering considerations as in the previous subsection, and the benefit from such a procedure is that within one year, more than one peak flow enters the calculation scene. Since there may appear two nearby peaks, this method takes into consideration the dependence between the peak discharges to a certain extent.

On the contrary, if the study of low flows is important in any area, then the low peak discharge selection procedure is just the reflection of the aforementioned flood selection procedure.

In practice, for short duration records (2–10 years) annual flood discharge time series is used. If the number of years is more than 10, annual partial flood discharge series comes into view. In case of lengthy records, the three methods yield almost the same result.



**Fig. 6.6**  Annual–partial flood discharge series

## 6.4 Flood Risk Calculations

For the purposes of mitigation against the flood danger, dams, culverts, bridges, and canals are designed on the basis of the return periods (safety life of the structure) for 50-year, 100-year, 200-year, or 500-year. Flood data are treated with the combination of two methods, namely empirical and theoretical. In the theoretical calculations, the time duration between two flood occurrences is assumed independent from each other. The arithmetic average of these durations is referred to as the recurrence interval, $T$. On the average, if only one flood appears, then one expects the next one after the average return period. This concept implies that there is an inverse relationship between the flood risk, $R$, and the return period as,

$$R = \frac{1}{T} \tag{6.9}$$

The theoretical probability of a flood to occur in any future year is equal to $1/T$, and its non-occurrence probability is $(1 - 1/T)$; i.e., safety, $S$, is the complementary event to $R$.

$$S = 1 - R = \left(1 - \frac{1}{T}\right) \tag{6.10}$$
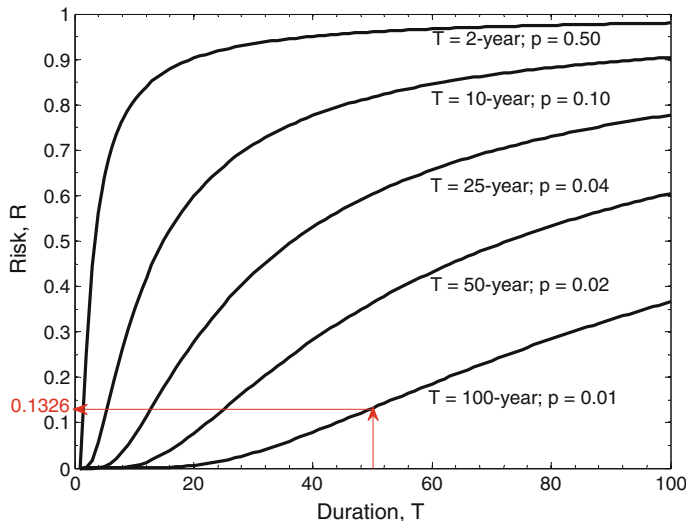
During $n$-year period, provided that the flood occurrences are independent from each other, the safety of water structure over n-years is a function of each year's safety. Independence in the probability theory corresponds to multiplication operation (Benjamin and Cornell 1970), and therefore, $n$-year safety, $S_n$, of a structure is,

$$S_n = \left(1 - \frac{1}{T}\right)^n \tag{6.11}$$

The complementary $n$-year risk, $R_n$, becomes,

$$R_n = 1 - \left(1 - \frac{1}{T}\right)^n \tag{6.12}$$

In these equations, $n$ corresponds to the planned life of water structure and the discharge expectation for the structure damage is referred to as the design discharge calculation, which is explained in Chap. 7. The graphical relationship between the structure design life (return period), $T$, and the risk level, $R$, is presented in Fig. 6.7. The risk, $R_n$, of an expected flood discharge over $n$-year can be read off from the graph for any given $T$-year return period. If design flood discharge is $Q_D$, then the risk for each year is $R = P(Q \geq Q_D)$ and the complementary safety is $S = P(Q < Q_D)$. The former (latter) corresponds to percentage of times that flood discharge, $Q$, is greater (smaller) than design discharge.

**Fig. 6.7** Structure life and flood risk graph

**Example 6.1:** At a site, the flood records are found to have independent structure or assumed to be so. At the same site, a dam construction is planned on the basis of 100-year flood expectation and the life of the structure is 50 year. What is the risk value for this design so that it is not subjected to flood damage? What is the design discharge value corresponding to the calculated risk level?

**Answer 6.1** The life, 50-year, of a water structure is fixed on the horizontal axis, the vertical line from this year is extended until it cuts 100-year curve, and then, the corresponding risk level is read off from the vertical axis, which yields $R_n = 0.1326$.

The second part of the question can be answered provided that the PDF of the flood discharges is determined theoretically.

## 6.5 Annual Flood Discharge Calculations

If the annual life of a water structure is $n$-year, then the probability of flood exceedence is equal to $1/n$. The first question at this stage is what is the probability of $i < n$ flood occurrence over $n$-year. The answer is similar to a single probability of occurrence, and it is defined on frequency basis as $i/n$. However, if the same question is repeated for n-year flood occurrence, then the probability becomes equal to $n/n = 1$. How could the probability become equal to one, which implies a complete determinism? This is against the idea that whatever are the circumstances, there must always remain a room for uncertainty. In general, the successive flood occurrences are independent and have the same PDF. In order to determine the empirical probabilities, the data are ranked in ascending order from the smallest to

the biggest. In this sequence, each one is given a rank, m, starting from the smallest one as $m = 1$ ($m = 1, 2, 3, \ldots,$ n). If the question is repeated as what is the probability of occurrence for the $i$th order flood, then the answer can be given logically based on the rank by employing the formulation of Weibull as already indicated in Table 6.1 as,

$$P(Q_m < Q_D) = \frac{m}{n+1} \quad (m = 1, 2, \ldots, n) \tag{6.13}$$

Herein, $P(Q_m < Q_T)$, indicates non-exceedence probability of design discharge at the $m$th rank. This empirical formulation provides opportunity to calculate probability value for each flood data. It implies that small (big) flood discharges have small (big) probabilities. The probability of non-exceedence is equivalent to safety. Figure 6.8 indicates the relationship between the sample length and exceedence probability. The result is linear and shows a directly proportional relationship.

This figure shows the change of exceedence probability with rank for sample lengths 10, 25, 50, and 100. It is to be noticed that whatever is the sample length, the exceedence probability does not reach 1 exactly. Each rank is attached with a magnitude of flood record; therefore, the main solution is to find the relationship between the flood magnitudes and exceedence probabilities as given in Eq. (6.13). This is achievable only through a theoretical PDF attachment to the scatter diagram of the actual flood discharges versus the empirical exceedence probabilities. Since the empirical probabilities are different from each other, the uniform PDF cannot represent the flood magnitudes. In general, small flood values are rather rare than medium-size floods, but extreme flood magnitudes are very rare, and therefore, the flood dangers lie within this last part of verbal flood classification as rare, medium,
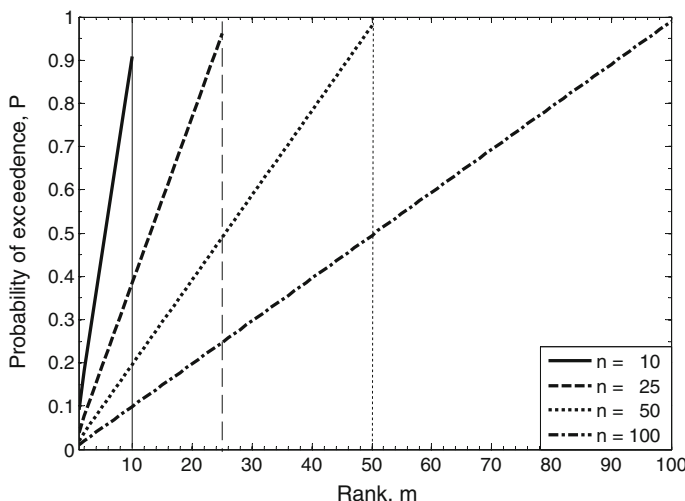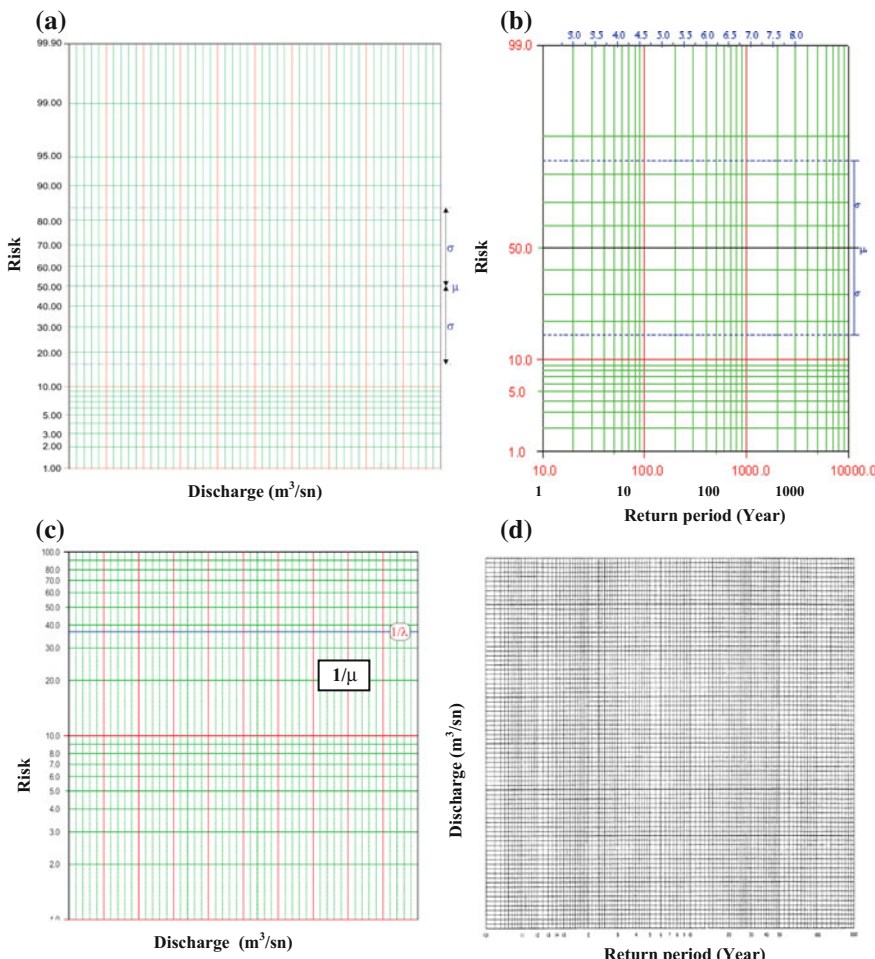


**Fig. 6.8** Risk sample length relationships

and extremely rare classes. This sentence brings to the mind a skewed PDF as in Fig. 6.1. Among different PDFs for flood discharges are the Gamma, log-normal, extreme value (Gumbel), and generalized extreme value (Pearson) PDFs (Sect. 6.6.2).

### 6.5.1   Probability Paper Plot Method

Practical applications can be achieved by the use of PDF papers. One of the axes on such papers is for the exceedence probability (risk) or non-exceedence probability (safety) and the other one (usually the horizontal axis) for the flood discharge magnitudes (Fig. 6.9).



**Fig. 6.9**   PDF papers: **a** normal, **b** log-normal, **c** exponential, **d** Gumbel papers

Among these papers, the normal PDF paper is the most extensively used in the probabilistic and statistical works; however, its fit to flood discharges is not valid practically. In case of extreme values, such as floods, most often used PDFs are generalized extreme value (GEV, Pearson), extreme value (Gumbel), Weibull, and Gamma PDFs. The flood data scatter according to aforementioned data plotting explanations yield to a straight line on the most suitable PDF paper. This requires the flood data plot on each PDF paper, and then, the most convenient one is selected with the straight-line appearance. The calculations according to Eq. (6.13) after the ranking procedure and the scatter diagram are referred in the literature as the Weibull plotting procedure.
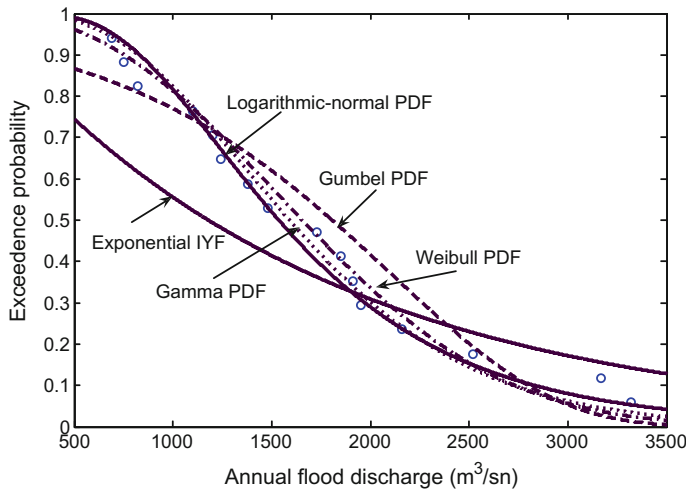
**Example 6.2:** The annual flood discharges are given in Table 6.2. Estimate the flood discharge that may emerge over 200-year period by making use of the Weibull plotting procedure.

**Answer 6.2** Under the light of what have been explained in the previous sections, annual flood discharge risk and return periods are presented in the same table. It is possible to deduct from this table that for 5.88% probability of exceedence corresponding annual flood is bigger than 3320 $m^3$/sec. Another meaning of this is that with 94.12% of exceedence the flood discharge is equal to 690 $m^3$/sec or bigger.

In our days, rather than handwork, the necessary software is available for all the calculations in addition to graphic representations. In Fig. 6.10, CDFs that are used mostly in the flood frequency analysis are given with data plots from Table 6.2.

**Table 6.2**  Annual flood discharges and necessary calculations

| Year | Annual flood ($m^3$/sec) | Observed flood ($m^3$/sec) | Rank | Risk, $r$ (%) | Return period, $1/r$ (year) |
|------|------|------|------|------|------|
| 1982 | 2520 | 3320 | 1  | 5.88  | 17   |
| 1983 | 1850 | 3170 | 2  | 11.76 | 8.5  |
| 1984 | 750  | 2520 | 3  | 17.65 | 5.62 |
| 1985 | 1100 | 2160 | 4  | 23.53 | 4.25 |
| 1986 | 1380 | 1950 | 5  | 29.41 | 3.40 |
| 1987 | 1910 | 1910 | 6  | 35.29 | 2.83 |
| 1988 | 3170 | 1850 | 7  | 41.18 | 2.43 |
| 1989 | 1200 | 1730 | 8  | 47.06 | 2.13 |
| 1990 | 820  | 1480 | 9  | 52.94 | 1.89 |
| 1991 | 690  | 1380 | 10 | 58.82 | 1.70 |
| 1992 | 1240 | 1240 | 11 | 64.71 | 1.55 |
| 1993 | 1730 | 1200 | 12 | 70.59 | 1.42 |
| 1994 | 1950 | 1100 | 13 | 76.47 | 1.31 |
| 1995 | 2160 | 820  | 14 | 82.35 | 1.21 |
| 1996 | 3320 | 750  | 15 | 88.24 | 1.13 |
| 1997 | 1480 | 690  | 16 | 94.12 | 1.06 |
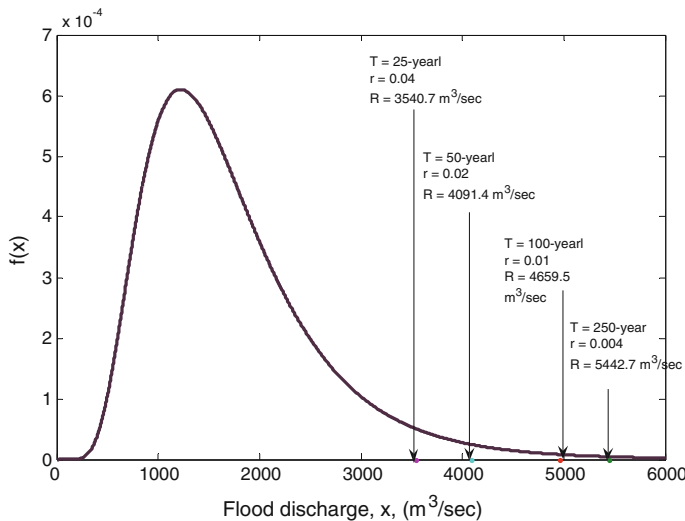
**Fig. 6.10** Various CDFs for annual flood discharges

**Table 6.3** MATLAB statements

| PDF | Parameter calculation | CDF (safety) | Risk = 1 − safety | Graphic |
|---|---|---|---|---|
| Weibull | *wblfit(data)*<br>A = 1930.4<br>B = 2.4 | *gw = wblcdf(data,A,B)* | rw = 1.0 − gw | *plot(data,rw)* |
| Gumbel | *evfit(data)*<br>A = 2111.9<br>B = 827.2 | *ggu = evcdf(data,A,B)* | rgu = 1.0 − ggu | *plot(data,rgu)* |
| Gamma | *gamfit(data)*<br>A = 4.994<br>B = 341.290 | *gga = gamcdf(data,A,B)* | rga = 1.0 − gga | *plot(data,rga)* |
| Exponential | *expfit(data)*<br>A = 1074.4 | *ge = expcdf(data,A)* | re = 1.0 − ge | *plot(data,re)* |
| Log-normal | *lognfit(data)*<br>A = 7.337<br>B = 0.477 | *gl = logncdf(data,A,B)* | rl = 1.0 − gl | *plot(data,rl)* |

Visual inspection of this figure reveals that the most suitable CDF for the data at hand is the Weibull type. This graph is obtained by a MATLAB program written by the author through the following steps, and the necessary statements are provided in Table 6.3.

(1) Sort the flood discharges given in the second column in Table 6.2 according to descending order, and write them into the third column. In the MATLAB program, this step is executed by the command *sort(data)*, after the reading of *data* file,

**Fig. 6.11** Safety–risk boundaries

(2) Attach a risk probability value to each one of the ranked data according to Eq. (6.13). The subtraction of these probability values from 1 gives the probability of exceedence, i.e., *risk*,

(3) Ranked data are shown on the horizontal axis and the corresponding probabilities on the vertical axis, and hence, the scatter diagram is obtained through another MATLAB statement as *scatter (data, risk),* and the scatter diagram is shown in Fig. 6.11 as small circles. This figure is in accordance with explanations and notations as in Sect. 6.2,

(4) The parameters of each PDF can be obtained by the MATLAB commands, and they are given in the second column of Table 6.3,

(5) By use of the calculated parameters with the commands on the third column of the table, CDFs can be calculated,

(6) Each risk value corresponding to the safety values can be calculated from the information that the risk and safety summation is equal to 1,

(7) On the top of the scatter diagram, each one of the CDFs is plotted as in Fig. 6.10. For this purpose, prior to plotting command "*hold on,*" MATLAB command is executed. Herein, not only the most convenient, but all the CDFs are plotted for the purpose of visual inspection opportunity to select the most suitable CDF selection,

(8) One can determine the most suitable straight line on the probability distribution paper by one of the following procedures (Benjamin and Cornell 1970).

(i) In practical applications, most often by rule of thumb and by eye,

(ii) Least squares technique,

(iii)  Method of moments,
(iv)  Maximum-likelihood principle.


## 6.5.2  Safety–Risk on PDF Curve

Key hydrological parameters in the safety–risk analysis for flood safety evaluations
are the probabilities for flood occurrence and magnitude, which are uncertain
variables. Uncertainty in the extreme flood magnitude is a function of the uncer-
tainty in a host of variables contributing to the flood estimation. Apart from the
man-made alterations in the environment, a particular focus is needed for quanti-
fying the uncertainty associated with hydrological variables that play significant
role in the estimation of the extreme floods, which also contribute to the uncertainty
in risk decision variables. The completion of flood hazard risk maps is achieved
with the view of perspective for effective planning, protection, operation, con-
struction, and maintenance against dangerous hydrological events.

In the previous sections, risk and safety calculation ways are explained on the
basis of flood discharge independence assumption. In the calculations, not the flood
peak discharge magnitudes, but only exceedence or non-exceedence probabilities
are considered. For flood discharge magnitude PDF, either the histogram is cal-
culated from a given set of flood discharges, and then, the most suitable PDF is
fitted to the histogram or a preliminary theoretical PDF is assumed for further
calculations.

In Fig. 6.11, the PDF is divided into two parts as shown on the right tail, which
is the representative area for floods. For instance, if the flood discharge magnitude
PDF is assumed as the log-normal PDF, then by considering the parameter values
from Table 6.3, the theoretical probability calculation is achieved by $y = logncdf$
$(x,7.3375,0.477)$ MATLAB command. It is important to notice that instead of the
CDF command, $logcdf$ (), PDF command $logpdf$ () is considered. Figure 6.11 is
plotted on the basis that from Table 6.4 for the flood discharge variation domain is
$0 < x < 6000$ m$^3$/sec.


**Table 6.4**  Frequency factor for various PDFs

| PDF | Return period (risk) | | | | | | | |
|---|---|---|---|---|---|---|---|---|
|  | 2 (0.5) | 5 (0.2) | 10 (0.1) | 25 (0.04) | 50 (0.02) | 100 (0.01) | 250 (0.004) | 500 (0.002) |
| Gumbel | −0.367 | 0.476 | 0.834 | 1.169 | 1.364 | 1.527 | 1.709 | 1.827 |
| Gamma | 0.693 | 1.609 | 2.303 | 3.219 | 3.912 | 4.605 | 5.522 | 6.215 |
| Normal | 0.500 | 1.342 | 1.782 | 2.251 | 2.554 | 2.826 | 3.152 | 3.378 |
| Log-normal | 1.000 | 2.320 | 3.602 | 5.759 | 7.797 | 10.240 | 14.183 | 17.782 |
| Weibull | 0.693 | 1.609 | 2.303 | 3.219 | 3.912 | 4.605 | 5.522 | 6.215 |

In this figure, the area below the PDF is divided into two parts. For instance, the risk of a flood occurrence once in 25 year is calculated from Eq. (6.9) as $R = 0.04$ and from Eq. (6.10) as $S = 0.996$. The flood discharge against these values can be calculated from the MATLAB log-normal PDF as ***logninv (0.96,7.337,0.477)***. The meaning of this command is that the probability is 0.996 with the parameters 7.377 and 0.477, and the result is the flood discharge magnitude. One can notice that this command is replaced by ***inv*** instead of the ***cdf*** in Table 6.3.

### *6.5.3 Frequency Factor*

It is obvious from the previous section that the calculations must be repeated for each risk (safety) value. Is it not possible to achieve these calculations in a more practical way? It is possible to calculate the flood discharge for standard statistical parameters and subsequently, the actual flood discharges. In the previous sections, the PDFs are employed without standardization. However, the standardization operation renders each PDF such that their arithmetic average is equal to zero and the standard deviation is 1. If the arithmetic average, $\mu_Q$, and the standard deviation, $\sigma_Q$, of a given flood discharge series, $Q_1, Q_2, \ldots, Q_n$, are calculated, then the standardization operation can be effected according to the following expression.

$$q_i = \frac{Q_i - \mu_Q}{\sigma_Q} \tag{6.14}$$

For instance, the arithmetic average and the standard deviation of the flood discharges in Table 6.2 are shown numerically in Fig. 6.12 as $\overline{Q}$, and, $S$, respectively.
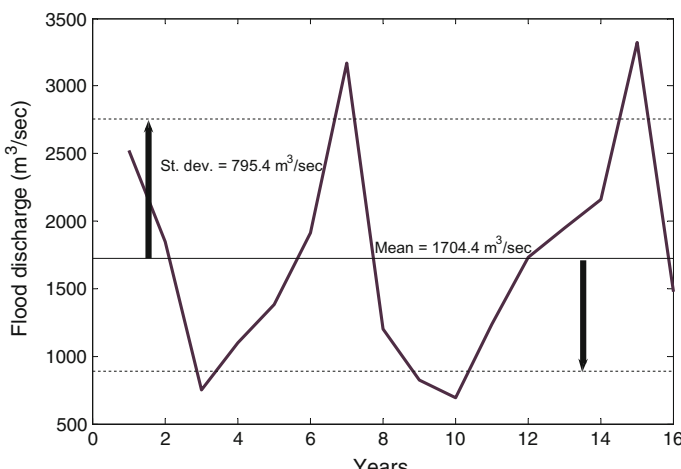


**Fig. 6.12** Annual flood discharge sequence

It is possible to express each flood discharge, $Q_i$, value in two parts as the arithmetic average, $\overline{Q}$, and additional positive or negative deviations, $S_i = Q_i - \overline{Q}$ (i = 1, 2, ..., n), as,

$$Q_i = \overline{Q} + S_i \tag{6.15}$$

If the arithmetic average value is regarded as the truncation level, then it is possible to attach all the variability to the underlying PDF.

The given flood discharge series is standardized by use of Eq. (6.14) with zero mean and unit standard deviation, and the graphical representation is given in Fig. 6.13.

Comparison of the two last figures indicates that there is no difference in the shape of time series, but the only difference is the shifted and scaled version of the former one such that the mean and standard deviation values are zero and one, respectively.

The explanations in this subsection bring to the mind the idea that the design flood discharge, $Q_{TD}$, can be expressed by the arithmetic average, $\overline{Q}$, and a certain fold, $k$, of the standard deviation, $S$, according to the following expression.

$$Q_D = \overline{Q} \pm kS \tag{6.16}$$

where $k$ is referred to as the frequency factor (Chap. 2). One can deduce that provided a flood discharge series is given after the arithmetic average and standard deviation calculation, the frequency factor can be determined from the CDF according to the return period. In this expression, + and − signs are for the calculation of extreme (flood) and low (drought) discharges, respectively. Hence, the
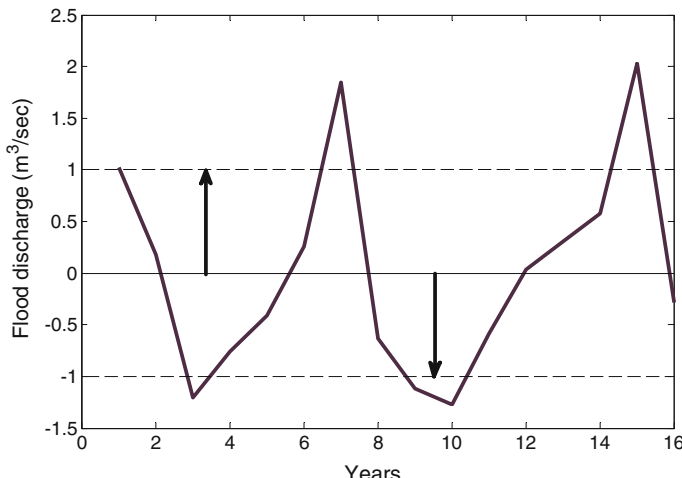


**Fig. 6.13** Standard flood discharge series

frequency factor is different for high and low discharges. In Fig. 6.11, the droughts are sought on the left-hand side of the PDF. The more is the frequency factor, the more are the deviations around the arithmetic average value. If its value is equal to zero, then there is not a random sequence. The size of the floods is dependent on the magnitude of this frequency factor similar to the PMP and PMF as explained in Chap. 2. The dimension of the last expression is the same as the given flood discharge series. In order to render it into a dimensionless form, it is sufficient to divide both sides by the arithmetic average.

$$\frac{Q_D}{\bar{Q}} = 1 \pm k\frac{S}{\bar{Q}} \tag{6.17}$$

or

$$Q_D = \bar{Q}(1 \pm kC_V) \tag{6.18}$$

Herein, $C_v$ indicates the coefficient of variation (Benjamin and Cornell 1970). There is a relationship between the frequency factor and the return period for a given PDF. It is possible to present such a relationship in the form of k versus T graph. For the application of this method, it is necessary first to calculate the summary statistics (arithmetic average, standard deviation, skewness coefficient, coefficient of variation) from the given data sequence. For a given return period, the probability can be obtained from Table 6.4 or from the relationship in Eq. (6.16). In this table, the calculation of the frequency factor is achieved after the following MATLAB steps.

(1) Extreme value (Gumbel) PDF: *Q = evinv (P, MU, SIGMA)* for MU = 0 and SIGMA = 1,
(2) Gamma PDF: *Q = gaminv (P, A, B)* for $A = 1$ and $B = 1$; in this case, Gamma PDF is equivalent to exponential PDF,
(3) Normal PDF: *Q = norminv (P, MU, SIGMA)* for MU = 0 and SIGMA = 1,
(4) Log-normal PDF: *Q = logninv (P, MU, SIGMA)* for MU = 0 and SIGMA = 1,
(5) Weibull PDF: *Q* = wblbinv (*P*, *A*, *B*) for $A = 1$ and $B = 1$.

### 6.5.3.1 Gumbel Method

For flood prediction at a site, most often either extreme value (EV, Gumbel) or generalized extreme value (GEV, Pearson) PDFs are employed. In the MATLAB software, it is given under the title of "gev." The Gumbel PDF has the following double exponential mathematical form.

$$f(Q) = \exp\left\{-\exp\left[-\frac{(Q-u)}{\alpha}\right]\right\} \tag{6.19}$$

Here, $u$ and $\alpha$ are the location and scale parameters, respectively. They are dependent on the arithmetic average, $\overline{Q}$, and standard deviation, $S_Q$, as,

$$\alpha = 0.7797 S_Q \tag{6.20}$$

and

$$u = \overline{Q} - 0.45 S_Q \tag{6.21}$$

This PDF is a specific form of the GEV PDF as given in Jenkins (1955). The GEV PDF expression is in the following form.

$$f(Q) = \exp\left\{-\left[1 - \frac{k(Q-u)}{\alpha}\right]\right\}^{1/k} \tag{6.22}$$

Herein, $k$ is a shape parameter, which is useful in finding the most suitable PDF to a given data series. It has three alternatives as follows:

(1)  For $k = 0$ extreme value, PDF is Gumbel PDF,
(2)  For $k<$ extreme value, PDF is Pearson type II PDF,
(3)  For $k > 0$ extreme value, PDF is Pearson type III PDF.

In different parts of the world, the most commonly used extreme value PDF is the Gumbel PDF. If the flood discharge predictions are sought for longer periods than the record length, the results may not be reliable due to the sampling errors. This is partly because the exact PDF cannot be identified from a finite length series.

The Gumbel PDF as obvious from Eq. (6.19) has double exponential form. The recurrence period is the reverse of the exceedence (risk) probability, and it becomes theoretically equal to the following expression.

$$\frac{1}{T} = 1 - \exp[-\exp(-q)] \tag{6.23}$$

where $q$ is named as the Gumbel small variable, and it is expressed as,

$$q = \frac{Q-u}{\alpha} \tag{6.24}$$

By taking double logarithm of both sides leads to,

$$q = \ln\left[\ln\left(\frac{T}{T-1}\right)\right] \tag{6.25}$$

The substitution of Eq. (6.24) into Eq. (6.19) gives,

$$f(x) = e^{-e^{-q}} \qquad (6.26)$$

On the other hand, according to the previously explained frequency factor from Eq. (6.16),

$$Q_T = \bar{Q} \pm qS \qquad (6.27)$$

Furthermore, the value of the arithmetic average in case of infinite series length is equal to Euler constant, which is 0.5772 (Spiegel 1965). For Gumbel PDF, return period and frequency factor relationship is presented in Table 6.5.

In order to make flood discharge prediction on the basis of Gumbel PDF, the following steps must be executed.

(a) Calculate the mean, $\bar{Q}$, and the standard deviation, $S_Q$, of the given flood discharge series,
(b) From Eqs. (6.20) and (6.21), find the $\alpha$ and $u$ parameters,
(c) From Eq. (6.26), take double logarithm and calculate $q$ value.

These calculation steps yield the discharge value as from an infinite length series, because throughout the calculations theoretical PDF is used. In the practical studies, there are finite length series. As a result of this, there is difference between the population and sample discharge values. For this reason, the q value must be adjusted as follows.

$$y = \frac{q - q_n}{s_n} \qquad (6.28)$$

where $q_n$ and $s_n$ are the mean value and the standard deviation of the Gumbel small value. The change of these parameters with the sample length is given in Table 6.6 (Bayazıt et al. 1997).

**Table 6.5** Gumbel frequency factor

| T | q |
|---|---|
| 1.5 | −0.523 |
| 2 | −0.164 |
| 5 | 0.720 |
| 10 | 1.305 |
| 25 | 2.044 |
| 50 | 2.5902 |
| 100 | 3.137 |
| 200 | 3.679 |
| 500 | 4.395 |

**Table 6.6** Gumbel small variable values

| n | $q_n$ | $s_n$ |
|---|---|---|
| 10 | 0.504 | 0.9050 |
| 15 | 0.513 | 1.021 |
| 20 | 0.524 | 1.063 |
| 25 | 0.531 | 1.092 |
| 30 | 0.536 | 1.112 |
| 35 | 0.540 | 1.128 |
| 40 | 0.544 | 1.141 |
| 45 | 0.546 | 1.152 |
| 50 | 0.549 | 1.161 |
| 60 | 0.552 | 1.175 |
| 70 | 0.555 | 1.185 |
| 80 | 0.557 | 1.1904 |
| 90 | 0.559 | 1.201 |
| 100 | 0.560 | 1.206 |
| 150 | 0.564 | 1.225 |
| 200 | 0.567 | 1.236 |
| 500 | 0.572 | 1.259 |
| 1000 | 0.575 | 1.269 |
| >1000 | 0.577 | 1.282 |

**Example 6.3** For Cizre station in the southeastern province of Turkey, annual maximum flow values are given by Bayazıt et al. (1997) for period 1956–1975 as in Table 6.7. The third column includes ranks.

**Answer 6.3** In the same table, columns 2 and 3 are for the ordered discharges and ranks, respectively. In the last column, non-exceedence risk probabilities are given and they are calculated by Eq. (6.13). The maximum discharge scatter diagram is presented in Fig. 6.14 together with Gumbel PDF.
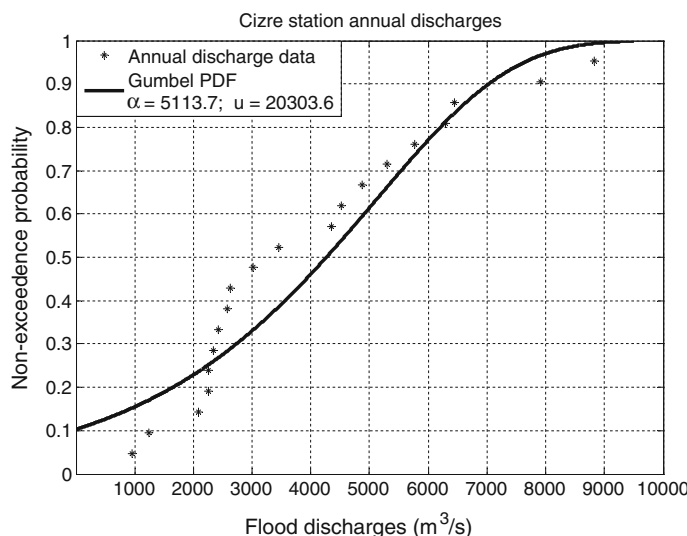
The scatter points are almost around the theoretical Gumbel PDF, and from this figure, one can find the non-exceedence probability for 50 year as $1 - 0.02 = 0.98$ corresponding to 6300 m³/s, and in the same manner for 100-year return period, flood discharge is 7050 m³/s. From Eqs. (6.20) and (6.21), one can calculate that $\alpha = 5113.7$ and $u = 2303.6$.

### 6.5.3.2   Log-Pearson Method

If the data have high skewness coefficient, then the logarithms of the data are taken, and hence, PDF is referred to as Log-Pearson PDF. The mathematical expression is as follows.

**Table 6.7** Annual flood values and calculations

| Natural sequence | | Artificial sequence | | Empirical probability |
|---|---|---|---|---|
| Year | Discharge (m³/s) | Rank | Sorted discharge (m³/s) | |
| 1956 | 2424 | 1 | 963 | 0.048 |
| 1956 | 6300 | 2 | 1250 | 0.095 |
| 1958 | 2340 | 3 | 2080 | 0.143 |
| 1959 | 2080 | 4 | 2250 | 0.190 |
| 1960 | 2262 | 5 | 2262 | 0.238 |
| 1961 | 1250 | 6 | 2340 | 0.286 |
| 1962 | 3014 | 7 | 2424 | 0.333 |
| 1963 | 7910 | 8 | 2571 | 0.381 |
| 1964 | 4350 | 9 | 2630 | 0.429 |
| 1965 | 2630 | 10 | 3014 | 0.476 |
| 1966 | 8820 | 11 | 3450 | 0.524 |
| 1967 | 4516 | 12 | 4350 | 0.571 |
| 1968 | 4866 | 13 | 4516 | 0.619 |
| 1969 | 6450 | 14 | 4866 | 0.667 |
| 1970 | 2250 | 15 | 5300 | 0.714 |
| 1971 | 3450 | 16 | 5772 | 0.762 |
| 1972 | 5300 | 17 | 6300 | 0.810 |
| 1973 | 963 | 18 | 6450 | 0.857 |
| 1974 | 5773 | 19 | 7910 | 0.905 |
| 1975 | 2571 | 20 | 8820 | 0.952 |



**Fig. 6.14** Gumbel PDF paper

$$f(Q) = \frac{1}{\beta^{\alpha}\Gamma(\alpha)}(Q-\gamma)^{\alpha-1}e^{-(Q-\gamma)/\beta} \quad (\gamma < Q < \infty) \qquad (6.29)$$

where $\gamma$ shows the lowest boundary; $\beta$ is the scale, and $\alpha$ is the shape parameters; and finally, $\Gamma(\alpha)$ indicates the Gamma function. This is a three-parameter PDF, with parameters dependence on the statistical parameters as follows:

$$\mu = \gamma + \alpha\beta \qquad (6.30)$$

$$\sigma^2 = \alpha\beta^2 \qquad (6.31)$$

and

$$\delta = 2/\sqrt{\alpha} \qquad (6.32)$$

where $\mu$, $\sigma$, and $\delta$ are the arithmetic average, standard deviation, and coefficient of skewness, respectively. The first application of this PDF to annual floods was by Foster (1924). Gamma and Log-Pearson type III PDF frequency factor values are presented in Table 6.8.

In flood frequency analysis, Log-Pearson PDF is used extensively. For its application, the completion of the following steps is necessary.

(1)  Calculate the logarithms of annual flood discharges,

$$Y_i = \log Q_i$$

**Table 6.8**  Log-Pearson and Gamma PDF frequency factors (Haan 1977, Table 7.7)

| Skewness coefficient | | Return period (year) | | | | | | | |
|---|---|---|---|---|---|---|---|---|---|
| | | 1.0101 | 2 | 5 | 10 | 25 | 50 | 100 | 200 |
| $\delta$ | Risk | | | | | | | | |
| | 99 | 50 | 20 | 10 | 4 | 2 | 1 | 0.5 |
| 3 | −0.667 | −0.396 | 0.42 | 1.18 | 2.278 | 3.152 | 4.051 | 4.97 |
| 2.5 | −0.799 | −0.36 | 0.518 | 1.25 | 2.262 | 3.048 | 3.845 | 4.652 |
| 2 | −0.99 | −0.307 | 0.609 | 1.302 | 2.219 | 2.912 | 3.605 | 4.298 |
| 1.5 | −1.256 | −0.24 | 0.69 | 1.333 | 2.146 | 2.743 | 3.33 | 3.91 |
| 1 | −1.588 | −0.164 | 0.758 | 1.34 | 2.043 | 2.542 | 3.022 | 3.489 |
| 0.5 | −1.955 | −0.083 | 0.808 | 1.323 | 1.91 | 2.311 | 2.686 | 3.041 |
| 0 | −2.326 | 0 | 0.842 | 1.282 | 1.751 | 2.054 | 2.326 | 2.576 |
| −0.5 | −2.686 | 0.083 | 0.856 | 1.216 | 1.567 | 1.777 | 1.955 | 2.108 |
| −1 | −3.022 | 0.164 | 0.852 | 1.128 | 1.366 | 1.492 | 1.588 | 1.664 |
| −1.5 | −3.33 | 0.24 | 0.825 | 1.018 | 1.157 | 1.217 | 1.256 | 1.282 |
| −2 | −3.605 | 0.307 | 0.777 | 0.895 | 0.959 | 0.98 | 0.99 | 0.995 |
| −2.5 | −3.845 | 0.36 | 0.711 | 0.711 | 0.793 | 0.798 | 0.799 | 0.8 |
| −3 | −4.051 | 0.396 | 0.636 | 0.66 | 0.666 | 0.666 | 0.667 | 0.667 |

(2) The arithmetic average, $\mu$, standard deviation, $\sigma$, and coefficient of skewness, $\delta$, are calculated according to the following expressions,

$$\mu = \frac{1}{n} \sum_{i=1}^{n} \log(Q_i) \tag{6.33}$$

$$\sigma = \sqrt{\frac{\sum_{i=1}^{n} \log(Q_i) - \mu^2}{n - 1}} \tag{6.34}$$

and

$$\delta = \frac{n \sum_{i=1}^{n} [\log(Q_i) - \mu^3]}{(n - 1)(n - 2)\sigma^3} \tag{6.35}$$

3) The design flood discharge estimation for any given recurrence period, $T$, can be calculated as,

$$\log(Q_D) = \mu + k\,\sigma \tag{6.36}$$

The frequency factor can be taken from Table 6.8.

**Example 6.4:** The annual flood discharge values are given in their natural sequence in the second column of Table 6.9 (Bayazıt et al. 1997).

**Solution 6.4:** The fit of the Log-Pearson PDF to the given annual flood discharges is presented in Fig. 6.15.

After the calculation by taking into consideration Eqs. (6.33)–(6.36), frequency analysis results are presented in Table 6.10.

## 6.6 Practical Flood Calculation Application

In this section, practical flood analysis calculations are presented based on data from Mutludere (Valika) stream at the international border between Turkey and Bulgaria on the Thrace Peninsula within the Marmara Sea region of Turkey (Fig. 6.16). This stream is in the Ergene drainage basin, which extends about 170 km from the Bulgarian border to the Durusu (Terkos) lake near Istanbul City, and the northern parts are on the medium elevation mountainous area next to the Black Sea.
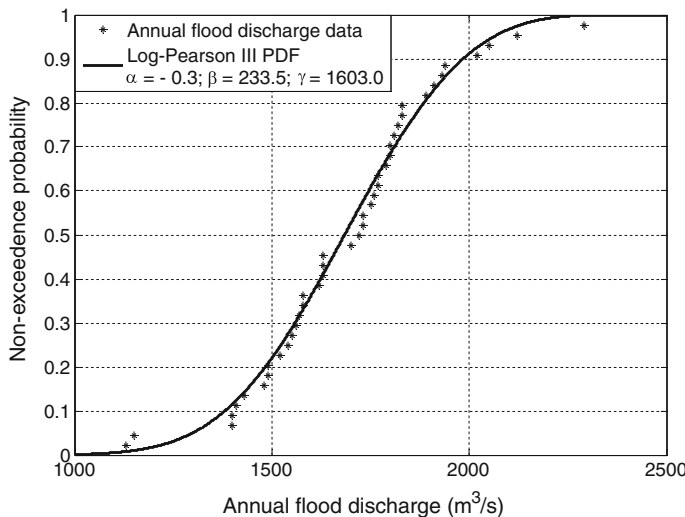
**Table 6.9**  Annual flood discharges and calculations

| Natural order | | Ranked order | | Return period (year) | Exceedence probability |
|---|---|---|---|---|---|
| Year | Discharge (m³/s) | Order | Discharge (m³/sn) | | |
| 1933 | 1930 | 1 | 2290 | 44.00 | 0.02 |
| 1934 | 2120 | 2 | 2120 | 22.00 | 0.04 |
| 1935 | 1400 | 3 | 2050 | 14.67 | 0.07 |
| 1936 | 1770 | 4 | 2020 | 11.00 | 0.09 |
| 1937 | 1750 | 5 | 1940 | 8.80 | 0.11 |
| 1938 | 1550 | 6 | 1930 | 7.33 | 0.13 |
| 1939 | 2050 | 7 | 1910 | 6.29 | 0.16 |
| 1940 | 1810 | 8 | 1890 | 5.50 | 0.18 |
| 1941 | 1580 | 9 | 1830 | 4.89 | 0.20 |
| 1942 | 1490 | 10 | 1830 | 4.40 | 0.22 |
| 1943 | 1630 | 11 | 1820 | 4.00 | 0.24 |
| 1944 | 1490 | 12 | 1810 | 3.67 | 0.27 |
| 1945 | 1760 | 13 | 1800 | 3.38 | 0.29 |
| 1946 | 1700 | 14 | 1800 | 3.14 | 0.31 |
| 1947 | 1730 | 15 | 1790 | 2.93 | 0.33 |
| 1948 | 1830 | 16 | 1770 | 2.75 | 0.36 |
| 1949 | 1910 | 17 | 1770 | 2.59 | 0.38 |
| 1950 | 1790 | 18 | 1760 | 2.44 | 0.40 |
| 1951 | 1940 | 19 | 1750 | 2.32 | 0.42 |
| 1952 | 2290 | 20 | 1730 | 2.20 | 0.44 |
| 1953 | 1620 | 21 | 1730 | 2.10 | 0.47 |
| 1954 | 1430 | 22 | 1720 | 2.00 | 0.49 |
| 1955 | 2020 | 23 | 1700 | 1.91 | 0.51 |
| 1956 | 1770 | 24 | 1630 | 1.83 | 0.53 |
| 1957 | 1890 | 25 | 1630 | 1.76 | 0.56 |
| 1958 | 1560 | 26 | 1630 | 1.69 | 0.58 |
| 1959 | 1480 | 27 | 1620 | 1.63 | 0.60 |
| 1960 | 1520 | 28 | 1580 | 1.57 | 0.62 |
| 1961 | 1630 | 29 | 1580 | 1.52 | 0.64 |
| 1962 | 1730 | 30 | 1570 | 1.47 | 0.67 |
| 1963 | 1410 | 31 | 1560 | 1.42 | 0.69 |
| 1964 | 1570 | 32 | 1550 | 1.38 | 0.71 |
| 1965 | 1800 | 33 | 1540 | 1.33 | 0.73 |
| 1966 | 1630 | 34 | 1520 | 1.29 | 0.76 |
| 1967 | 1130 | 35 | 1490 | 1.26 | 0.78 |
| 1968 | 1150 | 36 | 1490 | 1.22 | 0.80 |
| 1969 | 1800 | 37 | 1480 | 1.19 | 0.82 |
| 1970 | 1820 | 38 | 1430 | 1.16 | 0.84 |
| 1971 | 1830 | 39 | 1410 | 1.13 | 0.87 |

(continued)

**Table 6.9**   (continued)

| Natural order | | Ranked order | | Return period (year) | Exceedence probability |
|---|---|---|---|---|---|
| Year | Discharge (m³/s) | Order | Discharge (m³/sn) | | |
| 1972 | 1540 | 40 | 1400 | 1.10 | 0.89 |
| 1973 | 1580 | 41 | 1400 | 1.07 | 0.91 |
| 1974 | 1720 | 42 | 1150 | 1.05 | 0.93 |
| 1975 | 1400 | 43 | 1130 | 1.02 | 0.96 |



**Fig. 6.15**   Log-Pearson PDF fit

**Table 6.10**   Frequency analysis

| T (Year) | Risk (%) | y | $y\sigma_{\log Q}$ | $\log Q_T$ | $Q_T$ |
|---|---|---|---|---|---|
| 2 | 50 | 0.0953 | 0.0060 | 3.2302 | 1699 |
| 5 | 20 | 0.8568 | 0.0534 | 3.2776 | 1895 |
| 10 | 10 | 1.2032 | 0.0750 | 3.2992 | 1992 |
| 25 | 4 | 1.5358 | 0.0957 | 3.3199 | 2089 |
| 50 | 2 | 1.7314 | 0.1079 | 3.3321 | 2148 |
| 100 | 1 | 1.8950 | 0.1181 | 3.3423 | 2199 |
| 200 | 0.5 | 2.0344 | 0.1286 | 3.3510 | 2244 |

Average width is about 40 km in the northwest but 15 km in the southeast, and the highest hill is in the middle of the drainage area, which is Mahya Mountain with 1013 m peak above mean sea level (a.m.s.l). This massive mountain losses its height toward the southeast in pieces of 500 m elevation small hills.

**Fig. 6.16** Mutludere location

The Mutludere drainage is a transboundary basin between Turkey and Bulgaria with 70% on the Turkey side, and it extends in the west–east direction. Majority of waters originate from Turkey. Some of its geomorphological quantities (A, S, L, $\bar{h}$, and Lc) are given on the map in Fig. 6.17, where $A$ is the drainage area, $S$ is the main channel slope, $L$ is the main channel length, $\bar{h}$ is the average mean sea level (a. m.s.l.), and $L_c$ is the distance between the projection point of the drainage basin centroid on the main channel and the outlet.

The two surface water measurement stations that help for hydrological calculations are located at the inlet (high parts) and near the outlet area. According to these two stations, the drainage basin is thought of two parts as shown in Fig. 6.18.

Armutveren basin upstream and downstream geomorphological quantities are presented in Table 6.11.

In a simple manner by taking into consideration the ratio of the drainage areas (Chap. 5, Eq. 5.9), monthly flow model is used for the whole Mutludere drainage basin. The area ratio is 58/345 = 2.19. For the surface flow, the water volume resulting from rainfall is obtained by multiplying this ratio by the Armutveren monthly runoff records and the results are presented in Table 6.12.
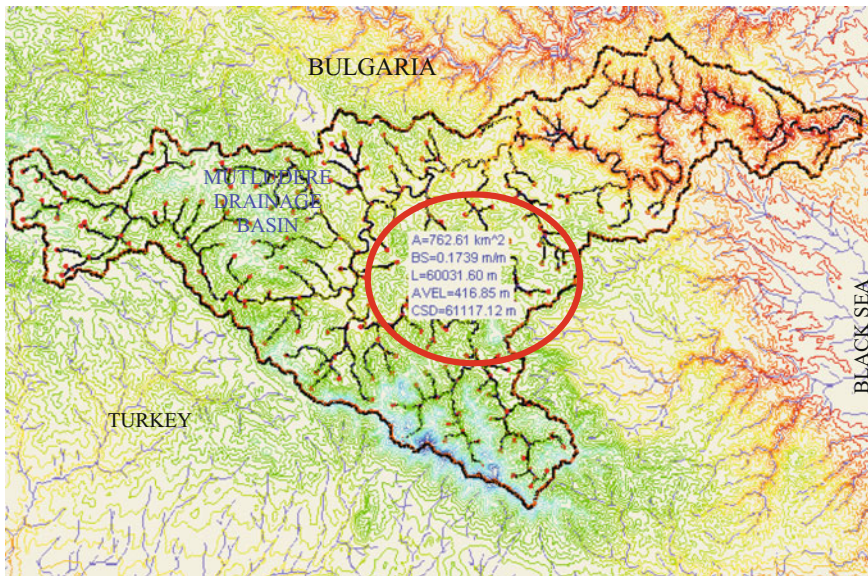
**Fig. 6.17** Mutludere drainage basin quantities
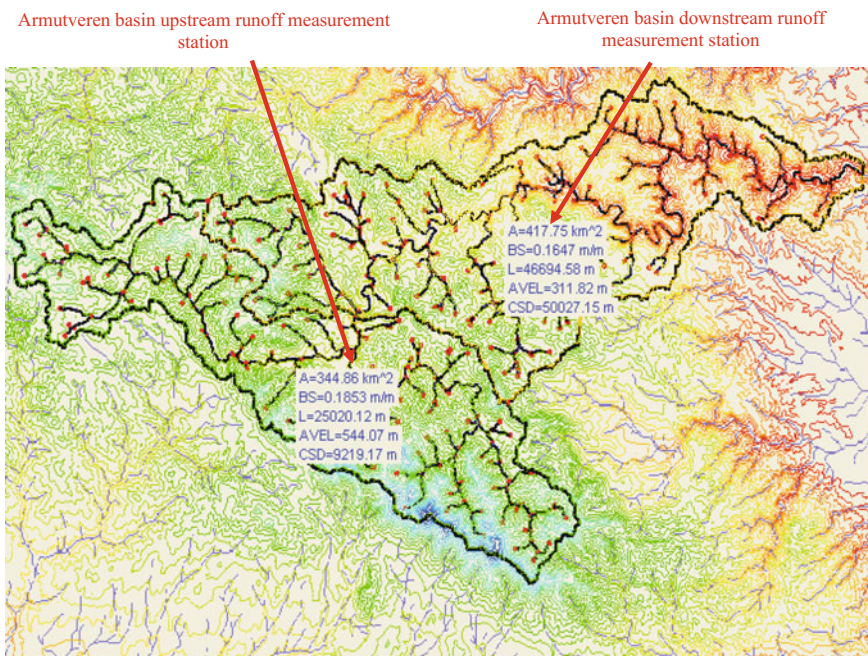


**Fig. 6.18** Upper and lower drainage basins
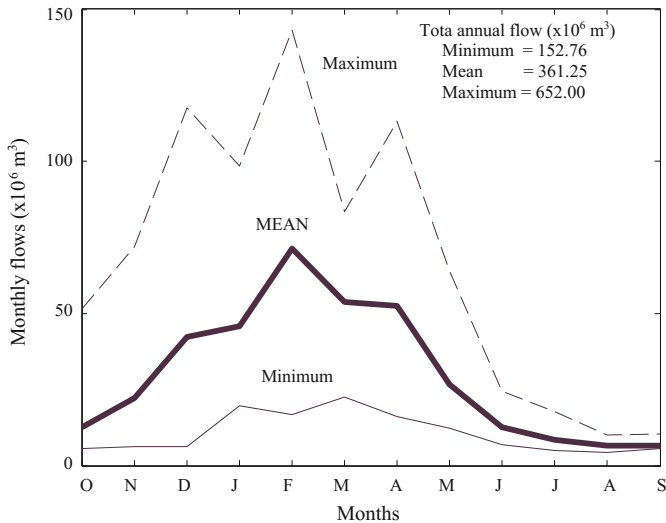
**Table 6.11**  Armutveren inlet and outlet quantities

| Drainage name | Area, $A$ (km$^2$) | Slope, $S$ (m/m) | Longest channel length, $L$ (km) | Average elevation, $\bar{h}$, (m) |
|---|---|---|---|---|
| Armutveren outlet | 345.00 | 0.1853 | 25.00 | 544.00 |
| Armutveren inlet | 418.00 | 0.1647 | 47.00 | 312.00 |
| Whole Mutludere | 758.00 | 0.1739 | 60.00 | 417.00 |

**Table 6.12**  Mutludere outlet monthly flows ($\times 10^6$ m$^3$)

| Year | October | November | December | January | February | March | |
|---|---|---|---|---|---|---|---|
| 1996 | 5.86 | 35.77 | 32.81 | 70.91 | 112.81 | 64.34 | |
| 1997 | 6.41 | 8.70 | 30.06 | 27.52 | 16.91 | 68.58 | |
| 1998 | 12.97 | 21.80 | 79.58 | 30.27 | 143.29 | 68.58 | |
| 1999 | 51.43 | 71.96 | 117.47 | 98.42 | 116.41 | 83.39 | |
| 2000 | 5.88 | 11.64 | 27.52 | 19.71 | 31.11 | 26.25 | |
| 2001 | 7.79 | 6.29 | 6.29 | 29.21 | 24.98 | 22.65 | |
| 2002 | 5.57 | 7.73 | 19.18 | 37.68 | 20.28 | 37.89 | |
| 2003 | 6.18 | 12.68 | 24.76 | 52.70 | 104.56 | 58.63 | |
| Minimum | 5.57 | 6.29 | 6.29 | 19.71 | 16.91 | 22.65 | |
| Mean | 12.76 | 22.07 | 42.21 | 45.80 | 71.30 | 53.79 | |
| Maximum | 51.43 | 71.96 | 117.47 | 98.42 | 143.29 | 83.39 | |
| St. Dev. | 15.81 | 22.39 | 37.11 | 26.85 | 52.60 | 22.14 | |
| | **April** | **May** | **June** | **July** | **August** | **September** | **Annual** |
| | 52.70 | 23.92 | 10.14 | 4.91 | 4.91 | 5.4608 | 424.54 |
| | 88.69 | 27.30 | 13.99 | 9.36 | 9.14 | 6.3286 | 312.99 |
| | 113.24 | 63.92 | 24.34 | 17.86 | 10.05 | 10.2232 | 596.12 |
| | 47.41 | 29.42 | 16.64 | 9.27 | 4.42 | 5.736 | 651.98 |
| | 16.93 | 16.66 | 9.52 | 5.31 | 4.76 | 5.482 | 180.77 |
| | 16.19 | 12.36 | 6.90 | 7.30 | 6.46 | 6.3498 | 152.77 |
| | 19.73 | 12.21 | 9.02 | 5.00 | 5.65 | 5.5032 | 185.44 |
| | 64.13 | 27.94 | 10.33 | 9.69 | 7.26 | 6.4768 | 385.34 |
| Minimum | 16.19 | 12.21 | 6.90 | 4.91 | 4.42 | 5.46 | 127.51 |
| Mean | 52.38 | 26.72 | 12.61 | 8.59 | 6.58 | 6.45 | 361.26 |
| Maximum | 113.24 | 63.92 | 24.34 | 17.86 | 10.05 | 10.22 | 805.59 |
| St. Dev. | 35.49 | 16.56 | 5.63 | 4.26 | 2.09 | 1.58 | 242.51 |

By means of these data, the change of minimum, mean, and maximum monthly surface flow variations are presented in Fig. 6.19.

**Fig. 6.19** Drainage basin monthly flow variations

Another independent approach is the use of the rational formulation in the flow calculations (Chap. 5). The two meteorology stations', Armağan and Sislioba, monthly rainfall records are taken into consideration. The calculations are made separately by means of the two station records, and then, their arithmetic average is adapted as the representative rainfall value. In this approach, the runoff coefficient is assumed as 0.35. Even though a constant runoff coefficient is not valid for whole year, it yields on the average acceptable results. The summary of the calculations is presented in Table 6.13.

The change of runoff volumes within a year is presented in Fig. 6.20 by benefiting from the calculations in this table.

**Table 6.13** Runoff volumes based on Mutludere rainfall amounts ($\times 10^6$ m$^3$)

|          | October | November | December | January | February | March     |        |
|----------|---------|----------|----------|---------|----------|-----------|--------|
| Sislioba | 33.598  | 31.061   | 33.655   | 28.208  | 20.497   | 22.165    |        |
| Armagan  | 16.835  | 21.647   | 20.422   | 16.127  | 14.373   | 13.489    |        |
| Mutludere| 25.2165 | 26.354   | 27.0385  | 22.1675 | 17.435   | 17.827    |        |
|          | **April** | **May** | **June** | **July** | **August** | **September** | **Annual** |
| Sislioba | 16.019  | 12.569   | 11.309   | 11.345  | 13.597   | 13.743    | 247.77 |
| Armagan  | 13.728  | 12.67    | 13.408   | 8.748   | 7.865    | 11.042    | 170.35 |
| Mutludere| 14.8735 | 12.6195  | 12.3585  | 10.0465 | 10.731   | 12.3925   | 209.06 |
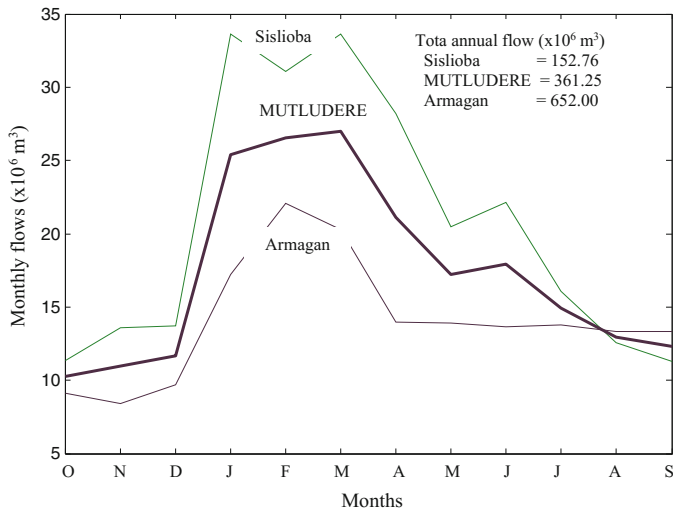
**Fig. 6.20** Runoff volumes from the rainfall amounts

### 6.6.1 Flood Analysis

It is also possible to calculate the possible flood discharges in the future in Mutludere drainage basin. For this purpose, runoff measurements at Armutveren are considered with two-year, five-year, 10-year, 50-year, 100-year, and 500-year return periods. The reverse of these periods yields the risk associated with the flood magnitudes (Eq. 6.9). The probability of flood can be calculated from Eq. (6.13). First of all, the maximum runoff measurements in each year are deduced from the monthly records as shown in Table 6.14.

On the basis of the theoretical log-normal, CDF and the probabilities for each flood are shown as scatter diagram and the theoretical curve in Fig. 6.21.

**Table 6.14** Annual maximum runoff volumes

| Year | Annual discharge ($\times 10^6$ m$^3$) |
|------|----------------------------------------|
| 1996 | 424.54 |
| 1997 | 312.99 |
| 1998 | 596.12 |
| 1999 | 651.98 |
| 2000 | 180.77 |
| 2001 | 152.77 |
| 2002 | 185.44 |
| 2003 | 385.34 |
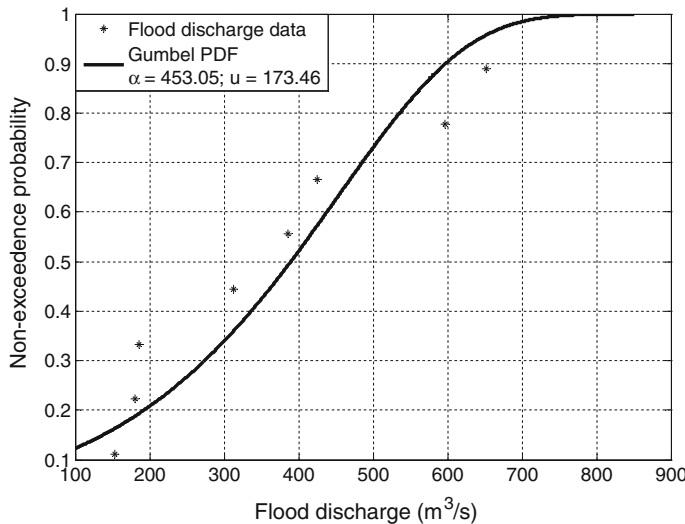
**Fig. 6.21** Flood model

It is obvious that there is a good agreement between the measurements and the theoretical curve. Table 6.15 indicates the calculation results.

The values in this table provide opportunity to decide on the design flood value provided that the life of the water structure is predetermined.

## 6.7   Regional Skewness Characteristics

According to the explanation in Chap. 2 and in Sect. 6.5.3, the frequency factor is dependent on the skewness coefficient at each meteorology station. In order to reduce the uncertainty contribution in the flood frequency analysis, it is preferred to consider the weighted average of all the stations' frequency factors. First, a

**Table 6.15** Annual flood calculations

| Recurrence interval (year) | Risk | Flood discharge ($\times 10^6$ m$^3$) |
| --- | --- | --- |
| 2 | 0.5 | 389.48 |
| 5 | 0.2 | 535.60 |
| 10 | 0.1 | 597.72 |
| 25 | 0.04 | 655.83 |
| 50 | 0.02 | 689.66 |
| 100 | 0.01 | 717.95 |
| 500 | 0.002 | 769.94 |

representative skewness coefficient for the region is obtained, and then, the skewness coefficient at a station is calculated according to the following expression.

$$\delta_w = \frac{(\text{AES})_{\text{st}}\delta_{\text{st}} + (\text{AES})_{\text{ar}}\delta_{\text{ar}}}{(\text{AES})_{\text{st}} + (\text{AES})_{\text{ar}}} \tag{6.37}$$

where $(\text{AES})_{\text{st}}$ and $(\text{AES})_{\text{ar}}$ are the average error squares at the station and region, respectively, and likewise, $\delta_{\text{st}}$ and $\delta_{\text{ar}}$ are the station and areal skewness coefficients, respectively. For areal works, it is necessary to take into consideration all the stations that fall within 160-km-radius circle or at least 40 stations are sufficient. At each station, there must be at least 25-year records. After computing the skewness coefficient at each station, the skewness coefficient contour maps can be prepared, and hence, general tendencies are determined. The square of the difference between the actual skewness coefficient and the regional skewness coefficient is average error square value at the station.

## 6.8 Relationship Between Extreme Values and Run-Lengths

The extreme values and run-lengths are the two most important variables in a water resources system design, and most often, they are investigated independently from each other. In this section, their joint properties are examined by considering first the PDF of extreme values in small samples originating from currently available hydrological models.

The generation of synthetic sequences statistically indistinguishable from the observed sequences has engaged the hydrologists over the last five decades. During the same period, a series of models for hydrological modeling has been proposed for rainfall, runoff (Chaps. 2 4, and 5), sedimentation (Chap. 7), lake level, etc., records. The main idea in any synthetic sequence generation is to match low-order statistical parameters between the observed and synthetic sequences. The very first model was due to Thomas and Fiering (1962), which preserves arithmetic mean, standard deviation, and cross-correlation coefficient between successive months. Later, long-term persistence started to play role in hydrological modeling, and hence, new models appeared such as the discrete fractional Gaussian noise by Mandelbrot and Wallis (1969a, b, c); the autoregressive integrated moving average (ARIMA) models (O'Connel 1971); the broken line process by Mejia et al. (1972), and white Markov process by Şen (1974).

It is possible to identify the suitable model provided that there is a sequence of historical records. In any hydrological modeling, low-order statistical parameters and long-term persistence are considered as basic similarity parameters between the synthetic and historical sequences, but as the historical observations increase by time, extreme events such as floods and run-lengths (wet and dry spells) show
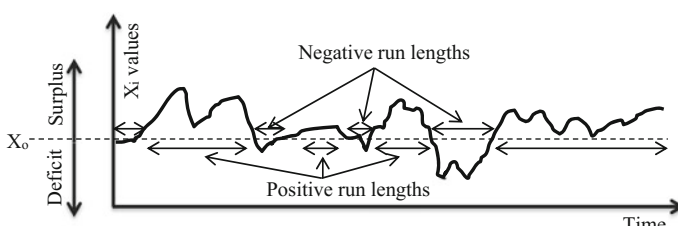
themselves more pronounced in a distinctive way, and these properties play significant role in water resources system design. For instance, the occurrence of a flood event over a given recurrence interval helps to design spillways. On the other hand, negative run-lengths (drought spells) can be adopted as objective descriptors for drought mitigation and adaptation (Şen 2015).

### 6.8.1 Extreme Values

So far, most extensively extreme values that originate from independent processes are studied by various authors (Gumbel 1958), but there exists slight information about the extreme value occurrences in dependent processes. It is important to keep in mind that any hydrological model must also preserve the extreme value properties of historical observations in addition to low-order statistical parameters. For instance, as stated by Rodrigues-Iturbe et al. (1987a, b), in using Markovian models for streamflow generation, it is quite common not to preserve the characteristics of the extreme events, floods, and droughts. The design period of a flood is equal to the expectation of the positive run-length in an infinite sequence. Therefore, one can conclude that the positive run-length is employed very extensively in flood frequency analysis (Şen 2015). Given the expected value of a positive run-length, one can calculate the size of a spillway to cope with the flood provided that a suitable PDF is assigned to the flood occurrence probabilities and magnitudes similar to Figs. 6.14, 6.15, and 6.21.

### 6.8.2 Run Properties

From the statistical point of view, a run is defined by Mood (1940) as a succession of similar kind of events preceded and succeeded by different kinds. It is obvious from this definition that two kinds of events are required for the run definition. Truncation of a sequence on a constant level gives rise to two kinds of events as surplus and deficit (Fig. 6.22, see also Figs. 6.5 and 6.6). If a given sequence of observation is $X_1, X_2, \ldots, X_n$ with a truncation level $X_o$, then the deficits and surplus sequences are $X_i - X_o \leq 0$ and $X_i - X_o > 0$, respectively.



**Fig. 6.22** Positive and negative run-lengths

A successive sequence of water surpluses (deficits) preceded and succeeded by deficits (surpluses) is a positive run-length (negative run-length) that corresponds to flood (drought) drought duration in water engineering. Hence, there are a number of runs, and the summation of surpluses or deficits over each run yields its magnitude. Among all the runs, there is one which is the longest and it will be referred to as maximum run-length. Similarly, among the same run-lengths, there is also one which is the shortest. It is important to preserve extreme run-lengths in the models so as to predict future possible run-lengths, and their simulation through the autoregressive (Markov) models is well explained by Mandelbrot and Wallis (1968) as:

*"For droughts the point is that if an independent Gauss process or Gauss-Markov process is chosen to fit best the other aspects of precipitation, it will greatly underestimate the durations of the longest drought. Therefore, such processes must be modified by considering more durable after effects (for example through multiple lag models)."*

The analytical expressions that appear in the literature are mostly for run properties in infinite sequences. The probability of positive run-length, $n_p$, of an independent process has been given by Feller (1968) as:

$$P(n_p = n) = q p^{n-1} \tag{6.38}$$

where

$$p = \int_{X_o}^{+\infty} P(x)dx$$

and

$$q = 1 - p = \int_{-\infty}^{X_o} P(x)dx$$

Herein, $P(x)$ is the PDF of the underlying event. A general approximate method in deriving various statistical properties of autoregressive processes has been developed by Saldarriaga and Yevjevich (1970) for an infinite sequence. Later, Şen (1976) obtained exact analytical expressions for the properties of a lag-one Markov process by making use of a bivariate normal PDF, which leads to the positive run-length as,

$$P(n_p = n) = (1 - r)r^{n-1} \tag{6.39}$$

where
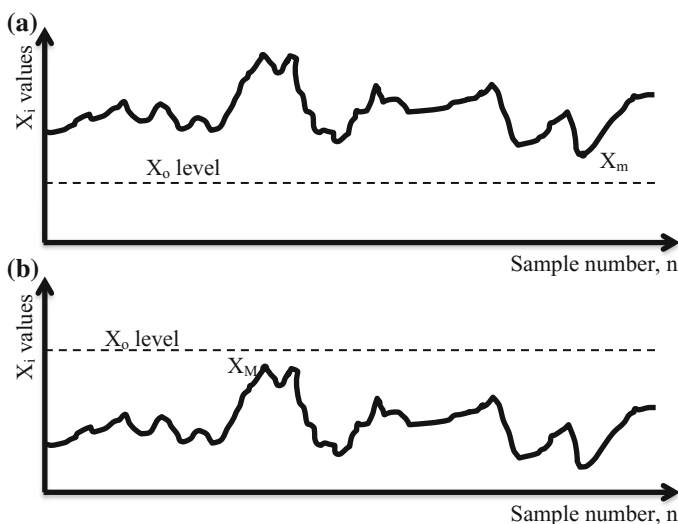
$$r = P(X_i > X_o | X_{i-1} > X_o)$$ (6.40)

It is possible to obtain r values from a bivariate PDF tables (Şen 1976, 2015). In the case of stationary and ergodic stochastic processes, the run-length properties for infinite sequences are synonymous with the first run. Another useful information for further investigation is that in the case of independent process, $r = p$, Eq. (6.39) reduces to Eq. (6.37).

### 6.8.3   Extreme Values of Small Samples

In water engineering, the failure of a hydraulic structure is intimately related to the largest or smallest value of the underlying event over the economic life, n, of the project. Thus, it is necessary to know the statistical performance of these extreme values in small samples. Consider a sequence of observations, $X_1, X_2, \ldots, X_n$, of length $n$. The probability of the minimum of these observations, $X_m$, to be greater than a base level, $X_o$, can be simply written by considerations from Fig. 6.23 as,

$$P(X_m > X_o) = P(n^+)$$ (6.41)



**Fig. 6.23** Positive run-length and minimum

where

$$X_m = \min(X_1, X_2, \ldots, X_n)$$

It is obvious from Fig. 6.23a that $P(n^+)$ is the probability of n observations to be greater than $X_o$. In other words, $P(n^+)$ can be interpreted as the probability of positive run-length to be at least greater than $n$. Its general expression is given by Feller (1968) as,

$$P(n^+) = p^n \tag{6.42}$$

which is valid only for the independent processes. However, corresponding probability for the lag-one Markov process has been obtained by Şen (1976) as,

$$P(n^+) = pr^{n-1} \tag{6.43}$$

The substitution of Eq. (6.43) into Eq. (6.41) leads to,

$$P(X_m > X_o) = pr^{n-1} \tag{6.44}$$

In the case of an independent process $r = p$, and therefore, Eq. (6.44) reduces to,

$$P(X_m > X_o) = p^n \tag{6.45}$$

In a similar way, the probability of the maximum among $n$ observations to be less than or equal to $X_o$ can be written as,

$$P(X_M \leq X_o) = P(n^-) \tag{6.46}$$

where

$$X_M = \mathrm{Max}(X_1, X_2, \ldots, X_n)$$

On the other hand, $P(n^-)$ is the probability of negative run-length to be at least equal to $n$ (see Fig. 6.23b). The explicit form of $P(n^{-1})$ for an independent process is,

$$P(n^-) = q^n \tag{6.47}$$

For the lag-one Markov process, after some manipulations, one can find,

$$P(n^-) = q(1 - r)^{n-1} \tag{6.48}$$

which is exactly equal to Eq. (6.47) for $r = p$. The substitution of Eq. (6.47) and Eq. (6.48) into Eq. (6.46) yields,

$$P(X_M \leq X_o) = q^n \tag{6.49}$$

and

$$P(X_M \leq X_o) = q(1-r)^{n-1} \tag{6.50}$$

for independent and dependent processes, respectively. It is also possible to obtain the joint PDF of the maximum and the minimum by considering the total run-length as in Fig. 6.24.

Thus,

$$P\big(X_{mi} > X_o, X_{M(n-i)} \leq X_o\big) = P(i^+)P(n-i)^- \tag{6.51}$$

where

$$X_{mi} = \min(X_1, X_2, \ldots, X_i)$$

$$X_{M(n-i)} = \text{Max}(X_{i+1}, X_{i+2}, \ldots, X_n)$$

$P(i^+)$ is the probability that the first successive observations are greater than $X_o$, and $P(n-i)^-$ is the probability that the subsequent $n-i$ observations are less than or equal to $X_o$. Equation (6.51) can be considered as a conditional probability for a given $i$ value. The conditional probability can be rendered into unconditional probability as follows.

$$P(X_m > X_o, X_M \leq X_o) = \sum_{i=1}^{n} P(i^+)P(n-i)^- \tag{6.52}$$
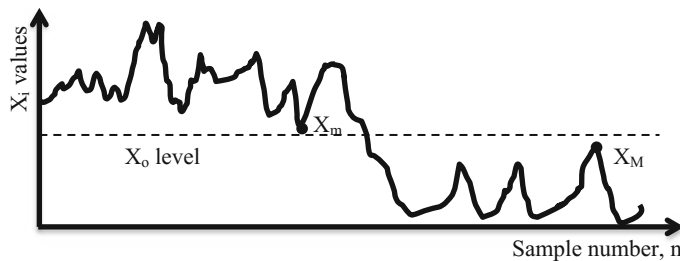


**Fig. 6.24**  Joint PDF

In the case of an independent process, Eq. (6.52) becomes,

$$P(X_m > X_o, X_M \leq X_o) = \sum_{i=1}^{n} p^i q^{n-i} = \frac{pq^n - qp^n}{q - p} \tag{6.53}$$

The right-hand side of Eq. (6.53) is the probability of total run-length by Feller (1968). In conclusion, one can say that the joint PDF of the maximum and the minimum in a sample of length n is equal to the PDF of the total run-length $n$ in an infinite sequence. Similar studies can be performed for the maximum and negative run-length. From Eqs. (6.39) and (6.44), one can easily observe the following relationship.

$$P(X_m > X_o) = \frac{p}{1 - r} P(n_p = n) \tag{6.54}$$

This for an independent process becomes

$$P(X_M > X_o) = \frac{p}{q} P(n_p = n) \tag{6.55}$$
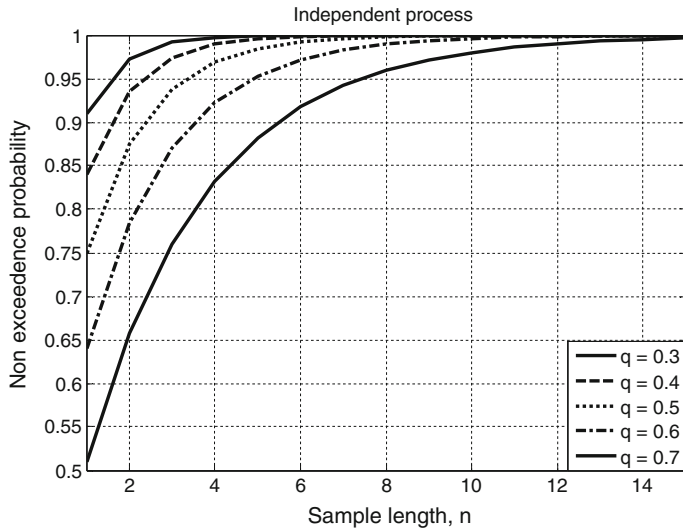
It is obvious from Eq. (6.54) that for a given level of truncation, $X_o$, the probability of the minimum to be greater than $X_o$ is proportional to the probability of positive run-length. Furthermore, it is a known fact from extreme value analysis that events with small probabilities have large magnitudes. An increase in run-length causes the magnitude of the extreme event to increase; i.e., for a given level of truncation, the magnitude of an extreme event is proportional to the run-length.

### 6.8.4  Application
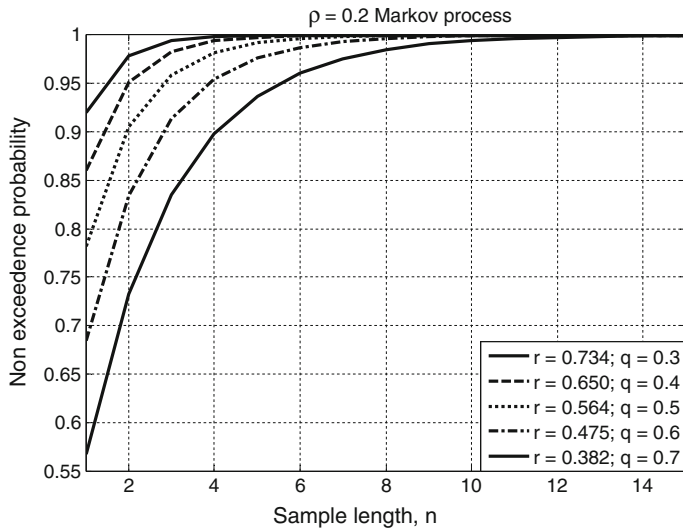
It is not possible to solve Eq. (6.50) analytically, but the numerical solution is possible on digital computers, for a given set of $\rho$ and $n$ values. In this way, the small sample distributions of the maximum have been obtained and plotted in Figs. 6.25, 6.26, 6.27, and 6.28. It can be seen from these figures that as the sample length increases so does the expected value of the maximum, which is enough to show that long sequences yield extreme values greater than the extreme values of shorter sequences.

A very useful interrelation can be obtained when the sample length is considered to be equal to the system's economic life, which is an important problem in water engineering. If the system is assumed to have a long life, the critical occurrences such as floods and droughts are more likely to happen with higher magnitudes than the system of a shorter life (Figure 6.25).

The comparison of these figures leads to the conclusion that as the linear dependence increases, the expected magnitude of the maxima increases. A very
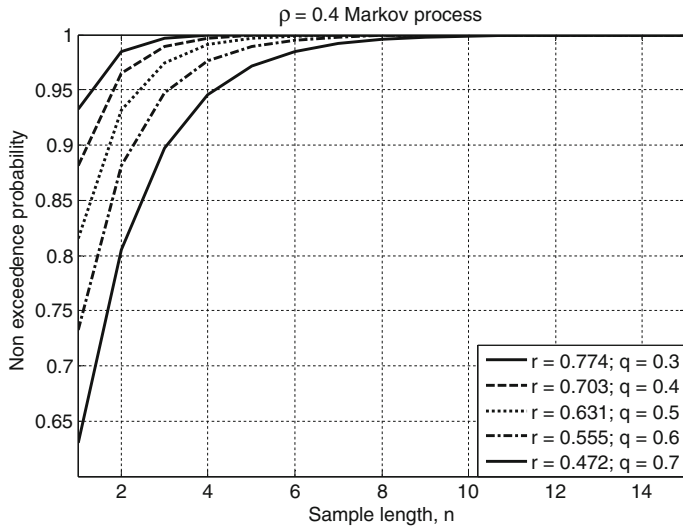
**Fig. 6.25** Cumulative probabilities of maxima in normal independent process
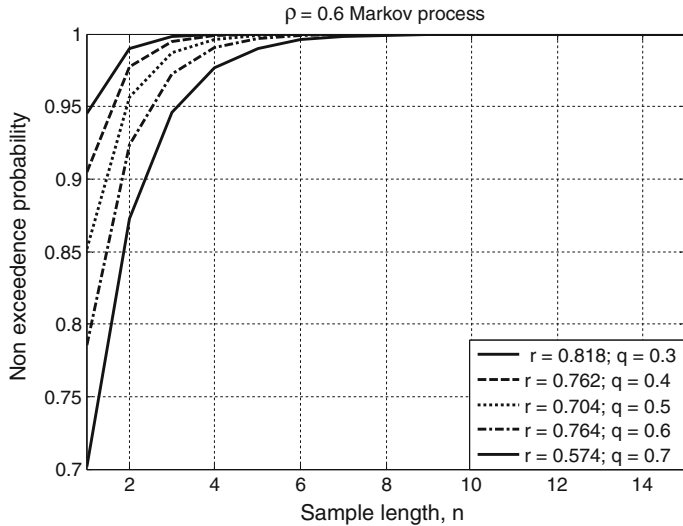


**Fig. 6.26** Cumulative probabilities of maxima in lag-one Markov process, $\rho = 0.2$

useful conclusion is that an increase in linear dependence between successive observations reduces the magnitude of the maximum event to occur over the system's economic life.

**Fig. 6.27** Cumulative probabilities of maxima in lag-one Markov process, $\rho = 0.4$



**Fig. 6.28** Cumulative probabilities of maxima in lag-one Markov process, $\rho = 0.6$

Finally, Monte Carlo simulation technique has been performed in order to find the expected value of maxima in various small samples of normal independent process, and the results are given in Table 6.16. On the other hand, the same expected values are calculated by the numerical solution of Eq. (6.50) and

**Table 6.16** Expected value of maxima of a normal independent process

| Sample size | 3 | 5 | 10 | 20 | 30 | 50 | 100 |
|---|---|---|---|---|---|---|---|
| Numerical | 0.896 | 1.212 | 1.587 | 1.914 | 2.08 | 2.290 | 2.535 |
| Simulation | 0.876 | 1.210 | 1.584 | 1.912 | 2.08 | 2.289 | 2.533 |

presented in the same table. An almost perfect correspondence is observed between the simulation and numerical result, which verifies the analytical derivations.

## 6.9   Simple Flood Risk Calculations in Dependent Time Series

Hydrological events have temporal and spatial uncertain variabilities, and therefore, their predictions cannot be achieved with certainty. Even the chaotic methodologies that can determine deterministic components in the uncertainty domain cannot make certainty predictions (Lorenz 1995; Lovejoy and Scherper 1986; Farmer and Sidorowich 1987, Jayawardena and Lai 1994). Due to the random variations, the future behavior of the hydrological events can be calculateable to a certain extent with remaining uncertainty. The prediction methodologies include probabilistic, statistical, stochastic, and chaotic approaches. The basis of such predictions is historical records. The shorter the record lengths, the more is the uncertainty component. Accordingly, the water structure dimensions may be bigger or smaller compared to the case with long records. In order to grasp the uncertainties in any design variable decision, a certain level of risk is taken into consideration.

The safety, $S$, is expressed as the succession of events that are all less than the design discharge, $Q_D$, throughout the water structure life. If annual occurrence of the flood event sequence, $Q_1$, $Q_2$, ..., $Q_n$, has the same probability distribution function, the exceedence probability can be expressed as,

$$S = P(x \le Q_D) = P(x_1 \le Q_D, x_2 \le Q_D, \ldots, x_n \le Q_D) \qquad (6.56)$$

On the other hand, simple risk, R, is the complementary of this value as explained earlier in Sect. 6.4, Eq. (6.10). The compound probability on the right-hand side of Eq. (6.56) can be expressed in terms of the equally likely PDF (Saldarriaga and Yevjevich 1970). In case of simply serially dependent process case, such as the first-order Markov process as explained by Şen (1976), the compound probability appears as the multiplication of a series of conditional probabilities. The general mathematical structure of a first-order Markov process similar to Eq. (5.30) is as follows.

$$Q_i - \mu = \rho(Q_{i-1} - \mu) + \sigma\sqrt{1 - \rho}\varepsilon_i \qquad (6.57)$$

where $Q_i$ is the random hydrological variable, $\rho$ is the first-order serial correlation coefficient, and $\varepsilon_i$ is the uncertainty random component, i.e., error, attached with the $i$th event. The arithmetic average of the error term is equal to zero. Simple safety or risk calculations can be achieved on the basis of design discharge and the life of water structure.

It is possible to model exceedence (flood) and non-exceedence (drought) probabilities by a two-state Markov chain (Şen 1991). In such processes, the non-exceedence of any discharge, $Q_i$, is represented by the event of discharge being less than or equal to the design discharge as $(Q_i \leq Q_D)$ and its complementary $(Q_i > Q_D)$. The probability calculations of these two-stage processes boil down to basic exceedence and non-exceedence probabilities as,

$$p = P\left(Q_i > Q_D\right)$$

and

$$q = 1 - p = P(Q_i \leq Q_D),$$

which are also regarded as state probabilities. Additionally, there are four transition probabilities as,

$$P(Q_i > Q_D|Q_{i-1} > Q_D),$$

$$P\left(Q_i > Q_D|Q_{i-1} \leq Q_D\right),$$

$$P\left(Q_i \leq Q_D|Q_{i-1} > Q_D\right),$$

and

$$P\left(Q_i \leq Q_D|Q_{i-1} \leq Q_D\right),$$

where $i = 2, 3, \ldots, n$. These probabilities have the following relationship among them.

$$P\left(Q_i > Q_D|Q_{i-1} > Q_D\right) + P\left(Q_i \leq Q_D|Q_{i-1} > Q_D\right) = 1.0$$

and

$$P\left(Q_i > Q_D|Q_{i-1} \leq Q_D\right), + P(Q_i \leq Q_D|Q_{i-1} \leq Q_D) = 1.0$$

Furthermore, for the safety and risk calculations, there are three probabilities $p$, $P\left(Q_i > Q_D \mid Q_{i-1} > Q_D\right)$, and $P\left(Q_i \leq Q_D \mid Q_{i-1} \leq Q_D\right)$ in the Markov chain. On the other hand, the first-order serial correlation coefficient, $\rho$, for the first-order

Markov process can be expressible in terms of the transition probabilities as (Şen 1991),

$$\rho = [P(Q_i > Q_D | Q_{i-1} > Q_D) - P(Q_i > Q_D | Q_{i-1} \leq Q_D)] + [P(Q_i \leq Q_D | Q_{i-1} > Q_D)$$
$$-P(Q_i > Q_D | Q_{i-1} \leq Q_D)]$$

On the other hand, Şen (1976) defined the transition probability, $P(Q_i > Q_D | Q_{i-1} \leq Q_D)$, as the first-order autorun, $r_1$, coefficient. By taking into account this point, the following equalities can be written as follows.

$$P(Q_i > Q_D | X_{i-1} > Q_D) = r_o \tag{6.58}$$

$$P(Q_i > Q_D | Q_{i-1} \leq Q_D) = (p/q)(1-r_o) \tag{6.59}$$

$$P(Q_i \leq Q_D | Q_{i-1} \leq Q_D) = 1 - (p/q)(1 - r_o) \tag{6.60}$$

and

$$P(Q_i \leq Q_D | Q_{i-1} > Q_D) = (1-r_o) \tag{6.61}$$

where $P(Q_i \leq Q_D \mid Q_{i-1} \leq Q_D)$ has been expressed by Cramer and Leadbetter (1967) as follows.

$$P(Q_i \leq Q_D | Q_{i-1} \leq Q_D) = q + \frac{1}{2\pi q} \int_0^\rho e^{-z^2/2(1+z)} \left(1 - z^2\right)^{1/2} dz \tag{6.62}$$

The numerical solution of this equation is given by Şen (1976) for different combinations of $\rho$ and $q$. Equation (6.56) can be separated into a series of multiplications for the first-order Markov process as,

$$S = P(Q \leq Q_D) \prod_{i=2}^{n} P(Q_i \leq Q_D | Q_{i-1} \leq Q_D) \tag{6.63}$$

The substitution of Eq. (6.62) into Eq. (6.63) leads to the following safety expression.

$$S = q \left[1 - \frac{p}{q}(1 - r_0)\right]^{n-1} \tag{6.64}$$
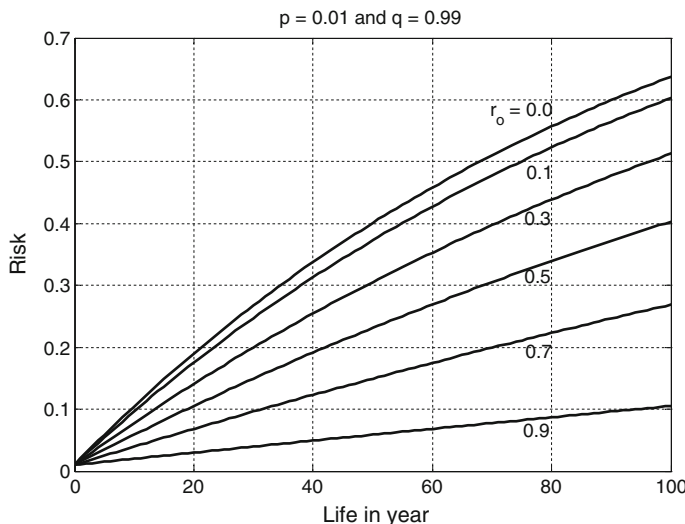
Herein, for $\rho = 0.0$, $r_1 = p$, and hence, $S = q^n$. The simplest form of this equation has been given by Yen (1970) for independent processes. The risk probability can be found as the complementary to Eq. (6.64),

$$R = 1 - q\left[1 - \frac{p}{q}(1 - r_0)\right]^{n-1} \tag{6.65}$$

In case of independent processes, it reduces down to $R = 1 - q^n$. At this stage, it is possible to ask how the correlation coefficient affects the risk? Some of the graphics from the last equation are given in Fig. 6.29, which provides the relationships among the $r_o$, $p$ ($q = 1 - p$), and the structural life, n. Similar graphs are also given for another set of parameters.

**Example 6.5** Calculate the risk value provided that the project has $n = 10$-year life with $p = 0.01$ exceedence probability and the runoff process abides by the first-order Markov process with the first-order serial correlation coefficient, $\rho = 0.2$

**Answer 6.5** If the runoff process is independent completely, then the risk is $R = 1 - (0.99)^{10} = 0.00956$. However, the process has $\rho = 0.2$, and therefore, from Eq. (6.65), $R = 0.0192$, and hence, one can find from Eq. (6.64) that $r_o = 0.0198$. This example indicates that increase in the serial correlation causes decrease in the risk level. This means that the safety of the structure increases. For this reason, in practice, calculations based on the independence assumption lead to bigger project dimensions and hence more money spending.



**Fig. 6.29** Water structure life–risk relationship

## 6.9.1 Flood Application

In practical studies, after the determination of the dependence structure and decision on the structural life, $T$, the way to risk calculation is open. In hydrology, as mentioned earlier, the return period is the average of the durations between two successive overcrossings of the threshold level. For instance, the time duration, $T_r$, between two overcrossing instances is a random variable. Its exceedence probability for independent process is given by Feller (1968) as,

$$P(T_r \geq j) = q^{j-1} \tag{6.66}$$

or

$$P(T_r = j) = pq^{j-1} \tag{6.67}$$

Hence, the arithmetic mean (expectation) of this duration (recurrence interval) is given as follows.

$$T = \sum_{j=1}^{\infty} jP(T_r = j) = p \sum_{j=1}^{\infty} jq^{j-1} = \frac{1}{p} \tag{6.68}$$
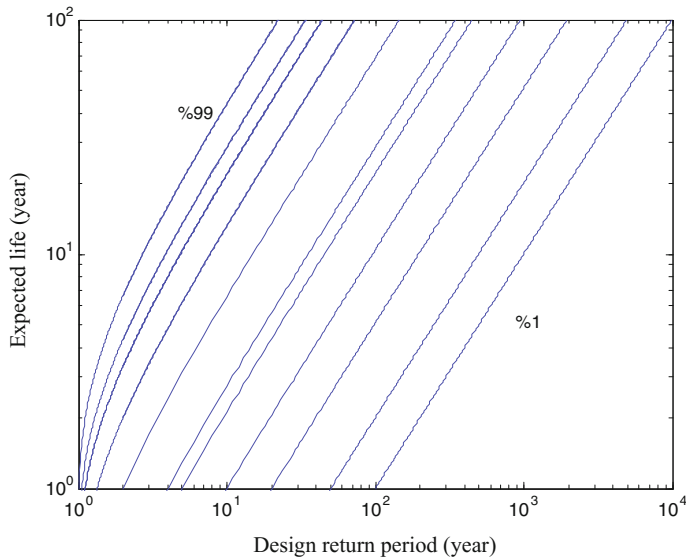
where $p = P(Q > Q_D)$ is the design discharge. This proves that there is a reverse relationship between the exceedence probability (risk) and the return period.

The theoretical return period probabilities are given in Table 11.2 (Linsley et al. 1982), but there is an error as for the real return period, $T_r$, is concerned. Gumbel (1958) stated that the return period cannot be less than 1. The theoretical probabilities of return period are given in Eq. (6.66). The solution of this equation is presented in Table 6.17. This is the corrected form of the table given by Linsley et al. (1982).

It is possible to deduce from this table that percentage of design duration to be less than 30 year is about 25%, but in the meantime, the exceedence of the same level corresponds to 139 year. In other words, if a water structure is designed for

Table 6.17 Theoretical return period probabilities for independent process

| Average return period | Exceedence time percentages for real return periods, $T_r$ | | | | | | |
|---|---|---|---|---|---|---|---|
| $T$ | 0.01 | 0.05 | 0.25 | 0.50 | 0.75 | 0.95 | 0.99 |
| 2 | 7.64 | 5.32 | 3.00 | 2.00 | 1.41 | 1.07 | 1.01 |
| 5 | 21.64 | 14.42 | 7.21 | 4.10 | 2.28 | 1.23 | 1.04 |
| 10 | 14.71 | 28.43 | 14.16 | 7.58 | 3.73 | 1.48 | 1.09 |
| 30 | 136.84 | 89.36 | 41.89 | 21.44 | 9.48 | 2.51 | 1.29 |
| 100 | 459.21 | 299.07 | 138.93 | 69.97 | 29.62 | 6.10 | 2.00 |
| 1000 | 4603.86 | 2995.23 | 1386.60 | 692.80 | 288.53 | 52.53 | 11.11 |

**Fig. 6.30** Return period and structural life relationship

100-year duration with 75% safety, it will be overcrossed within 30 years. The solution of Eq. (6.66) is presented graphically in Fig. 6.30.

The necessary table and graph for the application of Eq. (6.12) are given by Gupta (1973). On the other hand, in cases of dependent processes, Eqs. (6.11) and (6.12) are not valid. Theoretical return period PDF can be obtained from Eq. (6.64) by consideration of Eq. (6.66) as,

$$P(T_r \geq j) = q\left[1 - \frac{p}{q}(1 - r_0)\right]^{j-2} \tag{6.69}$$

or

$$P(T_r = j) = P(T_r \geq j) - P(T_r \geq j+1) = p(1 - r_0)\left[1 - \frac{p}{q}(1 - r_0)\right]^{j-2} \tag{6.70}$$

The substitution of $\rho = 0$ into the last expression implies that $r_0 = p$, which reduces down to Eq. (6.67). Furthermore, the expected value of the return period can be obtained from Eqs. (6.68) and (6.70) as follows.

$$T = \frac{q^2}{\left[1 - \frac{p}{q}(1 - r_0)\right]p(1 - r_0)} \tag{6.71}$$

**Table 6.18** Theoretical PDF of Markov process ($\rho = 0.2$) return period

| Average return period | Exceedence time percentages for real return periods, $T_r$ | | | | | | | | |
|---|---|---|---|---|---|---|---|---|---|
| $T$ | 0.01 | 0.05 | 0.25 | 0.50 | 0.75 | 0.95 | 0.99 | p | r |
| 2 | 8.83 | 6.02 | 3.21 | 2.00 | 1.29 | 0.88 | 0.80 | 0.500 | 0.5640 |
| 5 | 24.14 | 16.00 | 7.88 | 4.37 | 2.32 | 1.13 | 0.92 | 0.200 | 0.2818 |
| 10 | 48.39 | 31.80 | 15.20 | 8.06 | 3.88 | 1.44 | 1.00 | 0.100 | 0.1681 |
| 30 | 143.95 | 93.97 | 43.99 | 22.47 | 9.88 | 2.54 | 1.26 | 0.033 | 0.0810 |
| 100 | 471.22 | 306.88 | 142.53 | 71.75 | 30.35 | 6.21 | 2.00 | 0.010 | 0.0352 |
| 1000 | 4629.65 | 3012.00 | 1394.36 | 697.68 | 290.14 | 52.54 | 11.09 | 0.001 | 0.0065 |

This expression shows that the return period is not only dependent on the exceedence probability, $p$, but also it is a function of $r_0$ and hence of $\rho$. The theoretical PDF of the return period is presented in Table 6.18 for $\rho = 0.2$.

The comparison of this table with Table 6.16 indicates that in case of independence the return periods are longer than dependent case. The more the serial correlation coefficient, the longer is the return period. On the other hand, the safety, $S$, and risk, $R$, expressions for a dependent process can be obtained as follows.

$$S = q\left[\frac{q^2}{Tp(1 - r_0)}\right]^{n-1} \tag{6.72}$$

and

$$R = 1 - q\left[\frac{q^2}{Tp(1 - r_0)}\right]^{n-1} \tag{6.73}$$

The solution of Eqs. (6.72) and (6.73) for a set of $p$ and $\rho$ values is given in Table 6.19.

This is an expected result, because as the time between the appearances of the two events increases, the events become independent from each other, and finally, they are equal to each other. Uncertainty and risk increase in case of small sample size. The most advanced mathematics, statistics, and even the stochastic methodologies are not helpful to reduce the risk values.

## 6.10   Extreme Values in Small Sample-Dependent Processes

Since human life is very sensitive to extreme events, it is necessary to predict them by suitable models for safety protections. In meteorology and hydrology branches to arrive at a simple model and its use, the occurrences are assumed to be independent

**Table 6.19** Risk and safety values for Markov process ($\rho = 0.2$)

| $p$ | $D$ | $r_o$ | $T_r$ | Economic life of project, $n$ (year) | | | | | | | | | | | |
| | | | | $n = 10$ | | $n = 20$ | | $n = 30$ | | $n = 50$ | | $n = 100$ | |
| | | | | Safety | Risk | Safety | Risk | Safety | Risk | Safety | Risk | Safety | Risk |
| 0.33 | 0.67 | 0.414 | 3.26 | 0.031 | 0.969 | 0.001 | 0.999 | 0.000 | 1.000 | 0.000 | 1.000 | 0.000 | 1.000 |
| 0.25 | 0.75 | 0.334 | 4.34 | 0.078 | 0.992 | 0.006 | 0.994 | 0.000 | 1.000 | 0.000 | 1.000 | 0.000 | 1.000 |
| 0.20 | 0.80 | 0.282 | 5.43 | 0.134 | 0.866 | 0.018 | 0.982 | 0.003 | 0.997 | 0.000 | 1.000 | 0.000 | 1.000 |
| 0.10 | 0.90 | 0.168 | 10.72 | 0.375 | 0.625 | 0.158 | 0.842 | 0.060 | 0.940 | 0.008 | 0.992 | 0.000 | 1.000 |
| 0.05 | 0.95 | 0.104 | 21.14 | 0.615 | 0.385 | 0.400 | 0.600 | 0.234 | 0.766 | 0.089 | 0.911 | 0.008 | 0.992 |
| 0.03 | 0.97 | 0.083 | 35.22 | 0.772 | 0.228 | 0.561 | 0.439 | 0.434 | 0.566 | 0.237 | 0.763 | 0.056 | 0.944 |
| 0.01 | 0.99 | 0.035 | 102.5 | 0.906 | 0.094 | 0.822 | 0.278 | 0.745 | 0.255 | 0.613 | 0.687 | 0.375 | 0.625 |

from each other (Fisher ve Tippet 1928; Gumbel 1958). Structural features of the
historical records are adapted for derivation of convenient models for predictions.

Recent climate change event causes increase in the frequency of occurrence
rather than the magnitude of extreme values (Flohn 1989). On the other hand, the
climate change impact changes the roulette hat "past is the reflection of future" to
"past be not the reflection of future" (Milly et al. 2008). Unfortunately, in many
countries as for the design projects, still the classical approaches are employed
without climate change impact consideration. The more the frequency of extreme
events, the more they appear. This gives the impression that there may be depen-
dence more than the past between the successive occurrences of extreme events
related to the climate change. Herein, a new calculation method is suggested by
taking into consideration the frequency and the serial correlation in time series. In
the classical approaches, the following three points are taken into consideration.

(1) There must be numerous extreme value records preferably more than 30 records,
(2) There is not serial dependences in the meteorological and hydrological records,
(3) The PDF of variable remains the same throughout all durations.

### 6.10.1  Innovative Approach

All the values over a given threshold level, $X_o$, are regarded as extreme value
(Sect. 6.2.2). The basic principles of dependent flood frequency analyses are pre-
sented by Şen (1978). The two successive flood values that are independent have
the following conditional probability.

$$P(X_i > X_0 | X_{i-1} > X_0) = P(X_i > X_0) \tag{6.74}$$

Only in case of dependence, this probability renders into the inequality.

Given a sequence of meteorological measurements, Eqs. (6.74) can be verified at
any desired threshold value. Hence, the truncation level which satisfies Eq. (6.74)
approximately, say with 5% relative error, yields situation whereby the classical
extreme value statistics can be employed satisfactorily. Otherwise, if this inequality
form of Eq. (6.74) is valid, then the extreme values are dependent, and therefore,
the theory of extreme values must be employed.

If the structure of time series accords with the first-order Markov process, then
the probability of the maximum value, $X_{\max}$, to be smaller than $X_o$ is,

$$P_D(X_{\max} \leq X_0) = P(X_i \leq X_0) \prod_{i=2}^{n} P(X_i \leq X_0 | X_{i-1} \leq X_0) \tag{6.75}$$

where the subscript, $D$, stands for dependence. The conditional probability on the
right-hand side is defined as the autorun coefficient, $r_i(X_0)$, by Şen (1978), and it

assumes values as $0 < r_i(X_0) < 1$. On the other hand, since $q(X_0) = P(X_1 \leq X_0)$, Eq. (6.75) can be written as,

$$P_D(X_{\max} \leq X_0) = q(X_0) \prod_{i=2}^{n} r_i(X_0) \tag{6.76}$$

In case of extreme value non-variability by time, the process is in the steady state form, and therefore, this expression can be written as,

$$P_D(X_{\max} \leq X_0) = q(X_0) r^{n-1}(X_0) \tag{6.77}$$

It is useful in cases of dependent but finite length samples. Extreme value PDF can be derived from a given time series after the completion of the following steps.

(1) Find the minimum, $X_{\max}$, maximum, $X_{\min}$, and the variation domain of the data, i.e., the range,
(2) Starting from the minimum value takes a set of truncation levels systematically within the variation domain. For this purpose, the variation domain must be divided by a number of classes between 5 and 15. The more the data number, the higher is the class number,
(3) For each truncation level, calculate $q(X_0)$ and $r(X_0)$ values and plot them on the Cartesian coordinate system,
(4) Fit most suitable curve to the scatter diagram; hence, $[X_0, q(X_0)]$, $[X_0, r(X_0)]$ and if necessary $[q(X_0), r(X_0)]$ mathematical expressions are obtained. Under the assumption of independence $[X_0, q(X_0)]$ and $[X_0, r(X_0)]$ indicates the same graph, but $[q(X_0), r(X_0)]$ represents 1:1 (45°) straight line. In fact, this step is the matching of a PDF to given data. For this purpose, various tests can be applied such as Chi-square, Kolmogorov–Smirnov, Anderson–Darling,
(5) If the values of $q(X_0)$ and $r(X_0)$ are close to each other within the sampling error limits, the extreme value generation mechanism is a completely independent process, and hence, classical extreme value analysis methodologies can be applied. Otherwise, it is necessary to apply the next step,
(6) Finally, $q(X_0)$ and $r(X_0)$ functions are substituted in Eq. (6.77) leading to the extreme value PDF.

### 6.10.2 Application

It is not possible to solve Eq. (6.77) analytically, and therefore, simulation works are undertaken in computers. For this purpose, a set of serial correlation coefficients ($\rho = 0.2$; 0.4; ve 0.6) and sample lengths ($n = 2$; 10 ve 100) are considered. On the other hand, the stochastic variable is assumed to have zero mean and unit standard

deviation. The joint probability of two successive extreme values can be expressed from Cramer ve Leadbetter (1967) by the autorun coefficient as,

$$r(X_0) = q(X_0) + \frac{1}{2\pi \, q(X_0)} \int\limits_0^\rho \exp\left[-\frac{X_0^2}{2(1+z)}\right](1-z^2)^{1/2} dz \qquad (6.78)$$

where $z$ is an interim variable. The substitution of Eq. (6.78) into Eq. (6.77) leads to a complex expression, and its solution set is given for sample size and first-order serial correlation coefficient, $\rho$.

Consideration of Eq. (6.78) with the necessary simulation studies yields in Table 6.20 the arithmetic average values for a set of sample sizes.

As mentioned in the previous section, Eq. (6.76) can be transformed into a more simple and practical form by substitution of $q(X_0)$ with $r(X_0)$. This is possible after making simulations according to Eq. (6.78) and fitting regression lines to the scatter diagrams. In general, one can obtain,

$$r(X_0) = aq^{1-\rho}(X_0)[1 - q(X_0)]^b \qquad (6.79)$$

The value of regression parameters is given depending on the serial correlation coefficient in Table 6.21.

The substitution of the last expression into Eq. (6.77) leads simply to,

$$P(X_{\max} < X_0) = q(X_0)\left\{aq^{1-\rho}(X_0)[1 - q(X_0)]^b\right\}^{n-1} \qquad (6.80)$$

The numerical solution of this expression provides the change of $P(X_{\max} < X_0)$ with the truncation level, $X_0$. It is then possible to deduce the following points.

(1) As the sample length increases, the probability of the maximum event increases,

**Table 6.20** Extreme value arithmetic average

| Sample length, $n$ | 3 | 5 | 10 | 20 | 30 | 50 | 100 |
|---|---|---|---|---|---|---|---|
| Numerical | 0.895 | 1.212 | 1.587 | 1.914 | 2.087 | 2.290 | 2.535 |
| Simulation | 0.876 | 1.210 | 1.587 | 1.912 | 2.080 | 2.289 | 2.533 |

**Table 6.21** Regression line parameters

| $\rho$ | $a$ | $b$ |
|---|---|---|
| 0.0 | 1.00 | 0.00 |
| 0.2 | 3.10 | 1.65 |
| 0.4 | 2.20 | 1.25 |
| 0.6 | 1.65 | 0.65 |

(2) As the serial correlation coefficient increases, the probability of the maximum
    event increases significantly. This means that in a process with serial correlation
    structure, the appearance of extreme value is less than independent process.

The major drawbacks in the conventional extreme value statistics theory are that
finite sample length and the dependence structure of the available historical series
cannot be accounted. Therefore, the use of this classical theory in the evaluation of
extreme values leads to overestimation due to sample length and dependence.

# References

Al-Zhrani. (2007). *Bridge design*.

Bayazıt, M., Avcı, I., & Şen, Z. (1997). Hidroloji Uygulamaları. İstanbul Teknik Üniversitesi. Hydrology Applications, Istanbul Technical University, 280 pp.

Benjamin, J. R., & Cornell, C. A. (1970). *Probability, statistics, and decision for civil engineers*. Dover Books on Engineering.

Chow, V. T. (1964). *Handbook of applied hydrology*. New York: McGraw-Hill.

Cramer, H., & Leadbetter, M. R. (1967). *Stationary and related stochastic processes*. New York, USA: Wiley.

Farmer, J. D., & Sidorowich, J. J. (1987). Predicting chaotic time series. *Physical Review Letters, 59,* 845–848.

Feller, W. (1968). *An introduction to probability theory and its applications* (3rd ed., Vol. I). Wiley.

Fisher, R. A., & Tippett, L. H. C. (1928). Limiting forms of the frequency distribution of the largest or smallest member of a sample. *Proceedings of the Cambridge Philosophical Society, 24,* 180–290.

Flohn, H. (1989). *Ändert sich unser Klima? Mannheimer Forum, 88/89* (Boehringer Mannheim GmbH), 135–189.

Foster, H. A. (1924). Theoretical frequency curves and the application to engineering problems, *Transactions of the American Society of Civil Engineers*, *87*, 142– 203.

Gumbel, E. J. (1958). *Statistics of extremes*. New York: Columbia University Press.

Gupta, V. L. (1973). Information content of time-variant data. *Journal of Hydraulics Division, ASCE, 89*(HY3), Proc. Paper 9615:383–393.

Haan, C. T. (1977). *Statistical methods in hydrology*. Iowa state university press.

Hazen, A. (1914). Storage to be provided in impounding reservoirs for municipal water supply. *Trans. ASCE, 77,* 1308.

Jayawardena, A. W., & Lai, F. (1994). Analysis and prediction of chaos in rainfall and stream flow time series. *Journal of Hydrology, 153,* 23–52.

Jenkins, W. L. (1955). An improved method for tetrachoric r. *Psychometrika, 20*(3), 253–258.

Jenkinson, A. F. (1969). Estimation of maximum floods, chap. 5. World Meteorological Office Technical Note 98.

Kite, G. W. (1977). *Frequency and risk analysis in hydrology*. Fort Collins CO: Water Resources Publications.

Leopold, L. B., Wolman, M. C., & Miller, J. P. (1964). *Fluvial processes in geomorphology*. San Francisco (CA): W.H. Freeman and Co.

Linsley, R. K., Kohler, M. A., & Paulhus, J. L. H. (1982). *Hydrology for engineers* (3rd ed., 508 pp). New York: McGraw-Hill.

Lorenz, E. N. (1995). *Climate is what you expect*, edited, p. 55 pp, http://www.aps4.mit.edu/research/Lorenz/publications.htm. Available 16 May 2012.

Lovejoy, S., & Schertzer, D. (1986). Scale invariance in climatological temperatures and 165 the spectral plateau. *Annales Geophysicae, 4B,* 401–410.

Mandelbrot, B. B., & Wallis, J. R. (1968). Noah, Joseph, and operational hydrology. *Water Resources Research, 4*(5), 909–918.

Mandelbrot, B. B., & Wallis, J. R. (1969a). Computer experiments with fractional Gaussian noises. *Water Resource Research, 1,* 228–267.

Mandelbrot, B. B., & Wallis, J. R. (1969b). Robustness of the rescaled range R/S in the measurement of noncyclic long run statistical dependence. *Water Resource Research, 5*(5), 967–988.

Mandelbrot, B. B., & Wallis, J. R. (1969c). Some long-run properties of geophysical records". *Water Resource Research, 5*(2), 321–340.

Mejia, J. M., Rodriguez-Iturbe, I., & Dawdy, D. R. (1972). Streamflow simulation 2: The broken line process as a potential model for hydrologic simulation. *Water Resource Research, 8*(4), 931–941.

Milly, P. C. D., Betancourt, J., Falkenmark, M., Hirsch, R. M., Kundzewicz, Z. W., Lettenmaier, D. P., & Stouffer, R. J. (2008). Stationarity is dead: Whither water management? *Science, 319*, 573–574.

Mood, A. M. (1940). The distribution theory of runs. *The Annals of Mathematical Statistics, 11,* 367–392.

O'Connell, P. E. (1971). A simple stochastic modelling of Hurst's law. *Mathematical Models in Hydrology: Proceedings of the Warsaw Symposium, 1,* 169–187.

Pearson, K. (1930). *Tables of statisticians and biometricians, Part I* (3rd ed.). London: The Biometric Laboratory, University College; (printed by Cambridge University Press, London).

Rodriguez-Iturbe, I., Cox, D. R., & Isham, V. (1987a). Some models for rainfall based on stochastic point processes. *Proceedings of the Royal Society of London, Ser. A, 410,* 269–288.

Rodriguez-Iturbe, I., Febres de Power, B., & Valdes, J. B. (1987b). Rectangular pulse point process models for rainfall: Analysis of empirical data. *Journal Geophysical Research, 92*(D8), 9645–9656.

Saldarriaga, J., & Yevjevich, V. (1970). *Application of run lengths to hydrologic series*. Hydrology Paper no. 40. Fort Collins, Colorado, USA: Colorado State University.

Şen, Z. (1974) Small sample properties of stationary stochastic processes and the hurst phenomenon in hydrology. *Unpublished Ph. D. Dissertation*. University of London, Imperial College of Science and Technology, 257 pp.

Şen, Z., (1976). Wet and dry periods of annual flow series. *Journal of Hydraulics Division, ASCE, 102*(HY10), Proc. Paper 12457, 1503–1514.

Şen, Z. (1978). Autorun analysis of hydrologic time series. *Journal of Hydrology, 36,* 75–85.

Şen, Z. (1991). Probabilistic modeling of crossing in small samples and application of runs to hydrology. *Journal of Hydrology, 124,* 345–362.

Şen, Z. (2015). *Applied drought modeling, prediction, and mitigation* (p. 472). Elsevier Publication.

Spiegel, M.R. (1965). Schaum's outline series – Laplace transforms. McGraw Hill Book Co., New York, USA.

Thomas, H. A., & Fiering, M. B. (1962). Mathematical synthesis of streamflow sequences for the analysis of river basins by simulation. In: A. Maas et al. (Ed.), *Design of water resources systems* (Chapter 12). Harvard University Press, Cambridge, Mass.

Yen, B. C. (1970). Risks in hydrologic design of engineering projects. *Journal of Hydraulics Division, ASCE, 96*(HY4), Proc. Paper 7229, 959–966.

Yevjevich, V. (1972). *Probability and statistics in hydrology*. Fort Collins CO: Water Resources Publications.

# Chapter 7
# Flood Design Discharge and Case Studies

**Abstract** Protection against floods is possible by construction of some engineering structure, but their dimensioning needs to scientific calculations, where flood design discharge plays the major role. The definition of flood design discharge is given with different choices including probable maximum flood (PMF) as explained in Chap. 2, standard project flood, flood of a specific return period, and the use of intensity-duration-frequency curves. The causes of floods are explained in terms of landslides, rock falls, debris flow, and sediment yield with suitable calculation methodologies and design methodologies.

**Keywords** Debris flow · Design discharge · Flood assessment stages
Hydro-technical consideration · Land slide · Possible maximum flood
Rock fall · Sedimentation

## 7.1 General

Flood design discharge determination is very significant decision in water-related structure planning and construction. Water structures that require proper flood design discharge are canals, derivation tunnels, dams, culverts, bridges, and levees. Various scientific probability and statistical methods are used for determining the most accurate design flood quantity. Due to climate change impact, time series records that are taken into consideration in any flood discharge design also change, and therefore, it is necessary to revise the design quantities continuously for at least every 5-year or 10-year periods. The climate, land use, vegetation, and geomorphological changes bring significant dynamic uncertainties into the decisions and contribute severely to the flood risk calculation procedures.

Since the last 100 years, different engineering water structure designs are based on the currently best available scientific methodologies. Early design discharge calculations had rather verbal basis followed by the rational and logical methods (Chap. 5). This chapter will present the historical development of design discharge calculation methodologies with proper scientific methodologies.

As the volume of water in a catchment greatly increases during times of flood, its erosive power becomes more attractive with flood occurrence. Thus, the stream channels carry a much higher sediment load. Deposition of the sedimentation where it is not wanted also represents a serious problem. The influence of human activity can bring about changes in drainage basin characteristics. For example, the removal of the forest from parts of a drainage basin can lead to higher peak discharges, which may generate increased flood hazard.
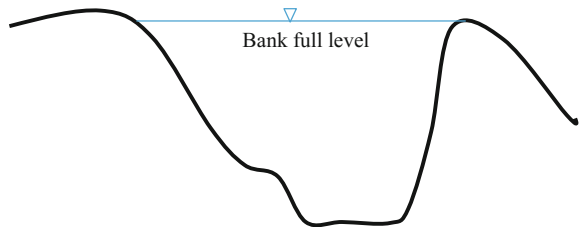
This chapter presents flood design discharge calculation methodologies and provides information about the erosion and sedimentation problems due to floods in cases of different engineering structures such as bridges, culverts, canals, dams.

## 7.2  Design Discharge Definition

The flood design discharge for a water structure has a number of definitions, the most significant five are explained below.

(1) Design discharge is the maximum flood that any hydraulic cross section allows to pass safely without inundation problems on the channel banks. Figure 7.1 indicates the bank-full level of a flood occurrence in a cross section,

(2) It is the amount of discharge that is calculated by taking into consideration the allowable and tolerable risk level. As already mentioned in Chap. 6, the risk is the reverse of design duration (see Eq. 6.9) or economically planned life of the structure,

(3) It is the flood discharge that can be sustainable by hydraulic structure (culvert, bridge, levee, dam, weir, diversions, drainage channels, and canal) without any significant damage. There must be damage neither to the structure itself nor to the surrounding environment,

(4) It is the maximum past flood discharge that is selected for safety design and evolution of the water structure,

(5) It is based either on the entire flood hydrograph as the values of discharge change along time or the peak discharge of the flood hydrograph.

**Fig. 7.1** Base flood definitions



Bank full level

## 7.2.1  Design Discharge Choice

One of the following alternatives is adapted as design discharge calculation procedure depending on the importance of the project and accordingly risk level.

### 7.2.1.1  Probable Maximum Flood (PMF)

It is a reasonable rare discharge that reflects the most extreme combinations of meteorological and hydrological conditions based on the rainfall and geomorphological drainage area features as explained in Chaps. 2 and 3. If the probable maximum precipitation (PMP) features are calculable physically by taking into consideration physical upper limits to storm rainfall in a region over a drainage basin, then the geomorphological features convert this storm rainfall event to flood and its calculation is possible through methodologies presented in Chaps. 4 and 5.

### 7.2.1.2  Standard Project Flood (SPF)

Depending on the reasonable characteristics of the region and drainage basin, it is the discharge amount that results from the most severe meteorological and hydrological conditions. It is computable from the standard project storm (SPS) over the drainage basin, and should be taken as the largest storm record in the drainage basin region. This alternative does not look for the maximization of the most critical atmospheric conditions. If SPS is not available over the drainage basin then it may be transferred from nearby regional drainage basins.

On the other hand, probabilistic and statistical methodologies, which are known as flood frequency analysis, provide calculation ways of flood design discharge of a given frequency (or return period) as explained in Chap. 6. For the calculations, long- and short-term data are necessary including rainfall and runoff values, annual flood peak discharge series, catchment physiographic characteristics.

The PMP or the SPS estimation is achievable according to the hydrometeorological approach, which leads to severe flood production effective factors. It is first necessary to have a design storm hyetograph from past long-term rainfall data and derivation of the catchment response function by means of either a lumped or distributed or distributed-lumped model (Chap. 5). In the former case, a unit hydrograph is assumed to represent the entire drainage area (Chap. 4). In the distributed-lumped model, the catchment is divided into smaller subregions or sub-catchment, and the unit hydrographs of each subregion are applied together with flood routing and sometimes reservoir routing to produce the drainage area response.

### 7.2.1.3  Flood of a Specific Return Period

In this case, flood frequency analysis is the basis of design flood calculation from the annual, partial, or hybrid past flood values of adequate lengths (see Chap. 6). If there is not adequate flood data, then the frequency analysis of available storm rainfall data helps to calculate the storm of a particular frequency through the application of the unit hydrograph in order to obtain the design flood as explained in Chap. 4. This alternative leads to flood discharge usually with a return period greater than the storm itself.

### 7.2.1.4  IDF Curves

As already explained in Chap. 2, IDF curves are helpful to decide on the rainfall intensity after the adaptation of design storm rainfall duration and the life (or the risk level) for water structure and they should be decided in some reliable manner.

Flood design discharge should help to maintain the safety of, say, a dam against overtopping, structural failures, and the spillway and energy dissipation arrangements. The following flood design criteria are valid, in general, at dam construction planning stage.

(1) Large dams are with gross storage greater than 60 million $m^3$ or hydraulic head greater than 30 m, and their design discharge calculation should be based on IDF curves leading to PMF (Chap. 2),
(2) In case of intermediate dams with gross storage between 10 and 60 million $m^3$ or hydraulic head between 12 and 30 m, IDF curves should be based on SPF,
(3) Small dams with gross storage between 0.5 and 10 million $m^3$ or hydraulic head between 7.5 and 12 m should be designed according to the IDF curves by taking into consideration 100-year return period.

In the flood planning, large or small magnitudes may be used if the expected eventual failure hazard is practically high or low. Apart from the size, other relevant factors that should be cared for in a proper design are the distance to settlement centers at the downstream and also the maximum hydraulic capacity of the downstream channel at a level without expectation of catastrophic damage.

IDF curves are also necessary for efficient operation of energy dissipation system by considering a design discharge, which may be lower than the IDF for dam safety. The use of this flood discharge with standard specifications or other factors affects the performance and the energy dissipation arrangements in the most efficient manner. IDF curves are also used for checking extent of upstream submergence, which depends on prevailing local conditions, type of property, and effects of the submergence for very important water structures like power house, mines. SPF or PMF levels are helpful to determine submergence effects. In general, for land and built up property acquisition, a 25-year or 50-year design flood is recommended for adaptation, respectively.

IDF curves are also useful for checking the extent of downstream damage, which depends on local conditions, the type of property, and effects of the submergence. For instance, in case of power house for safety of the dam with all spillway gates operation, outflows corresponding to the inflow design flood are relevant. Usually, physical flooding damage may not be allowed according to the prevailing conditions with disruption of operation.

### 7.2.1.5   Limitation of Calculations

Although theoretically sound, both PMF and SPF methodologies have restrictive boundaries.

(1) In many parts of the world, long-term hydrometeorological data are not available for reliable design storm parameter estimations,
(2) Unfortunately, physical rainfall modeling procedures to compute PMP is not fully available, and accordingly, as available today, the rainfall process knowledge and information have severe limitations,
(3) Currently, the historical storm maximization for probable maximum favorable conditions is based on the surface dew point data, which cannot represent moisture availability correct enough in the upper atmosphere,
(4) The drainage areas are not covered by self-recording rain gauges that reflect the historical individual thunderstorm data. The recording rain gauges provide information about the rainfall height change by time during each storm rainfall,
(5) There are a set of assumptions in the unit hydrograph theory, which are not valid in practical applications except on the average,
(6) Derivation of unit hydrographs suffers from the good quality and inadequate data quantity.

## 7.3   Discharge Magnitude Classification

Prior to any construction, in water structure dimensions calculation, local climate, hydrology, and morphology conditions should be considered in addition to possible future extreme events under a certain risk level. The amount of discharge calculation based on a certain level of risk is referred to as the hydrological design discharge. Dependence on early warning systems to reduce the flood hazards is very important, but unfortunately such warning software is not available in many parts of the world.

The design discharge can be calculated under a set of assumptions and prevailing conditions all of which can be taken into consideration in an effective planning, management, and mitigation principles. In flood analysis, the most important quantity is the flood design discharge. It is necessary to give dimension to a water structure such that throughout its life only one extremely hazardous flood occurs.

It is important not to select big design discharges that may cause to high economic investments or small discharge quantities to give way to more dangerous situations. Apart from the high economic investments and management programs, the water structure may not be resistant to such a discharge along its economic life. In case of small design discharge, it may be subjected to several hazardous occurrences during the economic life, which may lead to complete overture and destruction of the structure. Depending on the discharge magnitude, it is possible to classify floods into three categories.

(1) Common floods: These may overtop the water structure few times during its economic life,
(2) Standard project flood: It is decided by consideration of the whole drainage basin response to an extreme rainfall event. This discharge can overtop the reliable capacity of the water structure once or twice. Even though the standard project discharge is rather big, some of the levels in the cross sections can reach to inundation level from time to time. In general, it is smaller than the PMF magnitude, which is a consequence of the most possible big rainfall and hydrological conditions over a drainage basin (Şen 2004),
(3) Infrequent floods: These are not so much dangerous, and they have magnitudes between the SPF and the PMF.

In order to make the design of the PMF planning, it is necessary to have economic opportunities and the risk level that will be taken into consideration during the functioning life of water structure. The risk-level decision must be assumed at the beginning of all the planning and project design. There is a direct relationship between the risk level and the economy of the project. Any decrease in the risk implies increase in the project design flood discharge. In general, one can expect at least the following three functions from a water structure.

(1) Reliability performance,
(2) Low economic cost,
(3) Function throughout the design life with the least hazardous situation.

In the dimensioning of a water structure, the design discharge is quantified as the maximum possible discharge during the economic life. It may not be necessary to consider the probable maximum discharge in all the cases except the spillway and protection areas planning (regulators, weirs, discharge canals, etc.). These structures are allowed to dangerous discharges few times with some risk, because this provides significant reductions in the overall cost. This indicates the rule that rather than the absolute risk in the design of a water structure, the experts may allow slight reductions so as to bring the investment and capital costs to acceptable lower levels.

Especially, in subtropical regions, the floods appear, generally in winter, but in late spring months, snowmelt may also cause to dangerous floods. Most of the precipitation occurrences are due to frontal types. However, in summer season, floods are rather flash in behaviors and mostly born as a result of convective rainfall events (Chap. 2). One must not ignore the effect of the climate change depending

on the location (Chap. 8). For instance, in arid and semiarid regions, flash floods appear as a result of sudden and rather short duration rainfall instances. Especially, in places of insufficient infrastructure availability, they cause severe damages in urban and suburban areas. The impact of climate change is bound to appear more frequently in the future (IPCC 2007, 2013, 2014). Recently, one can observe that even the design discharges that are bound to appear once or twice over the economic life of water structure, they are bound to appear more frequently than before. This may imply that there may be dependences between successive flood events. As a result of this annual and partial duration, flood calculations become close to each other (Chap. 6). The differences are rather in the short and medium ranges.

## 7.4   Design Flood Prediction

Unfortunately, so far there is not an accurate formulation to calculate the rainfall intensity for precise estimation of flood design discharge. There are approximate formulations whatever the availability of the data, which lead to approximate evaluation of flood discharge and hazard assessment. Recently, apart from the formulations, it is also very helpful to depend on the expert views by fuzzy logic principles (Şen 2010).

Some of the design discharge formulations are empirical and dependent on the morphological features of the drainage basin. The most extensively employed formulation is the rational formula, which relates the discharge directly and linearly to the drainage area and the intensity of rainfall (Chap. 5). Some others take into consideration the theoretical PDF of the available records for the discharge calculation (Chap. 6). It is also possible in practice to employ few of these methodologies and then reach to a better flood design discharge magnitude. In general, an optimization approach is used by considering the costs and the incomes from the project. The University of Illinois's 1953 survey of the design practices of state highway departments showed little agreement on recurrence intervals for bridges and culverts at the start of the modern era (Chow 1962). The recurrence intervals for culverts, small bridges, and the drainage structures in the secondary highway system ranged from 5 to 100 years. The most common recurrence interval for these structures is 25 years. The most common recurrence interval for the larger or more important structures is 50 years.

Sometimes to be on the reliable side, in spite of the life as 100 years or 200 years, engineers may also take into account 500-year life flood design. For flood discharge, there are different approaches each with additional complement to others. These methodologies are explained in Chap. 6 in a detailed manner.

(1) Flood discharge estimation by means of empirical formulations that are based on gained experience in a region (Chap. 3),
(2) Flood estimation by use of envelop curves determined based on previous flood discharges (Chap. 3),

(3) Application of rational and logical formulations (Chaps. 3 and 4),
(4) Probability and statistical approaches also provide theoretical methodologies for flood discharge estimation (Chap. 6),
(5) Unit hydrographs are other means that help to estimate flood discharge (Chap. 4).

In the flood design discharge calculations in a drainage basin channel, the source of risk is extreme rainfall and/or snowmelt occurrences that lead to river discharge and surges. It is important to know the frequency of the rainfall and/or runoff discharge occurrences. In any flood assessment, not only record measurements and predictions are important but additionally social structure, urban expansion, and even political importance of the location also play significant role. All of these factors must be integrated through a systematic and effective programs and software.

## 7.5  Flood Design Discharge Calculation

There are many flood peak discharge estimation formulations that have been developed over the last 150 years. Some of them are much localized, but others have wider applicability all over the world. However, they must be applied with great prudence, and prior to the application, the basic assumptions must be verified as much as possible. Unfortunately, none of them provide precise result even for the applicable areas, and therefore, probability, statistical, and risk limits must be taken into consideration (Chaps. 6 and 9). The uncertainty is due to the fact that the flood peak discharge depends on many factors, and it is not possible to take all of them into consideration in one formulation. Most of the formulations involve few factors or at the maximum several ones. Some of the empirical flood peak discharge estimation formulations are explained in the following sequel.

In order to know the maximum water level, past flood marks on ancient monuments, bridges, sides along river banks can be observed by some persons, who live nearby the bank of the river. It is possible to obtain the following geometric measurements from a distinctive cross section with flood marks.

(a) Water flow area, $A$, through the cross section,
(b) Wetted perimeter length, $P$,
(c) Radius of influence, $R$, which is the ratio of the cross sectional area, $A$, to the wetted perimeter, $P$,
(d) It is possible to measure the cross sectional slope, $S$, by considering a certain distance toward upstream and downstream between two points; each one of them may be about 50 or 100 m away from the cross section along the main channel as shown in Chap. 3, Fig. 3.19.

All these quantities can be substituted into the Manning or Chezy equations with the determination of roughness coefficient from Chap. 3, Table 3.2, and then, the

resulting flood discharge can be determined empirically. The repetition of this procedure for different levels of water traces leads to the rating curve for the concerned cross section. Apart from this calculation method, there are several other empirical formulations for flood discharge calculation.

(1) Catchment area-based formulations: These take into consideration the catchment area, $A$, without any rainfall quantity concern, and the peak flood discharge can be calculated as,

$$Q = C A^n \tag{7.1}$$

where $C$ is the flood coefficient and $n$ is referred to as the flood index both of which depends on a set of factors such as the catchment size, shape, location, and topographic feature in addition to some rainfall descriptions as the duration and storm distribution patter. These two constant parameters remain the same for each drainage basin. Among the formula similar to Eq. (7.1) are the following alternatives.

(a) Dicken (1985) formulation: There is a nonlinear relationship between the peak discharge, $Q_P$, and the drainage area, $A$, through Dicken's constant, $C_D$, which assumes values between 5 and 30.

$$Q_p = C_D A^{3/4} \tag{7.2}$$

The peak discharge results in $m^3/s$, provided that the area is in $km^2$ (Table 7.1).

(b) Ryve (1884) formulation: This is similar to Eqs. (7.1) and (7.2) with the differences in the constant, $C_R$, and flood index value, 2/3.

$$Q_p = C_R A^{2/3} \tag{7.3}$$

The peak discharge, $Q_P$, is obtained in $m^3/s$, provided that the drainage area is in $km^2$. Ryve's expression is developed originally for Tamil Nadu region and also for parts of Karnataka and Andhra Pradesh. This formulation is also valid for Madras, India, regions. Ryve (1884) recommends the coefficient values as 6.8 for drainage areas within 80 km from the east coast; 8.5 for areas that are 80–60 km away from the same coast; and finally, 10.2 for limited areas near hills.

**Table 7.1** Dicken's flood constants

| Features | $C_D$ value |
|---|---|
| North Indian Plains | 6 |
| North Indian hilly regions | 11–14 |
| Central India | 14–28 |
| Coastal Andhra and Orissa | 22–28 |

(3) Inglis (1930) formulation: Again, this expression has been suggested for India depending on the local experience, and its differences from the previous ones are in the flood constant and flood index values.

$$Q_p = \frac{124\,A}{\overline{A} + 10.4} \tag{7.4}$$

where $A$ is the drainage area, and $\overline{A}$ is the average of the sub-areas. It is based on flood data of catchments in Western Ghats in Maharashtra.

(4) Nawab formulation: This has been derived for Hyderabad Deccan catchments. It expresses the peak flood discharge as,

$$Q_p = C_N\,A'^{\,[0.92 - (1/14\,\log A)]} \tag{7.5}$$

where $C_N$ varies between 48 and 60 and takes occasionally the maximum value of 86, $A'$ and $A$ are the drainage area in $m^2$ and $km^2$, respectively.

(5) Fanning formulation: This is regarded as valid for American drainage basins with the flood constant $C_F = 2.64$

$$Q_p = C_F\,A^{5/6} \tag{7.6}$$

(6) Creager formulation: This is developed during the flood peak discharge study in the USA, and its expression is given as,

$$Q_p = C_C A'\left(0.894\,A'^{\,-0.048}\right) \tag{7.7}$$

The peak discharge results in $m^3/s$, provided that $A'$ is the drainage area in $m^2$ and correspondingly, $0.39\,A$, where $A$ is the drainage area in $km^2$. The flood constant $C_C$ varies from 40 to 130; lower values are for ordinary floods, and higher values for intense and acute floods.

(7) Meyer et al. (2009) formulation: It is also developed for the USA drainage basins, which expresses the flood peak discharge as,

$$Q_p = 177\,p\sqrt{A} \text{ in cumecs} \tag{7.8}$$

where $p$ has a value of unity for stream that has the greatest flood flow of the area. For any other stream, $p$ is the fraction for the flood flow of stream. For different streams, values of $p$ vary from 0.002 to 1.0, usually taken as 1.

(8) Jarvis formulation: This is very similar to the previous formulation and comparatively simpler than it.

$$Q_p = C_J\,\sqrt{A} \tag{7.9}$$

where $C_J$ varies between 1.77 and 177. $Q_P$ is in $m^3/s$ if the drainage area is substituted in $km^2$.

(9) Fuller (1914) formulation: This is also empirical formula, which relates the peak discharge to the drainage basin area, and it includes also the flood frequency. It is developed for the USA typical drainage basins. Its expression is given as,

$$Q_p = C_F A^{0.8} (1 + 0.8 \log T) \tag{7.10}$$

where $Q_P$ is the peak discharge with maximum 24-h flood with a frequency of $T$ years, and it has $m^3$/s dimension with $A$ in $km^2$ and the Fuller constant values between 0.18 and 1.88.

### 7.5.1 Drainage Area- and Shape-Based Formulations

The aforementioned formulations had the drainage basin variable as the major factor. However, the following formulations take into consideration additional variables such as the shape factor (Chap. 3). For instance, Dredge or Burge formulation is based on Indian records and states that

$$Q_P = 19.6 \frac{A}{L^{2/3}} \tag{7.11}$$

where $L$ is the length of the drainage basin in km. On the other hand, if $W$ is the average width of the basin in km, then substitution of $A = WL$ into the previous expression leads to,

$$Q_P = 19.6 \, WL^{1/3} \tag{7.12}$$

### 7.5.2 Rainfall and Drainage Area-Based Formulation

The original developments of such formulations are from Northern USA, Ohio to Connecticut as,

$$Q_P = C_P \left( PW^{5/4} \right) \tag{7.13}$$

where $P$ is the probable 100-year maximum 1-day rainfall in cm, and $C_P$ is the flood constant equal to 1.5 for humid areas and 0.2 for desert areas. The formula requires in its application fairly uniform width with no storage effect. The application validity of this formulation is confined to areas from 1600 to 16,000 $km^2$. If the area is wider at the lower end, the formula gives too small results, and if it is wider

at its upper ends, the results obtained are too large. A correction of 10–13% may be required for width variations.

### 7.5.3   Total Runoff and Drainage Area-Based Formulation

The most widely known alternative to this group of formulations is the Boston Society of Civil Engineers Formula, which is suggested by the flood committee of Boston Society of Civil Engineers, per square kilometer that is based on the New England flood of November 1927. Its general formulation is as follows:

$$q_P = 0.0056 \frac{D}{t} \tag{7.14}$$

where $q_p$ is the peak flow m$^3$/s/km$^2$; $D$ is the flood runoff total depth in cm; $t$ is the total flood period in hours or the base of the flood hydrograph (Chap. 4). The evolution of this formulation started with a triangular hydrograph. It yields reasonable satisfactory results. It has been observed during the study that $t$ remains almost constant irrespective of the flood size. It has been suggested by the committee that if there is not flood hydrographs availability, then the following formulations should be used.

$$q_p = \frac{C_F D}{\sqrt{A}} \tag{7.15}$$

or

$$Q_p = \frac{C_F D A}{\sqrt{A}} = C_F D \sqrt{A} \tag{7.16}$$

Herein, $C_B$ is a coefficient of the stream or flood characteristics, which varies generally from 0.7 to 3.5, but up to 7 in mountains and less than 0.7 for very flat streams. For New England, values of $D$ generally vary from 7.5 to 15 cm for occasional floods to rare floods and are not over 20 cm even for maximum floods.

### 7.5.4   Rainfall Intensity and Drainage Area-Based Formulation

This is referred to as the rational formulation, which is the oldest and best known formula for determining peak flow from a given drainage area. It has already been explained in Chap. 5 in detail. The peak discharge, $Q_P$, formulation is given as follows:

$$Q_p = 0.28\,C\,I\,A \tag{7.17}$$

In the calculations, $Q_p$ is obtained in m$^3$/sec on the base that the rainfall intensity, $I$, is in mm/h and the drainage area, $A$, in km$^2$. The rational formulation for flood peak discharge estimation has the consideration of the entire drainage area as a single unit, flood peak discharge estimation at the most downstream point, and the assumption of uniformly distributed rainfall over the drainage area. General assumptions in the rational formula are that the predicted peak discharge, $Q_P$, has the same probability of occurrence (return period) as the used rainfall intensity, $I$; the runoff coefficient, $C$, is constant during the storm rainfall, and the recession time is equal to the time of rise.

On the other hand, in the modified version of the rational formula, a storage coefficient, $C_S$, is included to account for a recession time larger than the time the hydrograph takes to rise. Hence, enhanced formulation is

$$Q_p = 0.28\,C_S\,C\,I\,A \tag{7.18}$$

In a drainage basin, the peak flood discharge is reached when all parts of the watershed are contributing to the outflow, i.e., at the time of concentration, $t_c$, in min, which is given by Kirpich (1940) on the bases of main channel length, $L$, in m and the slope, $S$, as

$$t_c = 0.0195\,L^{0.77}S^{-0.385} \tag{7.19}$$

### 7.5.5  Envelope Curves

If in a region with same climatological characteristics the flood record data is scarcely available, then the envelope curve technique is adapted to develop a relationship between the peak flood discharge, $Q_P$, and drainage area, $A$ (Chap. 5). Hence, the available flood peak discharge data are collected from a large number of catchments that are meteorologically and topographically similar to each other. The data are then plotted on a log-log paper as $Q_P$ versus $A$ (see Figs. 5.1–5.4). If an enveloping curve can be fitted to encompass all the scatter data points, then it can be used to obtain peak discharge estimation, provided that the drainage area is known. Such envelop curves are very useful in getting quick estimations of peak flood design discharge values. If equations are fitted to the envelope curve, then it provides empirical flood formulae of the type, $Q = f(A)$. Such formulations are presented in Chap. 5.

## 7.6   Engineering Water Structure Design

Any water resource-related structural design necessitates the estimation and final decision on the design discharge value. Although there are different methodologies, each water-related problem has its specific formulation and calculation method.
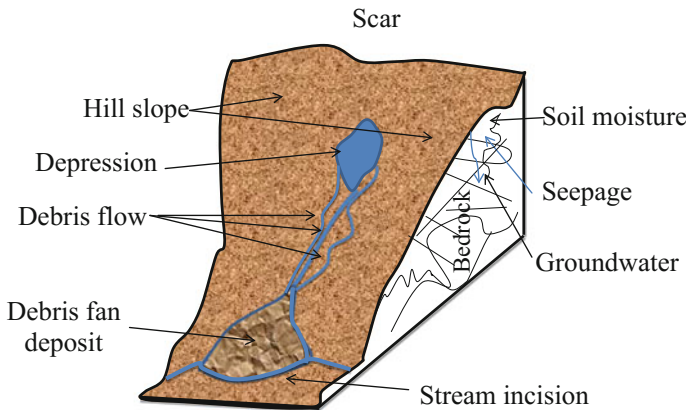
### 7.6.1   Debris Flow

During floods, these are liquefied fast-flowing landslide mixtures of unconsolidated water and debris. In arid regions due to exposition of necked land surfaces to hot and cold diurnal temperature changes, earth surface materials get broken into small masses, which are triggered for movement over sloppy regions during and after each storm rainfall and runoff. This is what happens along the elevated locations at road alignments, and therefore, after each storm rainfall depending on the rainfall intensity and consequent runoff or flood debris flow takes place. They are in the form of very dense fluids full of sands, gravels, cobbles, boulders, and fine grains. Their flow may endanger the traffic on the roads and highway. It is necessary to construct small dams, retaining walls, artificial stilling depressions, wire network, and similar hindrances against their flow in order to maintain usable structures safely. Depending on the sorting of fine and coarse material, they may appear in the form of mudflows and poorly sorted sediment forms. Mudflows can carry materials ranging in size from clay to boulders and may contain a large amount of woody debris such as logs and tree stumps. Especially after intensive rainfall events, runoff or floods are bound to trigger such flows. Speed of debris flows vary depending on the slope of the main channel and very high along road alignment. Accordingly, the volume of debris flow also increases depending not only on the slope but also exposition of surface to alternative wet and dry periods (Şen 2015). Among the most important debris flow impacting variables are slope angle, availability of loose sediment, and degree of land disturbance by natural or man-made activities. Debris flows may render extremely destructive impacts onto human life and property.

Debris and mudflows appear in the form of stream flows in the natural channels on the hill sides as shown in Fig. 7.2 including rock pieces, earth, and other materials within the surface flow. They develop when water rapidly accumulates in the ground, during intensive storm rainfalls, changing the earth into a flowing river of mud or "slurry." They can flow rapidly down slopes or through channels.

#### 7.6.1.1   Debris Flow Calculation

Logically, flood peak discharge is in direct relationship with the amount of debris flow. In fact, peak discharge associated with flow velocity is important when evaluating the conveyance capacity of stream channel reaches or critical cross

**Fig. 7.2** Debris flow components along hill sides

sections as, for example, under bridges or culverts. It has been shown that empirical relationships can be established between the peak discharge, $Qp$, of a debris flow and the debris flow volume (Hungr et al. 1984; Mizuyama et al. 1992; Takahashi 1991; Takahashi et al. 1994). In Table 7.2, a set of equations is proposed for debris flow calculation.

Rickenmann and Koch (1997) provided double logarithmic paper plot between the peak discharge and the debris flow volume as shown in Fig. 7.3. The red line is adopted in this book as the average of all the cases.

The red line in this graph yields average expression between the peak discharge, $Q_P$, and debris flow volume, $V$, as follows:

$$Q_P = 0.0375 \, V^{0.7143} \tag{7.20}$$
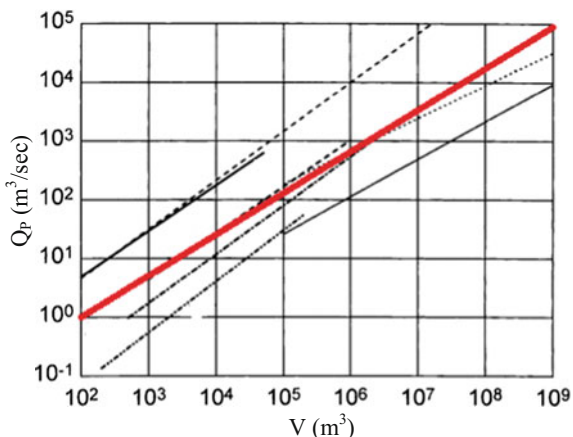
or the reverse of this expression as the debris flow volume subjects as

$$V = 26.57 \, Q_P^{1.4} \tag{7.21}$$

**Table 7.2** Debris flow volume, V, and peak discharge relationships

| Data basis | Equation | Source |
|---|---|---|
| Granular debris flow (Japan) | $Q_P = 0.135 \, V^{0.78}$ | Mizuyama et al. (1992) |
| Muddy debris flow (Japan) | $Q_P = 0.0188 \, V^{0.79}$ | Mizuyama et al. (1992) |
| Landslide dam failure | $Q_P = 0.293 \, V^{0.78}$ | Costa (1988a, b) |

## 7.6.2  Rock Falls

At the upstream of a drainage basin over the top of mountains, there are possibilities
of rock falls especially during wet periods with intensive rainfall and subsequent
flood events. Rock falls are only from the natural sloppy hill sides along the road
alignment, but also from insufficiently protected rock cuts. Stabilization forces on
rock masses can be disturbed by some climatic or biological event under the
gravitational effect over road cut or natural hill slopes. Among these events,
especially, in arid zones are also pore pressure increases due to rainfall intensity,
subsequent infiltration, and erosion of surrounding material during intensive storm
rainfalls, chemical degradation, rock weathering, plant root growth, and intensive
winds. The geometry of the hilly side slopes provides open domain for the
movement of the rock and its downward falling along the convenient potential
trajectories. For instance, in some of the project areas, road alignment dip slope
faces are created by the sheet joints in granites and they play major role in rock fall
events. The slope faces exert a horizontal component to the path taken by a rock
after it bounces on the slope or rolls off the slope. Especially, hard unweathered
rock faces are the most dangerous locations, because they do not retard the
movement of the falling or rolling rock to any significant degree. Existence of talus
material (loose sand, gravel, debris, etc.) over the hill surfaces helps to decelerate
the rock fall movement and even may stop the movement completely. It is,
therefore, advised to place gravel layers on catch benches in order to prevent further
bouncing of falling rocks.

Rock falls and slides involve a sudden rapid slide of bedrock along planes of
weakness. Rock slides are very common in the oversteepened hill slopes such as
along the case of Al-Hada road alignment in the Kingdom of Saudi Arabia. Such
occurrences are possible at a set of locations along the road alignment. Figure 7.4
indicates rock falls danger from a high elevation toward main channel of the
small-scale drainage basin.

**Fig. 7.4**  Different views of flow

After intensive rainfall events and subsequent ordinary floods, small rock fragments collapse and single block rock falls from highway sidehill slopes and may endanger transportation systems. In general, the volume sizes of rock blocks vary between 0.1 and 1.5 m$^3$. Along the highway alignments, there are both active and passive rock falls possibilities. Active cases must be prevented by protection, whereas passive rock falls possibilities may need further enhancement of stabilization.

### 7.6.2.1   Design Methodologies

In the following, the guidelines given by GHD are taken into consideration for rural areas not for urban areas.

(1) Before and during the project review of previous works related to the project area must be revised critically. Rainfall data, digital elevation model (DEM) data, satellite imagery, necessary topographic surveys (at each station very local 1/1000-scale topographic maps are prepared), soil, debris, and rock samplings should be collected,

(2) Preliminary work on meteorological data should be accomplished as for the wet and dry rainfall feature properties; daily, monthly, and annual rainfall analyses; IDF curve preparation; return period risk analyses must be completed. In doing

so experienced hydrometeorologists' views and scientific assessments should also be considered,

(3) Hydrological works should be completed as for the surface flow, floods, debris flow, mudflow, sedimentation, hydrograph analysis. Flood history of the region should also be recorded,

(4) Without any cost estimation, hydraulic capacities of side-ditches, culverts that affect the catchment must be assessed particularly at their intersections with the proposed road identifications. Conveyance characteristics of all the gullies (culverts, bridges) must be determined based on field observations and hydraulic works at the office. Hydraulic characteristics of each gully (rills) must be considered in the affected catchment areas and particularly at their intersections with the road,

(5) Engineering geological tasks must be completed as for the rock falls, side failures, and geotechnical aspects along the highway alignment. Soil classifications must be obtained through field and laboratory experimentations,

Storm water runoff from the roadway sloppy adjacent sides must be presented properly using topographic and digital elevation model (DEM) data through software. Surface drainage systems must be identified as gullies and their surface water capabilities are calculated based on available data from a set of rainfall measurement stations and the intensity-duration-frequency (IDF).

Rainwater falling on the road alignment adjacent sloppy sides must be modeled at different risk levels by taking into consideration the intersection with the road. In order to avoid overtopping of surface flow, necessary calculations must be performed with the checking of the side-ditches, culverts, and under-road crossings along the road alignment. Return periods of recurrence intervals must be used to rate the capacity and safety of drainage system including 10-year, 25-year, 50-year, 100-year, 250-year, and 500-year flood events. However, 50-year and 100-year return period calculations are recommended for use.

Recommendations are given as for the flood, debris flow, and mudflow and rock falls possibilities with necessary solution suggestions. Minor catchments should be defined from the surveys and DEM data.

In the assessment sound engineering expertise, judgment and experiences must be taken into consideration. Among the main topics are the following points.

(1) IDF curves,
(2) Dry period analysis,
(3) Wet period analysis,
(4) Risk calculation for debris and gullies along the road,
(5) Culvert capacity calculations,
(6) Rill and streamflow volume and risk calculations,
(7) Sediment transport calculation,
(8) Rock fall possibility and risk calculation,
(9) Morphological study and instability analysis,
(10) Infiltration, subsurface, and groundwater flow calculations.

After the general hydrological and hydrogeological assessment of the region, the necessary numerical data should be examined for its reliability in addition to periodic field trip study for tentative conclusions and recommendations. The treatment of data conditions must be specifically explained at gully sites through meteorological, hydrological, and hydrogeological methods.

## 7.7  Canals

These are necessary artificial engineering water structures that collect and transport surface flow to the sea or to any desirable outlet point. They are also used around any town or city in order to protect the settlement and industrial areas against possible flood danger and inundations. The surface water velocity calculation can be made by Manning formulation as explained in Chap. 4.

### 7.7.1  Groundwater Velocity Calculation

In the groundwater studies, velocity, $V$, calculation can be achieved according to Darcy law, where the necessary parameters are hydraulic gradient (slope), $i$, and hydraulic conductivity, $k$.

$$V = k\,i \tag{7.24}$$

One can obtain $k$ values from Internet as the hydraulic conductivity values as shown in Table 7.3.

Hydraulic gradient can be found from the groundwater-level measurements or groundwater table maps.

**Table 7.3**  Hydraulic conductivity values

| Rock type | Grain size (mm) | Hydraulic conductivity $k$ (m/day) |
|---|---|---|
| Clay | 0.0005–0.002 | $10^{-8}$–$10^{-2}$ |
| Silt | 0.002–0.06 | 10/02/2001 |
| Fine sand | 0.06–0.25 | 01-May |
| Medium sand | 0.25–0.50 | May-20 |
| Coarse sand | 0.50–2 | 20–100 |
| Gravel | Feb-64 | 100–1000 |
| Shale | small | $5 \times 10^{-8}$–$5 \times 10^{-6}$ |
| Sandstone | medium | 10/03/2001 |
| Limestone | variable | 10/05/2001 |
| Basalt | small | 0.0003–3 |
| Granite | large | 0.0003–0.03 |
| Slate | small | $10^{-8}$–$10^{-5}$ |
| Schist | medium | $10^{-7}$–$10^{-4}$ |

## 7.8   Culverts

A culvert is a closed conduit which connects two open channel segments in dry periods and two water bodies in wet periods. The most well-known type is box culverts, which are rectangular in cross section. Culverts have an entrance for water flows into the culvert and an exit for water discharge out of the culvert with a barrel as a closed conduit portion between the two ends. The tailwater implies the depth of water on the downstream side. Headwater represents the entrance part water. The selection of culvert length and slope must be in harmony with approximate existing topography. The culvert entrance should match the geometry of the roadway embankment.

In many areas of the world rather catastrophic slides due to heavy storm rainfall events and floods are well-known occurrences that may cause to road alignment hazard. They occur especially in areas with the following features:

(1) They may cause the slide in the relatively thin mantle of residual soil overlying bedrock along the road lines in the gullies,
(2) Steep gully slopes encourage the slides due to the gravity overland flow with high velocities, which start to trigger comparatively small grains, and hence, their movement causes a sort of chain effect by hitting the lower-lying loose rock pieces, gravel, and, in general, stagnant debris,
(3) Runoff and subsequent infiltration into superficial deposits may cause slide on the bedrock basement, which especially after each storm rainfall is exposed to partial or integrated massive slides and failures,
(4) The rock blocks along the runoff paths on the steep slopes of these gullies may gain momentum, and hence, fall downward, which may damage or block the road traffic for some period of time.

Depending on the geomorphology, geology, and especially hydrogeology of local gullies, small catchments, surface water, and floods, subsurface and groundwater flows may cause undesirable phenomenon along the road alignment due to the following cases.

(1) The mantle along each rill and gully may consist of residual sandy-gravelly and fine-grained porous material, which generates a pervious or semi-pervious medium that intakes surface water endangering the stability of the debris accumulation,
(2) Most often these residual mantle debris are underlain at several meters by weathered bedrocks, which may become more pervious and saturated due to percolation, and hence, provide an unstable base after each storm rainfall,
(3) The porous medium as mentioned in the previous steps provides groundwater storage generation, which provides additional pressure (pore pressure) on the steep base rock surface and may cause to debris flows and slides locally along the highway. The same pore pressure increases the horizontal force on the retain walls and gabions. This is due to the reduction in the shear stress between the debris accumulation and bedrock,

(4) Additional instability arises due to the saturation of the porous media in the debris volume leading to weight increments and consequent slide possibilities,

(5) As a result of the debris accumulation weight, most often shear cracks start to occur at the upstream parts hence reducing the tensile stress. The flow of surface or flood water into these cracks triggers the debris flow further. It is also possible that water enters the basement rock cracks, fissures, and fractures increasing the potentiality of wedge failure,

(6) Accumulation of water in pores as a result of subsequent and frequent storm rainfalls may lead to oversaturation and runoff over the slopes, which may liquefy the debris accumulation, and hence, spread out in the form of fans at the downstream parts of the rills, and even cause mudflow occurrences.

All of what have been explained in the above steps is bound to take place in various gullies along highway alignments. Walker and Fell (1987) in their soil slope instability and stabilization study gave Table 7.4, which provides empirical information based on the runoff depth, $d$, ratio to its extension, $e$ ($e/d$) about the type of failures.

Land slide and debris flows occur most often after each intensive, frequent, and durable storm rainfall and flood occurrences with the accelerations of steep topography and loose geological local mantle cover. Soil layers' mechanical features such as grain size, porosity, friction and hydraulic properties including permeability, infiltration, seepage play very significant role in the sliding or failure phenomena. It is for certain that the hazardous cases along the road alignment are due to storm rainfall impacts.

In any application study, reconnaissance field trips play very significant role, because they indicate on-to-one observation, interpretation, and idea generation for problem identification and the necessary solution in a verbal manner. In order to understand the mechanism, impacts and causes of possible slides during the field survey the following points are taken into consideration.

(1) Identification and investigation of the potential rills and gullies that may give damage to road infrastructure and traffic service stoppages,

(2) Inspection of already rock fall, debris flow locations, and remaining dangerous locations for the next intensive storm rainfall, surface runoff, and flood occurrences,

(3) Inspection of all the possible factors (geology, slopes, morphology, hindrances, etc.) by naked eye and make expert views and suggestions for each gully and associated rills,

(4) Identification of very local debris accumulations, rock hangings, fractures, rill depths, and especially surface water and groundwater possible flow lines and directions,

**Table 7.4**  Movement and slope instability

| Slide or flow depth ($d$)/extension ($e$) ratio. | $d/e$ (%) |
|---|---|
| Rotational deep slides–geomass (rock blocks, debris, earth) | 15–30 |
| Planar or shallow slides–saturated rock or soil mass | 5–10 |
| Supersaturated debris flow and mudflow | 0.5–3.0 |

(5) Identification of safety and dangerous portions of the road alignments and the association between these portions. This is especially true for highway, where there are few road cross sections at different elevations along a straight line perpendicular to the road axis,
(6) Depiction of segments' features that are delimited by the roads and gully or rill natural water divide lines.

## 7.8.1   Culvert Hydraulics

Guidance on culvert hydraulics in early highway engineering textbooks was incomplete at best. The fundamental differences in culvert performance under inlet control and outlet control were generally ignored. Several early textbooks advocate the sizing of culverts by a "uniform flow" method that considers barrel friction but not inlet or outlet conditions. However, certain authors did provide some sound qualitative guidance, for example, the efficiency of the culvert may be materially increased by so arranging the upper end that the water may enter it without being retarded. The discharging capacity of a culvert can also be increased by increasing the inclination of its bed, provided that the channel below will allow the water to flow away freely after having passed the culvert. The discharging capacity of the culvert can be greatly increased by allowing the water to dam up above it. A culvert will discharge twice as much under a head of four feet than under a head of one foot. This can be done safely only with a well-constructed culvert Byrne (1902). In 1922–1923, engineers from the Bureau of Public Roads and the University of Iowa conducted ground-breaking research on culvert hydraulics in the University of Iowa hydraulics laboratory. Articles in Public Roads in 1924 and 1926 summarized the findings from this research program for highway engineers. The introduction to the 1924 article provided the following overview of the key findings:

Three facts stand out from the results of the tests as worthy of the most serious consideration of highway engineers. The first is that highway engineers must pay more attention to the coefficient of roughness of the material forming the culvert. So long as the different materials used for culvert pipe did not differ greatly in roughness, and hence, in their frictional resistance to moving water, engineers were perhaps justified in not giving this factor much consideration. In recent years a new material, corrugated metal has been extensively manufactured into culvert pipes, which are shown by these tests to offer much greater frictional resistance to the flow of water than other materials, such as vitrified clay, cast iron, concrete, and timber.

The second fact brought out by the tests is that the quantity of water a culvert will discharge is directly proportional to the square root of the head and bears no relation to the grade at which the pipe is laid, if the pipe flows full, as it should at maximum capacity. The water in a pipe culvert under these conditions does not act as does that flowing in an open ditch, where the quantity of discharge is dependent upon the slope or grade of the water surface in the ditch, but as is the case in any

pipe flowing full, the discharge depends upon the water pressure available to force the water through the opening and the pipe. In the case of a culvert, the water pressure, which causes discharge, is furnished by the difference between the water level at the entrance and the outlet. The depth of submergence has no effect on this discharge, so long as the difference of the water levels at the two ends of the culvert remains the same.

The third observation is that the head loss at the culvert entrance is an important factor in determining the discharge and varies greatly with the type of entrance used. The data on the effect of different types of entrance on the entrance loss are among the most interesting of the findings from the tests.

The next and most recent, major advances in culvert hydraulics resulted from a research program at the National Bureau of Standards (NBS) hydraulics laboratory in the 1950s and 1960s. The NBS research program focused mainly on entrance conditions and their effects on culvert performance. This research produced dimensionless head–discharge relationships for inlet control and entrance-loss coefficients for outlet control for a large variety of entrance types. It also produced recommended designs for side-tapered and slope-tapered entrances.

In general, culverts are installed such that the grade-line coincides with the average streambed grade-line. This rule cannot be applied in very sloppy hill sides, and therefore, the culvert gradient must be determined according to experts' view by taking into consideration previous field experience, actual field studies, sedimentation possibilities, debris flow and mudflow cases, local geology, and storm rainfall consequent runoff amounts. Unfortunately, present-day culverts and their drop inlets are not designed properly, because topographic, meteorological, climatologic, engineering geologic, hydrological, and hydrogeological factors are not taken into consideration in an integrated manner. It is possible to see the consequences of wrong or incomplete design consequences or hazards through any field trip. The following points are the major drawbacks of the present drop inlets and culverts.

(1) Drop inlets may have vertical walls, which do not provide additional gravitational and culvert directed forces for debris flow and rock pieces falls,
(2) The bottom of drop inlets may be horizontal flat floor, which helps accumulation of debris flow and rock pieces without any support to enter the culvert head-water part,
(3) The horizontal dimensions of drop inlets may not have sufficient areal extend for the debris flow entrance,
(4) Culverts are of classical box culverts with rectangular cross sections, which do not show any distinctive performance during wet and dry periods,
(5) Culverts may not have enough longitudinal slopes for the assistance of rock fragment or debris gravel pieces rolling,
(6) Box culvert floor for fluid flow may be in the form of weakly inclined flat surface, which cannot support additional gravitational force to solid material flow in water transportation velocity.

In order to get rid of the abovementioned drawbacks, a very special drop inlet and box culvert water flow surface and cross section are suggested on the basis of the scientific study during this book. The special box culverts for highway should have the following important and distinctive features compared to any other parts in most of the highway water drainage system.

(1) Drop inlet part of the drainage system should be inclined walls on three sides except the entrance part to the box culvert,
(2) Drop inlet bottom should not be inclined, but at a reduced slope, which encourages the entrance of debris flow or rock fragments into the culvert head-water part,
(3) The horizontal dimension of drop inlets is calculated according to findings (peak discharge, debris flow volume, rock fragment amounts, and 50% safety factor) and suggestions based on the work,
(4) Culvert cross sections should not have rectangular shapes but triangular (or circular) shapes, so that the water, mud, debris, and rock fragment flows can be functional even at dry (or low intensity rainfall) runoff cases,
(5) Culvert longitudinal slopes should be kept as high as possible from the head-water to tailwater part, so that any debris that enter the culvert can be subjected to extra gravitational force to move downstream,
(6) Extra weight along the culvert length at the head-water part helps to stabilize the culvert underneath the road surface cover,
(7) Drop inlet and culvert system joint function may be enhanced through different slopes along the whole system.

## 7.9  Gully Sediment Yield Calculation

Sediment transport assessment in head-water areas of catchments in arid regions is a major concern for flash flood hazard control in watershed management. Under arid climates, sediment sources are often restricted to particular areas where shallow landslides and debris flow phenomena act as the principle sediment supply to sources and demand network and by the efficiency of downstream sediment routing. Under homogeneous conditions of climate, geology, and land use, the topographic control on erosion and deposition processes play a major role in landscape evolution.

Erosion and sedimentation phenomena are studied by various researchers, but there is no clearly defined and accepted method to the problem. According to Lal (1994a, b) either our conceptual understanding of the erosion–sedimentation problem on the earth surface is far from being complete, especially in arid and semiarid regions, or erosion–sedimentation research techniques are still more of an art than a science. Sediment yield was studied in the past by two basic types of analyses, namely hydrological and hydraulic approaches.

(1) The choice largely depends on the type of data used in the analysis. In the hydrological analysis, natural and anthropological factors such as the climate, catchment morphology, soil, vegetation, and man's activities are taken into consideration for sediment yield formulations (Task Committee on Handbook, ASCE, 1996).

(2) In the case of hydraulic analysis, fluid and grain size properties of the sediment factors are taken into account such as the fluid, entrained solids and geometric boundary characteristics, presence of density interfaces, etc.

Runoff and flood erosion largely concerns the transportation of loose materials by turbulent water flowing in sheets, rills, or gullies, although some detachment of particles can occur in runoff erosion (Cooke and Doornkamp 1974; Throne et al. 1987). A concise book about the theoretical approach for sediment yield problems in engineering has been written by Yalin (1972), where there are many empirical approaches. Wischmeier and Smith (1978) wrote a comprehensive book on the prediction of rainfall-erosion losses. Recently, Cheng (1997) demonstrated that the settling velocity is equivalent to the critical near-bed velocity, which is experienced by a typical bed sediment particle under the threshold condition, but only for large sediment sizes such as sand and gravel.

Semiarid and arid regions are distinctive in terms of erosion and sedimentation yield (Jansson 1982; Hadley 1986; Walling and Webb 1986). The most important agents are as follows:

(1) Erosion and transport characteristics,
(2) Basin morphological features,
(3) Geological layout and soil coverage,
(4) Vegetation covers factors,
(5) Land-use and management practices.

In arid regions, hill slopes are the primary source of erosion by occasional runoff and flood with channel bank and flood plains as secondary sources. The sediment yield phenomenon can be divided into two broad categories as

(1) The upland phase and
(2) The lowland stream or in-channel phase.

The upland phase emphasizes the erosion process of detachment and transport in rill and inter-rill areas where the mechanics of the rainfall event and surface flow are the major agents. Major variables influencing the yield in this phase are rock units, soil type, environmental conditions, and moisture content at the start of the event, in addition to the slope, vegetation, litter cover, rainfall amount, intensity, and duration.

In the in-channel phase, sediment transport and deposition processes predominate, and consequently, channel transport capacity becomes more important. Pertinent variables in this phase are the velocity, depth of flow, channel slope, wash-load, water temperature, grain size distribution, and median size of bed

material. Although not all of the sub-processes occur on all source areas, each has its part in the total sediment yield process.

In refined assessments, a drainage area is divided into sub-areas, similar in their degree of weathering and erosion intensity, which can be used as a basis for sediment yield evaluation. This technique is used for quick regional assessment of erosion in the absence of measurements. Accurate prediction of sediment yield rate in arid and semiarid regions is a difficult task that is not handled well by most models.

The relevant variables considered for sediment yield rate formulation are the runoff discharge, drainage area, mean channel slope, and drainage density. These variables are explained in any standard handbook on hydrology (Maidment 1993).

### 7.9.1　Sediment Yield Models

Few formulations are developed by Şen (2014) for arid region sediment transport yield, $S_y$, calculations through the dimensionless analysis.

$$S_y = k \frac{Q}{A} S \tag{7.22}$$

where $k$ is a constant, $Q$ is the discharge, $S$ is the slope, and $A$ is the area. This is the simplest sediment yield formulation, and it has completely logical basis. Provided that all the variables are measured for any drainage basin (wadi in arid lands), then the constant $k$ can be determined from Eq. (7.22). This constant is referred to also as the numerical factor of proportionality between the dependent variable and the combination of independent variables.
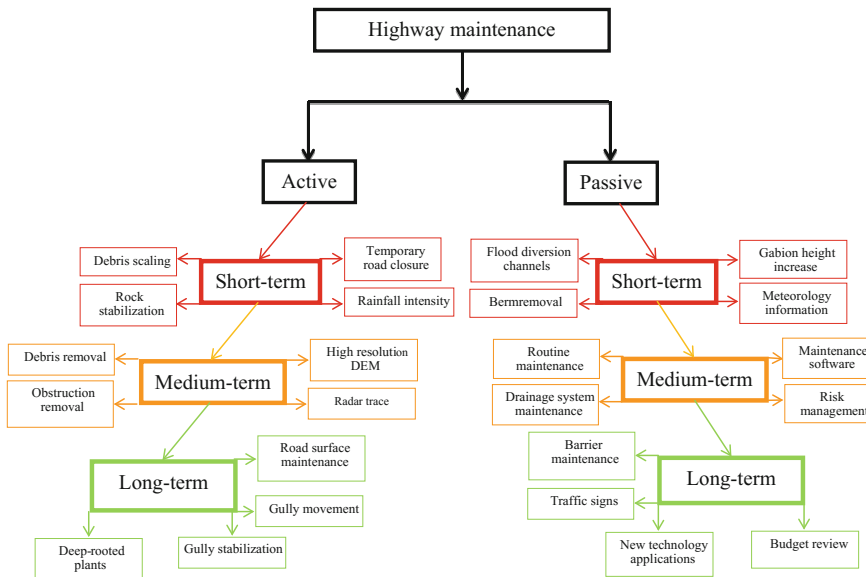
The term, $Q/A$, in Eq. (7.22) expresses the depth, $H$, of surface water per time, which in turn is related to the height of excess rainfall intensity, $I$. Since $Q/A = h = CI$, where $C$ is the runoff coefficient (Chap. 4), Equation (7.22) can be rewritten as

$$S_y = k \, C \, I \, S \tag{7.23}$$

## 7.10　Highway Safety Assessment and Recommendations

After whole geological, geotechnical, engineering geological, meteorological, hydrological, hydrogeological, hydraulics, and overall assessments, especially future safety measures and maintenance methodologies and practices can be viewed as shown in Fig. 7.5.

This figure provides many activities for highway maintenance throughout many years. The priority must be given to active maintenance, but in the meantime

**Fig. 7.5** Highway safety and maintenance

passive parts may also be executed simultaneously depending on time and financial support. Short-term implies daily and at the maximum up to 2 years activities, whereas medium-term should cover 2–5 years period, and the long-term planning includes more than 5-year period. In any case, a close inspection from all points is recommended for review after each 5 years under the light of information rose in this book. On the other hand, occasional but immediate maintenance based on the present conditions must be affected when it is possible to assess residual lives of the assets on basis of inspections or test results. The activities as shown in Fig. 7.5 can be categorized further into routine, periodic, and emergency (urgent) classes. The road maintenance should comprise of all the activities in the figure, but especially pavements, shoulders, slopes, drainage facilities, gully stability, rock fall occurrence possibility, structures (culverts, side canals, bridges, etc.). The road area must be observed at least weekly or in wet periods more frequently, say, daily, in order to visualize defect occurrences leading to minor repairs and improvements to eliminate the cause of defects and to avoid excessive repetition of maintenance efforts. Among the routine maintenance are small-scale works consisting of short-term (daily) activities such as to provide traffic passage and safety. Depending on visual daily inspection, the frequency of routine activities may change and generally at least once a week or month maintenance is necessary. In cases of unseen and unpredictable repair requirements, urgent maintenance must be undertaken immediately. Another medium-term maintenance type is of periodic maintenance, and it covers activities on a section of road at regular and relatively long intervals, which aims to provide permanent structural integrity of the road. Periodic maintenance is,

in general, at large scales and requires expert workers and operators for the completion of the work. Such a maintenance alternative is necessary at least once in each wet and dry season (Şen 2015).

An inventory of all the culverts, ditches, and drop inlets in any area must be kept, and accordingly, periodic inspections must be carried out for sustainable maintenance. Regular periodic inspections allow minor problems to be spotted and corrected before they become to yield serious problems. The road inspection agency must define full range of culvert inspection program on the basis of inspection frequency, size, and type of culverts to be inventoried and inspected, and the information to be collected. It is advised herein that each culvert must be inspected every two years. Lack of maintenance is a prime cause of improper functioning in culverts, bridges, and other drainage structures.

In active gullies, the floor lowers over time as more soil is scoured out. It is recommended to measure regularly the distance from the floor to natural land level and compare the measurements to check floor movement. After the necessary comparisons, and finally, the engineer can take decision and apply it in the field for improvement and safety of the road.

Regular checking should be done to identify whether the erosion is active; however, if the gully has stabilized, then it is better to leave it alone. Disturbing dispersive soils may reactivate the gully and cause more erosion. In order to check whether the erosion is active, it is necessary to look at the gully head, walls, and floor in comparison with their previous positions.

After each intense storm rainfall leading to strong surface flow (flood), it is possible that the gully may become active, and therefore, the inspectors should try and find out if the erosion is caused by surface water or groundwater. In a highway region, both the surface and subsurface (groundwater) play significant role on gully activities. It is possible to divert the surface water through properly designed canals and earthworks or vegetation plantation especially plants with deep-root possibilities. On the other hand, in case of subsurface and groundwater activity vertical holes with their connection through horizontal pipes may be one of the solutions. This is rather similar to Qanats, but in local and small scales (Şen 1995). Vegetation also helps to break the force of raindrops hitting the ground and slow the speed of surface runoff and hence, decelerate flood speed. In cases of sparse vegetation above, the gully there may be removing of stock from the area and it is recommended to fence it off so that plants can regenerate. Keeping stock out of gullies will encourage faster stabilization and natural re-vegetation.

Due to the geotechnical properties of the loose and unconsolidated debris along the gully slopes along the highway road, heavy and intense rainfall occurrences may trigger possible floods for land sliding. In order to reduce such events, it is recommended in this book to scale them immediately. The scaling of all types of debris could be done by pouring water over it to simulate the rainfall effect, where the slide took place for all the materials. A fire truck could be used to pour water from the higher road alignment on each loose and consolidated debris accumulation along the gully path.

## 7.11 Flood Hazard Reduction

In general, within the subtropical climate belt, and hence, in particular, arid and semiarid regions are prone to occasional floods due to unexpected weather and geomorphological effects. In addition to these natural effects, the human settlement and urbanization, highway network planning, etc., may also increase the flood hazard potential due to unconcise or improper planning without flood hazard and inundation maps availability. Under the light of aforementioned information, it is possible to deduce the general and specific recommendations for flood awareness studies, hazards and inundation areas.

(1) Individual storm rainfall intensity tables and associated risk levels for a set of duration including 5-year, 10-year, 25-year, 50-year, and 100-year must be calculated and made ready for any future flood assessment studies in the region (Chap. 2),

(2) Surface runoff measurement stations at a set of control cross sections must be established, because worth of even a single runoff measurement is very high for arid regions (Chap. 4),

(3) Humid region flood assessment formulations as available in the literature must be used with care in arid and semiarid regions (Şen 2008). It is necessary either to modify them according to the features of arid region and the availability of data or new approaches must be developed for these regions,

(4) High-resolution topographic maps (preferably digital elevation maps) must be prepared for the region in order to implement the flood inundation boundaries at different risk levels.

Depending on flood abatement and flood diversion alternatives, there are different individual and combination physical control structures and procedures in practical uses. Flood diversion is a direct solution for flood hazard reduction in an area. Flood abatement or flood reduction involves decreasing the amount of runoff potential that is able to create a flood peak in a drainage basin. This is a less reliable strategy than flood diversion. Flood abatement approaches are typical control strategies as watershed treatment include especially in rural areas, if possible, reforestation or reseeding of sparsely vegetated areas to increase evaporative losses, mechanical slope treatments within the watershed contour terracing, runoff coefficient reduction, comprehensive protection of vegetation from wildfires, overgrazing, clear-cutting of forest land, or any other practices likely to increase flood discharges and sediment loads. Furthermore, construction of small water and sediment holding areas especially in farm ponds also help to reduce the flood discharge in the downstream portions. Most flood reduction achievements are rather local and in small scales and restricted to flood flows from comparatively small basins.

The following protections are concerned with flood diversion measures whereby the floods may partially diverted from the risk areas.

(1) Embankments or stop banks that are terminologically referred to as the levees. They are designed for restriction of flood waters to well-defined, low value land on the floodplains. Their constructions are simple and mostly constructed from earth fills and

(2) Since one of the flood magnitude effective factors is the velocity and it is dependent on the cross sectional area, it is possible to enlarge the cross sectional area to reduce the flood velocity and to spread the waters over a larger area.

For the regulation of flood waters temporally impoundment structures such as reservoirs and large dams are constructed. These help to store the water during the flooding time and then to release the water to downstream after the flooding at desired locations, for instance, to groundwater recharge potential areas. In order to reduce the debris flow, mudflow, and possible partial or complete landslides, the following points are advised to stick.

(1) Continuous research support, information and knowledge collection, assessment, and dissemination,
(2) The area along the alignment must be mapped from hazard points of view as suggested in this chapter. This report provides the basic information,
(3) Real-time measurements,
(4) Guidelines and training principles for public awareness and education,
(5) Emergency preparedness.

## 7.12  Hydrological Flood Assessments

The following points are among the least stages for any water resource location assessment especially in arid regions such as the Arabian Peninsula and semiarid lands such as the southeastern Turkey.

### 7.12.1  First Stage

(1) Drainage area delamination (DEM) (Chap. 3),
(2) Geomorphological evaluation (area, main channel slope and length, drainage density, elevation difference) (DEM) (Chap. 3),
(3) Rainfall intensity-frequency-duration (IDF) curves for a set of years (2-year, 5-year, 10-year, 50-year, 100-year return periods) (Chap. 2),
(4) Hydrograph analysis (peak design discharge) (Chaps. 4 and 5),
(5) Channel hydraulics (transmittance capacity, runoff routing, overflooding),
(6) Transmission losses and groundwater recharge possibilities, if possible diversion location determinations.

## 7.12.2  Second Stage

(1) Suitable location for the dam:

  (a) Preparation of maps and cross sections on topographic map and/or DEM configuration in the office,
  (b) Geological setup of the area (geological and if possible subsurface maps),
  (c) Reconnaissance field survey without instrument (determination of few suitable locations),
  (d) Dam reservoir features' determination (water surface area-elevation and water volume-elevation curves),
  (e) Depending on the dam location aforementioned features, dam height determination by considering 5–10% overtopping possibilities in the future.

(2) Dam structure assessment:

  (a) Determination on the dam length, width, face slopes,
  (b) Determination of dam volume and accordingly material volumes,
  (c) Dam foundation prospection from engineering geological point,
  (d) Dam construction prospection from civil engineering point of view,
  (e) Dam seepage calculation from hydrogeology point of view.

(3) Environmental problems:

  (a) Flood and overtopping possibilities and risk assessments,
  (b) Dam break risk assessment and inundation map,
  (c) Determination of safety settlement locations from the possible risky areas,
  (d) Human health safety problem alleviations,
  (e) Pollution protection measures.

## 7.12.3  Third Stage

(1) Water transmission canal assessment:

  (a) Water transmission volume at the entrance point to the canal,
  (b) Water transmission loss evaluation along the canal,
  (c) Canal transmission capacity assessment,
  (d) Possible sedimentation calculation,

(2) Canal line assessment:

  (a) Hydraulic calculations for possible sub- and supercritical flows and their locations,
  (b) Sediment transport capacity calculations,
  (c) Canal width variation possibilities,

(d) Canal slope effect on the surface flow,
(e) Flood routing along the canal

(3) Transmission canal construction:

(a) Topographic features (elevation and slope profile along the canal,
(b) Geologic and soil characteristics determination along the canal line,
(c) Calculation of local material needs, cement, and gravel.

# References

Bradley, J. (1978). *Hydraulics of bridge waterways* (2nd ed.,) US Department of Transportation, FHWA, US (Published electronically in 1978).

Byrne, A. (1902). *Treatise on highway construction* (4th ed.,).

Cheng, N. S. (1997). Simplified settling velocity formula for sediment particle. *ASCE Journal of Hydraulic Engineering, 123*(8), 149–152.

Chow, V. T. (1962). Hydrologic determination of waterway areas for the design of drainage structures in small drainage basins. University of Illinois, Engrg. Experimental Station Bull.

Chow, V., Maidment, D., & Mays, L. (1988). *Applied hydrology* (p. 572). New York: McGraw-Hill.

Cooke, R. V., & Doornkamp, J. C. (1974). *Geomorphology in environmental management: An introduction* (p. 413). Oxford: Clarendon Press.

Costa, J. E. (1988a) Rheologic, geomorphic, and sedimentological differentiation of water floods, hyper concentrated flows, and debris flows, In: V. R. Baker et al. (Eds.), Flood Geomorphology, Wiley, New York, pp 113–122.

Costa, J. E. (1988b). Floods from dam failures. In V. R. Baker et al. (Eds.), *Flood geomorphology* (pp. 439–463). New York: Wiley.

FHW, A. (1988). Interim procedures for evaluating scour at bridges, U.S. Dep. of Trans., Fed. Highway Admin., Technical Advisory, "Scour at Bridges", Washington, DC.

FHW, A. (1989). Scour at Bridges, Hydraulic Engineering Circular No. 18, Washington DC.

Hadley, R. F. (1986). Fluvial transport of sediment in arid and semi-arid regions. In *Proceedings of International Symposium on Erosion and Sedimentation in Arab Countries*. Iraqi Journal of Water Research, Vol. 5: 335–348.

Hungr, O., Morgan, G. C., & Kellerhals, R. (1984). Quantitative analysis of debris torrent hazards for design of remedial measures. *Canadian Geotechnical Journal, 21,* 663–677.

IPCC. (2007). *Climate change 2007: Impacts, adaptation, and vulnerability*. (Contribution of Working Group II to the Fourth Assessment Report of the Intergovernmental Panel on Climate Change). Cambridge, UK: Cambridge University Press.

IPCC. (2013). *Climate change 2013: The physical science basis*. (Contribution of Working Group I to the Fifth Assessment Report of the Intergovernmental Panel on Climate Change). Cambridge, UK: Cambridge University Press.

IPCC. (2014). Climate change 2014: Impacts, adaptation, and vulnerability. (Contribution of Working Group II to the Fifth Assessment Report of the Intergovernmental Panel on Climate Change). Cambridge, UK: Cambridge University Press.

Jansson, M. B. (1982). Land erosion by water in different climates. Dept. Phys. Geography, Uppsala University, INGI Rapport, 57.

Kirpich, Z. P. (1940). Time of concentration of small agricultural watersheds. *Civil Engineering, 10*(6), 362.

Lal, R. (1994a). *Soil Erosion Research Methods*. Delray Beach, FL: Soil Water Conservation Society. St. Lucie Press.

Lal, R. (1994b). Sustainable land use system and soil resilience. In D. J. Greenland & I. Szabolc I (Eds.), *Soil resilience and sustainable land use*, (pp. 41–67) Walingford: CAB International.

Laursen, E. M. (1960). Scour at Bridge Crossings, ASCE Hyd. Div. Jour., Vol. 89, No. Hyd 3. Laursen, E. M., (1980). Predicting Scour at Bridge Piers and Abutments, Gen. Report No.3, Eng. Exp. Sta., College of Eng. Univ. of Arizona, AZ.

Maidment, D. R. (1993). *Handbook of hydrology*. New York, USA: McGraw-Hill.

Meyer, V., Haase, D., & Scheuer, S. (2009). Flood Risk Assessment in European River Basins—Concept, Methods and Challenges, exemplified at the Mulde River, *Integrated Environmental Assessment and Management*, Vol. 5, 17–26.

Mizuyama, T., Kobashi, S., & Ou, G. (1992). Prediction of debris flow peak discharge, Proc. Int. *Symposium Interpraevent, Bern, Switzerland, 4,* 99–108.

Nagler, F. A. (1918). Obstruction of bridge piers to the flow of water. Trans. ASCE, Vol. 82.

Rickenmann, D. & Koch, T. (1997). Comparison of debris flow modelling approaches, Proc. First Int. Conf. on Debris Flow Hazards Mitigation, San Francisco, USA, ASCE: 576–585.

Şen, Z. (1995). *Applied hydrogeology for scientists and engineers* (p. 496). New York: CRC Press.

Şen, Z. (2004). Saudi geological survey (SGS) hydrograph method—Arid regions (Wadi Baysh) (Technical Report), Saudi geological survey, p 40.

Şen, Z. (2008). *Wadi Hydrology* (p. 347). New York: Taylor and Francis Group, CRC Press.

Şen, Z. (2010). *Fuzzy logic and hydrological modeling* (p. 340). New York: Taylor and Francis Group, CRC Press.

Şen, Z. (2014). Sediment yield estimation formulations for arid regions. *Arabian Journal of Geosciences, 7*(4), 1627–1636.

Şen, Z. (2015a). *Applied drought modeling, prediction, and mitigation* (p. 472). Amsterdam: Elsevier.

Şen, Z. (2015b). *Applied drought modeling, prediction and mitigation* (p. 492). Amsterdam: Elsevier.

Takahashi, T. (1991). *Debris flow, IAHR monograph series*. The Netherlands: Balkema Publishers.

Takahashi, T., Sawada, T., Suwa, H., Mizuyama, T., Mizuhara, K., Wu, J. et al. (1994). *Japan–China joint research on the prevention from debris flow hazards*, (Research Report, Japanese Ministry of Education, Science and Culture, Int. Scientific Research Program No. 03044085).

Throne, C. R., Bathurst, J. C., & Hey, H. D. (1987). *Sediment transport in gravel-bed rivers*. New York: Wiley.

Walker, B., & Fell, R. (Eds.) (1987). Soil slope instability and stabilization, Balkema.

Walling, D. E., & Webb, B. W. (1986). Solute transport by rivers in arid environments: An overview. In: *Proceedings of International Symposium on Erosion and Sedimentation in Arab countries. Iraqi Journal of Water Research*, Vol. 5: 800–822.

Wischmeier, W. H., & Smith, D. D., (1978). Predicting rainfall erosion losses—A guide to conservation planning. U.S. Department of Agriculture, Agriculture Handbook No. 537.

Yalin, M. S. (1972). *Mechanics of sediment transport* (p. 290). Oxford, G.B.: Pergamon Press.

Yarnell, D. L. (1934). Bridge piers as channel obstructions. U.S. Dept. of Agriculture, Technical Bulletin No. 442.

# Chapter 8
# Climate Change Impact on Floods

**Abstract** One of the most effective climate change impacts is on the unexpected occurrences of floods and especially flash floods. The impact on water resources is the most concerned affair not only for water resources management but also on the food security of a region or country. Engineering risk management is very significant factor in climate change assessment and impact intensity calculations on engineering water structures. In order to enhance and perform a better idea about the impacts of the climate change fact, various exemplary application cases are presented in this chapter. Especially, innovative trend analysis provides whether there is an increasing trend in the past records to plan for future and additionally what are the positions of high and extreme rainfall cases that may give rise to flood occurrences?

**Keywords** Climate change · Impact · Innovative trend · Risk management Vulnerability · Water structure

## 8.1 General

During the last three decades, the climate change impact caused unprecedented flood and drought event occurrences with frequency, intensity, and duration increments that are comparatively different than the past records. Additionally, such events led to inflicting damages, and as a result of global warming, climate change started to impact water resources supply and demand, (IPCC 2007, 2013). It is by now well known that the climate change is due to increase in the atmospheric greenhouse gases (GHG) concentration that gives rise to causative effects and complicated relationship with flood and its risk. It is not only the occurrence of rainfall events that cause to flood events, but also unplanned land use and unreliability of precipitation predictions (especially sudden or in short time occurrences) through even by means of the most advanced numerical weather prediction models coupled with statistical and stochastic methodologies. Temporal and spatial variabilities of precipitation are other key factors that pour uncertainty ingredients into

the prediction affairs. Under the influence of climate change, present flood prediction methodologies must be revised in such a way that especially the database for future flood and risk analyses should cover not only temporal but also areal variabilities. Climate change-related flood risk calculations on the regional level can be improved by updating the present methodologies according to the environmental circumstances.

The atmospheric environment is conspicuous, and the daily life takes place in it with lithosphere, biosphere, and hydrosphere partners. The atmospheric dynamics can be appreciated through the natural extreme events such as volcanic activities, earthquakes, tornadoes, floods and droughts and normal meteorological, hydrological and environmental dynamics. In order to understand the causes of floods, one should take into consideration first the atmospheric (climate change) and tropospheric (meteorological) dynamisms. Conventional flood calculation methodologies are based on the meteorological events, and especially, the rainfall intensity, but the intensity must be revised with the climate change effect. Otherwise, the prediction of peak discharge and design discharge is bound to remain as underestimations. The climatological and meteorological studies have advanced tremendously during the last 100 years, but presently, they are rather stagnant, because the climate change-dependent methodologies are not yet sufficiently available for practical uses in many water-related projects. Climate change impact projections are available based on different scenarios, but their practical usages are not available for many parts of the world. The end products of such scenario studies must be brought to the attention of layman and practical engineering levels so that the knowledge and scientific information can be used beneficially in application projects. For instance, in the simplest rational method, the rainfall intensity is the sole variable for peak discharge calculation in small watershed areas, but the intensity–duration–frequency (IDF) curves are all based on the past records. Atmospheric research centers and meteorological services collect various objective meteorological data continuously for decades, which are fundamentals in understanding of the interconnectedness of atmospheric and tropospheric dynamics. Numerical and linguistic (verbal) information and data are abundant, but most methodologies use numerical database only. However, linguistic statements, rational and logical rule bases are also important in the model construction, and especially, in model modification studies to suit the local circumstances for reliable predictions (Şen 2010). All of the numerical records and linguistic knowledge help to sharpen vision concerning atmospheric and tropospheric processes. Furthermore, during the last 3–4 decades satellite imagery allows researchers to understand more comprehensively the atmospheric dynamic events and consequent earth surface occurrences such as floods and droughts. Even with the availability of all the scientific and methodological facilities, one cannot make predictions with complete safety, but with very small risk so that the human life and property are subjected to the least hazardous consequences. One may think that such qualitative and linguistic data are not important in the prediction of future similar event occurrences, but they help to adjust the objective numerical methodology results based on actual measurements.

Whatever the origin of the climate models, they all predict tropospheric global warming with some rainfall increases or decreases temporally and spatially at different parts of the world. In general, there is a direct effect of the global warming on the hydrological cycle, the main source of water resources (surface and groundwater) and accordingly, the engineering water structures must be managed or new ones must be planned by taking into account the climate change effects. The warmer becomes the climate of a region, the less will be the snowfall, and hence, reduction of natural water storages as snow cover will decrease especially at high elevations and polar regions, and in late spring and early summer, surface flow amounts will decrease. This will have a direct and very significant effect on the local and regional water resources collection and distribution systems. For instance, at the Euphrates–Tigris River basin upstream parts in Turkey, the snow falls are observed as decreasing trends during the last two decades, and hence, the river discharges are at reduction direction (Şen et al. 2010). With more than one-sixth of the earth's population relying on glaciers and seasonal snow packs for their water supply are likely to be severed by the consequences of these hydrological changes including future water availability (Barnett et al. 2005).

During the twenty-first century, the impacts of climate change might lead to crucial effects, if necessary precautions are not taken according to the global warming expected patterns. In many cases, flood waters are not used in beneficial way especially in developed countries. However, in some arid regions, flood waters are impounded behind small surface reservoirs and by a set of injection wells behind the reservoir; impoundment water is injected to underlying aquifers, which are of unconfined types. This is the one of the beneficial ways to render flood or flash flood waters as groundwater recharge sources in arid and semiarid regions (Şen et al. 2011).

Global change and consequent climate change impacts on the water, food, forest, lake, and environment have been searched intensively in the literature. However, the engineering structures subject to these effects are vague in an almost nonexistent manner. Each engineering water structure should be planned, designed, operated, and maintained according to the local and regional climate and future climate change impacts. The interdependencies between the climate change and infrastructure need to be managed well under the light of present and future global warming effects. The present capacity improvements and managements of any infrastructure are becoming more important due to the climate change impact.
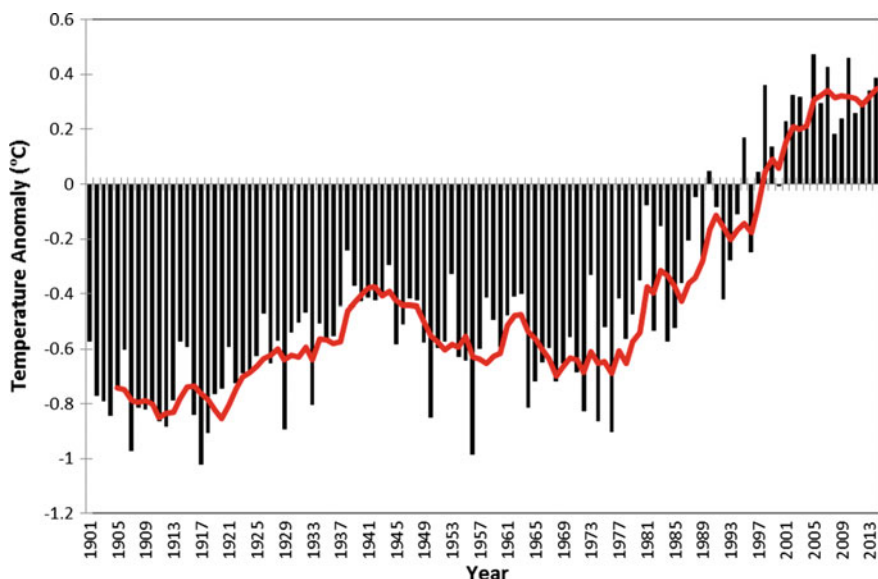
This chapter focuses on the floods within a wider context of climate change impact. The necessary concepts of global warming and the consequent climate change implications on the meteorological and hydrological aspects are explained for safer future predictions of floods.

## 8.2  Global Warming, Climate Change, and Water Resources

Current increase in the earth's average temperature is referred to as the global warming. The climate change does not focus only on the temperature increments, but also on precipitation, evaporation, wind speed and direction, sea-level changes, dry and wet periods concerning their extreme values, intensities and frequencies. In these contexts, climate change attracts more attention, because its changes are concerned directly with top significant human issues such as water resources, food security, forestry. Figure 8.1 reflects the global temperature anomalies for the past 110-year duration.

Water resources structures are major social and engineering units that are among the basic essentials for individuals, societies, countries, and humanity, in general. The development of any country is measured with the water resources system availability and adaptation to natural (droughts and floods) and man-induced (including climate change due to global warming) variations. Climate change can be regarded as one of the accumulating variability, and therefore, in any future project design, its impacts must be taken into consideration.

The potential impact of climate change on the hydrological regime is a crucial question for water resources engineering structures and system management.



**Fig. 8.1** Global mean air temperature anomaly (°C) obtained from Climatic Research Unit (CRU) monthly time series data for the period 1901–2014. The anomaly is calculated with respect to base period 1981–2010 and solid line (red) filters 5-year running mean

Potential change in hydrological regime resulting from climate change is an important topic in contemporary hydrology and water resources management.

Water supply systems and their managements are vulnerable for future climate change effects, and therefore, they need to essential engineering structures, which enable safe and reliable supply and distribution through properly designed infrastructures. Especially, summer and winter extreme weather events cause droughts and floods more frequently and severely than the past seasons affecting water structures.

As the climate continues to change, the difficulty in meeting the challenge of maintaining a robust and reliable infrastructure system increases. This is especially true as infrastructure sectors have developed into highly technical and interconnected systems. If one sector is at risk, so are the rest at different levels. If floods damage our energy supply, all other services can be affected, causing a cascade of failure (RAE 2011). These points indicate that engineers have a significant role in adaptation and mitigation works against the climate change impact through climate change-resistant water structural designs.

The IPCC (2007, 2013) reports on climate impact studies suggest large differences in the vulnerability of water resource systems to climate variables. Isolated single-reservoir systems in arid and semiarid areas are extremely sensitive to climate change. They lack the flexibility to adapt to the climate impacts that could vary from decreases in reservoir yields in excess of even more than 50% at one extreme to seasonal flooding increase at the other. In contrast, highly integrated regional systems are inherently more robust. Climate change will affect the complex infrastructure of engineering structural systems in place to manage the society's water demand and existing climate variability. It is not that the construction of additional dams that indicates the development level of a country, but rather an efficient management program of the existing water structures and from now on by taking into consideration the climate change impact.

Long-range water availability and short-term variability are expected under the climate impacts. Potential regional impacts of climate change could include increased frequency and magnitude of floods and long-term changes in mean renewable water supplies through changes in precipitation, temperature, humidity, wind intensity, duration of accumulated snowpack, nature and extent of vegetation, soil moisture, and runoff (Solomon et al. 2007).

After a detailed climate scenario models, Arnell (1999) showed that the climate change will cause to global average precipitation increases, but much of it will fall over the oceans. Additionally, increase in the evaporative demand is expected to be associated with higher temperatures leading to river runoff decreases across large parts of the world. However, especially in arid and semiarid regions, flash flood frequency and magnitude increases are expected.

As stated by Gleick (1998), climate change is one of the pressures facing water resources and their management over the next few years and decades. Herein, pressure means on water supply and demand sides. Especially, supply side is directly related to climate change, because after all, precipitation and runoff are the main sources of surface water engineering storage structures and groundwater

storage, and recharge to aquifers. On the demand-side pressure, there are social affairs such as population increase, extravagant life style, more consumption in almost all aspects of modern life, land use, energy generation. On the other hand, Kundzewicz and Somlyody (1997) provided a discussion on climate impact uncertainties analyses on water resources, water management planning, design, and adaptation. A detailed account has been given by Kundzewicz et al. (2008) on the implications of projected climate change for freshwater resources and their management. Climate change effects are the focus of many scientific, engineering, economic, social, cultural, and global nuisances, and these effects await cost-effective remedial solutions (Şen 2009).

One-third of the developing world will face severe water shortages in the twenty-first century even though large amounts of water will continue to flood annually to sea from arid regions (Keller et al. 2000).

Water supplies and quality are highly sensitive to climate variability and change. Relatively small changes in precipitation, evapotranspiration, snowmelt, sea-level rise, and other factors can have a substantial impact on the supply and quality of water resources.

Temperature will be an important factor in determining key vulnerabilities for water resources. Higher temperatures will speed the hydrological cycle, increasing evapotranspiration, and hence, increasing the risk of more intense droughts and precipitation events. Higher temperatures will also result in more precipitation as rain rather than snow and in a shorter season for precipitation as snow. This could have important consequences for regions dependent on snowpack (Stewart et al. 2004).

Clearly, changes in precipitation will have a very important impact on determining key vulnerabilities. In a Mediterranean climate, where most of the precipitation occurs in the winter half year, summer temperatures, which, as noted above, drive evapotranspiration, are a very important factor in determining key vulnerabilities in the hydrological sector. Thus, depending on circumstances' temperature, precipitation, or a combination of changes may be of paramount importance, and therefore, it is difficult to assign high confidence to broad generalizations on hydrological vulnerability to climate change, but rather a regional context is needed for projections of specific vulnerabilities. While global precipitation will rise with higher temperatures, and broad patterns of change in precipitation are becoming clearer, there is still substantial uncertainty about how regional patterns of precipitation might change. Nonetheless, some statements can be made about differences in vulnerability to changes in water supplies across some regions.

## 8.2.1  Climate Change Vulnerability

Changes in socioeconomic conditions, as population growth, improved technology, and application of practices such as detection of leaks from water systems can substantially affect the supply and demand for water resources. Thus, the effect of different socioeconomic factors in the climate change modeling scenarios can have

a larger effect on availability of demand for supply and quality of water resources than the change in climate itself. Other key vulnerabilities in water resources are the following.

(1) Reduction in the security of supply for public water systems, where either the volumes are reduced or the timing of streamflow and groundwater recharge changes. This is a particularly important vulnerability, where pressures on resources are already high such as in megacities in developing countries. As urbanization increases over the twenty-first century, the vulnerability of these areas to climate change may increase as well,

(2) Reduction in the availability of safe rural water supply in dry regions, where streamflow or recharge is reduced,

(3) Increases in the frequency and magnitude of flood losses due to increases in the volume or changes in the timing of river flows or flash floods. Poor countries and populations are particularly vulnerable and have limited ability to recover,

(4) Irrigation could be vulnerable through increases in demand and reductions in availability of suitable water at desired times as a result of higher temperatures and changes in the volume or timing of precipitation, streamflow, and groundwater recharge,

(5) Reduction in hydropower generation, if the volume of flows reduces and timing of flow changes. This could be a critical vulnerability for many nations or regions that draw a significant portion of their electricity production from hydropower,

(6) Sea-level rise will adversely affect water supplies in many coastal regions due to salinization of groundwater in estuaries, low-lying islands, and coastal plains,

(7) Decreased snowpack and melting of glaciers will adversely affect seasonal water storage in many mountainous regions, threatening water supplies in dependent communities and requiring management of water storages more for winter and spring flood controls than for summer irrigation.

Hitz and Smith (2004) reviewed global impact studies, but they could not find clear relationship between changes in water supply and increases in global mass transfer. They concluded that higher magnitudes of climate change are likely to increase stress for water resources. This is due in part to the fact that current water resource infrastructure is generally designed for today's climate. Results from global studies in this sector are highly inconsistent with some studies quite sensitive to the climate model and mode of aggregation (Arnell 1999, 2004) and others showing little net global impact (Vorosmarty et al. 2000; Doll and Siebert 2002).

## 8.3 Climate Change Effects on Floods

Factors other than average rainfall intensity can affect the PDF of flood peaks, and hence, the critical assumption of the design storm method is often not valid. The weaknesses of the design storm method are critical when it is used to evaluate complex strategies for flood mitigation.

Extreme events, such as floods are related to climate variability and change. The climate change causes some areas to suffer from more frequent and severe flooding. The impact of flood on groundwater resources is obvious (Şen et al. 2011). One impact of flooding causes a significant risk increase in groundwater contamination.

Hydrologists and climatologists have long been aware of the regional climate role in the floods predictions. With growing sense of a variable climate, it is appropriate to reassess the flood concepts, not as isolated events, but as phenomena connected on a worldwide scale.

Meteorological extremes are almost daily wonders in any society for social activities. Especially, floods must be taken into consideration in land use on the basis of flood-inundation risk levels (Chap. 3). Floods are conspicuous events and possible meteorological conditions for a given scale. They arise under uncommon meteorological and atmospheric conditions. Climate may not turn out to be a smooth continuum of meteorological possibilities after all, but rather the summation of multiple processes operating both regionally and globally on differing time scales. Floods are not periodic but rather random in the magnitude as well as temporal and spatial frequencies. Prior to flood assessment, the geomorphological, meteorological, and climate change impacts must be reviewed under the light of all available historical knowledge, information, and records. One must not confine the view only on the drainage basin, but also on the drainage transboundary, i.e., adjacent drainage basin features, and climate change effects for regional flood features must be taken into consideration.

Floods are also related to behavior of dry and especially wet years, but their comprehension and prediction are complex processes. The sequence of dry years is linked with droughts (Şen 2015), and wet years include floods in many places around the world. Floods in one location often exist within similar global climate configuration.

Some floods are typically many times as large as previous ones, but to find the hazardous floods and nearby inundation areas, field trips provide invaluable information for future planning and flood management studies. Such studies provide appreciation of a set of flood causes including channel slope, dangerous cross-sectional locations and specifications, and sediment load.

Prior to a quantitative model for flood discharge prediction, it is very helpful to look for rational reasons for various flood triggering mechanisms. As a version of flood, for instance, tsunamis occur as after effects of earthquakes and landslides. Natural or artificial (man-made) dam brakes give rise to flood at the downstream locations. Water levels in rivers can swell after each precipitation, but intensive precipitation occurrences cause further swell resulting in floods and inundations. River water level rises are most intimately tied to the whims of weather. Some floods are anticipated within hours or days, if not weeks. Floods as natural events do not provide enough warning time.

Flood occurrences are not just after effects of rainfall events. They occur due to rainfall on saturated grounds, which do not allow infiltration. Warm rainfall falls on snowpacks may cause to melting that may lead to flood triggering. Another reason for flood occurrence is due to some changes within the drainage basin

(urbanization, deforestation) with possible destruction flood hindrances so as to retain or heighten flood waters that would have otherwise rolled on through without making a mess.
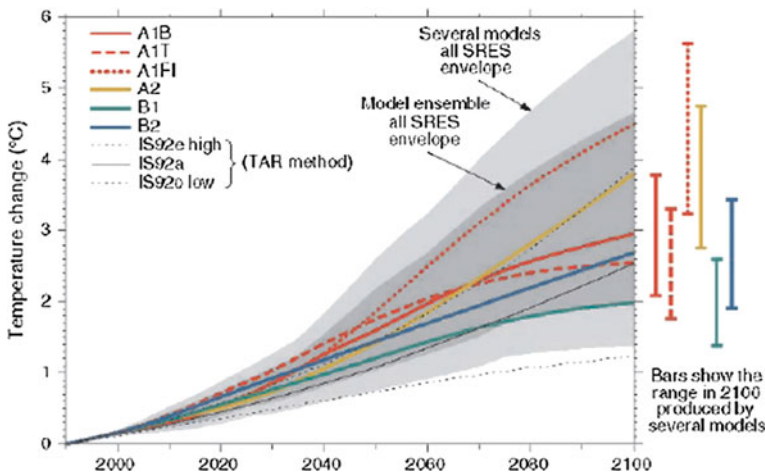
Melting of winter snow in spring is always a time of high river flow, and in many regions, river channels shape themselves to accommodate these annual flood events by building banks and gradually raising flood plain terraces in response to each year's high water. Melt waters will usually be released from the snow bound mountains in an orderly progression as spring time temperatures begin to rise. Floods will occur if temperatures rise faster than expected or if rain falls on snow that is already near its melting point.

In practice, there are many instances that a flood hits a drainage basin, but not adjacent ones. This is due to the geomorphological, urbanization and land-use practices that show difference from basin to another. In some of the drainage basins, villages, towns, and agricultural areas are wiped out. Floods are set up by large-scale atmospheric processes in local and regional scales.

For natural balance, greenhouse gases concentrations are essential for weather and climate dynamics. The effective radiation temperature of the earth–atmosphere system is equivalent to a mean radiative flux of about 342 $W/m^2$ (W per square meter). Due to industrialization, since 1850 the anthropogenic release of additional greenhouse gas amounts such as $CO_2$, $CH_4$, or $N_2O$ led to slight change in the atmospheric chemical composition. The radiative forcing of additional $CO_2$ amounts to 1.5 $W/m^2$, whereas for $CH_4$ to 0.5 $W/m^2$ and for $N_2O$ to 0.15 $W/m^2$. This is well below 1% of the effective exchange of radiant fluxes of the earth–atmosphere system, and therefore, difficult to measure or model. The inverse effects by aerosols, feed backs by clouds, and the biosphere increase further the challenges to correctly predict the climatic consequences of these additional greenhouse gas amounts. It is not yet known what will be the future emission rates, and this point also adds to the difficulty in predictions. In climate change modeling apart from the ground measurements, different scenarios are considered on the basis of population growth rate, energy needs and means of energy production, and geographical distribution of production and wealth. Climate change impact models rely on scenarios that include certain assumptions even on expected economic developments. Hence, the scenarios are the main source of the uncertainty of the IPCC forecast (IPCC 2007), and they predict about 1.4–5.8 °C temperature increase by 2100 as shown in Fig. 8.2.

## 8.4   Climate Change and Dams

After the entrance of "climate change impact" into calculation domain, the question about what is a "safe dam" cannot be answered properly. Engineers design dams and their spillways to cope with the extreme floods that they predict using past records of streamflow and precipitation (Chaps. 2 and 6). It is vital that spillways are adequately dimensioned; otherwise, a high risk of a dam break comes into view.

**Fig. 8.2** Predicted global changes in temperature for various scenarios predicted by different GCM (Global Circulation Models), from IPCC (2007)

So far in the calculations, it was assumed that there is a stable climate, which implied that the future is the reflection of the past, which is no longer a valid assumption since the start of climate change debates about three decades ago. Not only precipitation, but accordingly runoff volumes are also changing, and under the current aspects of the climate change, the present change is expected to continue.

As noted in a World Commission on Dams' background paper: "The major implications of climate change for dams and reservoirs are firstly that the future can no longer be assumed to be like the past, and secondly that the future is uncertain." The climatologists agree almost universally that more extreme storms and increasingly severe floods are expected to occur in the future. Unfortunately, the vast majority of dam proponents and operators do not care for the climate change impact on dam safety.

The world's more than 45,000 existing large dams have not been built to allow for a rapidly intensifying hydrological cycle due to climate change, and therefore, without the climate change impact consideration, many dams are unsafe. The several hundreds of billions of dollars that may be necessary to make existing dams "safe" under the existing climate would likely be dwarfed by the expenditure needed to upgrade the world's stock of dams to allow for floods far bigger than predicted by hydrological history.

There are so many societal, technological, ecological, and climatological variables to know with some degree of precision concerning the magnitude of future extreme floods. Risk management is intimately related to greenhouse effect, and many climate change assessments have alluded to risk, but only recently formal links have been made between climate change and risk management frameworks.

Climate change assessment and risk management have many elements in common including the need to manage uncertainty, the linking of hazards and

consequences, communication between technical experts and stakeholders, the mitigation of risk by reducing both the hazard and consequences of those hazards, and formal processes to link all of these activities. Risk management is an iterative process. Three iterations of risk management can be identified through the overriding questions being addressed through successive assessments. These are,

(1) Do greenhouse gas emissions pose a sufficient risk to warrant a significant response?
(2) What are the risks of unmanaged climate change and what type of responses may be needed? Climate modeling based on those scenarios has been conducted and impacts and adaptation assessments resulting from climate scenarios are derived from that information,
(3) How does one manage climate risks across appropriate scales, different groups, and at different locations?

The two major forms of risk treatment are the mitigation of climate change through the abatement of greenhouse gas emissions and sequestration of greenhouse gases, and adaptation to the consequences of a changing climate. Mitigation reduces the rate and magnitude of changing climate hazards associated with the enhanced greenhouse effect, whereas adaptation reduces the consequences of those hazards. This relationship has important ramifications for identifying and treating climate change risks. On the one hand, adaptation and mitigation treat different parts of climate risk, so they are complementary processes in risk reduction. On the other hand, their benefits will appreciate at different time scales, and in many cases, adaptation and mitigation measures can be assessed and implemented separately.

Many of the commonly recommended adaptation options to address climate change in the water resources sector, including water conservation and preparedness for extreme events, are based on strategies for dealing with current variability (coping with climate changes). Structural adaptations, such as dams, weirs, and drainage canals, tend to increase the flexibility of management operations, although these adaptation options generate social and environmental costs.

Since flood risk tends to rise in many areas, increasing attention is being paid to upgrade flood protection systems. In order to improve flood preparedness, one has to select adequate site-specific measures, both structural ("hard"), defenses such as dikes, dams and flood control reservoirs, diversions and non-structural ("soft") measures. The latter include watershed management (source control), i.e., modifying flood formation by "catching water where it falls." With certain practices of land-use control and soil conservation, one can enhance water storage on the land surface or underground. Improved preparedness can be achieved by advance in awareness, information, flood forecasting–warning system; regulations, zoning, and insurance. However, no flood protection measure guarantees perfect safety and complete protection. There is no single one-fits-all measure; hence, a site-specific set of measures is advisable (Kundzewicz et al. 2008).

## 8.5  Risk Management Frameworks
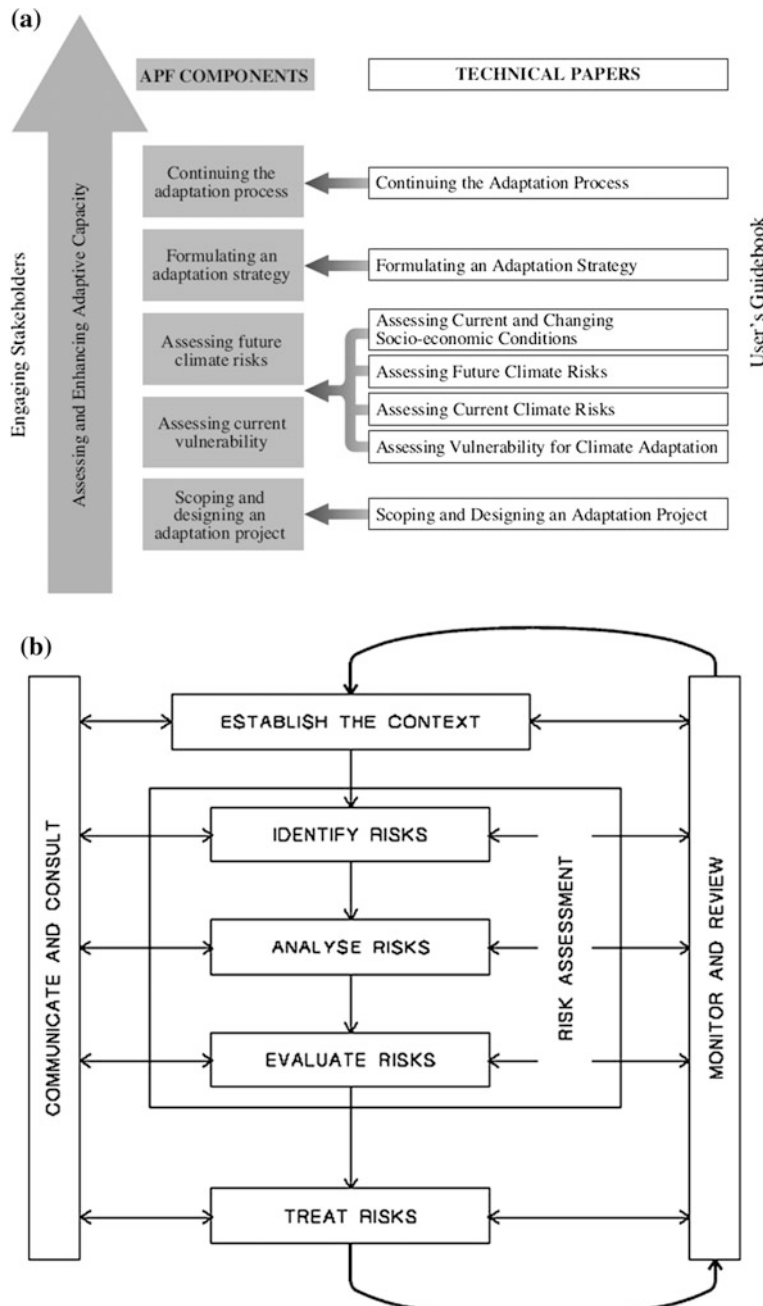
Risk management is defined as the culture, processes, and structures that are directed toward realizing potential opportunities while managing adverse effects. This definition also serves as an appropriate aim to guide adaptation to climate change-related risks. Risk itself is defined as the combination of the probability of an event and its consequences, and where it is recognized that there may be more than one event, consequences can range from positive to negative and probabilities, and they can be measured qualitatively or quantitatively.

The application of risk management in the past has been hampered by the wide range of different definitions for the same terms. Recent steps to standardize risk management internationally promise to remove some of the confusion caused by different nomenclature and approaches (Fig. 8.3). This figure as suggested by IPCC (2007) WGII Fourth Assessment Report compares the UNDP Adaptation Policy Framework and the AS/NZS 17 (2004) risk management standard. The two frameworks have a great deal in common including 18 scoping, risk analysis, evaluation of treatment measures and implementation, monitoring, and 19 stakeholder's involvement.

Risks associated with climate change take on a variety of forms. Primary climate risks include the direct effect of climate and climate-related hazards, which range in scale from small, local effects to dangerous climate change. Climate change impacts can also lead to secondary risks, such as those associated with land degradation or species loss, where climate change may be a partial, but not the sole factor. Tertiary risks are twice removed such as those occurring in business servicing sectors affected by climate change.

Climate-related risks can be identified by characterizing a particular climate hazard, or by identifying climate as a significant driver interacting with other factors. Main streaming is a process that integrates climate with other change factors for the purposes of management. Methods that focus directly on the assessment of adaptive capacity and specific adaptation measures will generally be based on an understanding of adaptation to current climate risks.

A further set of risks is associated with the implementation of policies or measures associated with climate change such as adaptation and mitigation. To date, such risks have generally not been explored through formal frameworks, but have been assessed in an ad hoc manner separately from the assessment of direct and indirect climate-related risks. A growing literature on integrated assessments and climate policy is addressing these issues. A significant advantage of risk management approaches is that such issues can be explored without any need to advocate a particular view or normative outcome, beyond the broad requirement to avoid dangerous anthropogenic interference.

**Fig. 8.3** Comparison of **a** the AS/NZS 4360:2004 risk management standard with **b** the UNDP Adaptation Policy Framework. *Note* The direction of analysis flows downwards in the former and builds upwards in the latter
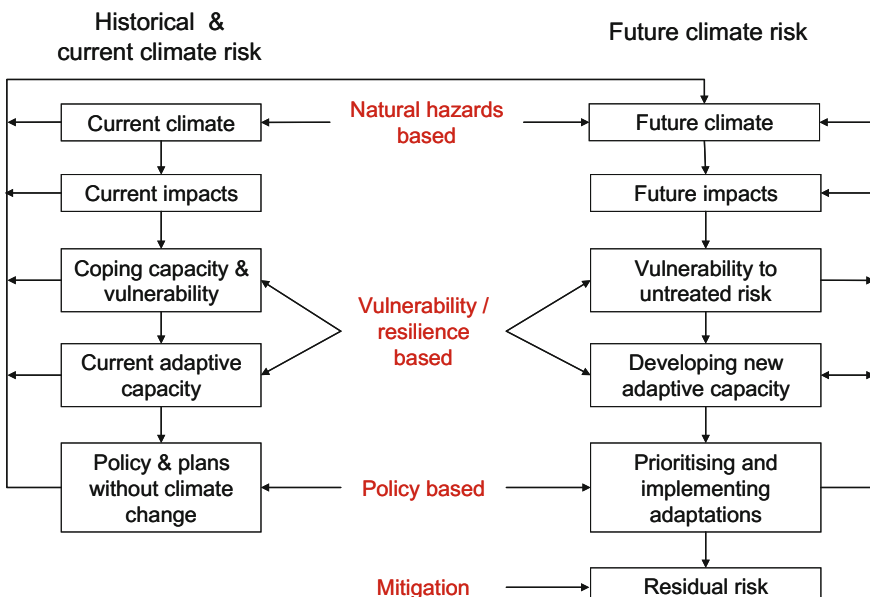
## 8.5.1  Methods of Climate Risk Management

A range of different orientations (describing approaches to space, subject matter, and time) can be applied to risk management. Here, one may classify three different templates according to their focus on the central subject matter. Figure 8.4 shows the major elements of the climate change impacts, adaptation, and vulnerability assessment processes, and positions of the main analytical approaches (IPCC 2007).

The left-hand side of the figure shows the rise in importance of the assessment of a range of historical and current factors, which progresses well beyond the construction of baseline data.

In any climate risk management, the following sequence of items must be taken into consideration.

(1) A conventional natural hazards approach, where climate scenarios are projected through impact models to assess outcomes. The natural hazards approach is so named after the process used in the discipline of the same name, which identifies the hazard, assesses its likelihood and impact before going on to define vulnerability. Treatment can then reduce the consequences of an event (e.g., adaptation), or modify the event itself (e.g., mitigation). Such methods are guided by coarse-scale scenarios, which may be downscaled to an appropriate resolution.



**Fig. 8.4** Flow chart showing relationship of different assessment approaches with the process of assessing current and future climate risks. Though highly simplified, the arrows aim to highlight how simple pathways through the assessment, cross-links, and inverse methods are all possible, depending on the project scope and context

(2) A vulnerability-based approach, where initial criteria such as critical thresholds are set and their levels of exceedance then assessed. Vulnerability and resilience-based approaches focus on socioeconomic or physical outcomes to which some value has been attached and can address either or both current and future states. Vulnerability concentrates on the downside of risk and resilience approaches focus on adaptation and adaptive capacity. Much of the assessment at the local scale is not specifically concerned with whether a particular level of change is dangerous, but instead deals with development pathways, researching the implementation of adaptation measures with different institutions and stakeholder groups.

(3) Vulnerability assessed at the global scale pursues the notion of dangerous anthropogenic interference, where risk approaches are applied in integrated assessments of the likelihood of exceeding dangerous levels of global warming or sea-level rise (Jones 2005; Wigley 2004). In this approach, lower and upper levels of global warming are identified, and the lower levels signifying climate changes that appear to be inevitable regardless of foreseeable actions to reduce greenhouse gases (GHG) emissions, and hence, requiring adaptation (either to exploit benefits or avoid damage), and the upper levels are maximum tolerable changes in climate beyond which unacceptable impacts would result, hence requiring mitigation. These approaches can either focus on the upside or downside of risk and take both exploratory and normative pathways.

(4) A policy-based or normative approach, where current or future policies are investigated to determine whether their aims are achieved under a changing climate. Policy-related assessments focus on how current or proposed policies and plans may be able to cope with climate change and how they may be modified to better meet their objectives. Several risk assessment frameworks have recently been developed that focus on adaptation. These frameworks are explicitly based on risk assessment methods but take a range of approaches.

Baseline adaptation, existing adaptive capacity, and adaptations to historically experienced climate risks are all utilized, especially when they have been developed to deal with climate variability and extremes, which are more difficult to simulate in climate models.

## 8.6 Impacts, Adaptation, and Vulnerability Assessments

Climate change adaptation requires learning from the past experiences linguistically and numerically compared to the present climate. Although the case for the use of risk management toward adaptation to climate change has been considered by many researchers among whom are Jones (2001, 2004a, b), UKCIP (2003) and UNDP (2005), it is increasingly being accepted that there remains a great deal of uncertainty about which approach to use (Carter et al. 2007).

Climate change adaptation has several different directions for assessment such as through a natural hazard approach, assessments according to current and/or future climate or by vulnerability assessments and resilience of different groups over time.

Majority of climate change impacts, vulnerability and combat are based on fossil energy (the main source of anthropogenic greenhouse gas emissions) sources assessments. Sinks and adaptation assessments are given less weights. Currently, energy supply relies predominantly on fossil fuels, and therefore, energy policy has the logical basis for mitigation. Among the policies, there are a wide range of options for sequestering carbon in vegetation, oceans, and geological formations, and hence, to reduce the sectoral vulnerability and impacts on the communities by means of adaptation.

There is a relationship between the climate policy and sustainable development. Reductions in greenhouse gas emissions might reduce the impact of air pollution and enhance the ecosystem integrity, which are significant ingredients of sustainable development. It is very essential to focus on the interrelationships between adaptation, mitigation, response capacity, and development patterns. If climate policy and sustainable development are combined in an integrated way, then it is possible not only simply to evaluate specific policy options that might accomplish both goals, but also to explore the determinants of response capacity that underlie those options and their connections to underlying socioeconomic and technological development paths.

Global scale climate change impact researchers have different opinions about formulation of the adaptation–mitigation linkages. Some consider them as substitutes and seek the optimal policy in cost–benefit frameworks, while others emphasize the diversity of impacts (with little scope for adaptation in some sectors) and the asymmetry of social actors who need to mitigate versus those who need to adapt.

Afforestation, reforestation, and forest conservation have been advocated for decades as essential mitigation options. Based on an extensive survey of dissolved carbon in the Amazonian river system, Mayorga et al. (2005) suggest that a small and rapidly cycling pool of organic carbon accounts for the large carbon fluxes from land to water to atmosphere in the humid tropics. Another study emphasizes that in arid and semiarid regions afforestation massively reduces water yields, which has direct and wide-ranging negative implications for adaptation options in several sectors such as agriculture (irrigation), power generation (cooling towers), and ecosystem protection (minimum flow to sustain ecosystems in rivers, wetlands, and on the banks). Afforestation and reforestation may also have negative impacts on biodiversity, as shown by Caparrós and Jacquemont (2003), due to the overplantation of fast-growing alien species. These studies demonstrate the intricate relationships between climate change mitigation, adaptation, and also linkages to other environmental concerns such as water resources and biodiversity with profound policy implications.

While the implications of some mitigation strategies for adaptation and other development and environment concerns have been recognized recently, the effects of adaptation on greenhouse emissions have been known much longer but have

remained largely unexplored. For example, many adaptation options are known to involve increased energy use, and hence, interfere with mitigation efforts if the energy is supplied from carbon-emitting sources. Yet it is not straightforward to separate the adaptation effects from those of other drivers in regional or national energy demand projections.

The IPCC Third Assessment Report (TAR; Smith et al. 2001) identified five "reasons for concern," which individually, or in combination, could be used to determine a "dangerous" level of climate change. The five reasons for concern each addressed the relationship between an increase in global mean temperature.

(1) Risks to unique and threatened systems,
(2) Risks from extreme climate events,
(3) Distribution of impacts,
(4) Aggregate impacts,
(5) Risks from future large-scale discontinuities.

## 8.6.1 Vulnerability Reduction in Climatic Variability

Some researchers recently reported that vulnerability reduction to current climatic variability can go a long way toward reducing vulnerability to hazard increment risk associated with climate change, emphasized the extra value to be gleaned if measures designed to reduce vulnerability are also sustainable. To a large extent, adaptation measures for climate variability and extremes already exist. Measures to reduce current vulnerability by capacity building rather than distribution of disaster relief, for example, will increase resilience to changes in hazard caused by climate change. Similarly, the implementation of improved warning and forecasting methods and the adoption of some land-use planning measures would reduce both current and future vulnerability. However, many responses to current climatic variability would not in themselves be a sufficient response to climate change. For example, a changing climate would alter the design standard of a physical defense, such as a realigned channel or a defense wall. It could alter the effectiveness of building codes based on designing against specified return period events (such as the 10-year return period gust). Finally, it could alter the area exposed to a potential hazard, meaning that development previously assumed to be "safe" was now located in a risky area.

Coping with current changes in climatic variability and extremes will build learning in dealing with future climate changes and will enhance coping abilities of communities. Since climate change will likely manifest itself through changes in variability as well as in overall trend, methods used to cope with past and emerging patterns in climatic variability will be a useful starting point for the design of future.

## 8.7 Risk Assessment Under Climate Change Effects

Global warming is a term used for the average temperature increase in the lower atmosphere (troposphere), and it triggers various hydrological elements and the hydrological cycle itself at different scales depending on the location on the world. Although there are numerous literature studies concerning the effect of climate change on the hydrological elements (temperature, precipitation, evaporation, wind, runoff, flood, drought, etc.), unfortunately, the performance of the engineering water structures are not taken into consideration. As an integral part of the whole water resources systems, the engineering structures such as dams, canals, culverts, wells are also subject to climate change impacts. This section examines the climate change performance of the engineering structures by taking into account the climate change impact on the risk assessment formulation. For this purpose, the risk concept is redefined, and the climate change impact is taken into account by a climate change factor depending on the historical record trend slope increment or decrement. The risk levels are revised for 10-year, 50-year, and 100-year return periods. The application of the proposed methodology is given for three separate meteorology station precipitation records from the northeastern European province of Turkey and the same number of stations from the Kingdom of Saudi Arabia (KSA).

All climate change models indicate that the Arabian Peninsula is bound to take more frequent and intensive rainfall occurrences with the impact of global warming and climate change, and therefore, the present water resources system must be adapted to this situation, or the new ones must be planned accordingly. On the other hand, the rainfall may increase in one area and decrease in other areas of the Arabian Peninsula in the future climate (Almazroui 2013).

### 8.7.1 Modified Engineering Risk Assessment Due to Global Warming

In general, risk is defined as the probability of an extreme event occurrence during specified time duration. Among the global warming climate-related extreme events are droughts or floods that are very important in the water resources structures design, planning, operation, and maintenance stages. In the risk definition, there are two important parts that imply quantities. These are "extreme events" that occur over various "time durations." An event gains its extreme character provided that it transgresses a certain level. Nature is expected to break records continuously, because humans cannot know what might be the future maximum rainfall at any point of the world. As the new record breaks come in, the duration is also renewed as the time duration for the last extreme event to occur. In all these explanations, there is no engineering structure involved with the rainfall or runoff amounts.

Acceptable risk is a level of any injury or loss from a disastrous situation that is considered to be tolerable by a society or authority in view of the social, political,

and economic cost–benefit analyses. In any uncertain study, the solution cannot be achieved absolutely without error. Hence, a level of vulnerability is considered to be "acceptable" and balancing factors such as cost, equity, public input, and the probability of drought (Şen 2015).

In case of an engineering structure such as engineering water structures, their capacity of dam is related to the level for extreme event and risk definition (Chap. 7). For instance, the risk is defined as the overtopping of the dam once during its economic life that will damage its stability or cause damages. This is not only related to rainfall or runoff, but also related to other dam effective factors, which must be taken into consideration such as the sedimentation rate. Global warming will cause some water structures to under-perform or overperform depending on the climate change effect in the region. In general, for the calculation purposes convenient formulations must be developed. Logically, since the simple and classical risk, R, without consideration of climate change is equal to the probability of dangerous event occurrence, P, only once during the whole life duration of the structure, R, as given in Chap. 6, Sect. 6.4, Eq. (6.9). In this equation, the global warming and climate change effects are not taken into consideration. Logical and rational deduction renders this expression into the following form.
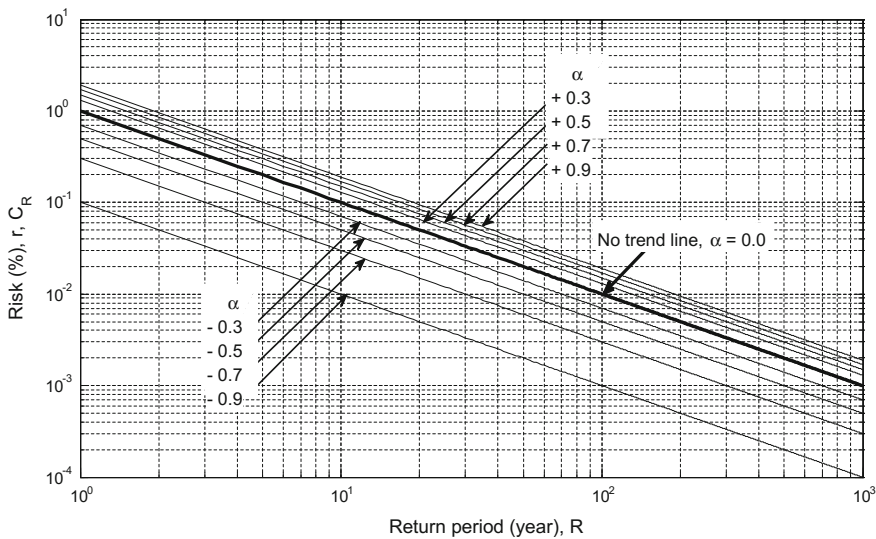
$$R_C = \frac{1 + \alpha}{R} \qquad (8.1)$$

Herein, $R_C$ is the simple risk under the climate change impact, and $\alpha$ is a climate change factor that reflects the climate change effect. If there is no climate change expectation, then $\alpha = 0$; otherwise, $\alpha$ might take positive or negative values. In this section, the climate factor is equivalent to the slope of trend component within the hydrometeorological time series. If there is no trend, then there is no climate change effect ($\alpha = 0$). However, in increasing and decreasing trend cases, $\alpha$ takes positive and negative values, respectively. Based on Eq. (8.1), Fig. 8.5 indicates the relationship between the climate change-incorporated risk and engineering structure life at different climate change factor values.

It is obvious from this figure that the severances are more pronounced in the dry (decreasing trend) case than the wet alternatives. This is logical because in the decreasing trend case, the demand on water amount, and hence, engineering water structures become more pronounced.

## 8.7.2  Applications

It is recommended that rather than the classical risk formulation, the simple and climate change effective risk approach, as suggested in this section, can be applied for future engineering structure designs. If sufficient storage capacities are not planned from now then much of the rainfall caused runoff and flood may end up as losses into the seas. It is observed that the inclusion of the climate change factor in

**Fig. 8.5** Climate change impacted risk-return period relationship

the risk calculation formulation generally leads to increase in the return period and risk compared to the conventional calculations.
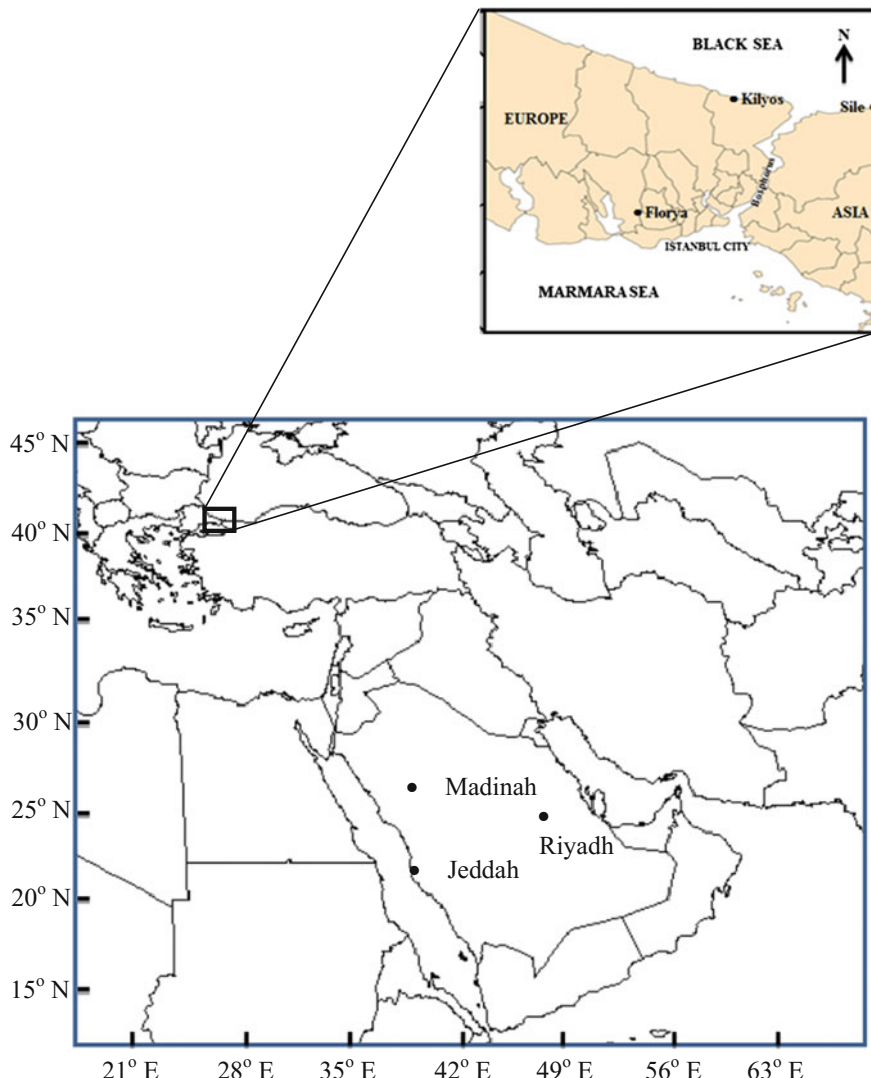
Application cases are given from two different countries, as representative of humid regions the northwestern part of Turkey and as arid country the KSA. The locations of the meteorology stations used in this study are shown in Fig. 8.6. Table 8.1 indicates the specific features of three meteorology stations from each country.

The time series of each station with trend component and the corresponding CDF for exceedence probability calculations reversal (rainfall amount calculation for any given probability level) are presented in Figs. 8.7 and 8.8 for Turkey and the KSA, respectively.

Table 8.2 presents global warming effect on each meteorology station in terms of climate change on the annual precipitation records also during the normal case (without climate change effect) statistics for 10-year, 50-year, and 100-year return periods. The comparisons between the climate change and normal cases are given quantitatively through the relative error percentages by use of Eq. (8.1). The relative error, $\beta$, is calculated by taking into consideration precipitation amounts under the effects of climate change, $P_c$, and no climate change, $P$, values into consideration according to the following expression.

$$\beta = 100\frac{P_c - P}{P_c} \tag{8.2}$$

In Table 8.2, the relative error percentages for Turkey are always greater than Saudi Arabia. This is a good indicator that Turkey will be more subjected to severe
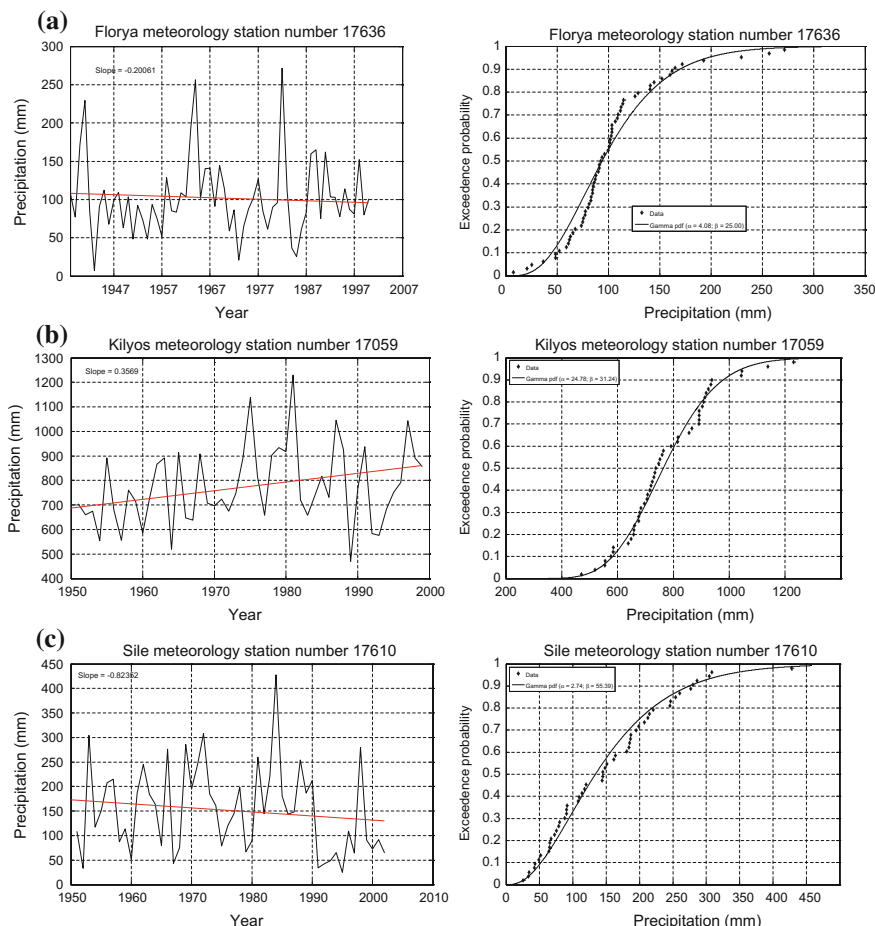
**Fig. 8.6** Meteorology station locations in Turkey and Saudi Arabia used in this study
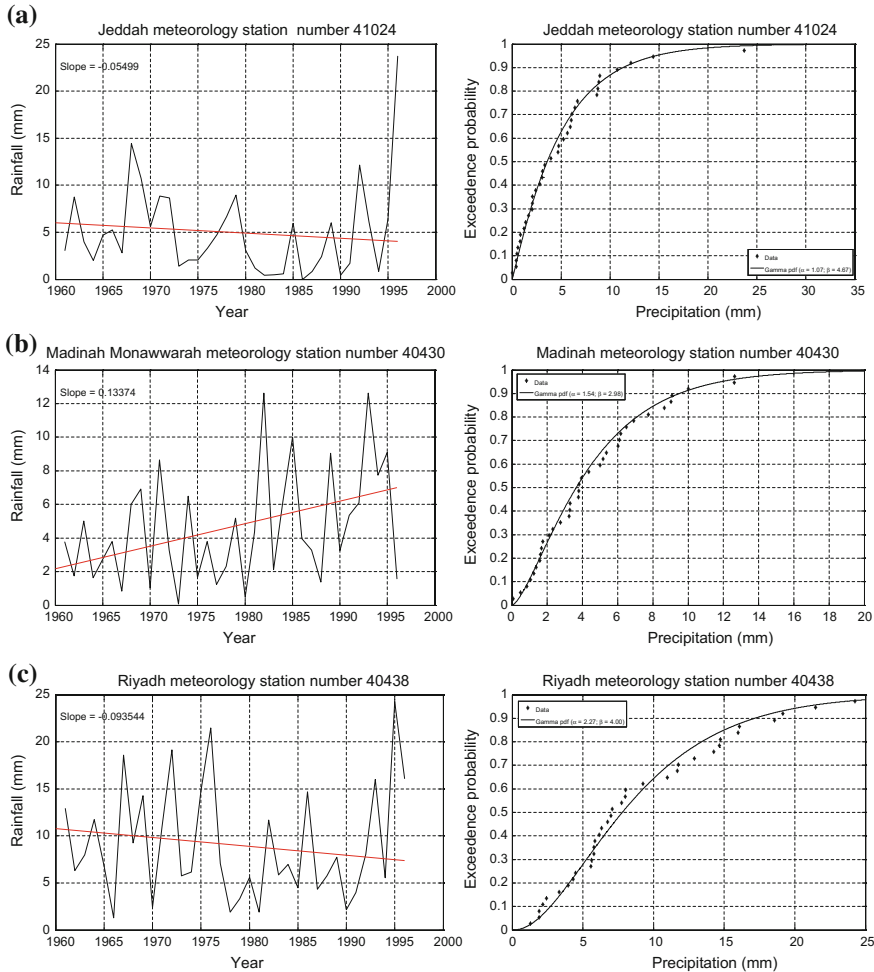
climate change impacts due to its location within the subtropical climate belt. Accordingly, more adaptation and mitigation works are necessary.

By taking into consideration the climate change risk level calculations from Eq. (8.1), one is then able to calculate the return periods according to the classical formulation in Eq. (6.9) as if there is no climate change impact. Hence, it is possible to see how the climate change impact causes for consideration of longer return periods than the classical calculations. The relative error percentages are calculated similar to Eq. (8.2) as,

**Table 8.1**  Station specifications

| Station name | Station number | Record duration | Arithmetic average (mm) | Standard deviation (mm) |
|---|---|---|---|---|
| *Turkey* | | | | |
| Florya | 17636 | 1937–2006 | 102.02 | 49.57 |
| Kilyos | 17059 | 1951–2006 | 774.09 | 159.09 |
| Sile | 17610 | 1950–2006 | 151.83 | 88.85 |
| *Kingdom of Saudi Arabia* | | | | |
| Jeddah | 41024 | 1961–1996 | 5.00 | 4.93 |
| Madinah | 40430 | 1961–1996 | 4.59 | 3.31 |
| Riyadh | 40438 | 1961–1996 | 9.08 | 5.96 |



**Fig. 8.7**  Turkish meteorology station trend and PDF graphs

**Fig. 8.8** Saudi Arabian meteorology station trend and PDF graphs

$$\gamma = 100 \frac{R_C - R}{R_C} \qquad (8.3)$$

where $R_C$ and $R$ are already defined earlier as the return periods with and without climate change impact, respectively. Table 8.3 includes all the quantitative values with the relative errors for comparison purposes.

A close inspection of this table indicates that the climate change impacted return periods are longer in Turkey than the KSA. This point indicates that the climate change impact is expected to be more pronounced and intensive in Turkey than the KSA. It is possible to generalize in saying that the tropical (arid regions) will not be affected as the subtropical regions from the climate change impact. From

**Table 8.2** Climate impact precipitation features

| Return period r | Climate effect | | Turkey | | | Kingdom of Saudi Arabia | | |
|---|---|---|---|---|---|---|---|---|
| | | | Florya | Kilyos | Sile | Jeddah | Madinah | Riyadh |
| | Climate change factor, $\alpha$ | | −0.200 | +0.357 | −0.923 | −0.055 | +0.134 | −0.094 |
| 10-year | Risk, $R_C$ | | 0.08000 | 0.0643 | 0.0177 | 0.0945 | 0.1134 | 0.0906 |
| | Precipitation (mm) | Climate change, $R_C$ | 178.61 | 1022.8 | 401.55 | 11.60 | 9.07 | 17.68 |
| | | No climate change, P | 169.71 | 978.9 | 274.75 | 11.33 | 9.50 | 17.16 |
| | Relative error (%), $\beta$ | | 4.98 | 4.29 | 31.57 | 2.28 | 4.53 | 2.95 |
| 50-year | Risk, $R_C$ | | 0.0160 | 0.0129 | 0.0035 | 0.0189 | 0.0227 | 0.0181 |
| | Precipitation (mm) | Climate change, $P_C$ | 238.07 | 1161.2 | 512.03 | 19.25 | 14.48 | 27.78 |
| | | No climate change, Pc | 230.19 | 1125.9 | 392.97 | 18.98 | 14.89 | 25.43 |
| | Relative error (%), $\beta$ | | 3.31 | 3.44 | 23.25 | 1.40 | 2.75 | 8.46 |
| 100-year | Risk, $R_C$ | | 0.0080 | 0.0064 | 0.0018 | 0.0095 | 0.0113 | 0.0091 |
| | Precipitation (mm) | Climate change, $P_C$ | 261.97 | 1214.8 | 556.02 | 22.51 | 16.76 | 29.01 |
| | | No climate change, P | 254.36 | 1181.0 | 441.10 | 22.26 | 17.15 | 28.56 |
| | Relative error (%), $\beta$ | | 2.90 | 2.77 | 20.67 | 1.11 | 2.27 | 1.55 |

**Table 8.3** Return period (year) comparison

| No climate change return period, r | Climate effect | Turkey | | | Kingdom of Saudi Arabia | | |
|---|---|---|---|---|---|---|---|
| | | Florya | Kilyos | Sile | Jeddah | Madinah | Riyadh |
| 10-year | Climate change risk, $R_C$ | 0.08000 | 0.0643 | 0.0177 | 0.0945 | 0.1134 | 0.0906 |
| | Climate change return period, Eq. (8.2) | 12.50 | 15.50 | 56.50 | 16.60 | 8.82 | 11.10 |
| | Difference | 2.50 | 5.50 | 46.50 | 6.60 | −1.18 | 1.10 |
| | Relative error (%), $\gamma$ | 20.00 | 35.48 | 82.30 | 39.76 | −13.38 | 9.91 |
| 50-year | Climate change risk, $R_C$ | 0.0160 | 0.0129 | 0.0035 | 0.0189 | −0.0227 | 0.0181 |
| | Climate change return period, Eq. (8.2) | 62.50 | 77.52 | 28.57 | 52.91 | 44.05 | 55.25 |
| | Difference | 12.50 | 27.52 | 21.43 | 2.91 | −5.95 | 5.25 |
| | Relative error (%), $\gamma$ | 20.00 | 35.50 | 75.01 | 5.50 | −13.51 | 9.50 |
| 100-year | Climate change risk, $R_C$ | 0.0080 | 0.0064 | 0.0018 | 0.0095 | 0.0113 | 0.0091 |
| | Climate change return period, Eq. (8.2) | 125 | 156.25 | 156.02 | 105.26 | 88.50 | 109.89 |
| | Difference | 25.00 | 56.25 | 56.55 | 5.26 | −11.50 | 9.89 |
| | Relative error (%), $\gamma$ | 20 | 34.04 | 36.25 | 4.99 | −12.99 | 9.00 |

engineering point of view, in water structure planning due to climate change impact longer return periods must be considered than the no business (without climate change) cases. This further implies that the constructions will be more costly, which also brings economic load as a result of climate change impact.

In the same table, Madinah location in the KSA has its distinctive feature, because instead of longer return periods shorter periods are dominant. This indicates that in the future less costly engineering structures are necessary at this location. Furthermore, present structures are expected to perform better in the future periods.

## 8.8   Climate Change Impacts on Water Structures in Arid Regions

Global warming impacts on many social, environmental, and health issues are examined by many researchers. Although climate change effects on hydrometeo-rological records are searched with objective methodologies quantitatively, but the

same cannot be said for engineering water structure (dams, culverts, canals, highways and their side drainage, levees, etc.) design variables. This section is concentrated on the features of design variables in terms of cumulative distribution functions (CDF), intensity–duration–frequency (IDF) curves and innovative trend analysis (ITA) procedures toward a better structural design in the future. For this purpose, instead of classical approaches to derive the design variable features from the whole available hydrometeorological records, two-half time series approach is suggested, applied and the results are compared with the classical approaches currently in use in water structural designs (Şen 2012, 2014).

### 8.8.1   Hydrometeorological Variables and Rainfall Records

In general, climate change is expected to lead to more precipitation coupled with more evaporation, but the important question is how much of this precipitation will end up at water deficit areas such as arid and semiarid zones? Hence, regional management of engineering water infrastructures comes into view with sustainable water distribution programs by taking into consideration the climate change impacts. On the other hand, probable precipitation increase in some areas or decrease in others is another indication for regional water resources distribution to demand areas through efficient management programs.

It is important to estimate the magnitude of potential changes in time at the land surface (lakes, seasonal snowpacks, soil moisture, groundwater, glaciers, and ice sheets), changes in fluxes of water (precipitation, evaporation, runoff, and groundwater recharge), and changes in atmospheric water storage and transport, all of which have profound influence on the earth's energy cycle, meteorology, climate dynamics, hydrological cycle, and global climate change processes. Toward this end, a better understanding is needed about what causes both short-term and long-term variability in these fluxes that integrate the engineering water structures with each other as well as with the oceans and atmosphere.

An understanding of mechanisms linking large-scale climate variability with regional conditions also forms the basis for reducing the uncertainty associated in assessing regional climate change impact over decadal-to-centennial periods. A region-specific ability to project the consequences of global change is now needed more than before. For example, decision makers who are concerned with long-term fixed capital investments on infrastructures such as dams, water diversion systems, and flood damage mitigation systems, look for information about vulnerable shifts in hydro-climatic regime.

Although climate change is appreciable on the average over rather long periods such as 30-year, but its shorter duration meteorology factors must be considered for better future predictions.

The most important and basic factor for water resources management and proper structural design in the future is the rainfall records, because it is the source of all surface and groundwater storages. The characteristics of the rainfall records are
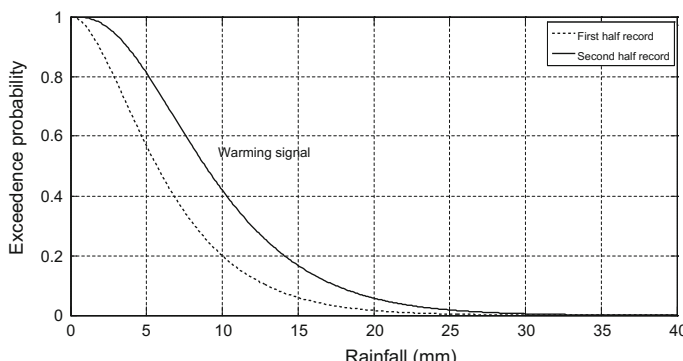
reflected in any engineering water structure design. For this purpose, apart from the CDF and IDF curves, ITA methodologies provide information about the possible trend component in a given record time series. The discharge of surface water from any drainage basin is also directly related to rainfall characteristics, especially in terms of rainfall intensity, duration and also risk calculation (Chaps. 2 and 6). In any design procedure for water structures, engineering structural life (return period) is adapted as 2-year (0.50 risk), 5-year (0.20 risk), 10-year (0.10 risk), 25-year (0.04 risk), 50-year (0.02 risk), and 100-year (0.01 risk); all of these are in direct relationship with the rainfall characteristics.

## 8.8.2 Climate Change Identification Methodologies

Classical methodologies are based on the consideration of all the available hydrometeorological time series features for scientific modeling and especially practical application works in any water-related project. Such an approach may offset the recent characteristics of the phenomenon concerned leading to biased and at times risky solutions.
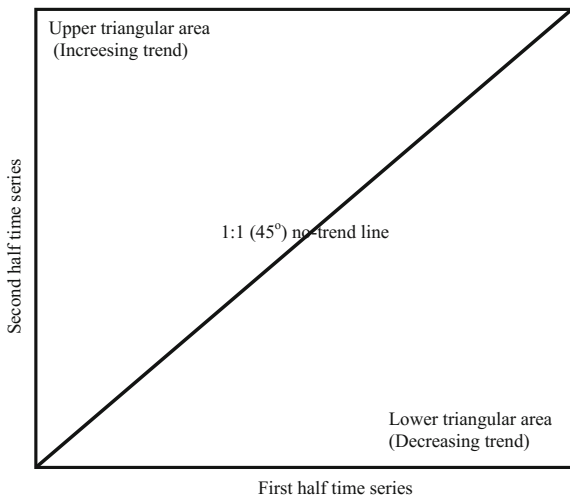
In this section, as already mentioned by Şen (2012) available hydrometeorological time series is divided into two halves each representing the older past and recent past periods. This procedure provides comparison of recent records in the second half with the older half and hence provides information about the possibility of any change in the record behavior. A similarity is available in the global warming assessment of temperature records by comparing two CDF's as in Fig. 8.9.

The difference between the two CDFs is an indication for the climate change. Şen (2012, 2014) has based the trend identification also on the two halves and their ascending order scatter against each other, which provides trend tendency information. The scatter graphs are referred to as ITA template as shown in Fig. 8.10.



**Fig. 8.9** Global warming signatures

**Fig. 8.10** Innovative trend
templates
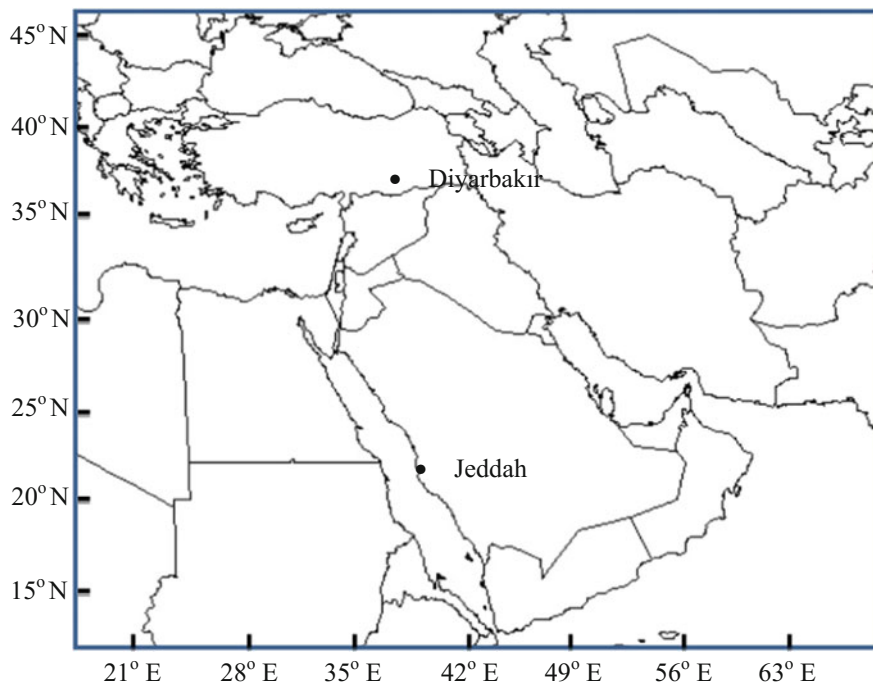


In this template, two axes have the same length, and the 1:1 (45°) straight line
corresponding to no trend case. Upper (lower) triangular area is for increasing
(decreasing) trend indications.

## 8.8.3  Application

In order to present detailed application of the climate change effect on water
resources structural design procedures, two different regions are selected as rep-
resentatives of semiarid and arid regions in southeast Turkey and western Saudi
Arabia. These are Diyarbakır and Jeddah meteorology stations, and their locations
are shown in Fig. 8.11.

Diyarbakır station has continental climate type, where summer seasons are dry
and very hot, and winters are cold and wet, and sometime nights may experience
frost. Its location is in the upper Mesopotamian plain and next to the Mediterranean
type of climate with continental effects. In some summer seasons, the maximum
temperature may reach to 45 °C, and the minimum temperature occasionally may
go down to 15–20 °C. This station represents a semiarid climate region.

Jeddah meteorology station lies next to the Red Sea, and it is under the effect of
different air movements. During winter seasons, Mediterranean type of climate
coverage extends to the south of this station along the Res Sea channel effect,
whereas during the late spring monsoon, air movement origination from the Indian
subcontinent reaches the location through the Arabian Sea with storm rainfall
effects. On the other hand, the hydrological cycle that originates from the Red Sea
penetrates toward the east and causes occasional convective and orographic rainfall
types. This station is a representative of arid region climate.
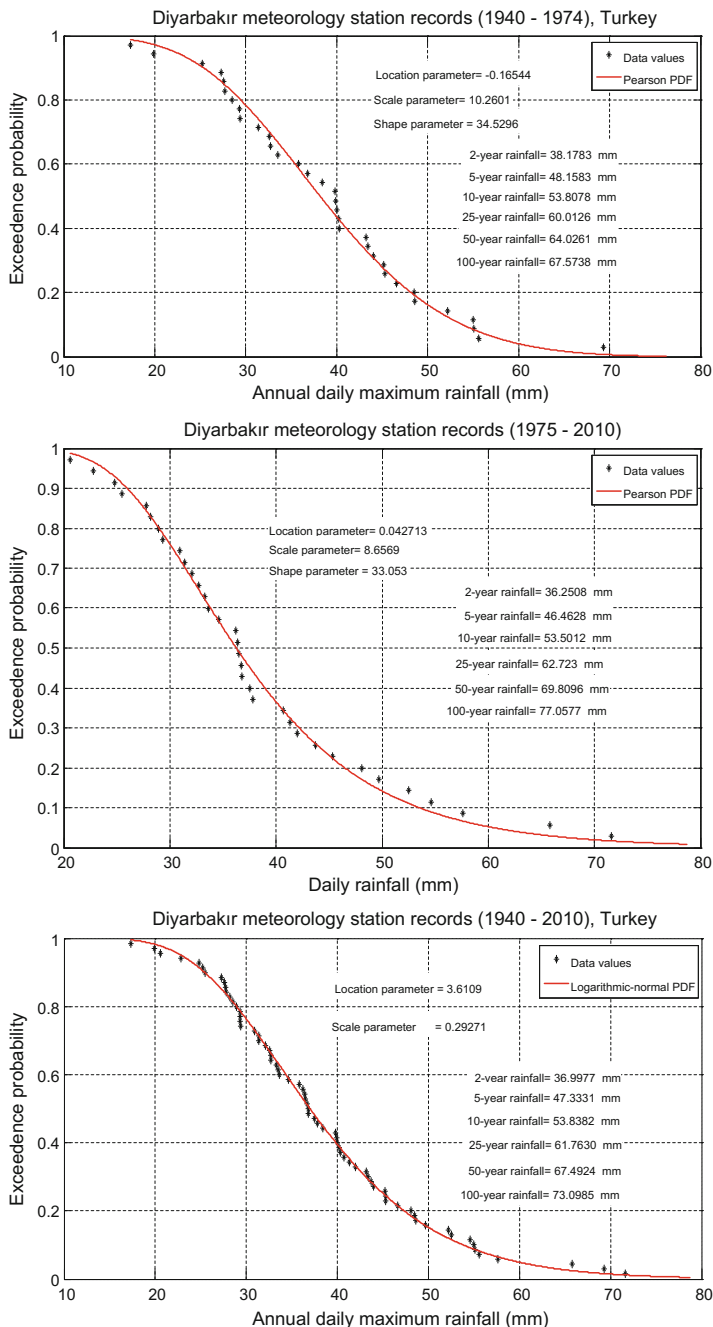
**Fig. 8.11** Study area

The applications of the design procedures based on the rainfall records are considered in three subsections. In both stations, annual daily maximum records are used. The data available at Diyarbakır station is from 1940 to 2010, whereas the same type of data is available for Jeddah station starting from 1970 up to 2014, inclusive.
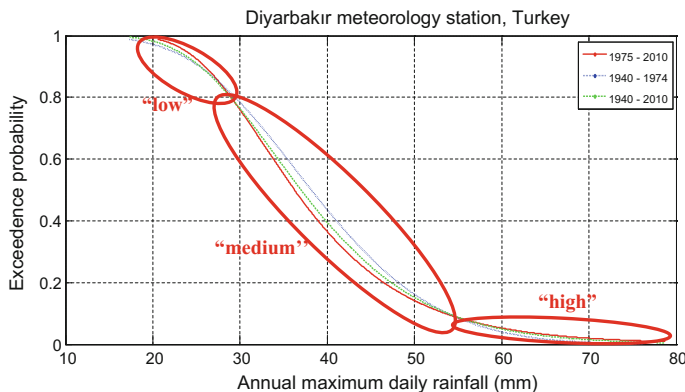
### 8.8.3.1  Probability Distribution Function (PDF)

The PDF is an essential feature of any hydrometeorological time series records, and accordingly, different works can be achieved such as the statistical evaluation, stochastic modeling, and drought and flood assessments. In this section, in addition to the classical whole record consideration, as stated before the available record is divided into two halves, and each one is sorted in ascending order. Hence, there are three PDFs, one for each half time series, and the third for the whole time series. These PDFs are shown in Fig. 8.12 for Diyarbakır station.

On the same figure, type of PDF, its parameters (location, scale and shape) are given in addition to the return periods (2-year, 5-year, 10-year, 25-year, 50-year, and 100-year) rainfall amounts corresponding to 0.50, 0.20, 0.10, 0.04, 0.02, and 0.01 risk levels. A comparison of the three graphs indicates that for 25-year (0.04),

**Fig. 8.12** PDFs for Diyarbakır meteorology station

**Fig. 8.13** PDFs comparison for Diyarbakır station

50-year (0.02), and 100-year (0.01) return periods (risk levels); the rainfall amounts have increased in the second half compared to the first half.

The comparison of each PDF with others is provided in Fig. 8.13, where during the second half (1975–2010) there are increases in the "low" and "high" rainfall values; however, "medium" rainfall amounts are in decrease compared with the whole record PDF and the first half (1940–1974).

Similar PDFs for Jeddah meteorology station in Saudi Araba are given in Fig. 8.14 for the whole and half periods.
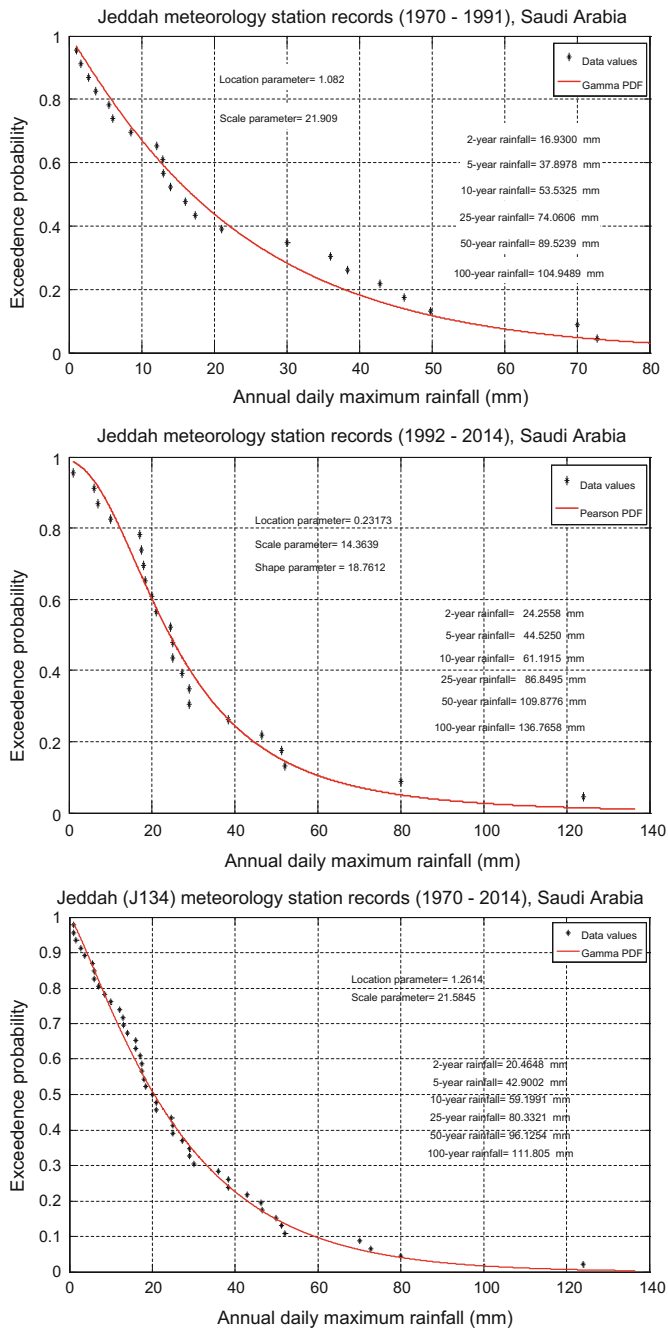
Again, it is obvious that during the second half (1970–1991), there is increase in the rainfall amounts especially at "low" record values. The comparison of these PDFs is presented in Fig. 8.15.

The second half records (1992–2014) are higher than the first half (1970–1991) especially at "low" values in a gradually decreasing rate toward the "medium" and "high" record ranges.
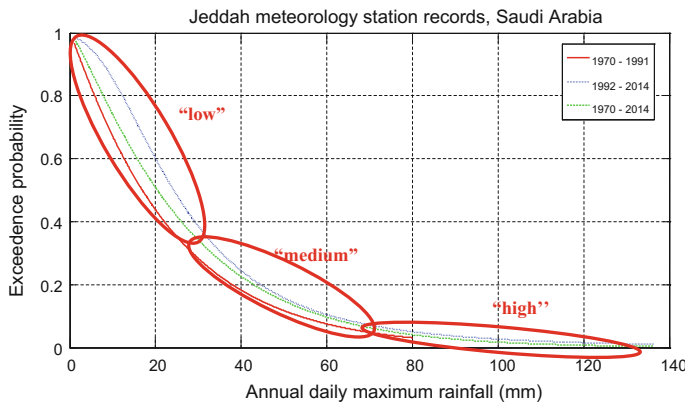
In any project planning, design, operation, and maintenance work, it is suggested that the second half values are taken as the basis, because they reflect the climate change impacts.

### 8.8.3.2  Intensity–Duration–Frequency (IDF) Curves

In any water resources system study, the most sought information is the intensity–duration–frequency (IDF) curves either in the form of graphs or preferably as tables. They help to find design rainfall intensity after deciding on the life (return period) of water structure and calculation of time of concentration from the features of concerned drainage basin, which falls outside the scope of this book Şen (2008). The IDF curves are also prepared for the two halves in addition to the whole record length. Figure 8.16 shows the IDF curves for Diyarbakır station.

**Fig. 8.14**  PDFs for Jeddah meteorology station

**Fig. 8.15**  Diyarbakır meteorology station ITA template

One can observe from these IDF curves that the rainfall intensities were higher during the early half duration (1940–1974) than others, and hence, at Diyarbakır region, rainfall intensities had a decreasing tendency. Figure 8.17 provides comparative information between the three cases (two halves and the complete time series) for 100-year and 2-year return period or 0.01 and 0.50 risk levels, respectively.

In each graphs, the highest rainfall intensities lie within the first half (1940–1974) period. On the same graphs, the relative differences between the first half and the whole period are also calculated according to the relative error, $\alpha$, formulation similar to Eq. (8.4) as,

$$\alpha = 100 \times \frac{R_{max} - R_{min}}{R_{max}} \tag{8.4}$$
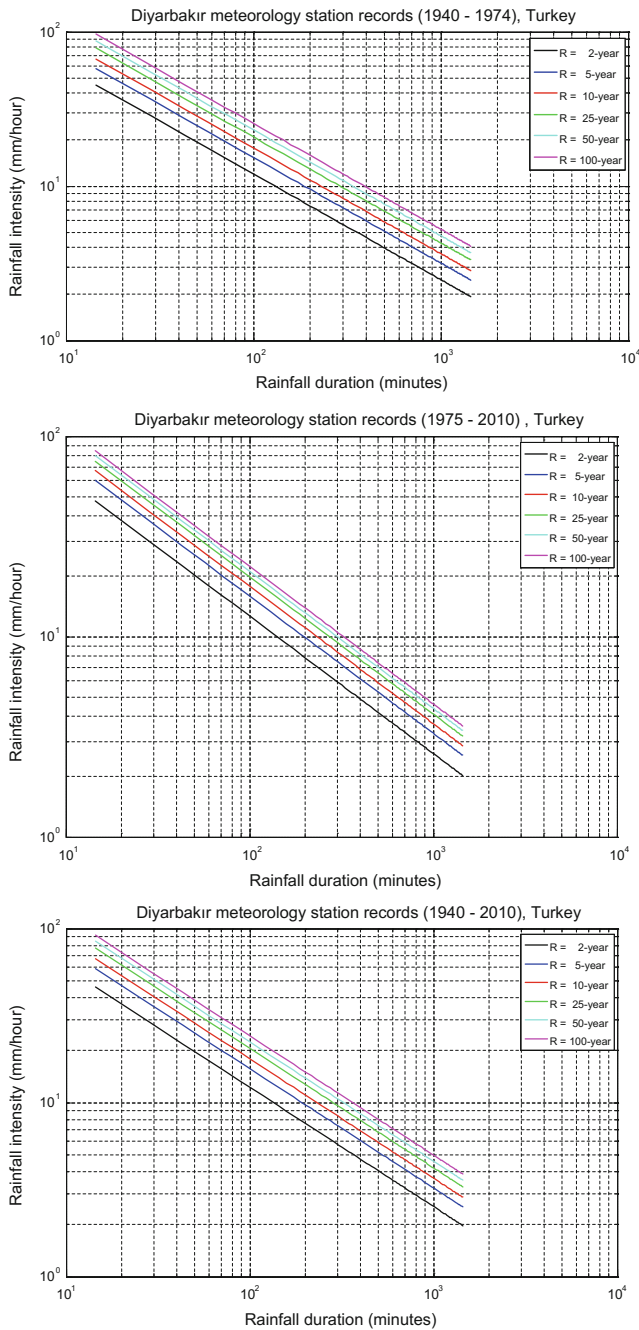
where $R_{max}$ and $R_{min}$ are the two extreme values for comparison. The relative differences are calculated as 5.4 and 3.1 for the 100-year and 2-year return periods, respectively. It is advised that in this region, precipitation amounts can be augmented on the average by 5% due to the climate change impact.
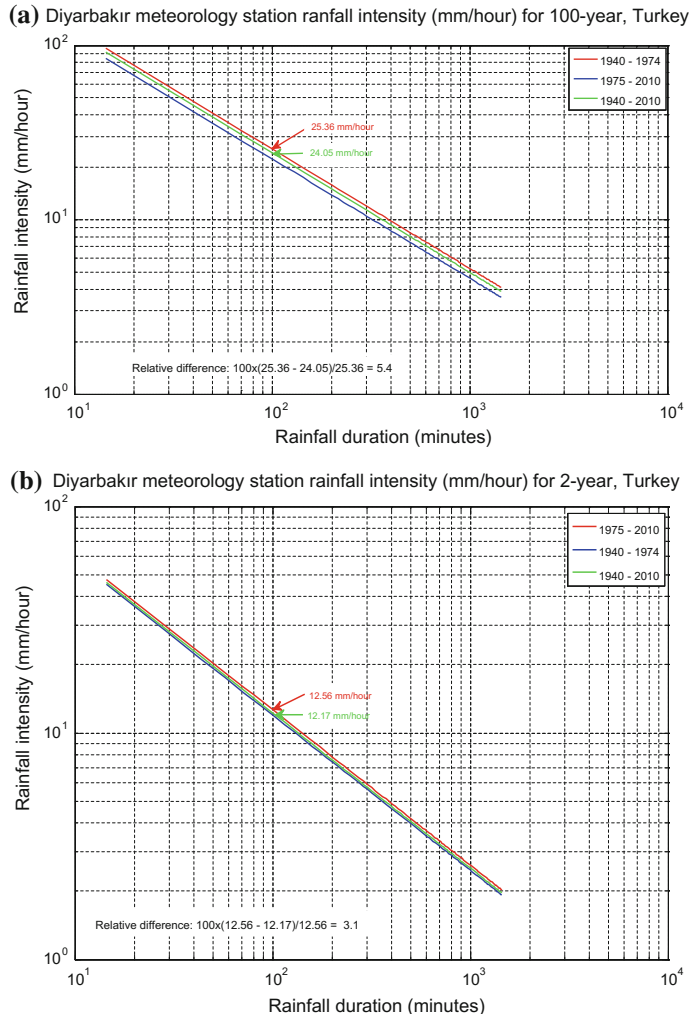
As for the Jeddah meteorology station, Figs. 8.18 and 8.19 give the IDF curves for each half series together with the whole record length and their comparisons, respectively.

The second half time series (1992–2014) yields the maximum rainfall intensity values, and hence, this indicates that there is climate change impact on this region with an increasing tendency.

One hundred-year and 2-year IDF curve comparisons indicate that in both cases, there is increase during the second half period with relative differences of 15.65 and 18.25%, respectively. It is, therefore, recommended that in any future water structure project, design value should be increased by 15 or 20%, depending on the project location and decision maker's preference.

**Fig. 8.16** IDF curves for Diyarbakır meteorology station

**(a)** Diyarbakır meteorology station ranfall intensity (mm/hour) for 100-year, Turkey

**(b)** Diyarbakır meteorology station rainfall intensity (mm/hour) for 2-year, Turkey
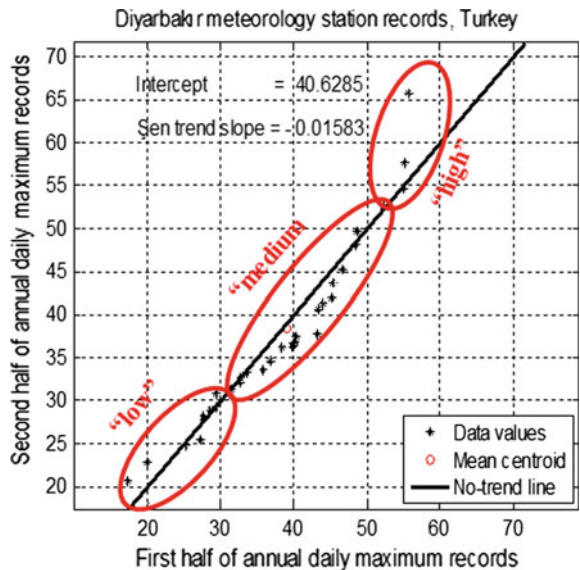
**Fig. 8.17**  IDFs comparison for Diyarbakır station

On the other hand, Tables 8.4 and 8.5 provide numerical rainfall intensity values for a set of return period (or risk, which is the inverse of return period) and duration.

#### 8.8.3.3  Innovative Trend Analysis (ITA)

Another important point in the assessment of rainfall records, as for the climate change impact effect, is the comparison of the two halves on the innovative trend template graph, which indicates the scatter of points as explained in Sect. 8.8.3. Figure 8.20 is the ITA for Diyarbakır meteorology station.

On this figure, the given trend slope value is for the whole rainfall record, and it indicates a slightly decreasing trend, which is explicitly shown in Fig. 8.21.

The slope, S, is calculated according to the following expression by taking into consideration the first and the second half series arithmetic averages as $\overline{R}_1$ and $\overline{R}_2$, respectively, as (Şen 2015),
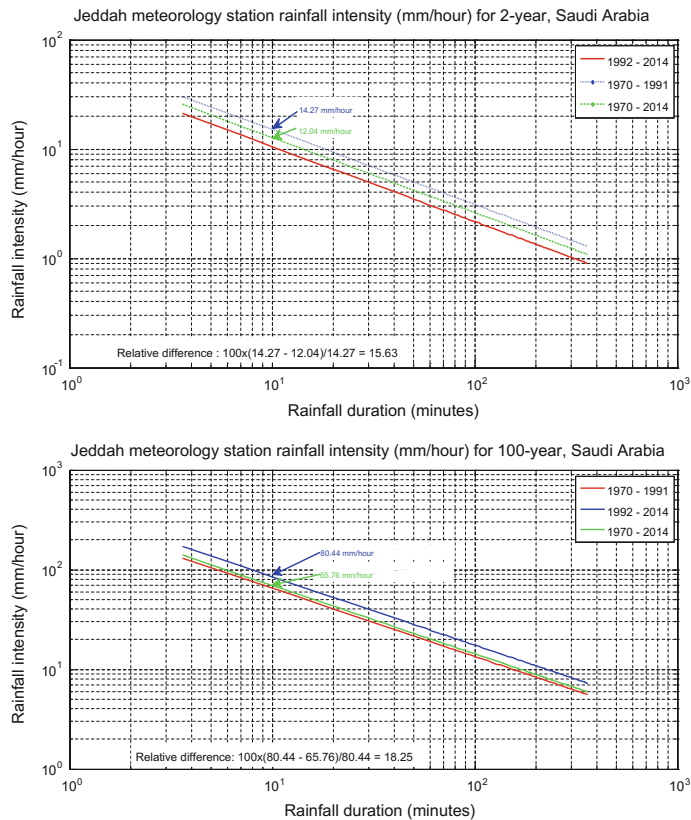
$$S = \frac{2(\overline{R}_2 - \overline{R}_1)}{n} \qquad (8.5)$$

where n is the length of the whole rainfall time series.

The attraction of the ITA is that it provides a visual inspection about the "low," "medium" and "high" rainfall values, whether they have trend component or not. The inspection of Fig. 8.20 yields that there is a slightly increasing trend at "low" values, because few points are above the 1:1 straight line; "medium" rainfall values have decreasing trend; but "high" values have a significantly increasing trend.

On the other hand, Jeddah meteorology station has ITA graph in Fig. 8.22, and the whole series trend component is given in Fig. 8.23.

There is a significantly increasing trend component with positive slope of 0.34335 in the whole series as obvious from Fig. 8.22. However, detailed trend component interpretations are available from the ITA graph, which implies that "low" values have an increasing trend, whereas "medium" rainfall values do not have significant trend value, because the scatter points are around the 1:1 straight line, but "high" rainfall range has very significant increasing trend component. It is possible to conclude that the trend component in Fig. 8.23 is an average of the "low," "medium," and "high" rainfall range trends.

**Fig. 8.19** IDFs comparison for Jeddah station

The global warming consequent climate change has impacts on social, environmental, health, agriculture, and many other sectors, which have been covered in detail in the literature. Unfortunately, the exposition of engineering design quantities under climate change impact on decision variables such as the rainfall intensity has not been investigated sufficiently. In this section, three different methodologies are presented to clarify this point, by the CDF, IDF curves, and ITA methods.

**Table 8.4**  Diyarbakır meteorology station numerical IDF values, Turkey

| Return period (year) | Time series duration (year) | Rainfall duration (mm) | | | | | | |
|---|---|---|---|---|---|---|---|---|
| | | 10 | 20 | 30 | 60 | 120 | 180 | 360 |
| 2 | 1940–1974 | *29.6524* | *15.8206* | *11.4623* | *7.1266* | *4.3383* | *3.2629* | *2.0286* |
| | 1975–2010 | 28.1553 | 15.0219 | 10.8836 | 6.7668 | 4.1193 | 3.0981 | 1.9262 |
| | 1940–2010 | 28.7354 | 15.3314 | 11.1079 | 6.9062 | 4.2042 | 3.162 | 1.9659 |
| 5 | 1940–1974 | *37.4037* | *19.9562* | *14.4586* | *8.9895* | *5.4724* | *4.1158* | *2.5589* |
| | 1975–2010 | 36.0868 | 19.2536 | 13.9496 | 8.673 | 5.2797 | 3.9709 | 2.4688 |
| | 1940–2010 | 36.7627 | 19.6142 | 14.2109 | 8.8354 | 5.3786 | 4.0453 | 2.5151 |
| 10 | 1940–1974 | 41.7916 | 22.2972 | 16.1548 | 10.044 | 6.1144 | 4.5986 | 2.8591 |
| | 1975–2010 | 41.5534 | 22.1702 | 16.0627 | 9.9868 | 6.0795 | 4.5724 | 2.8428 |
| | 1940–2010 | *41.8151* | *22.3098* | *16.1639* | *10.0497* | *6.1178* | *4.6012* | *2.8607* |
| 25 | 1940–1974 | 46.6108 | 24.8685 | 18.0177 | 11.2023 | 6.8195 | 5.1289 | 3.1888 |
| | 1975–2010 | *48.7158* | *25.9916* | *18.8314* | *11.7082* | *7.1274* | *5.3605* | *3.3328* |
| | 1940–2010 | 47.9702 | 25.5938 | 18.5432 | 11.529 | 7.0184 | 5.2785 | 3.2818 |
| 50 | 1940–1974 | 49.728 | 26.5316 | 19.2227 | 11.9514 | 7.2755 | 5.4719 | 3.4021 |
| | 1975–2010 | *54.2199* | *28.9282* | *20.9591* | *13.031* | *7.9327* | *5.9662* | *3.7094* |
| | 1940–2010 | 52.4202 | 27.968 | 20.2634 | 12.5985 | 7.6694 | 5.7682 | 3.5863 |
| 100 | 1940–1974 | 52.4834 | 28.0017 | 20.2878 | 12.6137 | 7.6787 | 5.7751 | 3.5906 |
| | 1975–2010 | *59.8493* | *31.9317* | *23.1352* | *14.384* | *8.7564* | *6.5856* | *4.0945* |
| | 1940–2010 | 56.7744 | 30.2911 | 21.9465 | 13.645 | 8.3065 | 6.2473 | 3.8842 |
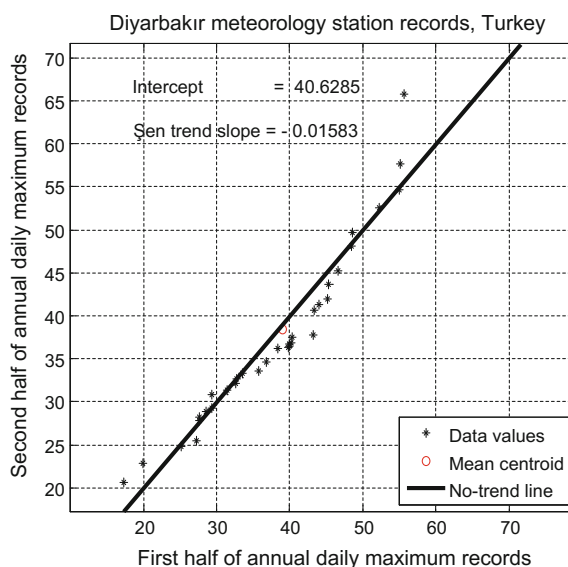
**Table 8.5**  Jeddah (J134) meteorology station numerical IDF values, Saudi Arabia
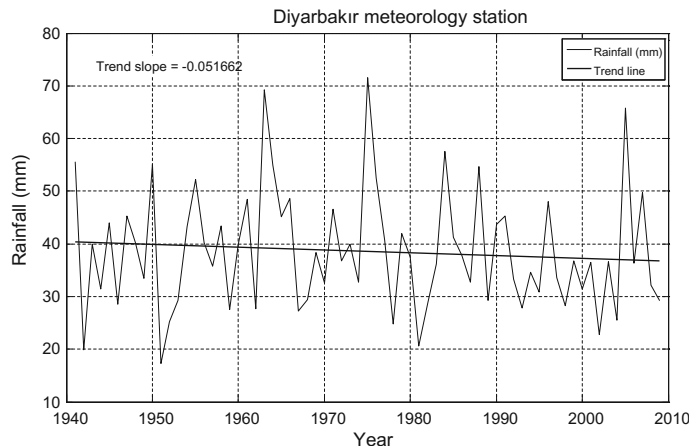
| Return period (year) | Time series duration (year) | Rainfall duration (year) | | | | | | |
|---|---|---|---|---|---|---|---|---|
| | | 10 | 20 | 30 | 60 | 120 | 180 | 360 |
| 2 | 1970–1992 | 13.1493 | 7.0156 | 5.0829 | 3.1603 | 1.9238 | 1.4469 | 0.8996 |
| | 1992–2014 | *18.8391* | *10.0513* | *7.2824* | *4.5277* | *2.7563* | *2.0730* | *1.2889* |
| | 1970–2014 | 15.8946 | 8.4803 | 6.1442 | 3.8201 | 2.3255 | 1.7490 | 1.0874 |
| 5 | 1970–1992 | 29.4345 | 15.7044 | 11.3781 | 7.0742 | 4.3065 | 3.2389 | 2.0137 |
| | 1992–2014 | *34.5818* | *18.4506* | *13.3678* | *8.3113* | *5.0595* | *3.8053* | *2.3659* |
| | 1970–2014 | 33.3198 | 17.7773 | 12.88 | 8.008 | 4.8749 | 3.6664 | 2.2795 |
| 10 | 1970–1992 | 41.5778 | 22.1832 | 16.0722 | 9.9927 | 6.0831 | 4.5751 | 2.8445 |
| | 1992–2014 | *47.5264* | *25.357* | *18.3716* | *11.4223* | *6.9534* | *5.2297* | *3.2515* |
| | 1970–2014 | 45.9789 | 24.5314 | 17.7735 | 11.0504 | 6.727 | 5.0594 | 3.1456 |
| 25 | 1970–1992 | 57.5215 | 30.6897 | 22.2353 | 13.8245 | 8.4158 | 6.3295 | 3.9353 |
| | 1992–2014 | *67.4545* | *35.9893* | *26.075* | *16.2118* | *9.869* | *7.4225* | *4.6148* |
| | 1970–2014 | 62.3926 | 33.2886 | 24.1183 | 14.9952 | 9.1284 | 6.8655 | 4.2685 |

<div align="right">(continued)</div>

**Table 8.5**  (continued)
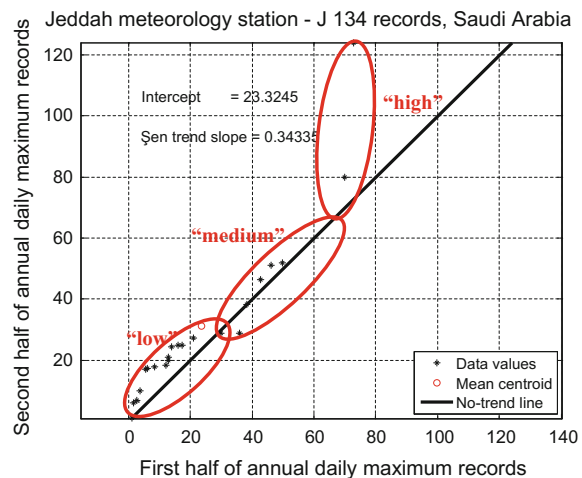
| Return period (year) | Time series duration (year) | Rainfall duration (year) | | | | | | |
|---|---|---|---|---|---|---|---|---|
| | | 10 | 20 | 30 | 60 | 120 | 180 | 360 |
| 50 | 1970–1992 | 69.5317 | 37.0976 | 26.8779 | 16.711 | 10.1729 | 7.6511 | 4.7569 |
| | 1992–2014 | *85.3400* | *45.5319* | *32.9888* | *20.5103* | *12.4858* | *9.3906* | *5.8385* |
| | 1970–2014 | 74.6589 | 39.8331 | 28.8599 | 17.9433 | 10.9231 | 8.2152 | 5.1077 |
| 100 | 1970–1992 | 81.512 | 43.4895 | 31.509 | 19.5903 | 11.9257 | 8.9693 | 5.5766 |
| | 1992–2014 | *106.2236* | *56.674* | *41.0614* | *25.5294* | *15.5412* | *11.6885* | *7.2672* |
| | 1970–2014 | 86.837 | 46.3306 | 33.5674 | 20.8701 | 12.7048 | 9.5553 | 5.9409 |
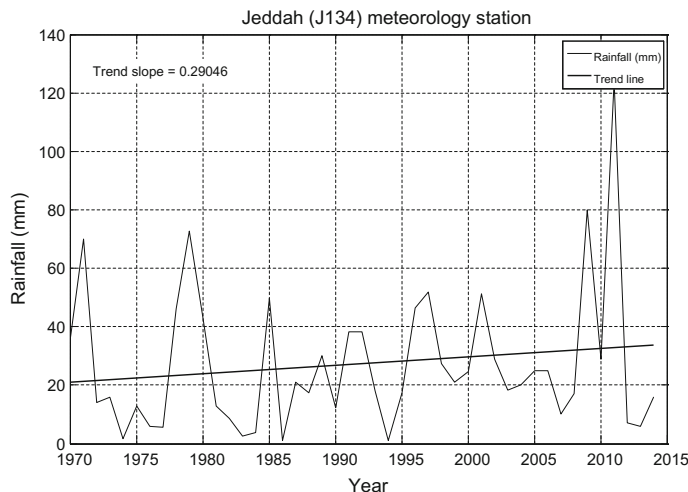


**Fig. 8.20**  Diyarbakır meteorology station ITA

**Fig. 8.21** Diyarbakır meteorology station rainfall record trends



**Fig. 8.22** Jeddah meteorology station ITA

**Fig. 8.23** Jeddah meteorology station rainfall record trends

# References

IPCC. (2007). Climate change 2007: Impacts, adaptation, and vulnerability. Contribution of working group II to the fourth assessment report of the intergovernmental panel on climate change. Cambridge, UK: Cambridge University Press.

IPCC. (2013). Climate change 2013: The physical science basis. contribution of working group i to the fifth assessment report of the intergovernmental panel on climate change. Cambridge, UK: Cambridge University Press.

Kundzewicz, Z. W., & Somlyódy, L. (1997). Climatic change impact on water resources in a systems perspective. *Water Resources Management, 11,* 407–435.

Almazroui, M. (2013). Simulation of present and future climate of Saudi Arabia using a regional climate model (PRECIS). *International Journal of Climatology, 33,* 2247–2259.

Arnell, N. W. (1999). Climate change and global water resources. *Global Environmental Change, 9,* 31–49.

Barnett, T. P., Adam, J. C., & Lettenmaier, D. P. (2005). Potential impacts of a warming climate on water availability in snow-dominated regions. *Nature, 438,* 303–309.

Caparrós, A., & Jacquemont, F. (2003). Conflicts between biodiversity and carbon offset programs: Economic and legal implications. *Ecological Economics, 46,* 143–157.

Carter, T. R., Jones, R. N., Lu, X., Bhadwal, S., Conde, C. & Mearns, L. et al. (2007). New assessment methods and the characterization of future conditions. In M. L., Parry, O. F., Canziani, J. P., Palutikof, P. J., van der Linden & C. E. Hanson, (Eds.), *Climate change 2007: Impacts, adaptation and vulnerability. Contribution of working group II to the fourth assessment report of the intergovernmental panel on climate change* (pp. 133–171). Cambridge, United Kingdom: Cambridge University Press,

Döll, P., & Lehner, B. (2002). Validation of a new global 30-min drainage direction map. *Journal of Hydrology, 258,* 214–231.

Gleick, P. H. (1998). *The world's water: the biennial report on freshwater resources 1998–1999.* San Francisco: Island Press.

Hitz, S., & Smith, J. (2004). Estimating global impacts from climate change. *Global Environmental Change, 14,* 201–218.

Jones, R. N. (2001). An environmental risk assessment/management framework for climate change. *Natural Hazards, 23,* 197–230.

Jones, R. N. (2004a). Incorporating agency into climate change risk assessments—An editorial comment. *Climate Change, 67,* 13–36.

Jones, R. N., (2004b). Managing climate change risks, In: J. Corfee Morlot & Agrawala, S. (Eds.), The Benefits of Climate Change Policies: Analytical and framework issues. Organization for Economic Co-operation and Development, Paris: 251-297.

Jones, R. N., & Boer, R. (2005). Assessing current climate risks. In B. Lim, E. Spanger-Siegfried, I. Burton, E. Malone, & S. Huq (Eds.), *Adaptation policy frameworks for climate change: Developing strategies, policies and measures* (pp. 91–118). Cambridge and NewYork: Cambridge University Press.

Keller, J., Sakthivadivel, R., & Seckler, D. (2000). Water scarcity and the role of storage development, Research Report 39, Colombia, Sri Lanka, International Water Management Institute.

Kundzewicz, Z. W., Mata, L. J., Arnell, N., Döll, P., Jiménez, B., Miller, K., et al. (2008). The implications of projected climate change for freshwater resources and their management. *Hydrological Sciences Journal, 53*(1), 3–10.

Mayorga, E., Logsdon, M. G., Ballester, M. V. R., & Richey, J. E. (2005). Estimating cell-to-cell land surface flow paths from digital channel networks, with an application to the Amazon basin. *Journal of Hydrology, 315,* 167–182.

RAE, Royal Academy of Engineering. (2011). Infrastructure, Engineering and climate change adaptation—ensuring services in an uncertain future. Published by The royal academy of engineering on behalf of engineering the future. The Royal Academy of Engineers.

Şen, Z. (2008). Wadi hydrology (p. 347). New York: Taylor and Francis Group, CRC Press.

Şen, Z. (2009). Global warming threat on water resources and environment: A review. *Environmental Geology, 57,* 321–329.

Şen, Z. (2012). Innovative trend analysis methodology. *Journal of Hydrologic Engineering, 17*(9), 1042–1046.

Şen, Z. (2014). Trend identification simulation and application. *Journal of Hydrologic Engineering, 19*(3), 635–642.

Şen, Z. (2015). Applied drought modeling, prediction, and mitigation (p. 472). Amsterdam: Elsevier.

Şen, Z., Alsheikh, A., Turbak, A. S., Al-Bassam, A. M., & Al-Dakheel, A. M. (2011). Climate change impact and runoff harvesting in arid regions. *Arabian Journal of Geosciences* . doi:10. 1007/s12517-011-0354-z.

Şen, Z., Uyumaz, A., Cebeci, M., Öztopal, A., Küçükmehmetoğlu, M., Özger, M., et al. (2010). *The impacts of climate change on Istanbul and Turkey Water resources* (p. 1500). Istanbul Water and Sewerage Administration: Istanbul Metropolitan Municipality.

Smith, S. J., Wigley, T. M. L., Nakicenovic´, N. & Raper, S. C. B. (2001). Climate implications of greenhouse gas emission scenarios. *Technological Forecasting and Social Change, 65*, 195–204.

Solomon, S., Qin, D., Manning, M., Alley, R. B., Berntsen, T., Bindoff, N. L. et al. (2007). Technical summary. In: Climate Change 2007: The physical science basis. Contribution of working group I to the fourth assessment report of the intergovernmental panel on climate change [Solomon, S., Qin, D., Manning, M., Chen, Z., Marquis, M., Averyt, K. B., Tignor, M., Miller H. L. (eds.)]. Cambridge, United Kingdom and New York, NY, USA: Cambridge University Press.

Stewart, I. T., Cayan, D. R., & Dettinger, M. D. (2004). Changes in snowmelt runoff timing in western North America under a 'business as usual' climate scenario. *Climatic Change, 62,* 217–232.

UKCIP. (2003). Climate adaptation: Risk, uncertainty and decision-making. In R. I. Willows & R. K.Connell (Eds.), UKCIP Technical Report. UKCIP, Oxford, 166 p. Available from: http:// www.ukcip.org.uk/images/stories/Pub_pdfs/Risk.pdf (Accessed 22 December 2009).

UNDP. (2005). Adaptation policy frameworks for climate change: Developing strategies, policies and measures. In B., Lim, E., Spanger-Siegfried, I., Burton, E., Malone & S. Huq, (Eds.), Cambridge and New York: Cambridge University Press, 266 p.

Vorosmarty, C. J., Green, P., Salisbury, J., & Lammers, R. B. (2000). Global water resources; vulnerability from climate change and population growth. *Science, 289,* 284–288.

Wigley, T. M. L. (2004). Choosing a stabilization target for CO2. *Climatic Change, 67,* 1–11.

# Chapter 9
# Flood Safety and Hazard

**Abstract** After all what have been explained in the previous chapters, it is necessary on the basis of the explained information to plan for the flood safety, reducing its hazardous character. There must be a common understanding on the basic definitions and for this purpose, the most common safety and flood hazard terminology is provided. Among the safety factors are defense against floods their measurements, proofing, controls and plans. Flood risk calculations in a different way from the previous chapters are presented with detailed explanations. Public awareness is one of the most significant educational ingredients in reducing flood hazard by consideration of flood resilience possibilities.

**Keywords** Awareness · Control · Hazard · Measurement · Plan
Public · Resilience · Risk · Safety

## 9.1 General

The flood hazard potentiality may have adverse effects on urban, industrial, infrastructural, and agricultural areas. This view emerges from the past experiences, and therefore, urges preparation of flood risk inundation maps. Availability of such maps is the key requirement in any urban development including dams, tunnels, highways, culverts, and bridges for sustainable future (Chap. 7). The main objective of this section is to present in detail the steps toward the preparation of risk maps starting by measurements. The completion of flood hazard risk maps is achieved with the view of perspective for effective planning, protection, operation, construction, and maintenance against dangerous hydrological events.

Floods are among the natural disasters that impact on many human activities in an undesirable manner. Agriculture, water resources, power generation, and industry are under the threat if necessary precautions are not planned against flood occurrences. Especially, anthropogenic agents force climate change impacts on flood-prone areas, and regional climate variability triggers flood occurrences and they are of primary importance for natural disaster vulnerability measures.

Mesoscale weather prediction models are used for extreme event predictions such as severe thunderstorms and heavy rainfall under the constraint on the future climate changes and the hydrological cycle (Allen and Ingram 2002), but it is not yet possible to make accurate extreme rainfall event predictions. Furthermore, mesoscale models cannot be utilized for prediction beyond 3–5 days. Thus, a long-term forecasting model would be very helpful for preparing disaster plans. The current numerical models supported even by satellite data need for steady improvements to digest the unexpected occurrences of floods at different locations. The general circulation or climate models (GCMs) are not sufficient for regional and local weather disaster occurrences and predictions, but they must be supported by local experiences, environmental circumstances, and administrative circles. As suggested by Romero et al. (1998) in the Mediterranean region, the simulations of excessive rainfall events by mesoscale models usually underestimate the rainfall peaks. This means that rainfall–runoff models even though they may be well advanced, it is not possible to make flood peak discharge estimations accurately.

Flooding is a major hazard in Mediterranean regions due to its extreme spatial and temporal variability. Furthermore, flood risk has increased over recent decades as socioeconomic factors have led to increasing urbanization and development along the Mediterranean coast that has resulted in ever larger flood-prone areas and societal vulnerability. On the other hand, especially the eastern Mediterranean region is mentioned among the worst climate change impact parts of the world (IPCC 2007). With regards to flood risk prevention in the region, the estimation of rare and large magnitude floods is rather unreliable due to short gauging station records and their scarce spatial distributions. A further problem with systematic flood records is that of accurately measuring extreme flood discharges, which in Mediterranean regimes are often 100 times greater than the mean flow (Baker et al. 2002). During these large floods, gauge stations are frequently either flooded or destroyed, and therefore, the flood discharges are estimated from streamflow measurements by using indirect methods (Chaps. 4 and 5) or statistical extrapolations (Chap. 6).

A convenient PDF to extreme rainfall records provides an opportunity to calculate the flood risks at a set of return periods such as 5-year, 10-year, 50-year, 100-year, or 250-year that correspond to life of water structure. As explained in Chap. 7 in case of any flood occurrence, debris flow, erosion, sedimentation, and other impacts on human activities must also be taken into account.

In any flood protection planning, management, and hazard assessment, possible flood variability should be taken into consideration rather than a single value yielded by models. The simplest measure of variability is the standard deviation, which covers the additional unwanted consequences of flood occurrence around a single value, say arithmetic average. The general understanding of the term "risk" dates from the initial risk research (Knight 1921). In terms of floods, it is interpreted as harm to flood-prone elements with a specific vulnerability ("elements at risk") due to probable flood events (Chap. 2). It should not be confused with risk in terms of reliability, which plays a major role for quantifying the safety of structural works for flood protection (Plate 1999).

In a flood risk assessment study, various events and quantities play joint role in the final causal impacts. These can be summarized as follows.

(1) Meteorological events,
(2) Hydrological events,
(3) Source area,
(4) Pathways under inundation expansion,
(5) Flood subject areas,
(6) Risky area identifications,
(7) Local and overall consequences.

Flood management can be achieved by consideration of flood risk assessment or without. In any region for flood assessment, hydrological features, responses, and existing flood defensive infrastructures must be taken into consideration prior to a detailed flood modeling study. The existing facilities provide the preliminary mitigation assessment movement for the management with necessary decisions and precautions. Marsalek (2000), Hooijer et al. (2004), and Oumeraci (2004) presented the bases of scientific methodologies for flood assessment and mitigation works. In case of flood management without the consideration of previously mentioned ingredients, at least risks associated with flood dangers and hazard reductions should be considered (Chap. 6). Along this line of consideration especially in practical applications, simple risk formulations must be adapted under the impact of climate change. There are many engineering equations as mentioned in almost all the previous chapters for rainfall and flood calculations, but unfortunately, they do not take into consideration the climate change impact and on their bases, it is not possible to achieve an effective adaptation of the engineering water structures. It is well-known presently that a range of impacts is related to mean global warming, which appears as trend effects and they provide a bridge between adaptation and mitigation uncertainties. Rahmstorf (2007) and Füssel (2010) stated that in case of mitigation expectation, planning adaptation responses for the highest projections of climate change may not be necessary over the long term. Although in the near-term, before mitigation policies can take effect, it would seem prudent to depend on the adaptation measures given that many variables are tracking at or above the level of Intergovernmental Panel on Climate Change (IPCC) projections.

To reduce risk associated with floods, there is a critical need to increase the length of the extreme flood record beyond that of the instrumental period. The flood record can be extended for hundreds to thousands of years by reconstructing past flood discharges using geomorphological indicators (paleo-floods) and documentary evidence. Paleo-flood hydrology, the reconstruction of the magnitude and frequency of large floods using geological evidence (Baker et al. 2002), has been employed in many regions of the world for compiling long-term flood records for improving flood risk estimation (House et al. 2002a, b). In particular, paleo-flood records have been reconstructed in the southwest USA (Kochel and Baker 1998; Kochel et al. 1982; Ely and Baker 1985; Partridge and Baker 1987; O'Connor et al. 1994), Australia (Baker and Pickup 1987; Pickup et al. 1988; Wohl et al. 1994),

Israel (Greenbaum et al. 2000), India (Kale et al. 2000), Japan (Jones et al. 2001), China (Yang et al. 2000), France (Sheffer et al. 2003), and central Spain (Benito et al. 2004, 2003a, b, c).

The main purpose of this chapter is to provide a forum concerning flood safety, hazard, vulnerability, resilience, control, risk and warning, and education aspects.

## 9.2  Flood Safety

Safety against flood danger is a matter of significant importance in many countries, because of the presence of a large number of human activities that cover a host of environmental problems. The safe operation of floods has significant social, economic, and environmental relevancies.

A flood safety review should include collection of all available historical records, field inspections, and investigations. It then proceeds with a check of environmental stability and operational safety of the flood prediction implementations beginning with a reappraisal of basic features and assumptions. The level of detail required in an early study must commensurate with the importance and complexity of flood occurrences and their consequent hazardous implications on the society and environment.

Flood safety analysis aims for determination of flood-causing system capacity to retain the flood water volume and to pass around and through the natural channels and environmental infrastructures in a safe and controlled manner with the maintenance of stability in every respect. A complete flood safety can be achieved by consideration of various interdisciplinary approaches in an integrated manner. Among such engineering disciplines are,

  (1)  Hydrology,
  (2)  Hydraulics,
  (3)  Meteorology,
  (4)  Land use,
  (5)  Morphology,
  (6)  Vegetation,
  (7)  Geology,
  (8)  Climate change impact,
  (9)  Remote sensing,
 (10)  Satellite images.

Flood safety decisions should include the following sequential activities, which are,

(1) Prevention: Possible extreme flood initiation related to any of the above-mentioned disciplines,
(2) Control: In case of any deteriorating situation,

(3)  Mitigation: If any failure cannot be prevented completely.

In general, flood safety methods are typically deterministic based on classification and standards, which may be also based on the probabilistic risk assessments (Chap. 6). In any flood safety analysis, the following points are important considerations.

(1)  Possible hazards and their analysis,
(2)  Possible failure modes and their effects,
(3)  Surface water operation reliability,
(4)  Infrastructure stability response,
(5)  Dangerous human effects,
(6)  Possible emergency scenarios.

For successful flood safety studies, the boundaries of the whole drainage area must be identified (Chap. 3). Sufficient and good quality as well as quantity data must be prepared for reliability and risk assessments. It is important that not only numerical but also verbal, linguistic, and expert views must be deposited in computer memories for ready use (Şen 2010). Flood hazards may change at different stages of human activities and at times suddenly in the form of flash floods (Chaps. 1 and 5). The following points are external hazards.

(1)  Meteorological and hydrological extreme events such as floods, droughts, intensive rainfalls, temperature extremes, icing and ice jams, windstorms, and lightning strikes,
(2)  Especially, upstream unstable slopes and the effects of upstream debris (Chap. 7).

However, additional internal hazards may also endanger the stability of flood passage channels causing suspicions about the flood safety, which are,

(1)  Design of the flood discharge canals,
(2)  Maintenance before and after the flood occurrence,
(3)  Flood water operation,
(4)  Future plans, procedures, and adaptations.

On the other hand, failure modes, sequences, and combinations of a flood path be identified in an expert manner, which may include,

(1)  During the flood occurrence, modes may change both in nature and surrounding environment,
(2)  The extend and rate of failure may change significant characteristics and these must be determined in an appropriate level of detail,
(3)  The analysis should address the manner in which failure modes and failure sequences can be detected.

### 9.2.1   Defense Against Floods

Many measures can be used by societies to cope with floods. They are usually classified into two major groups as structural measures and non-structural measures. Furthermore, these measures can be combined together in order to maximize the effects of the alleviation of the floods risks.

Structural measures of the flood management can be defined as the measures that alter the physical characteristics of the floods. They usually involve engineering works as diversions, reservoirs and retarding basins, channels and catchment modifications, levee-banks, flood proofing, etc.

On the other hand, non-structural measures alter the exposure of lives and properties to flooding (flood forecasting and early warning systems, flood insurance, planning controls, public information and education, etc.).

### 9.2.2   Flood Control Measures

They comprise major engineering works that can temporarily store or divert the flow of water and thus lowering the flood peak, such as dams, reservoirs and retarding basins, levee-banks, catchment modifications, etc. If they are used wisely, these measures can greatly reduce the level of flooding, even to the level where the river remains within its banks.

### 9.2.3   Flood Proofing

It consists in the modification of buildings and structures and their immediate surrounding to reduce damage in flooding. Flood proofing provides individual property owners with a means of reducing their risk of damage, although its effectiveness may be limited in the case of very serious floods.

### 9.2.4   Planning Control

Hydrologists can estimate the likelihood of a flood inundating an area to a given depth and flood risk maps can, therefore, be prepared showing high-risk areas. Moreover, the total designation of flood-prone areas into zones of different exposure to flooding may be used to enlighten potential users of their exposure to damage, to identify zones of insurance as well as to underlie compulsory statuary limits on land use in the area of exposition.

### *9.2.5   Emergency Plans*

Public authorities may arrange plans to be implemented upon receipt of warning. Planning includes the identification of responsible authorities, flood warning levels, targets and dissemination channels, evacuation, relief and rescue forces, repair and maintenance equipment and materials, emergency flow control mechanisms, and training requirements. It is worthy to remember that floods are periodical events, so that in between these events, people forget their effects. For this reason, it is important to increase awareness of flood problem.

## 9.3   Flood Hazard

Among all environmental hazards, flooding is the most common to many societies all over the world. The main reasons for this are the widespread geographical distribution of river valleys in humid regions and wadi courses in arid and semiarid regions and low-lying coasts, together with their long-standing attractions for human settlement and the surface and groundwater resources availability. Although in many cases the threat is limited to comparatively well-defined floodplain and low-lying areas such as estuaries, no country is immune from flood hazards (Smith 1992).

Generalized flood hazard zones and management strategies are explained by Kenny (1990) as follows.

(1) Flood hazard zone I (Active flood plain area):

   (a) Prohibit development (business and residential) within flood plain,
   (b) Maintain area in a natural state as an open space or for recreational uses only,

(2) Flood hazard zone II (Alluvial fans and plains with channels less than meter deep, bifurcating, and intricately interconnected systems subject to inundation from overbank flooding):

   (a) Flood proofing to reduce or prevent loss to structures is highly recommended,
   (b) Residential development densities should be relatively low; development in obvious drainage channels should be prohibited,
   (c) Dry stream channels should be maintained in a natural state and/or the density of the native vegetation should be increased to facilitate superior water drainage retention and infiltration capabilities,
   (d) Installation of upstream storm water retention basins to reduce peak water recharges,
   (e) Construction should be at the highest local elevation site where possible.

(3) Flood hazard zone III (Dissected upland and lowland slopes; drainage channels where both erosional and depositional processes are operative along gradients generally less than 5%):

  (1) Similar to flood hazard zone II,
  (2) Roadways that transverse channels should be reinforced to withstand the erosion power of a channeled streamflow.

(4) Flood hazard zone IV (Steep gradient drainages consisting of incised channels adjacent to outcrops and mountain fronts characterized by relatively coarse bedload material) (Chap. 7).

  (a) Bridges, roads, and culverts should be designed to allow unrestricted flow of boulders and debris up to a meter or more in diameter,
  (b) Abandon roadways that currently occupy the wash flood plain,
  (c) Restrict residential dwelling to relatively level building sites,
  (d) Provisions for subsurface and surface drainage on residential sites should be required,
  (e) Storm water retention basins in relatively confined upstream channels to migrate high peak discharges,
  (f) Land-use regulation seeks to obtain the beneficial use of flood plains with minimum flood damage and minimum expenditure on flood protection. The purchase of land by government agencies to reduce flood damage is rare,
  (g) Reforestation of slopes denude of woodland tends to reduce runoff and thereby lowers the intensity of flooding. As a consequence, forests are commonly used as a watershed management technique. They are most effective in relation to small floods, where the possibility exists of reducing flood volumes and delaying flood response. Agricultural practices such as contour plowing and strip cropping are designed to reduce soil erosion by reducing the rate of runoff,
  (h) Financial assistance in the form of government relief or insurance payouts does nothing to reduce flood hazard. Indeed, by attempting to reduce the economic and social impact of a flood, they encourage repair and rebuilding of damaged property, which may lead to the next flood of similar size giving rise to more damage.

The concept of flood hazard management includes flood control and flood plain managements. Traditional flood control measures have generally referred to various engineering projects aimed for flood water control such as building of levees and traditional flood plain management, which is aimed at controlling building in the flood plain. Current efforts are directed toward comprehensive flood hazard mitigation planning. Comprehensive flood hazard management is the most effective way to address flood control issues. It incorporates a variety of engineering, environmental protection, and planning measures with flood plain management, flood control maintenance activities, storm water management, and shoreline management, protection of frequently flooded areas under growth management,

watershed management, other flood hazard mitigation activities, and preparation for flood disasters, where mitigation activities cannot prevent flooding.

Environmental management studies against natural hazards and disasters should be based on the risk management, which has two components as the preparation for and reduction of exposure to potentially hazardous events including floods, droughts, hurricanes, or earthquakes; the next one is based on the development of a mechanism for recovery after an event strike. The literature on hazard and disaster management is huge, ranging from studies into the mechanisms, which generate hazards, engineering and management responses to hazard and the factors which determine vulnerability to hazard.

In a flood-prone region prior to any flood occurrence, the preliminary necessary steps must be put into action such as the alteration of the physical (hydraulic, hydrologic) manifestations of the hazard event, to reduce loss exposure and to facilitate subsequent recovery from loss. These activities require engineering works for river channel alterations, building planning to reduce susceptibility to damage, land-use planning to encourage wise use of hazard-prone areas, the development of early warning and forecasting systems, and the development of insurance to pay for losses. The following points are essential for preliminary works for preparation before the next flood occurrence in any area.

(1) The environmental physical situation must be arranged especially by encouraging development in risk zones such that it does not lead to an increase in exposure,
(2) During the flood protection preparation, community sectors must not be harmed differentially for benefit or harm,
(3) Preparation works must take place in such a way that they do not increase exposure to other type hazards and threats,
(4) Preparations in any area must not increase exposure to downstream communities. In fact, a joint cooperation is the most effective way between the upstream and downstream communities.
(5) In any planning and development within or nearby an urban area, flood impact possibilities must be taken into consideration.

At times and places, emergency measures and actions must be taken immediately after a disaster onset with inclusion of disaster relief provision and assistance. Sustainable disaster relief should not increase vulnerability to subsequent events or other hazards, and should be implemented equitably. Although the climate change is just one of the drivers behind an increasing interest in sustainable hazard management approaches, it is not necessarily the most important one. However, it does affect the performance and benefits of sustainable measures.

Not all the flood phenomena have destructive effects, and therefore, they are not dangerous. By definition, an ordinary flood cannot be described as hazardous unless it threatens human life and property. The damage potential of flood waters can increase exponentially with velocity and speeds above 3 m/s can undermine the foundations of buildings (Smith 1992). The physical stresses on structures are

raised further, probably by hundreds of times, when rapidly flowing water contains debris such as rock and sediment (Chap. 7). Rapid inundation by floods greatly increases the risk of life as well as property. This is because forecasting and warning systems can provide less time for evacuation or for emergency flood-proofing measures.

## 9.4  Risk Assessment

The risk is not only under the control of experts but also individuals, societal, and administrational agents must also be involved so as to try and reduce the certain risk levels. In this task, not only objective scientific methodologies but interactively subjective knowledge and information must also be taken into consideration. Societal experiences are significant ingredients in any risk reduction management. Risk perception and weighting procedures are two important stages in any risk assessment. Risk perception is concerned with the magnitude of risk of individuals or groups in flood hazard involvement risk management. Each shareholder should have a proper concept about the flood hazard and risk levels. It is a well-known fact that anybody, who has been involved in a previous flood event, should have a better conception about the flood risk and consequent hazard. Their accumulative knowledge provides a common basis for rational awareness and proper decision-makings. All these subjective and linguistic information coupled with proper scientific methodologies as explained in the previous chapters direct the early warning and the necessary precautions before, during, and after the flood occurrences.

Inclusion of rational and presumable correct flood risk concepts based on subjective awareness and decisions support objective approaches to match the objective information deduction, which is very significant for a society. Hence, the decision arrived based on two sources, namely subjective and objective information pave the way to better conception, understanding, preparedness, and mitigation possibilities against possible future flood occurrences and their hazards risks. In the overall flood assessment works, effective communication provides dissemination, analysis, and synthesis of the available information and their digestion by reliable scientific methodologies. Risk perception also depends on the feelings, experiences, and expert views. It is not possible to have effective risk perception prior to identification, assessment, analysis, and synthesis of every sort of knowledge and information sources. It is a continuous process, which builds up with time through knowledge and information accumulation and their objective evaluations. Risk analysis is concerned with scientific methodologies, whereas the risk perception is more cultural and societal activity responses.

Even though the risk perception ripens with time, it does not help to reach final decision, because there are fuzziness ingredients in the perceptions. The information for the risk analysis is vague, incomplete, and imperfect, and therefore, even the scientific methodology results are not free of uncertainty. However, in practice,

the main purpose is to reduce this uncertainty as much as possible. Risk is an option that is related to the probability of unwanted (negative) consequence, and it is not possible to clear the risk concept from all the uncertainties and fuzziness. For this reason, the best approach is to weight the flood risk based on possible pros and cons that affect the society. The risk assessment includes the weighting of individual risks that are identified due to different causes.

Flood risk is not a stagnant process, but it has temporal and spatial dynamism, which should be taken into account in the formulations and implementation strategies. Flood risk management can be achieved with the joint contribution of various experts, especially, water engineers, hydrologists, hydrogeologists, economists, social scientists, local administrators, environmentalists, and urban area planners.

Different scientific methodologies (probabilistic, statistical, and stochastic) help to define objectively the risk estimation with confined uncertainty (Chap. 6). There are four types of uncertainties in any risk assessment. These are knowledge uncertainty (linguistic information and simulation works), inherent natural uncertainty in the variability (meteorological and climate-related uncertainty), methodological uncertainty (adaptation of a convenient model), and final decision uncertainty. The best way of quantitative uncertainty is by means of probabilistic methodologies (Chap. 6). The improvement studies in the uncertainty are focused on climatological, hydrological, and hydraulic modeling with the involvement of relevant expert team. Each expert should try to maximize his/her scientific information on flood hazards and flood risk in order optimizing the effectiveness of flood protection measures. Politicians are the execution agents for the implementations of the decisions reached by scientific teams. The implementations must be approved by the local administrators and societies, who should be educated continuously for their region flood protection policies.

### 9.4.1   Risks and Uncertainties at All Levels

In an integrated management system, the risks must be considered collectively after the identification of individual risk components related to floods. Each time after certain durations, for instance, each year the responsible authority must ask the questions; is there additional uncertainties and risk? One must not forget that each component as social, natural, and economic aspects has their individual uncertainty sources. Integrated flood management (IFM) has specific rules in integrating water resources development in a drainage area including two main targets as maximization of efficient flood plain use and minimization of flood damage on human life and property. In addition to short-term, also long-term management strategies must be taken into planning framework. In such a management, especially flood plain location precious arable and fertile land pieces must have extra care by the decision makers. The flood plain productivity must be managed in such a way that by time the efficiency and productivity are maximized. In the meantime, economic

and human life loses must not be forgotten in any planning procedure. Although there are traditional mitigation procedures, they are rather local and not efficient. IFM procedures subsume all these activities under the umbrella of large-scale development and flood protection studies. For an efficient IFM, initial planning of the drainage basin must be set up with the vision of all the shareholders jointly and then accordingly, flood-prone areas are identified, and the necessary studies are started. In the IFM strategy, the surface (runoff) and subsurface flow toward the outlet points, erosion and sedimentation, and possible pollution alternatives should be taken into consideration (Chap. 7). Development requirements and the flood losses must be held in a balance with improvement of the river main channel and branches for protection against flood dangers. In the meantime, the harmonious balance must be kept among water, land use, and drainage basin environment. The main purpose is not only to reduce loses, but also to maximize the efficiency of the flood plains. Of course, the main objective is to reduce the loss of human life. It must not be forgotten that population and economic activities exert significant pressure on the flood plains, and therefore, enhanced economic activities must be planned in such a way that in the future there will be improvements. Especially, in populated regions, development of urban areas may trigger flood risk, and therefore, infrastructure construction must be based on the IFM reduction strategic planning works. Especially, in urban areas, extra care is necessary for flood risk augmentation structures. Flood inundation maps are one of the main guidance for efficient and successful IFM studies. Flood plains are gravitational locations for agricultural activities because of the fertile arable lands, haulages of fine sand and gravel material for constructions, technically suitable places for building constructions for easy livelihood opportunities.

Every society urges for water and food security and these are the most abundantly available along the main channels of the flood plains. The most flood subjective flood plains are attractive settlement areas for poor people and those who migrate from different places of the same country, and therefore, their security must be a part of the IFM program. Land and water interactions are the highest dynamic temporal and spatial activities at river basins; improvement in one may endanger the other to a certain extent. When the balance limits are transgressed then the river basin may behave in an unnatural manner giving rise to flood events that have not been observed in the past. Even the floods may be in flash forms that are more dangerous than common ones (Chaps. 1 and 5). In drainage basin farming, mining and urbanization are the main responsible activities that can cause unprecedented flood occurrences, if they are not planned and managed according to the potentiality of the drainage basin. Floods may cause landslides, erosion, sedimentation, and pollution effects. For instance, landslides or sedimentation may disturb surface flow regime. On the other hand, improper land use, deforestation, and urbanization may endanger the flood plain in favor of flood hazard and risk augmentation.

In any future flood vulnerability, mitigation and risk assessments, the following points must be taken into consideration.

(1) Population growth and economic activities are among the major factors that increase the flood occurrence potentiality of the flood plains,

(2) Flood assessment methodologies must be chosen carefully to suit the circumstances of the drainage basin, otherwise under estimation of flood design discharge may cause flood dangers and loses of human life and property,

(3) As a result of climate change impact, in many regions, the intensity, duration, and frequency of precipitation events are bound to increase, which means that in the future more frequent severe flood and flash flood occurrences may appear with augmented magnitudes.

Flood plains are, in general, those lands most subject to recurring floods, situated adjacent to rivers and streams. They are, therefore, "flood prone" and are hazardous for development activities if the vulnerability of those activities exceeds an acceptable level.

## 9.4.2   Risk Analysis

The risk management approach to decisions is not simply an application of the precautionary principle to decision analysis under uncertainty. It is, instead, as rooted in the precise definition of economic efficiency as the cost–benefit approach. In any IFM against the floods, the most significant points are as follows (Yadigaroglu and Chakraborty 1985; UNDRO 1991).

(1) Effective, rational, and logical risk analysis: This provides information on every type of risk calculations numerically and/or verbally so that the risk potential of the area is well established,

(2) The assessment of the risk analysis under the present circumstances with future considerations: It is necessary to grasp the basic concepts, perceptions, and their effective evaluation as preparation for risk reduction,

(3) To accommodate all the facilities toward risk reduction: This is also for further risk reduction activities by taking into consideration all available local and international knowledge, information, and expertise.

In any flood risk management, there are three risk-related tasks, namely, risk analysis, risk management, and risk reduction. Risk analyses try to determine hazard and vulnerability. Risk assessment has its main concern on perception and weighting of the risk, whereas risk reduction focuses on reductions prior to the flood occurrence, during the flood and after the flood subsidence.

An effective risk assessment and flood vulnerability study should include several information sources as meteorological, hydrological, hydraulic, economic, social science, and ecological modern methods. Collection, integration, generation, and dissemination of the knowledge from all these fields provide a common basis for effective flood risk evaluation. There are many theoretical probabilistic, statistical, and rational approaches that are used in practical applications and their basic

concepts, principles, and activations corporate altogether risk assessment scientifically and administrationally.

Floods are natural hazards that appear at different times and durations, and therefore, in their design, the duration must be taken into consideration. The duration is selected according to the significance and functionality of the location. For instance, within the city developments 5-year to 25-year; for road constructions 25-to 50-year; for agricultural areas 50- to 100-year; in spillway calculations 100- to 250-year; and in cases of extreme flood protections 500-year durations are preferable. The design duration, $T$, is in direct relationship with the design discharge, $Q_D$, but this relationship may not be linear. It can be expressed mathematically in an implicit form as,

$$Q_D = f(T) \tag{9.1}$$
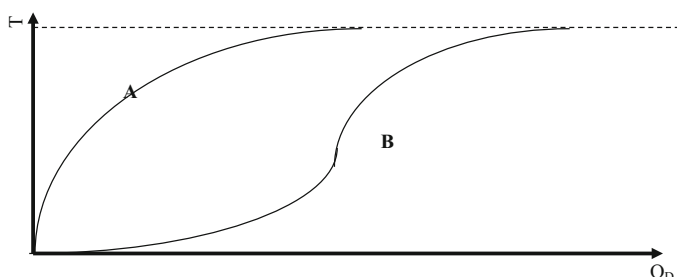
Rational thinking leads to the conclusion that as the design duration increases, although the design discharge amount also increases, but there are reductions in the design discharge increment rate, and therefore, consideration of the design discharge on the horizontal axis and the duration on the vertical one leads to the visualization of one of the curves in Fig. 9.1.

In this figure, curve A provides a quick response design discharge to duration, whereas in curve B the response is slow.
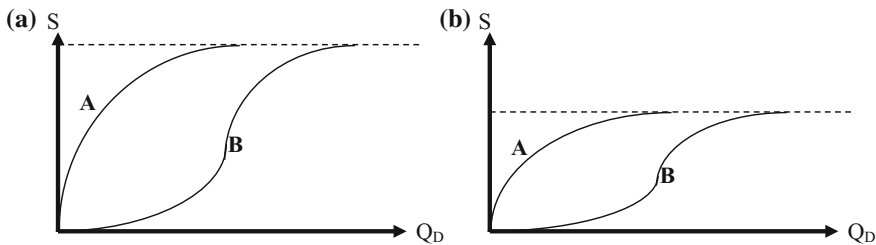
Another question is what is the relationship between the design discharge and the safety, S, against flood. Again rational logical thinking indicates that as the safety increases, the design discharge decreases. For instance, in case of a dam construction against flood hazard, does increase in the reservoir storage capacity reduce the damage at the downstream locations? Logic implies that there is again a nonlinear form of relationships as in Fig. 9.2 in two comparative graphs.

In Fig. 9.2a, the storage volume of the reservoir is bigger than the one in Fig. 9.2b, and consequently, it is safer but in both as the safety increases also the design discharge increases.

The most important quantity of floods is the risk concept from the engineering, social, and economy views. Flood risk, $R$, and the safety are two complementary



**Fig. 9.1** Duration and design–discharge relationships

**Fig. 9.2** Safety and design–discharge relationships

events. The more is the safety the less is the risk. For a given water structure, their summation is equal to a constant value, c, as (see Chap. 6),

$$S + R = c \qquad (9.2)$$
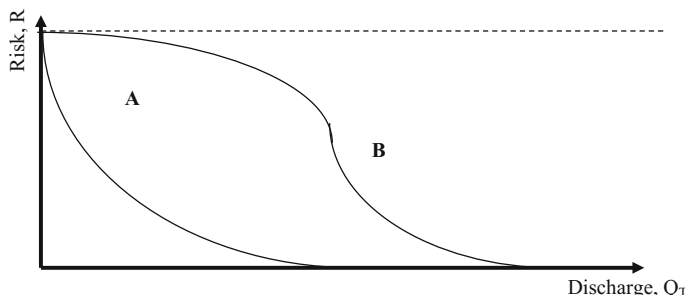
The constant implies all the possibilities of safety and risk. If both sides of this equation is divided by the total value, c, then one can obtain the percentages or probabilities of risk, $r$, and safety, $s$, as,

$$s + r = 1 \qquad (9.3)$$
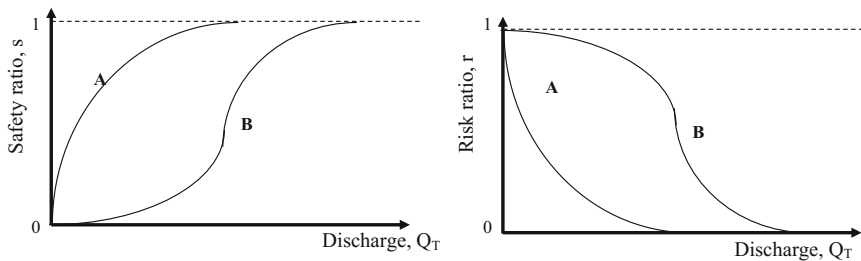
On the basis of Eq. (9.2) together with Fig. 9.1, there is an inverse relationship between the risk and the flood design discharge in a nonlinear manner as in Fig. 9.3.

The comparison of Figs. 9.1 and 9.2 leads to the conclusion that the risk is inversely related to design duration. For practical applications, Figs. 9.1 and 9.3 become standardized if the vertical axis is scaled down to 1 as in Fig. 9.4.

In these figures, the variation domain of risk (safety) is between 0 and 1 and for zero risk (unit safety) and vice versa. Multiplication of the values on the vertical axis by 100 yields percentages of safety and risk, if necessary. In practice, there is no case with 100% risk (or safety). There is never a methodology, which satisfies



**Fig. 9.3** Risk–discharge relationships

**Fig. 9.4** Design discharge-safety–risk standard curves

100% safety, which means that there is always risk percentage and in engineering works, this percentage is regarded as acceptable if it is less than 10%. The summary of all the rational and logical derivations leads to the following points.

(1) There is a direct relationship between the flood design discharge and duration of occurrences to the next flood but it is not linear (see Fig. 9.1),
(2) Safety and design discharge are inversely and nonlinearly related to each other (Fig. 9.2),
(3) Risk–design discharge relationship is also inversely and nonlinearly related, (Fig. 9.3),
(4) The summation of safety and risk ratios is equal to 1 (Fig. 9.4) because subtraction of safety-design discharge curve from 1 yields risk-design discharge curve,
(5) In practice, the risk (safety) cannot be equal to 1.
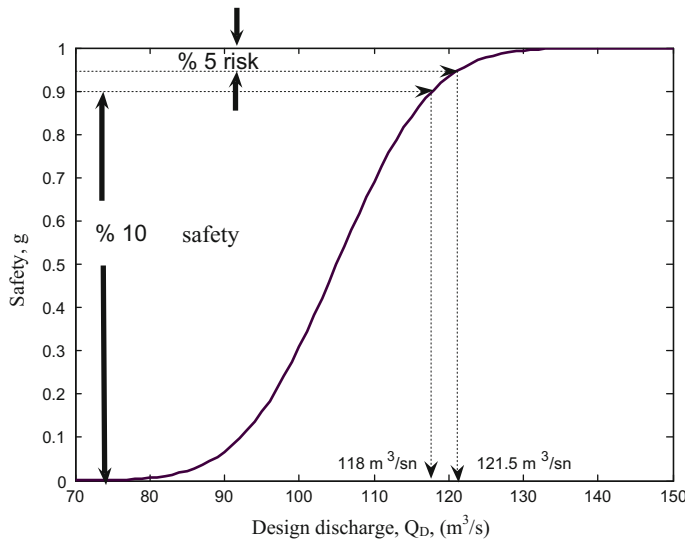
**Example 9.1:** If the safety–design discharges relationship is regarded as in Fig. 9.5, then answer to the following questions.

(1) What is the % 90 safety-design discharge?
(2) What is the % 5' risk-design discharge?

**Answer 9.1:** The given curve provides opportunity for the flood design discharge calculation for the region.

(1) Starting from the vertical axis corresponding to 90% safety, one can reach to given curve horizontally, and the design discharge is on the horizontal axis corresponding to the intersection point on the curve and the numerical value is 118 m$^3$/sec,
(2) Under the light of Eq. (9.3), 5% risk level is equivalent to 95% safety and similar to the previous calculation, one can read the flood design discharge on the horizontal axis as 121.5 m$^3$/sec.

Since flood design discharge calculation is based on the return duration; what is the relationship of safety (or risk) to the duration? The answer to this question can be found in the definition of design flood (Chap. 6). Over the design duration the

**Fig. 9.5** Safety ratio–design discharge relationships

flood is assumed to occur only once, and hence, during the time duration, $T$, the occurrence ratio, i.e., risk ratio, $r$, (probability) is,

$$r = \frac{1}{T} \tag{9.4}$$
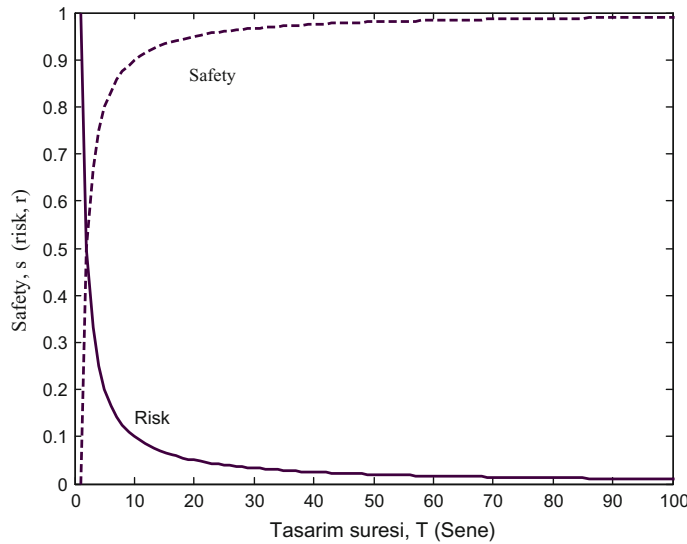
The safety ratio can be calculated from Eq. (9.3) as,

$$s = 1 - \frac{1}{T} \tag{9.5}$$

It is important to remember one very important point that the safety or risk represents only one occurrence at any time during the design duration. This leads to the conclusion that there is an inverse and nonlinear relationship between the risk and the duration. Figure 9.6 indicates the relationship between the risk, safety ratios, and the duration.

The rational and logical derivations of aforementioned equations also explain how they can be used in practical applications. The most important question is how one can obtain these curves for study area? These curves are functions of the regional climatology, morphology, and hydrometeorology.
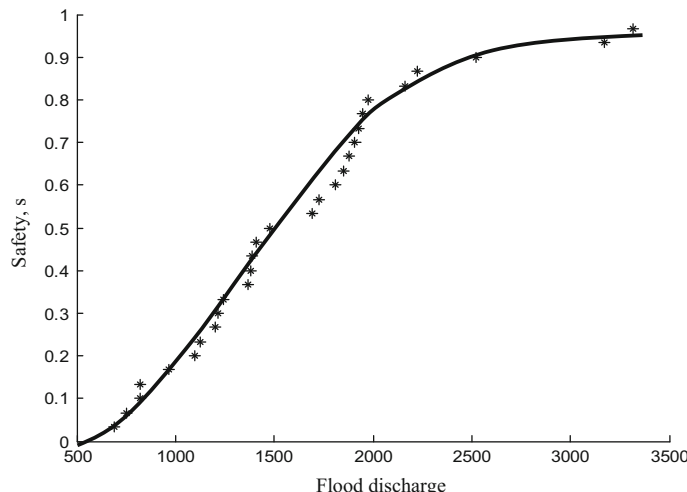
It is time to explain the derivation of these safety and risk curves empirically. For this purpose, one needs flood discharge historical record time series in the region. Such measurements are given in Chap. 6, Table 6.2.

**Fig. 9.6** Safety–risk-design discharge relationships

If one takes into account that the remaining life of the world is 5 billion years (in practical application, this is assumed as infinity), then in Chap. 6, Eq. (6.13) yields value almost equal to 1, i.e., $P(X_m < Q_D) = 1$.

The safety percentages can be obtained by subtracting the risk percentages in Table 6.2 from 1, and the relationship between the flood design discharge and safety is plotted in Fig. 9.7.



**Fig. 9.7** Flood discharge–safety relationships

The scatter points indicate never descending part and the best fit to this scatter gives the analytical expression for the flood design discharge–safety relationship. The functional form of the continuous curve is always in the form of CDF.

Under the light of the aforementioned explanations, Turkish Water Foundation has suggested similar procedure by considering some error, $e$, component in the duration value as follows,

$$s = \frac{m}{n(1+e)} \tag{9.6}$$

For the flood calculations according to Eq. (9.6), the flood data in Table 6.2 are adapted and the results are given in Table 9.1 for five error levels as 1–5%.

The relationship of flood design discharge-safety is given in Fig. 9.8 for each error amount, but they yield practically very close safety values.

This figure is similar to Fig. 9.7, but it differs in the sense that instead of only one safety level, there is a set of safety levels within a narrow band.

## 9.5   Probability Distribution Functions of Flood Data

As for the safety and risk probability definitions in the previous sections, the probability of exceedance and non-exceedance of a given flood design discharge, $Q_D$, can be expressed as,

$$s = P(Q \leq Q_D) = \frac{n_s}{n} \tag{9.7}$$

and

$$r = P(Q > Q_D) = \frac{n_b}{n} \tag{9.8}$$

where $P(Q \leq Q_D)$ and $P(Q > Q_D)$ are non-exceedance and exceedance probabilities, respectively; $n_s$ and $n_b$ are the numbers of discharges to be smaller and greater than flood design discharge. Similar to Eq. (9.3), the summation of the safety and risk statements is equal to one.

$$P(Q \leq Q_D) + P(Q > Q_D) = 1 \tag{9.9}$$
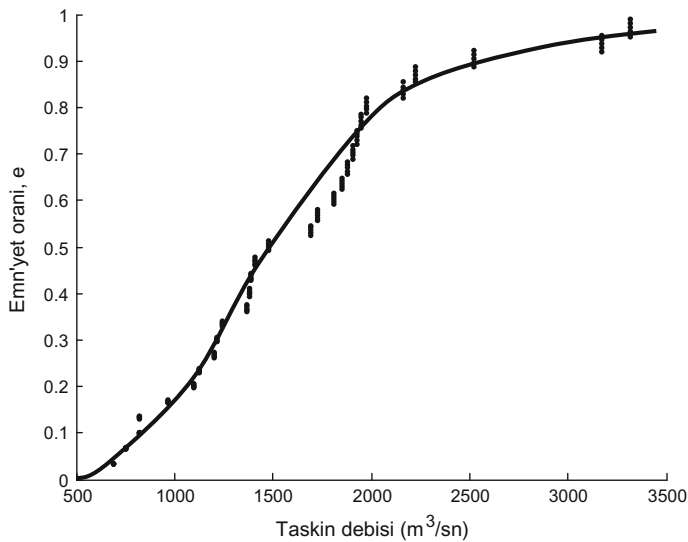
In Fig. 9.4, the design discharge-safety curve shows the probability of discharge to be less than design discharge and it is in the form of continuously increasing form, and therefore, named as the PDF. According to the theory of probability, the

**Table 9.1**  Turkish Water Foundation flood discharge calculations
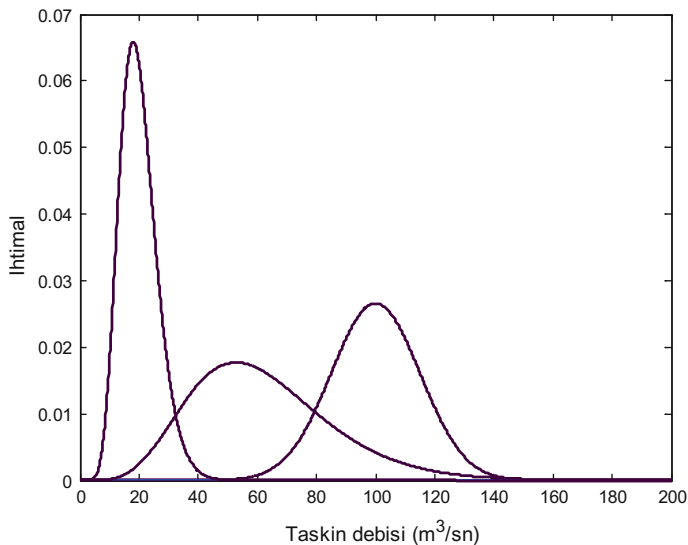
| Natural record | | Artificial ranks | | Safety with error ingredient | | | | |
|---|---|---|---|---|---|---|---|---|
| Year | Flood discharge (m³/sec) | Ranked flood discharge (m³/sec) | Rank, m | $e = 0.01$ | $e = 0.02$ | $e = 0.03$ | $e = 0.04$ | $e = 0.05$ |
| 1980 | 2520 | 690 | 1 | 0.034 | 0.034 | 0.033 | 0.033 | 0.033 |
| 1981 | 1850 | 750 | 2 | 0.068 | 0.068 | 0.067 | 0.066 | 0.066 |
| 1982 | 750 | 820 | 3 | 0.102 | 0.101 | 0.100 | 0.099 | 0.099 |
| 1983 | 1100 | 820 | 4 | 0.137 | 0.135 | 0.134 | 0.133 | 0.131 |
| 1984 | 1380 | 965 | 5 | 0.171 | 0.169 | 0.167 | 0.166 | 0.164 |
| 1985 | 1910 | 1100 | 6 | 0.205 | 0.203 | 0.201 | 0.199 | 0.197 |
| 1986 | 3170 | 1126 | 7 | 0.239 | 0.237 | 0.234 | 0.232 | 0.230 |
| 1987 | 1200 | 1200 | 8 | 0.273 | 0.270 | 0.268 | 0.265 | 0.263 |
| 1988 | 820 | 1212 | 9 | 0.307 | 0.304 | 0.301 | 0.298 | 0.296 |
| 1989 | 690 | 1240 | 10 | 0.341 | 0.338 | 0.335 | 0.332 | 0.328 |
| 1990 | 1240 | 1367 | 11 | 0.376 | 0.372 | 0.368 | 0.365 | 0.361 |
| 1991 | 1730 | 1380 | 12 | 0.410 | 0.406 | 0.402 | 0.398 | 0.394 |
| 1992 | 1950 | 1385 | 13 | 0.444 | 0.439 | 0.435 | 0.431 | 0.427 |
| 1993 | 2160 | 1410 | 14 | 0.478 | 0.473 | 0.469 | 0.464 | 0.460 |
| 1994 | 3320 | 1480 | 15 | 0.512 | 0.507 | 0.502 | 0.497 | 0.493 |
| 1995 | 1480 | 1695 | 16 | 0.546 | 0.541 | 0.536 | 0.531 | 0.525 |
| 1996 | 1812 | 1730 | 17 | 0.580 | 0.575 | 0.569 | 0.564 | 0.558 |
| 1997 | 1695 | 1812 | 18 | 0.615 | 0.609 | 0.603 | 0.597 | 0.591 |
| 1998 | 1926 | 1850 | 19 | 0.649 | 0.642 | 0.636 | 0.630 | 0.624 |
| 1999 | 820 | 1876 | 20 | 0.683 | 0.676 | 0.670 | 0.663 | 0.657 |
| 2000 | 965 | 1910 | 21 | 0.717 | 0.710 | 0.703 | 0.696 | 0.690 |
| 2001 | 1212 | 1926 | 22 | 0.751 | 0.744 | 0.737 | 0.729 | 0.722 |
| 2002 | 1385 | 1950 | 23 | 0.785 | 0.778 | 0.770 | 0.763 | 0.755 |
| 2003 | 1976 | 1976 | 24 | 0.819 | 0.811 | 0.803 | 0.796 | 0.788 |
| 2004 | 2225 | 2160 | 25 | 0.854 | 0.845 | 0.837 | 0.829 | 0.821 |
| 2005 | 1876 | 2225 | 26 | 0.888 | 0.879 | 0.870 | 0.862 | 0.854 |
| 2006 | 1126 | 2520 | 27 | 0.922 | 0.913 | 0.904 | 0.895 | 0.887 |
| 2007 | 1367 | 3170 | 28 | 0.956 | 0.947 | 0.937 | 0.928 | 0.920 |
| 2008 | 1410 | 3320 | 29 | 0.990 | 0.980 | 0.971 | 0.962 | 0.952 |

derivative of this curve provides PDF, which is shown in Fig. 9.9. The probability corresponds to the relative frequency of the observed discharge value.

This point indicates the importance of the PDF in the calculation of flood discharge. It also indicates that in order to make flood calculations, first of all the empirical frequency distribution function must be obtained from the observations (Chap. 6).

**Fig. 9.8** Turkish Water Foundation flood discharge–safety relationship



**Fig. 9.9** Probability distribution functions

## 9.6   Hazard and Safety Calculation

Among earth sciences, hydrology and meteorology phenomena are the rainfall, runoff, flood, drought, thunderstorm, fog, solar irradiation, and evaporation, wind velocity, in addition to soil and rock properties. Future occurrences and magnitudes of these phenomena should be predicted at high accuracy with the hope to reduce their disastrous consequences that may lead to floods and water structure damage. Successful predictions are based on the quantitative uncertainty methods such as probability, statistics, and stochastic approaches (Chap. 6) in addition to recent modern technique of qualitative analysis in terms of fuzzy logic (Şen 2004). It is the main purpose of this section to mention various applications of these techniques concerning the hydrometeorological-earth science aspects and regional risk properties. Although water structures have many benefits, they can also pose risk to communities without proper design, maintenance, operation, and management procedures.

In order to reduce the risks of the floods, the education and training programs must also be in cooperation with the common interest and usage of the available data. This is the only way how to reach to the scientific conclusions and consequent interpretations. In this manner, the quantitative data can be obtained linguistically for useful information extraction from local people even though they may not be experts. Along this line, the effects of the weather pattern on the human life and property must be kept alive in the daily agenda for the conservation of properties. Each country should have risk maps for floods, in particular, and for any natural events, in general. Although the gathering of the basic meteorological data is costly, their interpretations and coupled model usages are more important. By means of suitable procedures, useful information can be extracted from the quantitative data and they become very desirable by the policy makers, administrators, and the insurance companies.

Natural hazards are always a part of human history even in the modern world despite the scientific and technological achievements, there is a continuing death and destruction associated with the extreme events. The minimum is the hazard, the best is the safety. Scientific and technological designs and developments are not without hazard and they give rise to emergence of man-made threats, which may arise from the misapplication of technology failure and its application in engineering designs such as water structure constructions. Hazard is an ever-present and inescapable part of everyday life. Nobody can live in a risk-free environment. Risk is sometimes synonymous with hazard, and it has a particular chance of occurrence. The following definitions are meaningful.

Hazard:   It is a potential threat to humans and their welfare.
Risk:      It is the probability (chance) of hazard occurrence.
Safety:    It is a potential non-threat to humans and their welfare
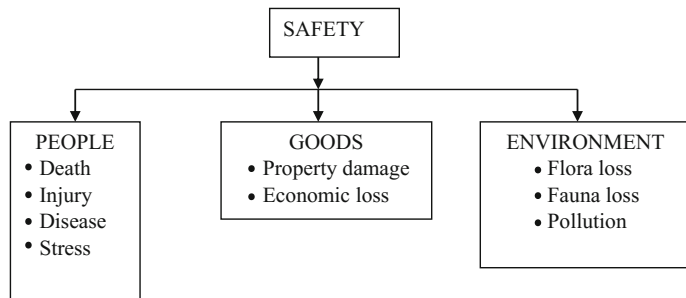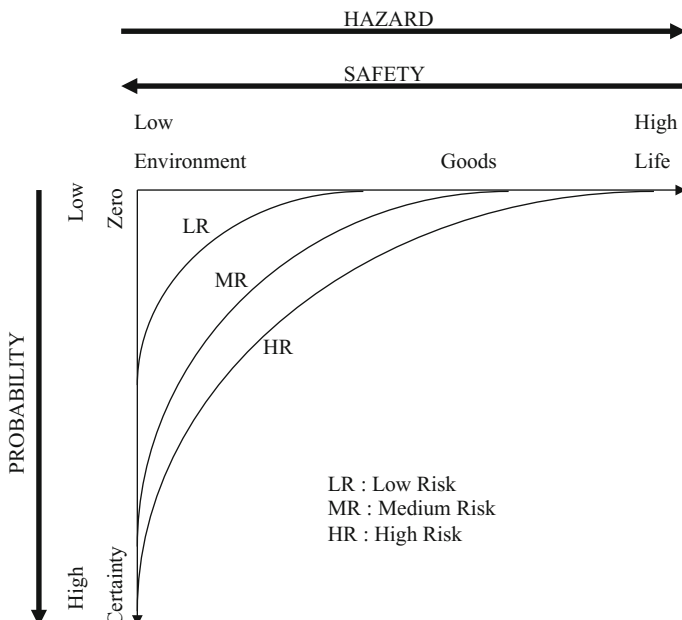
For example, at the same location, if two water structures, one small and the other one in big scale, are proposed for construction, then both of them will have

the same hazard for downstream environment but the risk (probability of damage) and safety are very different. This means that hazard, risk, and safety operate on varying scales. The threats in Fig. 9.10 should be decreased for hazard severity, i.e., for safety increase.

There is always a relationship between the hazard or safety and its probability, which shows the overall case as in Fig. 9.11 (Smith 1992).



Fig. 9.10 Safety threats



Fig. 9.11 Relationship between safety-hazard-probability

Most of the hazardous situations have several points in common at the same time and location. These may include,

(1) The origin of damage is clear with characteristic effects,
(2) The warning time is short, for instance, water structure failure may take place instantly,
(3) Most of the property and life losses are suffered very shortly after the occurrence of event,
(4) The risk of exposure is largely involuntary and in normal cases, it is due to location of people, which is mostly in risky, hazardous, and unsafe areas,
(5) The resulting disaster occurs with an intensity and scale.

The water structures are under the threat of different natural and man-made risks right from the construction onwards. These risks can be summarized as in Table 9.2.

The following are among the reasons why despite the development of science and technology, there are still possibilities of risk.

(1) Population growth at times by migrations that could not be accommodated with available facilities,
(2) Land use and planning pressure. Especially, land exploitation without taking into consideration proper planning considers possible future hazards,

**Table 9.2** Water structure safety and risks

| *Atmospheric* |
| --- |
| • Rainfall intensity and frequency |
| • Snow |
| *Hydrologic* |
| • Floods |
| • Runoff |
| • Wave action |
| • Glacier advance |
| • Snowmelt |
| • Erosion |
| *Geologic* |
| • Landslide |
| • Mudflows |
| • Subsidence |
| • Earthquake |
| • Silting |
| • Volcanic eruptions |
| *Hydrogeology* |
| • Groundwater |
| • Karstic media |
| • Fractures |
| *Technological* |
| • Material quality |
| • Design errors |
| • Engineering design |

(3) Economic growth, which led to increased leisure time with the construction of additional homes built in potentially dangerous locations,
(4) Technological innovations, which are used in dam and water structure construction,
(5) Social expectations, safety in services are expected by consumers from weather-born enterprises such as water supply,
(6) Growing interdependence, which adds to the increase of unsafe areal coverage of hazards.

In general, risk is an integral part of life and there is almost nothing without risk involvement. Even the best expertise, knowledge, science, and technology are collaborated in any water structure designs, still the safety of the final product must be monitored with time at a set of different control points.

## 9.6.1   Risk Calculations

For the safety of any engineering water structure, it is necessary to keep track on the performance records with qualitative and quantitative assessment procedures in addition to future predictions of the alternative dangerous possibilities, if any. Hence, a risk assessment procedure must be kept alive at all times, which must include the following steps.

(1) Possibility evaluation of a set of future disasters that may occur during the future life of a water structure,
(2) Probability evaluation of each possibility and the risk attachment (hence safety attachment),
(3) Social evaluation of possible and probable consequences of the risk (or safety). Here, the question is; what is the consequent loss by each possible and probable event so far as the human life and property are concerned?

If the probability of each event is p and the consequent loss is $L$, then the social attachment risk, $R_S$, of such an event can be expressed as,

$$R_S = p \times L \tag{9.10}$$

### 9.6.1.1   Historical Data Presence

If there are n historical events, $E_1$, $E_2$, ..., $E_n$ of a phenomenon, say floods, each with probability of occurrence, $p_1$, $p_2$, ..., $p_n$ such that

$$p_1 + p_2 + \ldots p_n = 1 \tag{9.11}$$

and respective losses, $L_1, L_2, \ldots, L_n$, then one can order the events in the increasing order of loss as,

$$L_1 \leq L_2 \leq \ldots \leq L_n \tag{9.12}$$

Based on the ordering, the cumulative probability for an individual event can be calculated as follows.

$$P_j = p_j + p_{j+1} + \ldots p_n \tag{9.13}$$

This enables one to decide the probability of the occurrence of an event for which the loss is as great as or greater than $L_j$ as in Table 9.3.

In order to calculate the overall loss, $L_o$ in a weighted average form the following expression is valid.

$$L_o = p_1 L_1 + p_2 L_2 \ldots + p_n L_n \tag{9.14}$$

On the other hand, without loss consideration, the probability of extreme event occurrence, $p_i$ ($i = 1, 2, \ldots, n$) can be calculated for n data values, $X_i$ ($i = 1, 2, \ldots, n$) according to Table 9.4.

In the formulation form, the probability of $m$-th ranking data value can be given similar to Eq. (9.8) as,

$$p_m = \frac{m}{n+1} \tag{9.15}$$

Table 9.3  Quantitative risk analysis

| Phenomenon | Probability | Loss | Cumulative probability |
|---|---|---|---|
| $E_1$ | $p_1$ | $L_1$ | $P_1 = p_1 + \ldots + p_n = 1$ |
| $E_2$ | $p_2$ | $L_2$ | $P_2 = p_2 + \ldots + p_n$ |
| . | . | . | . |
| . | . | . | . |
| . | . | . | . |
| $E_n$ | $p_n$ | $L_n$ | $P_n = p_n$ |

Table 9.4  Extreme event probability of occurrence calculations

| Data value | Ascending data | Rank | Probability |
|---|---|---|---|
| $X_1$ | $X_i$ (minimum) | 1 | $1/(n+1)$ |
| . | . | . | . |
| . | . | . | . |
| $X_2$ | $X_j$ | $m$ | $m/(n+1)$ |
| . | . | . | . |
| . | . | . | . |
| . | . | . | . |
| $X_n$ | $X_k$ (maximum) | $n$ | $n/(n+1)$ |

### 9.6.1.2   Historical Data Absence

The simple risk, $R$, can be defined as the probability of occurrence of the hydrological variable, $X$, to be greater than the design discharge, $Q_D$, at least once over the system's economic life, $n$. If the sequence of future likely occurrence of $X$ is $X_1$, $X_2$, …, $X_n$, then the joint probability of non-occurrence, i.e., safety, S, is defined as,

$$S = P(X \leq Q_D) = P(E_1 < Q_D, X_2 < Q_D, \ldots, X_n < Q_D) \qquad (9.16)$$

Hence, the simple risk, $R$, as a complementary event is defined as,

$$R = 1 - P(X_1 < Q_D, X_2 < Q_D, \ldots, X_n < Q_D) \qquad (9.17)$$

The calculation of the multivariate probability term on the right-hand side of Eq. (9.17) is dependent on the structure of the variate considered and, in general, can be calculated by multiple integration of the multivariate PDF through tetrachoric series expansion (Saldarriaga and Yevjevich 1970). However, in the case of simple dependence structure such as the first-order Markov dependence, the right-hand side of Eq. (9.16) factorizes into various terms which are explained in detail in Chap. 6 and by Şen (1976).

## 9.7   Flood Control Structures

Unfortunately, only engineering structural protections cannot serve the community, but more significantly the pre-flood warning through the flood inundation maps are very helpful for future planning by local and central authorities. The main rule considered in this section is that rather than the trust to an engineering structure and expansion of the activity within the flood plain, it is wiser to depend on the flood inundation maps in planning for future developments in a flood-prone area. Psychologically, the existence of such maps will hinder any administrator to allow land use in the floodplain even at his own risk.

Flood damage can be reduced by engineering works (dikes), flood-proofing techniques, pre-flood planning initiatives, and post-flood emergency measures. Engineering works, such as dams and dikes, do reduce the risk of flood damage. However, during severe floods dike failure may occur due to erosion (Chap. 7), overtopping, or seepage and flooding will occur. It is impractical and beyond our economic means to eliminate all flood damage with dams and dikes.

Depending on flood abatement and flood diversion alternatives, there are different individual and combination physical control structures and procedures in practical uses. Flood diversion is a direct solution for flood hazard reduction in an area. Flood abatement or flood reduction involves decrease in the amount of runoff

potential that is able to generate a flood peak in a drainage basin. This is a less reliable strategy than flood diversion. Flood abatement approaches are rather theoretical and they include either the weather modification or watershed treatment approaches. Weather modification methods and their impractical consequences are discussed by Şen (1997). Modification approaches cannot be successful due to different reasons, the major one being the cloud seeding sensitivity.

Typical control strategies as watershed treatment include especially in rural areas reforestation or reseeding of sparsely vegetation areas to increase evaporative losses; mechanical slope treatments within the watershed, contour plowing or terracing, runoff coefficient reduction, comprehensive protection of vegetation from wildfires, overgrazing, clear-cutting of forest land, or any other practices likely to increase flood discharges and sediment loads. Furthermore, construction of small water and sediment-holding areas especially in farm ponds also help to reduce the flood discharge in the downstream portions. Most flood reduction achievements are rather local and in small scales and restricted to flood flows from comparatively small basins.

The following protections are concerned with flood diversion measures whereby the floods may partially be diverted from the risk areas. Among these solutions are,

(1) Embankments or stop banks that are terminologically referred to as the levees. They are designed for restriction of flood waters to well-defined, low-value land on the floodplains. Their constructions are simple and mostly constructed from earth fills,

(2) Since one of the flood magnitude effective factors is the velocity and it is dependent on the cross sectional area, it is possible by enlarging the cross sectional area to reduce the flood velocity and to spread the waters over a larger area,

(3) For the regulation of flood waters, temporally impoundment structures such as reservoirs and large dams are constructed. These help to store the water during the flooding time and then to release the water to downstream after the flooding at desired safe amounts.

On the other hand, there are benefits in non-flood-prone areas such that they are the necessary parts of environmental, and catchment ecosystems help to maintain a wide range of wetland habitats, maintain fertile soil by silt deposition, and flush salts from the surface layers, provision of water for natural irrigation and for fisheries as protein source. It is possible to state that in normal years with balanced hydrological conditions floods bring benefit to a society rather than destruction. This is completely true if the necessary precautions in the forms of risk attached flood inundation maps are planned and their future predictions are completed. Even in developed countries, flood risk nature and scale varies greatly. In arid region countries, such as the Arabian Peninsula countries, sudden floods in the form of flash occurrences are the most dangerous hazards in the middle stream portion of the wadi system with inundation risks in the downstream (Şen 2008).

### 9.7.1  Land-Use Planning

Floodplain developments can be reduced by considering different and suitable land-use practices, which are convenient for the region. These developments reduce pressure through a mixed policy of land annexation, service extension, and zoning by-laws and the community made available an adequate supply of flood-free land. Land-use allocations and choices result mainly from a sustained political behavior, but not fully constrained by monetarized estimations. So if the maps of flood inundation with risk attachments are clear and relatively stable at least on the signs displayed (area clearly and simply mapped as having credit, or deficit, of relative security), then they could become a powerful and respected tool for land-use planning and could progressively lead to an actual and respected risk alleviation policy.

In land-use practices against the floods, it is customary to divide the risk into two components, which are more or less independent from each other. These are the vulnerability (the sensitivity of the land use and of the population) and the natural hazard. Such a division leads to a more adequate, flexible and manageable definition of risk. If a place is not vulnerable, then the risk will be small. The vulnerability is related to the exposition of any human activity to flood danger. If in a drainage basin there are no infrastructural elements, no settlement, no agricultural activity, in this case, the vulnerability is almost zero. Most of the drainage areas have negligible vulnerability, and therefore, their risk attachments are not vulnerability dependent.

This is possible only through quantitative and qualitative management of runoff with the aim to reduce the flood scale down to a minimum hazardous level. For this purpose, drainage basin measurements are essential tools, which include infiltration measures by means of infiltration trenches and ponds, detention basins, retention ponds, and wetland areas. In addition to these, other significant components are forestation, reduced impact logging practices, and less intensive agricultural practices so as to reduce soil erosion and landslides that may lead to channel siltation and flood level raisings. At local level, simple means are also effective to reduce the flood scale by means of small-scale runoff storages and drainage improvements all of which lead to flood mitigation.

In cases of afforestation consideration as part of a packet of measures, its full effects should be on the full range of hydrological function and downstream uses should be cared for. In the assessment of the likely effectiveness of source controls, pre-flood conditions must be considered. There are three stages for flood scale reduction.

(1) Flood scale reduction: Among these activities are runoff control, drainage basin management improvement, dam construction at suitable locations, detention basin expansions, and protection of wet lands,

(2) Flood threat isolation: These include flood proofing, flood plain development limitation, and flood embankment constructions,

(3) Human awareness: Emergency and evacuation plans, better forecasting facilities, early warning system establishment, compensation, and insurance policies.

The lowlands are convenient places for flood flow storages through detention basins, which are dry normally prior to storm rainfall occurrence. Lakes on the rivers can also be used as a solution to reduce the flood scale. Natural wetlands are also important assets for flood storage, and agricultural fields can be used for micro-storage.

## 9.8  Public Awareness About Floods

The most effective method of reducing the risk of flood damage is to regulate development on the floodplain. This requires the cooperation of all levels of government, developers, builders, and the public. Land-use decisions by local governments must take into account flood risks to ensure that development occurs on the least hazardous lands. Increased public safety and protection of property is achieved through the following points.

(1) Public awareness of flood hazards,
(2) Establishment of flood-proofing standards for new development,
(3) Local government land-use planning,
(4) Appropriate regulation of subdivision approvals.

Most experts blame the flooding on human activities such as human-induced to the region, and the clearing of forests and riverside vegetation have reduced natural barriers to flooding. Meanwhile, because people are building more on the flood plains, the effect of any flood is more devastating.

Compared to other natural hazards such as earthquakes, volcanic eruptions, and avalanches, which are more local in nature, flooding is the most widespread and most damaging natural risk. Thus, an efficient development of improved flood forecasting and warning systems should be performed by bringing together technical expertise and practical experience from different disciplines. Development and implementation of flood forecasting and warning systems require a multi-disciplinary approach, including hydrological and meteorological expertise as well as expertise in operational flood forecasting systems, flood warning dissemination, and emergency planning.

Over the past years, there has been a shift in both the societal expectation and the predictive capabilities and it is likely that this trend will continue over the next decade. The main societal changes in the context of floods have been an increase in the risk awareness and an increase in the targets for protection levels. Now floods need to be predicted more accurately, over longer lead times and in smaller catchments than in the past years. The predictive capabilities have also changed

tremendously. Accurate weather forecasts are playing an increasingly important role in hydrological predictions and the hydrological models are becoming more complex and data intensive. One of the cornerstones of the data needed for accurate hydrological predictions is satellite data from various platforms.

Many measures can be used by societies to cope with floods. They are usually classified into two major groups as engineering structural and non-structural measures. Furthermore, these measures can be combined together in order to maximize the effects of the alleviation of the floods risks.

Structural measures of the flood management can be defined as the measure that alters the physical characteristics of the floods. They usually involve engineering hydraulic structures as dams, reservoirs and retarding basins, channel and catchments modifications, levee-banks, flood proofing, etc. On the other hand, non-structural measures alter the exposure of lives and properties to flooding (flood forecasting and warning, flood insurance, planning controls, public information and education, etc.)
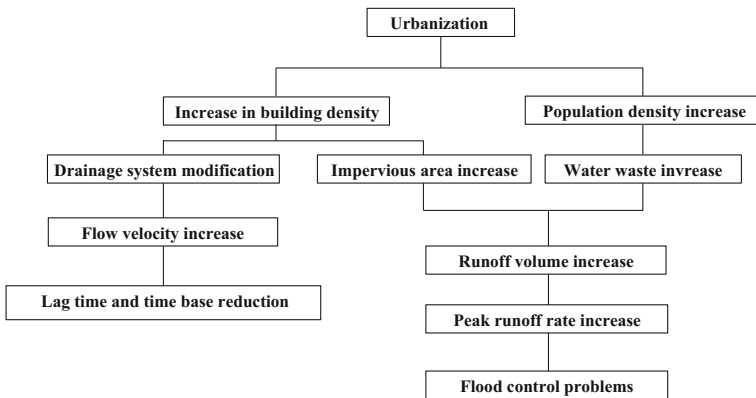
In many water-scarce regions, large amounts of water annually flood out to the sea. Some of this flood water is committed flow to flush salt and other harmful products out of the system and maintain the ecological aspects of estuaries and coastal areas (Seckler et al. 1998).

Even though there are significant improvements in engineering flood design discharge estimation methodologies and structural protections against the floods, they are not sufficient for an efficient flood management. Additionally, prior to flood occurrence, flood inundation maps at different risk levels must be ready (Chap. 3). The inundation boundaries must be known by local settlers so that they can take individual decisions at their own risk.

Urbanization in flood hazard zones creates a challenge as urban areas accommodate higher concentrations of people, buildings, and infrastructure (Wamsler 2004). Despite increasing flood risk awareness, human settlements continue to develop in flood-prone areas due to the need for land, and poverty. These conditions reflect reality for the urban poor who are faced with little option other than to illegally occupy public land or purchase affordable land in hazard zones (Montoya 2002).

The increase in flood frequency in urban area is largely due to the urbanization process, which is mostly reflected by the demand on urban facilities and change on land-use activities that are causing the development of more impervious surfaces (Fig. 9.12). The spread of urbanization has increased flood potential (Bilsborrow 1998). This increase is attributed to the population growth and of higher building density in urban areas. The focus of development in areas prone to hazard without the appropriate protective and maintenance measures will contribute to the increasing losses due to disasters.

Other flood-intensifying conditions arise from human actions such as land-use changes, which may be semi-deliberate, including the increase in agricultural land drainage designed to speed the runoff from productive fields.

**Fig. 9.12** Water quality aspects of hydrological cycle affected by both the rise in population and the increase in extent of the impervious areas (After Hall 1984)

## 9.9   Integrated Flood Management (IFM)

In nature, none of the floods has the same effect as the others because their characteristics change depending on the drainage basin features and their implications as flood plains cause various degrees of hazard to human life and property especially in concentrated settlement areas such as villages, towns, and cities. On the other hand, millions of people are dependent on floods for their livelihood. There are different scientific alternatives for flood peak discharge prediction, management, and inundation maps. If they are cared for properly, then there are social and economic sustainable benefits. This is mostly achieved through a properly planned, managed, and applied integrated flood management, which consists of flood alleviation and utilization, mitigation, and risk management rather than a strict reliance on structural flood control based on dykes, levees, and dams. For instance, the performance of dam structural response is not enough only for flood control but it must be supported by shift toward flood management.

Success in any flood intervention strategy depends on a number of factors that are related to each other in a complicated manner. Population and land-use systems are subject to different risks, which are intimately related to the flood event characteristics. The capacity of population settlement and land use are among the criteria to cope with and recover from risk if an effective flood management strategy is effective in the flood-prone region. Whatever are the facilities and the effectivity of the flood management programs, it is not absolutely possible to achieve a complete protection. It is not even desirable because the main purpose of a flood management program is to reduce the risk, damage, and hazard to a minimum level. For these achievements, reliable predictions, management, and synchronized responds are necessary to prevent widespread losses and obtain the best consequence.

From engineering point of view, although there are intervention strategies in flood management, there is also gradual shift toward flood control through introduction or expansion of non-structural responses as a part of integrated floodplain management strategy. It is possible to classify the basic strategy into three complementary approaches.

(1) The use of a number of structural and non-structural means for flood scale reduction so as to minimize possible unwanted consequences,
(2) Isolation of flood threats by means of structural, technological, and policy alternatives,
(3) Individuals' capacity increment to cope with effective flood management and control.

It is important to take into consideration the relationship between the floods and floodplains through structural measurements.

The primary objective of remote sensing methods for mapping flood-prone areas in developing countries is to provide planners and disaster management institutions with a practical and cost-effective way to identify floodplains and other susceptible areas and to assess the extent of disaster impact. The method can be used in sectoral planning activities, integrated planning studies, and for damage assessment.

Traditionally all over the world, dams, earthen embankments, levees, dykes, and bunds are used dominantly for flood control alternatives. These artificial structures must be in harmoniously functional with natural drainage basin. These precautional structures protect flooding due to local precipitation, tributary, and main channel flooding. If there is not adequate drainage, then they are prone to flood inundation and hazard as a result of waterlogging. Local morphological changes may take place after the embankment constructions as channel sedimentation and bank erosion, which leads to riverbed raise.

Dwelling structures help in a variety of ways to reduce flood water penetration risk through waterproofing walls; fitting openings with permanent or temporary doors, gates, or other closure devices; fitting one-way valves on sewer lines or building boundary walls around the house structure. Other possible measures are sump-pumps that begin operating in basements when water levels rise, and contingency plans and design facilities to operate flood anticipation. Reliable flood warning system is necessary for preparative. Provided that the limits of inundation are known another solution is to raise dwelling locations. In effective integrated flood approach alleviation, mitigation and flood risk management should take into consideration the following major points.

(1) Flood plains and coastal zones should be managed through an integrated catchment management system,
(2) Land use and development must be arranged in such a way that flood alleviation stays at the focal point,
(3) Reduction of human impact on the local environment through flood disaster resilience,

(4) Local capacity improvement and adaptation by means of the best adaptation possibility and its implementation,
(5) Flood vulnerability addressing with satisfactory activities.

Preparedness, response, and recovery are the three emergency planning and management stages. Individuals' capacity, households, groups; communities should work jointly to cope with flood occurrences and possible consequent disasters based on local knowledge, international information, and scientific approaches. The following points are among the prosperous solutions.

(1) It is necessary to have a set of local and central knowledge about possible flood, thread and how to mitigate the consequences before, during and after a flood, and accordingly, identification of flood causes and then mitigation activities,
(2) To have an inventory of presently available resources as physical assets and possibilities of various cooperative organizations with household neighboring groups, communities toward the best solution among different alternatives.

In an effective integrated flood management, the most necessary ingredients are a flood early warning system, flood mitigation strategies, possible evacuation plans, and after-flood evacuation plans. In an effective IFM study, inclusion of the following points is important for the success in an optimum manner. Enabling conditions that will promote an IFM approach to flood management must include the following.

(1) Public involvement promotion and support for integrated final decisions after the identification the characteristics of an IFM,
(2) For the success of an integrated drainage area, single functional operations must be integrated for in multi-operational activity,
(3) Any flood hazard management cannot be fully successful if institutional design system is not integrated into the overall management functionality. Especially, mutual cooperation between various institutions is a key factor for the common success in the mitigation against flood hazards,
(4) Local communities that cope with the possible flood subject, should be supported by practical knowledge for awareness and decision-making to minimize flood destructive aspects.

Before, during, and after flood occurrence energy, water, and food needs should be planned according to local circumstances. There are many alternative options for demand-side management and supply efficiency. The following items are some of the significant components for a successful flood management.

(1) In the demand-side management, important points are consumption reduction, recycling, technological means to promote water, and power efficiency at the user locations,
(2) Supply and conveyance efficiencies must be improved through rational and logically planned management strategies by taking into consideration new supply sources and conveyance possibilities. For instance, among such tasks are leakage reduction from the water distribution pipe network, periodic

maintenance, control upgradation, promotion, and application of refined and new technologies for transmission and distribution means,

(3) Especially, upstream drainage basin management to reduce erosion and downstream sedimentation by means of vegetation cover enhancement, local structural measures, peak discharge, and expected occurrence time predictions and contribution to groundwater storages by means of natural and artificial recharge augmentations,

(4) Search for the best local and environmentally effective, economically viable, acceptable solutions among local people by consensus, water recycling, water and runoff harvestings,

(5) Improvements in the performance of irrigation and agricultural activities for better productivities in an overall management system in addition to local, small-scale and traditional water management and harvesting systems, and groundwater recharge methods.

## 9.10 Flood Resilience

Resilience is the ability of a system with its component parts to anticipate, absorb, accommodate, or recover from the effects of any hazardous event in a timely and efficient manner. During this process preservation, restoration or improvement in essentially basic infrastructure and their components must be ensured for the safety of the community and society. Policy makers are facing increasing calls to consider the resilience of communities that rely on ecosystem goods and services, and the resilience of natural systems themselves. These calls are in response to increasing threats to communities in general from external factors such as environmental (possibly associated with climate change), social (reductions in natural resources), and economic (changes in local and regional economic conditions) hazards. Unfortunately, most communities have had little experience in explicitly managing for resilience (Şen 2015a). Resilience in few sectors is not enough for climate change adaptation and mitigation, but a complete success is possible with the cooperation of all sectors so that a cascade failure remains outside the circle.

Resilience is also thought as the opposite of vulnerability and its improvement and promotion are possible by means of knowledge accessibility and development processes and poverty reduction programs. The following three items are suggested by Dams and Development (2000) for successful resilience.

(a) The priority for achieving a sustainable and equitable global energy sector is for all societies to increase the efficiency of energy use and the use of renewable sources. High-consumption societies must also reduce their use of fossil fuels. Decentralized, small-scale options based on local renewable sources offer the greatest near-term and possibly long-term potential in rural areas.

(b) In the water supply sector, meeting the needs of those currently not served in both urban and rural areas through a range of efficient supply options is the priority. Further efforts to revitalize existing sources, introduce appropriate pricing strategies, encourage fair and sustainable water marketing and transfers, recycling and reuse, and local strategies such as rainwater harvesting also have great potential.

(c) In the case of floods, as absolute flood control may be neither achievable nor desirable, it is necessary to manage floods to minimize flood damage and maximize ecological benefits. An integrated approach to flood management will involve reducing a community's vulnerability to floods through structural, non-structural, technological and policy alternatives, and increasing people's capacity to cope with floods.

In front of a successive flood management, there are some regulatory hindrances that may be borne by a variety of contributors such as numerous markets, policy, institutional, and intellectual subjective suggestions, which may not be combined in the best possible manner for a common consensus. It is necessary to overcome the barriers of capacity and resource constraints, the dominance of conventional approaches and interests in development planning, a lack of awareness and experience with non-conventional alternatives, inadequate access to capital and a lack of openness in the planning system.

# References

Allen, M. R., & Ingram, W. J. (2002). Constraints on future changes in climate and the hydrologic cycle. *Nature*, Vol. *419*, 224–232.

Baker, V. R., & Kochel, R. C. (1988). Flood sedimentation in bedrock fluvial systems. In: V. R. Baker, R. C. Kochel, & P. C. Patton (Eds.), *Flood geomorphology* (pp. 123–137). New York, USA: Wiley.

Baker, V. R., & Pickup, G. (1987). Flood geomorphology of the Katherine Gorge, Northern Territory, Australia. *Geological Society of America Bulletin, 98,* 635–646.

Baker, V. R., Webb, R. H., & House, P. K. (2002). The Scientific and societal value of paleo flood hydrology. In: P. K. House, R. H. Webb, V. R. Baker, & D. R. Levish (Eds.), *Ancient floods, and modern hazards: Principles and applications of paleo flood hydrology, water science and application series* (Vol. 5, pp. 127–146).

Baker, J. D., Littnan, C. L., Johnston, D. W. (2006). Potential effects of sea level rise on the terrestrial habitats of endangered and endemic megafauna in the Northwestern Hawaiian Islands. *Endangered Species Research*, Vol. *2*, 21–30.

Benito, G., Díez-Herrero, A., & Fernández de Villalta, M. (2003a). Magnitude and frequency of flooding in the Tagus Basin (Central Spain) over the last millennium. *Climatic Change, 58,* 171–192.

Benito, G., Lang, M., Barriendos, M., Llasat, M. C., Francés, F., Ouarda, T., et al. (2003b). Use of systematic, paleoflood and historical data for the improvement of flood risk estimation. Review of scientific methods. *Natural Hazards, 31,* 623–643.

Benito, G., Sánchez-Moya, Y., & Sopeña, A. (2003c). Sedimentology of high-stage flood deposits of the Tagus River, Central Spain. *Sedimentary Geology, 157,* 107–132.

Benito, G., Sopeña, A., Sánchez, Y., Machado, M. J., & Pérez González, A. (2003d). Paleo flood Record of the Tagus River (Central Spain) during the Late Pleistocene and Holocene. *Quaternary Science Reviews, 22,* 1737–1756.

Benito, G., Lang, M., Barriendos, M., Llasat, M. C., Francés, F., Ouarda, T., Thorndycraft, V., Enzel, Y., Bardossy, A., Coeur, D., and Bobée, B. (2004). Systematic, paleoflood and historical data for the improvement of flood risk estimation, *Natural Hazards*, Vol. *31*, 623–643.

Bilsborrow, R. E. (1998). The state of the art and overview of the chapters. In R. E. Bilsborrow (Ed.), *Migration, urbanization and development: New directions and issues, proceedings of the symposium on internal migration and urbanization in developing countries*. January 22–24, 1996, New York, (Massachusetts, United Nations Population Fund and Kluwer Academic Publishers): pp. 1–56.

Dams and Development. (2000). *A new framework for decision-making the report of the world commission on dams*. London and Sterling, VA: Earth Scan Publications Ltd.

Ely, L. L., & Baker, V. R. (1985). Reconstructing paleo flood hydrology with slack water deposits: Verde River, Arizona. *Physical Geography, 6,* 103–126.

Füssel, H. M. (2010). How inequitable is the global distribution of responsibility, capability, and vulnerability to climate change: A comprehensive indicator-based assessment. *Global Environmental Change*, Vol. *20*(4), 597–611.

Greenbaum, N., Schick, A. P., & Baker, V. R. (2000). The paleo flood record of a hyper arid catchment, Nahal Zin, Negev Desert, Israel. *Earth Surface Processes and Landforms, 25,* 951–971.

Hall, M. J. (1984). *Urban hydrology*. New York: Elsevier Applied Science Publishers.

House, P. K., Pearthree, P. A., & Klawon, J. E. (2002b). Historical flood and paleo flood chronology of the Lower Verde River, Arizona: Stratigraphic evidence and related uncertainties. In: P. K. House, R. H. Webb, V. R. Baker, & D. R. Levish (Eds.), *Ancient floods, modern hazards: Principles and applications of paleo flood hydrology, water science and application series* (Vol. 5, pp. 267–293).

House, P. K., Webb, R. H., Baker, V. R., & Levish, D. R. (2002a). (Eds.). *Ancient floods, modern hazards: Principles and applications of paleo flood hydrology, water science and application series* (Vol. 5, 385p).

Hooijer, A., Klijn, F., Bas, G., Pedroli, M., & Van Os, A. (2004). Towards sustainable flood risk management in the Rhine and Meuse river basins: synopsis of the findings of IRMA-SPONGE, River research and applications, Vol. *20*, 343–357.

IPCC. (2007). *Climate change 2007: Impacts, adaptation, and vulnerability*. (Contribution of Working Group II to the Fourth Assessment Report of the Intergovernmental Panel on Climate Change). Cambridge, UK: Cambridge University Press.

Jones, A. P., Shimazu, H., Oguchi, T., Okuno, M., & Tokutake, M. (2001). Late Holocene slack water deposits on the Nakagawa River, Tochigi Prefecture, Japan. *Geomorphology, 39,* 39–51.

Kale, V. S., Singhvi, A. K., Mishra, P. K., & Banerjee, D. (2000). Sedimentary records and luminescence chronology of Late Holocene paleo floods in the Luna River, Thar Desert, northwest India. *CATENA, 40,* 337–358.

Kenny, R. (1990). Hydrogeomorphic flood hazard evaluation for semi-arid environments. *Quarterly Journal of Engineering Geology, 23,* 333–336.

Knight, F. H. (1921). Risk, Uncertainty and Profit. New York: Harper & Row. http://www.econlib.org/library/Knight/knRUPCover.html.

Kochel, R. C., & Baker, V. R. (1988). Paleo flood analysis using slack water deposits. In V. R. Baker, R. C. Kochel, & P. C. Patton (Eds.), *Flood Geomorphology* (pp. 357–376). New York, USA: Wiley.

Kochel, R. C., Baker, V. R., & Patton, P. C. (1982). Paleo-hydrology of Southwest Texas. *Water Resources Research, 18,* 1165–1183.

Marsalek, J. (2000) Overview of Flood Issues in Contemporary Water Management. In: Marsalek J., Watt W. E., Zeman E., Sieker F. (Eds.), *Flood Issues in Contemporary Water Management*. NATO Science Series (Series 2. Environment Security), Vol. *71*. Springer, Dordrecht.

Montoya, L. (2002). Urban disaster management: A case study of earthquake risk assessment in Cartago, Costa Rica. Enscheda, ITC Publication Series No. 96.

O'Connor, J. E., Ely, L. L., Stevens, L. E., Melisa, T. S., Kale, V. S., & Baker, V. R. (1994). A 4500-year record of large floods in the Colorado River in the Grand Canyon, Arizona. *The Journal of Geology, 102,* 1–9.

Oumeraci, H. (2004). Sustainable coastal flood defences: scientific and modelling challenges towards an integrated risk-based design concept. *Proc. First IMA International Conference on Flood Risk Assessment, IMA - Institute of Mathematics and its Applications, Session*, Vol. *1*, Bath, UK: 9–24.

Partridge, J. B., & Baker, V. R. (1987). Paleo flood hydrology of the Salt River, Arizona. *Earth Surface Processes and Landforms, 12,* 109–125.

Pickup, G., Allan, G., & Baker, V. R. (1988). History, paleo-channels and paleo floods of the Finke River, central Australia. In R. F. Warner (Ed.), *Fluvial geomorphology of Australia* (pp. 177–200). Sydney: Academic Press.

Plate, E. (1999). Flood risk management: A strategy to cope with floods. In: Bronstert, A., Ghazi A., Hladny J., Kundzewicz Z. W., Menzel L. (Eds.), *Proceedings of the European Expert Meeting on the Oder Flood 1997*. Luxembourg (European Communities), (pp. 115–128).

Rahmstorf, S. (2007). Sea-level rise a semi-empirical approach to projecting future. *Science*, Vol. *315*, 368–370. doi:10.1126/science.1135456.

Romero, R. J. A., Guijarro Ramis, C., & Alonso, S. (1998). A 30-year (1964–1993) daily rainfall data base for the Spanish Mediterranean regions: first exploratory study. *International Journal of Climatology, 18,* 541–560.

Saldarriaga, J., & Yevjevich, V. (1970). Application of run-lengths to hydrologic series. Hydrology Paper 40, Colorado State University, Fort Collins, Colorado.

Seckler, D., Molden, D., & Randolph, B., (1998). Water scarcity in the twenty-first century. IWMI Water Brief 1. Colombo, Sri Lanka: International Water Management Institute.

Şen, Z. (1976). Wet and dry periods of annual flow series. *Journal of the Hydraulics Division, ASCE, 102*, No. HY10, Proceedings Paper 12457, 1503–1514.

Şen, Z. (1997). Weather modification methods and their impractical consequences are discussed by Şen (1997).

Şen, Z. (2004). *Hydrograph methods, arid regions, Saudi Geological Survey (SGS)*, Technical Report.

Şen, Z. (2008). Wadi hydrology. New York: Taylor and Francis Group, CRC Press, 347 p.

Şen, Z. (2010). *Fuzzy logic and hydrological modeling*. New York: Taylor and Francis Group, CRC Press. 340p.

Şen, Z. (2015a). *Drought modeling, prediction and mitigation* (p. 472). Amsterdam, Netherlands: Elsevier.

Şen, Z. (2015b). Global warming quantification by innovative trend template method. International Journal of Global Warming (in print).

Sheffer, N. A., Enzel, Y., Benito, G., Grodek, T., Poart, N., Lang, M., et al. (2003). Historical and paleo floods of the Ardèche river, France. *Water Resources Research, 39,* 1376.

Smith, K. (1992). *Environmental hazards assessing risk and reducing disaster*. London: Routledge. 324p.

UNDRO, (1991). Office of the United Nations Disaster Relief Co-coordinator: Mitigation natural disasters: phenomena, effects and options. A manual for policy makers and planners, United Nations, New York.

Wamsler, C. (2004). Managing urban risk: Perceptions of housing and planning as a tool for reducing disaster risk. *Global Built Environmental Review (GBER), 4*(2), 11–28.

Wohl, E. E., Webb, R. H., Baker, V. R., & Pickup, G. (1994). Sedimentary flood records in the bedrock canyons of rivers in the monsoonal region of Australia. Water Resour. Papers 107, 102p.

Yadigaroğlu, G., & Chakraborty, S. (1985). Risikountersuchungen als Entscheidunsinstrument. (Risk analysis as decision tool). TUV Rheinland Publication.

Yang, H., Yu, G., Xie, Y., Zhan, D., & Li, Z. (2000). Sedimentary records of large Holocene floods from the middle reaches of the Yellow River, China. *Geomorphology, 33,* 73–88.

# Index